A Heat Transfer Textbook

Third Edition

by

John H. Lienhard IV

and

John H. Lienhard V

SHOUT
SHARE
IT

Professor John H. Lienhard IV
Department of Mechanical Engineering
University of Houston
Houston TX 77204-4792 U.S.A.

Professor John H. Lienhard V
Department of Mechanical Engineering
Massachusetts Institute of Technology
77 Massachusetts Avenue
Cambridge MA 02139-4307 U.S.A.

Copyright ©2000 by John H. Lienhard IV and John H. Lienhard V
All rights reserved

Please note that this material is copyrighted under U.S. Copyright Law. The authors grant you the right to download and print it for your personal use or for non-profit instructional use. Any other use, including copying, distributing or modifying the work for commercial purposes, is subject to the restrictions of U.S. Copyright Law. International copyright is subject to the Berne International Copyright Convention.

The authors have used their best efforts to ensure the accuracy of the methods, equations, and data described in this book, but they do not guarantee them for any particular purpose. The authors and publisher offer no warranties or representations, nor do they accept any liabilities with respect to the use of this information. Please report any errata to authors.

Lienhard, John H., 1930–
A heat transfer textbook / John H. Lienhard IV and
John H. Lienhard V — 3rd ed. — Cambridge, MA :
J.H. Lienhard V, c2000
Includes bibliographic references
1. Heat—Transmission 2. Mass Transfer
I. Lienhard, John H., V, 1961– II. Title
TJ260.L445 2000

Published by J.H. Lienhard V
Cambridge, Massachusetts, U.S.A.

This book was typeset in Lucida Bright and Lucida New Math fonts (designed by Bigelow & Holmes) using LaTeX under the Y&Y TeX System.

For updates and information, visit:

`http://web.mit.edu/lienhard/www/ahtt.html`

This copy is:

`Version 0.20 dated June 27, 2001`

Preface

Contents

I The General Problem of Heat Exchange **1**

1 Introduction **3**
- 1.1 Heat transfer . . . 3
- 1.2 Relation of heat transfer to thermodynamics . . . 6
- 1.3 Modes of heat transfer . . . 10
- 1.4 A look ahead . . . 35
- 1.5 Problems . . . 35
- Problems . . . 37
- References . . . 45

2 Heat conduction concepts, thermal resistance, and the overall heat transfer coefficient **49**
- 2.1 The heat diffusion equation . . . 49
- 2.2 Solutions of the heat diffusion equation . . . 58
- 2.3 Thermal resistance and the electrical analogy . . . 62
- 2.4 Overall heat transfer coefficient, U . . . 74
- 2.5 Summary . . . 82
- Problems . . . 83
- References . . . 91

3 Heat exchanger design **93**
- 3.1 Function and configuration of heat exchangers . . . 93
- 3.2 Evaluation of the mean temperature difference in a heat exchanger . . . 97
- 3.3 Heat exchanger effectiveness . . . 114
- 3.4 Heat exchanger design . . . 120
- Problems . . . 123
- References . . . 129

II Analysis of Heat Conduction **131**

4 Analysis of heat conduction and some steady one-dimensional problems **133**
4.1 The well-posed problem 133
4.2 The general solution 135
4.3 Dimensional analysis 142
4.4 An illustration of dimensional analysis in a complex steady conduction problem 151
4.5 Fin design 155
Problems 173
References 180

5 Transient and multidimensional heat conduction **181**
5.1 Introduction 181
5.2 Lumped-capacity solutions 182
5.3 Transient conduction in a one-dimensional slab 191
5.4 Temperature-response charts 196
5.5 One-term solutions 206
5.6 Transient heat conduction to a semi-infinite region 208
5.7 Steady multidimensional heat conduction 223
5.8 Transient multidimensional heat conduction 235
Problems 240
References 250

III Convective Heat Transfer **253**

6 Laminar and turbulent boundary layers **255**
6.1 Some introductory ideas 255
6.2 Laminar incompressible boundary layer on a flat surface 262
6.3 The energy equation 278
6.4 The Prandtl number and the boundary layer thicknesses . 282
6.5 Heat transfer coefficient for laminar, incompressible flow over a flat surface 286
6.6 The Reynolds analogy 297
6.7 Turbulent boundary layers 299
Problems 310
References 315

7 Forced convection in a variety of configurations 317
7.1 Introduction 317
7.2 Heat transfer to and from laminar flows in pipes 318
7.3 Turbulent pipe flow 330
7.4 Heat transfer surface viewed as a heat exchanger 340
7.5 Heat transfer coefficients for noncircular ducts 342
7.6 Heat transfer during cross flow over cylinders 342
7.7 Other configurations 352
Problems 354
References 359

8 Natural convection in single-phase fluids and during film condensation 363
8.1 Scope 363
8.2 The nature of the problems of film condensation and of natural convection 364
8.3 Laminar natural convection on a vertical isothermal surface 367
8.4 Natural convection in other situations 382
8.5 Film condensation 394
Problems 409
References 416

9 Heat transfer in boiling and other phase-change configurations 421
9.1 Nukiyama's experiment and the pool boiling curve 421
9.2 Nucleate boiling 428
9.3 Peak pool boiling heat flux 436
9.4 Film boiling 450
9.5 Minimum heat flux 452
9.6 Transition boiling and system influences 453
9.7 Forced convection boiling in tubes 460
9.8 Two-phase flow in horizontal tubes 466
9.9 Forced convective condensation heat transfer 469
9.10 Dropwise condensation 470
9.11 The heat pipe 473
Problems 475
References 478

IV Thermal Radiation Heat Transfer **485**

10 Radiative heat transfer **487**
10.1 The problem of radiative exchange 487
10.2 Kirchhoff's law 495
10.3 Simple radiant heat exchange between two surfaces 497
10.4 Heat transfer among gray bodies 512
10.5 Gaseous radiation 522
10.6 Solar energy 530
Problems 535
References 542

V Mass Transfer **545**

11 An Introduction to Mass Transfer **547**
11.1 Introduction 547
11.2 Mixture compositions and species fluxes 550
11.3 Diffusion fluxes and Fick's Law 558
11.4 Transport properties of mixtures 562
11.5 The equation of species conservation 576
11.6 Steady mass transfer through a stagnant layer 586
11.7 Mass transfer coefficients 593
11.8 Simultaneous heat and mass transfer 606
Problems 616
References 628

VI Appendices **631**

A Some thermophysical properties of selected materials **633**
References 636

B Units and conversion factors **663**
References 664

C Nomenclature **667**

Citation Index **673**

Subject Index **679**

Part I

The General Problem of Heat Exchange

1. Introduction

The radiation of the sun in which the planet is incessantly plunged, penetrates the air, the earth, and the waters; its elements are divided, change direction in every way, and, penetrating the mass of the globe, would raise its temperature more and more, if the heat acquired were not exactly balanced by that which escapes in rays from all points of the surface and expands through the sky. ***The Analytical Theory of Heat,*** **J. Fourier**

1.1 Heat transfer

People have always understood that something flows from hot objects to cold ones. We call that flow *heat.* In the eighteenth and early nineteenth centuries, scientists imagined that all bodies contained an invisible fluid which they called *caloric.* Caloric was assigned a variety of properties, some of which proved to be inconsistent with nature (e.g., it had weight and it could not be created nor destroyed). But its most important feature was that it flowed from hot bodies into cold ones. It was a very useful way to think about heat. Later we shall explain the flow of heat in terms more satisfactory to the modern ear; however, it will seldom be wrong to imagine caloric flowing from a hot body to a cold one.

The flow of heat is all-pervasive. It is active to some degree or another in everything. Heat flows constantly from your bloodstream to the air around you. The warmed air buoys off your body to warm the room you are in. If you leave the room, some small buoyancy-driven (or *convective*) motion of the air will continue because the walls can never be perfectly isothermal. Such processes go on in all plant and animal life and in the air around us. They occur throughout the earth, which is hot at its core and cooled around its surface. The only conceivable domain free from heat flow would have to be isothermal and totally isolated from any other

region. It would be "dead" in the fullest sense of the word — devoid of any process of any kind.

The overall driving force for these heat flow processes is the cooling (or leveling) of the thermal gradients within our universe. The heat flows that result from the cooling of the sun are the primary processes that we experience naturally. The conductive cooling of Earth's center and the radiative cooling of the other stars are processes of secondary importance in our lives.

The life forms on our planet have necessarily evolved to match the magnitude of these energy flows. But while "natural man" is in balance with these heat flows, "technological man"[1] has used his mind, his back, and his will to harness and control energy flows that are far more intense than those we experience naturally. To emphasize this point we suggest that the reader make an experiment.

Experiment 1.1

Generate as much power as you can, in some way that permits you to measure your own work output. You might lift a weight, or run your own weight up a stairwell, against a stopwatch. Express the result in watts (W). Perhaps you might collect the results in your class. They should generally be less than 1 kW or even 1 horsepower (746 W). How much less might be surprising.

Thus, when we do so small a thing as turning on a 150 W light bulb, we are manipulating a quantity of energy substantially greater than a human being could produce in sustained effort. The energy consumed by an oven, toaster, or hot water heater is an order of magnitude beyond our capacity. The energy consumed by an automobile can easily be three orders of magnitude greater. If all the people in the United States worked continuously like galley slaves, they could barely equal the power output of even a single city power plant.

Our voracious appetite for energy has steadily driven the intensity of actual heat transfer processes upward until they are far greater than those normally involved with life forms on earth. Until the middle of the

[1] Some anthropologists think that the term *Homo technologicus* (technological man) serves to define human beings, as apart from animals, better than the older term *Homo sapiens* (man, the wise). We may not be as much wiser than the animals as we think we are, but only we do serious sustained tool making.

thirteenth century, the energy we use was drawn indirectly from the sun using comparatively gentle processes — animal power, wind and water power, and the combustion of wood. Then population growth and deforestation drove the English to using coal. By the end of the seventeenth century, England had almost completely converted to coal in place of wood. At the turn of the eighteenth century, the first commercial steam engines were developed, and that set the stage for enormously increased consumption of coal. Europe and America followed England in these developments.

The development of fossil energy sources has been a bit like Jules Verne's description in *Around the World in Eighty Days* in which, to win a race, a crew burns the inside of a ship to power the steam engine. The combustion of nonrenewable fossil energy sources (and, more recently, the fission of uranium) has led to remarkably intense energy releases in power-generating equipment. The energy transferred as heat in a nuclear reactor is on the order of *one million watts per square meter.*

A complex system of heat and work transfer processes is invariably needed to bring these concentrations of energy back down to human proportions. We must understand and control the processes that divide and diffuse intense heat flows down to the level on which we can interact with them. To see how this works, consider a specific situation. Suppose we live in a town where coal is processed into fuel-gas and coke. Such power supplies used to be common, and they may return if natural gas supplies ever dwindle. Let us list a few of the process heat transfer problems that must be solved before we can drink a glass of iced tea.

- A variety of high-intensity heat transfer processes are involved with combustion and chemical reaction in the gasifier unit itself.

- The gas goes through various cleanup and pipe-delivery processes to get to our stoves. The heat transfer processes involved in these stages are generally less intense.

- The gas is burned in the stove. Heat is transferred from the flame to the bottom of the teakettle. While this process is small, it is intense because boiling is a very efficient way to remove heat.

- The coke is burned in a steam power plant. The heat transfer rates from the combustion chamber to the boiler, and from the wall of the boiler to the water inside, are very intense.

- The steam passes through a turbine where it is involved with many heat transfer processes, including some condensation in the last stages. The spent steam is then condensed in any of a variety of heat transfer devices.

- Cooling must be provided in each stage of the electrical supply system: the winding and bearings of the generator, the transformers, the switches, the power lines, and the wiring in our houses.

- The ice cubes for our tea are made in an electrical refrigerator. It involves three major heat exchange processes and several lesser ones. The major ones are the condensation of refrigerant at room temperature to reject heat, the absorption of heat from within the refrigerator by evaporating the refrigerant, and the balancing heat leakage from the room to the inside.

- Let's drink our iced tea quickly because heat transfer from the room to the water and from the water to the ice will first dilute, and then warm, our tea if we linger.

A society based on power technology teems with heat transfer problems. Our aim is to learn the principles of heat transfer so we can solve these problems and design the equipment needed to transfer thermal energy from one substance to another. In a broad sense, all these problems resolve themselves into collecting and focusing large quantities of energy for the use of people, and then distributing and interfacing this energy with people in such a way that they can use it on their own puny level.

We begin our study by recollecting how heat transfer was treated in the study of thermodynamics and by seeing why thermodynamics is not adequate to the task of solving heat transfer problems.

1.2 Relation of heat transfer to thermodynamics

The First Law with work equal to zero

The subject of thermodynamics, as taught in engineering programs, makes constant reference to the heat transfer between systems. The First Law of Thermodynamics for a closed system takes the following form on a

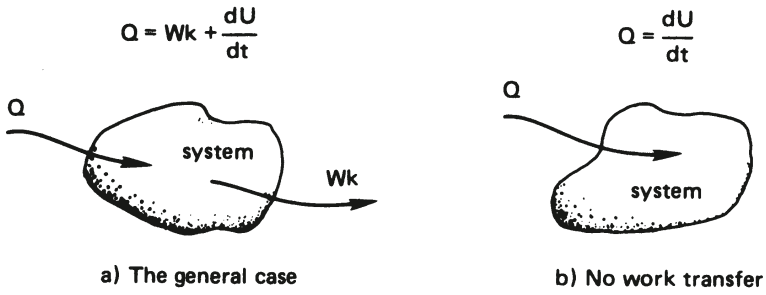

Figure 1.1 The First Law of Thermodynamics for a closed system.

rate basis:

$$\underbrace{Q}_{\substack{\text{positive toward}\\ \text{the system}}} = \underbrace{Wk}_{\substack{\text{positive away}\\ \text{from the system}}} + \underbrace{\frac{dU}{dt}}_{\substack{\text{positive when}\\ \text{the system's}\\ \text{energy increases}}} \tag{1.1}$$

where Q is the heat transfer rate and Wk is the work transfer rate. They may be expressed in joules per second (J/s) or watts (W). The derivative dU/dt is the rate of change of internal thermal energy, U, with time, t. This interaction is sketched schematically in Fig. 1.1a.

The analysis of heat transfer processes can generally be done without reference to any work processes, although heat transfer might subsequently be combined with work in the analysis of real systems. If $p\,dV$ work is the only work occuring, then eqn. (1.1) is

$$Q = p\frac{dV}{dt} + \frac{dU}{dt} \tag{1.2a}$$

This equation has two well-known special cases:

$$\text{Constant volume process:} \qquad Q = \frac{dU}{dt} = mc_v\frac{dT}{dt} \tag{1.2b}$$

$$\text{Constant pressure process:} \qquad Q = \frac{dH}{dt} = mc_p\frac{dT}{dt} \tag{1.2c}$$

where $H \equiv U + pV$ is the enthalpy, and c_v and c_p are the specific heat capacities at constant volume and constant pressure, respectively.

When the substance undergoing the process is incompressible (so that V is constant for any pressure variation), the two specific heats are equal: $c_v = c_p \equiv c$. The proper form of eqn. (1.2a) is then

$$\boxed{Q = \frac{dU}{dt} = mc\,\frac{dT}{dt}} \tag{1.3}$$

Since solids and liquids can frequently be approximated as being incompressible, we shall often make use of eqn. (1.3).

If the heat transfer were reversible, then eqn. (1.2a) would become[2]

$$\underbrace{T\,\frac{dS}{dt}}_{Q_{\text{rev}}} = \underbrace{p\,\frac{dV}{dt}}_{Wk_{\text{rev}}} + \frac{dU}{dt} \tag{1.4}$$

That might seem to suggest that Q can be evaluated independently for inclusion in either eqn. (1.1) or (1.3). However, it cannot be evaluated using $T\,dS$, because real heat transfer processes are all irreversible and S is not defined as a function of T in an irreversible process. The reader will recall that engineering thermodynamics might better be named thermo*statics*, because it only describes the equilibrium states on either side of irreversible processes.

Since the rate of heat transfer cannot be predicted using $T\,dS$, how can it be determined? If $U(t)$ were known, then (when $Wk = 0$) eqn. (1.3) would give Q, but $U(t)$ is seldom known *a priori*.

The answer is that a new set of physical principles must be introduced to predict Q. The principles are *transport laws*, which are not a part of the subject of thermodynamics. They include Fourier's law, Newton's law of cooling, and the Stefan-Boltzmann law. We introduce these laws later in the chapter. The important thing to remember is that a description of heat transfer requires that additional principles be combined with the First Law of Thermodynamics.

Reversible heat transfer as the temperature gradient vanishes

Consider a wall connecting two thermal reservoirs as shown in Fig. 1.2. As long as $T_1 > T_2$, heat will flow *spontaneously* and *irreversibly* from 1 to 2. In accordance with our understanding of the Second Law of Thermodynamics, we expect the entropy of the universe to increase as a consequence of this process. If $T_2 \longrightarrow T_1$, the process will approach being

[2] T = absolute temperature, S = entropy, V = volume, p = pressure, and "rev" denotes a reversible process.

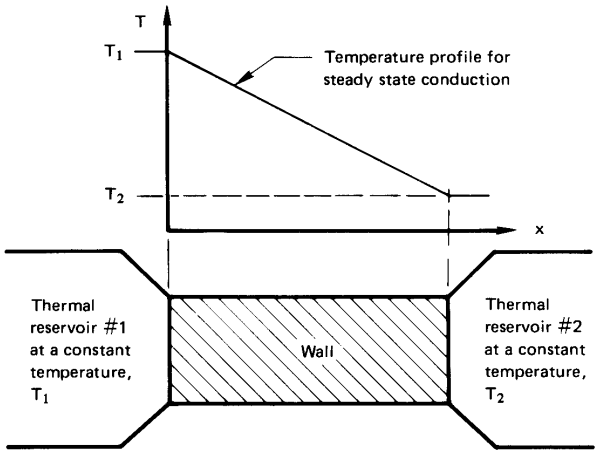

Figure 1.2 Irreversible heat flow between two thermal reservoirs through an intervening wall.

quasistatic and reversible. But the rate of heat transfer will also approach zero if there is no temperature difference to drive it. Thus all real heat transfer processes generate entropy.

Now we come to a dilemma: If the irreversible process occurs at steady state, the properties of the wall do not vary with time. We know that the entropy of the wall depends on its state and must therefore be constant. How, then, does the entropy of the universe increase? We turn to this question next.

Entropy production

The entropy increase of the universe as the result of a process is the sum of the entropy changes of *all* elements that are involved in that process. The *rate of entropy production* of the universe, $\dot{S}_{\mathrm{Un}}$, resulting from the preceding heat transfer process through a wall is

$$\dot{S}_{\mathrm{Un}} = \dot{S}_{\mathrm{res\ 1}} + \underbrace{\dot{S}_{\mathrm{wall}}}_{\substack{=0,\ \text{since } S_{\mathrm{wall}} \\ \text{must be constant}}} + \dot{S}_{\mathrm{res\ 2}} \tag{1.5}$$

where the dots denote time derivatives (i.e., $\dot{x} \equiv dx/dt$). Since the reservoir temperatures are constant,

$$\dot{S}_{\mathrm{res}} = \frac{Q}{T_{\mathrm{res}}}. \tag{1.6}$$

Now $Q_{\text{res }1}$ is negative and equal in magnitude to $Q_{\text{res }2}$, so eqn. (1.5) becomes

$$\dot{S}_{\text{Un}} = \left| Q_{\text{res }1} \right| \left(\frac{1}{T_2} - \frac{1}{T_1} \right). \tag{1.7}$$

The term in parentheses is positive, so $\dot{S}_{\text{Un}} > 0$. This agrees with Clausius's statement of the Second Law of Thermodynamics.

Notice an odd fact here: The rate of heat transfer, Q, and hence $\dot{S}_{\text{Un}}$, is determined by the wall's resistance to heat flow. Although the wall is the agent that causes the entropy of the universe to increase, its own entropy does not changes. Only the entropies of the reservoirs change.

1.3 Modes of heat transfer

Figure 1.3 shows an analogy that might be useful in fixing the concepts of heat conduction, convection, and radiation as we proceed to look at each in some detail.

Heat conduction

Fourier's law. Joseph Fourier[3] (see Fig. 1.4) published his remarkable book *Théorie Analytique de la Chaleur* in 1822. In it he formulated a very complete exposition of the theory of heat conduction.

He began his treatise by stating the empirical law that bears his name: *the heat flux,*[4] q (W/m^2), *resulting from thermal conduction is proportional to the magnitude of the temperature gradient and opposite to it in sign.* If

[3] Joseph Fourier lived a remarkable double life. He served as a high government official in Napoleonic France and he was also an applied mathematician of great importance. He was with Napoleon in Egypt between 1798 and 1801, and he was subsequently prefect of the administrative area (or "Department") of Isère in France until Napoleon's first fall in 1814. During the latter period he worked on the theory of heat flow and in 1807 submitted a 234-page monograph on the subject. It was given to such luminaries as Lagrange and Laplace for review. They found fault with his adaptation of a series expansion suggested by Daniel Bernoulli in the eighteenth century. Fourier's theory of heat flow, his governing differential equation, and the now-famous "Fourier series" solution of that equation did not emerge in print from the ensuing controversy until 1822.

[4] The heat flux, q, is a heat rate per unit area and can be expressed as Q/A, where A is an appropriate area.

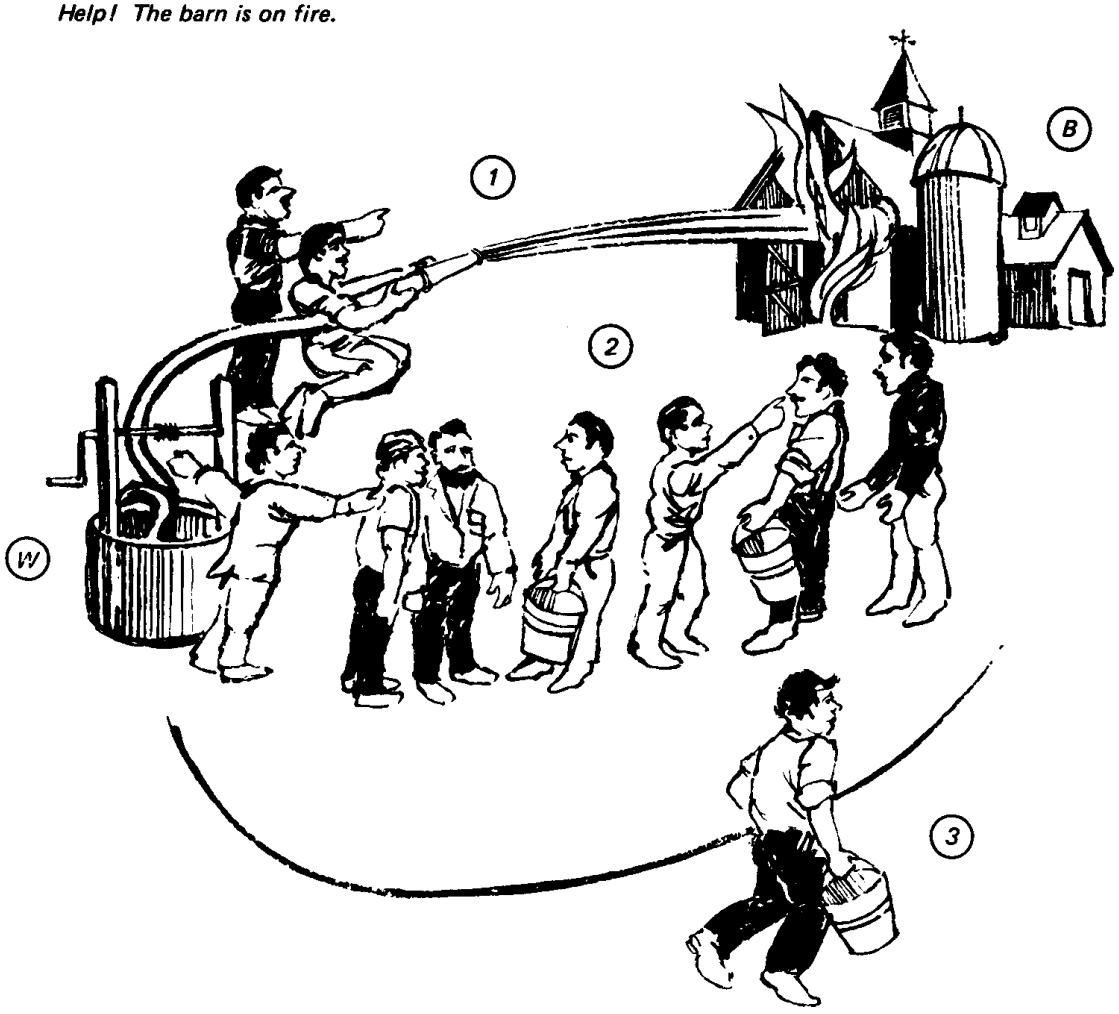

Let the *water* be analogous to *heat,* and let the *people* be analogous to the *heat transfer medium.* Then:

Case 1 **The hose directs water from (W) to (B) independently of the medium. This is analogous to *thermal radiation* in a vacuum or in most gases.**

Case 2 **In the bucket brigade, water goes from (W) to (B) through the medium. This is analogous to *conduction.***

Case 3 **A single runner, representing the medium, carries water from (W) to (B) . This is analogous to *convection.***

Figure 1.3 An analogy for the three modes of heat transfer.

Figure 1.4 Baron Jean Baptiste Joseph Fourier (1768–1830). (Courtesy of *Appl. Mech. Rev.*, vol. 26, Feb. 1973.)

we call the constant of proportionality, k, then

$$q = -k\frac{dT}{dx} \tag{1.8}$$

The constant, k, is called the *thermal conductivity*. It obviously must have the dimensions W/m·K, or J/m·s·K, or Btu/h·ft·°F if eqn. (1.8) is to be dimensionally correct.

The heat flux is a vector quantity. Equation (1.8) tells us that if temperature decreases with x, q will be positive—it will flow in the x-direction. If T increases with x, q will be negative—it will flow opposite the x-direction. In either case, q will flow from higher temperatures to lower temperatures. Equation (1.8) is the one-dimensional form of Fourier's law. We develop its three-dimensional form in Chapter 2, namely:

$$\vec{q} = -k\,\nabla T$$

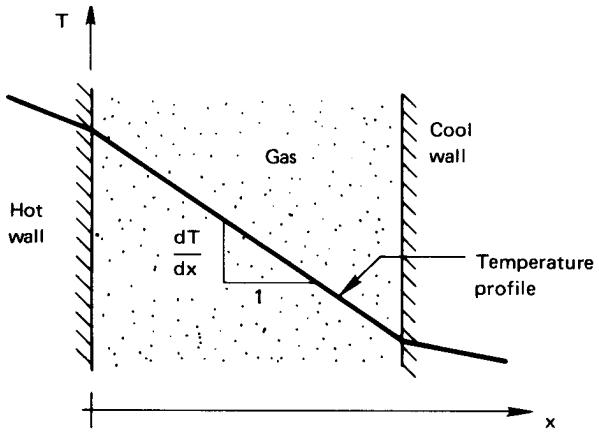

Figure 1.5 Heat conduction through gas separating two solid walls.

Example 1.1

The front of a slab of lead ($k = 35$ W/m·K) is kept at 110°C and the back is kept at 50°C. If the area of the slab is 0.4 m^2 and it is 0.03 m thick, compute the heat flux, q, and the heat transfer rate, Q.

SOLUTION. For the moment, we presume that dT/dx is a constant equal to $(T_{\text{back}} - T_{\text{front}})/(x_{\text{back}} - x_{\text{front}})$; we verify this in Chapter 2. Thus, eqn. (1.8) becomes

$$q = -35\left(\frac{50 - 110}{0.03}\right) = +70,000 \text{ W/m}^2 = 70 \text{ kW/m}^2$$

and

$$Q = qA = 70(0.4) = 28 \text{ kW}$$ ■

In one-dimensional heat conduction problems, there is never any real problem in deciding which way the heat should flow. It is therefore sometimes convenient to write Fourier's law in simple scalar form:

$$q = k\frac{\Delta T}{L} \tag{1.9}$$

where L is the thickness in the direction of heat flow and q and ΔT are both written as positive quantities. When we use eqn. (1.9), we must remember that q always flows from high to low temperatures.

Thermal conductivity values. It will help if we first consider how conduction occurs in, for example, a gas. We know that the molecular velocity depends on temperature. Consider conduction from a hot wall to

a cold one in a situation in which gravity can be ignored, as shown in Fig. 1.5. The molecules near the hot wall collide with it and are agitated by the molecules of the wall. They leave with generally higher speed and collide with their neighbors to the right, increasing the speed of those neighbors. This process continues until the molecules on the right pass their kinetic energy to those in the cool wall. Within solids, comparable processes occur as the molecules vibrate within their lattice structure and as the lattice vibrates as a whole. This sort of process also occurs, to some extent, in the electron "gas" that moves through the solid. The processes are more efficient in solids than they are in gases. Notice that

$$-\frac{dT}{dx} = \underbrace{\frac{q}{k} \propto \frac{1}{k}}_{\substack{\text{since, in steady} \\ \text{conduction, } q \text{ is} \\ \text{constant}}} \tag{1.10}$$

Thus solids, with generally higher thermal conductivities than gases, yield smaller temperature gradients for a given heat flux. In a gas, by the way, k is proportional to molecular speed and molar specific heat, and inversely proportional to the cross-sectional area of molecules.

This book deals almost exclusively with S.I. units, or *Système International d'Unités*. Since much reference material will continue to be available in English units, we should have at hand a conversion factor for thermal conductivity:

$$1 = \frac{\text{J}}{0.0009478\ \text{Btu}} \cdot \frac{\text{h}}{3600\ \text{s}} \cdot \frac{\text{ft}}{0.3048\ \text{m}} \cdot \frac{1.8^\circ\text{F}}{\text{K}}$$

Thus the conversion factor from W/m·K to its English equivalent, Btu/h·ft·°F, is

$$\boxed{1 = 1.731\ \frac{\text{W/m·K}}{\text{Btu/h·ft·°F}}} \tag{1.11}$$

Consider, for example, copper—the common substance with the highest conductivity at ordinary temperature:

$$k_{\text{Cu at room temp}} = (383\ \text{W/m·K}) \Big/ 1.731 \frac{\text{W/m·K}}{\text{Btu/h·ft·°F}} = 221\ \text{Btu/h·ft·°F}$$

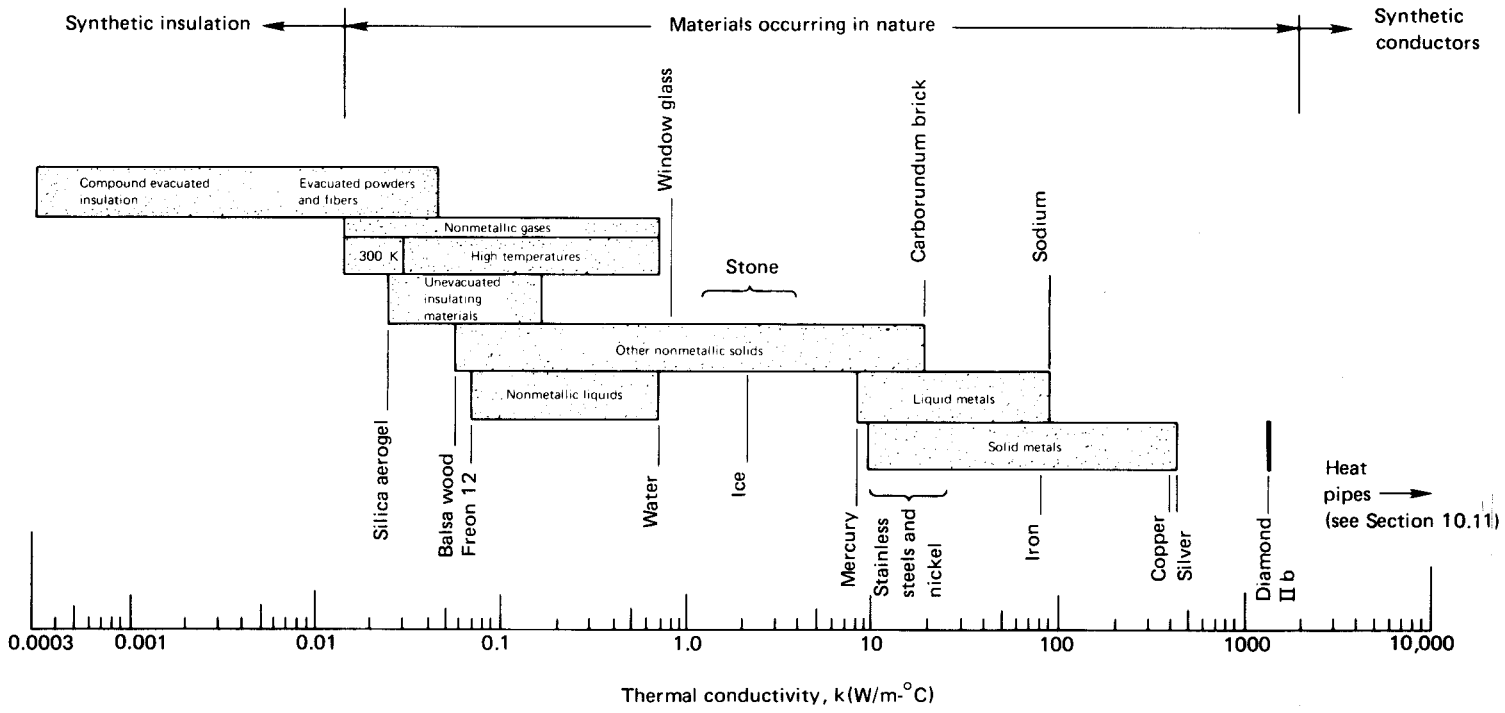

Figure 1.6 The approximate ranges of thermal conductivity of various substances.(All values are for the neighborhood of room temperature unless otherwise noted.)

The range of thermal conductivities is enormous. As we see from Fig. 1.6, k varies by a factor of about 10^5 between gases and diamond at room temperature. This variation can be increased to about 10^7 if we include the effective conductivity of various cryogenic "superinsulations." (These involve powders, fibers, or multilayered materials that have been evacuated of all air.) The reader should study and remember the order of magnitude of the thermal conductivities of different types of materials. This will be a help in avoiding mistakes in future computations, and it will be a help in making assumptions during problem solving. Actual numerical values of the thermal conductivity are given in Appendix A (which is a broad listing of many of the physical properties you might need in this course) and in Figs. 2.2 and 2.3.

Example 1.2

A copper slab (k = 372 W/m·K) is 3 mm thick. It is protected from corrosion by a 2-mm-thick layers of stainless steel (k = 17 W/m·K) on both sides. The temperature is 400°C on one side of this composite wall and 100°C on the other. Find the temperature distribution in the copper slab and the heat conduction through the wall (see Fig. 1.7).

Solution. If we recall Fig. 1.5 and eqn. (1.10), it should be clear that the temperature drop will take place almost entirely in the stainless steel, where k is less than 1/20 of k in the copper. Thus, the copper will be virtually isothermal at the average temperature of $(400 + 100)/2 = 250$°C. Furthermore, the heat conduction can be estimated in a 4 mm slab of stainless steel as though the copper were not even there. With the help of Fourier's law in the form of eqn. (1.8), we get

$$q = -k\frac{dT}{dx} \simeq 17 \text{ W/m·K} \cdot \left(\frac{400 - 100}{0.004}\right) \text{K/m} = 1275 \text{ kW/m}^2$$

The accuracy of this rough calculation can be improved by considering the copper. To do this we first solve for $\Delta T_{\text{s.s.}}$ and ΔT_{Cu} (see Fig. 1.7). Conservation of energy requires that the steady heat flux through all three slabs must be the same. Therefore,

$$q = \left(k\frac{\Delta T}{L}\right)_{\text{s.s.}} = \left(k\frac{\Delta T}{L}\right)_{\text{Cu}}$$

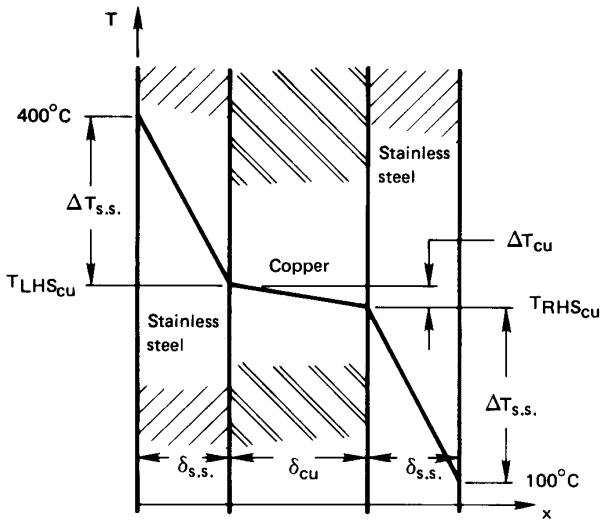

Figure 1.7 Temperature drop through a copper wall protected by stainless steel (Example 1.2).

but

$$\begin{aligned}(400-100)^\circ\text{C} &\equiv \Delta T_{\text{Cu}} + 2\Delta T_{\text{s.s.}} \\ &= \Delta T_{\text{Cu}}\left[1 + 2\frac{(k/L)_{\text{Cu}}}{(k/L)_{\text{s.s.}}}\right] \\ &= (30/18)\Delta T_{\text{Cu}}\end{aligned}$$

Solving this, we obtain $\Delta T_{\text{Cu}} = 9.94$ K. So $\Delta T_{\text{s.s.}} = (300 - 9.94)/2 = 145$ K. It follows that $T_{\text{Cu, left}} = 255^\circ$C and $T_{\text{Cu, right}} = 245^\circ$C.

The heat flux can be obtained by applying Fourier's law to any of the three layers. We consider either stainless steel layer and get

$$q = 17\frac{\text{W}}{\text{m}\cdot\text{K}}\frac{145\text{ K}}{0.002\text{ m}} = 1233\text{ kW/m}^2$$

Thus our initial approximation was accurate within a few percent. ■

One-dimensional heat diffusion equation. In Example 1.2 we had to deal with a major problem that arises in heat conduction problems. The problem is that Fourier's law involves two dependent variables, T and q. To eliminate q and first solve for T, we introduced the First Law of Thermodynamics implicitly: Conservation of energy required that q was the same in each metallic slab.

The elimination of q from Fourier's law must now be done in a more general way. Consider a one-dimensional element, as shown in Fig. 1.8.

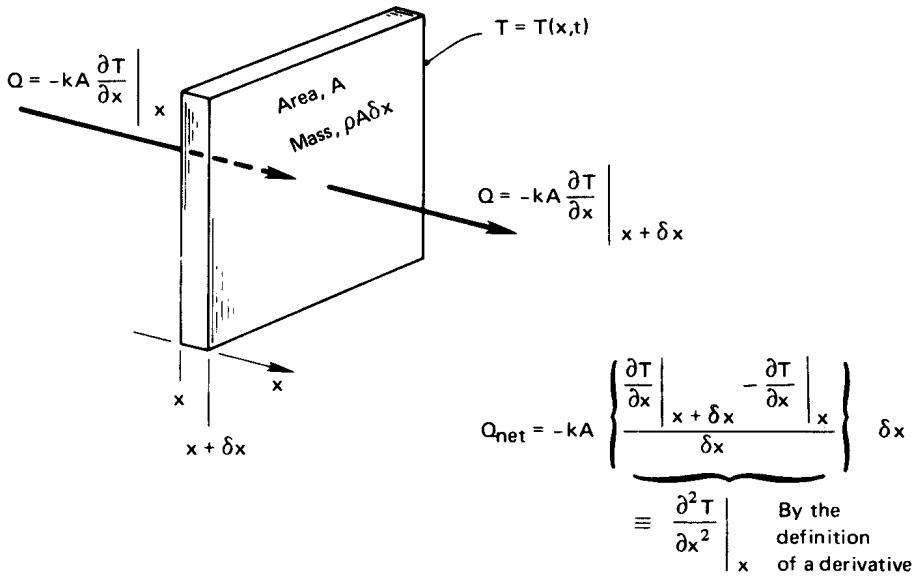

Figure 1.8 One-dimensional heat conduction through a differential element.

From Fourier's law applied at each side of the element, as shown, the net heat conduction out of the element during general unsteady heat flow is

$$q_{\text{net}}A = Q_{\text{net}} = -kA\frac{\partial^2 T}{\partial x^2}\,\delta x \tag{1.12}$$

To eliminate the heat loss Q_{net} in favor of T, we use the general First Law statement for closed, nonworking systems, eqn. (1.3):

$$-Q_{\text{net}} = \frac{dU}{dt} = \rho cA\frac{d(T - T_{\text{ref}})}{dt}\,\delta x = \rho cA\frac{dT}{dt}\delta x \tag{1.13}$$

where ρ is the density of the slab and c is its specific heat capacity.[5] Equations (1.12) and (1.13) can be combined to give

$$\boxed{\frac{\partial^2 T}{\partial x^2} = \frac{\rho c}{k}\frac{\partial T}{\partial t} \equiv \frac{1}{\alpha}\frac{\partial T}{\partial t}} \tag{1.14}$$

[5]The reader might wonder if c should be c_p or c_v. This is a strictly incompressible equation so $c_p = c_v = c$. The compressible equation involves additional terms, and this particular term emerges with c_p in it in the conventional rearrangements of terms.

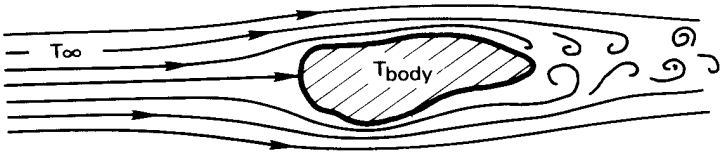

Figure 1.9 The convective cooling of a heated body.

This is the *one-dimensional heat diffusion equation*. Its importance is this: By combining the First Law with Fourier's law, we have eliminated the unknown Q and obtained a differential equation that can be solved for the temperature distribution, $T(x,t)$. It is the primary equation upon which all of heat conduction theory is based.

The heat diffusion equation includes a new property which is as important to transient heat conduction as k is to steady-state conduction. This is the thermal diffusivity, α:

$$\alpha \equiv \frac{k}{\rho c}\ \frac{\text{J}}{\text{m}\cdot\text{s}\cdot\text{K}}\ \frac{\text{m}^3}{\text{kg}}\ \frac{\text{kg}\cdot\text{K}}{\text{J}} = \alpha\ \text{m}^2/\text{s}\ \ (\text{or ft}^2/\text{hr}).$$

The thermal diffusivity is a measure of how quickly a material can carry heat away from a hot source. Since material does not just transmit heat but must be warmed by it as well, α involves both the conductivity, k, and the volumetric heat capacity, ρc.

Heat Convection

The physical process. Consider a typical convective cooling situation. Cool gas flows past a warm body, as shown in Fig. 1.9. The fluid immediately adjacent to the body forms a thin slowed-down region called a *boundary layer*. Heat is conducted into this layer, which sweeps it away and, farther downstream, mixes it into the stream. We call such processes of carrying heat away by a moving fluid *convection*.

In 1701, Isaac Newton considered the convective process and suggested that the cooling would be such that

$$\frac{dT_{\text{body}}}{dt} \propto T_{\text{body}} - T_\infty \tag{1.15}$$

where T_∞ is the temperature of the oncoming fluid. This statement suggests that energy is flowing from the body. But if the energy of the body

is constantly replenished, the body temperature need not change. Then with the help of eqn. (1.3) we get, from eqn. (1.15) (see Problem 1.2),

$$Q \propto T_{\text{body}} - T_\infty \tag{1.16}$$

This equation can be rephrased in terms of $q = Q/A$ as

$$\boxed{q = \overline{h}\left(T_{\text{body}} - T_\infty\right)} \tag{1.17}$$

This is the steady-state form of Newton's law of cooling, as it is usually quoted, although Newton never wrote such an expression.

The constant h is the *film coefficient* or *heat transfer coefficient*. The bar over h indicates that it is an average over the surface of the body. Without the bar, h denotes the "local" value of the heat transfer coefficient at a point on the surface. The units of h and $\overline{h}$ are $\text{W/m}^2\text{K}$ or $\text{J/s}\cdot\text{m}^2\cdot\text{K}$. The conversion factor for English units is:

$$1 = \frac{0.0009478\ \text{Btu}}{\text{J}} \cdot \frac{\text{K}}{1.8^\circ\text{F}} \cdot \frac{3600\ \text{s}}{\text{h}} \cdot \frac{(0.3048\ \text{m})^2}{\text{ft}^2}$$

or

$$\boxed{1 = 0.1761 \frac{\text{Btu/h}\cdot\text{ft}^2\cdot{}^\circ\text{F}}{\text{W/m}^2\text{K}}} \tag{1.18}$$

It turns out that Newton oversimplified the process of convection when he made his conjecture. Heat convection is complicated and $\overline{h}$ can depend on the temperature difference $T_{\text{body}} - T_\infty \equiv \Delta T$. In Chapter 6 we find that h really *is* independent of ΔT in situations in which fluid is forced past a body and ΔT is not too large. This is called *forced convection*.

When fluid buoys up from a hot body or down from a cold one, h varies as some weak power of ΔT—typically as $\Delta T^{1/4}$ or $\Delta T^{1/3}$. This is called *free* or *natural convection*. If the body is hot enough to boil a liquid surrounding it, h will typically vary as ΔT^2.

For the moment, we restrict consideration to situations in which Newton's law is either true or at least a reasonable approximation to real behavior.

We should have some idea of how large h might be in a given situation. Table 1.1 provides some illustrative values of h that have been

Table 1.1 Some illustrative values of convective heat transfer coefficients

Situation	$\overline{h}$, W/m^{2}K
Natural convection in gases	
• 0.3 m vertical wall in air, $\Delta T = 30°C$	4.33
Natural convection in liquids	
• 40 mm O.D. horizontal pipe in water, $\Delta T = 30°C$	570
• 0.25 mm diameter wire in methanol, $\Delta T = 50°C$	4,000
Forced convection of gases	
• Air at 30 m/s over a 1 m flat plate, $\Delta T = 70°C$	80
Forced convection of liquids	
• Water at 2 m/s over a 60 mm plate, $\Delta T = 15°C$	590
• Aniline-alcohol mixture at 3 m/s in a 25 mm I.D. tube, $\Delta T = 80°C$	2,600
• Liquid sodium at 5 m/s in a 13 mm I.D. tube at 370°C	75,000
Boiling water	
• During film boiling at 1 atm	300
• In a tea kettle	4,000
• At a peak pool-boiling heat flux, 1 atm	40,000
• At a peak flow-boiling heat flux, 1 atm	100,000
• At approximate maximum convective-boiling heat flux, under optimal conditions	10^6
Condensation	
• In a typical horizontal cold-water-tube steam condenser	15,000
• Same, but condensing benzene	1,700
• Dropwise condensation of water at 1 atm	160,000

observed or calculated for different situations. They are only illustrative and should not be used in calculations because the situations for which they apply have not been fully described. Most of the values in the table could be changed a great deal by varying quantities (such as surface roughness or geometry) that have not been specified. The determination of h or $\overline{h}$ is a fairly complicated task and one that will receive a great deal of our attention. Notice, too, that $\overline{h}$ can change dramatically from one situation to the next. Reasonable values of h range over about six orders of magnitude.

Example 1.3

The heat flux, q, is 6000 W/m^2 at the surface of an electrical heater. The heater temperature is 120°C when it is cooled by air at 70°C. What is the average convective heat transfer coefficient, $\overline{h}$? What will the heater temperature be if the power is reduced so that q is 2000 W/m^2?

SOLUTION.

$$\overline{h} = \frac{q}{\Delta T} = \frac{6000}{120 - 70} = 120 \text{ W/m}^2\text{K}$$

If the heat flux is reduced, $\overline{h}$ should remain unchanged during forced convection. Thus

$$\Delta T = T_{\text{heater}} - 70°\text{C} = q \Big/ \overline{h} = \frac{2000 \text{ W/m}^2}{120 \text{ W/m}^2\text{K}} = 16.67 \text{ K}$$

so $T_{\text{heater}} = 70 + 16.67 = 86.67°\text{C}$ ■

Lumped-capacity solution. We now wish to deal with a very simple but extremely important, kind of convective heat transfer problem. The problem is that of predicting the transient cooling of a convectively cooled object, such as is shown in Fig. 1.9. We begin with our now-familiar First law statement, eqn. (1.3):

$$\underbrace{Q}_{-\overline{h}A(T - T_\infty)} = \underbrace{\frac{dU}{dt}}_{\frac{d}{dt}[\rho c V (T - T_{\text{ref}})]} \tag{1.19}$$

where A and V are the surface area and volume of the body, T is the temperature of the body, $T = T(t)$, and T_{ref} is the arbitrary temperature at which U is defined equal to zero. Thus[6]

$$\frac{d(T - T_\infty)}{dt} = -\frac{\overline{h}A}{\rho c V}(T - T_\infty) \tag{1.20}$$

[6]Is it clear why $(T - T_{\text{ref}})$ has been changed to $(T - T_\infty)$ under the derivative? Remember that the derivative of a constant (like T_{ref} or T_∞) is zero. We can therefore introduce $(T - T_\infty)$ without invalidating the equation, and get the same dependent variable on both sides of the equation.

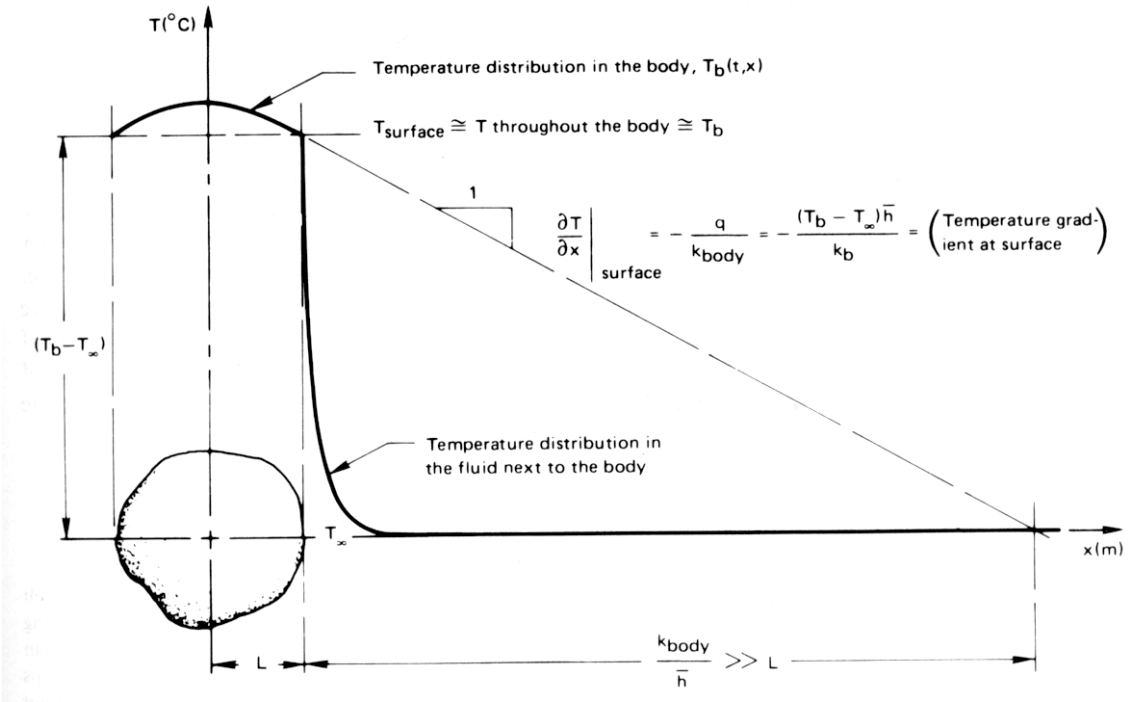
T(°C)
Temperature distribution in the body, $T_b(t,x)$
$T_{surface} \cong T$ throughout the body $\cong T_b$
1
$\left.\frac{\partial T}{\partial x}\right|_{surface} = -\frac{q}{k_{body}} = -\frac{(T_b - T_\infty)\bar{h}}{k_b}$ = (Temperature gradient at surface)
$(T_b - T_\infty)$
Temperature distribution in the fluid next to the body
T_∞
x(m)
L
$\frac{k_{body}}{\bar{h}} >> L$

Figure 1.10 The cooling of a body for which the Biot number, $\bar{h}L/k_b$, is small.

The general solution to this equation is

$$\ln(T - T_\infty) = -\frac{t}{(\rho cV/\bar{h}A)} + C \tag{1.21}$$

The group $\rho cV/\bar{h}A$ is the *time constant*, $\boldsymbol{T}$. If the initial temperature is $T(t = 0) \equiv T_i$, then $C = \ln(T_i - T_\infty)$, and the cooling of the body is given by

$$\boxed{\frac{T - T_\infty}{T_i - T_\infty} = e^{-t/\boldsymbol{T}}} \tag{1.22}$$

All of the physical parameters in the problem have now been "lumped" into the time constant. It represents the time required for a body to cool to $1/e$, or 37% of its initial temperature difference above (or below) T_∞.

The ratio $t/\boldsymbol{T}$ can also be interpreted as

$$\frac{t}{\boldsymbol{T}} = \frac{\overline{h}At\ (\text{J/°C})}{\rho cV\ (\text{J/°C})} = \frac{\text{capacity for convection from surface}}{\text{heat capacity of the body}} \tag{1.23}$$

Notice that the thermal conductivity is missing from eqns. (1.22) and (1.23). The reason is that we have assumed that the temperature of the body is nearly uniform, and this means that internal conduction is not important. We see in Fig. 1.10 that, if $L/(k_b/\overline{h}) \ll 1$, the temperature of the body, T_b, is almost constant within the body at any time. Thus

$$\frac{\overline{h}L}{k_b} \ll 1 \ \text{ implies that } \ T_b(x,t) \simeq T(t) \simeq T_{\text{surface}}$$

and the thermal conductivity, k_b, becomes irrelevant to the cooling process. This condition must be satisfied or the lumped-capacity solution will not be accurate.

We call the group $\overline{h}L/k_b$ the *Biot number*[7], Bi. If Bi were large, of course, the situation would be reversed, as shown in Fig. 1.11. In this case $\text{Bi} = hL/k_b \gg 1$ and the convection process offers little resistance to heat transfer. We could solve the heat diffusion equation

$$\frac{\partial^2 T}{\partial x^2} = \frac{1}{\alpha}\frac{\partial T}{\partial t}$$

subject to the simple boundary condition $T(x,t) = T_\infty$ when $x = L$, to determine the temperature in the body and its rate of cooling in this case. The Biot number will therefore be the basis for determining what sort of problem we have to solve.

To calculate the rate of entropy production in a lumped-capacity system, we note that the entropy change of the universe is the sum of the entropy decrease of the body and the more rapid entropy increase of the surroundings. The source of irreversibility is heat flow through the boundary layer. Accordingly, we write the time rate of change of entropy of the universe, $dS_{\text{Un}}/dt \equiv \dot{S}_{\text{Un}}$, as

$$\dot{S}_{\text{Un}} = \dot{S}_b + \dot{S}_{\text{surroundings}} = \frac{-Q_{\text{rev}}}{T_b} + \frac{Q_{\text{rev}}}{T_\infty}$$

[7]Pronounced **Bee**-oh. J.B. Biot, although younger than Fourier, worked on the analysis of heat conduction even earlier—in 1802 or 1803. He grappled with the problem of including external convection in heat conduction analyses in 1804 but could not see how to do it. Fourier read Biot's work and by 1807 had determined how to analyze the problem. (Later we encounter a similar dimensionless group called the Nusselt number, $\text{Nu} = hL/k_{\text{fluid}}$. The latter relates only to the boundary layer and not to the body being cooled. We deal with it extensively in the study of convection.)

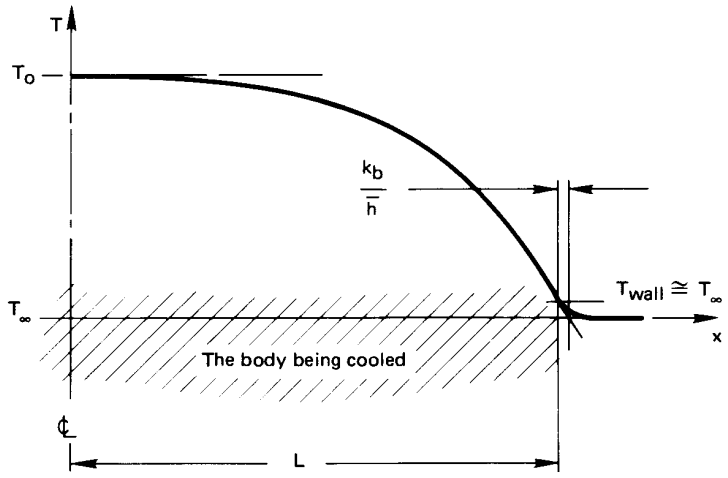

Figure 1.11 The cooling of a body for which the Biot number, $\overline{h}L/k_b$, is large.

or

$$\dot{S}_{\mathrm{Un}} = -\rho c V \frac{dT_b}{dt}\left(\frac{1}{T_\infty} - \frac{1}{T_b}\right).$$

We can multiply both sides of this equation by dt and integrate the right-hand side from $T_b(t = 0) \equiv T_{b0}$ to T_b at the time of interest:

$$\Delta S = -\rho c V \int_{T_{b0}}^{T_b} \left(\frac{1}{T_\infty} - \frac{1}{T_b}\right) dT_b. \tag{1.24}$$

Equation 1.24 will give a positive ΔS whether $T_b > T_\infty$ or $T_b < T_\infty$ because the sign of dT_b will always opposed the sign of the integrand.

Example 1.4

A thermocouple bead is largely solder, 1 mm in diameter. It is initially at room temperature and is suddenly placed in a 200°C gas flow. The heat transfer coefficient $\overline{h}$ is 250 W/m^{2}K, and the effective values of k, ρ, and c are 45 W/m·K, 9300 kg/m^3, and c = 0.18 kJ/kg·K, respectively. Evaluate the response of the thermocouple.

SOLUTION. The time constant, T, is

$$\begin{aligned} T &= \frac{\rho c V}{\overline{h} A} = \frac{\rho c}{\overline{h}} \frac{\pi D^3/6}{\pi D^2} = \frac{\rho c D}{6\overline{h}} \\ &= \frac{(9300)(0.18)(0.001)}{6(250)} \frac{\text{kg}}{\text{m}^3} \frac{\text{kJ}}{\text{kg}\cdot\text{K}} \text{m} \frac{\text{m}^2\cdot\text{K}}{\text{W}} \frac{1000\ \text{W}}{\text{kJ/s}} \\ &= 1.116\ \text{s} \end{aligned}$$

Therefore, eqn. (1.22) becomes

$$\frac{T - 200^\circ\text{C}}{(20 - 200)^\circ\text{C}} = e^{-t/1.116} \quad \text{or} \quad T = 200 - 180\, e^{-t/1.116}$$

This result is plotted in Fig. 1.12, where we see that, for all practical purposes, this thermocouple catches up with the gas stream in less than 5 s. Indeed, it should be apparent that any such system will come within 95% of the signal in three time constants. Notice, too, that if the response could continue at its initial rate, the thermocouple would reach the signal temperature in one time constant.

This calculation is based entirely on the assumption that $\text{Bi} \ll 1$ for the thermocouple. We must check that assumption:

$$\text{Bi} \equiv \frac{\overline{h} L}{k} = \frac{(250\ \text{W/m}^2\text{K})(0.001\ \text{m})/2}{45\ \text{W/m}\cdot\text{K}} = 0.00278$$

This is very small indeed, so the assumption is valid. ■

Experiment 1.2

Invent and carry out a simple procedure for evaluating the time constant of a fever thermometer in your mouth.

Radiation

Heat transfer by thermal radiation. All bodies constantly emit energy by a process of electromagnetic radiation. The intensity of such energy flux depends upon the temperature of the body and the nature of its surface. Most of the heat that reaches you when you sit in front of a fire is radiant energy. Radiant energy browns your toast in an electric toaster and it warms you when you walk in the sun.

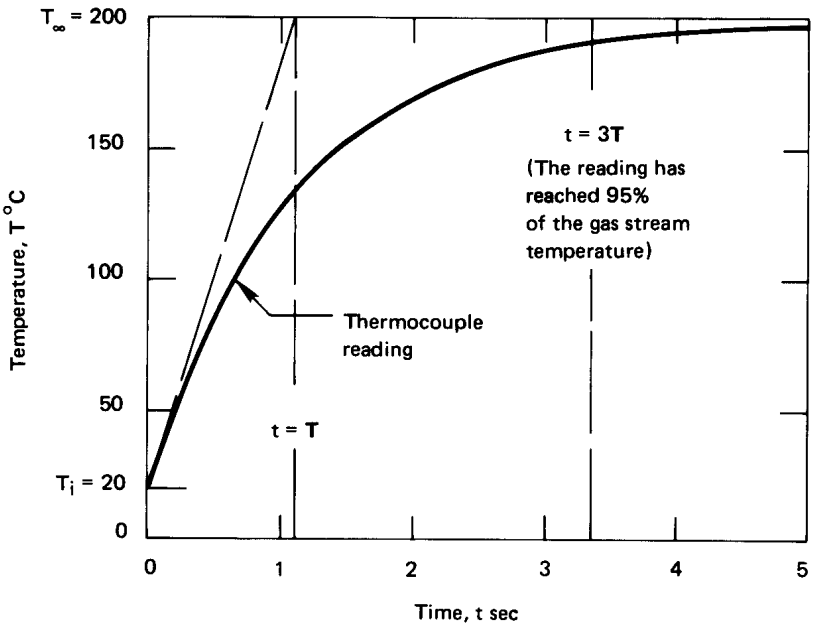

Figure 1.12 Thermocouple response to a hot gas flow.

Objects that are cooler than the fire, the toaster, or the sun emit much less energy because the energy emission varies as the fourth power of absolute temperature. Very often, the emission of energy, or *radiant heat transfer*, from cooler bodies can be neglected in comparison with convection and conduction. But heat transfer processes that occur at high temperature, or with conduction or convection suppressed by evacuated insulations, usually involve a significant fraction of radiation.

Experiment 1.3

Open the freezer door to your refrigerator. Put your face near it, but stay far enough away to avoid the downwash of cooled air. This way you cannot be cooled by convection and, because the air between you and the freezer is a fine insulator, you cannot be cooled by conduction. Still your face will feel cooler. The reason is that you radiate heat directly into the cold region and it radiates very little heat to you. Consequently, your face cools perceptibly.

Table 1.2 Forms of the electromagnetic wave spectrum

Characterization	*Wavelength, λ*	
Cosmic rays	< 0.3 pm	
Gamma rays	0.3–100 pm	
X rays	0.01–30 nm	
Ultraviolet light	3–400 nm	
Visible light	0.4–0.7 μm	***Thermal Radiation 0.1–1000 μm***
Near infrared radiation	0.7–30 μm	
Far infrared radiation	30–1000 μm	
Millimeter waves	1–10 mm	
Microwaves	10–300 mm	
Shortwave radio & TV	300 mm–100 m	
Longwave radio	100 m–30 km	

The electromagnetic spectrum. Thermal radiation occurs in a range of the electromagnetic spectrum of energy emission. Accordingly, it exhibits the same wavelike properties as light or radio waves. Each quantum of radiant energy has a wavelength, λ, and a frequency, ν, associated with it.

The full electromagnetic spectrum includes an enormous range of energy-bearing waves, of which heat is only a small part. Table 1.2 lists the various forms over a range of wavelengths that spans 24 orders of magnitude. Only the tiniest "window" exists in this spectrum through which we can *see* the world around us. Heat radiation, whose main component is usually the spectrum of infrared radiation, passes through the much larger window—about three orders of magnitude in λ or ν.

Black bodies. The model for the perfect thermal radiator is a so-called *black body*. This is a body which absorbs all energy that reaches it and reflects nothing. The term can be a little confusing, since such bodies *emit* energy. Thus, if we possessed infrared vision, a black body would glow with "color" appropriate to its temperature. of course, perfect radiators *are* "black" in the sense that they absorb all visible light (and all other radiation) that reaches them.

It is necessary to have an experimental method for making a perfectly

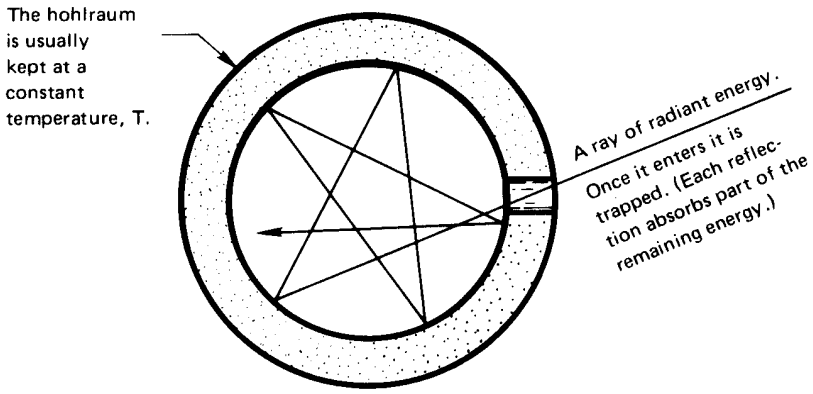
The hohlraum is usually kept at a constant temperature, T.
A ray of radiant energy. Once it enters it is trapped. (Each reflection absorbs part of the remaining energy.)

Figure 1.13 Cross section of a spherical hohlraum. The hole has the attributes of a nearly perfect thermal black body.

black body. The conventional device for approaching this ideal is called by the German term *hohlraum*, which literally means "hollow space". Figure 1.13 shows how a hohlraum is arranged. It is simply a device that traps all the energy that reaches the aperture.

What are the important features of a thermally black body? First consider a distinction between heat and infrared radiation. *Infrared radiation* refers to a particular range of wavelengths, while *heat* refers to the whole range of radiant energy flowing from one body to another. Suppose that a radiant heat flux, q, falls upon a translucent plate that is not black, as shown in Fig. 1.14. A fraction, α, of the total incident energy, called the *absorptance*, is absorbed in the body; a fraction, ρ, called the *reflectance*, is reflected from it; and a fraction, τ, called the *transmittance*, passes through. Thus

$$1 = \alpha + \rho + \tau \tag{1.25}$$

This relation can also be written for the energy carried by each wavelength in the distribution of wavelengths that makes up *heat* from a source at any temperature:

$$1 = \alpha_\lambda + \rho_\lambda + \tau_\lambda \tag{1.26}$$

All radiant energy incident on a black body is absorbed, so that α_b or $\alpha_{\lambda_b} = 1$ and $\rho_b = \tau_b = 0$. Furthermore, the energy emitted from a black body reaches a theoretical maximum, which is given by the Stefan-Boltzmann law. We look at this next.

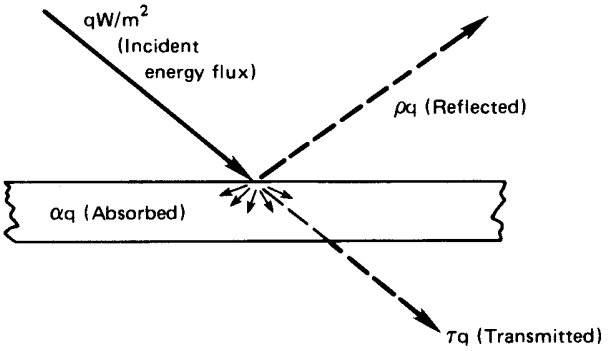

Figure 1.14 The distribution of energy incident on a translucent slab.

The Stefan-Boltzmann law. The flux of energy radiating from a body is commonly designated $e(T)$ W/m^2. The symbol $e_\lambda(\lambda, T)$ designates the distribution function of radiative flux in λ, or the *monochromatic emissive power:*

$$e_\lambda(\lambda, T) = \frac{de(\lambda, T)}{d\lambda} \quad \text{or} \quad e(\lambda, T) = \int_0^\lambda e_\lambda(\lambda, T)\, d\lambda \tag{1.27}$$

Thus

$$e(T) \equiv E(\infty, T) = \int_0^\infty e_\lambda(\lambda, T)\, d\lambda$$

The dependence of $e(T)$ on T for a black body was established experimentally by Stefan in 1879 and explained by Boltzmann on the basis of thermodynamics arguments in 1884. The Stefan-Boltzmann law is

$$\boxed{e_b(T) = \sigma T^4} \tag{1.28}$$

where the Stefan-Boltzmann constant, σ, is 5.670400×10^{-8} W/m$^2\cdot$K^4 or 1.714×10^{-9} Btu/hr$\cdot$ft$^2\cdot{}^\circ$R^4, and T is the absolute temperature.

e_λ vs. λ. Nature requires that, at a given temperature, a body will emit a unique distribution of energy in wavelength. Thus, when you heat a poker in the fire, it first glows a dull red—emitting most of its energy at long wavelengths and just a little bit in the visible regime. When it is white-hot, the energy distribution has been both greatly increased and shifted toward the shorter-wavelength visible range. At each temperature, a black body yields the highest value of e_λ that a body can attain.

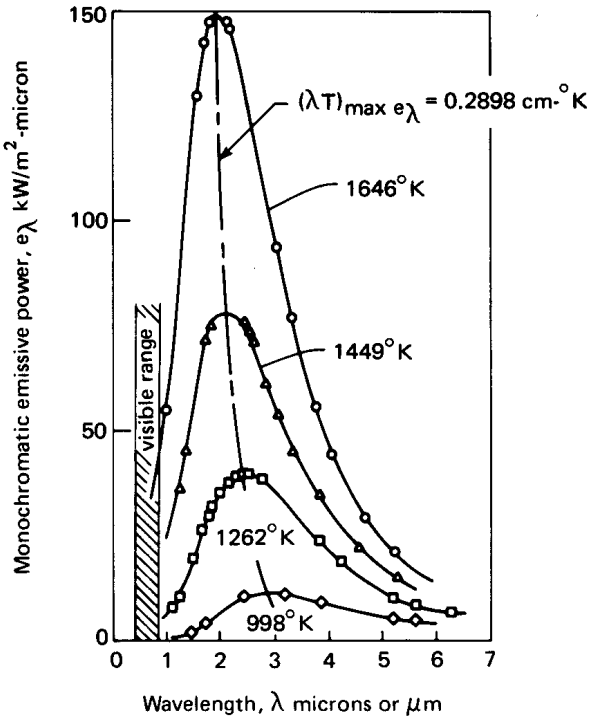

Figure 1.15 Emissive power of a black body at several temperatures—predicted and observed.

The very accurate measurements of the black-body energy spectrum by Lummer and Pringsheim (1899) are shown in Fig. 1.15. The locus of maxima of the curves is also plotted. It obeys a relation called *Wein's law:*

$$(\lambda T)_{e_{\lambda=\max}} = 2898\ \mu\text{m}\cdot\text{K} \tag{1.29}$$

About three-fourths of the radiant energy of a black body lies to the right of this line in Fig. 1.15. Notice that, while the locus of maxima leans toward the visible range at higher temperatures, only a small fraction of the radiation is visible even at the highest temperature.

Predicting how the monochromatic emissive power of a black body depends on λ was an increasingly serious problem at the close of the nineteenth century. The prediction was a keystone of the most profound scientific revolution the world has seen. In 1901, Max Planck made the prediction, and his work included the initial formulation of quantum me-

chanics. He found that

$$e_{\lambda_b} = \frac{2\pi h c_o^2}{\lambda^5 \left[\exp(hc_o/k_B T\lambda) - 1\right]} \tag{1.30}$$

where c_o is the speed of light, 2.99792458×10^8 m/s; h is Planck's constant, $6.62606876 \times 10^{-34}$ J·s; and k_B is Boltzmann's constant, $1.3806503 \times 10^{-23}$ J/K.

Radiant heat exchange. Suppose that a heated object (1 in Fig. 1.16) radiates to some other object (2). Then if both objects are thermally black, the net heat transferred from object 1 to object 2, Q_{net}, is the difference between Q_{1-2}

$$\boxed{Q_{\text{net}} = A_1 \left[e_1(T) - e_2(T)\right] = \sigma A_1 \left(T_1^4 - T_2^4\right)} \tag{1.31}$$

If the first object "sees" other objects in addition to object 2, as indicated in Fig. 1.16, then a *view factor* (sometimes called an *configuration factor* or a *shape factor*), F_{1-2}, must be included in eqn. (1.31):

$$Q_{\text{net}} = F_{1-2}\sigma A_1 \left(T_1^4 - T_2^4\right) \tag{1.32}$$

where F_{1-2} is the fraction of energy leaving object 1 that is intercepted by object 2. Finally, if the bodies are not black, then the view factor, F_{1-2}, must be replaced by a new *transfer factor*, $\mathcal{F}_{1-2}$, which depends on surface properties of the various objects as well as the geometrical "view".

Example 1.5

A black thermocouple measures the temperature in a chamber with black walls. If the air around the thermocouple is at 20°C, the walls are at 100°C, and the heat transfer coefficient between the thermocouple and the air is 15 W/m^{2}K, what temperature will the thermocouple read?

SOLUTION. The heat convected away from the thermocouple by the air must exactly balance that radiated to it by the hot walls if the system is steady. Furthermore, F_{1-2} is unity since the thermocouple is enclosed:

$$\overline{h}A\left(T_{tc} - T_{\text{air}}\right) = \sigma A \left(T_{\text{wall}}^4 - T_{tc}^4\right)$$

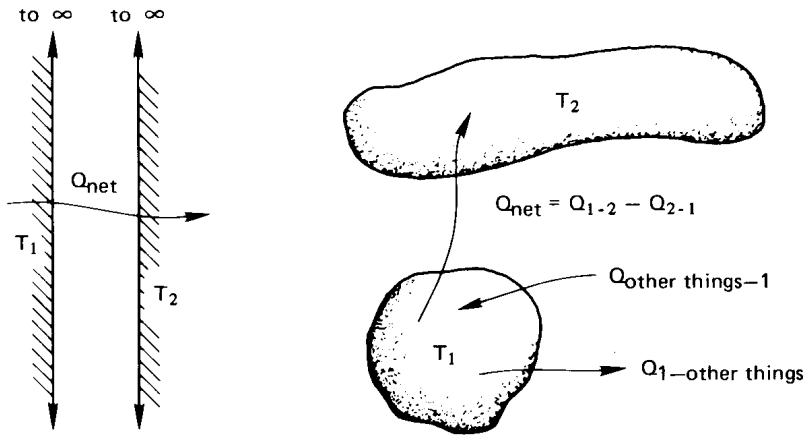

Figure 1.16 The net radiant heat transfer from one object to another.

or

$$15(T_{tc} - 20)\ \text{W/m}^2 = 5.6697 \times 10^{-8}\left[373^4 - (T_{tc} + 273)^4\right]\text{W/m}^2$$

Trial-and-error solution of this equation yields $T_{tc} = 51°\text{C}$. ■

Radiation shielding. The preceding example points out an important practical problem than can be solved with radiation shielding. The idea is as follows: If we want to measure the true air temperature, we can place a thin foil casing, or shield, around the thermocouple. The casing is shaped to obstruct the thermocouple's "view" of the room but to permit the free flow of the air around the thermocouple. Then the casing (or shield) will be closer to 50°C than to 100°C, and the thermocouple will be influenced by this much cooler radiator. if the shield is highly reflecting on the outside, it will assume a temperature still closer to that of the air and the error will be still less. Multiple layers of the shielding can further reduce the error.

Radiation shielding can take many forms and serve many purposes. it is an important element in superinsulations. A glass firescreen in a fireplace serves as a radiation shield because it is largely opaque to radiation. it absorbs energy and reradiates (ineffectively) at a temperature

much lower than that of the fire.

Example 1.6

A crucible of molten metal at 1800°C is placed on the foundry floor. The foundryman covers it with a metal sheet to reduce heat loss to the room. If the transfer factor, $\mathcal{F}$, between the melt and the sheet is 0.4, and that between the top of the sheet and the room is 0.8, how much will the heat loss to the room be reduced by the sheet if the transfer factor between the uncovered melt and the room had been 0.8?

SOLUTION. First find the sheet temperature by equating the heat transfer from the melt to the sheet to that from the sheet to the room:

$$q = (0.4)\sigma\left[(1800 + 273)^4 - T_{\text{sheet}}^4\right] = (0.8)\sigma\left[T_{\text{sheet}}^4 - (20 + 273)^4\right]$$

This gives $T_{\text{sheet}} = 1575$ K, so

$$\frac{q_{\text{with sheet}}}{q_{\text{without sheet}}} = \frac{0.8\sigma(1575^4 - 293^4)}{0.8\sigma(2073^4 - 293^4)} = 0.333$$

The shield therefore reduces the heat loss by 66.7%. ■

Experiment 1.4

Find a small open flame that produces a fair amount of soot. A candle, kerosene lamp, or a cutting torch with a rich mixture should work well. A clean blue flame will not work well because such gases do not radiate much heat. First, place your finger in a position about 1 to 2 cm to one side of the flame, where it becomes uncomfortably hot. Now take a piece of fine mesh screen and dip it in some soapy water, which will fill up the holes. Put it between your finger and the flame. You will see that your finger is protected from the heating until the water evaporates.

Water is relatively transparent to light. What does this experiment show you about the transmittance of water to infrared wavelengths?

1.4 A look ahead

What we have done up to this point has been no more than to reveal the tip of the iceberg. The basic mechanisms of heat transfer have been explained and some quantitative relations have been presented. However, this information will barely get you started when you are faced with a real heat transfer problem. Three tasks, in particular, must be completed to solve actual problems:

- The heat diffusion equation must be solved subject to appropriate boundary conditions if the problem involves heat conduction of any complexity.
- The convective heat transfer coefficient, h, must be determined if convection is important in a problem.
- The factor F_{1-2} or $\mathcal{F}_{1-2}$ must be determined to calculate radiative heat transfer.

Any of these determinations can involve a great deal of complication, and most of the chapters that lie ahead are devoted to these three basic problems.

Before becoming engrossed in these three questions, we shall first look at the archetypical applied problem of heat transfer–namely, the design of a heat exchanger. Chapter 2 sets up the elementary analytical apparatus that is needed for this, and Chapter 3 shows how to do such design if $\overline{h}$ is already known. This will make it easier to see the importance of undertaking the three basic problems in subsequent parts of the book.

1.5 Problems

We have noted that this book is set down almost exclusively in S.I. units. The student who has problems with dimensional conversion will find Appendix B helpful. The only use of English units appears in some of the problems as the end of each chapter. A few such problems are included to provide experience in converting back into English units, since such units will undoubtedly persist in this country for many more years.

Another matter often leads to some discussion between students and teachers in heat transfer courses. That is the question of whether a problem is “theoretical” or “practical”. Quite often the student is inclined to

view as "theoretical" a problem that does not involve numbers or that requires the development of algebraic results.

The problems assigned in this book are all intended to be useful in that they do one or more of five things:

1. They involve a calculation of a type that actually arises in practice (e.g., Problems 1.1, 1.3, 1.8 to 1.18, and 1.21 through 1.25).

2. They illustrate a physical principle (e.g., Problems 1.2, 1.4 to 1.7, 1.9, 1.20, 1.32, and 1.39). These are probably closest to having a "theoretical" objective.

3. They ask you to use methods developed in the text to develop other results that would be needed in certain applied problems (e.g., Problems 1.10, 1.16, 1.17, and 1.21). Such problems are usually the most difficult and the most valuable to you.

4. They anticipate development that will appear in subsequent chapters (e.g., Problems 1.16, 1.20, 1.40, and 1.41).

5. They require that you develop your ability to handle numerical and algebraic computation effectively. (This is the case with most of the problems in Chapter 1, but it is especially true of Problems 1.6 to 1.9, 1.15, and 1.17).

Partial numerical answers to some of the problems follow them in brackets. Tables of physical property data useful in solving the problems are given in Appendix A.

Actually, we wish to look at the *theory*, *analysis*, and *practice* of heat transfer—all three—according to Webster's definitions:

Theory: "a systematic statement of principles; a formulation of apparent relationships or underlying principles of certain observed phenomena."

Analysis: "the solving of problems by the means of equations; the breaking up of any whole into its parts so as to find out their nature, function, relationship, etc."

Practice: "the *doing* of something as an application of knowledge."

Problems

1.1 A composite wall consists of alternate layers of fir (5 cm thick), aluminum (1 cm thick), lead (1 cm thick), and corkboard (6 cm thick). The temperature is 60°C on the outside of the for and 10°C on the outside of the corkboard. Plot the temperature gradient through the wall. Does the temperature profile suggest any simplifying assumptions that might be made in subsequent analysis of the wall?

1.2 Verify eqn. (1.15).

1.3 $q = 5000$ W/m^2 in a 1 cm slab and $T = 140$°C on the cold side. Tabulate the temperature drop through the slab if it is made of

- Silver
- Aluminum
- Mild steel (0.5 % carbon)
- Ice
- Spruce
- Insulation (85 % magnesia)
- Silica aerogel

Indicate which situations would be unreasonable and why.

1.4 Explain in words why the heat diffusion equation, eqn. (1.13), shows that in transient conduction the temperature depends on the thermal diffusivity, α, but we can solve steady conduction problems using just k (as in Example 1.1).

1.5 A 1 m rod of pure copper 1 cm^2 in cross section connects a 200°C thermal reservoir with a 0°C thermal reservoir. The system has already reached steady state. What are the rates of change of entropy of (a) the first reservoir, (b) the second reservoir, (c) the rod, and (d) the whole universe, as a result of the process? Explain whether or not your answer satisfies the Second Law of Thermodynamics. [(d): +0.0120 W/K.]

1.6 Two thermal energy reservoirs at temperatures of 27°C and −43°C, respectively, are separated by a slab of material 10 cm thick and 930 cm^2 in cross-sectional area. The slab has a thermal conductivity of 0.14 W/m·K. The system is operating at

steady-state conditions. what are the rates of change of entropy of (a) the higher temperature reservoir, (b) the lower temperature reservoir, (c) the slab, and (d) the whole universe as a result of this process? (e) Does your answer satisfy the Second Law of Thermodynamics?

1.7 (a) If the thermal energy reservoirs in Problem 1.6 are suddenly replaced with adiabatic walls, determine the final equilibrium temperature of the slab. (b) what is the entropy change for the slab for this process? (c) Does your answer satisfy the Second Law of Thermodynamics in this instance? Explain. The density of the slab is 26 lb/ft^3 and the specific heat is 0.65 Btu/lb·°F. [(b): 30.81 J/K].

1.8 A copper sphere 2.5 cm in diameter has a uniform temperature of 40°C. The sphere is suspended is a slow-moving air stream at 0°C. The air stream produces a convection heat transfer coefficient of 15 W/m^{2}K. Radiation can be neglected. since copper is highly conductive, temperature gradients in the sphere will smooth out rapidly, and its temperature at any instant during the cooling process can be taken as uniform (i.e., Bi $\ll$ 1). Write the instantaneous energy balance between the sphere and the surrounding air. Solve this equation and plot the resulting temperatures as a function of time between 40°C and 0°C.

1.9 Determine the total heat transfer in Problem 1.8 as the sphere cools from 40°C to 0°C. Plot the net entropy increase resulting from the cooling process above, ΔS vs. T (K). [Total heat transfer = 1123 J.]

1.10 A truncated cone 30 cm high is constructed of Portland cement. The diameter at the top is 15 cm and at the bottom is 7.5 cm. The lower surface is maintained at 6°C and the top at 40°C. The other surface is insulated. Assume one-dimensional heat transfer and calculate the rate of heat transfer in watts from top to bottom. To do this, note that the heat transfer, Q, must be the same at every cross section. Write Fourier's law locally, and integrate it from top to bottom to get a relation between this unknown Q and the known end temperatures. [$Q = -1.70$ W.]

1.11 A hot water heater contains 100 kg of water at 75°C in a 20°C room. Its surface area is 1.3 m^2. Select an insulating material,

and specify its thickness, to keep the water from cooling more than 3°C/h. (Notice that this problem will be greatly simplified if the temperature drop in the steel casing and the temperature drop in the convective boundary layers are negligible. Can you make such assumptions? Explain.)

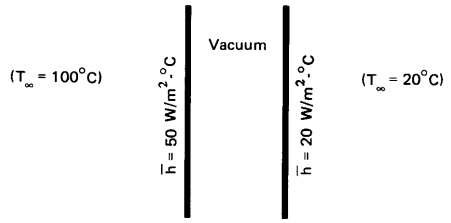

Figure 1.17 Configuration for Problem 1.12

1.12 What is the temperature at the left-hand wall shown in Fig. 1.17. Both walls are thin, very large in extent, highly conducting, and thermally black. [$T_{\text{right}} = 42.5$°C.]

1.13 Develop S.I. to English conversion factors for:

- The thermal diffusivity, α
- The heat flux, q
- The density, ρ
- The Stefan-Boltzmann constant, σ
- The view factor, F_{1-2}
- The molar entropy
- The specific heat per unit mass, c

In each case, begin with basic dimension J, m, kg, s, °C, and check your answers against Appendix B if possible.

1.14 Three infinite, parallel, black, opaque plates transfer heat by radiation, as shown in Fig. 1.18. Find T_2.

1.15 Four infinite, parallel, black, opaque plates transfer heat by radiation, as shown in Fig. 1.19. Find T_2 and T_3. [$T_2 = 75.53$°C.]

1.16 Two large, black, horizontal plates are spaced a distance L from one another. The top one is warm at a controllable temperature, T_h, and the bottom one is cool at a specified temperature, T_c. A gas separates them. The gas is stationary because it is

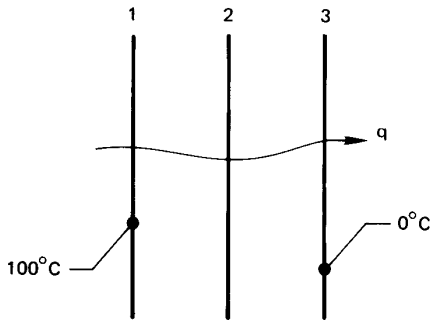

Figure 1.18 Configuration for Problem 1.14

warm on the top and cold on the bottom. Write the equation $q_{\text{rad}}/q_{\text{cond}} = \text{fn}(N, \Theta \equiv T_h/T_c)$, where N is a dimensionless group containing σ, k, L, and T_c. Plot N as a function of Θ for $q_{\text{rad}}/q_{\text{cond}} = 1$, 0.8, and 1.2 (and for other values if you wish).

Now suppose that you have a system in which $L = 10$ cm, $T_c = 100$ K, and the gas is hydrogen with an average k of 0.1 W/m·K . Further suppose that you wish to operate in such a way that the conduction and radiation heat fluxes are identical. Identify the operating point on your curve and report the value of T_h that you must maintain.

1.17 A blackened copper sphere 2 cm in diameter and uniformly at 200°C is introduced into an evacuated black chamber that is maintained at 20°C.

- Write a differential equation that expresses $T(t)$ for the sphere, assuming lumped thermal capacity.

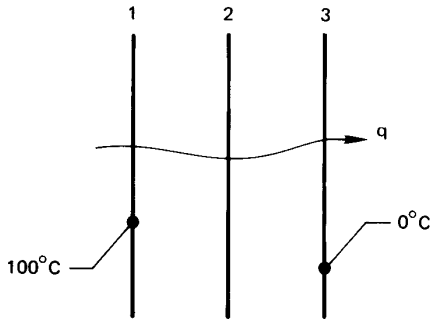

Figure 1.19 Configuration for Problem 1.15

- Identify a dimensionless group, analogous to the Biot number, than can be used to tell whether or not the lumped-capacity solution is valid.
- Show that the lumped-capacity solution is valid.
- Integrate your differential equation and plot the temperature response for the sphere.

1.18 As part of a space experiment, a small instrumentation package is released from a space vehicle. It can be approximated as a solid aluminum sphere, 4 cm in diameter. The sphere is initially at 30°C and it contains a pressurized hydrogen component that will condense and malfunction at 30 K. If we take the surrounding space to be at 0 K, how long may we expect the implementation package to function properly? Is it legitimate to use the lumped-capacity method in solving the problem? (*Hint:* See the directions for Problem 1.17.) [Time = 5.8 weeks.]

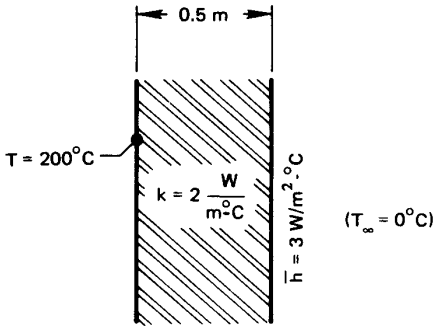

Figure 1.20 Configuration for Problem 1.19

1.19 Consider heat conduction through the wall as shown in Fig. 1.20. Calculate q and the temperature of the right-hand side of the wall.

1.20 Throughout Chapter 1 we have assumed that the steady temperature distribution in a plane uniform wall in linear. To prove this, simplify the heat diffusion equation to the form appropriate for steady flow. Then integrate it twice and eliminate the two constants using the known outside temperatures T_{left} and T_{right} at $x = 0$ and $x =$ wall thickness, L.

1.21 The thermal conductivity in a particular plane wall depends as follows on the wall temperature: $k = A + BT$, where A and B

are constants. The temperatures are T_1 and T_2 on either side if the wall, and its thickness is L. Develop an expression for q.

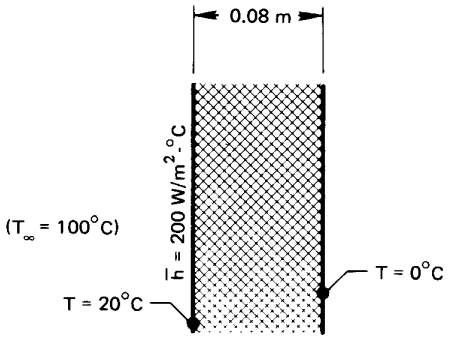

Figure 1.21 Configuration for Problem 1.22

1.22 Find k for the wall shown in Fig. 1.21. What might it be made of?

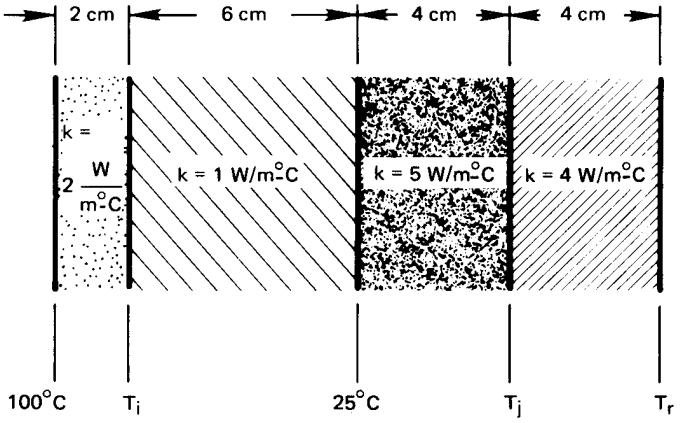

Figure 1.22 Configuration for Problem 1.23

1.23 What are T_i, T_j, and T_r in the wall shown in Fig. 1.22? [T_j = 16.44°C.]

1.24 An aluminum can of beer or soda pop is removed from the refrigerator and set on the table. If $\bar{h}$ is 13.5 W/m^{2}K, estimate when the beverage will be at 15°C. State all of your assumptions.

1.25 One large, black wall at 27°C faces another whose surface is 127°C. The gap between the two walls is evacuated. If the second wall is 0.1 m thick and has a thermal conductivity of 17.5 W/m·K, what is its temperature on the back side? (Assume steady state.)

1.26 A 1 cm diameter, 1% carbon steel sphere, initially at 200°C, is cooled by natural convection, with air at 20°C. In this case, $\overline{h}$ is not independent of temperature. Instead, $\overline{h} = 3.51(\Delta T°\text{C})^{1/4}$ W/m^{2}K. Plot T_{sphere} as a function of t. Verify the lumped-capacity assumption.

1.27 A 3 cm diameter, black spherical heater is kept at 1100°C. It radiates through an evacuated annulus to a surrounding spherical shell of Nichrome V. the shell has a 9 cm inside diameter and is 0.3 cm thick. It is black on the inside and is held at 25°C on the outside. Find (a) the temperature of the inner wall of the shell and (b) the heat transfer, Q. (Treat the shell as a plane wall.)

1.28 The sun radiates 650 W/m^2 on the surface of a particular lake. At what rate (in mm/hr) would the lake evaporate away if all of this energy went to evaporating water? Discuss as many other ways you can think of that this energy can be distributed (h_{fg} for water is 2,257,000 J/kg). Do you suppose much of the 650 W/m^2 goes to evaporation?

1.29 It is proposed to make picnic cups, 0.005 m thick, of a new plastic for which $k = k_o(1 + AT^2)$, where T is expressed in °C, $k_o = 0.15$ W/m·K, and $a = 10^{-4}$ °C^{-2}. We are concerned with thermal behavior in the extreme case in which $T = 100$°C in the cup and 0°C outside. Plot T against position in the cup wall and find the heat loss, q.

1.30 A disc-shaped wafer of diamond 1 lb is the target of a very high intensity laser. The disc is 5 mm in diameter and 1 mm deep. The flat side is pulsed intermittently with 10^{10} W/m^2 of energy for one microsecond. It is then cooled by natural convection from that same side until the next pulse. If $\overline{h} = 10$ W/m^{2}K and T_∞=30°C, plot T_{disc} as a function of time for pulses that are 50 s apart and 100 s apart. (Note that you must determine the temperature the disc reaches before it is pulsed each time.)

1.31 A 150 W light bulb is roughly a 0.006 m diameter sphere. Its steady surface temperature is room air is 90°C, and $\overline{h}$ on the outside is 7 W/m^{2}K. What fraction of the heat transfer from the bulb is by radiation *directly* from the filament through the glass? (State any additional assumptions.)

1.32 How much entropy does the light bulb in Problem 1.31 produce?

1.33 Air at 20°C flows over one side of a thin metal sheet ($\overline{h}$ = 10.6 W/m^{2}K). Methanol at 87°C flows over the other side ($\overline{h}$ = 141 W/m^{2}K). The metal functions as an electrical resistance heater, releasing 1000 W/m^2. Calculate (a) the heater temperature, (b) the heat transfer from the methanol to the heater, and (c) the heat transfer from the heater to the air.

1.34 A black heater is simultaneously cooled by 20°C air ($\overline{h}$ = 14.6 W/m^{2}K) and by radiation to a parallel black wall at 80°C. What is the temperature of the first wall if it delivers 9000 W/m^2.

1.35 An 8 oz. can of beer is taken from a 3°C refrigerator and placed in a 25°C room. The 6.3 cm diameter by 9 cm high can is placed on an insulated surface ($\overline{h}$ = 7.3 W/m^{2}K). How long will it take to reach 12°C? Discuss your assumptions.

1.36 A resistance heater in the form of a thin sheet runs parallel with 3 cm slabs of cast iron on either side of an evacuated cavity. The heater, which releases 8000 W/m^2, and the cast iron are very nearly black. The outside surfaces of the cast iron slabs are kept at 10°C. Determine the heater temperature and the inside slab temperatures.

1.37 A black wall at 1200°C radiates to the left side of a parallel slab of type 316 stainless steel, 5 mm thick. The right side of the slab is to be cooled convectively and is not to exceed 0°C. Suggest a convective process that will achieve this.

1.38 A cooler keeps one side of a 2 cm layer of ice at −10°C. The other side is exposed to air at 15°C. What is $\overline{h}$ just on the edge of melting? Must $\overline{h}$ be raised or lowered if melting is to progress?

1.39 At what minimum temperature does a black heater deliver its maximum monochromatic emissive power in the visible range? Compare your result with Fig. 10.2.

1.40 The local heat transfer coefficient during the laminar flow of fluid over a flat plate of length L is equal to $F/x^{1/2}$, where F is a function of fluid properties and the flow velocity. How does $\overline{h}$ compare with $H(x + L)$? (x is the distance from the leading edge of the plate.)

1.41 An object is initially at a temperature above that of its surroundings. We have seen that many kinds of convective processes will bring the object into equilibrium with its surroundings. Describe the characteristics of a process that will do so with the least net increase of the entropy of the universe.

1.42 A 250°C cylindrical copper billet, 4 cm in diameter and 8 cm long, is cooled in air at 25°C. The heat transfer coefficient is 5 W/m^{2}K. Can this be treated as lumped-capacity cooling? What is the temperature of the billet after 10 minutes?

1.43 The sun's diameter is 1,392,000 km, and it emits energy as if it were a black body at 5777 K. Determine the rate at which it emits energy. Compare this with a value from the literature. What is the sun's energy output in a year?

Bibliography of Historical and Advanced Texts

We include no specific references for the ideas introduced in Chapter 1 since these may be found in introductory thermodynamics or physics books. References 1–6 are some texts which have strongly influenced the field. The rest are relatively advanced texts or handbooks which go beyond the present textbook.

References

[1.1] J. Fourier. *The Analytical Theory of Heat.* Dover Publications, Inc., New York, 1955.

[1.2] L. M. K. Boelter, V. H. Cherry, H. A. Johnson, and R. C. Martinelli. *Heat Transfer Notes*. McGraw-Hill Book Company, New York, 1965. Originally issued as class notes at the University of California at Berkeley between 1932 and 1941.

[1.3] M. Jakob. *Heat Transfer*. John Wiley & Sons, New York, 1949.

[1.4] W. H. McAdams. *Heat Transmission*. McGraw-Hill Book Company, New York, 3rd edition, 1954.

[1.5] W. M. Rohsenow and H. Y. Choi. *Heat, Mass and Momentum Transfer*. Prentice-Hall, Inc., Englewood Cliffs, N.J., 1961.

[1.6] E. R. G. Eckert and R. M. Drake, Jr. *Analysis of Heat and Mass Transfer*. Hemisphere Publishing Corp., Washington, D.C., 1987.

[1.7] H. S. Carslaw and J. C. Jaeger. *Conduction of Heat in Solids*. Oxford University Press, New York, 2nd edition, 1959. Very comprehenisve, but quite dense.

[1.8] D. Poulikakos. *Conduction Heat Transfer*. Prentice-Hall, Inc., Englewood Cliffs, NJ, 1994. This book's approach is very accessible. Good coverage of solidification.

[1.9] V. S. Arpaci. *Conduction Heat Transfer*. Ginn Press/Pearson Custom Publishing, Needham Heights, Mass., 1991. Abridgement of the 1966 edition, omitting numerical analysis.

[1.10] W. M. Kays and M. E. Crawford. *Convective Heat and Mass Transfer*. McGraw-Hill Book Company, New York, 3rd edition, 1993. Coverage is mainly of boundary layers and internal flows.

[1.11] F.M. White. *Viscous Fluid Flow*. McGraw-Hill, Inc., New York, 2nd edition, 1991. Excellent development of fundamental results for boundary layers and internal flows.

[1.12] J.A. Schetz. *Foundations of Boundary Layer Theory for Momentum, Heat, and Mass Transfer*. Prentice-Hall, Inc., Englewood Cliffs, NJ, 1984. This book shows many experimental results in support of the theory.

[1.13] A. Bejan. *Convection Heat Transfer*. John Wiley & Sons, New York, 2nd edition, 1995. This book makes good use of scaling arguments.

[1.14] M. Kaviany. *Principles of Convective Heat Transfer*. Springer-Verlag, New York, 1995. This treatise is wide-ranging and quite unique. Includes multiphase convection.

[1.15] H. Schlichting and K. Gersten. *Boundary-Layer Theory*. Springer-Verlag, Berlin, 8th edition, 2000. Very comprehensive development of boundary layer theory. A classic.

[1.16] H. C. Hottel and A. F. Sarofim. *Radiative Transfer*. McGraw-Hill Book Company, New York, 1967.

[1.17] E. M. Sparrow and R. D. Cess. *Radiation Heat Transfer*. Hemisphere Publishing Corp./McGraw-Hill Book Company, Washington, D.C., 1978.

[1.18] R. Siegel and J. R. Howell. *Thermal Radiative Heat Transfer*. Hemisphere Publishing Corp., Washington, D.C., 3rd edition, 1992.

[1.19] M. F. Modest. *Radiative Heat Transfer*. McGraw-Hill, New York, 1993.

[1.20] J. G. Collier and J. R. Thome. *Convective Boiling and Condensation*. Oxford University Press, Oxford, 3rd edition, 1994.

[1.21] Y. Y. Hsu and R. W. Graham. *Transport Processes in Boiling and Two-Phase Systems Including Near-Critical Systems*. American Nuclear Society, LaGrange Park, IL, 1986.

[1.22] W. M. Kays and A. L. London. *Compact Heat Exchangers*. McGraw-Hill Book Company, New York, 3rd edition, 1984.

[1.23] G. F. Hewitt, editor. *Heat Exchanger Design Handbook 1998*. Begell House, New York, 1998.

[1.24] R. B. Bird, W. E. Stewart, and E. N. Lightfoot. *Transport Phenomena*. John Wiley & Sons, Inc., New York, 1960.

[1.25] A. F. Mills. *Mass Transfer*. Prentice-Hall, Inc., Upper Saddle River, 2001. Mass transfer from a mechanical engineer's perpective with strong coverage of convective mass transfer.

[1.26] D. S. Wilkinson. *Mass Transfer in Solids and Fluids*. Cambridge University Press, Cambridge, 2000. A systematic development of mass transfer with a materials science focus and an emphasis on modelling.

[1.27] W. M. Rohsenow, J. P. Hartnett, and Y. I. Cho, editors. *Handbook of Heat Transfer*. McGraw-Hill, New York, 3rd edition, 1998.

2. Heat conduction concepts, thermal resistance, and the overall heat transfer coefficient

It is the fire that warms the cold, the cold that moderates the heat...the general coin that purchases all things...

Don Quixote, **M. de Cervantes**

2.1 The heat diffusion equation

Objective

We must now develop some ideas that will be needed for the design of heat exchangers. The most important of these is the notion of an overall heat transfer coefficient. This is a measure of the general resistance of a heat exchanger to the flow of heat, and usually it must be built up from analyses of component resistances. In particular, we must know how to predict $\overline{h}$ and how to evaluate the conductive resistance of bodies more complicated than plane passive walls. The evaluation of $\overline{h}$ is a matter that must be deferred to Chapter 6 and 7. For the present, $\overline{h}$ values must be considered given information in any problem.

The heat conduction component of most heat exchanger problems is more complex than the simple planar analyses done in Chapter 1. To do such analyses, we must next derive the heat conduction equation and learn to solve it.

Consider the general temperature distribution in a three-dimensional body as depicted in Fig. 2.1. For some reason (heating from one side, in this case), there is a space- and time-dependent temperature field in the body. This field $T = T(x, y, z, t)$ or $T(\vec{r}, t)$, defines instantaneous

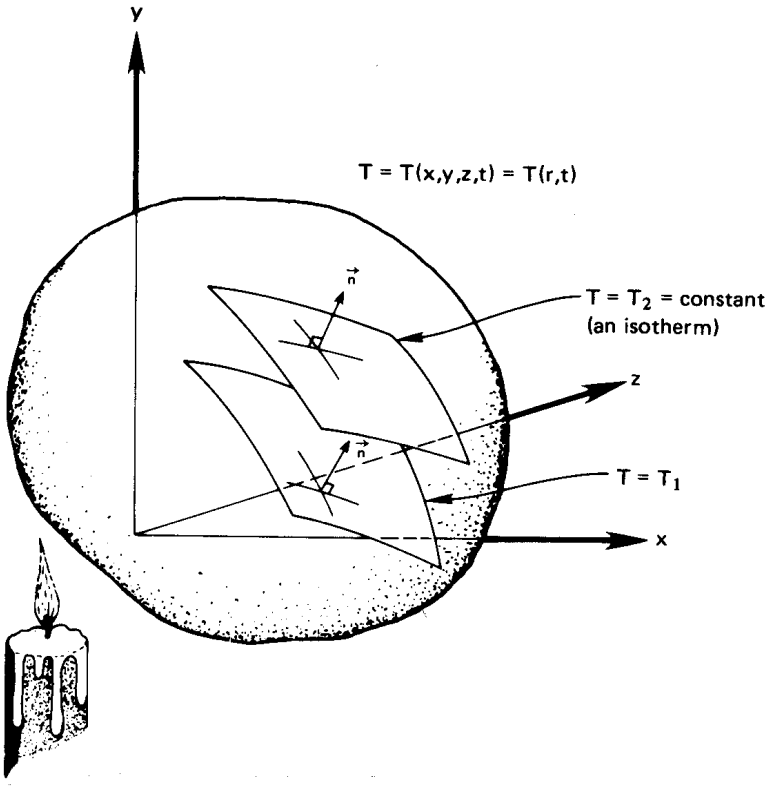

Figure 2.1 A three-dimensional, transient temperature field.

isothermal surfaces, T_1, T_2, and so on.

We next consider a very important vector associated with the scalar, T. The vector that has both the magnitude and direction of the maximum increase of temperature at each point is called the *temperature gradient*, ∇T:

$$\nabla T \equiv \vec{i}\frac{\partial T}{\partial x} + \vec{j}\frac{\partial T}{\partial y} + \vec{k}\frac{\partial T}{\partial z} \tag{2.1}$$

Fourier's law

"Experience"—that is, physical observation—suggests two things about the heat flow that results from temperature nonuniformities in a body.

These are:

$$\frac{\vec{q}}{|\vec{q}|} = -\frac{\nabla T}{|\nabla T|} \quad \left\{\begin{array}{l}\text{This says that } \vec{q} \text{ and } \nabla T \text{ are exactly opposite one}\\ \text{another in direction}\end{array}\right.$$

and

$$|\vec{q}| \propto |\nabla T| \quad \left\{\begin{array}{l}\text{This says that the magnitude of the heat flux is}\\ \text{directly proportional to the temperature gradient}\end{array}\right.$$

Notice that the heat flux is now written as a quantity that has a specified direction as well as a specified magnitude. Fourier's law summarizes this physical experience succinctly as

$$\boxed{\vec{q} = -k\nabla T} \tag{2.2}$$

which resolves itself into three components:

$$q_x = -k\frac{\partial T}{\partial x} \qquad q_y = -k\frac{\partial T}{\partial y} \qquad q_z = -k\frac{\partial T}{\partial z}$$

The "constant" k—the thermal conductivity—also depends on position and temperature in the most general case:

$$k = k[\vec{r}, T(\vec{r}, t)] \tag{2.3}$$

Fortunately, most materials (though not all of them) are very nearly homogeneous. Thus we can usually write $k = k(T)$. The assumption that we really want to make is that k is constant. Whether or not that is legitimate must be determined in each case. As is apparent from Fig. 2.2 and Fig. 2.3, k almost always varies with temperature. It always rises with T in gases at low pressures, but it may rise or fall in metals or liquids. The problem is that of assessing whether or not k is approximately constant in the range of interest. We could safely take k to be a constant for iron between 0° and 40°C (see Fig. 2.2), but we would incur error between −100° and 800°C.

It is easy to prove (Problem 2.1) that if k varies linearly with T, and if heat transfer is plane and steady, then $q = k\Delta T/L$, with k evaluated at the average temperature in the plane. If heat transfer is not planar or if it is not simply $A + BT$, it can be much more difficult to specify a single accurate effective value of k. If ΔT is not large, one can still make a reasonably accurate approximation using a constant average value of k.

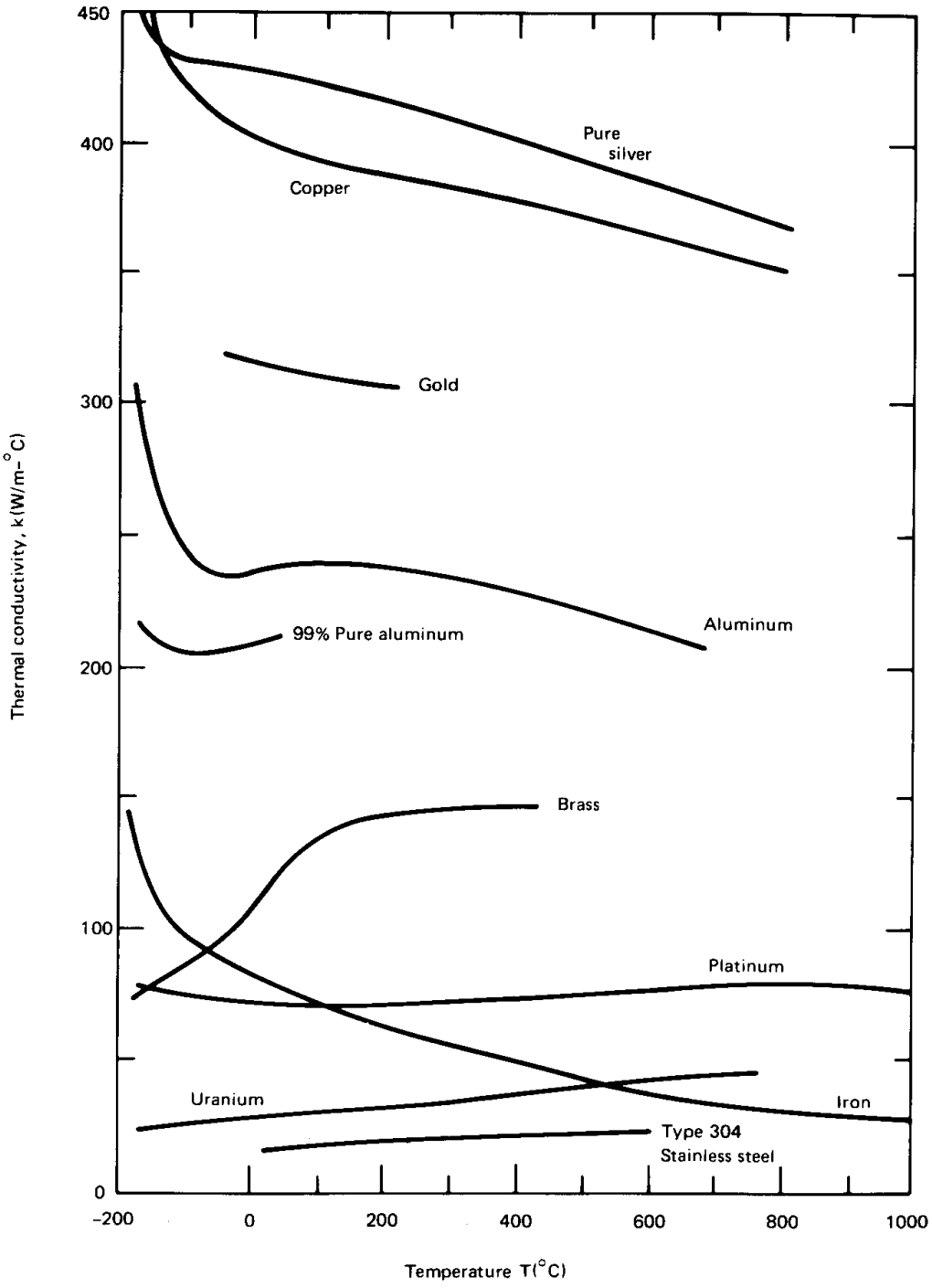

Figure 2.2 Variation of thermal conductivity of metallic solids with temperature

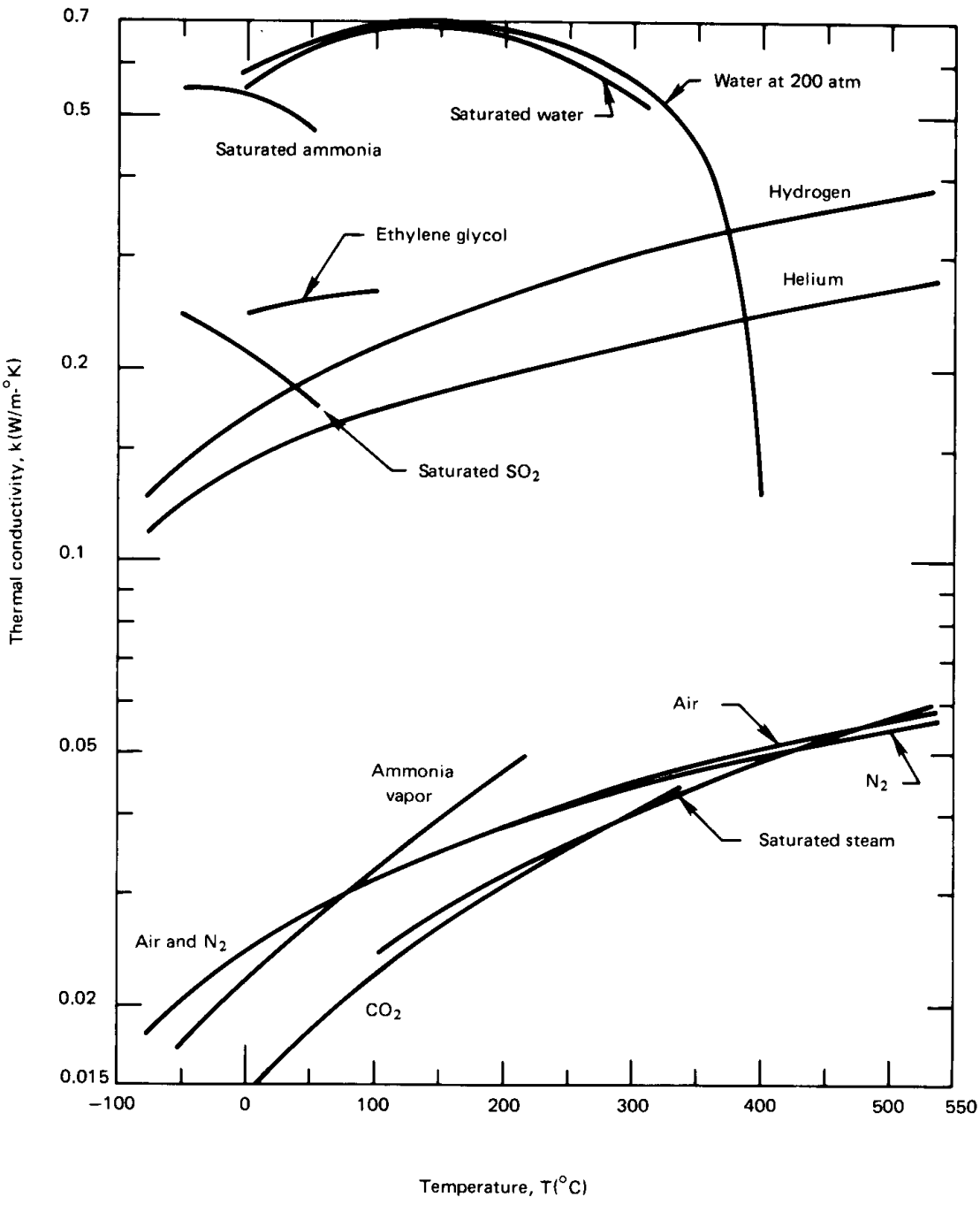

Figure 2.3 The temperature dependence of the thermal conductivity of liquids and gases that are either saturated or at 1 atm pressure.

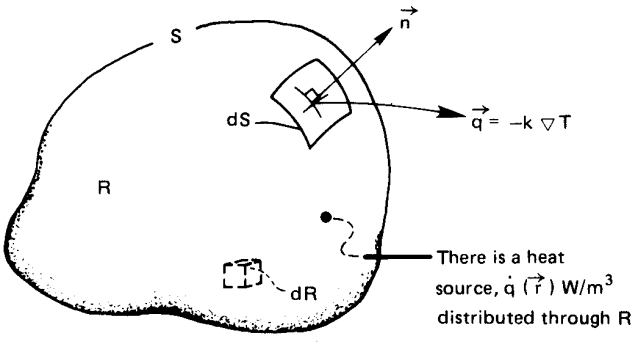

Figure 2.4 Control volume in a heat-flow field.

We have now revisited Fourier's law in three dimensions and found that there is more to it than we saw in Chapter 1. Next we write the heat conduction equation in three dimensions. We begin, as we did in Chapter 1, with the First Law statement, eqn. (1.3):

$$Q = \frac{dU}{dt}$$

This time we apply eqn. (1.3) to a three-dimensional control volume, as shown in Fig. 2.4.[1] The control volume is a finite region of a conducting body, which we set aside for analysis. The surface is denoted as S and the volume and the region as R; both are at rest. An element of the surface, dS, is identified and two vectors are shown on dS: one is the unit normal vector, $\vec{n}$ (with $|\vec{n}| = 1$), and the other is the heat flux vector, $\vec{q} = -k\nabla T$, at that point on the surface.

We also allow the possibility that a volumetric heat release equal to $\dot{q}(\vec{r})$ W/m^3 is distributed through the region. This might be the result of chemical or nuclear reaction, of electrical resistance heating, of external radiation into the region or of still other causes. With reference to Fig. 2.4, we can write the heat flux, dQ, out of dS as

$$dQ = (-k\nabla T) \cdot (\vec{n}\,dS) \tag{2.4}$$

If heat is also being generated (or consumed) within the region R, it must be added to eqn. (2.4) to get the *net* heat rate in R:

$$Q = -\int_S (-k\nabla T) \cdot (\vec{n}\,dS) + \int_R \dot{q}\,dR \tag{2.5}$$

[1] Figure 2.4 is the three-dimensional version of the control volume shown in Fig. 1.8.

The rate of energy increase of the region R is

$$\frac{dU}{dt} = \int_R \left(\rho c \frac{\partial T}{\partial t}\right) dR \tag{2.6}$$

where the derivative of T is in partial form because T is a function of both $\vec{r}$ and t.

Finally, we combine Q, as given by eqn. (2.5), and dU/dt, as given by eqn. (2.6), into eqn. (1.3). After rearranging the terms, we obtain

$$\int_S k\nabla T \cdot \vec{n} dS = \int_R \left[\rho c \frac{\partial T}{\partial t} - \dot{q}\right] dR \tag{2.7}$$

To get the left-hand side into a convenient form, we introduce Gauss's theorem, which converts a surface integral into a volume integral. Gauss's theorem says that if $\vec{A}$ is any continuous function of position, then

$$\int_S \vec{A} \cdot \vec{n} dS = \int_R \nabla \cdot \vec{A}\, dR \tag{2.8}$$

Therefore, if we identify $\vec{A}$ with $(k\nabla T)$, eqn. (2.7) reduces to

$$\int_R \left(\nabla \cdot k\nabla T - \rho c \frac{\partial T}{\partial t} + \dot{q}\right) dR = 0 \tag{2.9}$$

Next, since the region R is arbitrary, the integrand must vanish identically.[2] We therefore get the *heat diffusion equation* in three dimensions:

$$\boxed{\nabla \cdot k\nabla T + \dot{q} = \rho c \frac{\partial T}{\partial t}} \tag{2.10}$$

The limitations on this equation are:

- Incompressible medium. (This was implied when no expansion work term was included.)
- No convection. (The medium cannot undergo any relative motion. However, it *can* be a liquid or gas as long as it sits still.)

[2] Consider $\int f(x)\, dx = 0$. If $f(x)$ were, say, $\sin x$, then this could only be true over intervals of $x = 2\pi$ or multiples of it. For eqn. (2.9) to be true for *any* range of integration one might choose, the terms in parentheses must be zero everywhere.

If the variation of k with T is small, k can be factored out of eqn. (2.10) to get

$$\boxed{\nabla^2 T + \frac{\dot{q}}{k} = \frac{1}{\alpha}\frac{\partial T}{\partial t}} \tag{2.11}$$

This is a more complete version of the heat conduction equation [recall eqn. (1.14)] and α is the thermal diffusivity which was discussed after eqn. (1.14). The term $\nabla^2 T \equiv \nabla \cdot \nabla T$ is called the *Laplacian*. It arises thus in a Cartesian coordinate system:

$$\nabla \cdot k\nabla T \simeq k\nabla \cdot \nabla T = k\left(\vec{i}\frac{\partial}{\partial x} + \vec{j}\frac{\partial}{\partial y} + \vec{k}\frac{\partial}{\partial x}\right) \cdot \left(\vec{i}\frac{\partial T}{\partial x} + \vec{j}\frac{\partial T}{\partial y} + \vec{k}\frac{\partial T}{\partial z}\right)$$

or

$$\boxed{\nabla^2 T = \frac{\partial^2 T}{\partial x^2} + \frac{\partial^2 T}{\partial y^2} + \frac{\partial^2 T}{\partial z^2}} \tag{2.12}$$

The Laplacian can also be expressed in cylindrical or spherical coordinates. The results are:

- Cylindrical:

$$\nabla^2 T \equiv \frac{1}{r}\frac{\partial}{\partial r}\left(r\frac{\partial T}{\partial r}\right) + \frac{1}{r^2}\frac{\partial^2 T}{\partial \theta^2} + \frac{\partial^2 T}{\partial z^2} \tag{2.13}$$

- Spherical:

$$\nabla^2 T \equiv \frac{1}{r}\frac{\partial^2 (rT)}{\partial r^2} + \frac{1}{r^2 \sin\theta}\frac{\partial}{\partial \theta}\left(\sin\theta\frac{\partial T}{\partial \theta}\right) + \frac{1}{r^2 \sin^2\theta}\frac{\partial^2 T}{\partial \phi^2} \tag{2.14a}$$

or

$$\equiv \frac{1}{r^2}\frac{\partial}{\partial r}\left(r^2\frac{\partial T}{\partial r}\right) + \frac{1}{r^2 \sin\theta}\frac{\partial}{\partial \theta}\left(\sin\theta\frac{\partial T}{\partial \theta}\right) + \frac{1}{r^2 \sin^2\theta}\frac{\partial^2 T}{\partial \phi^2} \tag{2.14b}$$

where the coordinates are as described in Fig. 2.5.

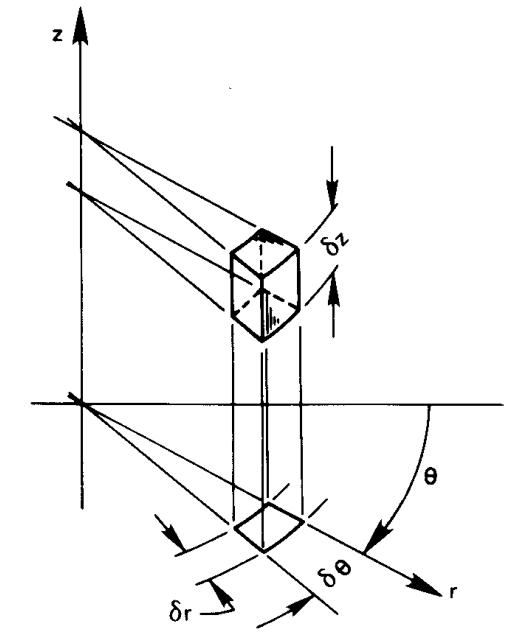

Polar coordinates

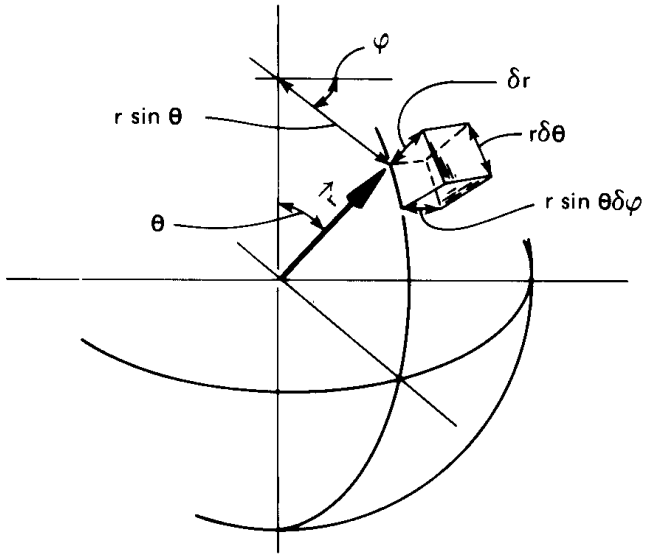

Spherical coordinates

Figure 2.5 Cylindrical and spherical coordinate schemes.

2.2 Solutions of the heat diffusion equation

We are now in position to calculate the temperature distribution and/or heat flux in bodies with the help of the heat diffusion equation. In every case, we first calculate $T(\vec{r}, t)$. Then, if we want the heat flux as well, we differentiate T to get q from Fourier's law.

The heat diffusion equation is a partial differential equation (p.d.e.) and the task of solving it may seem difficult, but we can actually do a lot with fairly elementary mathematical tools. For one thing, in one-dimensional steady-state situations the heat diffusion equation becomes an ordinary differential equation (o.d.e.); for another, the equation is linear and therefore not too formidable, in any case. Our procedure can be laid out, step by step, with the help of the following example.

Example 2.1 Basic Method

A large, thin concrete slab of thickness L is "setting." Setting is an exothermic process that releases $\dot{q}$ W/m^3. The outside surfaces are kept at the ambient temperature, so $T_w = T_\infty$. What is the maximum internal temperature?

SOLUTION.

Step 1. *Pick the coordinate scheme that best fits the problem and identify the independent variables that determine T.* In the example, T will probably vary only along the thin dimension, which we will call the x-direction. (We should want to know that the edges are insulated and that L was much smaller than the width or height. If they are, this assumption should be quite good.) Since the interior temperature will reach its maximum value when the process becomes steady, we write $T = T(x \text{ only})$.

Step 2. *Write the appropriate d.e., starting with one of the forms of eqn. (2.11).*

$$\frac{\partial^2 T}{\partial x^2} + \underbrace{\frac{\partial^2 T}{\partial y^2} + \frac{\partial^2 T}{\partial z^2}}_{\substack{=0, \text{ since} \\ T \neq T(y \text{ or } z)}} + \frac{\dot{q}}{k} = \underbrace{\frac{1}{\alpha}\frac{\partial T}{\partial t}}_{\substack{= 0, \text{ since} \\ \text{steady}}}$$

Therefore, since $T = T(x \text{ only})$, the equation reduces to the

ordinary d.e.

$$\frac{d^2T}{dx^2} = -\frac{\dot{q}}{k}$$

Step 3. *Obtain the general solution of the d.e.* (This is usually the easiest step.) We simply integrate the d.e. twice and get

$$T = -\frac{\dot{q}}{2k}x^2 + C_1x + C_2$$

Step 4. *Write the "side conditions" on the d.e.—the initial and boundary conditions.* This is always the hardest part for the beginning students; it is the part that most seriously tests their physical or "practical" understanding of problems.

Normally, we have to make two specifications of temperature on each position coordinate and one on the time coordinate to get rid of the constants of integration in the general solution. (These matters are discussed at greater length in Chapter 4.)

In this case there are two boundary conditions:

$$T(x = 0) = T_w \quad \text{and} \quad T(x = L) = T_w$$

Very Important Warning: Never, never introduce inaccessible information in a boundary or initial condition. Always stop and ask yourself, "Would I have access to a numerical value of the temperature (or other data) that I specify at a given position or time?" If the answer is no, then your result will be useless.

Step 5. *Substitute the general solution in the boundary and initial conditions and solve for the constants.* This process gets very complicated in the transient and multidimensional cases. Fourier series methods are typically needed to solve the problem. However, the steady one-dimensional problems are usually easy. In the example, by evaluating at $x = 0$ and $x = L$, we get:

$$T_w = -0 + 0 + C_2 \qquad \text{so} \qquad C_2 = T_w$$

$$T_w = -\frac{\dot{q}L^2}{2k} + C_1L + \underbrace{C_2}_{=T_w} \qquad \text{so} \qquad C_1 = \frac{\dot{q}L}{2k}$$

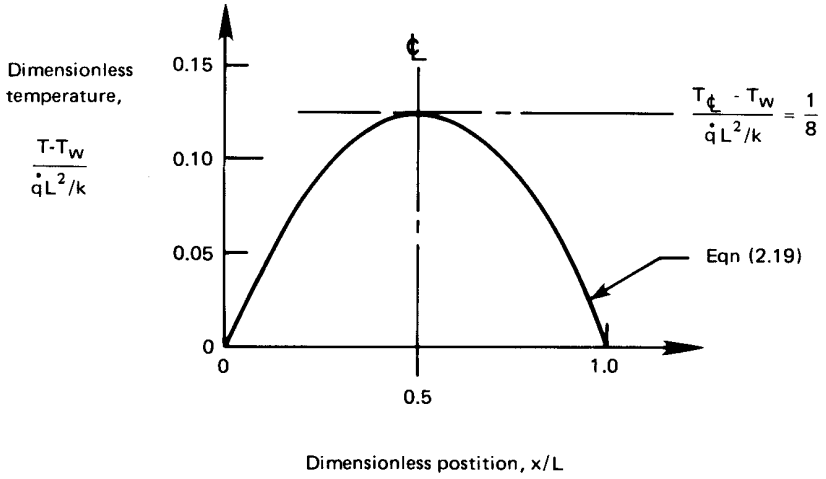

Figure 2.6 Temperature distribution in the setting concrete slab Example 2.1.

Step 6. *Put the calculated constants back in the general solution to get the particular solution to the problem.* In the example problem we obtain:

$$T = -\frac{\dot{q}}{2k}x^2 + \frac{\dot{q}}{2k}Lx + T_w$$

This should be put in neat dimensionless form:

$$\frac{T - T_w}{\dot{q}L^2/k} = \frac{1}{2}\left[\frac{x}{L} - \left(\frac{x}{L}\right)^2\right] \tag{2.15}$$

Step 7. *Play with the solution—look it over—see what it has to tell you. Make any checks you can think of to be sure it is correct.* In this case we plot eqn. (2.15) in Fig. 2.6. The resulting temperature distribution is parabolic and, as we would expect, symmetrical. It satisfies the boundary conditions at the wall and maximizes in the center. By nondimensionalizing the result, we have succeeded in representing all situations with a simple curve. That is highly desirable when the calculations are not simple, as they are here. (Notice that T actually depends on *five* different things, yet the solution is a single curve on a two-coordinate graph.)

Finally, we check to see if the heat flux at the wall is correct:

$$q_{\text{wall}} = -k\frac{\partial T}{\partial x}\bigg|_{x=0} = k\left[\frac{\dot{q}}{k}x - \frac{\dot{q}L}{2k}\right]_{x=0} = -\frac{\dot{q}L}{2}$$

Thus, half of the total energy generated in the slab comes out of the front side, as we would expect. The solution appears to be correct.

Step 8. *If the temperature field is now correctly established, you can, if you wish, calculate the heat flux at any point in the body by substituting $T(\vec{r}, t)$ back into Fourier's law.* We did this already, in Step 7, to check our solution. ■

We shall run through additional examples in this section and the following one. In the process, we shall develop some important results for future use.

Example 2.2 The Simple Slab

A slab shown in Fig. 2.7 is at a steady state with dissimilar temperatures on either side and no internal heat generation. We want the temperature distribution and the heat flux through it.

SOLUTION. These can be found quickly by following the steps set down in Example 2.1:

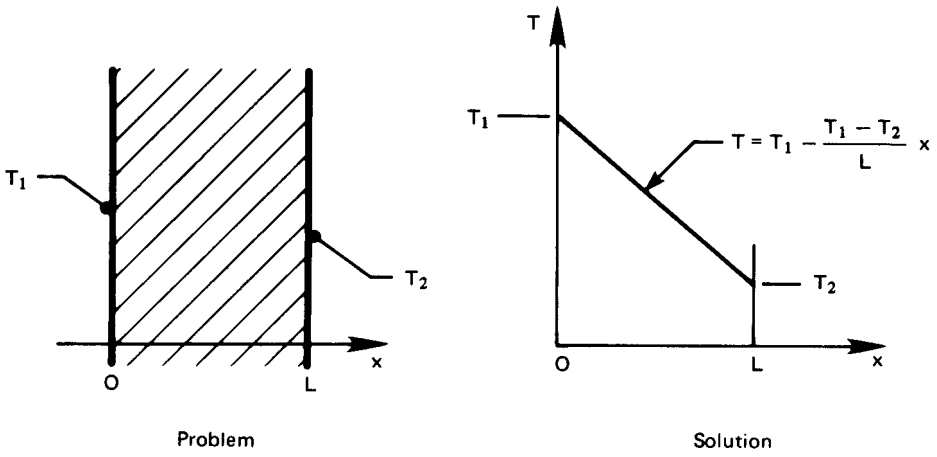

Figure 2.7 Heat conduction in a slab (Example 2.2).

Step 1. $T = T(x)$

Step 2. $\dfrac{d^2T}{dx^2} = 0$

Step 3. $T = C_1x + C_2$

Step 4. $T(x = 0) = T_1$; and $T(x = L) = T_2$

Step 5. $T_1 = 0 + C_2$, so $C_2 = T_1$; and $T_2 = C_1x + C_2$, so $C_1 = \dfrac{T_2 - T_1}{L}$

Step 6. $T = T_1 + \dfrac{T_2 - T_1}{L}x$; or $\dfrac{T - T_1}{T_2 - T_1} = \dfrac{x}{L}$

Step 7. We note that the solution satisfies the boundary conditions and that the temperature profile is linear.

Step 8. $q = -k\dfrac{dT}{dx} = -k\dfrac{d}{dx}\left(T_1 - \dfrac{T_1 - T_2}{L}x\right)_{x \text{ of interest}}$

so that $\boxed{q = k\dfrac{\Delta T}{L}}$ ■

This result, which is the simplest heat conduction solution, calls to mind Ohm's law. Thus, if we rearrange it:

$$Q = \frac{\Delta T}{L/kA} \qquad \text{is like} \qquad I = \frac{E}{R}$$

where L/kA assumes the role of a *thermal resistance*, to which we give the symbol R_t. R_t has the dimensions of $(\text{W/K})^{-1}$. Figure 2.8 shows how we can represent heat flow through the slab with a diagram that is perfectly analogous to an electric circuit.

2.3 Thermal resistance and the electrical analogy

Fourier's, Fick's, and Ohm's laws

Fourier's law has several extremely important analogies in other kinds of physical behavior, of which the electrical analogy is only one. These analogous processes provide us with a good deal of guidance in the solution of heat transfer problems And, conversely, heat conduction analyses can often be adapted to describe those processes.

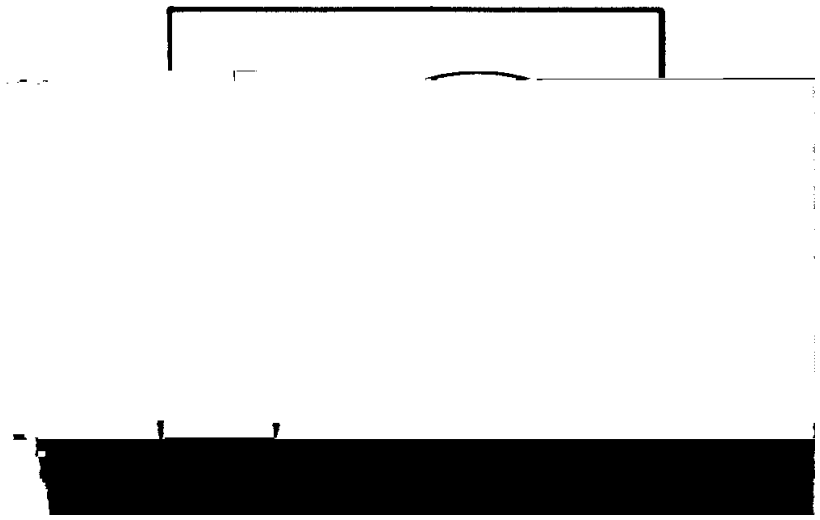

Figure 2.8 Ohm's law analogy to plane conduction.

Let us first consider *Ohm's law* in three dimensions:

$$\text{flux of electrical charge} = \frac{\vec{I}}{A} \equiv \vec{J} = -\gamma \nabla V \tag{2.16}$$

$\vec{I}$ amperes is the vectorial electrical current, A is an area normal to the current vector, $\vec{J}$ is the flux of current or *current density*, γ is the electrical conductivity in $\text{cm/ohm}\cdot\text{cm}^2$, and V is the voltage.

To apply eqn. (2.16) to a one-dimensional current flow situation, as pictured in Fig. 2.9, we write eqn. (2.16) as

$$J = -\gamma \frac{dV}{dx} = \gamma \frac{\Delta V}{L}, \tag{2.17}$$

but ΔV is the applied voltage, E, and the resistance of the wire is $R \equiv L/\gamma A$. Then, since $I = J A$, eqn. (2.17) becomes

$$I = \frac{E}{R} \tag{2.18}$$

which is the familiar, but restrictive, one-dimensional statement of Ohm's law.

Fick's law is another analogous relation. It states that during mass diffusion, the flux, $\vec{j}_1$, of a dilute component, 1, into a second fluid, 2, is

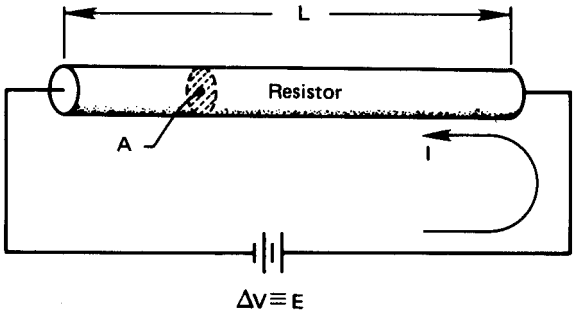

Figure 2.9 The one-dimensional flow of current.

proportional to the gradient of its mass concentration, m_1. Thus

$$\vec{j}_1 = -\rho D_{12} \nabla m_1 \tag{2.19}$$

where the constant D_{12} is the binary diffusion coefficient.

Example 2.3

Air fills a tube 1 m in length. There is a small water leak at one end where the water vapor concentration builds to a mass fraction of 0.01. A desiccator maintains the concentration at zero on the other side. What is the steady flux of water from one side to the other if D_{12} is 0.000284 m^2/s and $\rho = 1.18$ kg/m^3?

SOLUTION.

$$\left|\vec{j}_{\text{water vapor}}\right| = \left(0.000284 \frac{m^2}{s}\right)\left(1.18 \frac{kg}{m^3}\right)\left(\frac{0.01 \text{ kg } H_2O/\text{kg mixture}}{1 \text{ m}}\right)$$

$$= 0.00000335 \frac{kg}{m^2 \cdot s}$$

■

Contact resistance

One place in which the usefulness of the electrical resistance analogy becomes immediately apparent is at the interface of two conducting media. No two solid surfaces will ever form perfect thermal contact when they are pressed together. Since some roughness is always present, a typical plane of contact will always include tiny air gaps as shown in Fig. 2.10

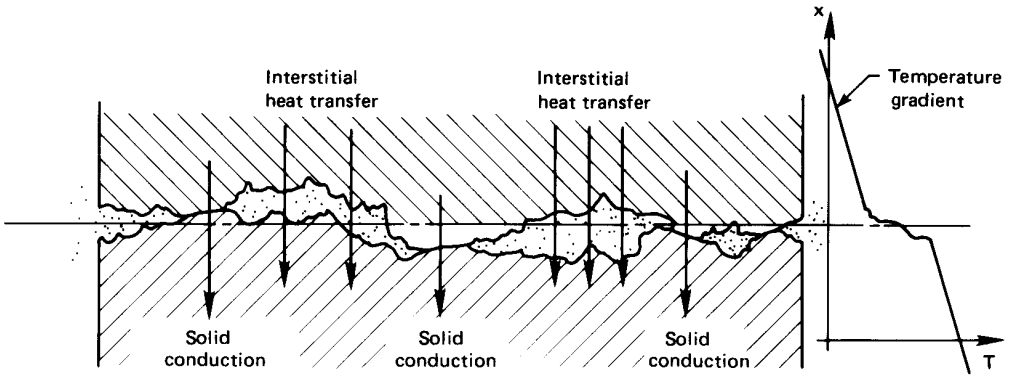

Figure 2.10 Heat transfer through the contact plane between two solid surfaces.

(which is drawn with a highly exaggerated vertical scale). Heat transfer follows two paths through such an interface. Conduction through points of solid-to-solid contact is very effective, but conduction through the gas-filled interstices, which have low thermal conductivity, can be very poor.

We treat the contact surface by placing a interfacial conductance, h_c, in series with the conducting materials on either side. The coefficient h_c is similar to a heat transfer coefficient and has the same units, $\mathrm{W/m^2K}$. Its inverse, $1/h_c$, is the contact resistance.

The interfacial conductance, h_c, depends on the following factors:

- The surface finish and cleanliness of the contacting solids.
- The materials that are in contact.
- The pressure with which the surfaces are forced together.
- the substance (or lack of it) in the interstitial spaces.
- the temperature at the contact plane.

The influence of pressure is usually a modest one up to around 10 atm in most metals. Beyond that, increasing plastic deformation of the local contact points causes h_c to increase more dramatically at high pressure. Table 2.1 gives typical values of contact resistances which bear out most of the preceding points. These values have been adapted from [2.1, Chap. 3] and [2.2].

Table 2.1 Some typical interfacial conductances (air gaps not evacuated)

Situation	h_c (W/m^{2}K)
Copper/copper (moderate pressure and normal finishes)	10,000 – 25,000
Aluminum/aluminum (moderate pressure and normal finishes)	2,200 – 12,000
Graphite/metals (moderate pressure and normal finishes)	3,000 – 6,000
Ceramic/metals (moderate pressure and normal finishes)	1,500 – 8,500
Ceramic/ceramic (moderate pressure and normal finishes)	500 – 3,000
Stainless steel/stainless steel (moderate pressure and normal finishes)	300 – 3,700
Rough aluminum/aluminum (low pressure and evacuated interstices)	~ 150
Iron/aluminum (70 atm pressure)	45,000

Example 2.4

Heat flows through two stainless steel slabs (k = 18 W/m·K) pressed together. How thin must the slabs be before contact resistance is important?

SOLUTION. With reference to Fig. 2.11, we can write

$$R_{\text{total}} = \frac{L}{18} + \frac{1}{h_c} + \frac{L}{18}$$

but h_c is about 2,500. Therefore,

$$\frac{2L}{18} \text{ must be } \gg \frac{1}{2500} = 0.0004$$

so L must be greater than 0.0036 m if contact resistance is to be ignored. A thickness of 4 cm would reduce the error to about 10%. ■

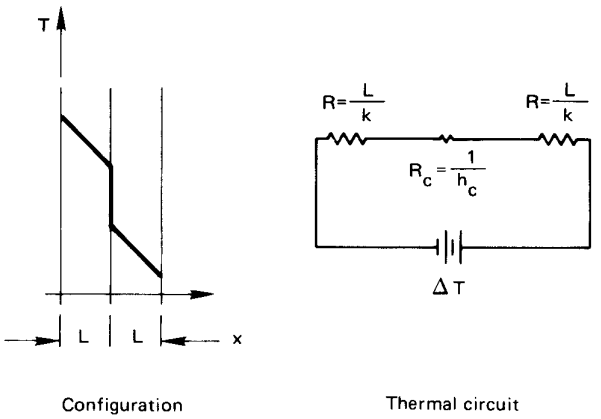

Figure 2.11 Conduction through two stainless steel slabs with a contact resistance.

Resistances for cylinders and for convection

As we continue developing our method of solving one-dimensional heat conduction problems, we find that other avenues of heat flow may also be expressed as thermal resistances, and introduced into the solutions that we obtain. We also find that, once the heat conduction equation has been solved, the results themselves may be used as new thermal resistance terms.

Example 2.5 Radial Heat Conduction in a Tube

Find the temperature distribution and the heat flux for the long hollow cylinder shown in Fig. 2.12.

SOLUTION.

Step 1. $T = T(r)$

Step 2.

$$\frac{1}{r}\frac{\partial}{\partial r}\left(r\frac{\partial T}{\partial r}\right) + \underbrace{\frac{1}{r^2}\frac{\partial^2 T}{\partial \phi^2} + \frac{\partial^2 T}{\partial z^2}}_{=0,\ \text{since } T \neq T(\phi, z)} + \underbrace{\frac{\dot{q}}{k}}_{=0} = \underbrace{\frac{1}{\alpha}\frac{\partial T}{\partial}}_{=0,\ \text{since steady}}$$

Step 3. Integrate once: $r\dfrac{\partial T}{\partial r} = C_1$; integrate again: $T = C_1 \ln r + C_2$

Step 4. $T(r = r_i) = T_i$ and $T(r = r_o) = T_o$

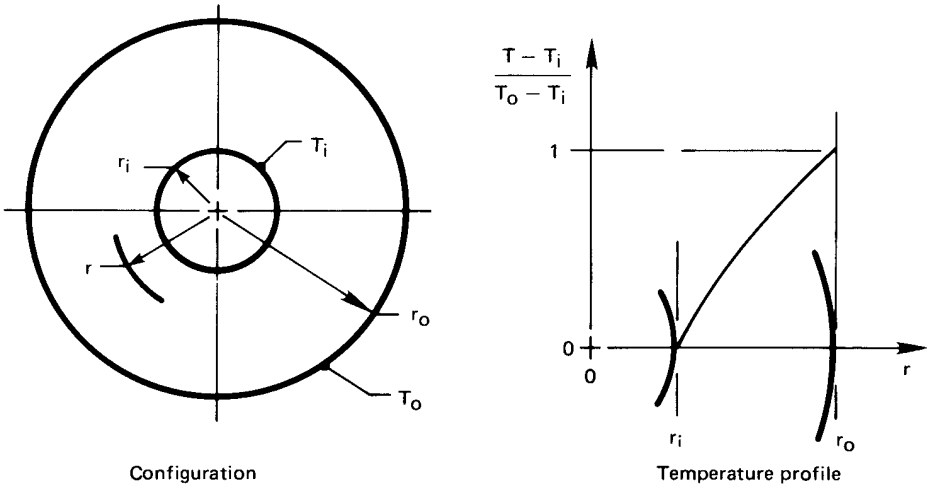

Figure 2.12 Heat transfer through a cylinder with a fixed wall temperature (Example 2.5).

Step 5.

$$\left.\begin{aligned} T_i &= C_1 \ln r_i + C_2 \\ T_o &= C_1 \ln r_o + C_2 \end{aligned}\right\} \Longrightarrow \begin{cases} C_1 = \dfrac{T_i - T_o}{\ln(r_i/r_o)} = -\dfrac{\Delta T}{\ln(r_o/r_i)} \\ C_2 = T_i + \dfrac{\Delta T}{\ln(r_o/r_i)} \ln r_i \end{cases}$$

Step 6. $T = T_i - \dfrac{\Delta T}{\ln(r_o/r_i)}(\ln r - \ln r_i)$ or

$$\boxed{\frac{T - T_i}{T_o - T_i} = \frac{\ln(r/r_i)}{\ln(r_o/r_i)}} \tag{2.20}$$

Step 7. The solution is plotted in Fig. 2.12. We see that the temperature profile is logarithmic and that it satisfies both boundary conditions. Furthermore, it is instructive to see what happens when the wall of the cylinder is very thin, or when r_i/r_o is close to 1. In this case:

$$\ln(r/r_i) \simeq \frac{r}{r_i} - 1 = \frac{r - r_i}{r_i}$$

and

$$\ln(r_o/r_i) \simeq \frac{r_o - r_i}{r_i}$$

Thus eqn. (2.20) becomes

$$\frac{T - T_i}{T_o - T_i} = \frac{r - r_i}{r_o - r_i}$$

which is a simple linear profile. This is the same solution that we would get in a plane wall.

Step 8. At any station, r:

$$q_{\text{radial}} = -k\frac{\partial T}{\partial r} = +\frac{l\Delta T}{\ln(r_o/r_i)}\frac{1}{r}$$

So the heat *flux* falls off inversely with radius. That is reasonable, since the same heat flow must pass through an increasingly large surface as the radius increases. Let us see if this is the case for a cylinder of length l:

$$Q\ (\text{W}) = (2\pi r l)\, q = \frac{2\pi k l \Delta T}{\ln(r_o/r_i)} \neq f(r) \tag{2.21}$$

Finally, we again recognize Ohm's law in this result and write the thermal resistance for a cylinder:

$$R_{t_{\text{cyl}}} = \frac{\ln(r_o/r_i)}{2\pi l k}\ \left(\frac{\text{K}}{\text{W}}\right) \tag{2.22}$$

This can be compared with the resistance of a plane wall:

$$R_{t_{\text{wall}}} = \frac{L}{kA}\ \left(\frac{\text{K}}{\text{W}}\right)$$

Both resistances are inversely proportional to k, but each reflects a different geometry. ■

In the preceding examples, the boundary conditions were all the same —a temperature specified at an outer edge. Next let us suppose that the temperature is specified in the environment away from a body, with a heat transfer coefficient between the environment and the body.

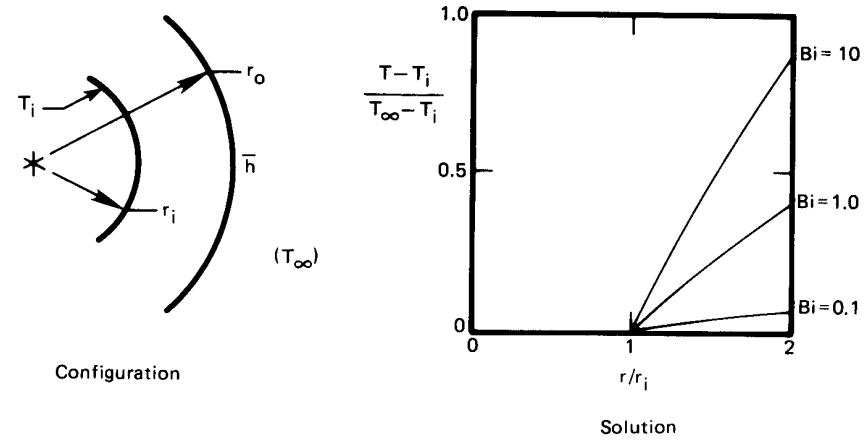

Figure 2.13 Heat transfer through a cylinder with a convective boundary condition (Example 2.6).

Example 2.6 A Convective Boundary Condition

A convective heat transfer coefficient around the outside of the cylinder in Example 2.5 provides thermal resistance between the cylinder and an environment at $T = T_\infty$, as shown in Fig. 2.13. Find the temperature distribution and heat flux in this case.

SOLUTION.

Step 1 through 3. These are the same as in Example 2.5.

Step 4. The first boundary condition is $T(r = r_i) = T_i$. The second boundary condition must be expressed as an energy balance at the outer wall (recall Section 1.3).

$$q_{\text{convection}} = q_{\substack{\text{conduction} \\ \text{at the wall}}}$$

or

$$\bar{h}(T - T_\infty)_{r=r_o} = -k \left.\frac{\partial T}{\partial r}\right|_{r=r_o}$$

Step 5. From the first boundary condition we obtain $T_i = C_1 \ln r_i + C_2$. It is easy to make mistakes when we substitute the general solution into the second boundary condition, so we will do it in

detail:

$$\overline{h}\Big[(C_1 \ln r + C_2) - T_\infty\Big]_{r=r_o} = -k\left[\frac{\partial}{\partial r}(C_1 \ln r + C_2)\right]_{r=r_o} \tag{2.23}$$

A common error is to substitute $T = T_o$ on the lefthand side instead of substituting the entire general solution. That will do no good, because T_o is not an accessible piece of information. Equation (2.23) reduces to:

$$\overline{h}(T_\infty - C_1 \ln r_o - C_2) = \frac{kC_1}{r_o}$$

When we combine this with the result of the first boundary condition to eliminate C_2:

$$C_1 = -\frac{T_i - T_\infty}{k/(\overline{h}r_o) + \ln(r_o/r_i)} = \frac{T_\infty - T_i}{1/\mathrm{Bi} + \ln(r_o/r_i)}$$

Then

$$C_2 = T_i - \frac{T_\infty - T_i}{1/\mathrm{Bi} + \ln(r_o/r_i)} \ln r_i$$

Step 6.

$$T = \frac{T_\infty - T_i}{1/\mathrm{Bi} + \ln(r_o/r_i)} \ln(r/r_i) + T_i$$

This can be rearranged in fully dimensionless form:

$$\frac{T - T_i}{T_\infty - T_i} = \frac{\ln(r/r_i)}{1/\mathrm{Bi} + \ln(r_o/r_i)} \tag{2.24}$$

Step 7. Let us fix a value of r_o/r_i—say, 2—and plot eqn. (2.24) for several values of the Biot number. The results are included in Fig. 2.13. Some very important things show up in this plot. When $\mathrm{Bi} \gg 1$, the solution reduces to the solution given in Example 2.5. It is as though the convective resistance to heat flow were not there. That is exactly what we anticipated in Section 1.3 for large Bi. When $\mathrm{Bi} \ll 1$, the opposite is true: $(T - T_i)/(T_\infty - T_i)$

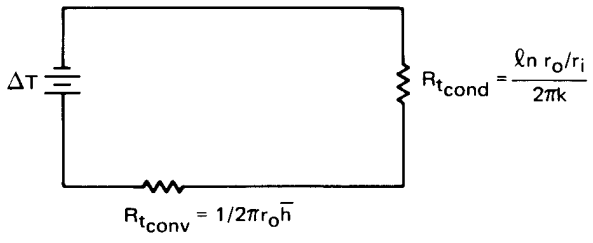

Figure 2.14 Thermal circuit with two resistances.

remains on the order of Bi, and internal conduction can be neglected. How big is big and how small is small? We do not really have to specify exactly. But in this case Bi < 0.1 signals constancy of temperature inside the cylinder with about $\pm 3\%$. Bi > 20 means that we can neglect convection with about 5% error.

Step 8. $q_{\text{radial}} = -k\dfrac{\partial T}{\partial r} = k\dfrac{T_i - T_\infty}{1/\text{Bi} + \ln(r_o/r_i)}\dfrac{1}{r}$

This can be written in terms of Q (W) $= q_{\text{radial}}\,(2\pi r l)$ for a cylinder of length l:

$$Q = \frac{T_i - T_\infty}{\dfrac{1}{\bar{h}\,2\pi r_o l} + \dfrac{\ln(r_o/r_i)}{2\pi k l}} = \frac{T_i - T_\infty}{R_{t_{\text{conv}}} + R_{t_{\text{cond}}}} \tag{2.25}$$

Equation (2.25) is once again analogous to Ohm's law. But this time the denominator is the sum of two thermal resistances, as would be the case in a series circuit. We accordingly present the analogous electrical circuit in Fig. 2.14.

The presence of convection on the outside surface of the cylinder causes a new thermal resistance of the form

$$R_{t_{\text{conv}}} = \frac{1}{\bar{h}A} \tag{2.26}$$

where A is the surface area over which convection occurs. ■

Example 2.7 Critical Radius of Insulation

An interesting consequence of the preceding result can be brought out with a specific example. Suppose that we insulate a 0.5 cm O.D. copper steam line with 85% magnesia to prevent the steam from condensing

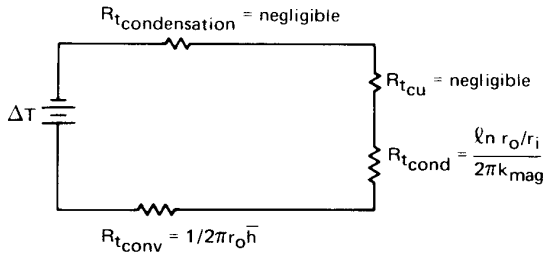

Figure 2.15 Thermal circuit for an insulated tube.

too rapidly. The steam is under pressure and stays at 150°C. The copper is thin and highly conductive—obviously a tiny resistance in series with the convective and insulation resistances, as we see in Fig. 2.15. The condensation of steam in the tube also offers very little resistance.[3] But a heat transfer coefficient of $\bar{h} = 20$ W/m^{2}K offers fairly high resistance on the outside. It turns out that insulation can actually *improve* heat transfer in this case. Figure 2.16 is a plot of the two significant resistances and their sum. A very interesting thing occurs here. $R_{t_{\text{conv}}}$ falls off rapidly when r_o is increased, because the outside area is increasing. Accordingly, the total resistance passes through a minimum in this case. Will it always do so? To find out, we differentiate eqn. (2.25), setting l equal to a unit length of 1 m:

$$\frac{dQ}{dr_o} = \frac{(T_i - T_\infty)}{\left(\dfrac{1}{2\pi r_o \bar{h}} + \dfrac{\ln(r_o/r_i)}{2\pi k}\right)^2}\left(-\frac{1}{2\pi r_o^2 \bar{h}} + \frac{1}{2\pi k r_o}\right) = 0$$

We solve this for the value of $r_o = r_{\text{crit}}$ at which R_t is minimum. Thus, we obtain

$$\text{Bi} = 1 = \frac{\bar{h} r_{\text{crit}}}{k} \tag{2.27}$$

at the maximum heat flux. In the present example, added insulation will *increase* heat loss instead of reducing it, until $r_{\text{crit}} = k/\bar{h} = 0.0037$ m or $r_{\text{crit}}/r_i = 1.48$. Indeed, insulation will not even start to do any good until r_o/r_i=2.32 or $r_o = 0.0058$ m. We call r_{crit} the *critical radius* of insulation. ■

[3]The question of how much resistance to heat transfer is offered by condensation inside the tube is the subject of Chapter 8. It turns out that $\bar{h}$ is generally enormous during condensation and that $R_{t_{\text{condensation}}}$ is tiny.

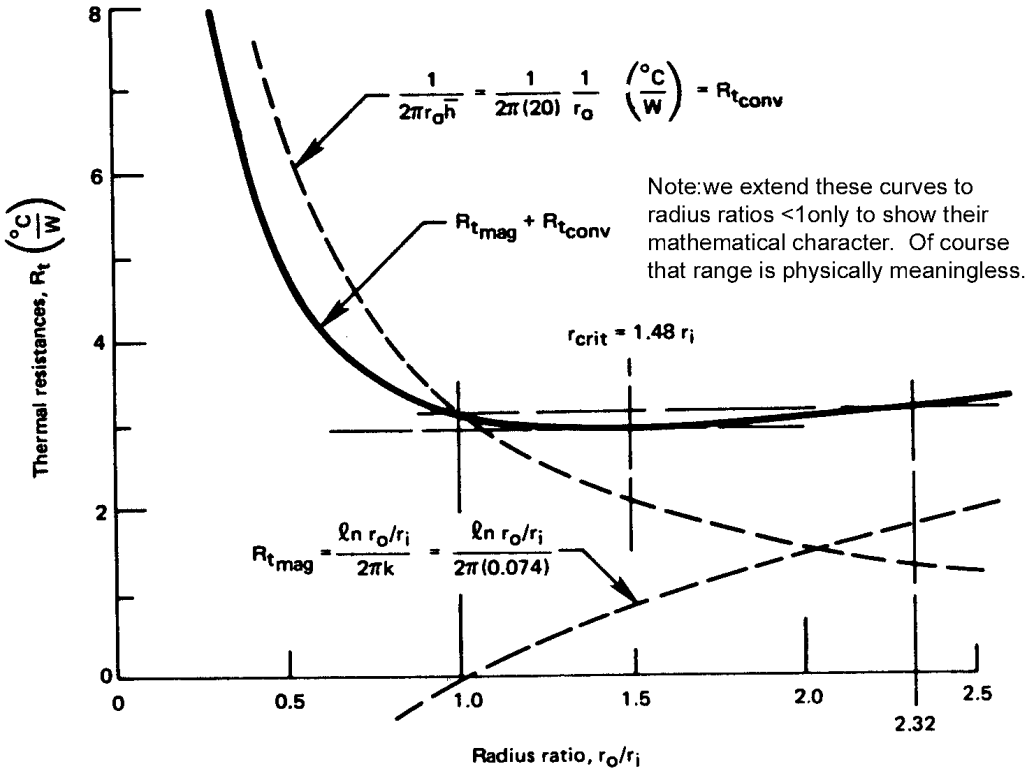

Figure 2.16 The critical radius of insulation (Example 2.7), written for a cylinder of unit length (l = 1 m).

There is an interesting catch here. For most cylinders, $r_{\text{crit}} < r_i$ and the critical radius idiosyncrasy is of no concern. If our steam line had a 1 cm outside diameter, the critical radius difficulty would not have arisen. The problem of cooling electrical wiring must be undertaken with this problem in mind, but one need not worry about the critical radius in the design of most large process equipment.

2.4 Overall heat transfer coefficient, U

Definition

We often want to transfer heat through composite resistances, as shown in Fig. 2.17. It is very convenient to have a number, U, that works like

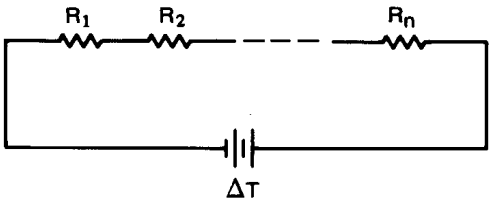

Figure 2.17 A thermal circuit with many resistances.

this[4]:

$$\boxed{Q = UA\,\Delta T} \tag{2.28}$$

This number, called the *overall heat transfer coefficient*, is defined largely by the system, and in many cases it proves to be insensitive to the operating conditions of the system. In Example 2.6, for example, we can use the value Q given by eqn. (2.25) to get

$$U = \frac{Q\,(\mathrm{W})}{[2\pi r_o l\,(\mathrm{m}^2)]\;\Delta T\,(^\circ\mathrm{C})} = \frac{1}{\dfrac{1}{\overline{\overline{h}}} + \dfrac{r_o \ln(r_o/r_i)}{k}} \quad (\mathrm{W/m^2K}) \tag{2.29}$$

We have based U on the outside area, r_o, in this case. We might also have based it on inside area and obtained

$$U = \frac{1}{\dfrac{r_i}{\overline{\overline{h}} r_o} + \dfrac{r_i \ln(r_o/r_i)}{k}} \tag{2.30}$$

It is therefore important to remember which area an overall heat transfer coefficient is based on. It is particularly important that A and U be consistent when we write $Q = UA\,\Delta T$.

Example 2.8

Estimate the overall heat transfer coefficient for the tea kettle shown in Fig. 2.18. Note that the flame convects heat to the thin aluminum. The heat is then conducted through the aluminum and finally convected by boiling into the water.

SOLUTION. We need not worry about deciding which area to base A on because the area normal to the heat flux vector does not change.

[4]This U must not be confused with internal energy. The two terms should always be distinct in context.

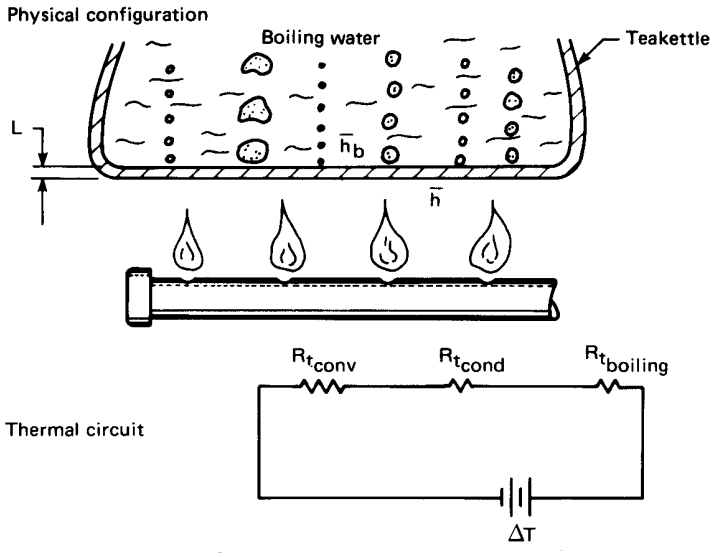

Figure 2.18 Heat transfer through the bottom of a tea kettle.

We simply write the heat flow

$$Q = \frac{\Delta T}{\sum R_t} = \frac{T_{\text{flame}} - T_{\text{boiling water}}}{\dfrac{1}{\bar{h}A} + \dfrac{L}{k_{\text{Al}}A} + \dfrac{1}{\bar{h}_b A}}$$

and apply the definition of U

$$U = \frac{Q}{A\Delta T} = \frac{1}{\dfrac{1}{\bar{h}} + \dfrac{L}{k_{\text{Al}}} + \dfrac{1}{\bar{h}_b}}$$

Let us see what typical numbers would look like in this example: $\bar{h}$ might be around 200 W/m^{2}K; L/k_{Al} might be 0.001 m/(160 W/m·K) or 1/160,000 W/m^{2}K; and $\bar{h}_b$ is quite large— perhaps about 5000 W/m^{2}K. Thus:

$$U \simeq \frac{1}{\dfrac{1}{200} + \dfrac{1}{160,000} + \dfrac{1}{5000}} = 192.1 \text{ W/m}^2\text{K} \qquad \blacksquare$$

It is clear that the first resistance is dominant, as is shown in Fig. 2.18. Notice that in such cases

$$U \longrightarrow 1/R_{t_{\text{dominant}}} \tag{2.31}$$

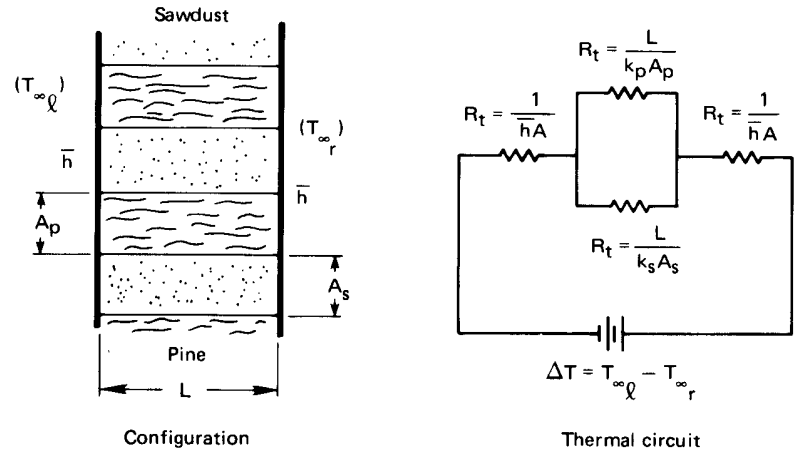

Figure 2.19 Heat transfer through a composite wall.

if we express R_t on a unit area basis (K/W per m^2 of heat exchanger area).

Experiment 2.1

Boil water in a paper cup over an open flame and explain why you can do so. [Recall eqn. (2.31) and see Problem 2.12.]

Example 2.9

A wall consists of alternating layers of pine and sawdust, as shown in Fig. 2.19). The sheathes on the outside have negligible resistance and $\bar{h}$ is known on the sides. Compute Q and U for the wall.

SOLUTION. So long as the wood and the sawdust do not differ dramatically from one another in thermal conductivity, we can approximate the wall as a parallel resistance circuit, as shown in the figure.[5] The total thermal resistance of such a circuit is

[5]For this approximation to be exact, the resistances must be equal. If they differ radically, the problem must be treated as two-dimensional.

$$R_{t_{\text{total}}} = R_{t_{\text{conv}}} + \frac{1}{\left(\frac{1}{R_{t_{\text{pine}}}} + \frac{1}{R_{t_{\text{sawdust}}}}\right)} + R_{t_{\text{conv}}}$$

Thus

$$Q = \frac{\Delta T}{R_{t_{\text{total}}}} = \frac{T_{\infty_1} - T_{\infty_r}}{\frac{1}{\overline{h}A} + \frac{1}{\left(\frac{k_p A_p}{L} + \frac{k_s A_s}{L}\right)} + \frac{1}{\overline{h}A}}$$

and

$$U = \frac{Q}{A\Delta T} = \frac{1}{\frac{2}{\overline{h}} + \frac{1}{\left(\frac{k_p}{L}\frac{A_p}{A} + \frac{k_s}{L}\frac{A_s}{A}\right)}}$$

■

Typical values of U

In a fairly general use of the word, a heat exchanger is anything that lies between two fluid masses at different temperatures. In this sense a heat exchanger might be designed either to impede or to enhance heat exchange. Consider some typical values of U in Table 2.2. These data were assembled from [2.3], [2.4], various manufacturers' literature, and other general sources listed at the end of Chapter 1. If the exchanger is intended to improve heat exchange, U will generally be much greater than 40 W/m^{2}K. If it is intended to impede heat flow, it will be less than 10 W/m^{2}K—anywhere down to almost perfect insulation. You should have some numerical concept of relative values of U, so we recommend that you scrutinize the numbers in Table 2.2. Some things worth bearing in mind are:

- The fluids with low thermal conductivities, such as tars, oils, or any of the gases, usually yield low values of $\overline{h}$. When such fluid flows on one side of an exchanger, U will generally be pulled down.
- Condensing and boiling are very effective heat transfer processes. They greatly improve U but they cannot override one very small value of $\overline{h}$ on the other side of the exchange. (Recall Example 2.8.)

Table 2.2 Typical values or ranges of U

Heat Exchange Configuration	U (W/m^{2}K)
Walls and roofs dwellings with a 24 km/h exterior wind velocity:	
• Insulated roofs	0.3–2
• Finished masonry walls	0.5–6
• Frame walls	0.8–5
• Uninsulated roofs	1.2–4
Single-pane windows	$\sim 6^{\dagger}$
Air to heavy tars and oils	As low as 45
Air to low-viscosity liquids	As high as 600
Air to various gases	60–550
Steam or water to oil	60–340
Liquids in coils immersed in liquids	110–2,000
Feedwater heaters	110–8,500
Air condensers	350–780
Steam-jacketed, agitated vessels	500–1,900
Shell-and-tube ammonia condensers	800–1,400
Steam condensers with 25°C water	1,500–5,000
Heat pipes	
• Cryogenic	$< 1,000$
• Water	3,000
• Liquid metal	50,000
Condensing steam to high-pressure boiling water	$\mathcal{O}(7,000)$

† Main heat loss is by infiltration.

In fact:

- For a high U, *all* resistances in the exchanger must be low.
- The highly conducting liquids, such as water and liquid metals, give high values of $\overline{h}$ and U.

Fouling resistance

Figure 2.20 shows one of the simplest forms of a heat exchanger—a pipe. The inside is new and clean on the left, but on the right it has built up a

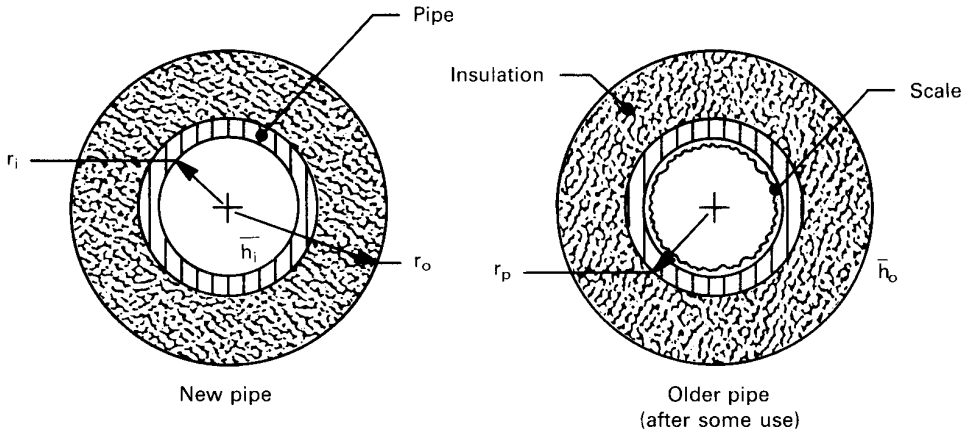

Figure 2.20 The fouling of a pipe.

layer of scale. In conventional freshwater preheaters, for example, this scale is typically $MgSO_4$ (magnesium sulfate) or $CaSO_4$ (calcium sulfate) which precipitates onto the pipe wall after a time. To account for the resistance offered by these buildups, we must include an additional, highly empirical resistance when we calculate U. Thus, for the pipe shown in Fig. 2.20,

$$U\Big|_{\substack{\text{older pipe}\\ \text{based on } r_i}} = \frac{1}{\dfrac{1}{h_i} + \dfrac{r_i \ln(r_o/r_p)}{k_{\text{insul}}} + \dfrac{r_i \ln(r_p/r_i)}{k_{\text{pipe}}} + \dfrac{r_i}{r_o h_o} + R_f}$$

And clearly

$$\boxed{R_f \equiv \frac{1}{U_{\text{old}}} - \frac{1}{U_{\text{new}}}} \tag{2.32}$$

Some typical values of R_f are given in Table 2.3. These values have been adapted from [2.5] and [2.6]. Notice that fouling has the effect of adding resistance on the order of 10^{-4} m^2·K/W in series. It is rather like another heat transfer coefficient, $\bar{h}_f$, on the order of 10,000 in series with the other resistances in the exchanger.

The tabulated values of R_f are given to only one significant figure because they are very approximate. Clearly, exact values would have to be referred to specific heat exchanger materials, to fluid velocities, to

Table 2.3 Some typical fouling resistances

Fluid and Situation	*Fouling Resistance* R_f ($m^2 \cdot °C/W$)
Distilled water	0.0001
Seawater	0.0001 – 0.0002
Treated boiler feedwater	0.0001 – 0.0002
Clean river or lake water	0.0002 – 0.0006
About the worst waters used in heat exchangers	< 0.0020
Fuel oil	0.0001
Transformer or lubricating oil	0.0002
Most industrial liquids	0.0002
Most refinery liquids	0.0002 – 0.0008
Non-oil-bearing steam	0.0001
Oil-bearing steam (e.g., turbine exhaust)	0.0005
Most stable gases	0.0005
Fuel gases	0.0020
Engine exhaust gases	0.0020

operating temperatures, and to age. The resistance generally drops with increased velocity and increases with temperature and age. The values given in the table are based on reasonable maintenance and the use of conventional heat exchangers. With misuse, a given heat exchanger can yield much higher values of R_f.

Notice too, that if $U \lesssim 1{,}000$ W/m^{2}K, fouling will be unimportant, because it will introduce small resistances in series. Thus in a water-to-water heat exchanger, in which U is on the order of 2000 W/m^{2}K, fouling might be important; but in a finned-tube heat exchanger with hot gas in the tubes and cold gas passing across them, U might be around 200 W/m^{2}K, and fouling should be insignificant.

Example 2.10

You have unpainted aluminum siding on your house and the engineer has based a heat loss calculation on $U = 5$ W/m^{2}K. You discover that

air pollution levels are such that R_t is 0.0005 m^2·K/W on the siding. Should the engineer redesign the siding?

SOLUTION. From eqn. (2.32) we get

$$\frac{1}{U_{\text{corrected}}} = \frac{1}{U_{\text{uncorrected}}} + R_f = 0.2000 + 0.0005$$

Therefore, fouling is irrelevant to the calculation of domestic heat loads. ■

Example 2.11

Since the engineer did not fail you in this calculation, you entrust him with the installation of a heat exchanger at your plant. He installs a water-cooled steam condenser with $U = 4000$ W/m^{2}K. You discover that he used water-side fouling resistance for distilled water but that the water flowing in the tubes is not clear at all. How did he do this time?

SOLUTION. Equation (2.32) and Table 2.3 give

$$\begin{aligned}\frac{1}{U_{\text{corrected}}} &= \frac{1}{4000} + (0.0006 \text{ to } 0.0020) \\ &= 0.00085 \text{ to } 0.00225 \text{ m}^2\text{·K/W}\end{aligned}$$

Thus, U is reduced from 4,000 to between 444 and 1,176 W/m^{2}K. Fouling is crucial in this case, and the engineer was in serious error. ■

2.5 Summary

Four things have been done in this chapter:

- The heat diffusion equation has been established. A method has been established for solving it in simple problems, and some important results have been presented. (We say much more about solving the heat diffusion equation in Part II of this book.)
- We have explored the electric analogy to steady heat flow, paying special attention to the concept of thermal resistance. We exploited the analogy to solve heat transfer problems in the same way we solve electrical circuit problems.

- The overall heat transfer coefficient has been defined, and we have seen how to build it up out of component resistances.
- Some practical problems encountered in the evaluation of overall heat transfer coefficients have been discussed.

Three very important things have *not* been considered in Chapter 2:

- In all evaluations of U that involve values of $\overline{h}$, we have taken these values as given information. In any real situation, we must determine correct values of $\overline{h}$ for the specific situation. Part III deals with such determinations.
- When fluids flow through heat exchangers, they give up or gain energy. Thus, the driving temperature difference varies through the exchanger. (Problem 2.14 asks you to consider this difficulty in its simplest form.) Accordingly, the design of an exchanger is complicated. We deal with this problem in Chapter 3.
- The heat transfer coefficients themselves vary with position inside many types of heat exchangers, causing U to be position-dependent.

Problems

2.1 Prove that if k varies linearly with T in a slab, and if heat transfer is one-dimensional and steady, then q may be evaluated precisely using k evaluated at the mean temperature in the slab.

2.2 Invent a numerical method for calculating the steady heat flux through a plane wall when $k(T)$ is an arbitrary function. Use the method to predict q in an iron slab 1 cm thick if the temperature varies from $-100°C$ on the left to $400°C$ on the right. How far would you have erred if you had taken $k_{\text{average}} = (k_{\text{left}} + k_{\text{right}})/2$?

2.3 The steady heat flux at one side of a slab is a known value q_o. The thermal conductivity varies with temperature in the slab, and the variation can be expressed with a power series as

$$k = \sum_{i=0}^{i=n} A_i T^i$$

(a) Start with eqn. (2.10) and derive an equation that relates T to position in the slab, x. (b) Calculate the heat flux at any position in the wall from this expression using Fourier's law. Is the resulting q a function of x?

2.4 Combine Fick's law with the principle of conservation of mass (of the dilute species) in such a way as to eliminate j_1, and obtain a second-order differential equation in m_1. Discuss the importance and the use of the result.

2.5 Solve for the temperature distribution in a thick-walled pipe if the bulk interior temperature and the exterior air temperature, T_{∞_i}, and T_{∞_o}, are known. The interior and the exterior heat transfer coefficients are $\overline{h}_i$ and $\overline{h}_o$, respectively. Follow the method in Example 2.1 and put your result in the dimensionless form:

$$\frac{T - T_{\infty_i}}{T_{\infty_i} - T_{\infty_o}} = \text{fn}\,(\text{Bi}_i, \text{Bi}_o, r/r_i, r_o/r_i)$$

2.6 Put the boundary conditions from Problem 2.5 into dimensionless form so that the Biot numbers appear in them. Let the Biot numbers approach infinity. This should get you back to the boundary conditions for Example 2.5. Therefore, the solution that you obtain in Problem 2.5 should reduce to the solution of Example 2.5 when the Biot numbers approach infinity. Show that this is the case.

2.7 Write an accurate explanation of the idea of *critical radius of insulation* that your kid brother or sister, who is still in grade school, could understand. (If you do not have an available kid, borrow one to see if your explanation really works.)

2.8 The slab shown in Fig. 2.21 is embedded on five sides in insulating materials. The sixth side is exposed to an ambient temperature through a heat transfer coefficient. Heat is generated in the slab at the rate of 1.0 kW/m^3 The thermal conductivity of the slab is 0.2 W/m·K. (a) Solve for the temperature distribution in the slab, noting any assumptions you must make. Be careful to clearly identify the boundary conditions. (b) Evaluate T at the front and back faces of the slab. (c) Show that your solution gives the expected heat fluxes at the back and front faces.

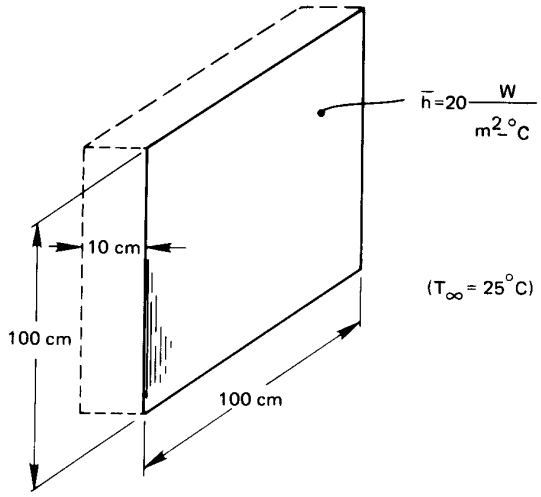

Figure 2.21 Configuration for Problem 2.8.

2.9 Consider the composite wall shown in Fig. 2.22. The concrete and brick sections are of equal thickness. Determine T_1, T_2, q, and the percentage of q that flows through the brick. To do this, approximate the heat flow as one-dimensional. Draw the thermal circuit for the wall and identify all four resistances before you begin.

2.10 Compute Q and U for Example 2.9 if the wall is 0.3 m thick. Five (each) pine and sawdust layers are 5 and 8 cm thick, respectively; and the heat transfer coefficients are 10 on the left and 18 on the right. $T_{\infty_1} = 30°C$ and $T_{\infty_r} = 10°C$.

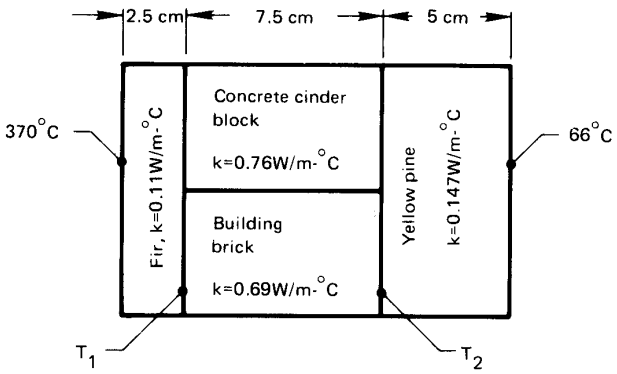

Figure 2.22 Configuration for Problem 2.9.

2.11 Compute U for the slab in Example 1.2.

2.12 Consider the tea kettle in Example 2.8. Suppose that the kettle holds 1 kg of water (about 1 liter) and that the flame impinges on 0.02 m^2 of the bottom. (a) Find out how fast the water temperature is increasing when it reaches its boiling point, and calculate the temperature of the bottom of the kettle immediately below the water if the gases from the flame are at 500°C when they touch the bottom of the kettle. (b) There is an old parlor trick in which one puts a *paper* cup of water over an open flame and boils the water without burning the paper (see Experiment 2.1). Explain this *using an electrical analogy*. [(a): $dT/dt = 0.37$°C/s.]

2.13 Copper plates 2 mm and 3 mm in thickness are processed rather lightly together. Non-oil-bearing steam condenses under pressure at $T_{sat} = 200$°C on one side ($\overline{h} = 12,000$ W/m^2K) and methanol boils under pressure at 130°Con the other ($\overline{h} =$ 9000 W/m^2K). Estimate U and q initially and after extended service. List the relevant thermal resistances in order of decreasing importance and suggest whether or not any of them can be ignored.

2.14 0.5 kg/s of air at 20°C moves along a channel that is 1 m from wall to wall. One wall of the channel is a heat exchange surface ($U = 300$ W/m^2K) with steam condensing at 120°C on its back. Determine (a) q at the entrance; (b) the rate of increase of temperature of the fluid with x at the entrance; (c) the temperature and heat flux 2 m downstream. [(c): $T_{2m} = 89.7$°C.]

2.15 An isothermal sphere 3 cm in diameter is kept at 80°C in a large clay region. The temperature of the clay far from the sphere is kept at 10°C. How much heat must be supplied to the sphere to maintain its temperature if $k_{clay} = 1.28$ W/m·K? (*Hint:* You must solve the boundary value problem not in the sphere but in the clay surrounding it.) [$Q = 16.9$ W.]

2.16 Is it possible to increase the heat transfer from a convectively cooled isothermal sphere by adding insulation? Explain fully.

2.17 A wall consists of layers of metals and plastic with heat transfer coefficients on either side. U is 255 W/m^2K and the overall

temperature difference is 200°C. One layer in the wall is stainless steel (k = 18 W/m·K) 3 mm thick. What is ΔT across the stainless steel?

2.18 A 1% carbon-steel sphere 20 cm in diameter is kept at 250°C on the outside. It has an 8 cm diameter cavity containing boiling water ($\overline{h}_{\text{inside}}$ is very high) which is vented to the atmosphere. What is Q through the shell?

2.19 A slab is insulated on one side and exposed to a surrounding temperature, T_∞, through a heat transfer coefficient on the other. There is nonuniform heat generation in the slab such that $\dot{q}$ =[A (W/m^4)][x (m)], where $x = 0$ at the insulated wall and $x = L$ at the cooled wall. Derive the temperature distribution in the slab.

2.20 800 W/m^3 of heat is generated within a 10 cm diameter nickel-steel sphere for which k = 10 W/m·K. The environment is at 20°C and there is a natural convection heat transfer coefficient of 10 W/m^{2}K around the outside of the sphere. What is its center temperature at the steady state? [21.37°C.]

2.21 An outside pipe is insulated and we measure its temperature with a thermocouple. The pipe serves as an electrical resistance heater, and $\dot{q}$ is known from resistance and current measurements. The inside of the pipe is cooled by the flow of liquid with a known bulk temperature. Evaluate the heat transfer coefficient, $\overline{h}$, in terms of known information. The pipe dimensions and properties are known. [*Hint:* Remember that $\overline{h}$ is not known and we cannot use a boundary condition of the third kind at the inner wall to get $T(r)$.]

2.22 Consider the hot water heater in Problem 1.11. Suppose that it is insulated with 2 cm of a material for which k = 0.12 W/m^{2}K, and suppose that $\overline{h}$ = 16 W/m^{2}K. Find (a) the time constant $\boldsymbol{T}$ for the tank, neglecting the casing and insulation; (b) the initial rate of cooling in °C/h; (c) the time required for the water to cool from its initial temperature of 75°C to 40°C; (d) the percentage of additional heat loss that would result if an outer casing for the insulation were held on by eight steel rods, 1 cm in diameter, between the inner and outer casings.

2.23 A slab of thickness L is subjected to a constant heat flux, q_1, on the left side. The right-hand side if cooled convectively by an environment at T_∞. (a) Develop a dimensionless equation for the temperature of the slab. (b) Present dimensionless equation for the left- and right-hand wall temperatures as well. (c) If the wall is firebrick, 10 cm thick, q_1 is 400 W/m^2, $\overline{h}$ = 20 W/m^{2}K, and T_∞ = 20°C, compute the lefthand and righthand temperatures.

2.24 Heat flows steadily through a stainless steel wall of thickness L_{ss} = 0.06 m, with a variable thermal conductivity of k_{ss} = 1.67 + 0.0143 T(°C). It is partially insulated on the right side with glass wool of thickness L_{gw} = 0.1 m, with a thermal conductivity of k_{gw} = 0.04. The temperature on the left-hand side of the stainless stell is 400°Cand on the right-hand side if the glass wool is 100°C. Evaluate q and T_i.

2.25 Rework Problem 1.29 with a heat transfer coefficient, $\overline{h}_o$ = 40 W/m^{2}K on the outside (i.e., on the cold side).

2.26 A scientist proposes an experiment for the space shuttle in which he provides underwater illumination in a large tank of water at 20°C, using a 3 cm diameter spherical light bulb. What is the maximum wattage of the bulb in zero gravity that will not boil the water?

2.27 A cylindrical shell is made of two layers– an inner one with inner radius = r_i and outer radius = r_c and an outer one with inner radius = r_c and outer radius = r_o. There is a contact resistance, h_c, between the shells. The materials are different, and $T_1(r = r_i) = T_i$ and $T_2(r = r_o) = T_o$. Derive an expression for the inner temperature of the outer shell (T_{2_c}).

2.28 A 1 kW commercial electric heating rod, 8 mm in diameter and 0.3 m long, is to be used in a highly corrosive gaseous environment. Therefore, it has to be provided with a cylindrical sheath of fireclay. The gas flows by at 120°C, and $\overline{h}$ is 230 W/m^{2}K outside the sheath. The surface of the heating rod cannot exceed 800°C. Set the maximum sheath thickness and the outer temperature of the fireclay. [*Hint:* use heat flux and temperature boundary conditions to get the temperature distribution. Then

use the additional convective boundary condition to obtain the sheath thickness.]

2.29 A very small diameter, electrically insulated heating wire runs down the center of a 7.5 mm diameter rod of type 304 stainless steel. The outside is cooled by natural convection ($\overline{h}$ = 6.7 W/m^{2}K) in room air at 22°C. If the wire releases 12 W/m, plot T_{rod} vs. radial position in the rod and give the outside temperature of the rod. (Stop and consider carefully the boundary conditions for this problem.)

2.30 A contact resistance experiment involves pressing two slabs of different materials together, putting a known heat flux through them, and measuring the outside temperatures of each slab. Write the general expression for h_c in terms of known quantities. Then calculate h_c if the slabs are 2 cm thick copper and 1.5 cm thick aluminum, if q is 30,000 W/m^2, and if the two temperatures are 15°C and 22.1°C.

2.31 A student working heat transfer problems late at night needs a cup of hot cocoa to stay awake. She puts milk in a pan on an electric stove and seeks to heat it as rapidly as she can, without burning the milk, by turning the stove on high and stirring the milk continuously. Explain how this works using an analogous electric circuit. Is it possible to bring the entire bulk of the milk up to the burn temperature without burning part of it?

2.32 A small, spherical hot air balloon, 10 m in diameter, weighs 130 kg with a small gondola and one passenger. How much fuel must be consumed (in kJ/h) if it is to hover at low altitude in still 27°C air? ($\overline{h}_{\text{outside}}$ = 215 W/m^{2}K, as the result of natural convection.)

2.33 A slab of mild steel, 4 cm thick, is held at 1,000°C on the back side. The front side is approximately black and radiates to black surroundings at 100°C. What is the temperature of the front side?

2.34 With reference to Fig. 2.3, develop an empirical equation for $k(T)$ for ammonia vapor. Then imagine a hot surface at T_w parallel with a cool horizontal surface at a distance H below it.

Develop equations for $T(x)$ and q. Compute q if $T_w = 350°C$, $T_{cool} = -5°C$, and $H = 0.15$ m.

2.35 A type 316 stainless steel pipe has a 6 cm inside diameter and an 8 cm outside diameter with a 2 mm layer of 85% magnesia insulation around it. Liquid at 112°C flows inside, so $\overline{h}_i = 346$ W/m^{2}K. The air around the pipe is at 20°C, and $\overline{h}_0 = 6$ W/m^{2}K. Calculate U based on the inside area. Sketch the equivalent electrical circuit, showing all known temperatures. Discuss the results.

2.36 Two highly reflecting, horizontal plates are spaced 0.0005 m apart. The upper one is kept at 1000°C and the lower one at 200°C. There is air in between. Neglect radiation and compute the heat flux and the midpoint temperature in the air. Use a power-law fit of the form $k = a(T°C)^b$ to represent the air data in Table A.6.

2.37 A 0.1 m thick slab with $k = 3.4$ W/m^{2}K is held at 100°C on the left side. The right side is cooled with air at 20°Cthrough a heat transfer coefficient, and $\overline{h} = (5.1\ \text{W/m}^2(K)^{-5/4})(T_{wall} - T_\infty)^{1/4}$. Find q and T_{wall} on the right.

2.38 Heat is generated at 54,000 W/m^3 in a 0.16 m diameter sphere. The sphere is cooled by natural convection with fluid at 0°C, and $\overline{h} = [2 + 6(T_{wall} - T_\infty)^{1/4}]$W/m^{2}K, $k_{sphere} = 9$ W/m^{2}K. Find the wall temperature and center temperature of the sphere.

2.39 Layers of equal thickness of spruce and pitch pine are laminated to make an insulating material. How should the laminations be oriented in a temperature gradient to achieve the best effect?

2.40 The resistances of a thick cylindrical layer of insulation must be increased. Will Q be lowered more by a small increase of the outside diameter or by the same decrease in the inside diameter?

2.41 You are in charge of energy conservation at your plant. There is a 300 m run of 6 in. O.D. pipe carrying steam at 250°C. The company requires that any insulation must pay for itself in one year. The thermal resistances are such that the surface of the

pipe will stay close to 250°C in air at 25°C when $\overline{h} = 10\ \mathrm{W/m^2K}$. Calculate the annual energy savings in kW·h that will result if a 1 in layer of 85% magnesia insulation is added. If energy is worth 6 cents per kW·h and insulation costs $75 per installed linear meter, will the insulation pay for itself in one year?

References

[2.1] W. M. Rohsenow and J. P. Hartnett, editors. *Handbook of Heat Transfer*. McGraw-Hill Book Company, New York, 1973.

[2.2] R. F. Wheeler. Thermal conductance of fuel element materials. US-AEC Rep. HW-60343, April 1959.

[2.3] C. Strock, editor. *Handbook of Air Conditioning, Heating and Ventilating*. The Industrial Press, New York, 1959.

[2.4] R. H. Perry, editor. *Chemical Engineer's Handbook*. McGraw-Hill Book Company, New York, 2nd edition, 1941.

[2.5] R.K. Shah and D.P. Sekulic. Heat exchangers. In W. M. Rohsenow, J. P. Hartnett, and Y. I. Cho, editors, *Handbook of Heat Transfer*, chapter 17. McGraw-Hill, New York, 3rd edition, 1998.

[2.6] Tubular Exchanger Manufacturer's Association. *Standards of Tubular Exchanger Manufacturer's Association*. New York, 4th and 6th edition, 1959 and 1978.

Most of the ideas in Chapter 2 are also dealt with at various levels in the general references following Chapter 1.

3. Heat exchanger design

The great object to be effected in the boilers of these engines is, to keep a small quantity of water at an excessive temperature, by means of a small amount of fuel kept in the most active state of combustion...No contrivance can be less adapted for the attainment of this end than one or two large tubes traversing the boiler, as in the earliest locomotive engines.
The Steam Engine Familiarly Explained and Illustrated,
Dionysus Lardner, 1836

3.1 Function and configuration of heat exchangers

The archetypical problem that any heat exchanger solves is that of getting energy from one fluid mass to another, as we see in Fig. 3.1. A simple or composite wall of some kind divides the two flows and provides an element of thermal resistance between them. There is an exception to this configuration in the direct-contact form of heat exchanger. Figure 3.2 shows one such arrangement in which steam is bubbled into water. The steam condenses and the water is heated at the same time. In other arrangements, immiscible fluids might contact each other or noncondensible gases might be bubbled through liquids.

This discussion will be restricted to heat exchangers with a dividing wall between the two fluids. There is an enormous variety of such configurations, but most commercial exchangers reduce to one of three basic types. Figure 3.3 shows these types in schematic form. They are:

- *The simple parallel or counterflow configuration.* These arrangements are versatile. Figure 3.4 shows how the counterflow arrangement is bent around in a so-called Heliflow compact heat exchanger configuration.
- *The shell-and-tube configuration.* Figure 3.5 shows the U-tubes of a

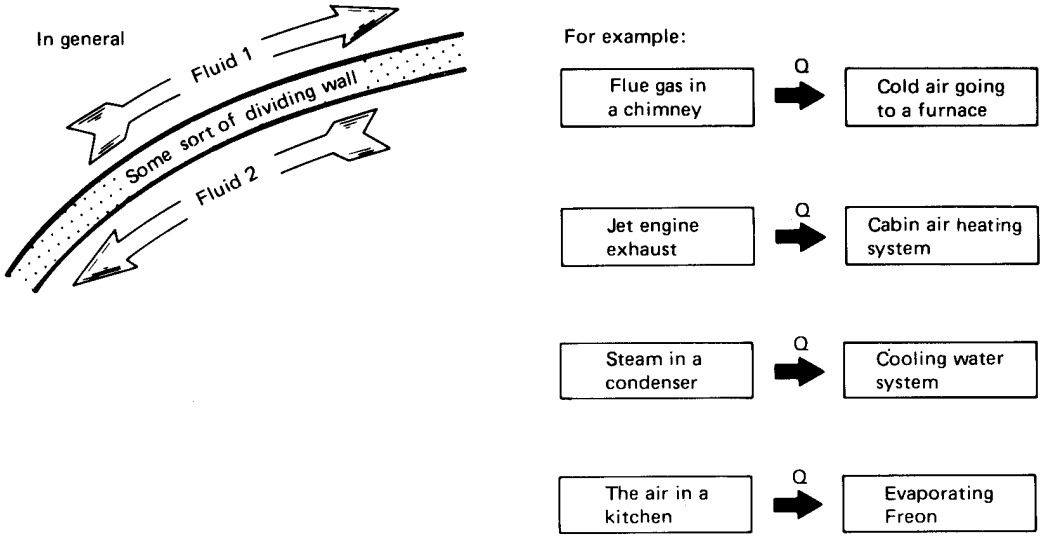

Figure 3.1 Heat exchange.

two-tube-pass, one-shell-pass exchanger being installed in the supporting baffles. The shell is yet to be added. Most of the really large heat exchangers are of the shell-and-tube form.

- *The cross-flow configuration.* Figure 3.6 shows typical cross-flow units. In Fig. 3.6a and c, both flows are *unmixed*. Each flow must stay in a prescribed path through the exchanger and is not allowed to "mix" to the right or left. Figure 3.6b shows a typical plate-fin cross-flow element. Here the flows are also unmixed.

Figure 3.7, taken from the standards of the Tubular Exchanger Manufacturer's Association (TEMA) [3.1], shows four typical single-shell-pass heat exchangers and establishes nomenclature for such units.

These pictures also show some of the complications that arise in translating simple concepts into hardware. Figure 3.7 shows an exchanger with a single tube pass. Although the shell flow is baffled so that it crisscrosses the tubes, it still proceeds from the hot to cold (or cold to hot) end of the shell. Therefore, it is like a simple parallel (or counterflow) unit. The kettle reboiler in Fig. 3.7d involves a divided shell-pass flow configuration over two tube passes (from left to right and back to the "channel header"). In this case, the isothermal shell flow could be flowing in any direction—it makes no difference to the tube flow. Therefore, this

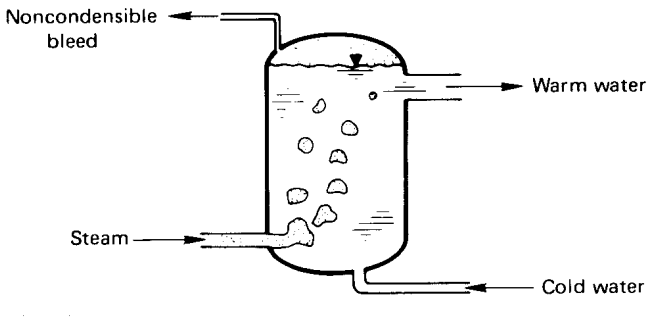

Figure 3.2 A direct-contact heat exchanger.

exchanger is also equivalent to either the simple parallel or counterflow configuration.

Notice that a salient feature of shell-and-tube exchangers is the presence of baffles. Baffles serve to direct the flow normal to the tubes. We find in Part III that heat transfer from a tube to a flowing fluid is usually better when the flow moves across the tube than when the flow moves along the tube. This augmentation of heat transfer gives the complicated shell-and-tube exchanger an advantage over the simpler single-pass parallel and counterflow exchangers.

However, baffles bring with them a variety of problems. The flow patterns are very complicated and almost defy analysis. A good deal of the shell-side fluid might unpredictably leak through the baffle holes in the axial direction, or it might bypass the baffles near the wall. In certain shell-flow configurations, unanticipated vibrational modes of the tubes might be excited. Many of the cross-flow configurations also baffle the fluid so as to move it across a tube bundle. The plate-and-fin configuration (Fig. 3.6b) is such a cross-flow heat exchanger.

In all of these heat exchanger arrangements, it becomes clear that a dramatic investment of human ingenuity is directed towards the task of augmenting the heat transfer from one flow to another. The variations are endless, as you will quickly see if you try Experiment 3.1.

Experiment 3.1

Carry a notebook with you for a day and mark down every heat exchanger you encounter in home, university, or automobile. Classify each

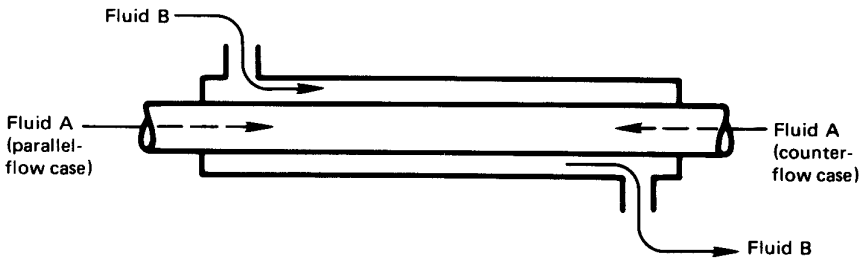

a) Parallel and counterflow heat exchangers

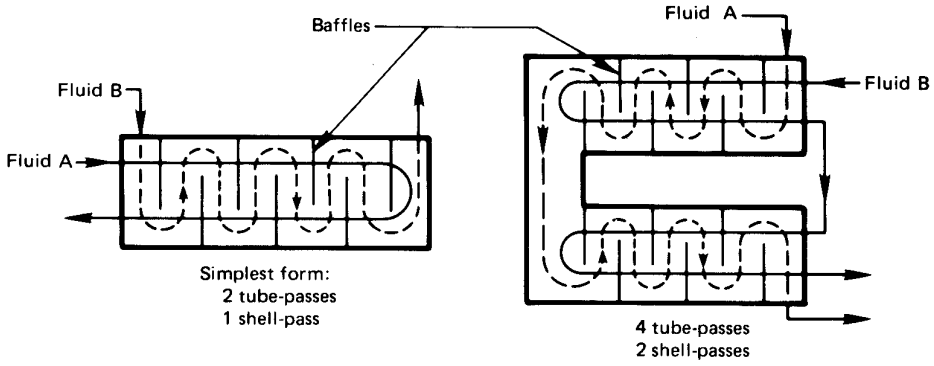

b) Two kinds of shell-and-tube heat exchangers

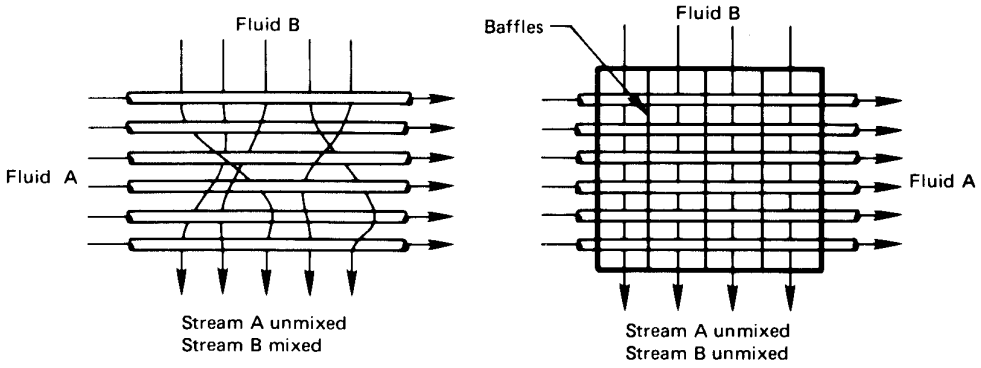

c) Two kinds of cross-flow exchangers

Figure 3.3 The three basic types of heat exchangers.

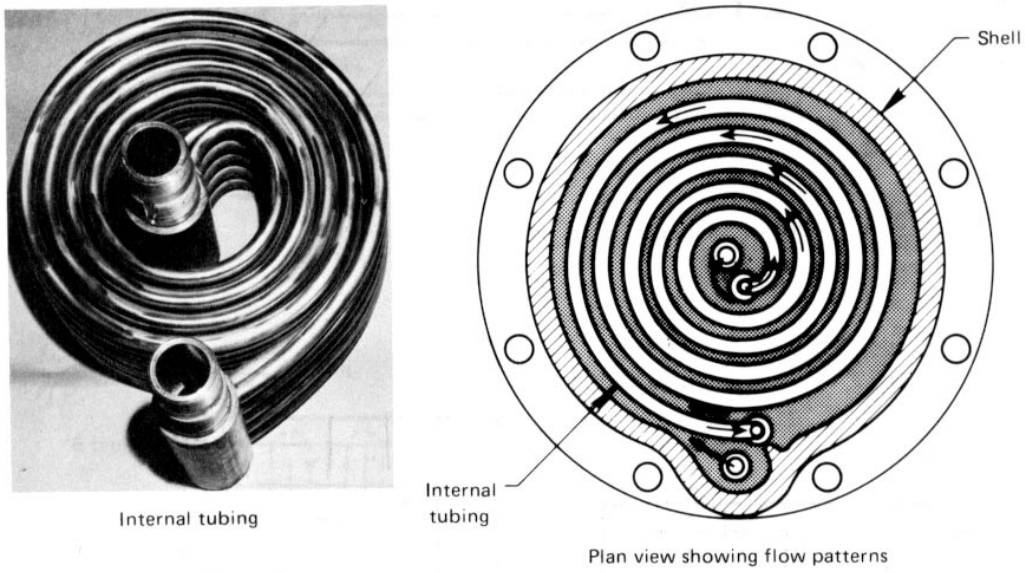

Figure 3.4 Heliflow compact counterflow heat exchanger. (Photograph coutesy of Graham Manufacturing Co., Inc., Batavia, New York.)

according to type and note any special augmentation features.

The analysis of heat exchangers first becomes complicated when we account for the fact that two flow streams change one another's temperature. It is to the problem of predicting an appropriate mean temperature difference that we address ourselves in Section 3.2. Section 3.3 then presents a strategy to use when this mean cannot be determined initially.

3.2 Evaluation of the mean temperature difference in a heat exchanger

Logarithmic mean temperature difference (LMTD)

To begin with, we take U to be a constant value. This is fairly reasonable in compact single-phase heat exchangers. In larger exchangers, particularly in shell-and-tube configurations and large condensers, U is apt to vary with position in the exchanger and/or with local temperature. But

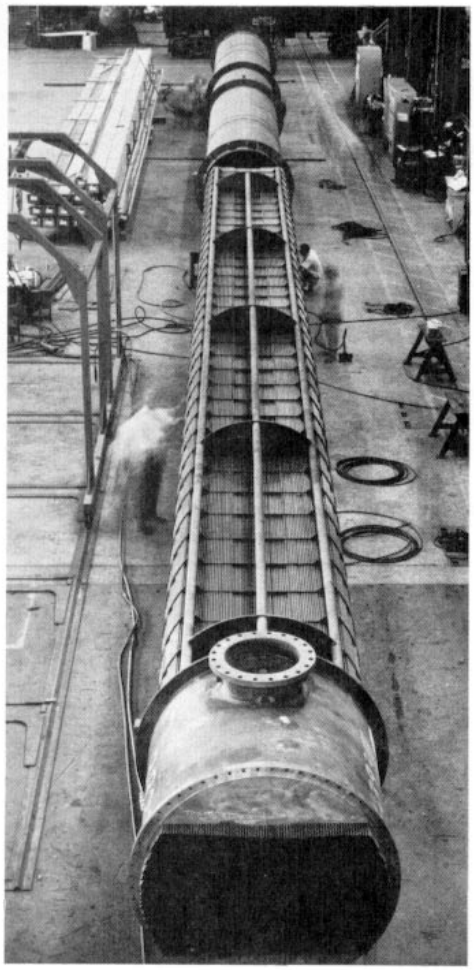

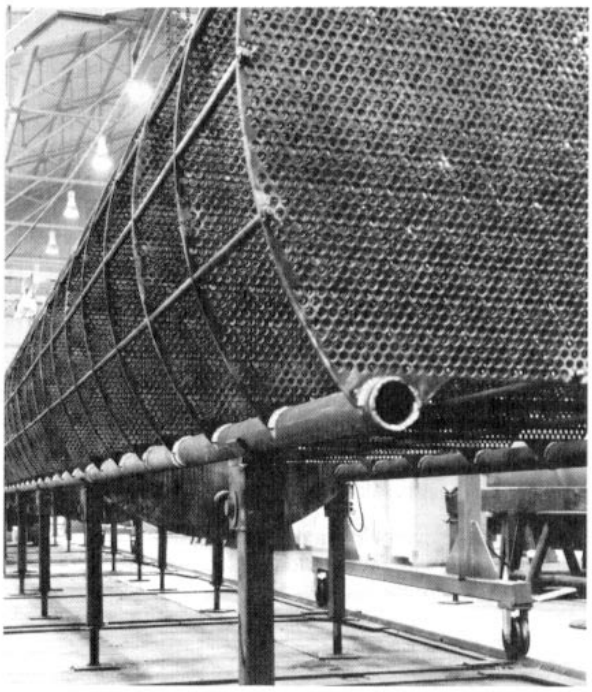

Above and left: A very large feed-water preheater. Tubes are shown withdrawn from the shell on the left. Inset above shows baffles before tubes are inserted. (Photos courtesy of Southwest Engineering Co., Subsidiary of Cronus Industries, Inc., Los Angeles, Calif.)

Below: Small "Swinglok" exchanger with tube-bundle removed from shell. (Photo courtesy of Graham Manufacturing Co. Inc., Batavia, New York.)

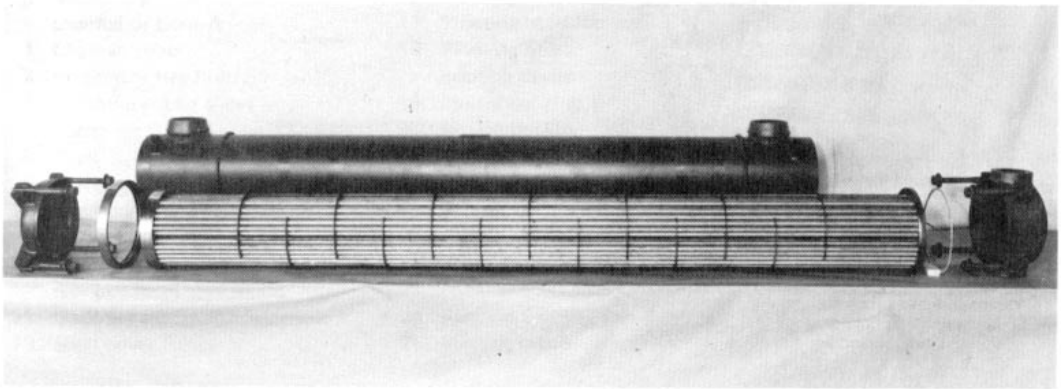

Figure 3.5 Typical commercial one-shell-pass, two-tube-pass heat exchangers.

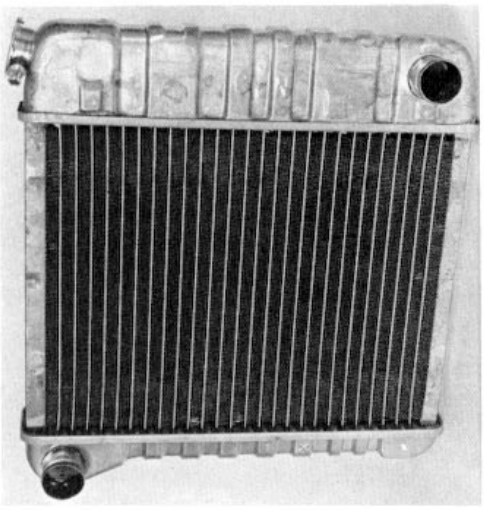

a) A 1980 Chevette radiator. Cross-flow exchanger with neither flow mixed. Vertical tubes cannot be seen.

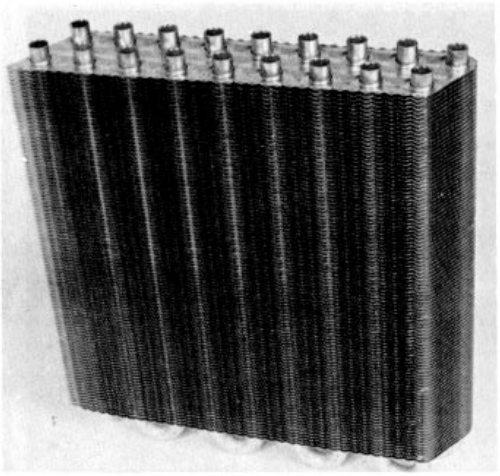

b) A section of an automotive air conditioning condenser. The flow through the horizontal wavy fins is allowed to mix with itself while the two-pass flow through the U-tubes remains unmixed

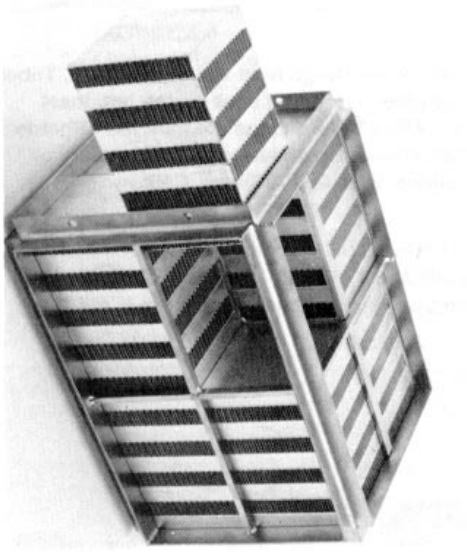

c) The basic 1 ft. × 1 ft. × 2 ft. module for a waste heat recuperator. It is a plate-fin, gas-to-air cross-flow heat exchanger with neither flow mixed.

Figure 3.6 Several commercial cross-flow heat exchangers. (Photographs courtesy of Harrison Radiator Division, General Motors Corporation.)

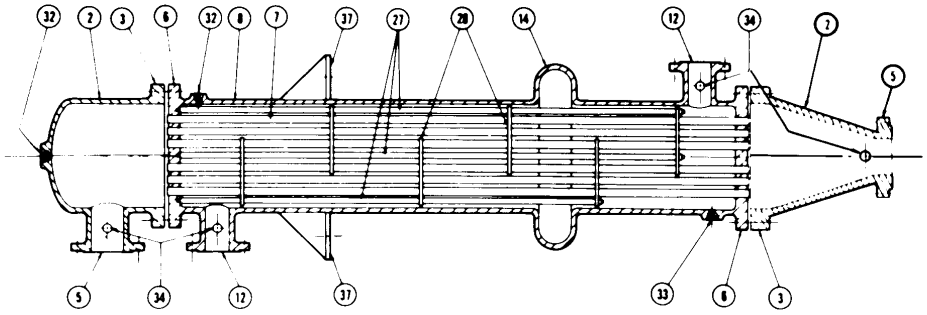

a) Single shell-pass, single tube-pass exchanger

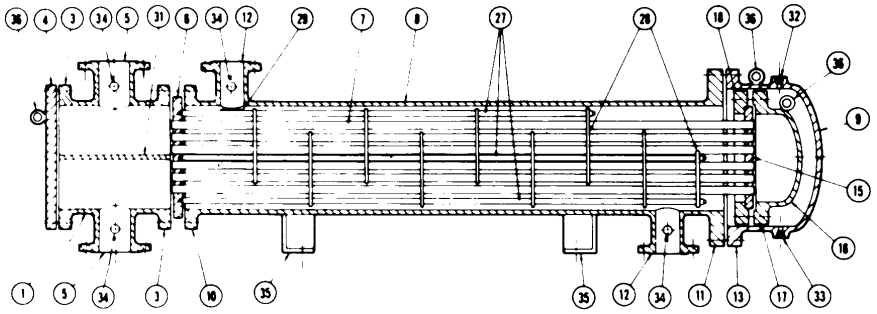

b) One shell-pass, two tube-pass exchanger

1. Stationary head-channel
2. Stationary head-bonnet
3. Stationary head-flange-channel or bonnet
4. Channel cover
5. Stationary head nozzle
6. Stationary tube sheet
7. Tubes
8. Shell
9. Shell cover
10. Shell flange-stationary head end
11. Shell flange-rear head end
12. Shell nozzle
13. Shell cover flange
14. Expansion joint
15. Floating tube sheet
16. Floating head cover
17. Floating head flange
18. Floating head backing device
19. Split shear ring
20. Slip-on backing flange
21. Floating head cover-external
22. Floating tube sheet skirt
23. Packing box
24. Packing
25. Packing gland
26. Lantern ring
27. Tie rods and spacers
28. Transverse baffles or support plates
29. Impingement plate
30. Longitudinal baffle
31. Pass partition
32. Vent connection
33. Drain connection
34. Instrument connection
35. Support saddle
36. Lifting lug
37. Support bracket
38. Weir
39. Liquid level connection

Figure 3.7 Four typical heat exchanger configurations (continued on next page). (Drawings courtesy of the Tubular Exchanger Manufacturers' Association.)

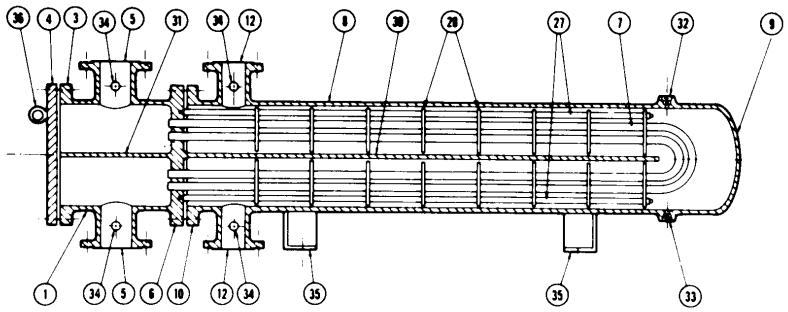

c) Two tube-pass, two shell-pass exchanger

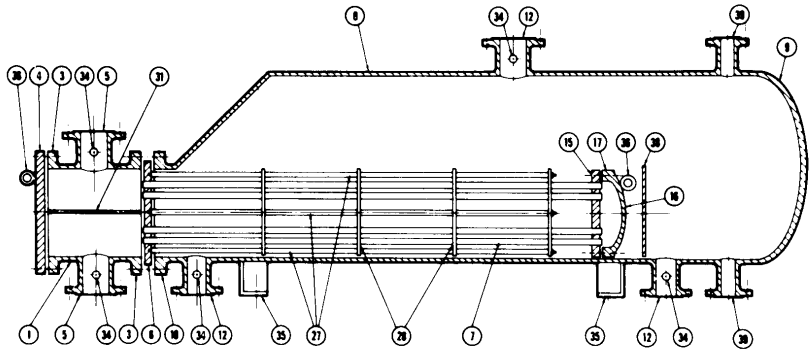

d) One split shell-pass, two tube-pass, kettle type of exchanger

Figure 3.7 Continued

in situations in which U is fairly constant, we can deal with the varying temperatures of the fluid streams by writing the overall heat transfer in terms of a mean temperature difference between the two fluid streams:

$$Q = UA\,\Delta T_{\text{mean}} \tag{3.1}$$

Our problem then reduces to finding the appropriate mean temperature difference that will make this equation true. Let us do this for the simple parallel and counterflow configurations, as sketched in Fig. 3.8.

The temperature of both streams is plotted in Fig. 3.8 for both single-pass arrangements—the parallel and counterflow configurations—as a function of the length of travel (or area passed over). Notice that, in the parallel-flow configuration, temperatures tend to change more rapidly

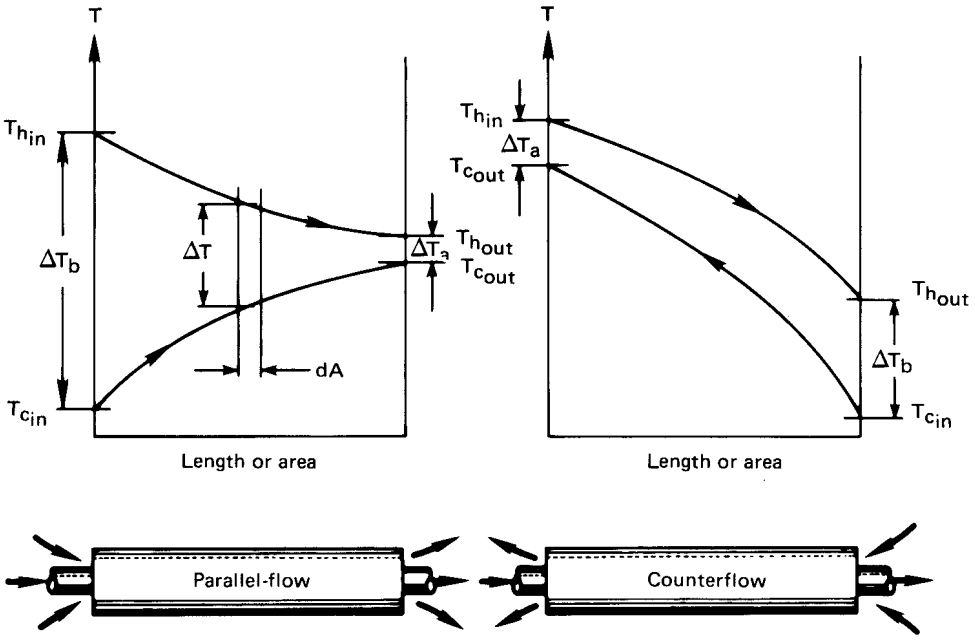

Figure 3.8 The temperature variation through single-pass heat exchangers.

with position and less length is required. But the counterflow arrangement achieves generally more complete heat exchange from one flow to the other.

Figure 3.9 shows another variation on the single-pass configuration. This is a condenser in which one stream flows through with its temperature changing, but the other simply condenses at uniform temperature. This arrangement has some special characteristics, which we point out shortly.

The determination of ΔT_{mean} for such arrangements proceeds as follows: the differential heat transfer within either arrangement (see Fig. 3.8) is

$$dQ = U\Delta T\, dA = -(\dot{m}c_p)_h\, dT_h = \pm(\dot{m}c_p)_c\, dT_c \tag{3.2}$$

where the subscripts h and c denote the hot and cold streams, respectively; the upper and lower signs are for the parallel and counterflow cases, respectively; and dT denotes a change from left to right in the exchanger. We give symbols to the total heat capacities of the hot and

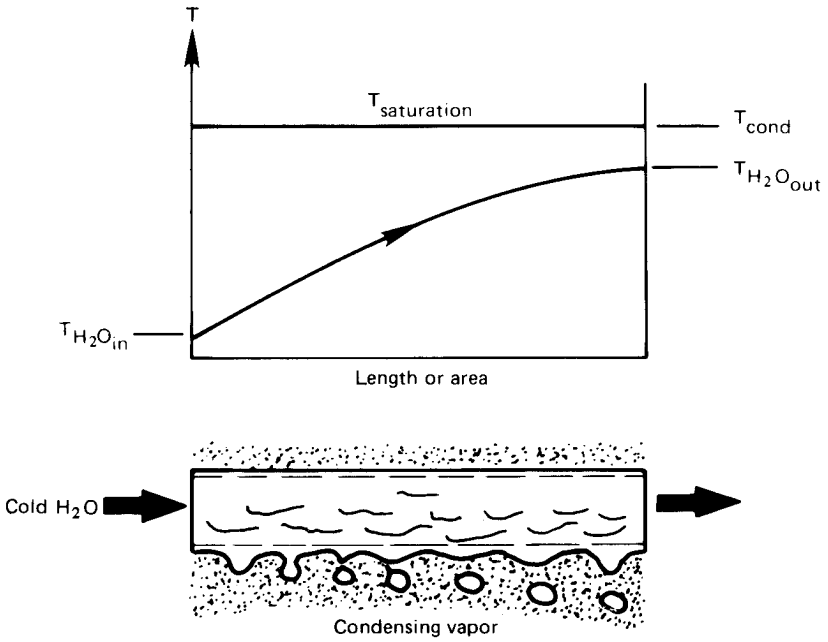

Figure 3.9 The temperature distribution through a condenser.

cold streams:

$$C_h \equiv (\dot{m}c_p)_h \text{ W/K} \qquad \text{and} \qquad C_c \equiv (\dot{m}c_p)_c \text{ W/K} \tag{3.3}$$

Thus, for either heat exchanger, $\mp C_h dT_h = C_c dT_c$. This equation can be integrated from the lefthand side, where $T_h = T_{h_{\text{in}}}$ and $T_c = T_{c_{\text{in}}}$ for parallel flow or $T_h = T_{h_{\text{in}}}$ and $T_c = T_{c_{\text{out}}}$ for counterflow, to some arbitrary point inside the exchanger. The temperatures inside are thus:

$$\begin{aligned} &\text{parallel flow:} \quad T_h = T_{h_{\text{in}}} - \frac{C_c}{C_h}(T_c - T_{c_{\text{in}}}) \quad = T_{h_{\text{in}}} - \frac{Q}{C_h} \\ &\text{counterflow:} \quad T_h = T_{h_{\text{in}}} - \frac{C_c}{C_h}(T_{c_{\text{out}}} - T_c) \quad = T_{h_{\text{in}}} - \frac{Q}{C_h} \end{aligned} \tag{3.4}$$

where Q is the total heat transfer from the entrance to the point of interest. Equations (3.4) can be solved for the local temperature differences:

$$\begin{aligned} \Delta T_{\text{parallel}} &= T_h - T_c = T_{h_{\text{in}}} - \left(1 + \frac{C_c}{C_h}\right) T_c + \frac{C_c}{C_h} T_{c_{\text{in}}} \\ \Delta T_{\text{counter}} &= T_h - T_c = T_{h_{\text{in}}} - \left(1 - \frac{C_c}{C_h}\right) T_c - \frac{C_c}{C_h} T_{c_{\text{out}}} \end{aligned} \tag{3.5}$$

Substitution of these in $dQ = C_c dT_c = U\Delta T\, dA$ yields

$$\left.\frac{U dA}{C_c}\right|_{\text{parallel}} = \frac{dT_c}{\left[-\left(1+\frac{C_c}{C_h}\right)T_c + \frac{C_c}{C_h}T_{c_{\text{in}}} + T_{h_{\text{in}}}\right]}$$
$$\left.\frac{U dA}{C_c}\right|_{\text{counter}} = \frac{dT_c}{\left[-\left(1-\frac{C_c}{C_h}\right)T_c - \frac{C_c}{C_h}T_{c_{\text{out}}} + T_{h_{\text{in}}}\right]} \tag{3.6}$$

Equations (3.6) can be integrated across the exchanger:

$$\int_0^A \frac{U}{C_c} dA = \int_{T_{c\,\text{in}}}^{T_{c\,\text{out}}} \frac{dT_c}{[---]} \tag{3.7}$$

If U and C_c can be treated as constant, this integration gives

$$\text{parallel:}\quad \ln\left[\frac{-\left(1+\frac{C_c}{C_h}\right)T_{c_{\text{out}}} + \frac{C_c}{C_h}T_{c_{\text{in}}} + T_{h_{\text{in}}}}{-\left(1+\frac{C_c}{C_h}\right)T_{c_{\text{in}}} + \frac{C_c}{C_h}T_{c_{\text{in}}} + T_{h_{\text{in}}}}\right] = -\frac{UA}{C_c}\left(1+\frac{C_c}{C_h}\right)$$
$$\text{counter:}\quad \ln\left[\frac{-\left(1-\frac{C_c}{C_h}\right)T_{c_{\text{out}}} - \frac{C_c}{C_h}T_{c_{\text{out}}} + T_{h_{\text{in}}}}{-\left(1-\frac{C_c}{C_h}\right)T_{c_{\text{in}}} - \frac{C_c}{C_h}T_{c_{\text{out}}} + T_{h_{\text{in}}}}\right] = -\frac{UA}{C_c}\left(1-\frac{C_c}{C_h}\right) \tag{3.8}$$

If U were variable, the integration leading from eqn. (3.7) to eqns. (3.8) is where its variability would have to be considered. Any such variability of U can complicate eqns. (3.8) terribly. Presuming that eqns. (3.8) are valid, we can simplify them with the help of the definitions of ΔT_a and ΔT_b, given in Fig. 3.8:

$$\text{parallel:}\quad \ln\left[\frac{(1+C_c/C_h)(T_{c_{\text{in}}} - T_{c_{\text{out}}}) + \Delta T_b}{\Delta T_b}\right] = -UA\left(\frac{1}{C_c}+\frac{1}{C_h}\right)$$
$$\text{counter:}\quad \ln\frac{\Delta T_a}{(-1+C_c/C_h)(T_{c_{\text{in}}} - T_{c_{\text{out}}}) + \Delta T_a} = -UA\left(\frac{1}{C_c}-\frac{1}{C_h}\right) \tag{3.9}$$

Conservation of energy ($Q_c = Q_h$) requires that

$$\boxed{\frac{C_c}{C_h} = -\frac{T_{h_{\text{out}}} - T_{h_{\text{in}}}}{T_{c_{\text{out}}} - T_{c_{\text{in}}}}} \tag{3.10}$$

Then eqn. (3.9) and eqn. (3.10) give

$$\text{parallel:}\quad \ln\left[\frac{\overbrace{(T_{c_{\text{in}}}-T_{c_{\text{out}}})+(T_{h_{\text{out}}}-T_{h_{\text{in}}})}^{\Delta T_a-\Delta T_b}+\Delta T_b}{\Delta T_b}\right] = \ln\left(\frac{\Delta T_a}{\Delta T_b}\right) = -UA\left(\frac{1}{C_c}+\frac{1}{C_h}\right)$$

$$\text{counter:}\quad \ln\left(\frac{\Delta T_a}{\Delta T_b-\Delta T_a+\Delta T_a}\right) = \ln\left(\frac{\Delta T_a}{\Delta T_b}\right) = -UA\left(\frac{1}{C_c}-\frac{1}{C_h}\right) \tag{3.11}$$

Finally, we write $1/C_c = (T_{c_{\text{out}}} - T_{c_{\text{in}}})/Q$ and $1/C_h = (T_{h_{\text{in}}} - T_{h_{\text{out}}})/Q$ on the right-hand side of either of eqns. (3.11) and get for either parallel or counterflow,

$$\boxed{Q = UA\left(\frac{\Delta T_a - \Delta T_b}{\ln(\Delta T_a/\Delta T_b)}\right)} \tag{3.12}$$

The appropriate ΔT_{mean} for use in eqn. (3.11) is thus the *logarithmic mean temperature difference* (LMTD):

$$\boxed{\Delta T_{\text{mean}} = \text{LMTD} \equiv \frac{\Delta T_a - \Delta T_b}{\ln\left(\frac{\Delta T_a}{\Delta T_b}\right)}} \tag{3.13}$$

Example 3.1

The idea of a logarithmic mean difference is not new to us. We have already encountered it in Chapter 2. Suppose that we had asked, "What mean radius of pipe would have allowed us to compute the conduction through the wall of a pipe as though it were a slab of thickness $L = r_o - r_i$?" (see Fig. 3.10). To answer this, we compare

$$Q = kA\frac{\Delta T}{L} = 2\pi kl\Delta T\left(\frac{r_{\text{mean}}}{r_o - r_i}\right)$$

with eqn. (2.21):

$$Q = 2\pi kl\Delta T\,\frac{1}{\ln(r_o/r_i)}$$

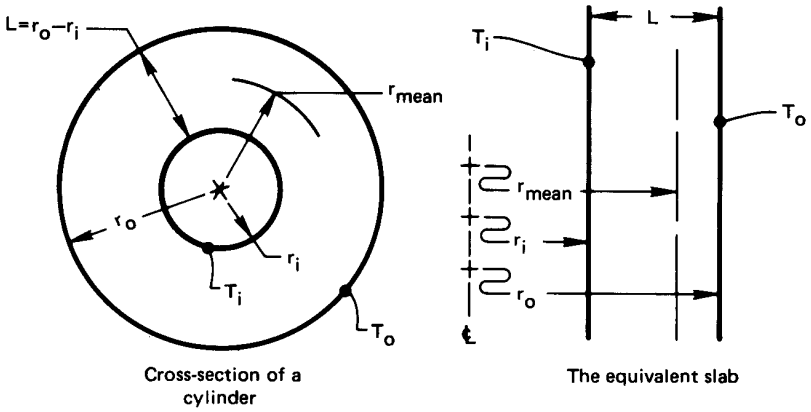

Figure 3.10 Calculation of the mean radius for heat conduction through a pipe.

It follows that

$$r_{\text{mean}} = \frac{r_o - r_i}{\ln(r_o/r_i)} = \text{logarithmic mean radius} \qquad \blacksquare$$

Example 3.2

Suppose that the temperature difference on either end of a heat exchanger, ΔT_a, and ΔT_b, are equal. Clearly, the effective ΔT must equal ΔT_a and ΔT_b in this case. Does the LMTD reduce to this value?

SOLUTION. If we substitute $\Delta T_a = \Delta T_b$ in eqn. (3.13), we get

$$\text{LMTD} = \frac{\Delta T_b - \Delta T_b}{\ln(\Delta T_b/\Delta T_b)} = \frac{0}{0} = \text{indeterminate}$$

Therefore it is necessary to use L'Hospital's rule:

$$\begin{aligned}\lim_{\Delta T_a \to \Delta T_b} \frac{\Delta T_a - \Delta T_b}{\ln(\Delta T_a/\Delta T_b)} &= \frac{\dfrac{\partial}{\partial \Delta T_a}(\Delta T_a - \Delta T_b)\Big|_{\Delta T_a = \Delta T_b}}{\dfrac{\partial}{\partial \Delta T_a}\ln\left(\dfrac{\Delta T_a}{\Delta T_b}\right)\Big|_{\Delta T_a = \Delta T_b}} \\ &= \left(\frac{1}{1/\Delta T_a}\right)\Big|_{\Delta T_a = \Delta T_b} = \Delta T_a = \Delta T_b\end{aligned}$$

It follows that the LMTD reduces to the intuitively obvious result in the limit. ■

Example 3.3

Water enters the tubes of a small single-pass heat exchanger at 20°C and leaves at 40°C. On the shell side, 25 kg/min of steam condenses at 60°C. Calculate the overall heat transfer coefficient and the required flow rate of water if the area of the exchanger is 12 m^2. (The latent heat, h_{fg}, is 2358.7 kJ/kg at 60°C.)

SOLUTION.

$$Q = \dot{m}_{\text{condensate}} \cdot h_{fg}\Big|_{60^\circ\text{C}} = \frac{25(2358.7)}{60} = 983 \text{ kJ/s}$$

and with reference to Fig. 3.9, we can calculate the LMTD without naming the exchanger "parallel" or "counterflow", since the condensate temperature is constant.

$$\text{LMTD} = \frac{(60-20)-(60-40)}{\ln\left(\dfrac{60-20}{60-40}\right)} = 28.85 \text{ K}$$

Then

$$U = \frac{Q}{A(\text{LMTD})} = \frac{983(1000)}{12(28.85)} = 2839 \text{ W/m}^2\text{K}$$

and

$$\dot{m}_{H_2O} = \frac{Q}{c_p \Delta T} = \frac{983,000}{4174(20)} = 11.78 \text{ kg/s}$$ ■

Extended use of the LMTD

Limitations. There are two basic limitations on the use of an LMTD. The first is that it is restricted to the single-pass parallel and counterflow configurations. This restriction can be overcome by adjusting the LMTD for other configurations—a matter that we take up in the following subsection.

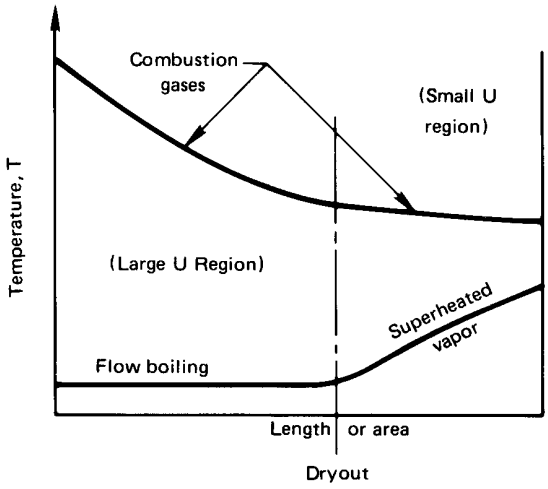

Figure 3.11 A typical case of a heat exchanger in which U varies dramatically.

The second limitation—our use of a constant value of U— is more serious. The value of U must be negligibly dependent on T to complete the integration of eqn. (3.7). Even if $U \neq \text{fn}(T)$, the changing flow configuration and the variation of temperature can still give rise to serious variations of U within a given heat exchanger. Figure 3.11 shows a typical situation in which the variation of U within a heat exchanger might be great. In this case, the mechanism of heat exchange on the water side is completely altered when the liquid is finally boiled away. If U were uniform in each portion of the heat exchanger, then we could treat it as two different exchangers in series.

However, the more common difficulty that we face is that of designing heat exchangers in which U varies continuously with position within it. This problem is most severe in large industrial shell-and-tube configurations[1] (see, e.g., Fig. 3.5 or Fig. 3.12) and less serious in compact heat exchangers with less surface area. If U depends on the location, analyses such as we have just completed [eqn. (3.1) to eqn. (3.13)] must be done using an average U defined as $\int_0^A U dA/A$.

[1]Actual heat exchangers can have areas well in excess of 10,000 m^2. Large power plant condensers and other large exchangers are often remarkably big pieces of equipment.

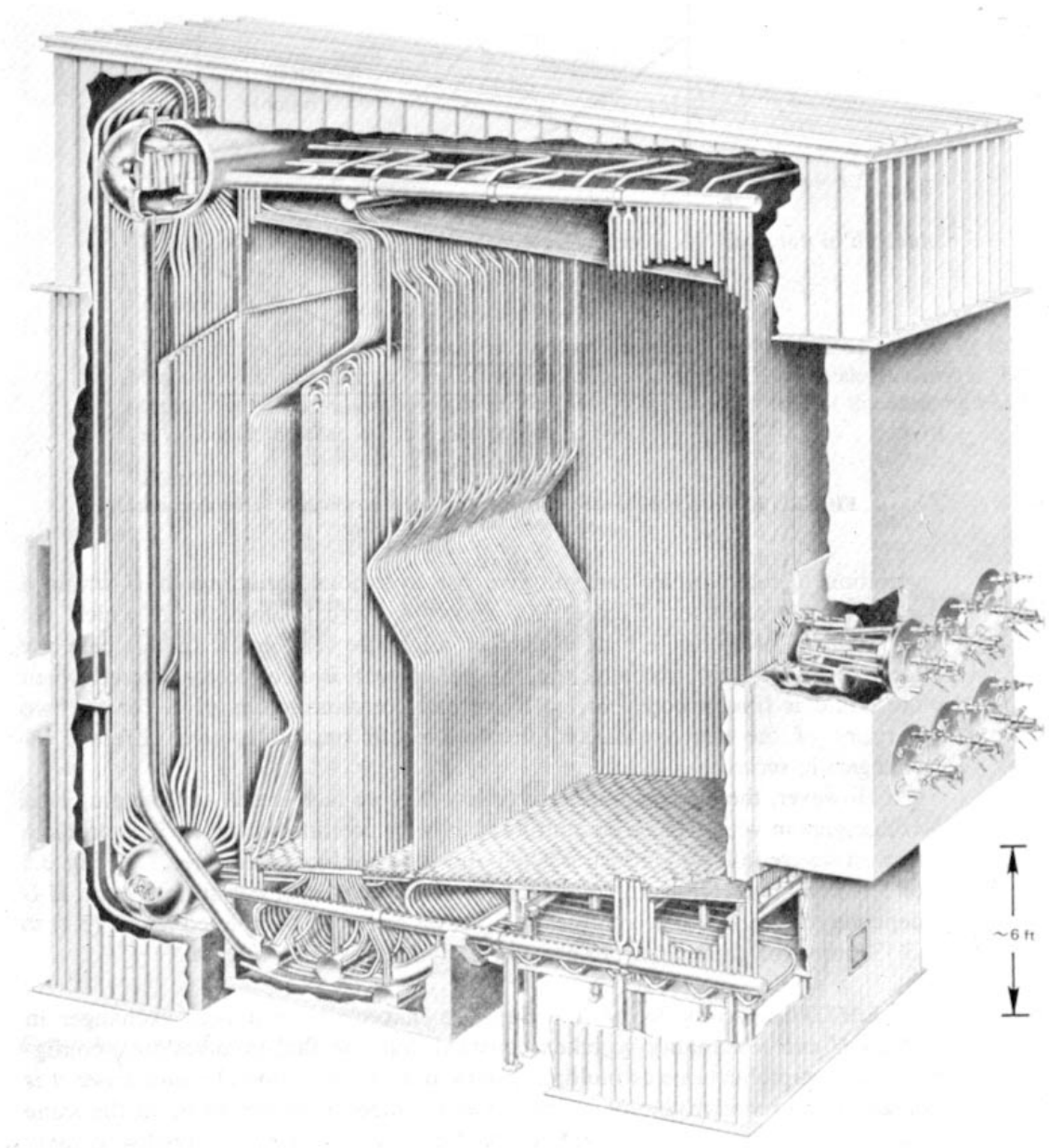

Figure 3.12 The heat exchange surface for a steam generator. This PFT-type integral-furnace boiler, with a surface area of 4560 m^2, is not particularly large. About 88% of the area is in the furnace tubing and 12% is in the boiler (Photograph courtesy of Babcock and Wilcox Co.)

LMTD correction factor, *F*. Suppose that we have a heat exchanger in which U can reasonably be taken constant, but one that involves such configurational complications as multiple passes and/or cross-flow. In such cases it is necessary to rederive the appropriate mean temperature difference in the same way as we derived the LMTD. Each configuration must be analyzed separately and the results are generally more complicated than eqn. (3.13).

This task was undertaken on an *ad hoc* basis during the early twentieth century. In 1940, Bowman, Mueller and Nagle [3.2] organized such calculations for the common range of heat exchanger configurations. In each case they wrote

$$Q = UA(\text{LMTD}) \cdot F\left(\underbrace{\frac{T_{t_{\text{out}}} - T_{t_{\text{in}}}}{T_{s_{\text{in}}} - T_{t_{\text{in}}}}}_{P}, \underbrace{\frac{T_{s_{\text{in}}} - T_{s_{\text{out}}}}{T_{t_{\text{out}}} - T_{t_{\text{in}}}}}_{R}\right) \tag{3.14}$$

where T_t and T_s are temperatures of tube and shell flows, respectively. The factor F is an LMTD correction that varies from unity to zero, depending on conditions. The dimensionless groups P and R have the following physical significance:

- P is the relative influence of the overall temperature difference $(T_{s_{\text{in}}} - T_{t_{\text{in}}})$ on the tube flow temperature. It must obviously be less than unity.
- R, according to eqn. (3.10), equals the heat capacity ratio C_t/C_s.
- If one flow remains at constant temperature (as, for example, in Fig. 3.9), then either P or R will equal zero. In this case the simple LMTD will be the correct ΔT_{mean} and F must go to unity.

The factor F is defined in such a way that *the LMTD should always be calculated for the equivalent counterflow single-pass exchanger with the same hot and cold temperatures.* This is explained in Fig. 3.13.

Bowman *et al.* [3.2] summarized all the equations for F, in various configurations, that had been dervied by 1940. They presented them graphically in not-very-accurate figures that have been widely copied. The TEMA [3.1] version of these curves has been recalculated for shell-and-tube heat exchangers, and it is more accurate. We include two of these curves in Fig. 3.14(a) and Fig. 3.14(b). TEMA presents many additional curves for more complex shell-and-tube configurations. Figures 3.14(c) and 3.14(d)

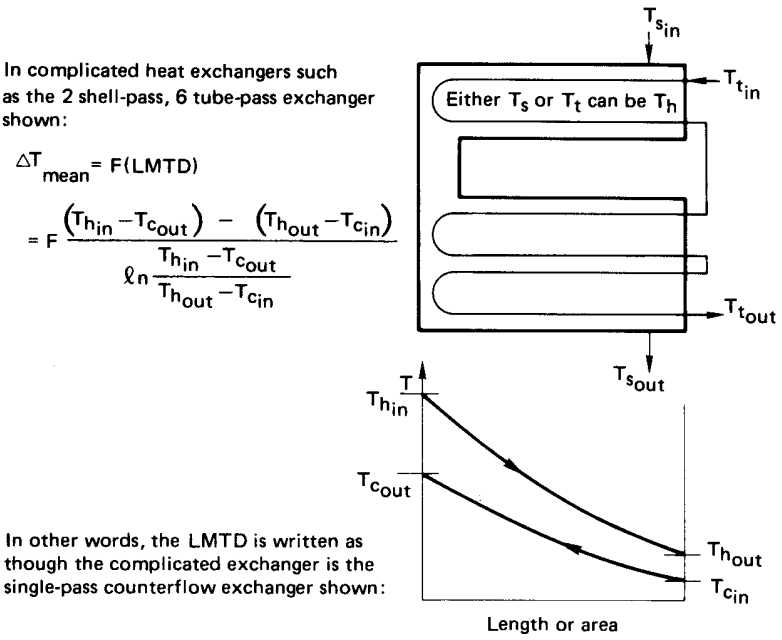
In complicated heat exchangers such as the 2 shell-pass, 6 tube-pass exchanger shown:
$\Delta T_{mean} = F(LMTD)$
$= F \dfrac{(T_{h_{in}} - T_{c_{out}}) - (T_{h_{out}} - T_{c_{in}})}{\ell n \dfrac{T_{h_{in}} - T_{c_{out}}}{T_{h_{out}} - T_{c_{in}}}}$
$T_{s_{in}}$
$T_{t_{in}}$
Either T_s or T_t can be T_h
$T_{t_{out}}$
$T_{s_{out}}$
T
$T_{h_{in}}$
$T_{c_{out}}$
$T_{h_{out}}$
$T_{c_{in}}$
In other words, the LMTD is written as though the complicated exchanger is the single-pass counterflow exchanger shown:
Length or area

Figure 3.13 The basis of the LMTD in a multipass exchanger, prior to correction.

are the Bowman *et al.* curves for the simplest cross-flow configurations. Gardner and Taborek [3.3] redeveloped Fig. 3.14(c) over a different range of parameters. They also showed how Fig. 3.14(a) and Fig. 3.14(b) must be modified if the number of baffles in a tube-in-shell heat exchanger is large enough to make it behave like a series of cross-flow exchangers.

We have simplified Figs. 3.14(a) through 3.14(d) by including curves only for $R \leqslant 1$. Shamsundar [3.4] noted that for $R > 1$, one may obtain F using a simple reciprocal rule. He showed that so long as a heat exchanger has a uniform heat transfer coefficient and the fluid properties are constant,

$$F(P, R) = F(PR, 1/R) \tag{3.15}$$

Thus, if R is greater than unity, one need only evaluate F using PR in place of P and $1/R$ in place of R.

Example 3.4

5.795 kg/s of oil flows through the shell side of a two-shell pass, four-

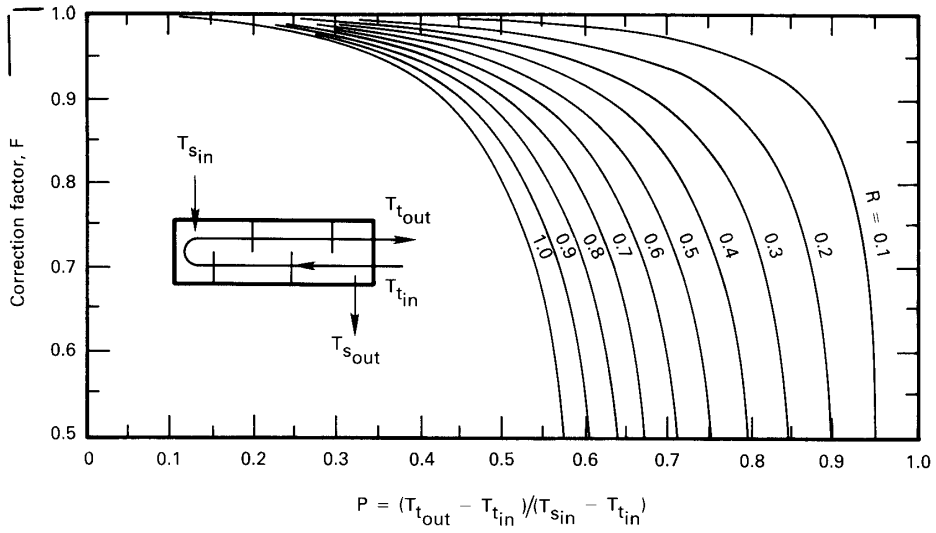

a. *F* for a one-shell-pass, four, six-, . . . tube-pass exchanger.

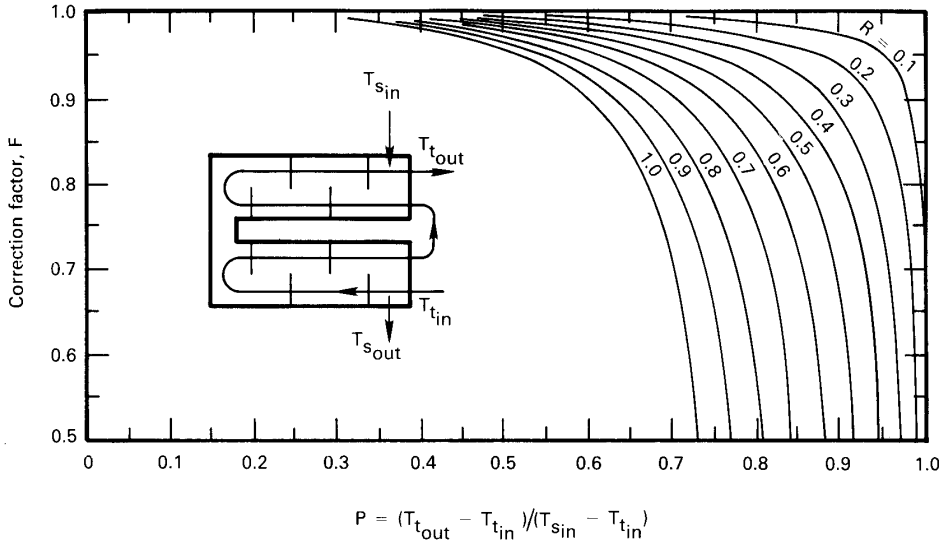

b. *F* for a two-shell-pass, four or more tube-pass exchanger.

Figure 3.14 LMTD correction factors, *F*, for multipass shell-and-tube heat exchangers and one-pass cross-flow exchangers.

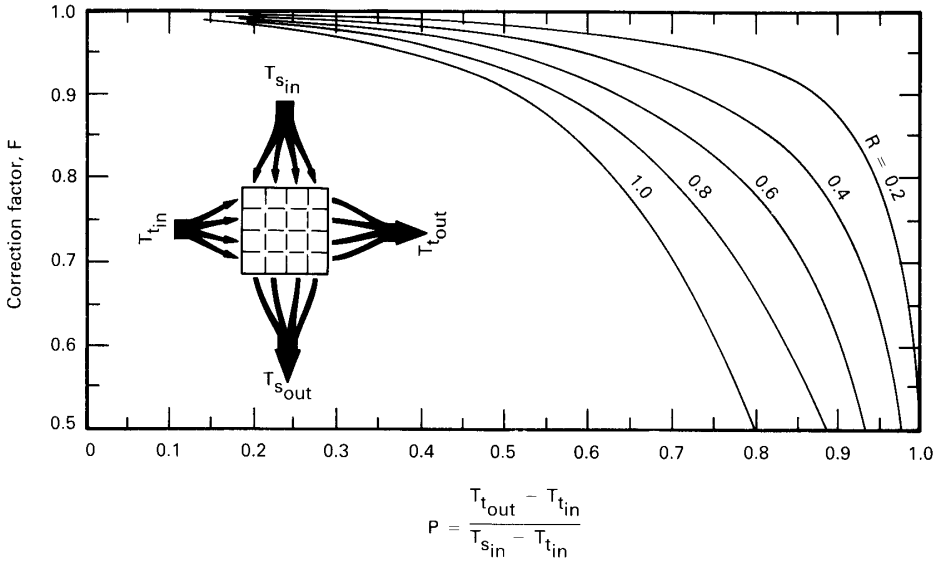

c. *F* for a one-pass cross-flow exchanger with both passes unmixed.

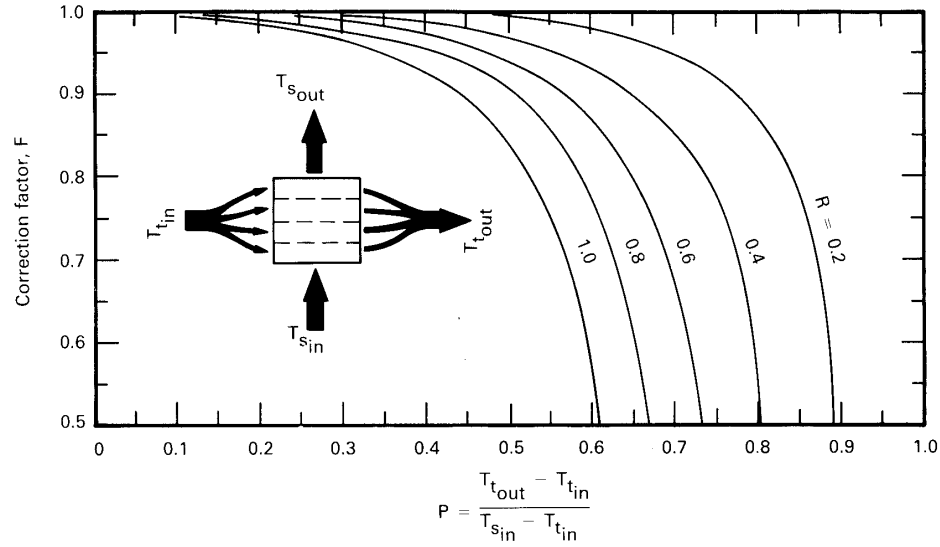

d. *F* for a one-pass cross-flow exchanger with one pass mixed.

Figure 3.14 LMTD correction factors, *F*, for multipass shell-and-tube heat exchangers and one-pass cross-flow exchangers.

tube-pass oil cooler. The oil enters at 181°C and leaves at 38°C. Water flows in the tubes, entering at 32°C and leaving at 49°C. In addition, $c_{p_{\text{oil}}} = 2282$ J/kg·K and $U = 416$ W/m^{2}K. Find how much area the heat exchanger must have.

SOLUTION.

$$\text{LMTD} = \frac{(T_{h_{\text{in}}} - T_{c_{\text{out}}}) - (T_{h_{\text{out}}} - T_{c_{\text{in}}})}{\ln\left(\dfrac{T_{h_{\text{in}}} - T_{c_{\text{out}}}}{T_{h_{\text{out}}} - T_{c_{\text{in}}}}\right)}$$

$$= \frac{(181 - 49) - (38 - 32)}{\ln\left(\dfrac{181 - 49}{38 - 32}\right)} = 40.76 \text{ K}$$

$$R = \frac{181 - 38}{49 - 32} = 8.412 \qquad P = \frac{49 - 32}{181 - 32} = 0.114$$

Since $R > 1$, we enter Fig. 3.14(b) using $P = 8.412(0.114) = 0.959$ and $R = 1/8.412 = 0.119$ and obtain $F = 0.92$.[2] It follows that:

$$Q = UAF(\text{LMTD})$$
$$5.795(2282)(181 - 38) = 416(A)(0.92)(40.76)$$
$$A = 121.2 \text{ m}^2$$

■

3.3 Heat exchanger effectiveness

We are now in a position to predict the performance of an exchanger once we know its configuration *and* the imposed differences. Unfortunately, we do not often know that much about a system before the design is complete.

Often we begin with information such as is shown in Fig. 3.15. If we sought to calculate Q in such a case, we would have to do so by guessing an exit temperature such as to make $Q_h = Q_c = C_h\Delta T_h = C_c\Delta T_c$. Then we could calculate Q from UA(LMTD) or UAF(LMTD) and check it against Q_h. The answers would differ, so we would have to guess new exit temperatures and try again.

Such problems can be greatly simplified with the help of the so-called *effectiveness-NTU method*. This method was first developed in full detail

[2]Notice that, for a 1 shell-pass exchanger, these R and P lines do not quite intersect [see Fig. 3.14(a)]. Therefore, one could not obtain these temperatures with any single-shell exchanger.

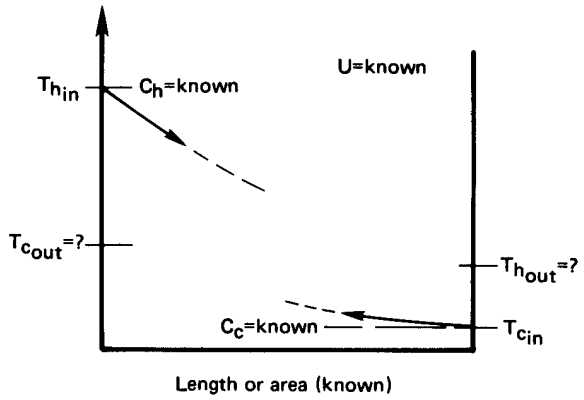

Figure 3.15 A design problem in which the LMTD cannot be calculated a priori.

by Kays and London [3.5] in 1955, in a book titled *Compact Heat Exchangers*. We should take particular note of the title. It is with compact heat exchangers that the present method can reasonably be used, since the overall heat transfer coefficient is far more likely to remain fairly uniform.

The heat exchanger effectiveness is defined as

$$\varepsilon \equiv \frac{C_h(T_{h_{\text{in}}} - T_{h_{\text{out}}})}{C_{\min}(T_{h_{\text{in}}} - T_{c_{\text{in}}})} = \frac{C_c(T_{c_{\text{out}}} - T_{c_{\text{in}}})}{C_{\min}(T_{h_{\text{in}}} - T_{c_{\text{in}}})} \tag{3.16}$$

where $C_{\min}$ is the smaller of C_c and C_h. The effectiveness can be interpreted as

$$\varepsilon = \frac{\text{actual heat transferred}}{\begin{array}{c}\text{maximum heat that could possibly be} \\ \text{transferred from one stream to the other}\end{array}}$$

It follows that

$$Q = \varepsilon C_{\min}(T_{h_{\text{in}}} - T_{c_{\text{in}}}) \tag{3.17}$$

A second definition that we will need was originally made by E.K.W. Nusselt, whom we meet again in Part III. This is the *number of transfer units* (NTU):

$$\text{NTU} \equiv \frac{UA}{C_{\min}} \tag{3.18}$$

This dimensionless group can be viewed as a comparison of the heat capacity of the heat exchanger, expressed in W/°C, with the heat capacity of the flow.

We can immediately reduce the parallel-flow result from eqn. (3.9) to the following equation, based on these definitions:

$$-\left(\frac{C_{\min}}{C_c}+\frac{C_{\min}}{C_h}\right)\mathrm{NTU}=\ln\left[-\left(1+\frac{C_c}{C_h}\right)\varepsilon\frac{C_{\min}}{C_c}+1\right] \tag{3.19}$$

We solve this for ε and, regardless of whether $C_{\min}$ is associated with the hot or cold flow, obtain for the parallel single-pass heat exchanger:

$$\varepsilon\equiv\frac{1-\exp\left[-(1+C_{\min}/C_{\max})\mathrm{NTU}\right]}{1+C_{\min}/C_{\max}}=\mathrm{fn}\left(\frac{C_{\min}}{C_{\max}},\mathrm{NTU\ only}\right) \tag{3.20}$$

The corresponding expression for the counterflow case is

$$\varepsilon=\frac{1-\exp\left[-(1-C_{\min}/C_{\max})\mathrm{NTU}\right]}{1-(C_{\min}/C_{\max})\exp\left[-(1-C_{\min}/C_{\max})\mathrm{NTU}\right]} \tag{3.21}$$

Equations (3.20) and (3.21) are given in graphical form in Fig. 3.16. Similar calculations give the effectiveness for the other heat exchanger configurations (see [3.5]) and we include some of the resulting effectiveness plots in Fig. 3.17. To see how the effectiveness can conveniently be used to complete a design, consider the following two examples.

Example 3.5

Consider the following parallel-flow heat exchanger specification:

$$\text{cold flow enters at } 40^\circ\text{C:}\quad C_c=20{,}000\ \text{W/K}$$
$$\text{hot flow enters at } 150^\circ\text{C:}\quad C_h=10{,}000\ \text{W/K}$$
$$A=30\ \text{m}^2\qquad U=500\ \text{W/m}^2\text{K}.$$

Determine the heat transfer and the exit temperatures.

SOLUTION. In this case we do not know the exit temperatures, so it is not possible to calculate the LMTD. Instead, we can go either to the parallel-flow effectiveness chart in Fig. 3.16 or to eqn. (3.20), using

$$\mathrm{NTU}=\frac{UA}{C_{\min}}=\frac{500(30)}{10{,}000}=1.5$$

$$\frac{C_{\min}}{C_{\max}}=0.5$$

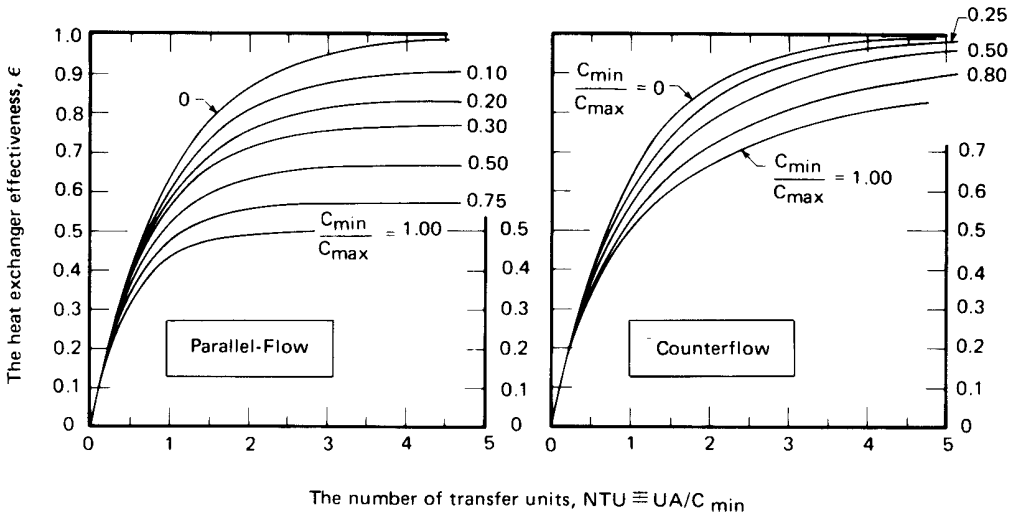

Figure 3.16 The effectiveness of parallel and counterflow heat exchangers. (Data provided by A.D. Krauss.)

and we obtain $\varepsilon = 0.596$. Now from eqn. (3.17), we find that

$$Q = \varepsilon C_{\min}(T_{h_{\text{in}}} - T_{c_{\text{in}}}) = 0.596(10,000)(110)$$
$$= 655,600 \text{ W} = 655.6 \text{ kW}$$

Finally, from energy balances such as are expressed in eqn. (3.4), we get

$$T_{h_{\text{out}}} = T_{h_{\text{in}}} - \frac{Q}{C_h} = 150 - \frac{655,600}{10,000} = 84.44^\circ\text{C}$$
$$T_{c_{\text{out}}} = T_{c_{\text{in}}} + \frac{Q}{C_c} = 40 + \frac{655,600}{20,000} = 72.78^\circ\text{C}$$ ■

Example 3.6

Suppose that we had the same kind of exchanger as we considered in Example 3.5, but that the area remained unspecified as a design variable. Then calculate the area that would bring the hot flow out at 90°C.

SOLUTION. Once the exit cold fluid temperature is known, the problem can be solved with equal ease by either the LMTD or the effective-

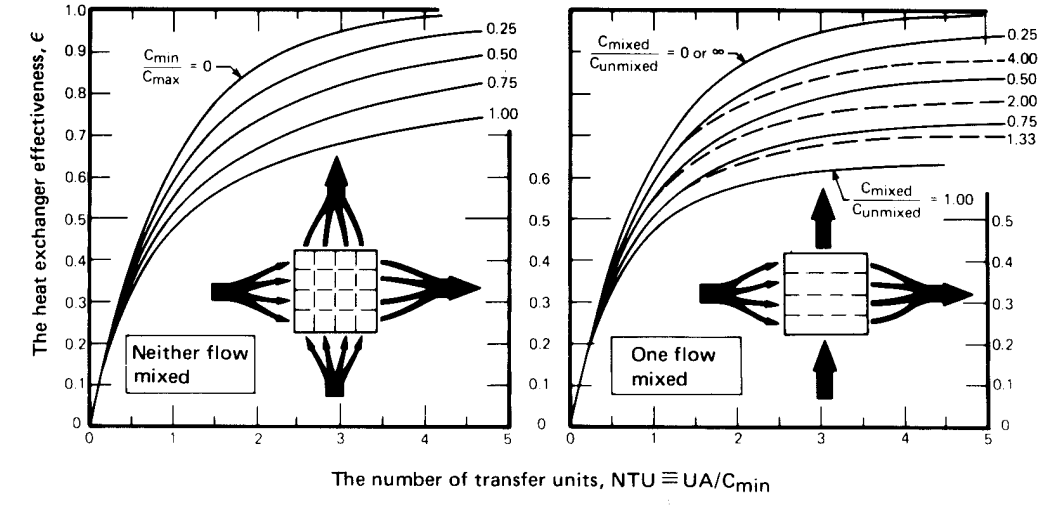

a.) Cross-flow exchanger, neither fluid mixed

b.) Cross-flow exchanger, one fluid mixed

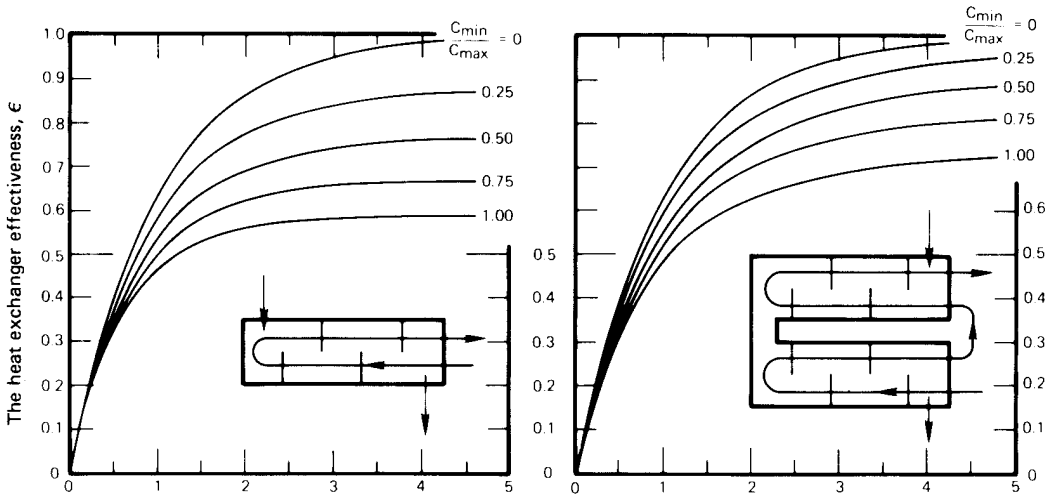

c.) One shell pass, two tube pass exchanger. (Can also be used for 4, 6, 8, 10, 12 tube passes with a maximum error in ϵ, of 0.040 at $C_{min}/C_{max} = 1$ and large NTU.)

d.) Two shell pass 4 tube pass exchanger. (Can also be used for 4, 6, 8, ... tube passes with reasonable accuracy if there are equal numbers of tube passes in each shell pass.)

Figure 3.17 The effectiveness of some other heat exchanger configurations. (Data provided by A.D. Krauss.)

ness approach.

$$T_{c_{\text{out}}} = T_{c_{\text{in}}} + \frac{C_h}{C_c}(T_{h_{\text{in}}} - T_{h_{\text{out}}}) = 40 + \frac{1}{2}(150 - 90) = 70^\circ\text{C}$$

Then, using the effectiveness method,

$$\varepsilon = \frac{C_h(T_{h_{\text{in}}} - T_{h_{\text{out}}})}{C_{\min}(T_{h_{\text{in}}} - T_{c_{\text{in}}})} = \frac{10,000(150 - 90)}{10,000(150 - 40)} = 0.5455$$

so from Fig. 3.16 we read NTU $\simeq 1.15 = UA/C_{\min}$. Thus

$$A = \frac{10,000(1.15)}{500} = 23.00 \text{ m}^2$$

We could also have calculated the LMTD:

$$\text{LMTD} = \frac{(150 - 40) - (90 - 70)}{\ln(110/20)} = 52.79 \text{ K}$$

so from $Q = UA(\text{LMTD})$, we obtain

$$A = \frac{10,000(150 - 90)}{500(52.79)} = 22.73 \text{ m}^2$$

The answers differ by 1%, which reflects graph reading inaccuracy. ■

When the temperature of either fluid in a heat exchanger is uniform, the problem of analyzing heat transfer is greatly simplified. We have already noted that no F-correction is needed to adjust the LMTD in this case. The reason is that when only one fluid changes in temperature, the configuration of the exchanger becomes irrelevant. Any such exchanger is equivalent to a single fluid stream flowing through an isothermal pipe.[3]

Since all heat exchangers are equivalent in this case, it follows that the equation for the effectiveness in any configuration must reduce to the same common expression as $C_{\max}$ approaches infinity. The volumetric heat capacity rate might *approach* infinity because the flow rate or specific heat is very large, or it might *be* infinite because the flow is absorbing or giving up latent heat (as in Fig. 3.9). The limiting effectiveness expression can also be derived directly from energy-balance considerations (see Problem 3.11), but we obtain it here by letting $C_{\max} \to \infty$ in either eqn. (3.20) or eqn. (3.21). The result is

$$\lim_{C_{\max} \to \infty} \varepsilon = 1 - e^{-\text{NTU}} \tag{3.22}$$

[3] We make use of this notion in Section 7.4, when we analyze heat convection in pipes and tubes.

Eqn. (3.22) defines the curve for $C_{\min}/C_{\max} = 0$ in all six of the effectiveness graphs in Fig. 3.16 and Fig. 3.17.

3.4 Heat exchanger design

The preceding sections provided means for designing heat exchangers that generally work well in the design of smaller exchangers—typically, the kind of compact cross-flow exchanger used in transportation equipment. Larger shell-and-tube exchangers pose two kinds of difficulty in relation to U. The first is the variation of U through the exchanger, which we have already discussed. The second difficulty is that convective heat transfer coefficients are very hard to predict for the complicated flows that move through a baffled shell.

We shall achieve considerable success in using analysis to predict $\overline{h}$'s for various convective flows in Part III. The determination of $\overline{h}$ in a baffled shell remains a problem that cannot be solved analytically. Instead, it is normally computed with the help of empirical correlations or with the aid of large commercial computer programs that include relevant experimental correlations. The problem of predicting $\overline{h}$ when the flow is boiling or condensing is even more complicated. A great deal of research is at present aimed at perfecting such empirical predictions.

Apart from predicting heat transfer, a host of additional considerations must be addressed in designing heat exchangers. The primary ones are the minimization of pumping power and the minimization of fixed costs.

The pumping power calculation, which we do not treat here in any detail, is based on the principles discussed in a first course on fluid mechanics. It generally takes the following form for each stream of fluid through the heat exchanger:

$$\begin{aligned}\text{pumping power} = \left(\dot{m}\,\frac{\text{kg}}{\text{s}}\right)\left(\frac{\Delta p}{\rho}\,\frac{\text{N/m}^2}{\text{kg/m}^3}\right) &= \frac{\dot{m}\Delta p}{\rho}\left(\frac{\text{N}\cdot\text{m}}{\text{s}}\right) \\ &= \frac{\dot{m}\Delta p}{\rho}\ (\text{W})\end{aligned} \tag{3.23}$$

where $\dot{m}$ is the mass flow rate of the stream, Δp the pressure drop of the stream as it passes through the exchanger, and ρ the fluid density.

Determining the pressure drop can be relatively straightforward in a single-pass pipe-in-tube heat exchanger or extremely difficulty in, say, a

shell-and-tube exchanger. The pressure drop in a straight run of pipe, for example, is given by

$$\Delta p = f\left(\frac{L}{D_h}\right)\frac{\rho u_{\text{av}}^2}{2} \tag{3.24}$$

where L is the length of pipe, D_h is the hydraulic diameter, u_{av} is the mean velocity of the flow in the pipe, and f is the Darcy-Weisbach friction factor (see Fig. 7.6).

Optimizing the design of an exchanger is not just a matter of making Δp as small as possible. Often, heat exchange can be augmented by employing fins or roughening elements in an exchanger. (We discuss such elements in Chapter 4; see, e.g., Fig. 4.6). Such augmentation will invariably increase the pressure drop, but it can also reduce the fixed cost of an exchanger by increasing U and reducing the required area. Furthermore, it can reduce the required flow rate of, say, coolant, by increasing the effectiveness and thus balance the increase of Δp in eqn. (3.23).

To better understand the course of the design process, faced with such an array of trade-offs of advantages and penalties, we follow Taborek's [3.6] list of design considerations for a large shell-and-tube exchanger:

- Decide which fluid should flow on the shell side and which should flow in the tubes. Normally, this decision will be made to minimize the pumping cost. If, for example, water is being used to cool oil, the more viscous oil would flow in the shell. Corrosion behavior, fouling, and the problems of cleaning fouled tubes also weigh heavily in this decision.
- Early in the process, the designer should assess the cost of the calculation in comparison with:
  (a) The converging accuracy of computation.
  (b) The investment in the exchanger.
  (c) The cost of miscalculation.
- Make a rough estimate of the size of the heat exchanger using, for example, U values from Table 2.2 and/or anything else that might be known from experience. This serves to circumscribe the subsequent trial-and-error calculations; it will help to size flow rates and to anticipate temperature variations; and it will help to avoid subsequent errors.

- Evaluate the heat transfer, pressure drop, and cost of various exchanger configurations that appear reasonable for the application. This is usually done with large-scale computer programs that have been developed and are constantly being improved as new research is included in them.

The computer runs suggested by this procedure are normally very complicated and might typically involve 200 successive redesigns, even when relatively efficient procedures are used.

However, most students of heat transfer will not have to deal with such designs. Many, if not most, *will* be called upon at one time or another to design smaller exchangers in the range 0.1 to 10 m^2. The heat transfer calculation can usually be done effectively with the methods described in this chapter. Some useful sources of guidance in the pressure drop calculation are Kern's classic treatment, *Process Heat Transfer* [3.7], the TEMA design book [3.1], *Perry's Chemical Engineers' Handbook* [3.8], and some of the other references at the end of this chapter.

In such a calculation, we start off with one fluid to heat and one to cool. Perhaps we know the flow heat capacity rates (C_c and C_h), certain temperatures, and/or the amount of heat that is to be transferred. The problem can be annoyingly wide open, and nothing can be done until it is somehow delimited. The normal starting point is the specification of an exchanger configuration, and to make this choice one needs experience. The descriptions in this chapter provide a kind of first level of experience. References [3.5, 3.7, 3.8, 3.9, 3.10, 3.11, 3.12] provide a second level. Manufacturer's catalogues are an excellent source of more advanced information.

Once the exchanger configuration is set, U will be approximately set and the area becomes the basic design variable. The design can then proceed along the lines of Section 3.2 or 3.3. If it is possible to begin with a complete specification of inlet and outlet temperatures,

$$\underbrace{Q}_{C\Delta T} = \underbrace{U}_{\text{known}} \underbrace{AF(\text{LMTD})}_{\text{calculable}}$$

Then A can be calculated and the design completed. Usually, a reevaluation of U and some iteration of the calculation is needed.

More often, we begin without full knowledge of the outlet temperatures. In such cases, we normally have to invent an appropriate trial-and-error method to get the area and a more complicated sequence of trials if we seek to optimize pressure drop and cost by varying the configuration

as well. If the C's are design variables, the U will change significantly, because $\overline{h}$'s are generally velocity-dependent and more iteration will be needed.

We conclude Part I of this book facing a variety of incomplete issues. Most notably, we face a serious need to be able to determine convective heat transfer coefficients. The prediction of $\overline{h}$ depends on a knowledge of heat conduction. We therefore turn, in Part II, to a much more thorough study of heat conduction analysis than was undertaken in Chapter 2. In addition to setting up the methodology ultimately needed to predict $\overline{h}$'s, Part II will also deal with many other issues that have great practical importance in their own right.

Problems

3.1 Can you have a cross-flow exchanger in which both flows are mixed? Discuss.

3.2 Find the appropriate mean radius, $\overline{r}$, that will make $Q = kA(\overline{r})\Delta T/(r_o - r_i)$, valid for the one-dimensional heat conduction through a thick spherical shell, where $A(\overline{r}) = 4\pi\overline{r}^2$ (*cf.* Example 3.1).

3.3 Rework Problem 2.14, using the methods of Chapter 3.

3.4 2.4 kg/s of a fluid have a specific heat of 0.81 kJ/kg·K enter a counterflow heat exchanger at 0°C and are heated to 400°C by 2 kg/s of a fluid having a specific heat of 0.96 kJ/kg·K entering the unit at 700°C. Show that to heat the cooler fluid to 500°C, all other conditions remaining unchanged, would require the surface area for a heat transfer to be increased by 87.5%.

3.5 A cross-flow heat exchanger with both fluids unmixed is used to heat water (c_p = 4.18 kJ/kg·K) from 40°C to 80°C, flowing at the rate of 1.0 kg/s. What is the overall heat transfer coefficient if hot engine oil (c_p = 1.9 kJ/kg·K), flowing at the rate of 2.6 kg/s, enters at 100°C? The heat transfer area is 20 m^2. (Note that you can use either an effectiveness or an LMTD method. It would be wise to use both as a check.)

3.6 Saturated non-oil-bearing steam at 1 atm enters the shell pass of a two-tube-pass shell condenser with thirty 20 ft tubes in

each tube pass. They are made of schedule 160, ¾ in. steel pipe (nominal diameter). A volume flow rate of 0.01 ft^3/s of water entering at 60°F enters each tube. The condensing heat transfer coefficient is 2000 Btu/h·ft^2·°F, and we calculate $\overline{h}$ = 1380 Btu/h·ft^2·°F for the water in the tubes. Estimate the exit temperature of the water and mass rate of condensate [$\dot{m}_c \simeq$ 8393 lb_m/h.]

3.7 Consider a counterflow heat exchanger that must cool 3000 kg/h of mercury from 150°F to 128°F. The coolant is 100 kg/h of water, supplied at 70°F. If U is 300 W/m^2K, complete the design by determining reasonable value for the area and the exit-water temperature. [A = 0.147 m^2.]

3.8 An automobile air-conditioner gives up 18 kW at 65 km/h if the outside temperature is 35°C. The refrigerant temperature is constant at 65°C under these conditions, and the air rises 6°C in temperature as it flows across the heat exchanger tubes. The heat exchanger is of the finned-tube type shown in Fig. 3.6b, with $U \simeq$ 200 W/m^2K. If $U \sim$ (air velocity)$^{0.7}$ and the mass flow rate increases directly with the velocity, plot the percentage reduction of heat transfer in the condenser as a function of air velocity between 15 and 65 km/h.

3.9 Derive eqn. (3.21).

3.10 Derive the infinite NTU limit of the effectiveness of parallel and counterflow heat exchangers at several values of $C_{\min}/C_{\max}$. Use common sense and the First Law of Thermodynamics, and refer to eqn. (3.2) and eqn. (3.21) only to check your results.

3.11 Derive the equation $\varepsilon = (\text{NTU}, C_{\min}/C_{\max})$ for the heat exchanger depicted in Fig. 3.9.

3.12 A single-pass heat exchanger condenses steam at 1 atm on the shell side and heats water from 10°C to 30°C on the tube side with U = 2500 W/m^2K. The tubing is thin-walled, 5 cm in diameter, and 2 m in length. (a) Your boss asks whether the exchanger should be counterflow or parallel-flow. How do you advise her? Evaluate: (b) the LMTD; (c) $\dot{m}_{H_2O}$; (d) ε. [$\varepsilon \simeq$0.222.]

3.13 Air at 2 kg/s and 27°C and a stream of water at 1.5 kg/s and 60°C each enter a heat exchanger. Evaluate the exit temperatures if $A = 12$ m^2, $U = 185$ W/m^{2}K, and:

a. The exchanger is parallel flow;

b. The exchanger is counterflow [$T_{h_{\text{out}}} \simeq 54.0$°C.];

c. The exchanger is cross-flow, one stream mixed;

d. The exchanger is cross-flow, neither stream mixed. [$T_{h_{\text{out}}} = 53.62$°C.]

3.14 Air at 0.25 kg/s and 0°C enters a cross-flow heat exchanger. It is to be warmed to 20°C by 0.14 kg/s of air at 50°C. The streams are unmixed. As a first step in the design process, plot U against A and identify the approximate range of area for the exchanger.

3.15 A particular two shell-pass, four tube-pass heat exchanger uses 20 kg/s of river water at 10°C on the shell side to cool 8 kg/s of processed water from 80°C to 25°C on the tube side. At what temperature will the coolant be returned to the river? If U is 800 W/m^{2}K, how large must the exchanger be?

3.16 A particular cross-flow process heat exchanger operates with the fluid mixed on one side only. When it is new, $U = 2000$ W/m^{2}K, $T_{c_{\text{in}}} = 25$°C, $T_{c_{\text{out}}} = 80$°C, $T_{h_{\text{in}}} = 160$°C, and $T_{h_{\text{out}}} = 70$°C. After 6 months of operation, the plant manager reports that the hot fluid is only being cooled to 90°C and that he is suffering a 30% reduction in total heat transfer. What is the fouling resistance after 6 months of use? (Assume no reduction of cold-side flow rate by fouling.)

3.17 Water at 15°C is supplied to a one-shell-pass, two-tube-pass heat exchanger to cool 10 kg/s of liquid ammonia from 120°C to 40°C. You anticipate a U on the order of 1500 W/m^{2}K when the water flows in the tubes. If A is to be 90 m^2, choose the correct flow rate of water.

3.18 Suppose that the heat exchanger in Example 3.5 had been a two shell-pass, four tube-pass exchanger with the hot fluid moving in the tubes. (a) What would be the exit temperature in this case? [$T_{c_{\text{out}}} = 75.09$°C.] (b) What would be the area if we wanted

the hot fluid to leave at the same temperature that it does in the example?

3.19 Plot the maximum tolerable fouling resistance as a function of U_{new} for a counterflow exchanger, with given inlet temperatures, if a 30% reduction in U is the maximum that can be tolerated.

3.20 Water at 0.8 kg/s enters the tubes of a two-shell-pass, four-tube-pass heat exchanger at 17°C and leaves at 37°C. It cools 0.5 kg/s of air entering the shell at 250°C with $U = 432$ W/m^{2}K. Determine: (a) the exit air temperature; (b) the area of the heat exchanger; and (c) the exit temperature if, after some time, the tubes become fouled with $R_f = 0.0005$ m^{2}K/W. [(c) $T_{\text{air}_{\text{out}}} = 140.5$°C.]

3.21 You must cool 78 kg/min of a 60%-by-mass mixture of glycerin in water from 108°C to 50°C using cooling water available at 7°C. Design a one-shell-pass, two-tube-pass heat exchanger if $U = 637$ W/m^{2}K. Explain any design decision you make and report the area, $T_{\text{H}_2\text{O}_{\text{out}}}$, and any other relevant features.

3.22 A mixture of 40%-by-weight glycerin, 60% water, enters a smooth 0.113 m I.D. tube at 30°C. The tube is kept at 50°C, and $\dot{m}_{\text{mixture}} = 8$ kg/s. The heat transfer coefficient inside the pipe is 1600 W/m^{2}K. Plot the liquid temperature as a function of position in the pipe.

3.23 Explain in physical terms why all effectiveness curves Fig. 3.16 and Fig. 3.17 have the same slope as NTU → 0. Obtain this slope from eqns. (3.20) and (3.21).

3.24 You want to cool air from 150°C to 60°C but you cannot afford a custom-built heat exchanger. You find a used cross-flow exchanger (both fluids unmixed) in storage. It was previously used to cool 136 kg/min of NH_3 vapor from 200°C to 100°C using 320 kg/min of water at 7°C; U was previously 480 W/m^{2}K. How much air can you cool with this exchanger, using the same water supply, if U is approximately unchanged? (Actually, you would have to modify U using the methods of Chapters 6 and 7 once you had the new air flow rate, but that is beyond our present scope.)

3.25 A one tube-pass, one shell-pass, parallel-flow, process heat exchanger cools 5 kg/s of gaseous ammonia entering the shell side at 250°C and boils 4.8 kg/s of water in the tubes. The water enters subcooled at 27°C and boils when it reaches 100°C. U = 480 W/m^{2}K before boiling begins and 964 W/m^{2}K thereafter. The area of the exchanger is 45 m^2, and h_{fg} for water is 2.257×10^6 J/kg. Determine the quality of the water at the exit.

3.26 0.72 kg/s of superheated steam enters a crossflow heat exchanger at 240°C and leaves at 120°C. It heats 0.6 kg/s of water entering at 17°C. U = 612 W/m^{2}K. By what percentage will the area differ if a both-fluids-unmixed exchanger is used instead of a one-fluid-unmixed exchanger? [−1.8%]

3.27 Compare values of F from Fig. 3.14(c) and Fig. 3.14(d) for the same conditions of inlet and outlet temperatures. Is the one with the higher F automatically the more desirable exchanger? Discuss.

3.28 Compare values of ε for the same NTU and C_{min}/C_{max} in parallel and counterflow heat exchangers. Is the one with the higher ε automatically the more desirable exchanger? Discuss.

3.29 The *irreversibility rate* of a process is equal to the rate of entropy production times the lowest absolute sink temperature accessible to the process. Calculate the irreversibility (or lost work) for the heat exchanger in Example 3.4. What kind of configuration would reduce the irreversibility, given the same end temperatures.

3.30 Plot T_{oil} and T_{H_2O} as a function of position in a very long counterflow heat exchanger where water enters at 0°C, with C_{H_2O} = 460 W/K, and oil enters at 90°C, with C_{oil} = 920 W/·C, U = 742 W/m^{2}K, and A = 10 m^2. Criticize the design.

3.31 Liquid ammonia at 2 kg/s is cooled from 100°C to 30°C in the shell side of a two shell-pass, four tube-pass heat exchanger by 3 kg/s of water at 10°C. When the exchanger is new, U = 750 W/m^{2}K. Plot the exit ammonia temperature as a function of the increasing tube fouling factor.

3.32 A one shell-pass, two tube-pass heat exchanger cools 0.403 kg/s of methanol from 47°C to 7°C on the shell side. The

coolant is 2.2 kg/s of Freon 12, entering the tubes at −33°C, with U = 538 W/m^{2}K. A colleague suggests that this arrangement wastes Freon. She thinks you could do almost as well if you cut the Freon flow rate all the way down to 0.8 kg/s. Calculate the new methanol outlet temperature that would result from this flow rate, and evaluate her suggestion.

3.33 The factors dictating the heat transfer coefficients in a certain two shell-pass, four tube-pass heat exchanger are such that U increases as $(\dot{m}_{\text{shell}})^{0.6}$. The exchanger cools 2 kg/s of air from 200°C to 40°C using 4.4 kg/s of water at 7°C, and U = 312 W/m^{2}K under these circumstances. If we double the air flow, what will its temperature be leaving the exchanger? [$T_{\text{air}_{\text{out}}}$ = 61°C.]

3.34 A flow rate of 1.4 kg/s of water enters the tubes of a two-shell-pass, four-tube-pass heat exchanger at 7°C. A flow rate of 0.6 kg/s of liquid ammonia at 100°C is to be cooled to 30°C on the shell side; U = 573 W/m^{2}K. (a) How large must the heat exchanger be? (b) How large must it be if, after some months, a fouling factor of 0.0015 will build up in the tubes, and we still want to deliver ammonia at 30°C? (c) If we make it large enough to accommodate fouling, to what temperature will it cool the ammonia when it is new? (d) At what temperature does water leave the new, enlarged exchanger? [(d) T_{H_2O} = 49.9°C.]

3.35 Both C's in a parallel-flow heat exchanger are equal to 156 W/K, U = 327 W/m^{2}K and A = 2 m^2. The hot fluid enters at 140°C and leaves at 90°C. The cold fluid enters at 40°C. If both C's are halved, what will be the exit temperature of the hot fluid?

3.36 A 1.68 ft^2 cross-flow heat exchanger with one fluid mixed condenses steam at atmospheric pressure ($\overline{h}$ = 2000 Btu/h·ft^2·°F) and boils methanol (T_{sat} = 170°F and $\overline{h}$ = 1500 Btu/h·ft^2·°F) on the other side. Evaluate U (neglecting resistance of the metal), LMTD, F, NTU, ε, and Q.

3.37 Eqn. (3.21) is troublesome when $C_{\min}/C_{\max} = 1$. Develop a working equation for ε in this case. Compare it with Fig. 3.16.

3.38 The effectiveness of a cross-flow exchanger with neither fluid mixed can be calculated from the following approximate for-

mula:

$$\varepsilon = 1 - \exp\left[\exp(-\mathrm{NTU}^{0.78} r) - 1\right](\mathrm{NTU}^{0.22}/r)\Big]$$

where $r \equiv C_{\min}/C_{\max}$. How does this compare with correct values?

3.39 Calculate the area required in a two-tube-pass, one-shell-pass condenser that is to condense 10^6 kg/h of steam at 40°C using water at 17°C. Assume that $U = 4700$ W/m^{2}K, the maximum allowable temperature rise of the water is 10°C, and $h_{fg} = 2406$ kJ/kg.

3.40 An engineer wants to divert 1 gal/min of water at 180°F from his car radiator through a small cross-flow heat exchanger with neither flow mixed, to heat 40°F water to 140°F for shaving when he goes camping. If he produces a pint per minute of hot water, what will be the area of the exchanger and the temperature of the returning radiator coolant if $U = 720$ W/m^{2}K?

References

[3.1] Tubular Exchanger Manufacturer's Association. *Standards of Tubular Exchanger Manufacturer's Association*. New York, 4th and 6th edition, 1959 and 1978.

[3.2] R. A. Bowman, A. C. Mueller, and W. M. Nagle. Mean temperature difference in design. *Trans. ASME*, 62:283–294, 1940.

[3.3] K. Gardner and J. Taborek. Mean temperature difference: A reappraisal. *AIChE J.*, 23(6):770–786, 1977.

[3.4] N. Shamsundar. A property of the log-mean temperature-difference correction factor. *Mechanical Engineering News*, 19(3): 14–15, 1982.

[3.5] W. M. Kays and A. L. London. *Compact Heat Exchangers*. McGraw-Hill Book Company, New York, 3rd edition, 1984.

[3.6] J. Taborek. Evolution of heat exchanger design techniques. *Heat Transfer Engineering*, 1(1):15–29, 1979.

[3.7] D. Q. Kern. *Process Heat Transfer*. McGraw-Hill Book Company, New York, 1950.

[3.8] R. H. Perry, D. W. Green, and J. Q. Maloney, editors. *Perry's Chemical Engineers' Handbook*. McGraw-Hill Book Company, New York, 7th edition, 1997.

[3.9] A. P. Fraas. *Heat Exchanger Design*. John Wiley & Sons, Inc., New York, 2nd edition, 1989.

[3.10] D. M. Considine. *Energy Technology Handbook*. McGraw-Hill Book Company, New York, 1975.

[3.11] G. F. Hewitt, editor. *Heat Exchanger Design Handbook 1998*. Begell House, New York, 1998.

[3.12] R.K. Shah and D.P. Sekulic. Heat exchangers. In W. M. Rohsenow, J. P. Hartnett, and Y. I. Cho, editors, *Handbook of Heat Transfer*, chapter 17. McGraw-Hill, New York, 3rd edition, 1998.

Part II

Analysis of Heat Conduction

4. Analysis of heat conduction and some steady one-dimensional problems

The effects of heat are subject to constant laws which cannot be discovered without the aid of mathematical analysis. The object of the theory which we are about to explain is to demonstrate these laws; it reduces all physical researches on the propagation of heat to problems of the calculus whose elements are given by experiment.

The Analytical Theory of Heat, **J. Fourier**

4.1 The well-posed problem

The heat diffusion equation was derived in Section 2.1 and some attention was given to its solution. Before we go further with heat conduction problems, we must describe how to state such problems so they can really be solved. This is particularly important in approaching the more complicated problems of transient and multidimensional heat conduction that we have avoided up to now.

A well-posed heat conduction problem is one in which all the relevant information needed to obtain a unique solution is stated. A well-posed and hence solvable heat conduction problem will always read as follows:

Find $T(x, y, z, t)$ such that:

1. $$\nabla \cdot (k \nabla T) + \dot{q} = \rho c \frac{\partial T}{\partial t}$$

   for $0 < t < \mathcal{T}$ (where $\mathcal{T}$ can $\longrightarrow \infty$), and for (x, y, z) belonging to

some region, R, which might extend to infinity.[1]

2. $T = T_i(x, y, z)$ at $t = 0$

   This is called an *initial condition*, or i.c.

   (a) Condition 1 above is not imposed at $t = 0$.

   (b) Only one i.c. is required. However,

   (c) The i.c. is not needed:

      i. In the steady-state case: $\nabla \cdot (k\nabla T) + \dot{q} = 0$.

      ii. For "periodic" heat transfer, where $\dot{q}$ or the boundary conditions vary periodically with time, and where we ignore the starting transient behavior.

3. T must also satisfy two *boundary conditions*, or b.c.'s, for each coordinate. The b.c.'s are very often of three common types.

   (a) *Dirichlet conditions*, or b.c.'s of the *first kind*:

   T is specified on the boundary of R for $t > 0$. We saw such b.c.'s in Examples 2.1, 2.2, and 2.5.

   (b) *Neumann conditions*, or b.c.'s of the *second kind*:

   The derivative of T normal to the boundary is specified on the boundary of R for $t > 0$. Such a condition arises when the heat flux, $k(\partial T/\partial x)$, is specified on a boundary or when , with the help of insulation, we set $\partial T/\partial x$ equal to zero.[2]

   (c) b.c.'s of the *third kind*:

   A derivative of T in a direction normal to a boundary is proportional to the temperature on that boundary. Such a condition most commonly arises when convection occurs at a boundary, and it is typically expressed as

$$-k \left.\frac{\partial T}{\partial x}\right|_{\text{bndry}} = \overline{h}(T - T_\infty)_{\text{bndry}}$$

   when the body lies to the left of the boundary on the x-coordinate. We have already used such a b.c. in Step 4 of Example 2.6, and we have discussed it in Section 1.3 as well.

[1] (x, y, z) might be any coordinates describing a position $\vec{r}$: $T(x, y, z, t) = T(\vec{r}, t)$.

[2] Although we write $\partial T/\partial x$ here, we understand that this might be $\partial T/\partial z$, $\partial T/\partial r$, or any other derivative in a direction locally normal to the surface on which the b.c. is specified.

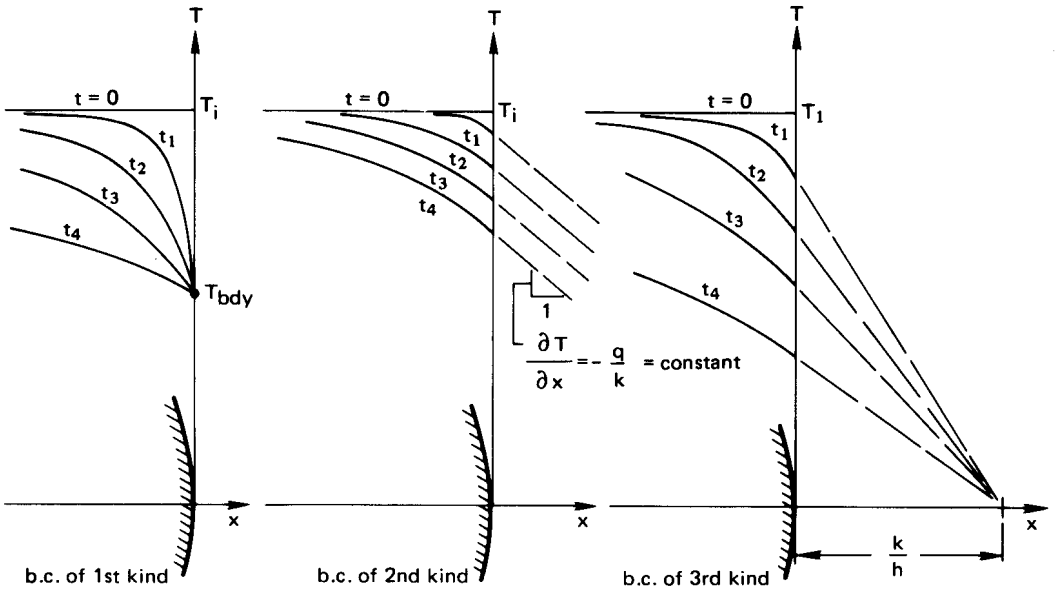

Figure 4.1 The transient cooling of a body as it might occur, subject to boundary conditions of the first, second, and third kinds.

This list of b.c.'s is not complete, by any means, but it includes a great number of important cases.

Figure 4.1 shows the transient cooling of body from a constant initial temperature, subject to each of the three b.c.'s described above. Notice that the initial temperature distribution is not subject to the boundary condition, as pointed out previously under 2(a).

The eight-point procedure that was outlined in Section 2.2 for solving the heat diffusion equation was contrived in part to assure that a problem will meet the preceding requirements and will be well posed.

4.2 The general solution

Once the heat conduction problem has been posed properly, the first step in solving it is to find the general solution of the heat diffusion equation. We have remarked that this is usually the easiest part of the problem. We next consider some examples of general solutions.

One-dimensional steady heat conduction

Problem 4.1 emphasizes the simplicity of finding the general solutions of linear ordinary differential equations, by asking for a table of all general solutions of one-dimensional heat conduction problems. We shall work out some of those results to show what is involved. We begin the heat diffusion equation with constant k and $\dot{q}$:

$$\nabla^2 T + \frac{\dot{q}}{k} = \frac{1}{\alpha}\frac{\partial T}{\partial t} \tag{2.11}$$

Cartesian coordinates: Steady conduction in the y-direction. Equation (2.11) reduces as follows:

$$\underbrace{\frac{\partial^2 T}{\partial x^2}}_{=0} + \frac{\partial^2 T}{\partial y^2} + \underbrace{\frac{\partial^2 T}{\partial z^2}}_{=0} + \frac{\dot{q}}{k} = \underbrace{\frac{1}{\alpha}\frac{\partial T}{\partial t}}_{=0,\text{ since steady}}$$

Therefore,

$$\frac{d^2 T}{dy^2} = -\frac{\dot{q}}{k}$$

which we integrate twice to get

$$T = -\frac{\dot{q}}{2k}y^2 + C_1 y + C_2$$

or, if $\dot{q} = 0$,

$$T = C_1 y + C_2$$

Cylindrical coordinates with a heat source: Tangential conduction. This time, we look at the heat flow that results in a ring when two points are held at different temperatures. We now express eqn. (2.11) in cylindrical coordinates with the help of eqn. (2.13):

$$\underbrace{\frac{1}{r}\frac{\partial}{\partial r}\left(r\frac{\partial T}{\partial r}\right)}_{=0} + \underbrace{\frac{1}{r^2}\frac{\partial^2 T}{\partial \phi^2}}_{r=\text{constant}} + \underbrace{\frac{\partial^2 T}{\partial z^2}}_{=0} + \frac{\dot{q}}{k} = \underbrace{\frac{1}{\alpha}\frac{\partial T}{\partial t}}_{=0,\text{ since steady}}$$

Two integrations give

$$T = -\frac{r^2\dot{q}}{2k}\phi^2 + C_1\phi + C_2 \tag{4.1}$$

This would describe, for example, the temperature distribution in the thin ring shown in Fig. 4.2. Here the b.c.'s might consist of temperatures specified at two angular locations, as shown.

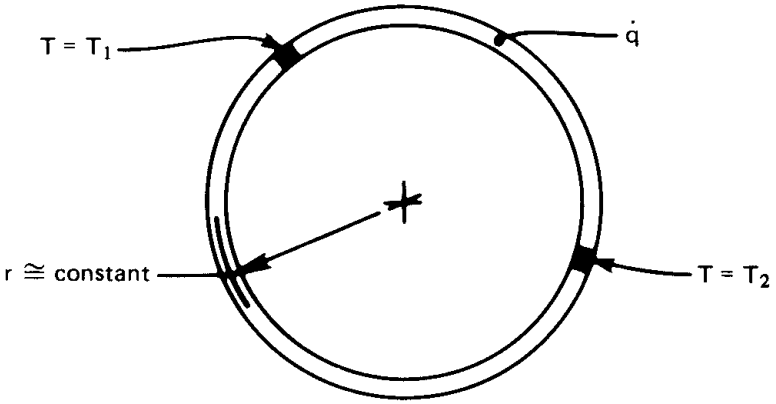

Figure 4.2 One-dimensional heat conduction in a ring.

T = T(t only)

If T is spatially uniform, it can still vary with time. In such cases

$$\underbrace{\nabla^2 T}_{=0} + \frac{\dot{q}}{k} = \frac{1}{\alpha}\frac{\partial T}{\partial t}$$

and $\partial T/\partial t$ becomes an ordinary derivative. Then, since $\alpha = k/\rho c$,

$$\frac{dT}{dt} = \frac{\dot{q}}{\rho c} \tag{4.2}$$

This result is consistent with the lumped-capacity solution described in Section 1.3. If the Biot number is low and internal resistance is unimportant, the convective removal of heat from the boundary of a body can be *prorated* over the volume of the body and interpreted as

$$\dot{q}_{\text{effective}} = -\frac{\overline{h}(T_{\text{body}} - T_\infty)A}{\text{volume}} \text{ W/m}^3 \tag{4.3}$$

and the heat diffusion equation for this case, eqn. (4.2), becomes

$$\frac{dT}{dt} = -\frac{\overline{h}A}{\rho c V}(T - T_\infty) \tag{4.4}$$

The general solution in this situation was given in eqn. (1.21). [A particular solution was also written in eqn. (1.22).]

Separation of variables: A general solution of multidimensional problems

Suppose that the physical situation permits us to throw out all but one of the spatial derivatives in a heat diffusion equation. Suppose, for example, that we wish to predict the transient cooling in a slab as a function of the location within it. If there is no heat generation, the heat diffusion equation is

$$\frac{\partial^2 T}{\partial x^2} = \frac{1}{\alpha}\frac{\partial T}{\partial t} \tag{4.5}$$

A common trick is to ask: "Can we find a solution in the form of a product of functions of t and x: $T = \mathcal{T}(t) \cdot \mathcal{X}(x)$?" To find the answer, we substitute this in eqn. (4.5) and get

$$\mathcal{X}''\mathcal{T} = \frac{1}{\alpha}\mathcal{T}'\mathcal{X} \tag{4.6}$$

where each prime denotes one differentiation of a function with respect to its argument. Thus $\mathcal{T}' = d\mathcal{T}/dt$ and $\mathcal{X}'' = d^2\mathcal{X}/dx^2$. Rearranging eqn. (4.6), we get

$$\frac{\mathcal{X}''}{\mathcal{X}} = \frac{1}{\alpha}\frac{\mathcal{T}'}{\mathcal{T}} \tag{4.7a}$$

This is an interesting result in that the left-hand side depends only upon x and the right-hand side depends only upon t. Thus, we set *both* sides equal to the same constant, which we call $-\lambda^2$, instead of, say, λ, for reasons that will be clear in a moment:

$$\frac{\mathcal{X}''}{\mathcal{X}} = \frac{1}{\alpha}\frac{\mathcal{T}'}{\mathcal{T}} = -\lambda^2 \quad \text{a constant} \tag{4.7b}$$

It follows that the differential eqn. (4.7a) can be resolved into two ordinary differential equations:

$$\mathcal{X}'' = -\lambda^2\mathcal{X} \quad \text{and} \quad \mathcal{T}' = -\alpha\lambda^2\mathcal{T} \tag{4.8}$$

The general solution of both of these equations are well known and are among the first ones dealt with in any study of differential equations. They are:

$$\begin{aligned} \mathcal{X}(x) &= A\sin\lambda x + B\cos\lambda x \quad \text{for} \quad \lambda \neq 0 \\ \mathcal{X}(x) &= Ax + B \qquad\qquad\qquad\quad \text{for} \quad \lambda = 0 \end{aligned} \tag{4.9}$$

and

$$\begin{array}{lll} \mathcal{T}(t) = Ce^{-\alpha\lambda^2 t} & \text{for} & \lambda \neq 0 \\ \mathcal{T}(t) = C & \text{for} & \lambda = 0 \end{array} \tag{4.10}$$

where we use capital letters to denote constants of integration. [In either case, these solutions can be verified by substituting them back into eqn. (4.8).] Thus the general solution of eqn. (4.5) can indeed be written in the form of a product, and that product is

$$\begin{array}{lll} T = \mathcal{X}\mathcal{T} = e^{-\alpha\lambda^2 t}(D\sin\lambda x + E\cos\lambda x) & \text{for} & \lambda \neq 0 \\ T = \mathcal{X}\mathcal{T} = Dx + E & \text{for} & \lambda = 0 \end{array} \tag{4.11}$$

The usefulness of this result depends on whether or not it can be fit to the b.c.'s and the i.c. In this case, we made the function $\mathcal{X}(t)$ take the form of sines and cosines (instead of exponential functions) by placing a minus sign in front of λ^2. The sines and cosines make it possible to fit the b.c.'s using Fourier series methods. These general methods are not developed in this book; however, a complete Fourier series solution is presented for one problem in Section 5.3.

The preceding simple methods for obtaining general solutions of linear partial d.e.'s is called the method of *separation of variables*. It can be applied to all kinds of linear d.e.'s. Consider, for example, two-dimensional steady heat conduction without heat sources:

$$\frac{\partial^2 T}{\partial x^2} + \frac{\partial^2 T}{\partial y^2} = 0 \tag{4.12}$$

Set $T = \mathcal{X}\mathcal{Y}$ and get

$$\frac{\mathcal{X}''}{\mathcal{X}} = -\frac{\mathcal{Y}''}{\mathcal{Y}} = -\lambda^2$$

where λ can be an imaginary number. Then

$$\left.\begin{array}{l} \mathcal{X} = A\sin\lambda x + B\cos\lambda x \\ \mathcal{Y} = Ce^{\lambda y} + De^{-\lambda y} \end{array}\right\} \text{for } \lambda \neq 0$$

$$\left.\begin{array}{l} \mathcal{X} = Ax + B \\ \mathcal{Y} = C\mathcal{y} + D \end{array}\right\} \text{for } \lambda = 0$$

The general solution is

$$\begin{array}{lll} T = (E\sin\lambda x + F\cos\lambda x)(e^{-\lambda y} + Ge^{\lambda y}) & \text{for } \lambda \neq 0 \\ T = (Ex + F)(\mathcal{y} + G) & \text{for } \lambda = 0 \end{array} \tag{4.13}$$

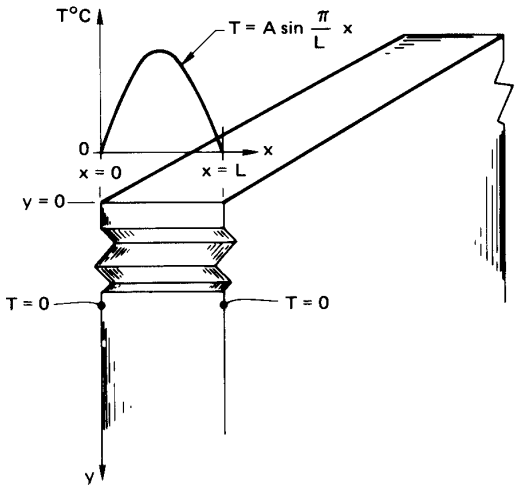

Figure 4.3 A two-dimensional slab maintained at a constant temperature on the sides and subjected to a sinusoidal variation of temperature on one face.

Example 4.1

A long slab is cooled to 0°C on both sides and a blowtorch is turned on the top edge, giving an approximately sinusoidal temperature distribution along the top, as shown in Fig. 4.3. Find the temperature distribution within the slab.

SOLUTION. The general solution is given by eqn. (4.13). We must therefore identify the appropriate b.c.'s and then fit the general solution to it. Those b.c.'s are:

$$\begin{aligned} \text{on the top surface}: &\quad T(x,0) = A\sin\pi\frac{x}{L} \\ \text{on the sides}: &\quad T(0 \text{ or } L, y) = 0 \\ \text{as } y \longrightarrow \infty: &\quad T(x, y\to\infty) = 0 \end{aligned}$$

Substitute eqn. (4.13) in the third b.c.:

$$(E\sin\lambda x + F\cos\lambda x)(0 + G\cdot\infty) = 0$$

The only way that this can be true for all x is if $G = 0$. Substitute eqn. (4.13), with $G = 0$, into the second b.c.:

$$(O + F)e^{-\lambda y} = 0$$

so F also equals 0. Substitute eqn. (4.13) with $G = F = 0$, into the first b.c.:

$$E(\sin \lambda x) = A \sin \pi \frac{x}{L}$$

It follows that $A = E$ and $\lambda = \pi/L$. Then eqn. (4.13) becomes the particular solution that satisfies the b.c.'s:

$$T = A \left(\sin \pi \frac{x}{L} \right) e^{-\pi y/L}$$

Thus, the sinusoidal variation of temperature at the top of the slab is attenuated exponentially at lower positions in the slab. At a position of $y = 2L$ below the top, T will be $0.0019\,A \sin \pi x/L$. The temperature distribution in the x-direction will still be sinusoidal, but it will have less than $1/500$ of the amplitude at $y = 0$. ■

Consider some important features of this and other solutions:

- The b.c. at $y = 0$ is a special one that works very well with this particular general solution. If we had tried to fit the equation to a general temperature distribution, $T(x, y = 0) = \text{fn}(x)$, it would not have been obvious how to proceed. Actually, this is the kind of problem that Fourier solved with the help of his Fourier series method. We discuss this matter in more detail in Chapter 5.

- Not all forms of general solutions lend themselves to a particular set of boundary and/or initial conditions. In this example, we made the process look simple, but more often than not, *it is in fitting a general solution to a set of boundary conditions that we get stuck.*

- Normally, on formulating a problem, we must *approximate* real behavior in stating the b.c.'s. It is advisable to consider what kind of assumption will put the b.c.'s in a form compatible with the general solution. The temperature distribution imposed on the slab by the blowtorch in Example 4.1 might just as well have been approximated as a parabola. But as small as the difference between a parabola and a sine function might be, the latter b.c. was far easier to accommodate.

- The twin issues of existence and uniqueness of solutions require a comment here: It has been established that solutions to all well-posed heat diffusion problems are unique. Furthermore, we know

from our experience that if we describe a physical process correctly, a unique outcome exists. Therefore, we are normally safe to leave these issues to a mathematician—at least in the sort of problems we discuss here.

- Given that a unique solution exists, we accept any solution as correct since we have carved it to fit the boundary conditions. In this sense, the solution of differential equations is often more of an incentive than a formal operation. The person who does it best is often the person who has done it before and so has a large assortment of tricks up his or her sleeve.

4.3 Dimensional analysis

Introduction

Most universities place the first course in heat transfer after an introduction to fluid mechanics: and most fluid mechanics courses include some dimensional analysis. This is normally treated using the familiar *method of indices*, which is seemingly straightforward to teach but is cumbersome and sometimes misleading to use. It is rather well presented in [4.1].

The method we develop here is far simpler to use than the method of indices, and it does much to protect us from the common errors we might fall into. We refer to it as the *method of functional replacement*.

The importance of dimensional analysis to heat transfer can be made clearer by recalling Example 2.6, which (like most problems in Part I) involved several variables. Theses variables included the dependent variable of temperature, $(T_\infty - T_i)$;[3] the major independent variable, which was the radius, r; and five system parameters, $r_i, r_o, \overline{h}, k$, and $(T_\infty - T_i)$. By reorganizing the solution into dimensionless groups [eqn. (2.24)], we reduced the total number of variables to only four:

$$\underbrace{\frac{T - T_i}{T_\infty - T_i}}_{\text{dependent variable}} = \text{fn}\left[\underbrace{r/r_i,}_{\text{indep. var.}} \underbrace{r_o/r_i, \quad \text{Bi}}_{\text{two system parameters}}\right] \tag{2.24a}$$

[3] Notice that we do not call T_i a variable. It is simply the reference temperature against which the problem is worked. If it happened to be 0°C, we would not notice its subtraction from the other temperatures.

This solution offered a number of advantages over the dimensional solution. For one thing, it permitted us to plot *all* conceivable solutions for a particular shape of cylinder, (r_o/r_i), in a single figure, Fig. 2.13. For another, it allowed us to study the simultaneous roles of $\overline{h}$, k and r_o in defining the character of the solution. By combining them as a Biot number, we were able to say—even before we had solved the problem—whether or not external convection really had to be considered.

The nondimensionalization made it possible for us to consider, simultaneously, the behavior of all *similar* systems of heat conduction through cylinders. Thus a large, highly conducting cylinder might be *similar* in its behavior to a small cylinder with a lower thermal conductivity.

Finally, we shall discover that, by nondimensionalizing a problem *before* we solve it, we can often greatly simplify the process of solving it.

Our next aim is to map out a method for nondimensionalization problems before we have solved then, or, indeed, before we have even written the equations that must be solved. The key to the method is a result called the *Buckingham pi-theorem*.

The Buckingham pi-theorem

The attention of scientific workers was apparently drawn very strongly toward the question of similarity at about the beginning of World War I. Buckingham first organized previous thinking and developed his famous theorem in 1914 in the *Physical Review* [4.2], and he expanded upon the idea in the *Transactions of the ASME* one year later [4.3]. Lord Rayleigh almost simultaneously discussed the problem with great clarity in 1915 [4.4]. To understand Buckingham's theorem, we must first overcome one conceptual hurdle, which, if it is clear to the student, will make everything that follows extremely simple. Let us explain that hurdle first.

Suppose that y depends on r, x, z and so on:

$$y = y(r, x, z, \dots)$$

We can take any one variable—say, x—and arbitrarily multiply it (or it raised to a power) by any other variables in the equation, without altering the truth of the functional equation, like this:

$$\frac{y}{x} = \frac{y}{x}\left(x^2 r, x, xz\right)$$

To see that this is true, consider an arbitrary equation:

$$y = y(r, x, z) = r(\sin x)e^{-z}$$

This need only be rearranged to put it in terms of the desired modified variables and x itself ($y/x, x^2r, x,$ and xz):

$$\frac{y}{x} = \frac{x^2 r}{x^3} (\sin x) \exp\left[-\frac{xz}{x}\right]$$

We can do any such multiplying or dividing of powers of any variable we wish without invalidating any functional equation that we choose to write. This simple fact is at the heart of the important example that follows:

Example 4.2

Consider the heat exchanger problem described in Fig. 3.15. The "unknown," or dependent variable, in the problem is either of the exit temperatures. Without any knowledge of heat exchanger analysis, we can write the functional equation on the basis of our physical understanding of the problem:

$$\underbrace{T_{c_{\text{out}}} - T_{c_{\text{in}}}}_{^\circ\text{C}} = \text{fn}\left[\underbrace{C_{\max}}_{\text{W}/^\circ\text{C}}, \underbrace{C_{\min}}_{\text{W}/^\circ\text{C}}, \underbrace{(T_{h_{\text{in}}} - T_{c_{\text{in}}})}_{^\circ\text{C}}, \underbrace{U}_{\text{W/m}^2\cdot^\circ\text{C}}, \underbrace{A}_{\text{m}^2}\right] \tag{4.14}$$

where the dimensions of each term are noted under the quotation.

We want to know how many dimensionless groups the variables in eqn. (4.14) should reduce to. To determine this number, we use the idea explained above—that is, that we can arbitrarily pick one variable from the equation and divide or multiply it into other variables. Then—one at a time—we select a variable that has one of the dimensions. We divide or multiply it by the other variables in the equation that have that dimension in such a way as to eliminate the dimension from them.

We do this first with the variable $(T_{h_{\text{in}}} - T_{c_{\text{in}}})$, which has the dimension of °C.

$$\underbrace{\frac{T_{c_{\text{out}}} - T_{c_{\text{in}}}}{T_{h_{\text{in}}} - T_{c_{\text{in}}}}}_{\text{dimensionless}} = \text{fn}\left[\underbrace{C_{\max}(T_{h_{\text{in}}} - T_{c_{\text{in}}})}_{\text{W}}, \underbrace{C_{\min}(T_{h_{\text{in}}} - T_{c_{\text{in}}})}_{\text{W}}, \underbrace{(T_{h_{\text{in}}} - T_{c_{\text{in}}})}_{^\circ\text{C}}, \underbrace{U(T_{h_{\text{in}}} - T_{c_{\text{in}}})}_{\text{W/m}^2}, \underbrace{A}_{\text{m}^2}\right]$$

The interesting thing about the equation in this form is that the only remaining term in it with the units of °C is $(T_{h_{\text{in}}} - T_{c_{\text{in}}})$. No such term *can* exist in the equation because it is impossible to achieve dimensional homogeneity without another term in °C to balance it. Therefore, we must remove it.

$$\underbrace{\frac{T_{c_{\text{out}}} - T_{c_{\text{in}}}}{T_{h_{\text{in}}} - T_{c_{\text{in}}}}}_{\text{dimensionless}} = \text{fn}\left[\underbrace{C_{\max}(T_{h_{\text{in}}} - T_{c_{\text{in}}})}_{\text{W}}, \underbrace{C_{\min}(T_{h_{\text{in}}} - T_{c_{\text{in}}})}_{\text{W}}, \underbrace{U(T_{h_{\text{in}}} - T_{c_{\text{in}}})}_{\text{W/m}^2}, \underbrace{A}_{\text{m}^2}\right]$$

Now the equation has only two dimensions in it—W and m^2. Next, we multiply $U(T_{h_{\text{in}}} - T_{c_{\text{in}}})$ by A to get rid of m^2 in the second-to-last term. Accordingly, the term A (m^2) can no longer stay in the equation, and we have

$$\underbrace{\frac{T_{c_{\text{out}}} - T_{c_{\text{in}}}}{T_{h_{\text{in}}} - T_{c_{\text{in}}}}}_{\text{dimensionless}} = \text{fn}\left[\underbrace{C_{\max}(T_{h_{\text{in}}} - T_{c_{\text{in}}})}_{\text{W}}, \underbrace{C_{\min}(T_{h_{\text{in}}} - T_{c_{\text{in}}})}_{\text{W}}, \underbrace{UA(T_{h_{\text{in}}} - T_{c_{\text{in}}})}_{\text{W}},\right]$$

Next, we divide the first and third terms on the right by the second. This leaves only $C_{\min}(T_{h_{\text{in}}} - T_{c_{\text{in}}})$, with the dimensions of W. That term must then be removed, and we are left with the completely dimensionless result:

$$\frac{T_{c_{\text{out}}} - T_{c_{\text{in}}}}{T_{h_{\text{in}}} - T_{c_{\text{in}}}} = \text{fn}\left(\frac{C_{\max}}{C_{\min}}, \frac{UA}{C_{\min}}\right) \tag{4.15}$$

■

Equation (4.15) has exactly the same functional form as eqn. (3.21), which we obtained by direct analysis.

Notice that we removed one variable from eqn. (4.14) for each dimension in which the variables are expressed. If there are n variables—including the dependent variable—expressed in m dimensions, we then expect to be able to express the equation in $(n - m)$ dimensionless groups, or *pi-groups*, as Buckingham called them.

This fact is expressed by the *Buckingham pi-theorem*, which we state formally in the following way:

> A physical relationship among n variables, which can be expressed in *a minimum* of m dimensions, can be rearranged into a relationship among $(n-m)$ *independent* dimensionless groups of the original variables.

Two important qualifications have been italicized. They will be explained in detail in subsequent examples.

Buckingham called the dimensionless groups pi-groups and identified them as $\Pi_1, \Pi_2, ..., \Pi_{n-m}$. Normally we call Π_1 the dependent variable and retain $\Pi_{2\to(n-m)}$ as independent variables. Thus, the dimension*al* functional equation reduces to a dimension*less* functional equation of the form

$$\Pi_1 = \text{fn}\,(\Pi_2, \Pi_3, \ldots, \Pi_{n-m}) \tag{4.16}$$

Applications of the pi-theorem

Example 4.3

Is eqn. (2.24) consistent with the pi-theorem?

SOLUTION. To find out, we first write the dimensional functional equation for Example 2.6:

$$\underbrace{T - T_i}_{^\circ\text{C}} = \text{fn}\Big[\underbrace{r}_{\text{m}}, \underbrace{r_i}_{\text{m}}, \underbrace{r_o}_{\text{m}}, \underbrace{\overline{h}}_{\text{W/m}^2\cdot{}^\circ\text{C}}, \underbrace{k}_{\text{W/m}\cdot{}^\circ\text{C}}, \underbrace{(T_\infty - T_i)}_{^\circ\text{C}}\Big]$$

There are seven variables ($n = 7$) in three dimensions, °C, m, and W ($m = 3$). Therefore, we look for $7 - 3 = 4$ pi-groups. There *are* four pi-groups in eqn. (2.24):

$$\Pi_1 = \frac{T - T_i}{T_\infty - T_i}, \quad \Pi_2 = \frac{r}{r_i}, \quad \Pi_3 = \frac{r_o}{r_i}, \quad \Pi_4 = \frac{\overline{h} r_o}{k} \equiv \text{Bi}. \qquad \blacksquare$$

Consider two features of this result. First, the minimum number of dimensions was three. If we had written watts as J/s, we would have had four dimensions instead. But Joules never appear in that particular problem independently of seconds. They always appear as a ratio and should not be separated. (If we had worked in English units, this would have seemed more confusing, since there is no name for Btu/sec unless

we first convert it to horsepower.) The failure to identify dimensions that are consistently grouped together is one of the major errors that the beginner makes in using the pi-theorem.

The second feature is the *independence* of the groups. This means that we may pick any four dimensionless arrangements of variables, so long as no group or groups can be made into any other group by mathematical manipulation. For example, suppose that someone suggested that there was a fifth pi-group in Example 4.3:

$$\Pi_5 = \sqrt{\frac{\bar{h}r}{k}}$$

It is easy to see that Π_5 can be written as

$$\Pi_5 = \sqrt{\frac{\bar{h}r_o}{k}}\sqrt{\frac{r}{r_i}}\sqrt{\frac{r_i}{r_o}} = \sqrt{\mathrm{Bi}\,\frac{\Pi_2}{\Pi_3}}$$

Therefore Π_5 is not independent of the existing groups, nor will we ever find a fifth grouping that is.

Another matter that is frequently made much of is that of identifying the pi-groups once the variables are identified for a given problem. (The method of indices [4.1] is a cumbersome arithmetic strategy for doing this but it is perfectly correct.) We shall find the groups by using either of two methods:

1. The groups can always be obtained formally by repeating the simple elimination-of-dimensions procedure that was used to derive the pi-theorem in Example 4.2.

2. One may simply arrange the variables into the required number of independent dimensionless groups by inspection.

In any method, one must make judgments in the process of combining variables and these decisions can lead to different arrangements of the pi-groups. Therefore, if the problem can be solved by inspection, there is no advantage to be gained by the use of a more formal procedure.

The methods of dimensional analysis can be used to help find the solution of many physical problems. We offer the following example, not entirely with tongue in cheek:

Example 4.4

Einstein might well have noted that the energy equivalent, e, of a rest

mass, m_o, depended on the velocity of light, c_o, before he developed the special relativity theory. He wold then have had the following dimensional functional equation:

$$\left(e \ \text{N}\cdot\text{m} \quad \text{or} \quad e \ \frac{\text{kg}\cdot \text{m}^2}{\text{s}^2}\right) = \text{fn}\,(c_o \ \text{m/s},\ m_o \ \text{kg})$$

The minimum number of dimensions is only two: kg and m/s, so we look for $3 - 2 = 1$ pi-group. To find it formally, we eliminated the dimension of mass from e by dividing it by m_o (kg). Thus,

$$\frac{e}{m_o}\ \frac{\text{m}^2}{\text{s}^2} = \text{fn}\Big[\ c_o \ \text{m/s},\ \underbrace{m_o \ \text{kg}}_{\substack{\text{this must be removed}\\ \text{because it is the only}\\ \text{term with mass in it}}}\ \Big]$$

Then we eliminate the dimension of velocity (m/s) by dividing e/m_o by c_o^2:

$$\frac{e}{m_o c_o^2} = \text{fn}\,(c_o \ \text{m/s})$$

This time c_o must be removed from the function on the right, since it is the only term with the dimensions m/s. This gives the result (which could have been written by inspection once it was known that there could only be one pi-group):

$$\Pi_1 = \frac{e}{m_o c_o^2} = \text{fn}\,(\text{no other groups}) = \text{constant}$$

or

$$e = \text{constant} \cdot \left(m_o c_o^2\right)$$

Of course, it required Einstein's relativity theory to tell us that the constant is unity. ■

Example 4.5

What is the velocity of efflux of liquid from the tank shown in Fig. 4.4?

SOLUTION. In this case we can guess that the velocity, V, might depend on gravity, g, and the head H. We might be tempted to include

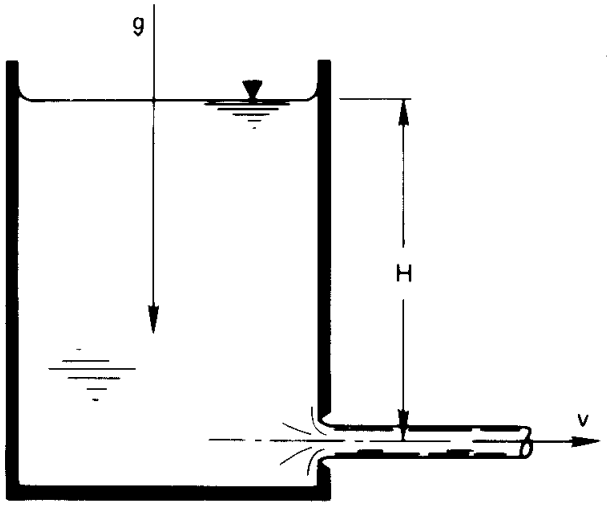

Figure 4.4 Efflux of liquid from a tank.

the density as well until we realize that g is already a *force per unit mass*. To understand this, we can use English units and divide g by the conversion factor,[4] g_c. Thus $(g \text{ ft/s}^2)/(g_c \text{ lb}_\text{m}\cdot\text{ft/lb}_\text{f} \text{ s}^2) = g \text{ lb}_\text{f}/\text{lb}_\text{m}$. Then

$$\underbrace{V}_{\text{m/s}} = \text{fn}\left[\underbrace{H}_{\text{m}}, \underbrace{g}_{\text{m/s}^2}\right]$$

so there are three variables in two dimensions, and we look for $3-2=1$ pi-groups. It would have to be

$$\Pi_1 = \frac{V}{\sqrt{gH}} = \text{fn (no other pi-groups)} = \text{constant}$$

or

$$V = \text{constant} \cdot \sqrt{gH}$$

The analytical study of fluid mechanics tells us that this form is correct and that the constant is $\sqrt{2}$. The group V^2/gh, by the way, is called a *Froude number*, Fr (pronounced "Frood"). It compares inertial forces to gravitational forces. Fr is about 1000 for a pitched baseball, and it is between 1 and 10 for the water flowing over the spillway of a dam. ■

[4] One can always divide any variable by a conversion factor without changing it.

Example 4.6

Obtain the dimensionless functional equation for the temperature distribution during steady conduction in a slab with a heat source, $\dot{q}$.

SOLUTION. In such a case, there might be one or two specified temperatures in the problem: T_1 or T_2. Thus the dimensional functional equation is

$$\underbrace{T - T_1}_{^\circ\mathrm{C}} = \mathrm{fn}\left[\underbrace{(T_2 - T_1)}_{^\circ\mathrm{C}}, \underbrace{x, L}_{\mathrm{m}}, \underbrace{\dot{q}}_{\mathrm{W/m^3}}, \underbrace{k}_{\mathrm{W/m\cdot{}^\circ C}}, \underbrace{\overline{h}}_{\mathrm{W/m^2\cdot{}^\circ C}}\right]$$

where we presume that a convective b.c. is involved and we identify a characteristic length, L, in the x-direction. There are seven variables in three dimensions, or $7 - 3 = 4$ pi-groups. Three of these groups are ones we have dealt with in the past in one form or another:

$$\Pi_1 = \frac{T - T_1}{T_2 - T_1} \qquad \text{dimensionless temperature, which we shall give the name } \Theta$$

$$\Pi_2 = \frac{x}{L} \qquad \text{dimensionless length, which we call } \xi$$

$$\Pi_3 = \frac{\overline{h}L}{k} \qquad \text{which we recognize as the Biot number, Bi}$$

The fourth group is new to us:

$$\Pi_4 = \frac{\dot{q}L^2}{k(T_2 - T_1)} \qquad \text{which compares the heat generation rate to the rate of heat loss; we call it } \Gamma$$

Thus, the solution is

$$\Theta = \mathrm{fn}\,(\xi, \mathrm{Bi}, \Gamma) \tag{4.17}$$

■

In Example 2.1, we undertook such a problem, but it differed in two respects. There was no convective boundary condition and hence, no $\overline{h}$, and only one temperature was specified in the problem. In this case, the dimensional functional equation was

$$(T - T_1) = \mathrm{fn}\,(x, L, \dot{q}, k)$$

so there were only five variables in the same three dimensions. The resulting dimensionless functional equation therefore involved only two

pi-groups. One was $\xi = x/L$ and the other is a new one equal to Θ/Γ. We call it Φ:

$$\Phi \equiv \frac{T - T_1}{\dot{q}L^2/k} = \text{fn}\left(\frac{x}{L}\right) \tag{4.18}$$

And this is exactly the form of the analytical result, eqn. (2.15).

Finally, we must deal with dimensions that convert into one another. For example, kg and N are defined in terms of one another through Newton's Second Law of Motion. Therefore, they cannot be identified as separate dimensions. The same would appear to be true of J and N·m, since both are dimensions of energy. However, we must discern whether or not a mechanism exists for interchanging them. If mechanical energy remains distinct from thermal energy in a given problem, then J should not be interpreted as N·m.

This issue will prove important when we do the dimensional analysis of several heat transfer problems. See, for example, the analyses of laminar convection problem at the beginning of Section 6.4, of natural convection in Section 8.3, of film condensation in Section 8.5, and of pool boiling burnout in Section 9.3. In all of these cases, heat transfer normally occurs without any conversion of heat to work or work to heat and it would be misleading to break J into N·m.

Additional examples of dimensional analysis appear throughout this book. Dimensional analysis is, indeed, our court of first resort in solving most of the new problems that we undertake.

4.4 An illustration of the use of dimensional analysis in a complex steady conduction problem

Heat conduction problems with convective boundary conditions can rapidly grow difficult, even if they start out simple, and so we look for ways to avoid making mistakes. For one thing, it is wise to take great care that dimensions are consistent at each stage of the solution. The best way to do this, and to eliminate a great deal of algebra at the same time, is to nondimensionalize the heat conduction equation before we apply the b.c.'s. This nondimensionalization should be consistent with the pi-theorem. We illustrate this idea with a fairly complex example.

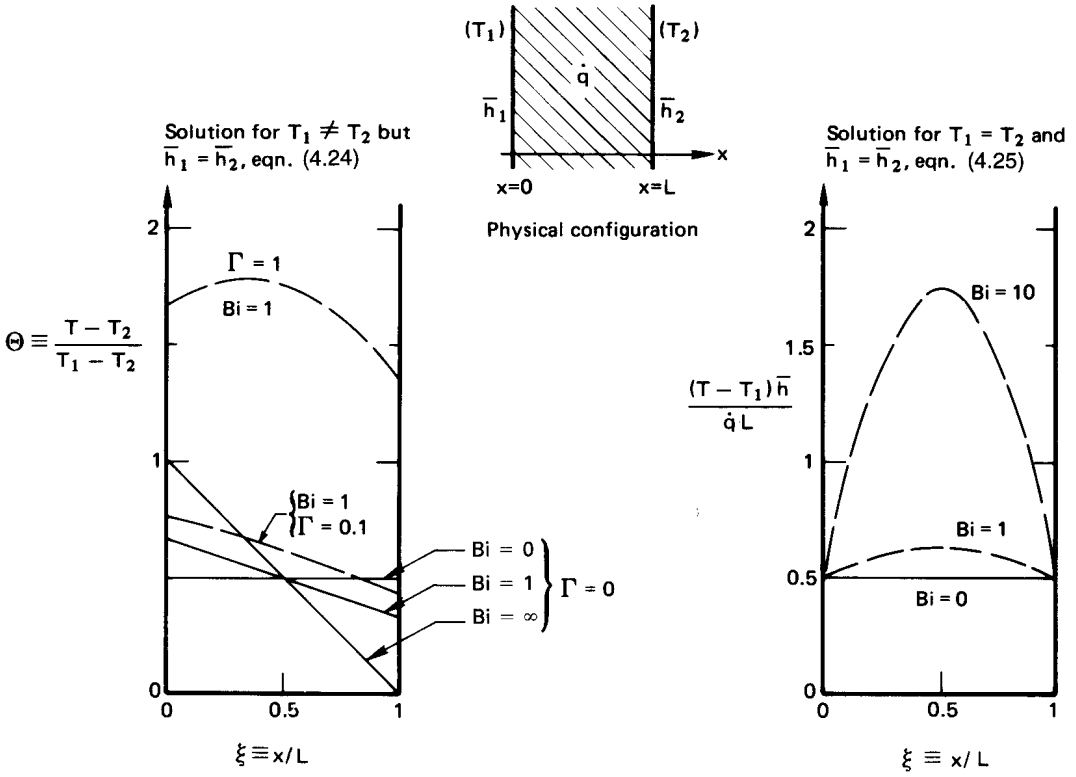

Figure 4.5 Heat conduction through a heat-generating slab with asymmetric boundary conditions.

Example 4.7

A slab shown in Fig. 4.5 has different temperatures and different heat transfer coefficients on either side and the heat is generated within it. Calculate the temperature distribution in the slab.

SOLUTION. The differential equation is

$$\frac{d^2T}{dx^2} = -\frac{\dot{q}}{k}$$

and the general solution is

$$T = -\frac{\dot{q}x^2}{2k} + C_1x + C_2 \tag{4.19}$$

with b.c.'s

$$\overline{h}_1(T_1 - T)_{x=0} = -k\left.\frac{dT}{dx}\right|_{x=0}, \qquad \overline{h}_2(T - T_2)_{x=L} = -k\left.\frac{dT}{dx}\right|_{x=L}. \tag{4.20}$$

There are eight variables involved in the problem: $(T - T_2)$, $(T_1 - T_2)$, x, L, k, $\overline{h}_1$, $\overline{h}_2$, and $\dot{q}$; and there are three dimensions: °C , W, and m. This results in $8 - 3 = 5$ pi-groups. For these we choose

$$\Pi_1 \equiv \Theta = \frac{T - T_2}{T_1 - T_2}, \qquad \Pi_2 \equiv \xi = \frac{x}{L}, \qquad \Pi_3 \equiv \mathrm{Bi}_1 = \frac{\overline{h}_1 L}{k},$$

$$\Pi_4 \equiv \mathrm{Bi}_2 = \frac{\overline{h}_2 L}{k}, \qquad \text{and} \qquad \Pi_5 \equiv \Gamma = \frac{\dot{q}L^2}{2k(T_1 - T_2)},$$

where Γ can be interpreted as a comparison of the heat generated in the slab to that which could flow through it.

Under this nondimensionalization, eqn. (4.19) becomes[5]

$$\Theta = -\Gamma\,\xi^2 + C_3\xi + C_4 \tag{4.21}$$

and b.c.'s become

$$\mathrm{Bi}_1(1 - \Theta_{\xi=0}) = -\Theta'_{\xi=0}, \qquad \mathrm{Bi}_2\Theta_{\xi=1} = -\Theta'_{\xi=1} \tag{4.22}$$

where the primes denote differentiation with respect to ξ. Substituting eqn. (4.21) in eqn. (4.22), we obtain

$$\mathrm{Bi}_1(1 - C_4) = -C_3, \qquad \mathrm{Bi}_2(-\Gamma + C_3 + C_4) = 2\Gamma - C_3. \tag{4.23}$$

Substituting the first of eqns. (4.23) in the second we get

$$C_4 = 1 + \frac{-\mathrm{Bi}_1 + 2(\mathrm{Bi}_1/\mathrm{Bi}_2)\Gamma + \mathrm{Bi}_1\Gamma}{\mathrm{Bi}_1 + \mathrm{Bi}_1^2/\mathrm{Bi}_2 + \mathrm{Bi}_1^2}$$

$$C_3 = \mathrm{Bi}_1(C_4 - 1)$$

Thus, eqn. (4.21) becomes

$$\Theta = 1 + \Gamma\left[\frac{2(\mathrm{Bi}_1/\mathrm{Bi}_2) + \mathrm{Bi}_1}{1 + \mathrm{Bi}_1/\mathrm{Bi}_2 + \mathrm{Bi}_1}\xi - \xi^2 + \frac{2(\mathrm{Bi}_1/\mathrm{Bi}_2) + \mathrm{Bi}_1}{\mathrm{Bi}_1 + \mathrm{Bi}_1^2/\mathrm{Bi}_2 + \mathrm{Bi}_1^2}\right] - \frac{\mathrm{Bi}_1}{1 + \mathrm{Bi}_1/\mathrm{Bi}_2 + \mathrm{Bi}_1}\xi - \frac{\mathrm{Bi}_1}{\mathrm{Bi}_1 + \mathrm{Bi}_1^2/\mathrm{Bi}_2 + \mathrm{Bi}_1^2} \tag{4.24}$$

■

[5]The rearrangement of the dimensional equations into dimensionless form is straightforward algebra. If the results shown here are not immediately obvious to you, sketch the calculation on a piece of paper.

This is a complicated result and one that would have required enormous patience and accuracy to obtain without first simplifying the problem statement as we did. If the heat transfer coefficients were the same on either side of the wall, then $\mathrm{Bi}_1 = \mathrm{Bi}_2 \equiv \mathrm{Bi}$, and eqn. (4.24) would reduce to

$$\Theta = 1 + \Gamma\left(\xi - \xi^2 + 1/\mathrm{Bi}\right) - \frac{\xi + 1/\mathrm{Bi}}{1 + 2/\mathrm{Bi}} \tag{4.25}$$

which is a very great simplification.

Equation (4.25) is plotted on the left-hand side of Fig. 4.5 for Bi equal to 0, 1, and ∞ and for Γ equal to 0, 0.1, and 1. The following features should be noted:

- When $\Gamma \ll 0.1$, the heat generation can be ignored.
- When $\Gamma \gg 1, \Theta \to \Gamma/\mathrm{Bi} + \Gamma(\xi - \xi^2)$. This is a simple parabolic temperature distribution displaced upward an amount that depends on the relative external resistance, as reflected in the Biot number.
- If both Γ and $1/\mathrm{Bi}$ become large, $\Theta \to \Gamma/\mathrm{Bi}$. This means that when internal resistance is low and the heat generation is great, the slab temperature is constant and quite high.

If T_2 were equal to T_1 in this problem, Γ would go to infinity. In such a situation, we should redo the dimensional analysis of the problem. The dimensional functional equation now shows $(T - T_1)$ to be a function of x, L, k, $\overline{h}$, and $\dot{q}$. There are six variables in three dimensions, so there are three pi-groups

$$\frac{T - T_1}{\dot{q}L/h} = \mathrm{fn}\,(\xi, \mathrm{Bi})$$

where the dependent variable is like Φ [recall eqn. (4.18)] multiplied by Bi. We can put eqn. (4.25) in this form by multiplying both sides of it by $\overline{h}(T_1 - T_2)/\dot{q}\delta$. The result is

$$\frac{\overline{h}(T - T_1)}{\dot{q}L} = \frac{1}{2}\mathrm{Bi}\left(\xi - \xi^2\right) + \frac{1}{2} \tag{4.26}$$

The result is plotted on the right-hand side of Fig. 4.5. The following features of the graph are of interest:

- Heat generation is the only "force" giving rise to temperature nonuniformity. Since it is symmetric, the graph is also symmetric.

- When Bi $\ll$ 1, the slab temperature approaches a uniform value equal to $T_1 + \dot{q}L/2h$. (In this case, we would have solved the problem with far greater ease by using a simple lumped-capacity heat balance, since it is no longer a heat conduction problem.)

- When Bi > 100, the temperature distribution is a very large parabola with ½ added to it. In this case, the problem could have been solved using boundary conditions of the first kind because the surface temperature stays very close to T_∞ (recall Fig. 1.11).

4.5 Fin design

The purpose of fins

The convective removal of heat from a surface can be substantially improved if we put extensions on that surface to increase its area. These extensions can take a variety of forms. Figure 4.6, for example, shows many different ways in which the surface of commercial heat exchanger tubing can be extended with protrusions of a kind we call *fins*.

Figure 4.7 shows another very interesting application of fins in a heat exchanger design. This picture is taken from an issue of *Science* magazine [4.5], which presents an intriguing argument by Farlow, Thompson, and Rosner. They offered evidence suggesting that the strange rows of fins on the back of the *Stegosaurus* were used to shed excess body heat after strenuous activity, which is consistent with recent suspicions that *Stegosaurus* was warm-blooded.

These examples involve some rather complicated fins. But the analysis of a straight fin protruding from a wall displays the essential features of all fin behavior. This analysis has direct application to a host of problems.

Analysis of a one-dimensional fin

The equations. Figure 4.8 shows a one-dimensional fin protruding from a wall. The wall—and the roots of the fin—are at a temperature T_0, which is either greater or less than the ambient temperature, T_∞. The length of the fin is cooled or heated through a heat transfer coefficient, $\overline{h}$, by the ambient fluid. The heat transfer coefficient will be assumed uniform, although (as we see in Part III) that can introduce serious error in boil-

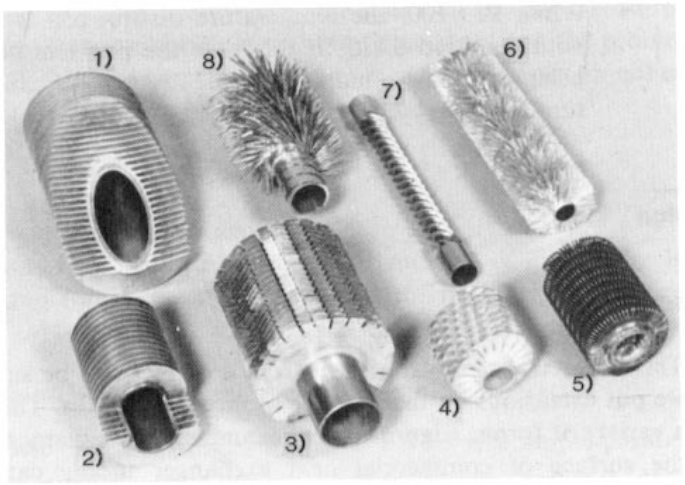

a) Eight examples of externally finned tubing.
1) and 2) Typical commercial circular fins of constant thickness;
3) and 4) Serrated circular fins and dimpled spirally-wound circular fins, both intended to improve convection.
5) Spirally-wound copper coils outside and inside.
6) and 8) Bristle fins, spirally wound and machined from base metal.
7) A spirally indented tube to improve convection as well as to increase surface area.

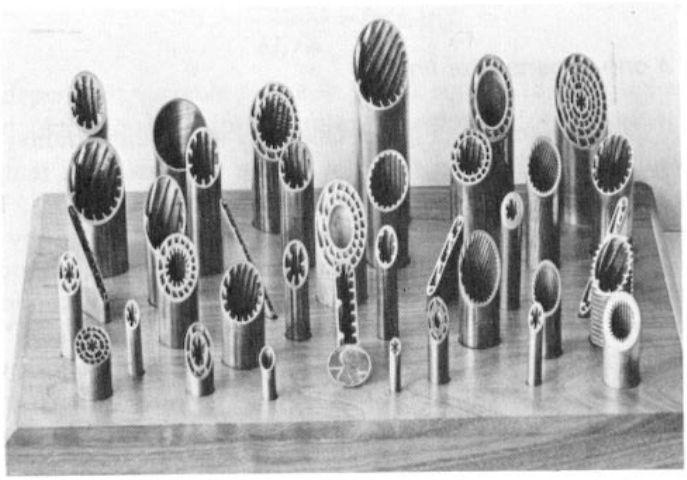

b) An array of commercial internally finned tubing (photo courtesy of Noranda Metal Industries, Inc.)

Figure 4.6 Some of the many varieties of finned tubes.

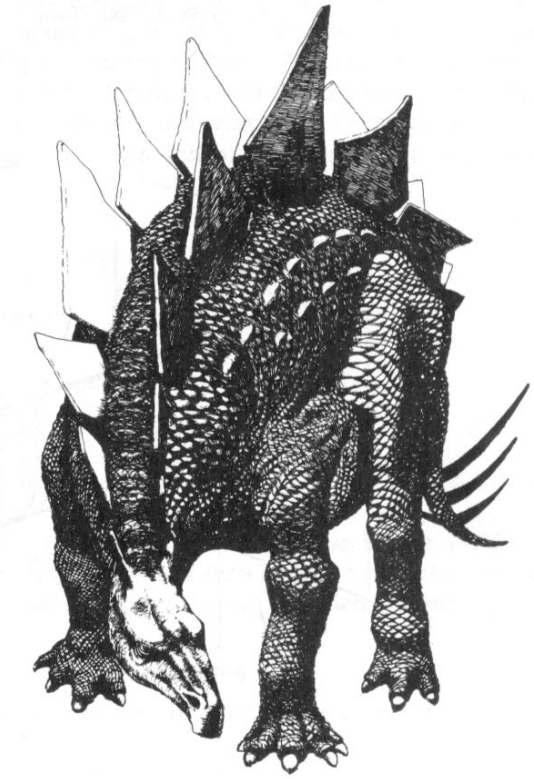

Figure 4.7 The Stegosaurus with what might have been cooling fins (etching by Daniel Rosner).

ing, condensing, or other natural convection situations, and will not be strictly accurate even in forced convection.

The tip may or may not exchange heat with the surroundings through a heat transfer coefficient, $\overline{h}_L$, which would generally differ from $\overline{h}$. The length of the fin is L, its uniform cross-sectional area is A, and its circumferential perimeter is P.

The characteristic dimension of the fin in the transverse direction (normal to the x-axis) is taken to be A/P. Thus, for a circular cylindrical fin, $A/P = \pi(\text{radius})^2/(2\pi \text{ radius}) = (\text{radius}/2)$. We define a Biot number for conduction in the transverse direction, based on this dimension, and require that it be small:

$$\text{Bi}_{\text{fin}} = \frac{\overline{h}(A/P)}{k} \ll 1 \tag{4.27}$$

This condition means that the transverse variation of T at any axial position, x, is much less than $(T_{\text{surface}} - T_\infty)$. Thus, $T \simeq T(x \text{ only})$ and the

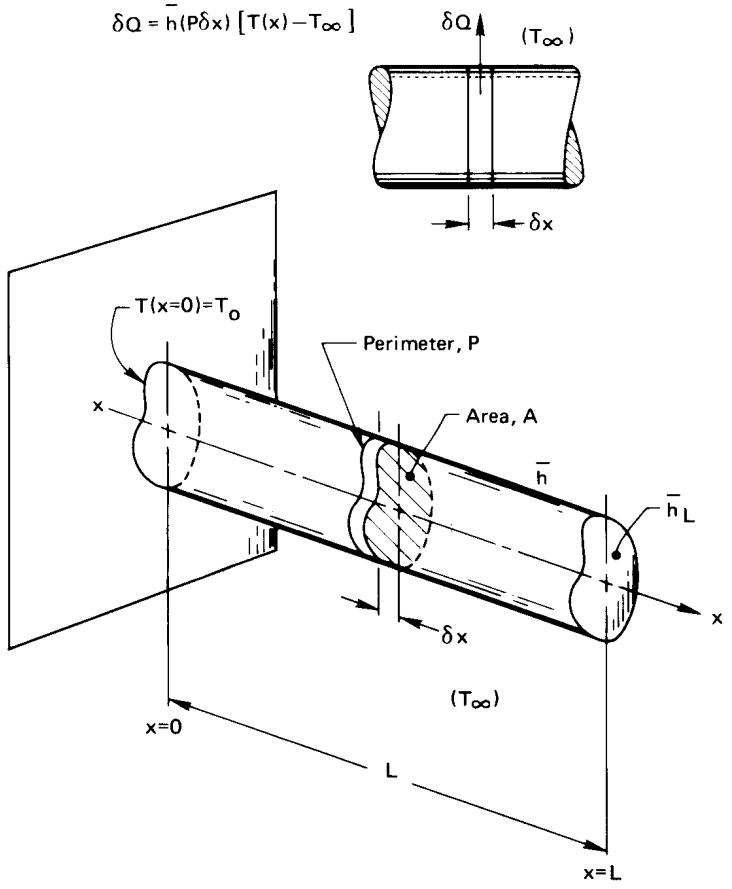

Figure 4.8 The analysis of a one-dimensional fin.

heat flow can be treated as one-dimensional.

An energy balance on the thin slice of the fin shown in Fig. 4.8 gives

$$-kA\left.\frac{dT}{dx}\right|_{x+\delta x} + kA\left.\frac{dT}{dx}\right|_{x} + \overline{h}(P\delta x)(T-T_\infty)_x = 0 \tag{4.28}$$

but

$$\frac{dT/dx|_{x+\delta x} - dT/dx|_x}{\delta x} \longrightarrow \frac{d^2T}{dx^2} = \frac{d^2(T-T_\infty)}{dx^2} \tag{4.29}$$

so

$$\frac{d^2(T-T_\infty)}{dx^2} = \frac{\overline{h}P}{kA}(T-T_\infty) \tag{4.30}$$

The b.c.'s for this equation are

$$\begin{aligned}(T-T_\infty)_{x=0} &= T_0 - T_\infty \\ -kA\left.\frac{d(T-T_\infty)}{dx}\right|_{x=L} &= \overline{h}_L A (T-T_\infty)_{x=L}\end{aligned} \tag{4.31a}$$

Alternatively, if the tip is insulated, or if we can guess that $\overline{h}_L$ is small enough to be unimportant, the b.c.'s are

$$(T-T_\infty)_{x=0} = T_0 - T_\infty \quad \text{and} \quad \left.\frac{d(T-T_\infty)}{dx}\right|_{x=L} = 0 \tag{4.31b}$$

Before we solve this problem, it will pay to do a dimensional analysis of it. The dimensional functional equation is

$$T - T_\infty = \text{fn}\left[(T_0 - T_\infty), x, L, kA, \overline{h}P, \overline{h}_L A\right] \tag{4.32}$$

Notice that we have written kA, $\overline{h}P$, and $\overline{h}_L A$ as single variables. The reason for doing so is subtle but important. Setting $h(A/P)/k \ll 1$, erases any geometric detail of the cross section from the problem. The *only* place where P and A enter the problem is as product of $k, \overline{h}$, or $\overline{h}_L$. If they showed up elsewhere, they would have to do so in a physically incorrect way. Thus, we have just seven variables in W, °C, and m. This gives four pi-groups if the tip is uninsulated:

$$\frac{T-T_\infty}{T_0-T_\infty} = \text{fn}\left(\frac{x}{L}, \sqrt{\frac{\overline{h}P}{kA}L^2}, \underbrace{\frac{\overline{h}_L AL}{kA}}_{=\overline{h}_L L/k}\right)$$

or if we rename the groups,

$$\Theta = \text{fn}\,(\xi, mL, \text{Bi}_{\text{axial}}) \tag{4.33a}$$

where we call $\sqrt{\overline{h}PL^2/kA} \equiv mL$ because that terminology is common in the literature on fins.

If the tip of the fin is insulated, $\overline{h}_L$ will not appear in eqn. (4.32). There is one less variable but the same number of dimensions; hence, there will be only three pi-groups. The one that is removed is Bi_{axial}, which involves $\overline{h}_L$. Thus, for the insulated fin,

$$\Theta = \text{fn}(\xi, mL) \tag{4.33b}$$

We put eqn. (4.30) in these terms by multiplying it by $L^2/(T_0 - T_\infty)$. The result is

$$\boxed{\frac{d^2\Theta}{d\xi^2} = (mL)^2\Theta} \tag{4.34}$$

This equation is satisfied by $\Theta = Ce^{\pm(mL)\xi}$. The sum of these two solutions forms the general solution of eqn. (4.34):

$$\boxed{\Theta = C_1 e^{mL\xi} + C_2 e^{-mL\xi}} \tag{4.35}$$

Temperature distribution in a one-dimensional fin with the tip insulated The b.c.'s [eqn. (4.31b)] can be written as

$$\Theta_{\xi=0} = 1 \quad \text{and} \quad \left.\frac{d\Theta}{d\xi}\right|_{\xi=1} = 0 \tag{4.36}$$

Substituting eqn. (4.35) into both eqns. (4.36), we get

$$C_1 + C_2 = 1 \qquad \text{and} \qquad C_1 e^{mL} - C_2 e^{-mL} = 0 \tag{4.37}$$

Mathematical Digression 4.1

To put the solution of eqn. (4.37) for C_1 and C_2 in the simplest form, we need to recall a few properties of hyperbolic functions. The four basic functions that we need are defined as

$$\begin{aligned} \sinh x &\equiv \frac{e^x - e^{-x}}{2} \\ \cosh x &\equiv \frac{e^x + e^{-x}}{2} \\ \tanh x &\equiv \frac{\sinh x}{\cosh x} = \frac{e^x - e^{-x}}{e^x + e^{-x}} \\ \coth x &\equiv \frac{e^x + e^{-x}}{e^x - e^{-x}} \end{aligned} \tag{4.38}$$

where x is the independent variable. Additional functions are defined by analogy to the trigonometric counterparts. The differential relations

can be written out formally, and they also resemble their trigonometric counterparts.

$$\begin{aligned} \frac{d}{dx}\sinh x &= \frac{1}{2}\left[e^{x} - (-e^{-x})\right] = \cosh x \\ \frac{d}{dx}\cosh x &= \frac{1}{2}\left[e^{x} + (-e^{-x})\right] = \sinh x \end{aligned} \tag{4.39}$$

These are analogous to the familiar results, $d\sin x/dx = \cos x$ and $d\cos x/dx = -\sin x$, but without the latter minus sign.

The solution of eqns. (4.37) is then

$$C_1 \frac{e^{-mL}}{2\cosh mL} \quad \text{and} \quad C_2 = 1 - \frac{e^{-ml}}{2\cosh mL} \tag{4.40}$$

Therefore, eqn. (4.35) becomes

$$\Theta = \frac{e^{-mL(1-\xi)} + (2\cosh mL)e^{-mL\xi} - e^{-mL(1+\xi)}}{2\cosh mL}$$

which simplifies to

$$\boxed{\Theta = \frac{\cosh mL(1-\xi)}{\cosh mL}} \tag{4.41}$$

for a one-dimensional fin with its tip insulated.

One of the most important design variables for a fin is the rate at which it removes (or delivers) heat the wall. To calculate this, we write Fourier's law for the heat flow into the base of the fin:[6]

$$Q = -kA\left.\frac{d(T - T_\infty)}{dx}\right|_{x=0} \tag{4.42}$$

We multiply eqn. (4.42) by $L/kA(T - T_\infty)$ and obtain, after substituting eqn. (4.41) on the right-hand side,

$$\frac{QL}{kA(T_0 - T_\infty)} = mL\frac{\sinh mL}{\cosh mL} = mL\tanh mL \tag{4.43}$$

[6]We could also integrate $\overline{h}(T - T_\infty)$ over the outside area of the fin to get Q. The answer would be the same, but the calculation would be a little more complicated.

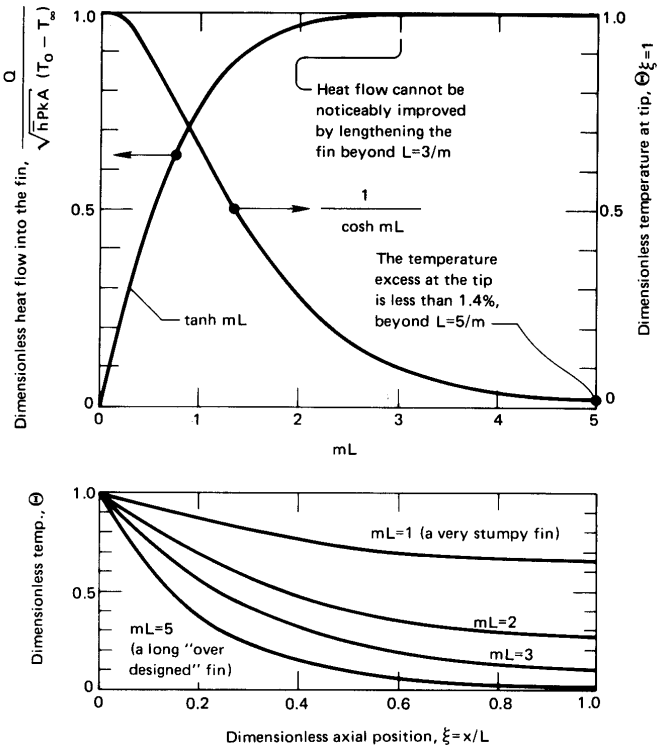
Dimensionless heat flow into the fin, $\frac{Q}{\sqrt{\bar{h}PkA}\,(T_0 - T_\infty)}$
Heat flow cannot be noticeably improved by lengthening the fin beyond L=3/m
$\frac{1}{\cosh mL}$
The temperature excess at the tip is less than 1.4%, beyond L=5/m
tanh mL
Dimensionless temperature at tip, $\Theta_{\xi=1}$
mL
Dimensionless temp., Θ
mL=1 (a very stumpy fin)
mL=2
mL=3
mL=5 (a long "over designed" fin)
Dimensionless axial position, ξ=x/L

Figure 4.9 The temperature distribution, tip temperature, and heat flux in a straight one-dimensional fin with the tip insulated.

which can be written

$$\frac{Q}{\sqrt{(kA)(\bar{h}P)}(T_0 - T_\infty)} = \tanh mL \tag{4.44}$$

Figure 4.9 includes two graphs showing the behavior of one-dimensional fin with an insulated tip. The top graph shows how the heat removal increases with mL to a virtual maximum at $mL \simeq 3$. This means that no such fin should have a length in excess of $2/m$ or $3/m$ if it is being used to cool (or heat) a wall. Additional length would simply increase the cost without doing any good.

Also shown in the top graph is the temperature of the tip of such a fin. Setting $\xi = 1$ in eqn. (4.41), we discover that

$$\Theta_{\text{tip}} = \frac{1}{\cosh mL} \tag{4.45}$$

This dimensionless temperature drops to about 0.014 at the tip when mL reaches 5. This means that the end is $0.014(T_0 - T_\infty)$°C above T_∞ at the end. Thus, if the fin is actually functioning as a holder for a thermometer or a thermocouple that is intended to read T_∞, the reading will be in error if mL is not significantly greater than five.

The lower graph in Fig. 4.9 hows how the temperature is distributed in insulated-tip fins for various values of mL.

Experiment 4.1

Clamp a 20 cm or so length of copper rod by one end in a horizontal position. Put a candle flame very near the other end and let the arrangement come to a steady state. Run your finger along the rod. How does what you feel correspond to Fig. 4.9? (The diameter for the rod should not exceed about 3 mm. A larger rod of metal with a lower conductivity will also work.)

Exact temperature distribution in a fin with an uninsulated tip. The approximation of an insulated tip may be avoided using the b.c's given in eqn. (4.31a), which take the following dimensionless form:

$$\Theta_{\xi=0} = 1 \quad \text{and} \quad -\left.\frac{d\Theta}{d\xi}\right|_{\xi=1} = \text{Bi}_{\text{ax}}\Theta_{\xi=1} \tag{4.46}$$

Substitution of the general solution, eqn. (4.35), in these b.c.'s yields

$$\begin{aligned} C_1 + C_2 &= 1 \\ -mL(C_1 e^{mL} - C_2 e^{-mL}) &= \text{Bi}_{\text{ax}}(C_1 e^{mL} + C_2 e^{-mL}) \end{aligned} \tag{4.47}$$

It requires some manipulation to solve eqn. (4.47) for C_1 and C_2 and to substitute the results in eqn. (4.35). We leave this as an exercise (Problem 4.11). The result is

$$\Theta = \frac{\cosh mL(1-\xi) + (\text{Bi}_{\text{ax}}/mL)\sinh mL(1-\xi)}{\cosh mL + (\text{Bi}_{\text{ax}}/mL)\sinh mL} \tag{4.48}$$

which is the form of eqn. (4.33a), as we anticipated. The corresponding heat flux equation is

$$\frac{Q}{\sqrt{(kA)(\bar{h}P)}(T_0 - T_\infty)} = \frac{(\text{Bi}_{\text{ax}}/mL) + \tanh mL}{1 + (\text{Bi}_{\text{ax}}/mL)\tanh mL} \tag{4.49}$$

We have seen that mL is not too much greater than unity in a well-designed fin with an insulated tip. Furthermore, when $\overline{h}_L$ is small (as it might be in natural convection), Bi_{ax} is normally much less than unity. Therefore, in such cases, we expect to be justified in neglecting terms multiplied by Bi_{ax}. Then eqn. (4.48) reduces to

$$\Theta = \frac{\cosh mL(1-\xi)}{\cosh mL} \tag{4.41}$$

which we obtained by analyzing an insulated fin.

It is worth pointing out that we are in serious difficulty if $\overline{h}_L$ is so large that we cannot assume the tip to be insulated. The reason is that $\overline{h}_L$ is nearly impossible to predict in most practical cases.

Example 4.8

A 2 cm diameter aluminum rod with $k = 205$ W/m°C, 8 cm in length, protrudes from a 150°C wall. Air at 26°C flows by it, and $\overline{h} = 120$ W/m°C. Determine whether or not tip conduction is important in this problem. To do this, make the very crude assumption that $\overline{h} \simeq \overline{h}_L$. Then compare the tip temperatures as calculated with and without considering heat transfer from the tip.

SOLUTION.

$$mL = \sqrt{\frac{\overline{h}PL^2}{kA}} = \sqrt{\frac{120(0.08)^2}{205(0.01/2)}} = 0.8656$$

$$\text{Bi}_{\text{ax}} = \frac{\overline{h}L}{k} = \frac{120(0.08)}{205} = 0.0468$$

Therefore, eqn. (4.48) becomes

$$\Theta\,(\xi = 1) = \Theta_{\text{tip}} = \frac{\cosh 0 + (0.0468/0.8656)\sinh 0}{\cosh(0.8656) + (0.0468/0.8656)\sinh(0.8656)}$$

$$= \frac{1}{1.3986 + 0.0529} = 0.6886$$

so the exact tip temperature is

$$T_{\text{tip}} = T_\infty + 0.6886(T_0 - T_\infty)$$

$$= 26 + 0.6886(150 - 26) = 111.43°\text{C}$$

Equation (4.41) or Fig. 4.9, on the other hand, gives

$$\Theta_{\text{tip}} = \frac{1}{1.3986} = 0.7150$$

so the approximate tip temperature is

$$T_{\text{tip}} = 26 + 0.715(150 - 26) = 114.66^\circ\text{C}$$

Thus the insulated-tip approximation is adequate for the computation in this case. ■

Very long fin. If a fin is so long that $mL \gg 1$, then eqn. (4.41) becomes

$$\lim_{mL\to\infty} \Theta = \lim_{mL\to\infty} \frac{e^{mL(1-\xi)} + e^{-mL(1-\xi)}}{e^{mL} + e^{-mL}} = \frac{e^{mL(1-\xi)}}{e^{mL}}$$

or

$$\lim_{mL\to\text{large}} \Theta = e^{-mL\xi} \tag{4.50}$$

Substituting this result in eqn. (4.42), we obtain [cf. eqn. (4.44)]

$$Q = \sqrt{(kA)(\bar{h}P)}(T_0 - T_\infty) \tag{4.51}$$

A heating or cooling fin would have to be terribly overdesigned for these results to apply—that is, mL would have been made much larger than necessary. Very long fins are common, however, in a variety of situations related to undesired heat losses. In practice, a fin may be regarded as "infinitely long" in computing its temperature if $mL \gtrsim 5$; in computing Q, $mL \gtrsim 3$ is sufficient for the infinite fin approximation.

Physical significance of mL. The group mL has thus far proved to be extremely useful in the analysis and design of fins. We should therefore say a brief word about its physical significance. Notice that

$$(mL)^2 = \frac{L/kA}{1/\bar{h}(PL)} = \frac{\text{internal resistance in } x\text{-direction}}{\text{gross external resistance}}$$

Thus $(mL)^2$ is a hybrid Biot number. When it is big, $\Theta|_{\xi=1} \to 0$ and we can neglect tip convection. When it is small, the temperature drop along the axis of the fin becomes small (see the lower graph in Fig. 4.9).

The group $(mL)^2$ also has a peculiar similarity to the NTU (Chapter 3) and the dimensionless time, $t/\boldsymbol{T}$, that appears in the lumped-capacity solution (Chapter 1). Thus,

$$\frac{\overline{h}(PL)}{kA/L} \quad \text{is like} \quad \frac{UA}{C_{\min}} \quad \text{is like} \quad \frac{\overline{h}A}{\rho cV/t}$$

In each case a convective heat rate is compared with a heat rate that characterizes the capacity of a system; and in each case the system temperature asymptotically approaches its limit as the numerator becomes large. This was true in eqn. (1.22), eqn. (3.21), eqn. (3.22), and eqn. (4.50).

The problem of specifying the root temperature

Thus far, we have assmed the root temperature of a fin to be given information. There really are many circumstances in which it might be known; however, if a fin protrudes from a wall of the same material, as sketched in Fig. 4.10a, it is clear that for heat to flow, there must be a temperature gradient in the neighborhood of the root.

Consider the situation in which the surface of a wall is kept at a temperature T_s. Then a fin is placed on the wall as shown in the figure. If $T_\infty < T_s$, the wall temperature will be depressed in the neighborhood of the root as heat flows into the fin. The fin's performance should then be predicted using the lowered root temperature, T_{root}.

This heat conduction problem has been analyzed for several fin arrangements by Sparrow and co-workers. Fig. 4.10b is the result of Sparrow and Hennecke's [4.6] analysis for a single circular cylinder. They give

$$1 - \frac{Q_{\text{actual}}}{Q_{\text{no temp. depression}}} = \frac{T_s - T_{\text{root}}}{T_s - T_\infty} = \text{fn}\left[\frac{\overline{h}r}{k}, (mr)\tanh(mL)\right] \tag{4.52}$$

where r is the radius of the fin. From the figure we see that the actual heat flux into the fin, Q_{actual}, and the actual root temperature are both reduced when the Biot number, $\overline{h}r/k$, is large and the fin constant, m, is small.

Example 4.9

Neglect the tip convection from the fin in Example 4.8 and suppose that it is embedded in a wall of the same material. Calculate the error in Q and the actual temperature of the root if the wall is kept at 150°C.

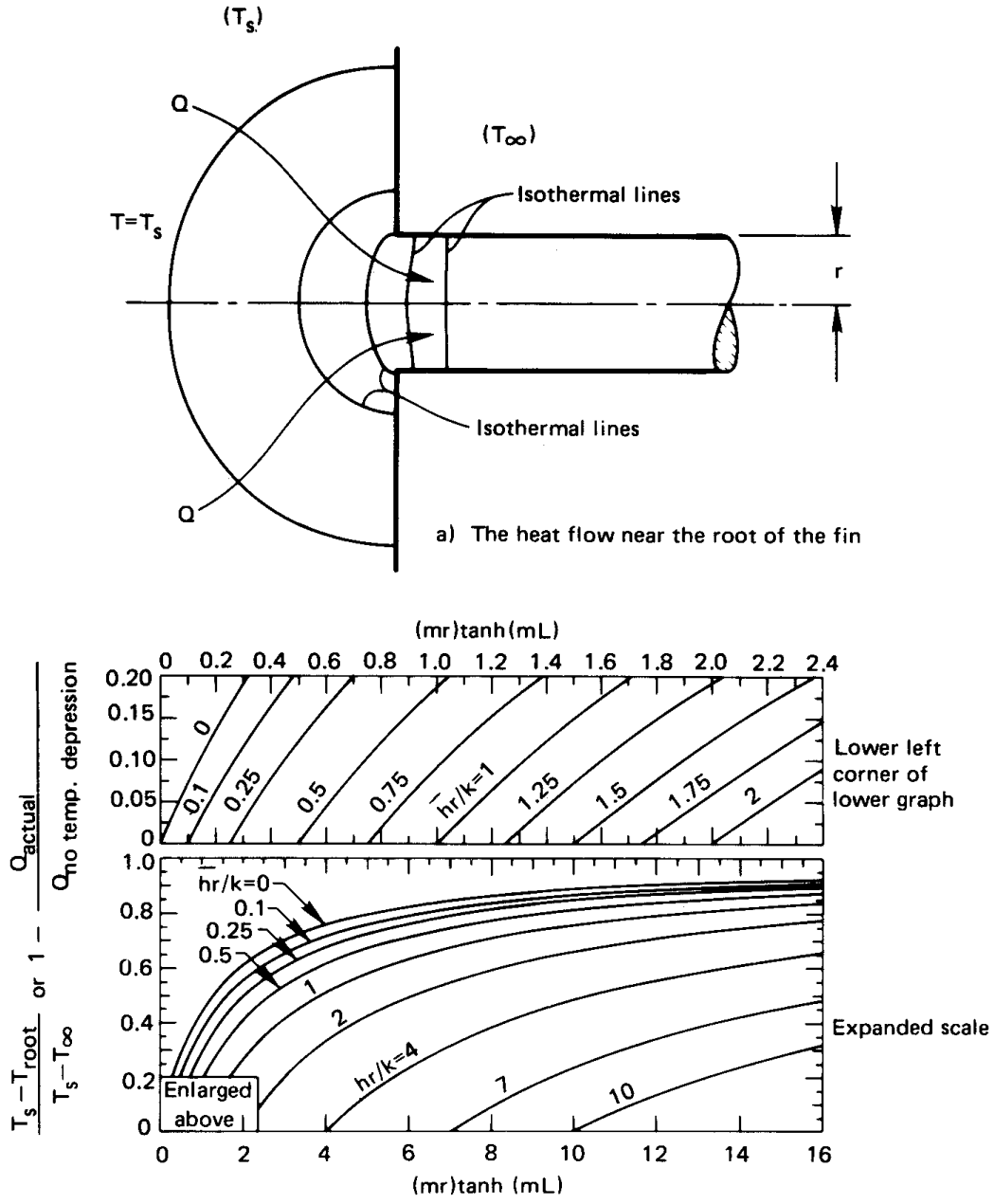

Figure 4.10 The influence of heat flow into the root of circular cylindrical fins [4.6].

SOLUTION. From Example 4.8 we have $mL = 0.8656$ and $\bar{h}r/k = 120(0.010)/205 = 0.00586$. Then, with $mr = mL(r/L)$, we have $(mr)\tanh(mL) = 0.8656(0.010/0.080)\tanh(0.8656) = 0.0756$. The lower portion of Fig. 4.10b then gives

$$1 - \frac{Q_{\text{actual}}}{Q_{\text{no temp. depression}}} = \frac{T_s - T_{\text{root}}}{T_s - T_\infty} = 0.05$$

so the heat flow is reduced by 5% and the actual root temperature is

$$T_{\text{root}} = 150 - (150 - 26)0.05 = 143.8^\circ\text{C}$$

The correction is modest in this case. ■

Fin design

Two basic measures of fin performance are particularly useful in a fin design. The first is called the *efficiency*, η_f.

$$\eta_f \equiv \frac{\text{actual heat transferred by a fin}}{\text{heat that would be transferred if the entire fin were at } T = T_0} \tag{4.53}$$

To see how this works, we evaluate η_f for a one-dimensional fin with an insulated tip:

$$\eta_f = \frac{\sqrt{(\bar{h}P)(kA)}(T_0 - T_\infty)\tanh mL}{\bar{h}(PL)(T_0 - T_\infty)} = \frac{\tanh mL}{mL} \tag{4.54}$$

This says that, under the definition of efficiency, a very long fin will give $\tanh mL/mL \to 1/\text{large number}$, so the fin will be inefficient. On the other hand, the efficiency goes up to 100% as the length is reduced to zero, because $\tanh(mL)_{\text{small}} \to mL$. While a fin of zero length would accomplish litte, a fin of small m might be designed in order to keep the tip temperature near the root temperature; this, for example, is desirable if the fin is the tip of a soldering iron.

It is therefore clear that, while η_f provides some useful information as to how well a fin is contrived, it is not possible to design toward any particular value of η_f.

A second measure of fin performance is called the *effectiveness*, ε:

$$\varepsilon \equiv \frac{\text{heat flux from the wall with the fin}}{\text{heat flux from the wall without the fin}} \tag{4.55}$$

This can easily be computed from the efficiency:

$$\varepsilon = \eta_f \frac{\text{surface area of the fin}}{\text{cross-sectional area of the fin}} \tag{4.56}$$

Normally, we want the effectiveness to be as high as possible, But this can always be done by extending the length of the fin, and that—as we have seen—rapidly becomes a losing proposition.

The measures η_f and ε probably attract the interest of designers not because their absolute values guide the designs, but because they are useful in characterizing fins with more complex shapes. In such cases the solutions are often so complex that η_f and ε plots serve as labor-saving graphical solutions. We deal with some of these curves in the following section.

The design of a fin thus becomes an open-ended matter of optimizing, subject to many factors. Some of the factors that have to be considered include:

- The weight of material added by the fin. This might be a cost factor or it might be an important consideration in its own right.
- The possible dependence of $\overline{h}$ on $(T - T_\infty)$, flow velocity past the fin, or other influences.
- The influence of the fin (or fins) on the heat transfer coefficient, $\overline{h}$, as the fluid moves around it (or them).
- The geometric configuration of the channel that the fin lies in.
- The cost and complexity of manufacturing fins.
- The pressure drop introduced by the fins.

Fins of variable cross section

Let us consider what is involved is the design of a fin for which A and P are functions of x. Such a fin is shown in Fig. 4.11. We restrict our attention to fins for which

$$\frac{\overline{h}(A/P)}{k} \ll 1 \quad \text{and} \quad \frac{d(a/P)}{d(x)} \ll 1$$

so the heat flow will be approximately one-dimensional in x.

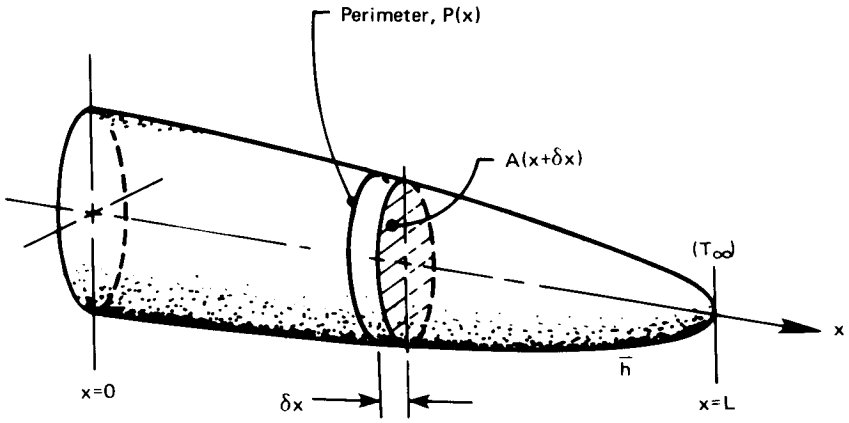

Figure 4.11 A general fin of variable cross section.

We begin the analysis, as always, with the First Law statement:

$$Q_{\text{net}} = Q_{\text{cond}} - Q_{\text{conv}} = \frac{dU}{dt}$$

or[7]

$$\underbrace{\left[kA(x+\delta x)\left.\frac{dT}{dx}\right|_{x=\delta x} - kA(x)\left.\frac{dT}{dx}\right|_{x}\right]}_{=\dfrac{d}{dx}kA(x)\dfrac{dT}{dx}\,\delta x} - \bar{h}P\,\delta x\,(T-T_\infty) = \underbrace{\rho c A(x)\delta x\frac{dT}{dt}}_{=0,\text{ since steady}}$$

Therefore,

$$\boxed{\frac{d}{dx}\left[A(x)\frac{d(T-T_\infty)}{dx}\right] - \frac{\bar{h}P}{k}(T-T_\infty) = 0} \tag{4.57}$$

If $A(x)$ = constant, this reduces to $\Theta'' - (mL)^2\Theta = 0$, which is the straight fin equation.

[7]Note that we approximate the external area of the fin as horizontal when we write it as $P\,\delta x$. The actual area is negligibly larger than this in most cases. An exception would be the tip of the fin in Fig. 4.11.

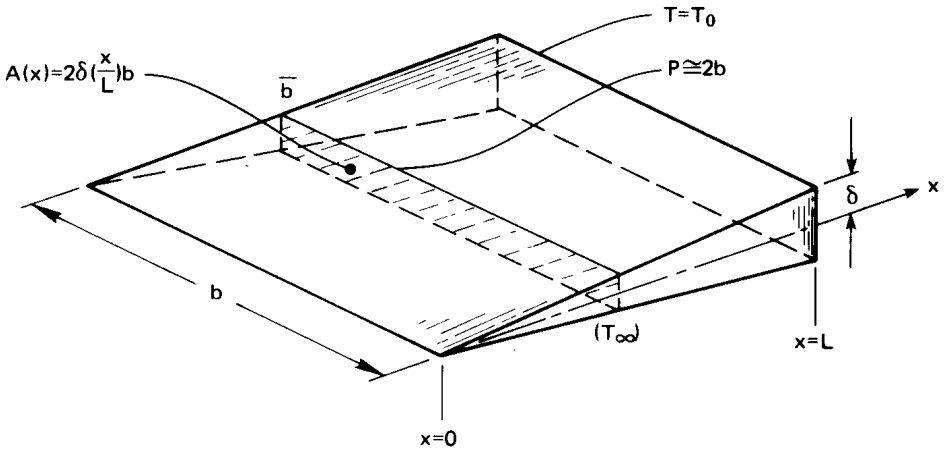

Figure 4.12 A two-dimensional wedge-shaped fin.

To see how eqn. (4.57) works, consider the triangular fin shown in Fig. 4.12. In this case eqn. (4.57) becomes

$$\frac{d}{dx}\left[2\delta\left(\frac{x}{L}\right)b\,\frac{d(T-T_\infty)}{dx}\right]-\frac{2\bar{h}b}{k}(T-T_\infty)=0$$

or

$$\xi\frac{d^2\Theta}{d\xi^2}+\frac{d\Theta}{d\xi}-\underbrace{\frac{\bar{h}L^2}{k\delta}}_{\substack{\text{a kind}\\ \text{of } (mL)^2}}\Theta=0 \tag{4.58}$$

This second-order linear differential equation is difficult to solve because it has a variable coefficient. Its solution is expressible in Bessel functions:

$$\Theta=\frac{I_o\left(2\sqrt{\bar{h}Lx/k\delta}\right)}{I_o\left(2\sqrt{\bar{h}L^2/k\delta}\right)} \tag{4.59}$$

where the modified Bessel function of the first kind, I_o, can be looked up in appropriate tables.

Rather than explore the mathematics of solving eqn. (4.57), we simply show the result for several geometries in terms of the fin efficiency, η_f, in Fig. 4.13. These curves were given by Schneider [4.7]. Kern and Kraus [4.8] provide a very complete discussion of fins and show a great many additional efficiency curves.

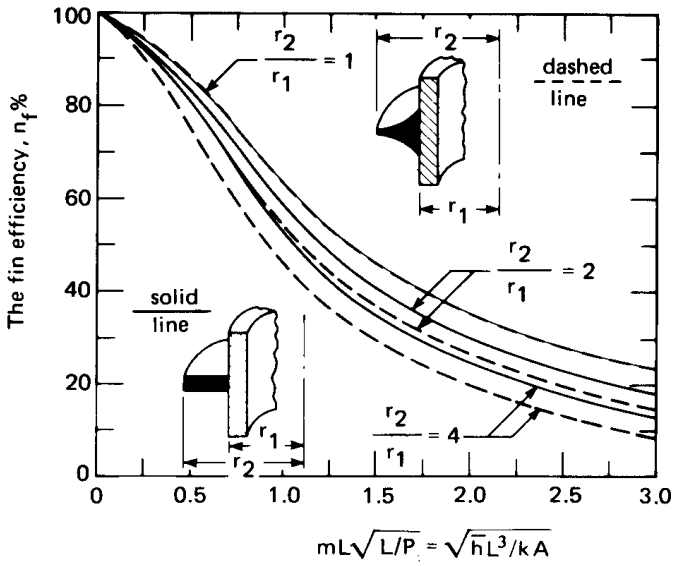

Comparison of a constant thickness circular fin, and a hyperbolic fin with thickness inversely proportional to radius. ($L \equiv r_2 - r_1$ and m is based on the area, A, shown in black.)

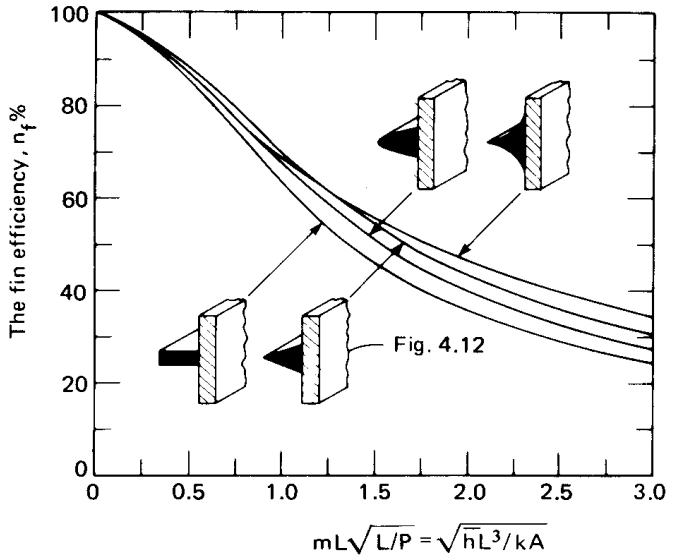

Comparison of four straight fins: constant thickness, triangular, parabolic, and hyperbolic. (m is based on A shown in black.)

Figure 4.13 The efficiency of several fins with variable cross section.

Example 4.10

A thin brass pipe, 3 cm in outside diameter, carries hot water at 85°C. It is proposed to place 0.8 mm thick straight circular fins on the pipe to cool it. The fins are 8 cm in diameter and are spaced 2 cm apart. It is determined that $\overline{h}$ will equal 20 W/m^2·°C on the pipe and 15 W/m^2·°C on the fins, when they have been added. If $T_\infty = 22°C$, compute the heat loss per meter of pipe before and after the fins are added.

SOLUTION. Before the fins are added,

$$Q = \pi(0.03\text{ m})(20\text{ W/m}^2\cdot°\text{C})(85-22)°\text{C} = 199\text{ W/m}$$

where we set $T_{\text{wall}} - T_{\text{water}}$ since the pipe is thin. Notice that, since the wall is constantly heated by the water, we should not have a root-temperature depression problem after the fins are added. Then we can enter Fig. 4.13a with

$$\frac{r_2}{r_1} = 2.67 \quad \text{and} \quad mL\sqrt{\frac{L}{P}} = \sqrt{\frac{\overline{h}L^3}{kA}} = \sqrt{\frac{15(0.04-0.15)^3}{125(0.025)(0.0008)}} = 0.306$$

and we obtain $\eta_f = 89\%$. Thus, the actual heat transfer given by

$$\underbrace{Q_{\text{without fin}}}_{119\text{ W/m}}\ \underbrace{\left(\frac{0.02-0.0008}{0.02}\right)}_{\text{fraction of unfinned area}} + 0.89\underbrace{[2\pi(0.04^2-0.015^2)]}_{\text{area per fin (both sides), m}^2}\left(50\frac{\text{fins}}{\text{m}}\right)\left(15\ \frac{\text{W}}{\text{m}^2\,°\text{C}}\right)[(85-22)°\text{C}]$$

so

$$Q_{\text{net}} = 478\text{ W/m} = 4.02\ Q_{\text{without fins}}$$ ■

Problems

4.1 Make a table listing the general solutions of all steady, unidimensional constant-properties heat conduction problemns in Cartesian, cylindrical and spherical coordinates, with and without uniform heat generation. This table should prove to be a

very useful tool in future problem solving. It should include a total of 18 solutions. State any restrictions on your solutions. Do not include calculations.

4.2 The left side of a slab of thickness L is kept at 0°C. The right side is cooled by air at T_∞°C blowing on it. $\overline{h}_{\text{RHS}}$ is known. An exothermic reaction takes place in the slab such that heat is generated at $A(T - T_\infty)$ W/m^3, where A is a constant. Find a fully dimensionless expression for the temperature distribution in the wall.

4.3 A long, wide plate of known size, material, and thickness L is connected across the terminals of a power supply and serves as a resistance heater. The voltage, current and T_∞ are known. The plate is insulated on the bottom and transfers heat out the top by convection. The temperature, T_{tc}, of the botton is measured with a thermocouple. Obtain expressions for (a) temperature distribution in the plate; (b) $\overline{h}$ at the top; (c) temperature at the top. (Note that your answers must depend on *known information* only.) [$T_{\text{top}} = T_{\text{tc}} - EIL^2/2k$ Vol.]

4.4 The heat tansfer coefficient, $\overline{h}$, resulting from a forced flow over a flat plate depends on the fluid velocity, viscosity, density, specific heat, and thermal conductivity, as well as on the length of the plate. Develop the dimensionless functional equation for the heat transfer coefficient (cf. Section 6.5).

4.5 Water vapor condenses on a cold pipe and drips off the bottom in regularly spaced nodes as sketched in Fig. 3.9. The wavelength of these nodes, λ, depends on the liquid-vapor density difference, $\rho_{\text{f}} - \rho_{\text{g}}$, the surface tension, σ, and the gravity, g. Find how λ varies with its dependent variables.

4.6 A thick film flows down a vertical wall. The local film velocity at any distance from the wall depends on that distance, gravity, the liquid kinematic viscosity, and the film thickness. Obtain the dimensionless functional equation for the local velocity (cf. Section 8.5).

4.7 A steam preheater consists of a thick, electrically conducting, cylindrical shell insulated on the outside, with wet stream flowing down the middle. The inside heat transfer coefficient is

highly variable, depending on the velocity, quality, and so on, but the flow temperature is constant. Heat is released at $\dot{q}$ J/m^{3}s within the cylinder wall. Evaluate the temperature within the cylinder as a function of position. Plot Θ against ρ, where Θ is an appropriate dimensionless temperature and $\rho = r/r_o$. Use $\rho_i = 2/3$ and note that Bi will be the parameter of a family of solutions. *On the basis of this plot*, recommend criteria (in terms of Bi) for (a) replacing the convective boundary condition on the inside with a constant temperature condition; (b) neglecting temperature variations within the cylinder.

4.8 Steam condenses on the inside of a small pipe, keeping it at a specified temperature, T_i. The pipe is heated by electrical resistance at a rate $\dot{q}$ W/m^3. The outside temperature is T_∞ and there is a natural convection heat transfer coefficient, $\overline{h}$ around the outside. (a) Derive an expression for the dimensionless expression temperature distribution, $\Theta = (T - T_\infty)/(T_i - T_\infty)$, as a function of the radius ratios, $\rho = r/r_o$ and $\rho_i = r_i/r_o$; a heat generation number, $\Gamma = \dot{q}r_o^2/k(T_i - T_\infty)$; and the Biot number. (b) Plot this result for the case $\rho_i = 2/3$, Bi = 1, and for several values of Γ. (c) Discuss any interesting aspects of your result.

4.9 Solve Problem 2.5 if you have not already done so, putting it in dimensionless form before you begin. Then let the Biot numbers approach infinity in the solution. You should get the same solution we got in Example 2.5, using b.c.'s of the first kind. Do you?

4.10 Complete the algebra that is missing between eqns. (4.30) and eqn. (4.31b) and eqn. (4.41).

4.11 Complete the algebra that is missing between eqns. (4.30) and eqn. (4.31a) and eqn. (4.48).

4.12 Obtain eqn. (4.50) from the general solution for a fin [eqn. (4.35)], using the b.c.'s $T(x = 0) = T_0$ and $T(x = L) = T_\infty$. Comment on the significance of the computation.

4.13 What is the minimum length, l, of a thermometer well necessary to ensure an error less than 0.5% of the difference between the pipe wall temperature and the temperature of fluid flowing in

a pipe? Assume that the fluid is steam at 260°C and that the coefficient between the steam and the tube wall is 300 W/m^2·°C. The well consists of a tube with the end closed. It has a 2 cm O.D. and a 1.88 cm I.D. The material is type 304 stainless steel. [3.44 cm.]

4.14 Thin fins with a 0.002 m by 0.02 m rectangular cross section and a thermal conductivity of 50 W/m^2·°C protrude from a wall and have $\overline{h} \simeq 600$ W/m^2·°C and $T_0 = 170$°C. What is the heat flow rate into each fin and what is the effectiveness? $T_\infty = 20$°C.

4.15 A thin rod is anchored at a wall at $T = T_0$ on one end and is insulated at the other end. Plot the dimensionless temperature distribution in the rod as a function of dimensionless length: (a) if the rod is exposed to an environment at T_∞ through a heat transfer coefficient; (b) if the rod is insulated but heat is removed from the fin material at the unform rate $-\dot{q} = \overline{h}P(T_0 - T_\infty)/A$. Comment on the implications of the comparison.

4.16 A tube of outside diameter d_o and inside diameter d_i carries fluid at $T = T_1$ from one wall at temperature T_1 to another wall a distance L away, at T_r. Outside the tube $\overline{h}_o$ is negligible, and inside the tube $\overline{h}_i$ is substantial. Treat the tube as a fin and plot the dimensionless temperature distribution in it as a function of dimensionless length.

4.17 (If you have had some applied mathematics beyond the usual two years of calculus, this problem will not be difficult.) The shape of the fin in Fig. 4.12 is changed so that $A(x) = 2\delta(x/L)^2 b$ instead of $2\delta(x/L)b$. Calculate the temperature distribution and the heat flux at the base. Plot the temperature distribution and fin thickness against x/L. Derive an expression for η_f.

4.18 Work Problem 2.21, if you have not already done so, nondimensionalizing the problem before you attempt to solve it. It should now be much simpler.

4.19 One end of a copper rod 30 cm long is held at 200°C, and the other end is held at 93°C. The heat transfer coefficient in between is 17 W/m^2·°C. If $T_\infty = 38$°C and the diameter of the rod is 1.25 cm, what is the net heat removed by the air around the rod? [19.13 W.]

4.20 How much error will the insulated-tip assumption give rise to in the calculation of the heat flow into the fin in Example 4.8?

4.21 A straight cylindrical fin 0.6 cm in diameter and 6 cm long protrudes from a magnesium block at 300°C. Air at 35°C is forced past the fin so that $\overline{h}$ is 130 W/m^2·°C. Calculate the heat removed by the fin, considering the temperature depression of the root.

4.22 Work Problem 4.19 considering the temperature depression in both roots. To do this, find mL for the two fins with insulated tips that would give the same temperature gradient at each wall. Base the correction on these values of mL.

4.23 A fin of triangular axial section (cf. Fig. 4.12) 0.1 m in length and 0.02 m wide at its base is used to extend the surface area of a mild steel wall. If the wall is at 40°C and heated gas flows past at 200°C ($\overline{h}$ = 230 W/m^2·°C), compute the heat removed by the fin per meter of breadth, b, of the fin. Neglect temperature distortion at the root.

4.24 Consider the concrete slab in Example 2.1. Suppose that the heat generation were to cease abruptly at time $t = 0$ and the slab were to start cooling back toward T_w. Predict $T = T_w$ as a function of time, noting that the intitial parabolic temperature profile can be nicely approximated as a sine function. (Without the sine approximation, this problem would require the series methods of Chapter 5.)

4.25 Steam condenses in a 2 cm I.D. thin-walled tube of 99% aluminum at 10 atm pressure. There are circular fins of constant thickness, 3.5 cm in diameter, every 0.5 cm. The fins are 0.8 mm thick and the heat transfer coefficient $\overline{h}$ = 6 W/m^2·°C on the outside. What is the mass rate of condensation if the pipe is 1.5 m in length, the ambient temperature is 18°C, and $\overline{h}$ for condensation is very large? [$\dot{m}_{\text{cond}}$ = 0.802 kg/hr.]

4.26 How long must a copper fin, 0.4 cm in diameter, be if the temperature of its insulated tip is to exceed the surrounding air temperature by 20% of $(T_0 - T_\infty)$? T_{air} = 20°C and $\overline{h}$ = 28 W/m^2·°C.

4.27 A 2 cm ice cube sits on a shelf of aluminum rods, 3 mm in diameter, in a refrigerator at 10°C. How rapidly, in mm/min, does the ice cube melt through the wires if $\overline{h}$ between the wires and the air is 10 W/m^2·°C. (Be sure that you understand the physical mechanism before you make the calculation.) Check your result experimentally. $h_{sf} = 333,300$ J/kg.

4.28 The highest heat flux that can be achieved in nucleate boiling (called q_{max}—see the qualitative discussion in Section 9.1) depends upon ρ_g, the saturated vapor density; h_{fg}, the latent heat vaporization; σ, the surface tension; a characteristic length, l; and the gravity force per unit volume, $g(\rho_f - \rho_g)$, where ρ_f is the saturated liquid density. Develop the dimensionless functional equation for q_{max} in terms of dimensionless length.

4.29 You want to rig a handle for a door in the wall of a furnace. The door is at 160°C. You consider bending a 16 in. length of ¼ in. mild steel rod into a U-shape and welding the ends to the door. Surrounding air at 24°C will cool the handle ($\overline{h} = 12$ W/m^2·°C). What is the coolest temperature of the handle? How close to the door can you grasp it without being burned? How might you improve the handle?

4.30 A 14 cm long by 1 cm square brass rod is supplied with 25 W at its base. The other end is insulated. It is cooled by air at 20°C, with $\overline{h} = 68$ W/m^2·°C. Develop a dimensionless expression for Θ as a function of ε and other known information. Calculate the base temperature.

4.31 A cylindrical fin has a constant imposed heat flux of q_1 at one end and q_2 at the other end, and it is cooled convectively along its length. Develop the dimensionless temperature distribution in the fin. Specialize this result for $q_2 = 0$ and $L \to \infty$, and compare it with eqn. (4.50).

4.32 A thin metal cylinder of radius r_o serves as an electrical resistance heater. The temperature along an axial line in one side is kept at T_1. Another line, θ_2 radians away, is kept at T_2. Develop dimensionless expressions for the temperature distributions in the two sections.

4.33 Heat transfer is augmented, in a particular heat exchanger, with a field of 0.007 m diameter fins protruding 0.02 m into a flow. The fins are arranged in a hexagonal array, with a minimum spacing of 1.8 cm. The fins are bronze, and $\overline{h}_f$ around the fins is 168 W/m^2·°C. On the wall itself, $\overline{h}_w$ is only 54 W/m^2·°C. Calculate $\overline{h}_{eff}$ for the wall with its fins. ($\overline{h}_{eff} = Q_{wall}$ divided by A_{wall} and $[T_{wall} - T_\infty]$.)

4.34 Evaluate $d(\tanh x)/dx$.

4.35 An engineer seeks to study the effect of temperature on the curing of concrete by controlling the temperature of curing in the following way. A sample slab of thickness L is subjected to a heat flux, q_w, on one side, and it is cooled to temperature T_1 on the other. Derive a dimensionless expression for the steady temperature in the slab. Plot the expression and offer a criterion for neglecting the internal heat generation in the slab.

4.36 Develop the dimensionless temperature distribution in a spherical shell with the inside wall kept at one temperature and the outside wall at a second temperature. Reduce your solution to the limiting cases in which $r_{outside} \gg r_{inside}$ and in which $r_{outside}$ is very close to r_{inside}. Discuss these limits.

4.37 Does the temperature distribution during steady heat transfer in an object with b.c.'s of only the first kind depend on k? Explain.

4.38 A long, 0.005 m diameter duralumin rod is wrapped with an electrical resistor over 3 cm of its length. The resistor imparts a surface flux of 40 kW/m^2. Evaluate the temperature of the rod in either side of the heated section if $\overline{h} = 150$ W/m^2·°C around the unheated rod, and $T_{ambient} = 27$°C.

4.39 The heat transfer coefficient between a cool surface and a saturated vapor, when the vapor condenses in a film on the surface, depends on the liquid density and specific heat, the temperature difference, the buoyant force per unit volume ($g[\rho_f - \rho_g]$), the latent heat, the liquid conductivity and the kinematic viscosity, and the position (x) on the cooler. Develop the dimensionless functional equation for $\overline{h}$.

4.40 A duralumin pipe through a cold room has a 4 cm I.D. and a 5 cm O.D. It carries water that sometimes sits stationary. It is proposed to put electric heating rings around the pipe to protect it against freezing during cold periods of $-7°C$. The heat transfer coefficient outside the pipe is 9 $W/m^{2}\cdot°C$. Neglect the presence of the water in the conduction calculation, and determine how far apart the heaters would have to be if they brought the pipe temperature to 40°C locally. How much heat do they require?

4.41 The specific entropy of an ideal gas depends on its specific heat at constant pressure, its temperature and pressure, the ideal gas constant and reference values of the temperature and pressure. Obtain the dimensionless functional equation for the specific entropy and compare it with the known equation.

References

[4.1] V. L. Streeter and E.B. Wylie. *Fluid Mechanics*. McGraw-Hill Book Company, New York, 7th edition, 1979. Chapter 4.

[4.2] E. Buckingham. *Phy. Rev.*, 4:345, 1914.

[4.3] E. Buckingham. Model experiments and the forms of empirical equations. *Trans. ASME*, 37:263–296, 1915.

[4.4] Lord Rayleigh, John Wm. Strutt. The principle of similitude. *Nature*, 95:66–68, 1915.

[4.5] J. O. Farlow, C. V. Thompson, and D. E. Rosner. Plates of the dinosaur stegosaurus: Forced convection heat loss fins? *Science*, 192(4244): 1123–1125 and cover, 1976.

[4.6] D. K. Hennecke and E. M. Sparrow. Local heat sink on a convectively cooled surface—application to temperature measurement error. *Int. J. Heat Mass Transfer*, 13:287–304, 1970.

[4.7] P. J. Schneider. *Conduction Heat Transfer*. Addison-Wesley Publishing Co., Inc., Reading, Mass., 1955.

[4.8] D. Q. Kern and A. D. Kraus. *Extended Surface Heat Transfer*. McGraw Hill Book Company, New York, 1972.

5. Transient and multidimensional heat conduction

When I was a lad, winter was really cold. It would get so cold that if you went outside with a cup of hot coffee it would freeze. I mean it would freeze fast. That cup of hot coffee would freeze so fast that it would still be hot after it froze. Now that's cold! ***Old North-woods tall-tale***

5.1 Introduction

James Watt, of course, did not invent the steam engine. What he did do was to eliminate a destructive transient heating and cooling process that wasted a great amount of energy. By 1763, the great puffing engines of Savery and Newcomen had been used for over half a century to pump the water out of Cornish mines and to do other tasks. In that year the young instrument maker, Watt, was called upon to renovate the Newcomen engine model at the University of Glasgow. The Glasgow engine was then being used as a demonstration in the course on natural philosophy. Watt did much more than just renovate the machine—he first recognized, and eventually eliminated, its major shortcoming.

The cylinder of Newcomen's engine was cold when steam entered it and nudged the piston outward. A great deal of steam was wastefully condensed on the cylinder walls until they were warm enough to accommodate it. When the cylinder was filled, the steam valve was closed and jets of water were activated inside the cylinder to cool it again and condense the steam. This created a powerful vacuum, which sucked the piston back in on its working stroke. First, Watt tried to eliminate the wasteful initial condensation of steam by insulating the cylinder. But that simply reduced the vacuum and cut the power of the working stroke.

Then he realized that, if he led the steam outside to a *separate condenser*, the cylinder could stay hot while the vacuum was created.

The separate condenser was the main issue in Watt's first patent (1769), and it immediately doubled the thermal efficiency of steam engines from a maximum of 1.1% to 2.2%. By the time Watt died in 1819, his invention had led to efficiencies of 5.7%, and his engine had altered the face of the world by powering the Industrial Revolution. And from 1769 until today, the steam power cycles that engineers study in their thermodynamics courses are accurately represented as steady flow—rather than transient—processes.

The repeated transient heating and cooling that occurred in Newcomen's engine was the kind of process that today's design engineer might still carelessly ignore, but the lesson that we learn from history is that transient heat transfer can be of overwhelming importance. Today, for example, designers of food storage enclosures know that such systems need relatively little energy to keep food cold at steady conditions. The real cost of operating them results from the consumption of energy needed to bring the food down to a low temperature and the losses resulting from people entering and leaving the system with food. The *transient* heat transfer processes are a dominant concern in the design of food storage units.

We therefore turn our attention, first, to an analysis of unsteady heat transfer, beginning with a more detailed consideration of the lumped-capacity system that we looked at in Section 1.3.

5.2 Lumped-capacity solutions

We begin by looking briefly at the dimensional analysis of transient conduction in general and of lumped-capacity systems in particular.

Dimensional analysis of transient heat conduction

We first consider a fairly representative problem of one-dimensional transient heat conduction:

$$\frac{\partial^2 T}{\partial x^2} = \frac{1}{\alpha}\frac{\partial T}{\partial t} \quad \text{with} \quad \begin{cases} \text{i.c.:} & T(t=0) = T_i \\ \text{b.c.:} & T(t>0, x=0) = T_1 \\ \text{b.c.:} & -k\left.\dfrac{\partial T}{\partial x}\right|_{x=L} = \overline{h}\,(T - T_1)_{x=L} \end{cases}$$

The solution of this problem must take the form of the following dimensional functional equation:

$$T - T = \text{fn}\left[(T_i - T_1), x, L, t, \alpha, \overline{h}, k\right]$$

There are eight variables in four dimensions (°C, s, m, W), so we look for $8 - 4 = 4$ pi-groups. We anticipate, from Section 4.3, that they will include

$$\Theta \equiv \frac{(T - T_1)}{(T_i - T_1)}, \quad \xi \equiv \frac{x}{L}, \quad \text{and Bi} \equiv \frac{\overline{h}L}{k},$$

and we write

$$\Theta = \text{fn}\,(\xi, \text{Bi}, \Pi_4) \tag{5.1}$$

One possible candidate for Π_4, which is independent of the other three, is

$$\Pi_4 \equiv \text{Fo} = \alpha t / L^2 \tag{5.2}$$

where Fo is the *Fourier number*. Another candidate that we use later is

$$\Pi_4 \equiv \zeta = \frac{x}{\sqrt{\alpha t}} \quad \left(\text{this is exactly } \frac{\xi}{\sqrt{\text{Fo}}}\right) \tag{5.3}$$

If the problem involved only b.c.'s of the first kind, the heat transfer coefficient, $\overline{h}$—and hence the Biot number—would go out of the problem. Then the dimensionless function eqn. (5.1) is

$$\Theta = \text{fn}\,(\xi, \text{Fo}) \tag{5.4}$$

By the same token, if the b.c.'s had introduced different values of $\overline{h}$ at $x = 0$ and $x = L$, *two* Biot numbers would appear in the solution.

The lumped-capacity problem is particularly interesting from the standpoint of dimensional analysis. In this case, neither k nor x enters the problem because we do not retain any features of the internal conduction problem. Therefore, we keep only the denominator of α, namely ρc. Furthermore, we do not have to separate ρ and c because they only appear as a product. Finally, we use the volume-to-external-area ratio, V/A, as a characteristic length. Thus, for the transient lumped-capacity problem, the dimensional equation is

$$T - T_\infty = \text{fn}\left[(T_i - T_\infty), \rho c, V/A, \overline{h}, t\right] \tag{5.5}$$

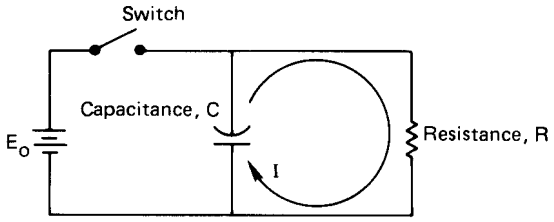

Figure 5.1 A simple resistance-capacitance circuit.

With six variables in the dimensions J, °C, m, and s, only two pi-groups will appear in the dimensionless function equation.

$$\Theta = \text{fn}\left(\frac{\overline{h}At}{\rho cV}\right) = \text{fn}\left(\frac{t}{\boldsymbol{T}}\right) \tag{5.6}$$

This is exactly the form of the simple lumped-capacity solution, eqn. (1.22). Notice, too, that the group $t/\boldsymbol{T}$ can be viewed as

$$\frac{t}{\boldsymbol{T}} = \frac{hk(V/A)t}{\rho c(V/A)^2 k} = \frac{\overline{h}(V/A)}{k} \cdot \frac{\alpha t}{(V/A)^2} = \text{Bi Fo} \tag{5.7}$$

Electrical and mechanical analogies to the lumped-thermal-capacity problem

The term *capacitance* is adapted from electrical circuit theory to the heat transfer problem. Therefore, we sketch a simple resistance-capacitance circuit in Fig. 5.1. The capacitor is initially charged to a voltage, E_o. When the switch is suddenly opened, the capacitor discharges through the resistor and the voltage drops according to the relation

$$\frac{dE}{dt} + \frac{E}{RC} = 0 \tag{5.8}$$

The solution of eqn. (5.8) with the i.c. $E(t = 0) = E_o$ is

$$E = E_o\, e^{-t/RC} \tag{5.9}$$

and the current can be computed from Ohm's law, once $E(t)$ is known.

$$I = \frac{E}{R} \tag{5.10}$$

Normally, in a heat conduction problem the *thermal* capacitance, ρcV, is distributed in space. But when the Biot number is small, $T(t)$

is uniform in the body and we can *lump* the capacitance into a single circuit element. The thermal resistance is $1/\overline{h}A$, and the temperature difference $(T - T_\infty)$ is analogous to $E(t)$. Thus, the thermal response, analogous to eqn. (5.9), is [see eqn. (1.22)]

$$T - T_\infty = (T_i - T_\infty) \exp\left(-\frac{\overline{h}At}{\rho cV}\right)$$

Notice that the electrical time constant, analogous to $\rho cV/\overline{h}A$, is RC.

Now consider a slightly more complex system. Figure 5.2 shows a spring-mass-damper system. The well-known response equation (actually, a force balance) for this system is

$$\underbrace{m}\frac{d^2x}{dt^2} + \underbrace{c}\frac{dx}{dt} + \underbrace{k}x = F(t) \qquad (5.11)$$

where k is analogous to $1/C$ or to $\overline{h}A$

the damping coefficient is analogous to R or to ρcV

What is the mass analogous to?

A term analogous to mass would arise from electrical inductance, but we

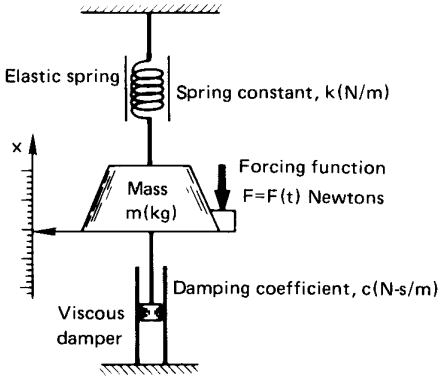

Figure 5.2 A spring-mass-damper system with a forcing function.

did not include it in the electrical circuit. Mass has the effect of carrying the system beyond its final equilibrium point. Thus, in an underdamped mechanical system, we might obtain the sort of response shown in Fig. 5.3 if we specified the velocity at $x = 0$ and provided no forcing function. Electrical inductance provides a similar effect. But the Second Law of Thermodynamics does not permit temperatures to overshoot their equilibrium values spontaneously. *There are no physical elements analogous to mass or inductance in thermal systems.*

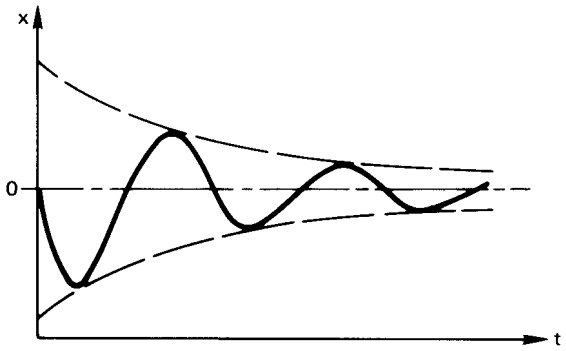

Figure 5.3 Response of an unforced spring-mass-damper system with an initial velocity.

Next, consider another mechanical element that does have a thermal analogy—namely, the forcing function, F. We consider a (massless) spring-damper system with a forcing function F that probably is time-dependent, and we ask: "What might a thermal forcing function look like?"

Lumped-capacity solution with a variable ambient temperature

To answer the preceding question, let us suddenly immerse an object at a temperature $T = T_i$, with Bi $\ll 1$, into a cool bath whose temperature is rising as $T_\infty(t) = T_i + bt$, where T_i and b are constants. Then eqn. (1.20) becomes

$$\frac{d(T - T_i)}{dt} = -\frac{T - T_\infty}{\boldsymbol{T}} = -\frac{T - T_i - bt}{\boldsymbol{T}}$$

where we have arbitrarily subtracted T_i under the differential. Then

$$\frac{d(T - T_i)}{dt} + \frac{T - T_i}{\boldsymbol{T}} = \frac{bt}{\boldsymbol{T}} \tag{5.12}$$

To solve eqn. (5.12) we must first recall that the general solution of a linear ordinary differential equation with constant coefficients is equal to the sum of any particular integral of the complete equation and the general solution of the homogeneous equation. We know the latter; it is $T - T_i = (\text{constant}) \exp(-t/\boldsymbol{T})$. A particular integral of the complete equation can often be formed by guessing solutions and trying them in the complete solution. Here we discover that

$$T - T_i = bt - b\boldsymbol{T}$$

satisfies eqn. (5.12). The general solution of the complete eqn. (5.12) is thus

$$T - T_i = C_1 e^{-t/\boldsymbol{T}} + b(t - \boldsymbol{T}) \tag{5.13}$$

Example 5.1

The flow rates of hot and cold water are regulated into a mixing chamber. We measure the temperature of the water as it leaves, using a thermometer with a time constant, $\boldsymbol{T}$. On a particular day, the system started with cold water at $T = T_i$ in the mixing chamber. Then hot water is added in such a way that the outflow temperature rises linearly, as shown in Fig. 5.4, with $T_{\text{exit flow}} = T_i + bt$. How will the thermometer report the temperature variation?

Solution. The initial condition in eqn. (5.13), which describes this process, is $T - T_i = 0$ at $t = 0$. Substituting eqn. (5.13) in the i.c., we get

$$0 = C_1 - b\boldsymbol{T} \quad \text{so} \quad C_1 = b\boldsymbol{T}$$

and the response equation is

$$T - (T_i + bt) = b\boldsymbol{T}\left(e^{-t/\boldsymbol{T}} - 1\right) \tag{5.14}$$

This result is graphically shown in Fig. 5.4. Notice that the thermometer reading reflects a transient portion, $b\boldsymbol{T}e^{-t/\boldsymbol{T}}$, which decays for a few time constants and then can be neglected, and a steady portion, $T_i + b(t - \boldsymbol{T})$, which persists thereafter. When the steady response is established, the thermometer follows the bath with a temperature lag of $b\boldsymbol{T}$. This constant error is reduced when either $\boldsymbol{T}$ or the rate of temperature increase, b, is reduced. ■

Second-order lumped-capacity systems

Now we look at situations in which two lumped-thermal-capacity systems are connected in series. Such an arrangement is shown in Fig. 5.5. Heat is transferred through two slabs with an interfacial resistance, h_c^{-1} between them. We shall require that $h_c L_1/k_1$, $h_c L_2/k_2$, and $\overline{h}L_2/k_2$ are all much less than unity so that it will be legitimate to lump the thermal capacitance of each slab. The differential equations dictating the temperature

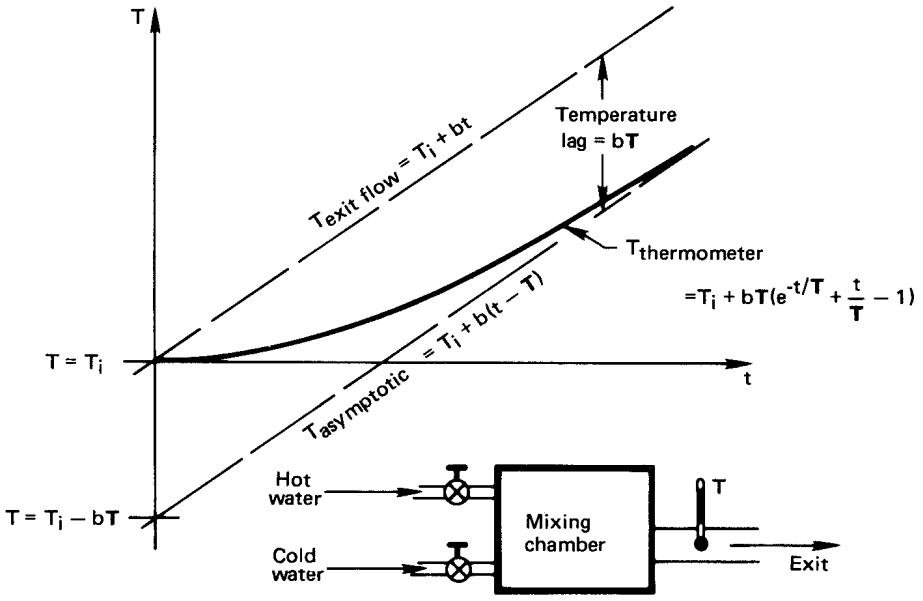

Figure 5.4 Response of a thermometer to a linearly increasing ambient temperature.

response of each slab are then

$$\text{slab 1}: \quad -(\rho cV)_1 \frac{dT_1}{dt} = h_c A(T_1 - T_2) \tag{5.15}$$

$$\text{slab 2}: \quad -(\rho cV)_2 \frac{dT_2}{dt} = \overline{h} A(T_2 - T_\infty) - h_c A(T_1 - T_2) \tag{5.16}$$

and the initial conditions on the temperatures T_1 and T_2 are

$$T_1(t = 0) = T_2(t = 0) = T_i \tag{5.17}$$

We next identify two time constants for this problem:[1]

$$\boldsymbol{T}_1 \equiv (\rho cV)_1 / h_c A \quad \text{and} \quad \boldsymbol{T}_2 \equiv (\rho cV)_2/ \overline{h} A$$

Then eqn. (5.15) becomes

$$T_2 = \boldsymbol{T}_1 \frac{dT_1}{dt} + T_1 \tag{5.18}$$

[1]Notice that we could also have used $(\rho cV)_2/h_c A$ for T_2 since both h_c and $\overline{h}$ act on slab 2. The choice is arbitrary.

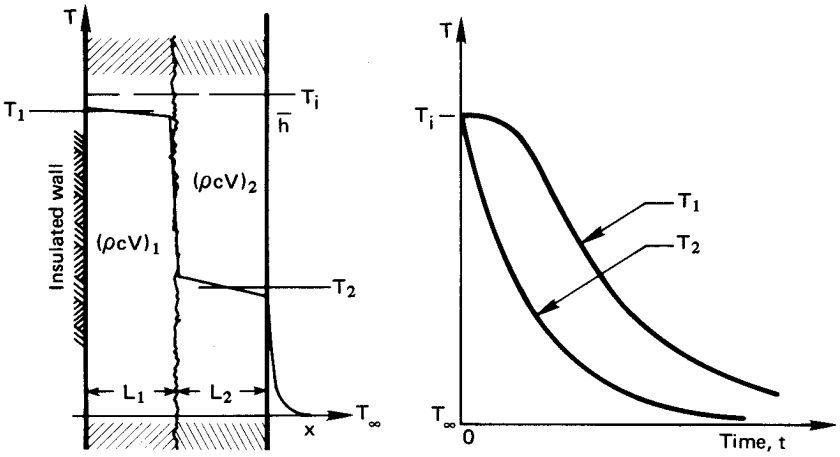

Figure 5.5 Two slabs conducting in series through an interfacial resistance.

which we substitute in eqn. (5.16) to get

$$\left(\boldsymbol{T}_1\frac{dT_1}{dt}+T_1-T_\infty\right)+\frac{h_c}{\overline{h}}\boldsymbol{T}_1\frac{dT_1}{dt}=\boldsymbol{T}_1\boldsymbol{T}_2\frac{d^2T_1}{dt^2}-\boldsymbol{T}_2\frac{dT_1}{dt}$$

or

$$\frac{d^2T_1}{dt^2}+\left[\underbrace{\frac{1}{\boldsymbol{T}_1}+\frac{1}{\boldsymbol{T}_2}+\frac{h_c}{\overline{h}\boldsymbol{T}_2}}_{\equiv b}\right]\frac{dT_1}{dt}+\underbrace{\frac{T_1-T_\infty}{\boldsymbol{T}_1\boldsymbol{T}_2}}_{c(T_1-T_\infty)}=0 \tag{5.19a}$$

if we call $T_1 - T_\infty \equiv \theta$, then eqn. (5.19a) can be written as

$$\frac{d^2\theta}{dt^2}+b\frac{d\theta}{dt}+c\theta=0 \tag{5.19b}$$

Thus we have reduced the pair of first-order equations, eqn. (5.15) and eqn. (5.16), to a single second-order equation, eqn. (5.19b).

The general solution of eqn. (5.19b) is obtained by guessing a solution of the form $\theta = C_1 e^{Dt}$. Substitution of this guess into eqn. (5.19b) gives

$$D^2+bD+c=0 \tag{5.20}$$

from which we find that $D = -(b/2) \pm \sqrt{(b/2)^2 - c}$. This gives us two values of D, from which we can get two exponential solutions. By adding

them together, we form a general solution:

$$\theta = C_1 \exp\left[-\frac{b}{2} + \sqrt{\left(\frac{b}{2}\right)^2 - c}\right] t + C_2 \exp\left[-\frac{b}{2} - \sqrt{\left(\frac{b}{2}\right)^2 - c}\right] t \tag{5.21}$$

To solve for the two constants we first substitute eqn. (5.21) in the first of i.c.'s (5.17) and get

$$T_i - T_\infty = \theta_i = C_1 + C_2 \tag{5.22}$$

The second i.c. can be put into terms of T_1 with the help of eqn. (5.15):

$$-\left.\frac{dT_1}{dt}\right|_{t=0} = \frac{h_c A}{(\rho c V)_1}(T_1 - T_2)_{t=0} = 0$$

We substitute eqn. (5.21) in this and obtain

$$0 = \left[-\frac{b}{2} + \sqrt{\left(\frac{b}{2}\right)^2 - c}\right] C_1 + \left[-\frac{b}{2} - \sqrt{\left(\frac{b}{2}\right)^2 - c}\right] \underbrace{C_2}_{= \theta_i - C_1}$$

so

$$C_1 = -\theta_i \left[\frac{-b/2 - \sqrt{(b/2)^2 - c}}{2\sqrt{(b/2)^2 - c}}\right]$$

and

$$C_2 = \theta_i \left[\frac{-b/2 + \sqrt{(b/2)^2 - c}}{2\sqrt{(b/2)^2 - c}}\right]$$

So we obtain at last:

$$\boxed{\begin{aligned}\frac{T_1 - T_\infty}{T_i - T_\infty} \equiv \frac{\theta}{\theta_i} = {} & \frac{b/2 + \sqrt{(b/2)^2 - c}}{2\sqrt{(b/2)^2 - c}} \exp\left[-\frac{b}{2} + \sqrt{\left(\frac{b}{2}\right)^2 - c}\right] t \\ & + \frac{-b/2 + \sqrt{(b/2)^2 - c}}{2\sqrt{(b/2)^2 - c}} \exp\left[-\frac{b}{2} - \sqrt{\left(\frac{b}{2}\right)^2 - c}\right] t\end{aligned}} \tag{5.23}$$

This is a pretty complicated result—all the more complicated when we remember that b involves three algebraic terms [recall eqn. (5.19a)]. Yet there is nothing very sophisticated about it; it is easy to understand. A system involving three capacitances in series would similarly yield a third-order equation of correspondingly higher complexity, and so forth.

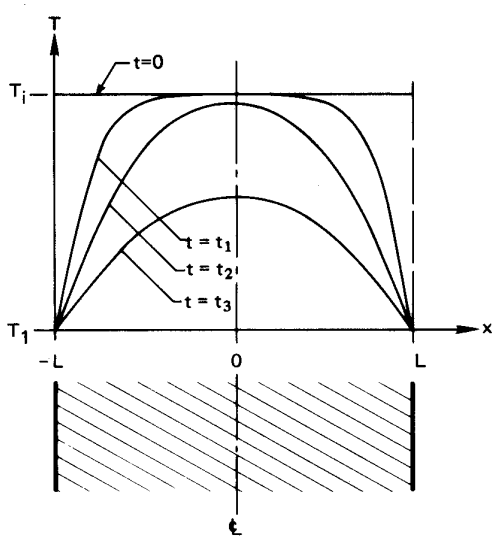

Figure 5.6 The transient cooling of a slab; $\xi = (x/L) + 1$.

5.3 Transient conduction in a one-dimensional slab

We next extend consideration to heat flow in bodies whose internal resistance is significant—to situations in which the lumped capacitance assumption is no longer appropriate. When the temperature within, say, a one-dimensional body varies with position as well as time, we must solve the heat diffusion equation for $T(x, t)$. We shall do this somewhat complicated task for the simplest case and then look at the results of such calculations in other situations.

A simple slab, shown in Fig. 5.6, is initially at a temperature T_i. The temperature of the surface of the slab is suddenly changed to T_i, and we wish to calculate the interior temperature profile as a function of time. The heat conduction equation is

$$\frac{\partial^2 T}{\partial x^2} = \frac{1}{\alpha}\frac{\partial T}{\partial t} \tag{5.24}$$

with the following b.c.'s and i.c.:

$$T(-L, t > 0) = T(L, t > 0) = T_1 \quad \text{and} \quad T(x, t = 0) = T_i \tag{5.25}$$

In fully dimensionless form, eqn. (5.24) and eqn. (5.25) are

$$\frac{\partial^2 \Theta}{\partial \xi^2} = \frac{\partial \Theta}{\partial \text{Fo}} \tag{5.26}$$

and

$$\Theta(0, \mathrm{Fo}) = \Theta(2, \mathrm{Fo}) = 0 \quad \text{and} \quad \Theta(\xi, 0) = 1 \tag{5.27}$$

where we have nondimensionalized the problem in accordance with eqn. (5.4), using $\Theta \equiv (T - T_1)/(T_i - T_1)$ and $\mathrm{Fo} \equiv \alpha t/L^2$; but for convenience in solving the equation, we have set ξ equal to $(x/L) + 1$ instead of x/L.

The general solution of eqn. (5.26) may be found using the separation of variables technique described in Sect. 4.2, leading to the dimensionless form of eqn. (4.11):

$$\Theta = e^{-\hat{\lambda}^2 \mathrm{Fo}} \left[G \sin(\hat{\lambda}\xi) + E \cos(\hat{\lambda}\xi) \right] \tag{5.28}$$

Direct nondimensionalization of eqn. (4.11) would show that $\hat{\lambda} \equiv \lambda L$, since λ had units of (length)$^{-1}$. The solution therefore appears to have introduced a fourth dimensionless group, $\hat{\lambda}$. This needs explanation. The number λ, which was introduced in the separation-of-variables process, is called an *eigenvalue*.[2] In the present problem, $\hat{\lambda} = \lambda L$ will turn out to be a number—or rather a sequence of numbers—that is independent of system parameters.

Substituting the general solution, eqn. (5.28), in the first b.c. gives

$$0 = e^{-\hat{\lambda}^2 \mathrm{Fo}} (0 + E) \quad \text{so} \quad E = 0$$

and substituting it in the second yields

$$0 = e^{-\hat{\lambda}^2 \mathrm{Fo}} [G \sin 2\hat{\lambda}] \quad \text{so either} \quad G = 0$$

or

$$2\hat{\lambda} = 2\hat{\lambda}_n = n\pi, \quad n = 0, 1, 2, \ldots$$

In the second case, we are presented with two choices. The first, $G = 0$, would give $\Theta \equiv 0$ in all situations, so that the initial condition could never be accommodated. (This is what mathematicians call a *trivial* solution.) The second choice, $\hat{\lambda}_n = n\pi/2$, actually yields a string of solutions, each of the form

$$\Theta = G_n \, e^{-n^2 \pi^2 \mathrm{Fo}/4} \sin\left(\frac{n\pi}{2}\xi\right) \tag{5.29}$$

[2]The word *eigenvalue* is a curious hybrid of the German term *eigenwert* and its English translation, *characteristic value*.

where G_n is the constant appropriate to the nth one of these solutions.

We still face the problem that none of eqns. (5.29) will fit the initial condition, $\Theta(\xi, 0) = 1$. To get around this, we remember that the sum of any number of solutions of a linear differential equation is also a solution. Then we write

$$\Theta = \sum_{n=1}^{\infty} G_n \, e^{-n^2\pi^2 \mathrm{Fo}/4} \sin\left(n\frac{\pi}{2}\xi\right) \tag{5.30}$$

where we drop $n = 0$ since it gives zero contribution to the series. And we arrive, at last, at the problem of choosing the G_n's so that eqn. (5.30) will fit the initial condition.

$$\Theta\,(\xi, 0) = \sum_{n=1}^{\infty} G_n \sin\left(n\frac{\pi}{2}\xi\right) = 1 \tag{5.31}$$

The problem of picking the values of G_n that will make this equation true is called "making a Fourier series expansion" of the function $f(\xi) = 1$. We shall not pursue strategies for making Fourier series expansions in any general way. Instead, we merely show how to accomplish the task for the particular problem at hand. We begin with a mathematical trick. We multiply eqn. (5.31) by $\sin(m\pi/2)$, where m may or may not equal n, and we integrate the result between $\xi = 0$ and 2.

$$\int_0^2 \sin\left(\frac{m\pi}{2}\xi\right) d\xi = \sum_{n=1}^{\infty} G_n \int_0^2 \sin\left(\frac{m\pi}{2}\xi\right) \sin\left(\frac{n\pi}{2}\xi\right) d\xi \tag{5.32}$$

(The interchange of summation and integration turns out to be legitimate, although we have not proved, here, that it is.[3]) With the help of a table of integrals, we find that

$$\int_0^2 \sin\left(\frac{m\pi}{2}\xi\right) \sin\left(\frac{n\pi}{2}\xi\right) d\xi = \begin{cases} 0 & \text{for } n \neq m \\ 1 & \text{for } n = m \end{cases}$$

Thus, when we complete the integration of eqn. (5.32), we get

$$-\frac{2}{m\pi} \cos\left(\frac{m\pi}{2}\xi\right)\Bigg|_0^2 = \sum_{n=1}^{\infty} G_n \times \begin{cases} 0 & \text{for } n \neq m \\ 1 & \text{for } n = m \end{cases}$$

[3] What is required is that the series in eqn. (5.31) be *uniformly convergent*.

This reduces to

$$-\frac{2}{m\pi}\left[(-1)^n - 1\right] = G_n$$

so

$$G_n = \frac{4}{n\pi} \quad \text{where } n \text{ is an odd number}$$

Substituting this result into eqn. (5.30), we finally obtain the solution to the problem:

$$\boxed{\Theta(\xi, \mathrm{Fo}) = \frac{4}{\pi} \sum_{n=\text{odd}}^{\infty} \frac{1}{n} e^{-(n\pi/2)^2 \mathrm{Fo}} \sin\left(\frac{n\pi}{2}\xi\right)} \tag{5.33}$$

Equation (5.33) admits a very nice simplification for large time (or at large Fo). Suppose that we wish to evaluate Θ at the outer center of the slab—at $x = 0$ or $\xi = 1$. Then

$$\Theta(0, \mathrm{Fo}) = \frac{4}{\pi} \times$$

$$\left\{ \underbrace{\exp\left[-\left(\frac{\pi}{2}\right)^2 \mathrm{Fo}\right]}_{\substack{= 0.085 \text{ at Fo} = 1 \\ = 0.781 \text{ at Fo} = 0.1 \\ = 0.976 \text{ at Fo} = 0.01}} - \underbrace{\frac{1}{3}\exp\left[-\left(\frac{3\pi}{2}\right)^2 \mathrm{Fo}\right]}_{\substack{\simeq 10^{-10} \text{ at Fo} = 1 \\ = 0.036 \text{ at Fo} = 0.1 \\ = 0.267 \text{ at Fo} = 0.01}} + \underbrace{\frac{1}{5}\exp\left[-\left(\frac{5\pi}{2}\right)^2 \mathrm{Fo}\right]}_{\substack{\simeq 10^{-27} \text{ at Fo} = 1 \\ = 0.0004 \text{ at Fo} = 0.1 \\ = 0.108 \text{ at Fo} = 0.01}} + \cdots \right\}$$

Thus for values of Fo somewhat greater than 0.1, only the first term in the series need be used in the solution (except at points very close to the boundaries). We discuss these one-term solutions in Sect. 5.5. Before we move to this matter, let us see what happens to the preceding problem if the slab is subjected to b.c.'s of the third kind.

Suppose that the walls of the slab had been cooled by symmetrical convection such that the b.c.'s were

$$\overline{h}(T_\infty - T)_{x=-L} = -k\frac{\partial T}{\partial x}\bigg|_{x=-L} \quad \text{and} \quad \overline{h}(T - T_\infty)_{x=L} = -k\frac{\partial T}{\partial x}\bigg|_{x=L}$$

or in dimensionless form, using $\Theta \equiv (T - T_\infty)/(T_i - T_\infty)$ and $\xi = (x/L) + 1$,

$$-\Theta\Big|_{\xi=0} = -\frac{1}{\mathrm{Bi}}\frac{\partial\Theta}{\partial\xi}\bigg|_{\xi=0} \quad \text{and} \quad \frac{\partial\Theta}{\partial\xi}\bigg|_{\xi=1} = 0$$

Table 5.1 Terms of series solutions for slabs, cylinders, and spheres.

	A_n	f_n	Equation for $\hat{\lambda}_n$
Slab	$\dfrac{2\sin\hat{\lambda}_n}{\hat{\lambda}_n + \sin\hat{\lambda}_n\cos\hat{\lambda}_n}$	$\cos\left(\hat{\lambda}_n \dfrac{x}{L}\right)$	$\cot\hat{\lambda}_n = \dfrac{\hat{\lambda}_n}{\mathrm{Bi}_L}$
Cylinder	$\dfrac{2J_1(\hat{\lambda}_n)}{\hat{\lambda}_n\left[J_0^2(\hat{\lambda}_n) + J_1^2(\hat{\lambda}_n)\right]}$	$J_0\left(\hat{\lambda}_n \dfrac{r}{r_o}\right)$	$\hat{\lambda}_n J_1(\hat{\lambda}_n) = \mathrm{Bi}_{r_o} J_0(\hat{\lambda}_n)$
Sphere	$2\dfrac{\sin\hat{\lambda}_n - \hat{\lambda}_n\cos\hat{\lambda}_n}{\hat{\lambda}_n - \sin\hat{\lambda}_n\cos\hat{\lambda}_n}$	$\left(\dfrac{r_o}{\hat{\lambda}_n r}\right)\sin\left(\dfrac{\hat{\lambda}_n r}{r_o}\right)$	$\hat{\lambda}_n\cot\hat{\lambda}_n = 1 - \mathrm{Bi}_{r_o}$

The solution is somewhat harder to find than eqn. (5.33) was, but the result is[4]

$$\boxed{\Theta = \sum_{n=1}^{\infty} \exp\left(-\hat{\lambda}_n^2\,\mathrm{Fo}\right)\left(\frac{2\sin\hat{\lambda}_n\cos[\hat{\lambda}_n(\xi-1)]}{\hat{\lambda}_n + \sin\hat{\lambda}_n\cos\hat{\lambda}_n}\right)} \tag{5.34}$$

where the values of $\hat{\lambda}_n$ are given as a function of n and Bi by the transcendental equation

$$\cot\hat{\lambda}_n = \frac{\hat{\lambda}_n}{\mathrm{Bi}} \tag{5.35}$$

The successive positive roots of this equation, which are $\hat{\lambda}_n = \hat{\lambda}_1, \hat{\lambda}_2, \hat{\lambda}_3, \ldots$, depend upon Bi. Thus, $\Theta = \mathrm{fn}(\xi, \mathrm{Fo}, \mathrm{Bi})$, as we would expect. This result, although more complicated than the result for b.c.'s of the first kind, still reduces to a single term for $\mathrm{Fo} \gtrsim 0.2$.

Similar series solutions can be constructed for cylinders and spheres that are convectively cooled at their outer surface, $r = r_o$. The solutions for slab, cylinders, and spheres all have the form

$$\boxed{\Theta = \frac{T - T_\infty}{T_0 - T_\infty} = \sum_{n=1}^{\infty} A_n \exp\left(-\hat{\lambda}_n^2\,\mathrm{Fo}\right) f_n} \tag{5.36}$$

where the coefficients A_n, the functions f_n, and the equations for the dimensionless eigenvalues $\hat{\lambda}_n$ are given in Table 5.1.

[4] See, for example, [5.1, §2.3.4] or [5.2, §3.4.3] for details of this calculation.

5.4 Temperature-response charts

Figure 5.7 is a graphical presentation of eqn. (5.34) for $0 \leqslant \text{Fo} \leqslant 1.5$ and for six x-planes in the slab. (Remember that the x-coordinate goes from zero in the center to L on the boundary, while ξ goes from 0 up to 2 in the preceding solution.)

Notice that, with the exception of points for which $1/\text{Bi} < 0.25$ on the outside boundary, the curves are all straight lines when $\text{Fo} \gtrsim 0.2$. Since the coordinates are semilogarithmic, this portion of the graph corresponds to the lead term—the only term that retains any importance—in eqn. (5.34). When we take the logarithm of the one-term version of eqn. (5.34), the result is

$$\ln\Theta \cong \ln\Bigg[\underbrace{\frac{2\sin\hat{\lambda}_1\cos[\hat{\lambda}_1(\xi-1)]}{\hat{\lambda}_1+\sin\hat{\lambda}_1\cos\hat{\lambda}_1}}_{\substack{\Theta\text{-intercept at Fo = 0 of}\\ \text{the straight portion of}\\ \text{the curve}}}\Bigg] - \underbrace{\hat{\lambda}_1^2\,\text{Fo}}_{\substack{\text{slope of the}\\ \text{straight portion}\\ \text{of the curve}}}$$

If Fo is greater than 1.5, the following options are then available to us for solving the problem:

- Extrapolate the given curves using a straightedge.
- Evaluate Θ using the first term of eqn. (5.34), as discussed in Sect. 5.5.
- If Bi is small, use a lumped-capacity result.

Figure 5.8 and Fig. 5.9 are similar graphs for cylinders and spheres. Everything that we have said in general about Fig. 5.7 is also true for these graphs. They were simply calculated from different solutions, and the numerical values on them are somewhat different. These charts are from [5.3, Chap. 5], although such charts are often called Heisler charts, after a collection of related charts subsequently published by Heisler [5.4].

Another useful kind of chart derivable from eqn. (5.34) is one that gives heat removal from a body up to a time of interest:

$$\begin{aligned}\int_0^t Q\,dt &= -\int_0^t kA\,\frac{\partial T}{\partial x}\bigg|_{\text{surface}} dt \\ &= -\int_0^{\text{Fo}} kA\,\frac{T_i - T_\infty}{L}\,\frac{\partial\Theta}{\partial\xi}\bigg|_{\text{surface}}\left(\frac{L^2}{\alpha}\right) d\text{Fo}\end{aligned}$$

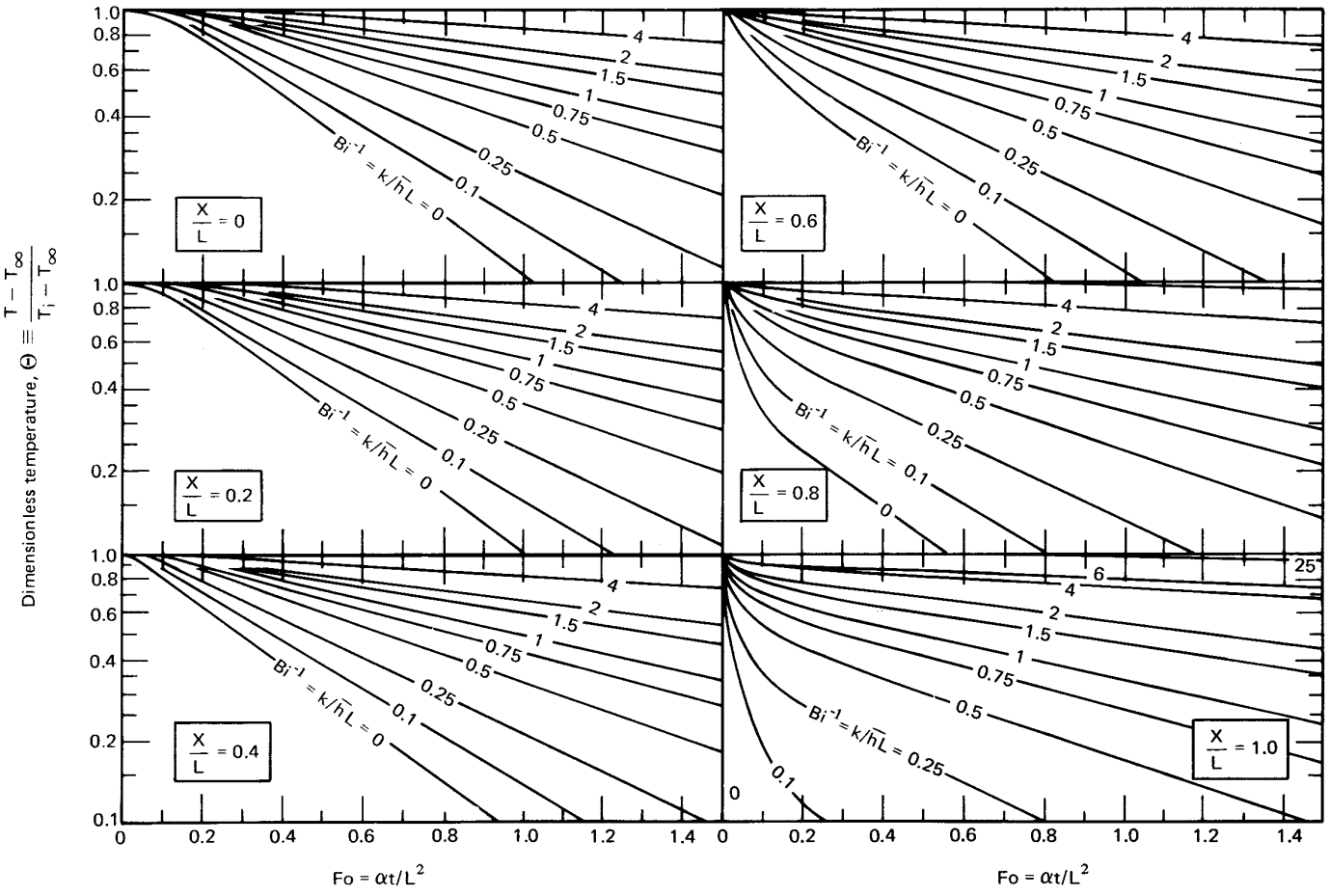

Figure 5.7 The transient temperature distribution in a *slab* at six positions: $x/L = 0$ is the center, $x/L = 1$ is one outside boundary.

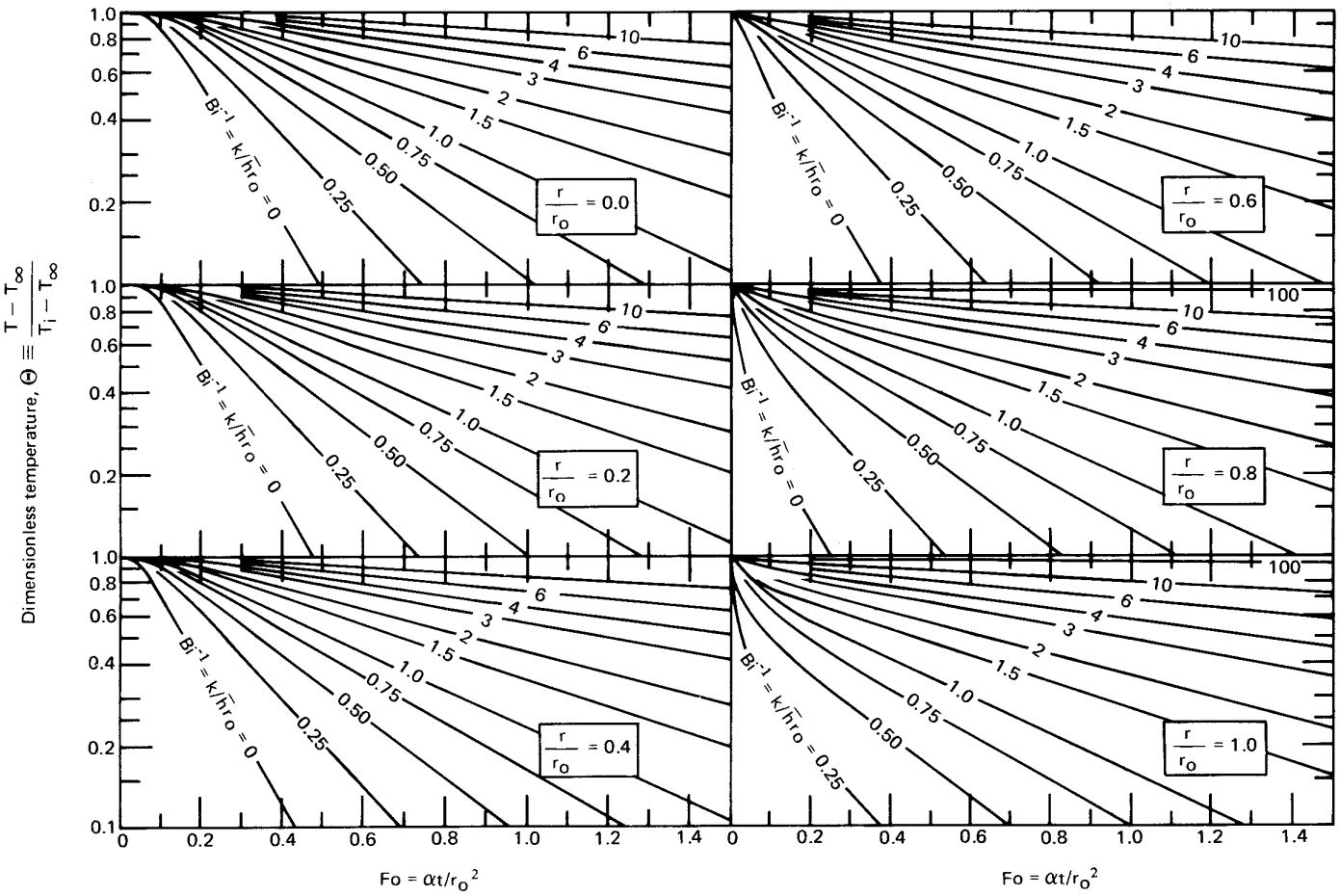

Figure 5.8 The transient temperature distribution in a long *cylinder* of radius r_o at six positions: $r/r_o = 0$ is the centerline; $r/r_o = 1$ is the outside boundary.

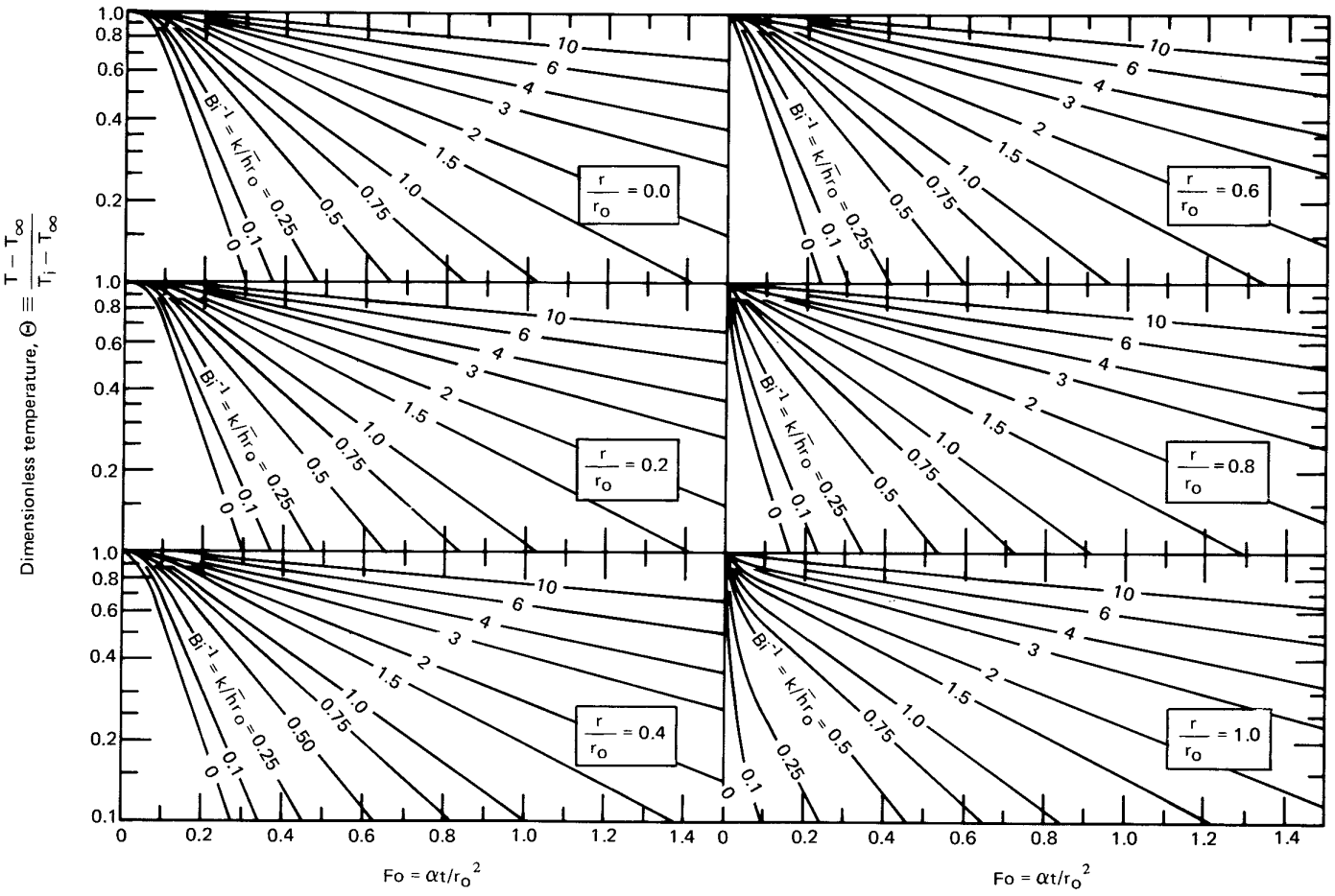

Figure 5.9 The transient temperature distribution in a *sphere* of radius r_o at six positions: $r/r_o = 0$ is the center; $r/r_o = 1$ is the outside boundary.

Dividing this by the total energy of the body above T_∞, we get a quantity, Φ, which approaches unity as $t \to \infty$ and the energy is all transferred to the surroundings:

$$\Phi \equiv \frac{\int_0^t Q\,dt}{\rho c V (T_i - T_\infty)} = -\int_0^{\text{Fo}} \left.\frac{\partial \Theta}{\partial \xi}\right|_{\text{surface}} d\text{Fo} \tag{5.37}$$

where the volume, $V = AL$. Substituting the appropriate temperature distribution [e.g., eqn. (5.34) for a slab] in eqn. (5.37), we obtain $\Phi(\text{Fo}, \text{Bi})$ in the form of an infinite series

$$\Phi\,(\text{Fo, Bi}) = 1 - \sum_{n=1}^{\infty} D_n \exp\left(-\hat{\lambda}_n^2\,\text{Fo}\right) \tag{5.38}$$

The coefficients D_n are different functions of $\hat{\lambda}_n$ — and thus of Bi — for slabs, cylinders, and spheres (e.g., for a slab $D_n = A_n \sin\hat{\lambda}_n/\hat{\lambda}_n$). These functions can be used to plot $\Phi(\text{Fo}, \text{Bi})$ once and for all. Such curves are given in Fig. 5.10.

The quantity Φ has a close relationship to the mean temperature of a body at any time, $\overline{T}(t)$. Specifically, the energy lost as heat by time t determines the difference between the initial temperature and the mean temperature at time t

$$\rho c V\,[T_i - \overline{T}(t)] = \int_0^t Q\,dt. \tag{5.39}$$

Thus, if we define $\overline{\Theta}$ as shown,

$$\overline{\Theta} \equiv \frac{\overline{T}(t) - T_\infty}{T_i - T_\infty} = 1 - \frac{\int_0^t Q(t)\,dt}{\rho c V (T_i - T_\infty)} = 1 - \Phi. \tag{5.40}$$

Example 5.2

A dozen approximately spherical apples, 10 cm in diameter are taken from a 30°C environment and laid out on a rack in a refrigerator at 5°C. They have approximately the same physical properties as water, and $\overline{h}$ is approximately 6 W/m^{2}K as the result of natural convection. What will be the temperature of the centers of the apples after 1 hr? How long will it take to bring the centers to 10°C? How much heat will the refrigerator have to carry away to get the centers to 10°C?

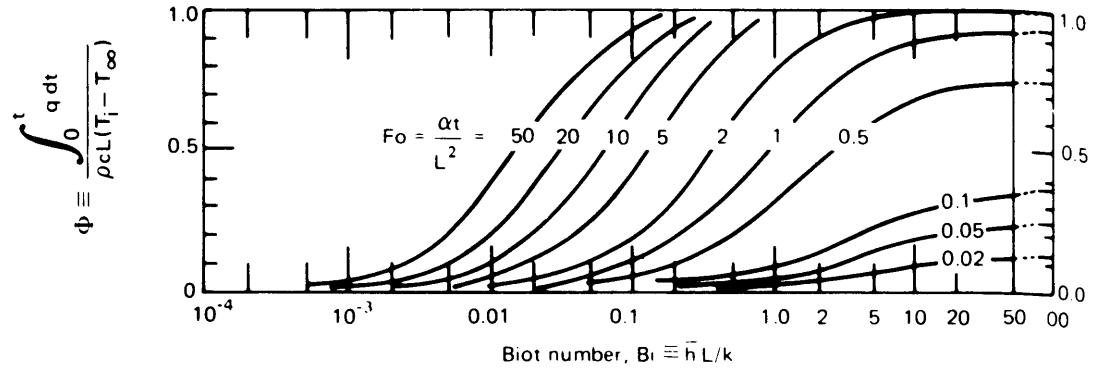
$\Phi \equiv \frac{\int_0^t q\,dt}{\rho c L(T_i - T_\infty)}$
Fo = $\frac{\alpha t}{L^2}$ = 50 20 10 5 2 1 0.5 0.1 0.05 0.02
1.0
0.5
0
10^{-4} 10^{-3} 0.01 0.1 1.0 2 5 10 20 50 00
Biot number, Bi ≡ $\bar{h}$ L/k

a.) *Slab* of thickness, L, insulated on one side

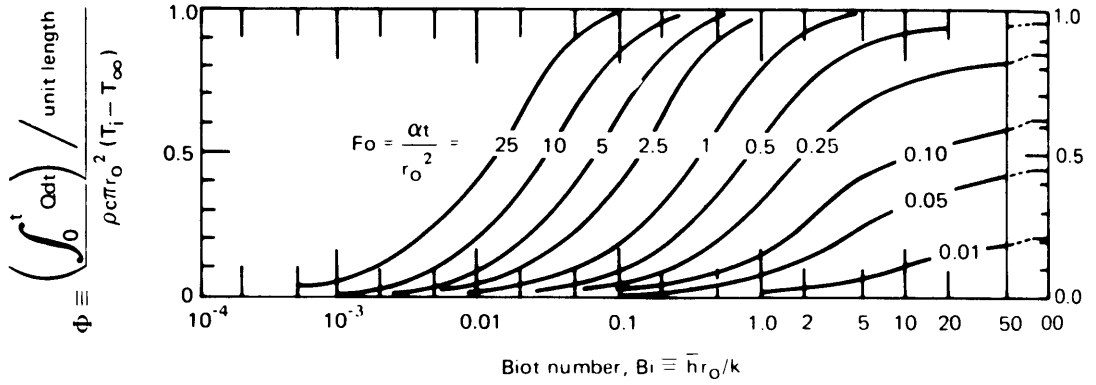
$\Phi \equiv \frac{\left(\int_0^t Q\,dt\right) / \text{unit length}}{\rho c \pi r_o^2 (T_i - T_\infty)}$
Fo = $\frac{\alpha t}{r_o^2}$ = 25 10 5 2.5 1 0.5 0.25 0.10 0.05 0.01
1.0
0.5
0
10^{-4} 10^{-3} 0.01 0.1 1.0 2 5 10 20 50 00
Biot number, Bi ≡ $\bar{h} r_o/k$

b.) *Cylinder*, of radius, r_o

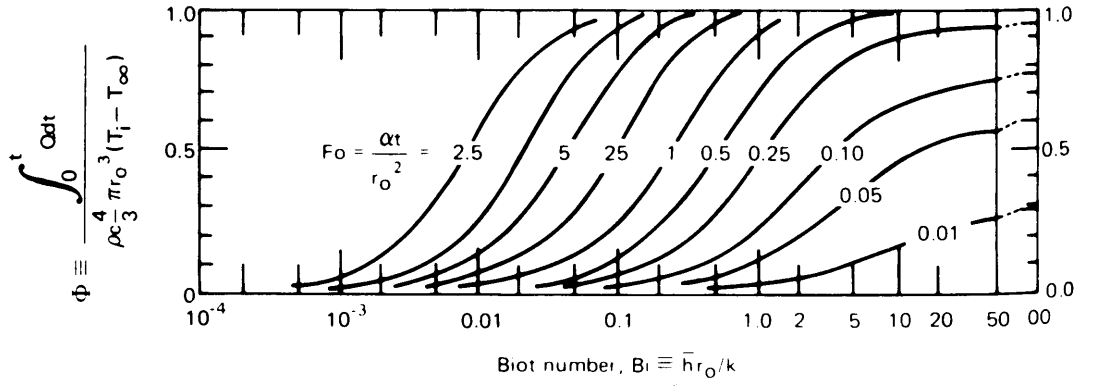
$\Phi \equiv \frac{\int_0^t Q\,dt}{\rho c \frac{4}{3} \pi r_o^3 (T_i - T_\infty)}$
Fo = $\frac{\alpha t}{r_o^2}$ = 2.5 5 25 1 0.5 0.25 0.10 0.05 0.01
1.0
0.5
0
10^{-4} 10^{-3} 0.01 0.1 1.0 2 5 10 20 50 00
Biot number, Bi ≡ $\bar{h} r_o/k$

c.) *Sphere*, of radius, r_o

Figure 5.10 The heat removal from suddenly-cooled bodies as a function of $\bar{h}$ and time.

SOLUTION. After 1 hr, or 3600 s:

$$\text{Fo} = \frac{\alpha t}{r_o^2} = \left(\frac{k}{\rho c}\right)_{20^\circ\text{C}} \frac{3600 \text{ s}}{(0.05 \text{ m})^2}$$
$$= \frac{(0.603 \text{ J/m·s·K})(3600 \text{ s})}{(997.6 \text{ kg/m}^3)(4180 \text{ J/kg·K})(0.0025 \text{ m}^2)} = 0.208$$

Furthermore, $\text{Bi}^{-1} = (\bar{h}r_o/k)^{-1} = [6(0.05)/0.603]^{-1} = 2.01$. Therefore, we read from Fig. 5.9 in the upper left-hand corner:

$$\Theta = 0.85$$

After 1 hr:

$$T_{\text{center}} = 0.85(30 - 5)^\circ\text{C} + 5^\circ\text{C} = 26.3^\circ\text{C}$$

To find the time required to bring the center to 10°C, we first calculate

$$\Theta = \frac{10 - 5}{30 - 5} = 0.2$$

and Bi^{-1} is still 2.01. Then from Fig. 5.9 we read

$$\text{Fo} = 1.29 = \frac{\alpha t}{r_o^2}$$

so

$$t = \frac{1.29(997.6)(4180)(0.0025)}{0.603} = 22,300 \text{ s} = 6 \text{ hr } 12 \text{ min}$$

Finally, we look up Φ at $\text{Bi} = 1/2.01$ and $\text{Fo} = 1.29$ in Fig. 5.10, for spheres:

$$\Phi = 0.80 = \frac{\int_0^t Q\, dt}{\rho c \left(\frac{4}{3}\pi r_0^3\right)(T_i - T_\infty)}$$

so

$$\int_0^t Q\, dt = 997.6(4180)\left(\frac{4}{3}\pi(0.05)^3\right)(25)(0.80) = 43,668 \text{ J/apple}$$

Therefore, for the 12 apples,

$$\text{total energy removal} = 12(43.67) = 524 \text{ kJ}$$ ■

The temperature-response charts in Fig. 5.7 through Fig. 5.10 are without doubt among the most useful available since they can be adapted to a host of physical situations. Nevertheless, hundreds of such charts have been formed for other situations, a number of which have been cataloged by Schneider [5.5]. Analytical solutions are available for hundreds more problems, and any reader who is faced with a complex heat conduction calculation should consult the literature before trying to solve it. An excellent place to begin is Carslaw and Jaeger's comprehensive treatise on heat conduction [5.6].

Example 5.3

A 1 mm diameter Nichrome (20% Ni, 80% Cr) wire is simultaneously being used as an electric resistance heater and as a resistance thermometer in a liquid flow. The laboratory workers who operate it are attempting to measure the boiling heat transfer coefficient, $\overline{h}$, by supplying an alternating current and measuring the difference between the average temperature of the heater, T_{av}, and the liquid temperature, T_∞. They get $\overline{h} = 30,000$ W/m^{2}K at a wire temperature of 100°C and are delighted with such a high value. Then a colleague suggests that $\overline{h}$ is so high because the surface temperature is rapidly oscillating as a result of the alternating current. Is this hypothesis correct?

SOLUTION. Heat is being generated in proportion to the product of voltage and current, or as $\sin^2 \omega t$, where ω is the frequency of the current in rad/s. If the boiling action removes heat rapidly enough in comparison with the heat capacity of the wire, the surface temperature may well vary significantly. This transient conduction problem was first solved by Jeglic in 1962 [5.7]. It was redone in a different form two years later by Switzer and Lienhard (see, e.g. [5.8]), who gave response curves in the form

$$\frac{T_{\max} - T_{\text{av}}}{T_{\text{av}} - T_\infty} = \text{fn}\,(\text{Bi}, \psi) \tag{5.41}$$

where the left-hand side is the dimensionless range of the temperature oscillation, and $\psi = \omega\delta^2\alpha$, where δ is a characteristic length. Because this problem is common and the solution is not widely available, we include the curves for flat plates and cylinders in Fig. 5.11 and Fig. 5.12 respectively.

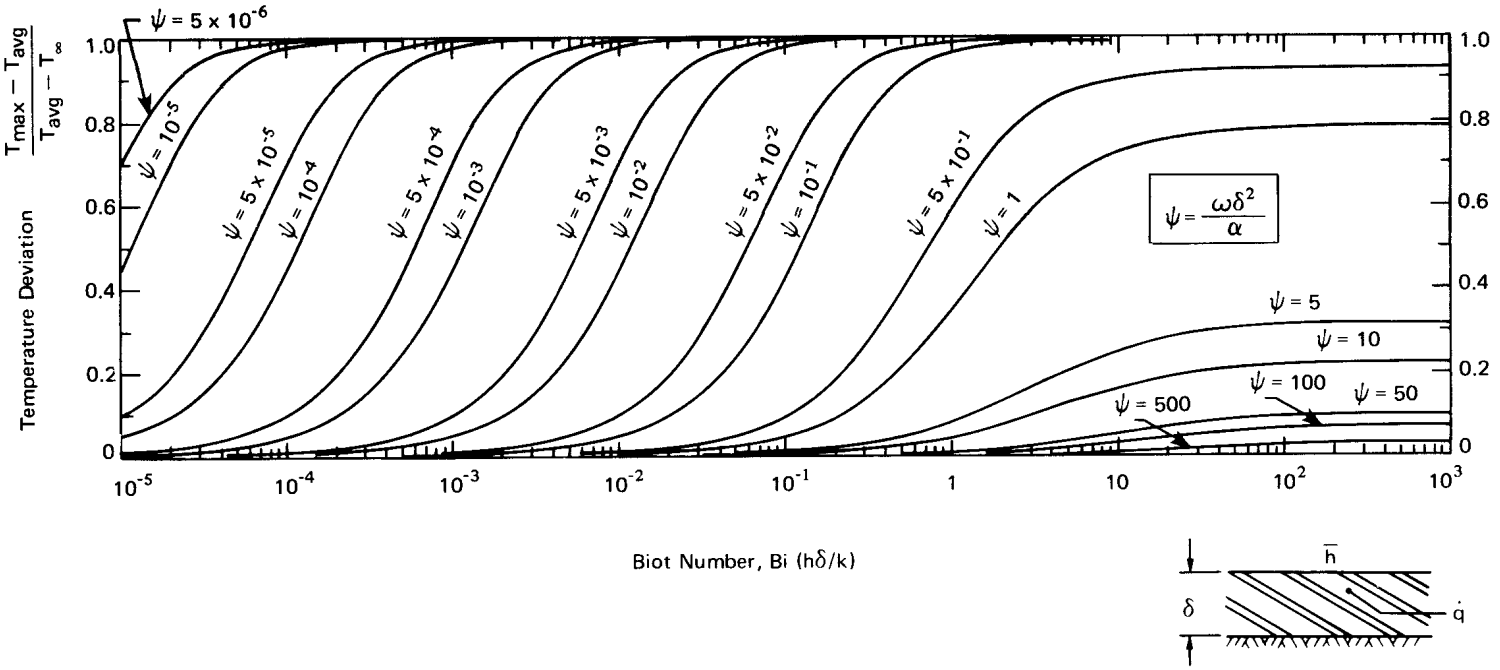

Figure 5.11 Temperature deviation at the surface of a *flat plate* heated with alternating current.

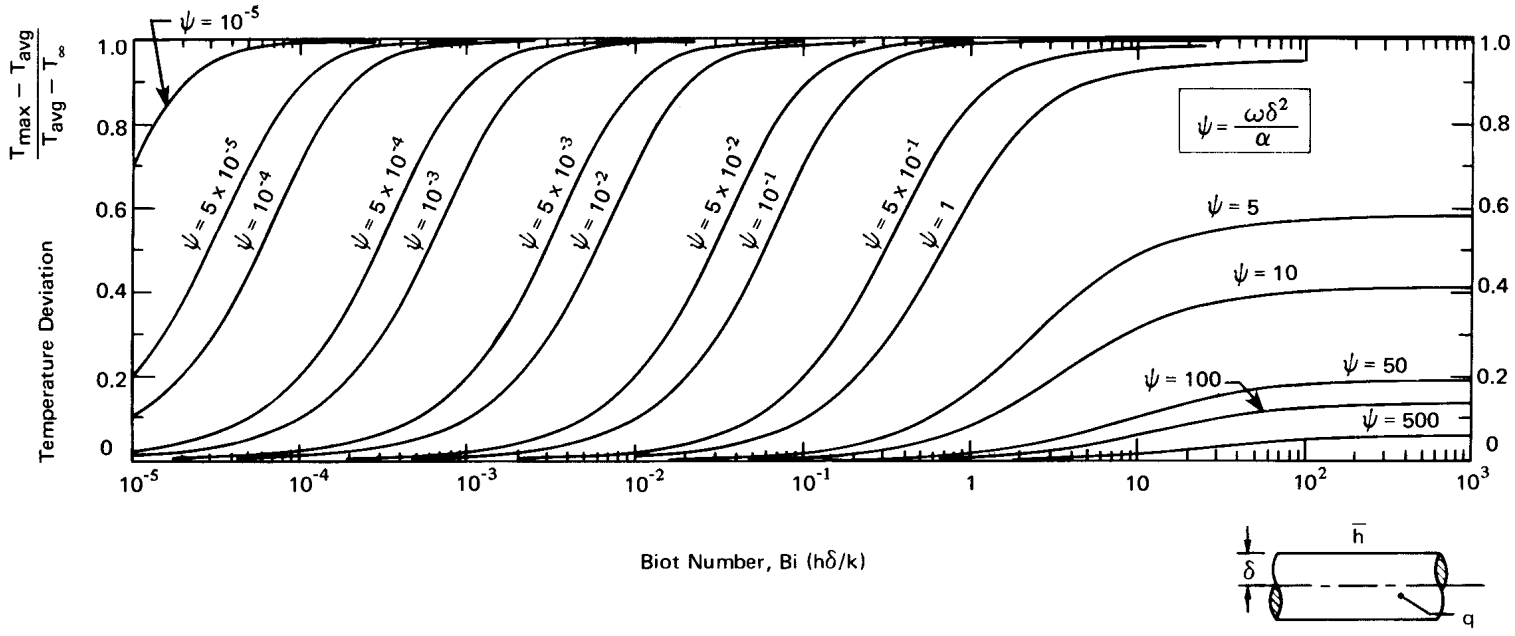

Figure 5.12 Temperature deviation at the surface of a *cylinder* heated with alternating current.

In the present case:

$$\text{Bi} = \frac{\overline{h}\ \text{radius}}{k} = \frac{30,000(0.0005)}{13.8} = 1.09$$
$$\frac{\omega r^2}{\alpha} = \frac{[2\pi(60)](0.0005)^2}{0.00000343} = 27.5$$

and from the chart for cylinders, Fig. 5.12, we find that

$$\frac{T_{\max} - T_{\text{av}}}{T_{\text{av}} - T_\infty} \simeq 0.04$$

A temperature fluctuation of only 4% is probably not serious. It therefore appears that the experiment was valid. ■

5.5 One-term solutions

As we have noted previously, when the Fourier number is greater than 0.2 or so, the series solutions from eqn. (5.36) may be approximated using only their first term:

$$\Theta \approx A_1 \cdot f_1 \cdot \exp\left(-\hat{\lambda}_1^2 \,\text{Fo}\right). \tag{5.42}$$

Likewise, the fractional heat loss, Φ, or the mean temperature $\overline{\Theta}$ from eqn. 5.40, can be approximated using just the first term of eqn. (5.38):

$$\overline{\Theta} = 1 - \Phi \approx D_1 \exp\left(-\hat{\lambda}_1^2 \,\text{Fo}\right). \tag{5.43}$$

Table 5.2 lists the values of $\hat{\lambda}_1$, A_1, and D_1 for slabs, cylinders, and spheres as a function of the Biot number. The one-term solution's error in Θ is less than 0.1% for a sphere with Fo $\geq$ 0.28 and for a slab with Fo $\geq$ 0.43. These errors are largest for Biot numbers near unity. If high accuracy is not required, these one-term approximations may generally be used whenever Fo $\geq$ 0.2

Table 5.2 One-term coefficients for convective cooling [5.1].

Bi	*Plate*			*Cylinder*			*Sphere*		
	$\hat{\lambda}_1$	A_1	D_1	$\hat{\lambda}_1$	A_1	D_1	$\hat{\lambda}_1$	A_1	D_1
0.01	0.09983	1.0017	1.0000	0.14124	1.0025	1.0000	0.17303	1.0030	1.0000
0.02	0.14095	1.0033	1.0000	0.19950	1.0050	1.0000	0.24446	1.0060	1.0000
0.05	0.22176	1.0082	0.9999	0.31426	1.0124	0.9999	0.38537	1.0150	1.0000
0.10	0.31105	1.0161	0.9998	0.44168	1.0246	0.9998	0.54228	1.0298	0.9998
0.15	0.37788	1.0237	0.9995	0.53761	1.0365	0.9995	0.66086	1.0445	0.9996
0.20	0.43284	1.0311	0.9992	0.61697	1.0483	0.9992	0.75931	1.0592	0.9993
0.30	0.52179	1.0450	0.9983	0.74646	1.0712	0.9983	0.92079	1.0880	0.9985
0.40	0.59324	1.0580	0.9971	0.85158	1.0931	0.9970	1.05279	1.1164	0.9974
0.50	0.65327	1.0701	0.9956	0.94077	1.1143	0.9954	1.16556	1.1441	0.9960
0.60	0.70507	1.0814	0.9940	1.01844	1.1345	0.9936	1.26440	1.1713	0.9944
0.70	0.75056	1.0918	0.9922	1.08725	1.1539	0.9916	1.35252	1.1978	0.9925
0.80	0.79103	1.1016	0.9903	1.14897	1.1724	0.9893	1.43203	1.2236	0.9904
0.90	0.82740	1.1107	0.9882	1.20484	1.1902	0.9869	1.50442	1.2488	0.9880
1.00	0.86033	1.1191	0.9861	1.25578	1.2071	0.9843	1.57080	1.2732	0.9855
1.10	0.89035	1.1270	0.9839	1.30251	1.2232	0.9815	1.63199	1.2970	0.9828
1.20	0.91785	1.1344	0.9817	1.34558	1.2387	0.9787	1.68868	1.3201	0.9800
1.30	0.94316	1.1412	0.9794	1.38543	1.2533	0.9757	1.74140	1.3424	0.9770
1.40	0.96655	1.1477	0.9771	1.42246	1.2673	0.9727	1.79058	1.3640	0.9739
1.50	0.98824	1.1537	0.9748	1.45695	1.2807	0.9696	1.83660	1.3850	0.9707
1.60	1.00842	1.1593	0.9726	1.48917	1.2934	0.9665	1.87976	1.4052	0.9674
1.80	1.04486	1.1695	0.9680	1.54769	1.3170	0.9601	1.95857	1.4436	0.9605
2.00	1.07687	1.1785	0.9635	1.59945	1.3384	0.9537	2.02876	1.4793	0.9534
2.20	1.10524	1.1864	0.9592	1.64557	1.3578	0.9472	2.09166	1.5125	0.9462
2.40	1.13056	1.1934	0.9549	1.68691	1.3754	0.9408	2.14834	1.5433	0.9389
3.00	1.19246	1.2102	0.9431	1.78866	1.4191	0.9224	2.28893	1.6227	0.9171
4.00	1.26459	1.2287	0.9264	1.90808	1.4698	0.8950	2.45564	1.7202	0.8830
5.00	1.31384	1.2402	0.9130	1.98981	1.5029	0.8721	2.57043	1.7870	0.8533
6.00	1.34955	1.2479	0.9021	2.04901	1.5253	0.8532	2.65366	1.8338	0.8281
8.00	1.39782	1.2570	0.8858	2.12864	1.5526	0.8244	2.76536	1.8920	0.7889
10.00	1.42887	1.2620	0.8743	2.17950	1.5677	0.8039	2.83630	1.9249	0.7607
20.00	1.49613	1.2699	0.8464	2.28805	1.5919	0.7542	2.98572	1.9781	0.6922
50.00	1.54001	1.2727	0.8260	2.35724	1.6002	0.7183	3.07884	1.9962	0.6434
100.00	1.55525	1.2731	0.8185	2.38090	1.6015	0.7052	3.11019	1.9990	0.6259
∞	1.57080	1.2732	0.8106	2.40483	1.6020	0.6917	3.14159	2.0000	0.6079

5.6 Transient heat conduction to a semi-infinite region

Introduction

Bronowksi's classic television series, *The Ascent of Man* [5.9], included a brilliant reenactment of the ancient ceremonial procedure by which the Japanese forged Samurai swords (see Fig. 5.13). The metal is heated, folded, beaten, and formed, over and over, to create a blade of remarkable toughness and flexibility. When the blade is formed to its final configuration, a tapered sheath of clay is baked on the outside of it, so the cross section is as shown in Fig. 5.13. The red-hot blade with the clay sheath is then subjected to a rapid quenching, which cools the uninsulated cutting edge quickly and the back part of the blade very slowly. The result is a layer of case-hardening that is hardest at the edge and less hard at points farther from the edge.

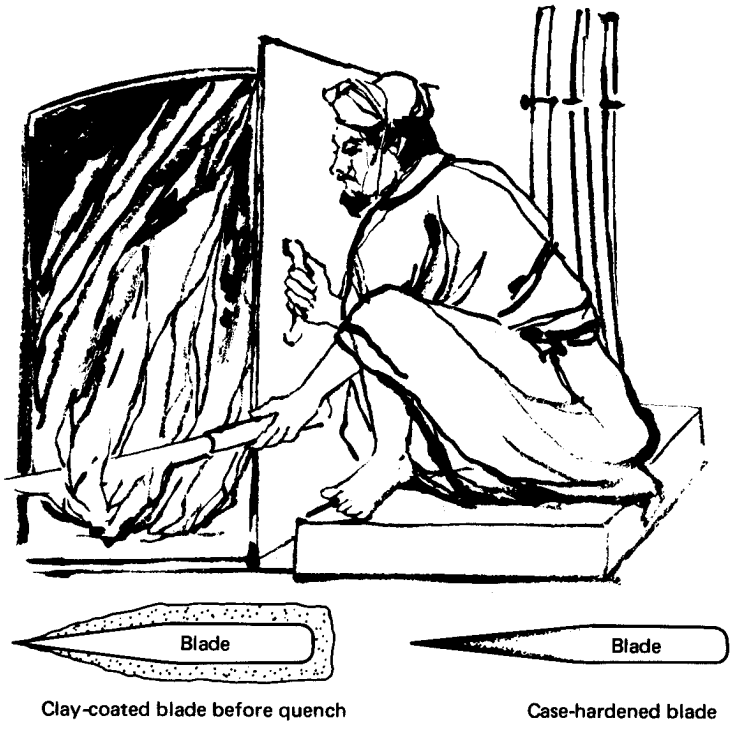

Figure 5.13 The ceremonial case-hardening of a Samurai sword.

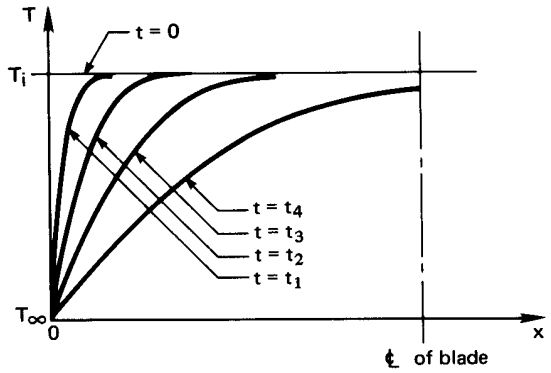

Figure 5.14 The initial cooling of a thin sword blade. Prior to $t = t_4$, the blade might as well be infinitely thick insofar as cooling is concerned.

The blade is then tough and ductile, so it will not break, but has a fine hard outer shell that can be honed to sharpness. We need only look a little way up the side of the clay sheath to find a cross section that was thick enough to prevent the blade from experiencing the sudden effects of the cooling quench. The success of the process actually relies on the *failure* of the cooling to penetrate the clay very deeply in a short time.

Now we wish to ask: "How can we say whether or not the influence of a heating or cooling process is restricted to the surface of a body?" Or if we turn the question around: "Under what conditions can we view the depth of a body as *infinite* with respect to the thickness of the region that has felt the heat transfer process?"

Consider next the cooling process within the blade in the absence of the clay retardant and when $\overline{h}$ is very large. Actually, our considerations will apply initially to any finite body whose boundary suddenly changes temperature. The temperature distribution, in this case, is sketched in Fig. 5.14 for four sequential times. Only the fourth curve—that for which $t = t_4$—is noticeably influenced by the opposite wall. Up to that time, the wall might as well have infinite depth.

Since any body subjected to a sudden change of temperature is infinitely large in comparison with the initial region of temperature change, we must learn how to treat heat transfer in this period.

Solution aided by dimensional analysis

The calculation of the temperature distribution in a semi-infinite region poses a difficulty in that we can impose a definite b.c. at only one position—the exposed boundary. We shall be able to get around that difficulty in a nice way with the help of dimensional analysis.

When the one boundary of a semi-infinite region, initially at $T = T_i$, is suddenly cooled (or heated) to a new temperature, T_∞, as in Fig. 5.14, the dimensional function equation is

$$T - T_\infty = \text{fn}\,[t, x, \alpha, (T_i - T_\infty)]$$

where there is *no characteristic length or time*. Since there are five variables in °C, s, and m, we should look for two dimensional groups.

$$\underbrace{\frac{T - T_\infty}{T_i - T_\infty}}_{\Theta} = \text{fn}\left(\underbrace{\frac{x}{\sqrt{\alpha t}}}_{\zeta}\right) \tag{5.44}$$

The very important thing that we learn from this exercise in dimensional analysis is that position and time collapse into one independent variable. This means that the heat conduction equation and its b.c.s must transform from a partial differential equation into a simpler ordinary differential equation in the single variable, $\zeta = x/\sqrt{\alpha t}$. Thus, we transform each side of

$$\frac{\partial^2 T}{\partial x^2} = \frac{1}{\alpha}\frac{\partial T}{\partial t}$$

as follows, where we call $T_i - T_\infty \equiv \Delta T$:

$$\frac{\partial T}{\partial t} = (T_i - T_\infty)\frac{\partial \Theta}{\partial t} = \Delta T \frac{\partial \Theta}{\partial \zeta}\frac{\partial \zeta}{\partial t} = \Delta T \left(-\frac{x}{2t\sqrt{\alpha t}}\right)\frac{\partial \Theta}{\partial \zeta};$$

$$\frac{\partial T}{\partial x} = \Delta T \frac{\partial \Theta}{\partial \zeta}\frac{\partial \zeta}{\partial x} = \frac{\Delta T}{\sqrt{\alpha t}}\frac{\partial \Theta}{\partial \zeta};$$

$$\text{and} \quad \frac{\partial^2 T}{\partial x^2} = \frac{\Delta T}{\sqrt{\alpha t}}\frac{\partial^2 \Theta}{\partial \zeta^2}\frac{\partial \zeta}{\partial x} = \frac{\Delta T}{\alpha t}\frac{\partial^2 \Theta}{\partial \zeta^2}.$$

Substituting the first and last of these derivatives in the heat conduction equation, we get

$$\frac{d^2\Theta}{d\zeta^2} = -\frac{\zeta}{2}\frac{d\Theta}{d\zeta} \tag{5.45}$$

Notice that we changed from partial to total derivative notation, since Θ now depends solely on ζ. The i.c. for eqn. (5.45) is

$$T(t = 0) = T_i \quad \text{or} \quad \Theta\,(\zeta \to \infty) = 1 \tag{5.46}$$

and the one known b.c. is

$$T(x=0) = T_\infty \quad \text{or} \quad \Theta(\zeta = 0) = 0 \tag{5.47}$$

If we call $d\Theta/d\zeta \equiv \chi$, then eqn. (5.45) becomes the first-order equation

$$\frac{d\chi}{d\zeta} = -\frac{\zeta}{2}\chi$$

which can be integrated once to get

$$\chi \equiv \frac{d\Theta}{d\zeta} = C_1 e^{-\zeta^2/4} \tag{5.48}$$

and we integrate this a second time to get

$$\Theta = C_1 \int_0^\zeta e^{-\zeta^2/4}\, d\zeta + \underbrace{\Theta(0)}_{\substack{=0 \text{ according} \\ \text{to the b.c.}}} \tag{5.49}$$

The b.c. is now satisfied, and we need only substitute eqn. (5.49) in the i.c., eqn. (5.46), to solve for C_1:

$$1 = C_1 \int_0^\infty e^{-\zeta^2/4}\, d\zeta$$

The definite integral is given by integral tables as $\sqrt{\pi}$, so

$$C_1 = \frac{1}{\sqrt{\pi}}$$

Thus the solution to the problem of conduction in a semi-infinite region, subject to a b.c. of the first kind is

$$\boxed{\Theta = \frac{1}{\sqrt{\pi}} \int_0^\zeta e^{-\zeta^2/4}\, d\zeta = \frac{2}{\sqrt{\pi}} \int_0^{\zeta/2} e^{-s^2}\, ds \equiv \operatorname{erf}(\zeta/2)} \tag{5.50}$$

The second integral in eqn. (5.50), obtained by a change of variables, is called the *error function* (erf). Its name arises from its relationship to certain statistical problems related to the Gaussian distribution, which describes random errors. In Table 5.3, we list values of the error function and the complementary error function, $\operatorname{erfc}(x) \equiv 1 - \operatorname{erf}(x)$. Equation (5.50) is also plotted in Fig. 5.15.

Table 5.3 Error function and complementary error function.

$\zeta/2$	$\text{erf}(\zeta/2)$	$\text{erfc}(\zeta/2)$	$\zeta/2$	$\text{erf}(\zeta/2)$	$\text{erfc}(\zeta/2)$
0.00	0.00000	1.00000	1.10	0.88021	0.11980
0.05	0.05637	0.94363	1.20	0.91031	0.08969
0.10	0.11246	0.88754	1.30	0.93401	0.06599
0.15	0.16800	0.83200	1.40	0.95229	0.04771
0.20	0.22270	0.77730	1.50	0.96611	0.03389
0.30	0.32863	0.67137	1.60	0.97635	0.02365
0.40	0.42839	0.57161	1.70	0.98379	0.01621
0.50	0.52050	0.47950	1.80	0.98909	0.01091
0.60	0.60386	0.39614	1.8214	*0.99000*	*0.01000*
0.70	0.67780	0.32220	1.90	0.99279	0.00721
0.80	0.74210	0.25790	2.00	0.99532	0.00468
0.90	0.79691	0.20309	2.50	0.99959	0.00041
1.00	0.84270	0.15730	3.00	0.99998	0.00002

In Fig. 5.15 we see the early-time curves shown in Fig. 5.14 collapse into a single curve. This is accomplished by the *similarity transformation*, as we call it[5]: $\zeta/2 = x/2\sqrt{\alpha t}$. Under this transformation, we see immediately that the local value of $(T - T_\infty)$ is more than 99% of $(T_i - T_\infty)$ so long as

$$\frac{\zeta}{2} > 1.8214 \quad \text{or} \quad x > 3.64\sqrt{\alpha t} \tag{5.51}$$

Thus, slabs with a half-thickness in excess of $3.64\sqrt{\alpha t}$ are still effectively semi-infinite.

Example 5.4

For what maximum time can a samurai sword be analyzed as a semi-infinite region after it is quenched, if it has no clay coating and $\overline{h}_{\text{external}} \cong \infty$?

SOLUTION. First, we must guess the half-thickness of the sword (say, 3 mm) and its material (probably wrought iron with an average α

[5]The transformation is based upon the "similarity" of spatial an temporal changes in this problem.

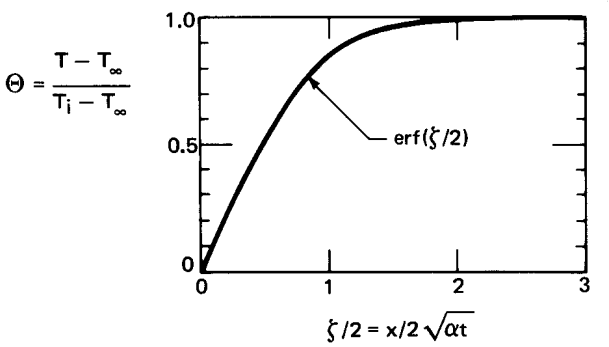

Figure 5.15 Temperature distribution in a semi-infinite region.

around 1.5×10^{-5} m^2/s). Then we invert eqn. (5.51) and set x equal to the half-thickness, so

$$t \leqslant \frac{x^2}{3.64^2 \alpha} = \frac{(0.003 \text{ m})^2}{13.3(1.5)(10)^{-5} \text{ m}^2/\text{s}} = 0.045 \text{ s}$$

Thus the quench would be felt at the centerline of the sword within only 1/20 s. The thermal diffusivity of clay is smaller than that of steel by a factor of about 30, so the quench time of the coated steel must continue for over 1 s before the temperature of the steel is affected at all, if the clay and the sword thicknesses are comparable. ■

Equation (5.51) provides an interesting foretaste of the notion of a fluid boundary layer. In the context of Fig. 1.9 and Fig. 1.10, we observe that free stream flow around an object is disturbed in a thick layer near the object because the fluid adheres to it. It turns out that the thickness of this boundary layer of altered flow velocity increases in the downstream direction. For flow over a flat plate, this thickness is approximately $4.92\sqrt{\nu t}$, where t is the time required for an element of the stream fluid to move from the leading edge of the plate to a point of interest. This is quite similar to eqn. (5.51), except that the thermal diffusivity, α, has been replaced by its counterpart, the kinematic viscosity, ν, and the constant is a bit larger. The velocity profile will resemble Fig. 5.15.

If we repeated the problem with a boundary condition of the third kind, we would expect to get $\Theta = \Theta(\text{Bi}, \zeta)$, except that there is no length, L, upon which to build a Biot number. Therefore, we must replace L with $\sqrt{\alpha t}$, which has the dimension of length, so

$$\Theta = \Theta\left(\zeta, \frac{\overline{h}\sqrt{\alpha t}}{k}\right) \equiv \Theta(\zeta, \beta) \tag{5.52}$$

The term $\zeta \equiv \overline{h}\sqrt{\alpha t}/k$ is like the product: $\mathrm{Bi}\sqrt{\mathrm{Fo}}$. The solution of this problem (see, e.g., [5.6], §2.7) can be conveniently written in terms of the complementary error function, $\mathrm{erfc}(x) \equiv 1 - \mathrm{erf}(x)$:

$$\boxed{\Theta = \mathrm{erf}\,\frac{\zeta}{2} + \exp\left(\beta\zeta + \beta^2\right)\left[\mathrm{erfc}\left(\frac{\zeta}{2} + \beta\right)\right]} \tag{5.53}$$

This result is plotted in Fig. 5.16.

Example 5.5

Most of us have passed our finger through an 800°C candle flame and know that if we limit exposure to about 1/4 s we will not be burned. Why not?

Solution. The short exposure to the flame causes only a *very* superficial heating, so we consider the finger to be a semi-infinite region and go to eqn. (5.53) to calculate $(T_{\text{burn}} - T_{\text{flame}})/(T_i - T_{\text{flame}})$. It turns out that the burn threshold of human skin, T_{burn}, is about 65°C. (That is why 140°F or 60°C tap water is considered to be "scalding.") Therefore, we shall calculate how long it will take for the surface temperature of the finger to rise from body temperature (37°C) to 65°C, when it is protected by an assumed $\overline{h} \cong 100$ W/m^2·°C. We shall assume that the thermal conductivity of human flesh equals that of its major component—water—and that the thermal diffusivity is equal to the known value for beef. Then

$$\Theta = \frac{65 - 800}{37 - 800} = 0.963$$

$$\beta\zeta = \frac{\overline{h}x}{k} = 0 \quad \text{since } x = 0 \text{ at the surface}$$

$$\beta^2 = \frac{\overline{h}^2\alpha t}{k^2} = \frac{100^2(0.135x10^{-6})t}{0.63^2} = 0.0034(t \text{ s})$$

The situation is quite far into the corner of Fig. 5.16. We read $\beta^2 \cong 0.001$, which corresponds with $t \cong 0.3$ s. For greater accuracy, we must go to eqn. (5.53):

$$0.963 = \underbrace{\mathrm{erf}\,0}_{=0} + e^{0.0034t}\left[\mathrm{erfc}\left(0 + \sqrt{0.0034\,t}\right)\right]$$

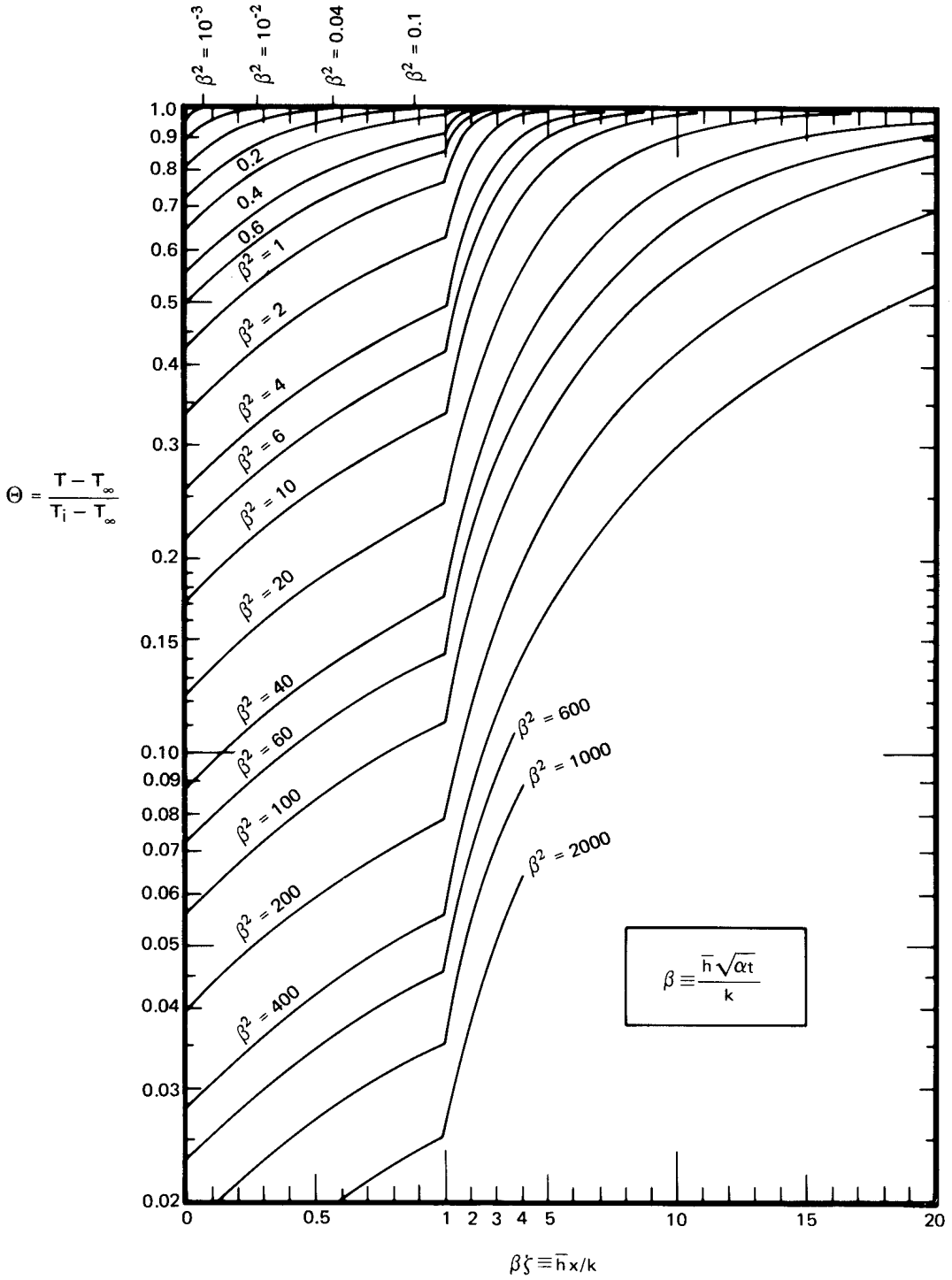

Figure 5.16 The cooling of a semi-infinite region by an environment at T_∞, through a heat transfer coefficient, $\bar{h}$.

so

$$0.963 = e^{0.0034t} \operatorname{erfc} \sqrt{0.0034\, t}$$

By trial and error, we get $t \cong 0.33$ s.

Thus it would require about $1/3$ s to bring the skin to the burn point. ■

Experiment 5.1

Immerse your hand in the subfreezing air in the freezer compartment of your refrigerator. Next immerse your finger in a mixture of ice cubes and water, but do not move it. Then, immerse your finger in a mixture of ice cubes and water , swirling it around as you do so. Describe your initial sensation in each case, and explain the differences in terms of Fig. 5.16. What variable has changed from one case to another?

Heat transfer

Heat will be removed from the exposed surface of a semi-infinite region, with a b.c. of either the first or the third kind, in accordance with Fourier's law:

$$q = -k \left.\frac{\partial T}{\partial x}\right|_{x=0} = \frac{k(T_\infty - T_i)}{\sqrt{\alpha t}} \left.\frac{d\Theta}{d\zeta}\right|_{\zeta=0}$$

Differentiating Θ as given by eqn. (5.50), we obtain, for the b.c. of the first kind,

$$\boxed{q = \frac{k(T_\infty - T_i)}{\sqrt{\alpha t}} \left(\frac{1}{\sqrt{\pi}} e^{-\zeta^2/4}\right)_{\zeta=0} = \frac{k(T_\infty - T_i)}{\sqrt{\pi\, \alpha t}}} \tag{5.54}$$

Thus, q decreases with increasing time, as $t^{-1/2}$. When the temperature of the surface is first changed, the heat removal rate is enormous. Then it drops off rapidly.

It often occurs that we suddenly apply a specified input heat flux, q_w, at the boundary of a semi-infinite region. In such a case, we can differentiate the heat diffusion equation with respect to x, so

$$\alpha \frac{\partial^3 T}{\partial x^3} = \frac{\partial^2 T}{\partial t \partial x}$$

When we substitute $q = -k\,\partial T/\partial x$ in this, we obtain

$$\alpha \frac{\partial^2 q}{\partial x^2} = \frac{\partial q}{\partial t}$$

with the b.c.'s:

$$q(x = 0, t > 0) = q_w \qquad \text{or} \qquad \left.\frac{q_w - q}{q_w}\right|_{x=0} = 0$$

$$q(x \geqslant 0, t = 0) = 0 \qquad \text{or} \qquad \left.\frac{q_w - q}{q_w}\right|_{t=0} = 1$$

What we have done here is quite elegant. We have made the problem of predicting the local heat flux q into exactly the same form as that of predicting the local temperature in a semi-infinite region subjected to a step change of wall temperature. Therefore, the solution must be the same:

$$\frac{q_w - q}{q_w} = \operatorname{erf}\left(\frac{x}{2\sqrt{\alpha t}}\right). \tag{5.55}$$

The temperature distribution is obtained by integrating Fourier's law. At the wall, for example:

$$\int_{T_i}^{T_w} dT = -\int_{\infty}^{0} \frac{q}{k}\,dx$$

where $T_i = T(x \to \infty)$ and $T_w = T(x = 0)$. Then

$$T_w = T_i + \frac{q_w}{k} \int_0^{\infty} \operatorname{erfc}(x/2\sqrt{\alpha t})\,dx$$

This becomes

$$T_w = T_i + \frac{q_w}{k}\sqrt{\alpha t} \underbrace{\int_0^{\infty} \operatorname{erfc}(\zeta/2)\,d\zeta}_{=2/\sqrt{\pi}}$$

so

$$T_w(t) = T_i + 2\frac{q_w}{k}\sqrt{\frac{\alpha t}{\pi}} \tag{5.56}$$

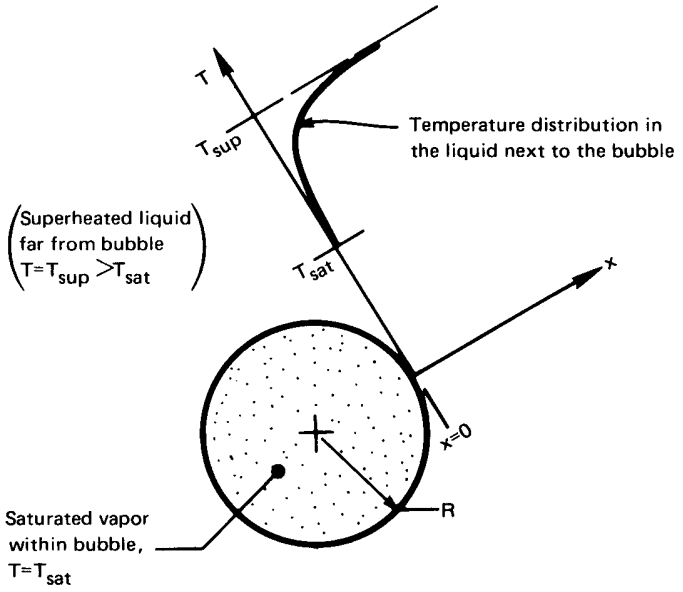

Figure 5.17 A bubble growing in a superheated liquid.

Example 5.6 Predicting the Growth Rate of a Vapor Bubble in an Infinite Superheated Liquid

This prediction is relevant to a large variety of processes, ranging from nuclear thermodynamics to the direct-contact heat exchange. It was originally presented by Max Jakob and others in the early 1930s (see, e.g., [5.10, Chap. I]). Jakob (pronounced Yah′-kob) was an important figure in heat transfer during the 1920s and 1930s. He left Nazi Germany in 1936 to come to the United States. We encounter his name again later.

Figure 5.17 shows how growth occurs. When a liquid is superheated to a temperature somewhat above its boiling point, a small gas or vapor cavity in that liquid will grow. (That is what happens in the superheated water at the bottom of a teakettle.)

This bubble grows into the surrounding liquid because its boundary is kept at the saturation temperature, T_{sat}, by the near-equilibrium coexistence of liquid and vapor. Therefore, heat must flow from the superheated surroundings to the interface, where evaporation occurs. So long as the layer of cooled liquid is thin, we should not suffer too much error by using the one-dimensional semi-infinite region solution to predict the heat flow.

Thus, we can write the energy balance at the bubble interface:

$$\underbrace{\left(-q\,\frac{\mathrm{W}}{\mathrm{m}^2}\right)\left(4\pi R^2\,\mathrm{m}^2\right)}_{Q \quad \text{into bubble}} = \underbrace{\left(\rho_g h_{\mathrm{fg}}\,\frac{\mathrm{J}}{\mathrm{m}^3}\right)\left(\frac{dV}{dt}\,\frac{\mathrm{m}^3}{\mathrm{s}}\right)}_{\substack{\text{rate of energy increase} \\ \text{of the bubble}}}$$

and then substitute eqn. (5.54) for q and $4\pi R^3/3$ for the volume, V. This gives

$$\frac{k(T_{\mathrm{sup}} - T_{\mathrm{sat}})}{\sqrt{\alpha \pi t}} = \rho_g h_{\mathrm{fg}} \frac{dR}{dt} \tag{5.57}$$

Integrating eqn. (5.57) from $R = 0$ at $t = 0$ up to R at t, we obtain Jakob's prediction:

$$R = \frac{2}{\sqrt{\pi}} \frac{k\Delta T}{\rho_g h_{\mathrm{fg}} \sqrt{\alpha}} \sqrt{t} \tag{5.58}$$

■

This analysis was done without assuming the curved bubble interface to be plane, 24 years after Jakob's work, by Plesset and Zwick [5.11]. It was verified in a more exact way after another 5 years by Scriven [5.12]. These calculations are more complicated, but they lead to a very similar result:

$$R = \frac{2\sqrt{3}}{\sqrt{\pi}} \frac{k\Delta T}{\rho_g h_{\mathrm{fg}} \sqrt{\alpha}} \sqrt{t} = \sqrt{3}\, R_{\mathrm{Jakob}}. \tag{5.59}$$

Both predictions are compared with some of the data of Dergarabedian [5.13] in Fig. 5.18. The data and the exact theory match almost perfectly. The simple theory of Jakob et al. shows the correct dependence on R on all its variables, but it shows growth rates that are low by a factor of $\sqrt{3}$. This is because the expansion of the spherical bubble causes a relative motion of liquid toward the bubble surface, which helps to thin the region of thermal influence in the radial direction. Consequently, the temperature gradient and heat transfer rate are higher than in Jakob's model, which neglected the liquid motion. Therefore, the temperature profile flattens out more slowly than Jakob predicts, and the bubble grows more rapidly.

Experiment 5.2

Touch various objects in the room around you: glass, wood, corkboard, paper, steel, and gold or diamond, if available. Rank them in

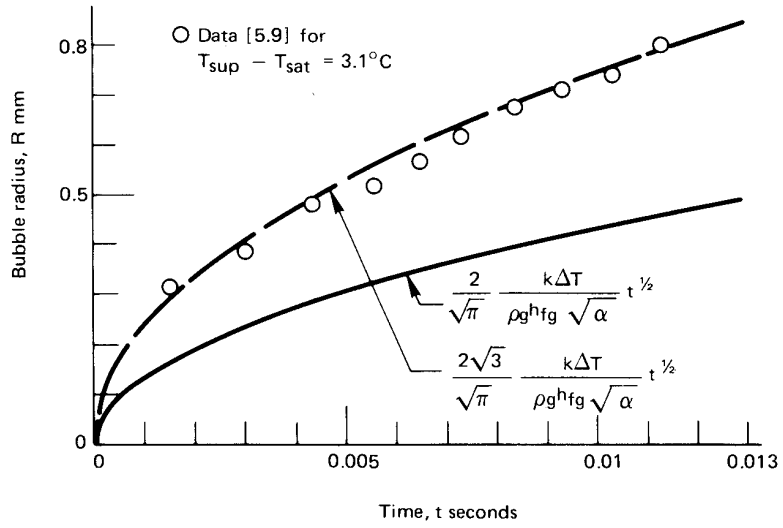

Figure 5.18 The growth of a vapor bubble—predictions and measurements.

order of which feels coldest at the first instant of contact (see Problem 5.29).

The more advanced theory of heat conduction (see, e.g., [5.6]) shows that if two semi-infinite regions at uniform temperatures T_1 and T_2 are placed together suddenly, their interface temperature, T_s, is given by[6]

$$\frac{T_s - T_2}{T_1 - T_2} = \frac{\sqrt{(k\rho c_p)_2}}{\sqrt{(k\rho c_p)_1} + \sqrt{(k\rho c_p)_2}}$$

If we identify one region with your body ($T_1 \cong 37°C$) and the other with the object being touched ($T_2 \simeq 20°C$), we can determine the temperature, T_s, that the surface of your finger will reach upon contact. Compare the ranking you obtain experimentally with the ranking given by this equation.

[6]For semi-infinite regions, initially at uniform temperatures, T_s does not vary with time. For finite bodies, T_s will eventually change. A constant value of T_s means that each of the two bodies independently behaves as a semi-infinite body whose surface temperature has been changed to T_s at time zero. Consequently, our previous results—eqns. (5.50), (5.51), and (5.54)—apply to each of these bodies while they may be treated as semi-infinite. We need only replace T_∞ by T_s in those equations.

Notice that your bloodstream and capillary system provide a heat source in your finger, so the equation is valid only for a moment. Then you start replacing heat lost to the objects. If you included a diamond among the objects that you touched, you will notice that it warmed up almost instantly. Most diamonds are quite small but are possessed of the highest known value of α. Therefore, they can behave as a semi-infinite region only for an instant, and they usually feel warm to the touch.

Conduction to a semi-infinite region with a harmonically oscillating temperature at the boundary

Suppose that we approximate the annual variation of the ambient temperature as sinusoidal and then ask what the influence of this variation will be beneath the ground. We want to calculate $T - \overline{T}$ (where $\overline{T}$ is the average surface temperature) as a function of: depth, x; thermal diffusivity, α; frequency of oscillation, ω; amplitude of oscillation, ΔT; and time, t. There are six variables in °C, m, and s, so the problem can be represented in three dimensionless variables:

$$\Theta \equiv \frac{T - \overline{T}}{\Delta T}; \qquad \Omega \equiv \omega t; \qquad \xi \equiv x\sqrt{\frac{\omega}{2\alpha}}.$$

We pose the problem as follows in these variables. The heat conduction equation is

$$\frac{1}{2}\frac{\partial^2 \Theta}{\partial \xi^2} = \frac{\partial \Theta}{\partial \Omega} \tag{5.60}$$

and the b.c.'s are

$$\Theta\Big|_{\xi=0} = \cos \omega t \qquad \text{and} \qquad \Theta\Big|_{\xi>0} = \text{finite} \tag{5.61}$$

No i.c. is needed because, after the initial transient decays, the remaining steady oscillation must be periodic.

The solution is given by Carslaw and Jaeger (see [5.6, §2.6] or work Problem 5.16). It is

$$\Theta(\xi, \Omega) = e^{-\xi} \cos(\Omega - \xi) \tag{5.62}$$

This result is plotted in Fig. 5.19. It shows that the surface temperature variation decays exponentially into the region and suffers a phase shift as it does so.

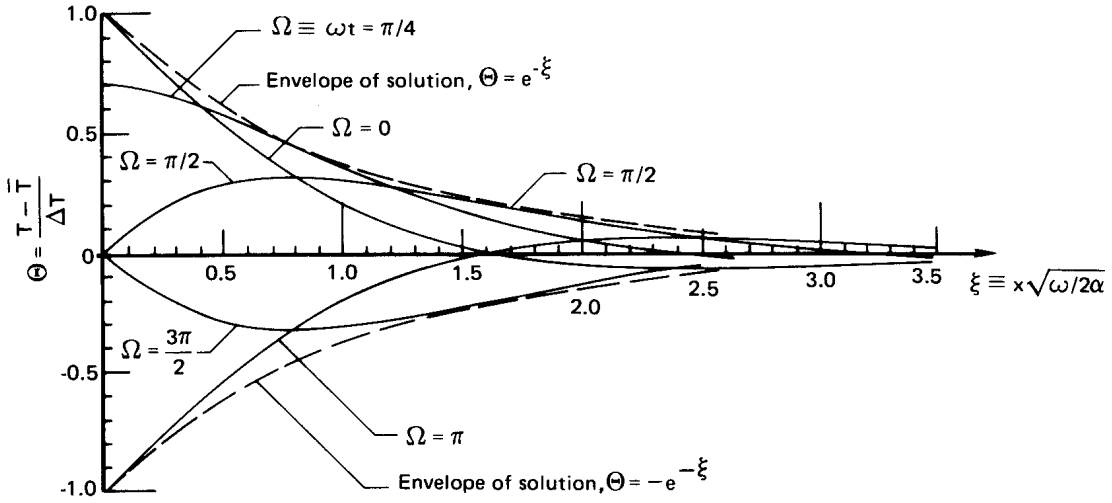

Figure 5.19 The temperature variation within a semi-infinite region whose temperature varies harmonically at the boundary.

Example 5.7

How deep in the earth must we dig to find the temperature wave that was launched by the coldest part of the last winter if it is now high summer?

SOLUTION. $\omega = 2\pi$ rad/yr, and $\Omega = \omega t = 0$ at the present. First, we must find the depths at which the $\Omega = 0$ curve reaches its local extrema. (We pick the $\Omega = 0$ curve because it gives the highest temperature at $t = 0$.)

$$\left.\frac{d\Theta}{d\xi}\right|_{\Omega=0} = -e^{-\xi}\cos(0-\xi) + e^{-\xi}\sin(0-\xi) = 0$$

This gives

$$\tan(0-\xi) = 1 \quad \text{so} \quad \xi = \frac{3\pi}{4}, \frac{7\pi}{4}, \ldots$$

and the first minimum occurs where $\xi = 3\pi/4 = 2.356$, as we can see in Fig. 5.19. Thus,

$$\xi = x\sqrt{\omega/2\alpha} = 2.356$$

or, if we take $\alpha = 0.139\times10^{-6}$ m^2/s (given in [5.14] for coarse, gravelly earth),

$$x = 2.356 \Big/ \sqrt{\frac{2\pi}{2\,(0.139\times10^{-6})}\,\frac{1}{365(24)(3600)}} = 2.783 \text{ m}$$

If we dug in the earth, we would find it growing older and colder until it reached a maximum coldness at a depth of about 2.8 m. Farther down, it would begin to warm up again, but not much. In midwinter ($\Omega = \pi$), the reverse would be true. ■

5.7 Steady multidimensional heat conduction

Introduction

The general equation for $T(\vec{r})$ during steady conduction in a region of constant thermal conductivity, without heat sources, is called Laplace's equation:

$$\nabla^2 T = 0 \tag{5.63}$$

It looks easier to solve than it is, since [recall eqn. (2.12) and eqn. (2.14)] the Laplacian, $\nabla^2 T$, is a sum of several second partial derivatives. We solved one two-dimensional heat conduction problem in Example 4.1, but this was not difficult because the boundary conditions were made to order. Depending upon your mathematical background and the specific problem, the analytical solution of multidimensional problems can be anything from straightforward calculation to a considerable challenge. The reader who wishes to study such analyses in depth should refer to [5.6] or [5.15], where such calculations are discussed in detail.

Faced with a steady multidimensional problem, three routes are open to us:

- Find out whether or not the analytical solution is already available in a heat conduction text or in other published literature.
- Solve the problem.
  (a) Analytically.
  (b) Numerically.
- Obtain the solution graphically if the problem is two-dimensional.

It is to the last of these options that we give our attention next.

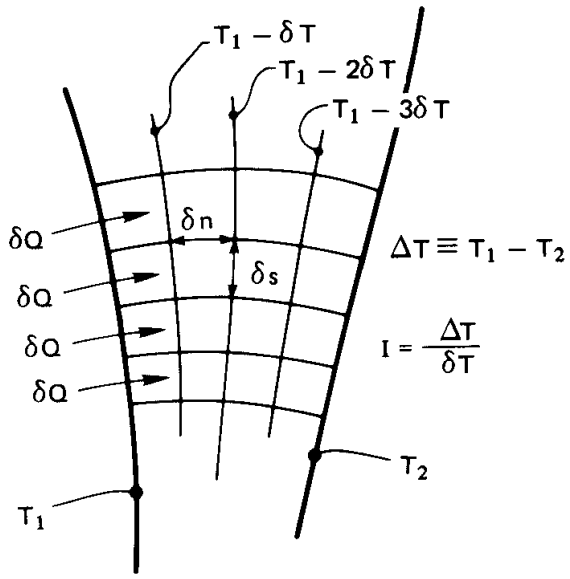

Figure 5.20 The two-dimensional flow of heat between two isothermal walls.

The flux plot

The method of *flux plotting* will solve all steady planar problems in which all boundaries are held at either of two temperatures or are insulated. With a little skill, it will provide accuracies of a few percent. This accuracy is almost always greater than the accuracy with which the b.c.'s and k can be specified; and it displays the physical sense of the problem very clearly.

Figure 5.20 shows heat flowing from one isothermal wall to another in a regime that does not conform to any convenient coordinate scheme. We identify a series of channels, each which carries the same heat flow, δQ W/m. We also include a set of equally spaced isotherms, δT apart, between the walls. Since the heat fluxes in all channels are the same,

$$\left|\delta Q\right| = k\frac{\delta T}{\delta n}\delta s \tag{5.64}$$

Notice that if we arrange things so that δQ, δT, and k are the same for flow through each rectangle in the flow field, then $\delta s/\delta n$ must be the same for each rectangle. We therefore arbitrarily set the ratio equal to unity, so all the elements appear as distorted *squares*.

The objective then is to sketch the isothermal lines and the adiabatic,[7]

[7]These are lines *in the direction of heat flow*. It immediately follows that there can

or heat flow, lines which run perpendicular to them. This sketch is to be done subject to two constraints

- Isothermal and adiabatic lines must intersect at right angles.
- They must subdivide the flow field into elements that are nearly square—"nearly" because they have slightly curved sides.

Once the grid has been sketched, the temperature anywhere in the field can be read directly from the sketch. And the heat flow per unit depth into the paper is

$$\boxed{Q \text{ W/m} = Nk\,\delta T\,\frac{\delta s}{\delta n} = \frac{N}{I}\,k\Delta T} \tag{5.65}$$

where N is the number of heat flow channels and I is the number of temperature increments, $\Delta T/\delta T$.

The first step in constructing a flux plot is to draw the boundaries of the region accurately *in ink*, using either drafting software or a straightedge. The next is to obtain a soft pencil (such as a no. 2 grade) and a soft eraser. We begin with an example that was executed nicely in the influential *Heat Transfer Notes* [5.3] of the mid-twentieth century. This example is shown in Fig. 5.21.

The particular example happens to have an axis of symmetry in it. We immediately interpret this as an adiabatic boundary because heat cannot cross it. The problem therefore reduces to the simpler one of sketching lines in only one half of the area. We illustrate this process in four steps. Notice the following steps and features in this plot:

- Begin by dividing the region, by sketching in either a single isothermal or adiabatic line.
- Fill in the lines perpendicular to the original line so as to make squares. Allow the original line to move in such a way as to accommodate squares. This will *always* require some erasing. Therefore:
- *Never* make the original lines dark and firm.
- By successive subdividing of the squares, make the final grid. *Do not make the grid very fine.* If you do, you will lose accuracy because the lack of perpendicularity and squareness will be less evident to the eye. Step IV in Fig. 5.21 is as fine a grid as should ever be made.

be no component of heat flow normal to them; they must be adiabatic.

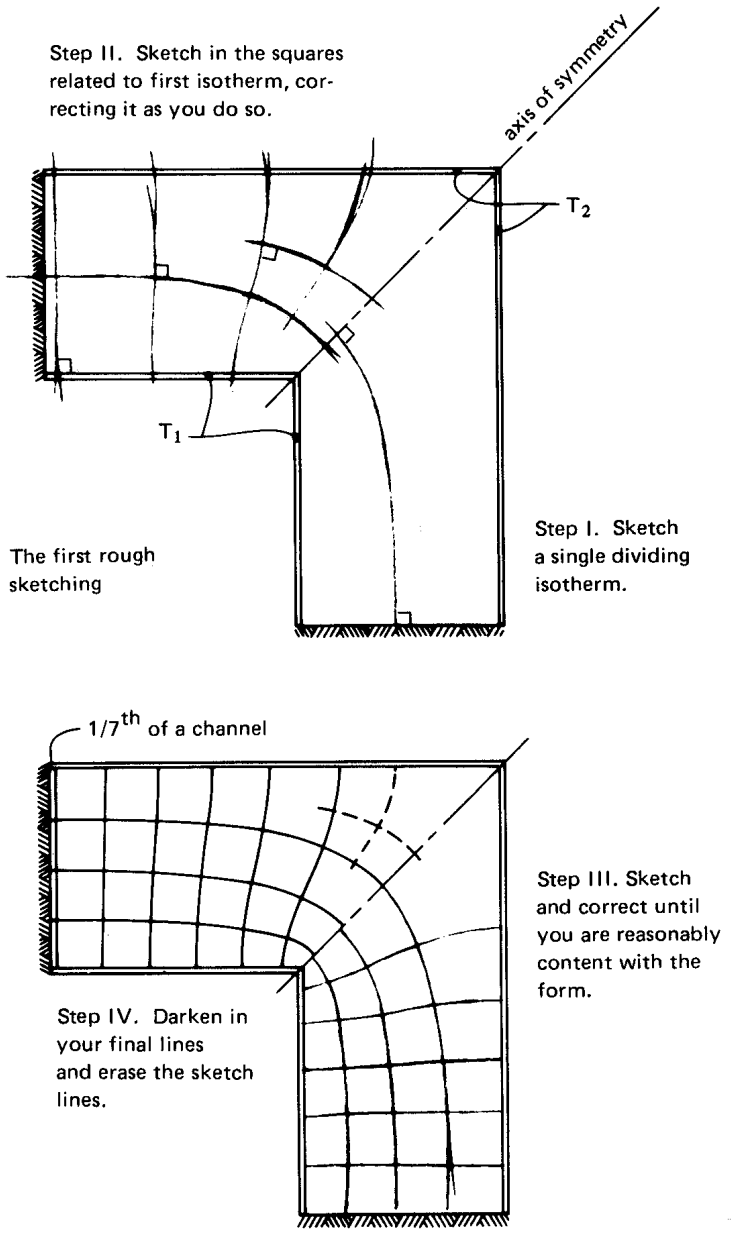
Step II. Sketch in the squares related to first isotherm, correcting it as you do so.
axis of symmetry
T_2
T_1
The first rough sketching
Step I. Sketch a single dividing isotherm.
1/7th of a channel
Step III. Sketch and correct until you are reasonably content with the form.
Step IV. Darken in your final lines and erase the sketch lines.

Figure 5.21 The evolution of a flux plot.

- If you have doubts about whether any large, ill-shaped regions are correct, fill them in with an extra isotherm and adiabatic line to be sure that they resolve into appropriate squares (see the dashed lines in Fig. 5.21).
- Fill in the final grid, when you are sure of it, either in hard pencil or pen, and erase any lingering background sketch lines.
- Your flow channels need not come out even. Notice that there is an extra 1/7 of a channel in Fig. 5.21. This is simply counted as 1/7 of a square in eqn. (5.65).
- Never allow isotherms or adiabatic lines to intersect themselves.

When the sketch is complete, we can return to eqn. (5.65) to compute the heat flux. In this case

$$Q = \frac{N}{I}\, k\Delta T = \frac{2(6.14)}{4}\, k\Delta T = 3.07\, k\Delta T$$

When the authors of [5.3] did this problem, they obtained $N/I = 3.00$—a value only 2% below ours. This kind of agreement is typical when flux plotting is done with care.

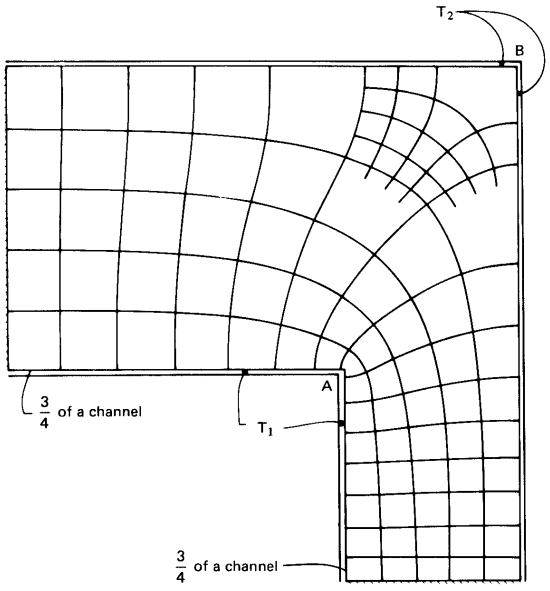

Figure 5.22 A flux plot with no axis of symmetry to guide construction.

One must be careful not to grasp at a false axis of symmetry. Figure 5.22 shows a shape similar to the one that we just treated, but with unequal legs. In this case, no lines must enter (or leave) the corners A and B. The reason is that since there *is* no symmetry, we have no guidance as to the direction of the lines at these corners. In particular, we know that a line leaving A will no longer arrive at B.

Example 5.8

A structure consists of metal walls, 8 cm apart, with insulating material (k = 0.12 W/m·K) between. Ribs 4 cm long protrude from one wall every 14 cm. They can be assumed to stay at the temperature of that wall. Find the heat flux through the wall if the first wall is at 40°C and the one with ribs is at 0°C. Find the temperature in the middle of the wall, 2 cm from a rib, as well.

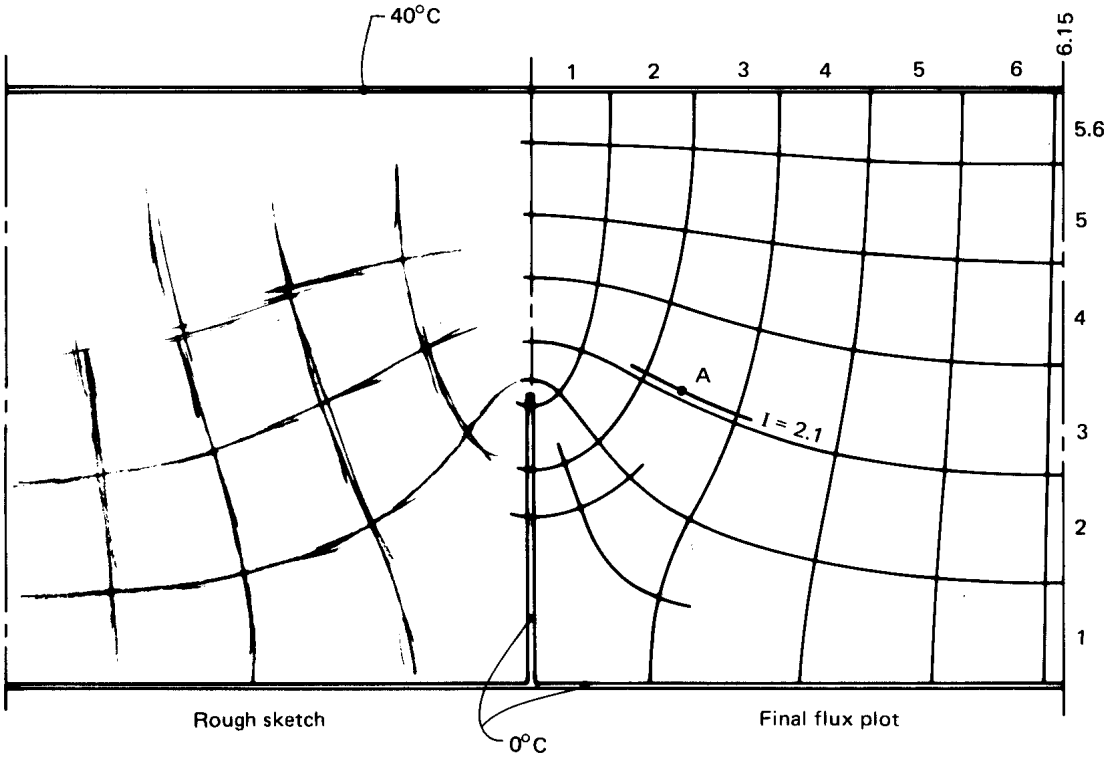

Figure 5.23 Heat transfer through a wall with isothermal ribs.

SOLUTION. The flux plot for this configuration is shown in Fig. 5.23. For a typical section, there are approximately 5.6 isothermal increments and 6.15 heat flow channels, so

$$Q = \frac{N}{I}\, k\Delta T = \frac{2(6.15)}{5.6}(0.12)(40-0) = 10.54 \text{ W/m}$$

where the factor of 2 accounts for the fact that there are two halves in the section. We deduce the temperature for the point of interest, A, by a simple proportionality:

$$T_{\text{point } A} = \frac{2.1}{5.6}(40-0) = 15^\circ\text{C} \qquad \blacksquare$$

The shape factor

A heat conduction *shape factor* S may be defined for steady problems involving two isothermal surfaces as follows:

$$Q \equiv S\, k\Delta T. \tag{5.66}$$

Thus far, every steady heat conduction problem we have done has taken this form. For these situations, the heat flow always equals a function of the geometric shape of the body multiplied by $k\Delta T$.

The shape factor can be obtained analytically, numerically, or through flux plotting. For example, let us compare eqn. (5.65) and eqn. (5.66):

$$Q\,\frac{\text{W}}{\text{m}} = (S \text{ dimensionless})\left(k\Delta T\,\frac{\text{W}}{\text{m}}\right) = \frac{N}{I}\, k\Delta T \tag{5.67}$$

This shows S to be dimensionless in a two-dimensional problem, but in three dimensions S has units of meters:

$$Q\ \text{W} = (S\ \text{m})\left(k\Delta T\,\frac{\text{W}}{\text{m}}\right). \tag{5.68}$$

It also follows that the thermal resistance of a two-dimensional body is

$$R_t = \frac{1}{kS} \qquad \text{where} \qquad Q = \frac{\Delta T}{R_t} \tag{5.69}$$

For a three-dimensional body, eqn. (5.69) is unchanged except that the dimensions of Q and R_t differ.[8]

[8] Recall that we noted after eqn. (2.22) that the dimensions of R_t changed, depending on whether or not Q was expressed in a unit-length basis.

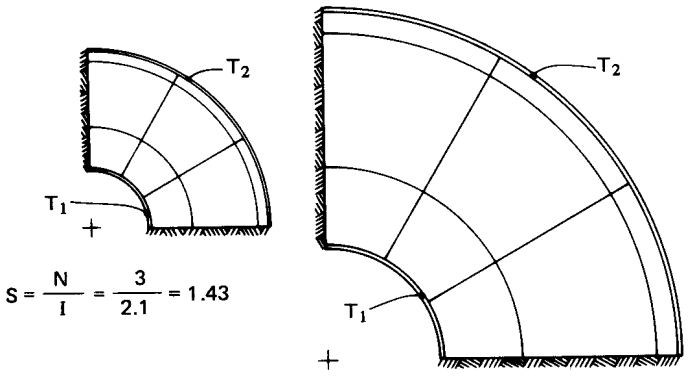

Figure 5.24 The shape factor for two similar bodies of different size.

The virtue of the shape factor is that it summarizes a heat conduction solution in a given configuration. Once S is known, it can be used again and again. That S is nondimensional in two-dimensional configurations means that Q is independent of the size of the body. Thus, in Fig. 5.21, S is always 3.07—regardless of the size of the figure—and in Example 5.8, S is $2(6.15)/5.6 = 2.196$, whether or not the wall is made larger or smaller. When a body's breadth is increased so as to increase Q, its thickness in the direction of heat flow is also increased so as to decrease Q by the same factor.

Example 5.9

Calculate the shape factor for a one-quarter section of a thick cylinder.

SOLUTION. We already know R_t for a thick cylinder. It is given by eqn. (2.22). From it we compute

$$S_{\text{cyl}} = \frac{1}{kR_t} = \frac{2\pi}{\ln(r_o/r_i)}$$

so on the case of a quarter-cylinder,

$$S = \frac{\pi}{2\ln(r_o/r_i)}$$

The quarter-cylinder is pictured in Fig. 5.24 for a radius ratio, $r_o/r_i = 3$, but for two different sizes. In both cases $S = 1.43$. (Note that the same S is also given by the flux plot shown.) ■

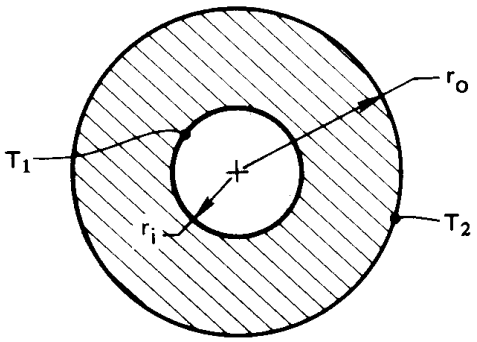

Figure 5.25 Heat transfer through a thick, hollow sphere.

Example 5.10

Calculate S for a thick hollow sphere, as shown in Fig. 5.25.

SOLUTION. The general solution of the heat diffusion equation in spherical coordinates for purely radial heat flow is:

$$T = \frac{C_1}{r} + C_2$$

when $T = \text{fn}(r \text{ only})$. The b.c.'s are

$$T(r = r_i) = T_i \quad \text{and} \quad T(r = r_o) = T_o$$

substituting the general solution in the b.c.'s we get

$$\frac{C_1}{r_i} + C_2 = T_i \quad \text{and} \quad \frac{C_1}{r_o} + C_1 = T_o$$

Therefore,

$$C_1 = \frac{T_i - T_o}{r_o - r_i} r_i r_o \quad \text{and} \quad C_2 = T_i - \frac{T_i - T_o}{r_o - r_i} r_o$$

Putting C_1 and C_2 in the general solution, and calling $T_i - T_o \equiv \Delta T$, we get

$$T = T_i + \Delta T \left[\frac{r_i r_o}{r(r_o - r_i)} - \frac{r_o}{r_o - r_i} \right]$$

Then

$$Q = -kA \frac{dT}{dr} = \frac{4\pi(r_i r_o)}{r_o - r_i} k\Delta T$$

$$S = \frac{4\pi(r_i r_o)}{r_o - r_i} \text{ m}$$

where S now has the dimensions of m. ■

Table 5.4 includes a number of analytically derived shape factors for use in calculating the heat flux in different configurations. Notice that these results will not give local temperatures. To obtain that information, one must solve the Laplace equation, $\nabla^2 T = 0$, by one of the methods listed at the beginning of this section. Notice, too, that this table is restricted to bodies with isothermal and insulated boundaries.

In the two-dimensional cases, both a hot and a cold surface must be present in order to have a steady-state solution; if only a single hot (or cold) body is present, steady state is never reached. For example, a hot isothermal cylinder in a cooler, infinite medium never reaches steady state with that medium. Likewise, in situations 5, 6, and 7 in the table, the medium far from the isothermal plane must also be at temperature T_2 in order for steady state to occur; otherwise the isothermal plane and the medium below it would behave as an unsteady, semi-infinite body. Of course, since no real medium is truly infinite, what this means in practice is that steady state only occurs after the medium "at infinity" comes to a temperature T_2. Conversely, in three-dimensional situations (such as 4, 8, 12, and 13), a body *can* come to steady state with a surrounding infinite or semi-infinite medium at a different temperature.

Example 5.11

A spherical heat source of 6 cm in diameter is buried 30 cm below the surface of a very large box of soil and kept at 35°C. The surface of the soil is kept at 21°C. If the steady heat transfer rate is 14 W, what is the thermal conductivity of this sample of soil?

SOLUTION.

$$Q = S\,k\Delta T = \left(\frac{4\pi R}{1 - R/2h}\right) k\Delta T$$

where S is that for situation 7 in Table 5.4. Then

$$k = \frac{14\ \text{W}}{(35 - 21)\text{K}} \frac{1 - (0.06/2)/2(0.3)}{4\pi(0.06/2)\ \text{m}} = 2.545\ \text{W/m·K}$$ ■

Readers who desire a broader catalogue of shape factors should refer to [5.16], [5.18], or [5.19].

Table 5.4 Conduction shape factors: $Q = S\,k\Delta T$.

Situation	*Shape factor, S*	*Dimensions*	*Source*
1. Conduction through a slab	A/L	meter	Example 2.2
2. Conduction through wall of a long thick cylinder	$\dfrac{2\pi}{\ln(r_o/r_i)}$	none	Example 5.9
3. Conduction through a thick-walled hollow sphere	$\dfrac{4\pi(r_o r_i)}{r_o - r_i}$	meter	Example 5.10
4. The boundary of a spherical hole of radius R conducting into an infinite medium 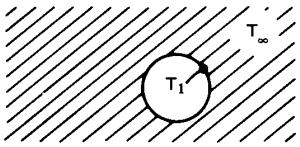	$4\pi R$	meter	Problems 5.19 and 2.15
5. Cylinder of radius R and length L, transferring heat to a parallel isothermal plane; $h \ll L$ 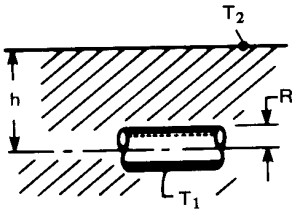	$\dfrac{2\pi L}{\cosh^{-1}(h/R)}$	meter	[5.16]
6. Same as item 5, but with $L \longrightarrow \infty$ (two-dimensional conduction)	$\dfrac{2\pi}{\cosh^{-1}(h/R)}$	none	[5.16]
7. An isothermal sphere of radius R transfers heat to an isothermal plane; $R/h < 0.8$ (see item 4) 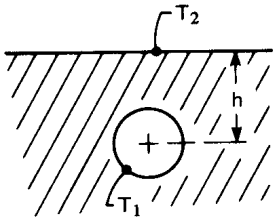	$\dfrac{4\pi R}{1 - R/2h}$	meter	[5.16, 5.17]

Table 5.4 Conduction shape factors: $Q = S\,k\Delta T$ *(con't).*

Situation	*Shape factor, S*	*Dimensions*	*Source*
8. An isothermal sphere of radius R, near an insulated plane, transfers heat to a semi-infinite medium at T_∞ (see items 4 and 7) 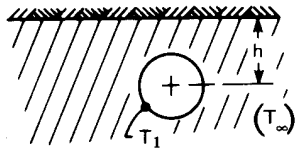	$\dfrac{4\pi R}{1 + R/2h}$	meter	[5.18]
9. Parallel cylinders exchange heat in an infinite conducting medium 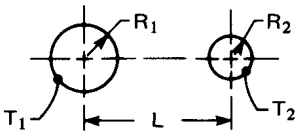	$\dfrac{2\pi}{\cosh^{-1}\left(\dfrac{L^2 - R_1^2 - R_2^2}{2R_1R_2}\right)}$	none	[5.6]
10. Same as 9, but with cylinders widely spaced; $L \gg R_1$ and R_2	$\dfrac{2\pi}{\cosh^{-1}\left(\dfrac{L}{2R_1}\right) + \cosh^{-1}\left(\dfrac{L}{2R_2}\right)}$	none	[5.16]
11. Cylinder of radius R_i surrounded by eccentric cylinder of radius $R_o > R_i$; centerlines a distance L apart (see item 2)	$\dfrac{2\pi}{\cosh^{-1}\left(\dfrac{R_o^2 + R_i^2 - L^2}{2R_oR_i}\right)}$	none	[5.6]
12. Isothermal disc of radius R on an otherwise insulated plane conducts heat into a semi-infinite medium at T_∞ below it	$4R$	meter	[5.6]
13. Isothermal ellipsoid of semimajor axis b and semiminor axes a conducts heat into an infinite medium at T_∞; $b > a$ (see 4)	$\dfrac{4\pi b\sqrt{1 - a^2/b^2}}{\tanh^{-1}\left(\sqrt{1 - a^2/b^2}\right)}$	meter	[5.16]

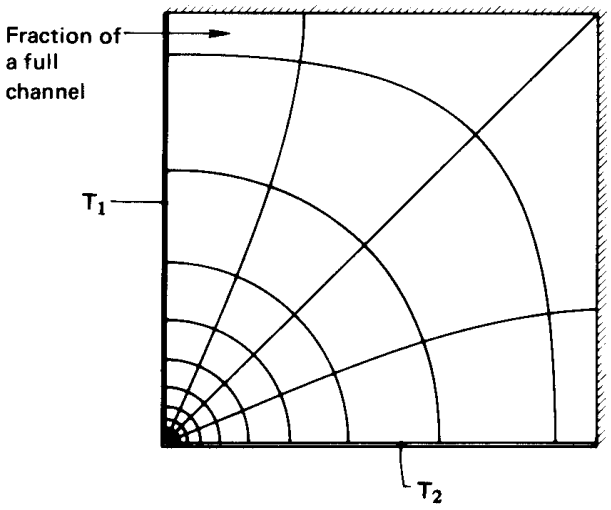

Figure 5.26 Resistance vanishes where two isothermal boundaries intersect.

The problem of locally vanishing resistance

Suppose that two different temperatures are specified on adjacent sides of a square, as shown in Fig. 5.26. The shape factor in this case is

$$S = \frac{N}{I} = \frac{\infty}{4} = \infty$$

(It is futile to try and count channels beyond $N \simeq 10$, but it is clear that they multiply without limit in the lower left corner.) The problem is that we have violated our rule that isotherms cannot intersect and have created a $1/r$ singularity. If we actually tried to sustain such a situation, the figure would be correct at some distance from the corner. However, where the isotherms are close to one another, they will necessarily influence and distort one another in such a way as to avoid intersecting. And S will never really be infinite, as it appears to be in the figure.

5.8 Transient multidimensional heat conduction— The tactic of superposition

Consider the cooling of a stubby cylinder, such as the one shown in Fig. 5.27a. The cylinder is initially at $T = T_i$, and it is suddenly subjected to a common b.c. on all sides. It has a length $2L$ and a radius r_o. Finding the temperature field in this situation is inherently complicated.

It requires solving the heat conduction equation for $T = \text{fn}(r, z, t)$ with b.c.'s of the first, second, or third kind.

However, Fig. 5.27a suggests that this can somehow be viewed as a combination of an infinite cylinder and an infinite slab. It turns out that the problem *can be analyzed* from that point of view.

If the body is subject to uniform b.c.'s of the first, second, or third kind, and if it has a uniform initial temperature, then its temperature response is simply the product of an infinite slab solution and an infinite cylinder solution each having the same boundary and initial conditions. For the case shown in Fig. 5.27a, if the cylinder begins convective cooling into a medium at temperature T_∞ at time $t = 0$, the dimensional temperature response is

$$T(r, z, t) - T_\infty = \left[T_{\text{slab}}(z, t) - T_\infty\right] \times \left[T_{\text{cyl}}(r, t) - T_\infty\right] \tag{5.70a}$$

Observe that the slab has as a characteristic length L, its half thickness, while the cylinder has as its characteristic length R, its radius. In dimensionless form, we may write eqn. (5.70a) as

$$\Theta \equiv \frac{T(r, z, t) - T_\infty}{T_i - T_\infty} = \left[\Theta_{\text{inf slab}}(\xi, \text{Fo}_s, \text{Bi}_s)\right] \left[\Theta_{\text{inf cyl}}(\rho, \text{Fo}_c, \text{Bi}_c)\right] \tag{5.70b}$$

For the cylindrical component of the solution,

$$\rho = \frac{r}{r_o}, \quad \text{Fo}_c = \frac{\alpha t}{r_o^2}, \quad \text{and} \quad \text{Bi}_c = \frac{\overline{h} r_o}{k},$$

while for the slab component of the solution

$$\xi = \frac{z}{L} + 1, \quad \text{Fo}_s = \frac{\alpha t}{L^2}, \quad \text{and} \quad \text{Bi}_s = \frac{\overline{h} L}{k}.$$

The component solutions are none other than those discussed in Sections 5.3–5.5. The proof of the legitimacy of such product solutions is given by Carlsaw and Jaeger [5.6, §1.15].

Figure 5.27b shows a point inside a one-eighth-infinite region, near the corner. This case may be regarded as the product of three semi-infinite bodies. To find the temperature at this point we write

$$\Theta \equiv \frac{T(x_1, x_2, x_3, t) - T_\infty}{T_i - T_\infty} = \left[\Theta_{\text{semi}}(\zeta_1, \beta)\right] \left[\Theta_{\text{semi}}(\zeta_2, \beta)\right] \left[\Theta_{\text{semi}}(\zeta_3, \beta)\right] \tag{5.71}$$

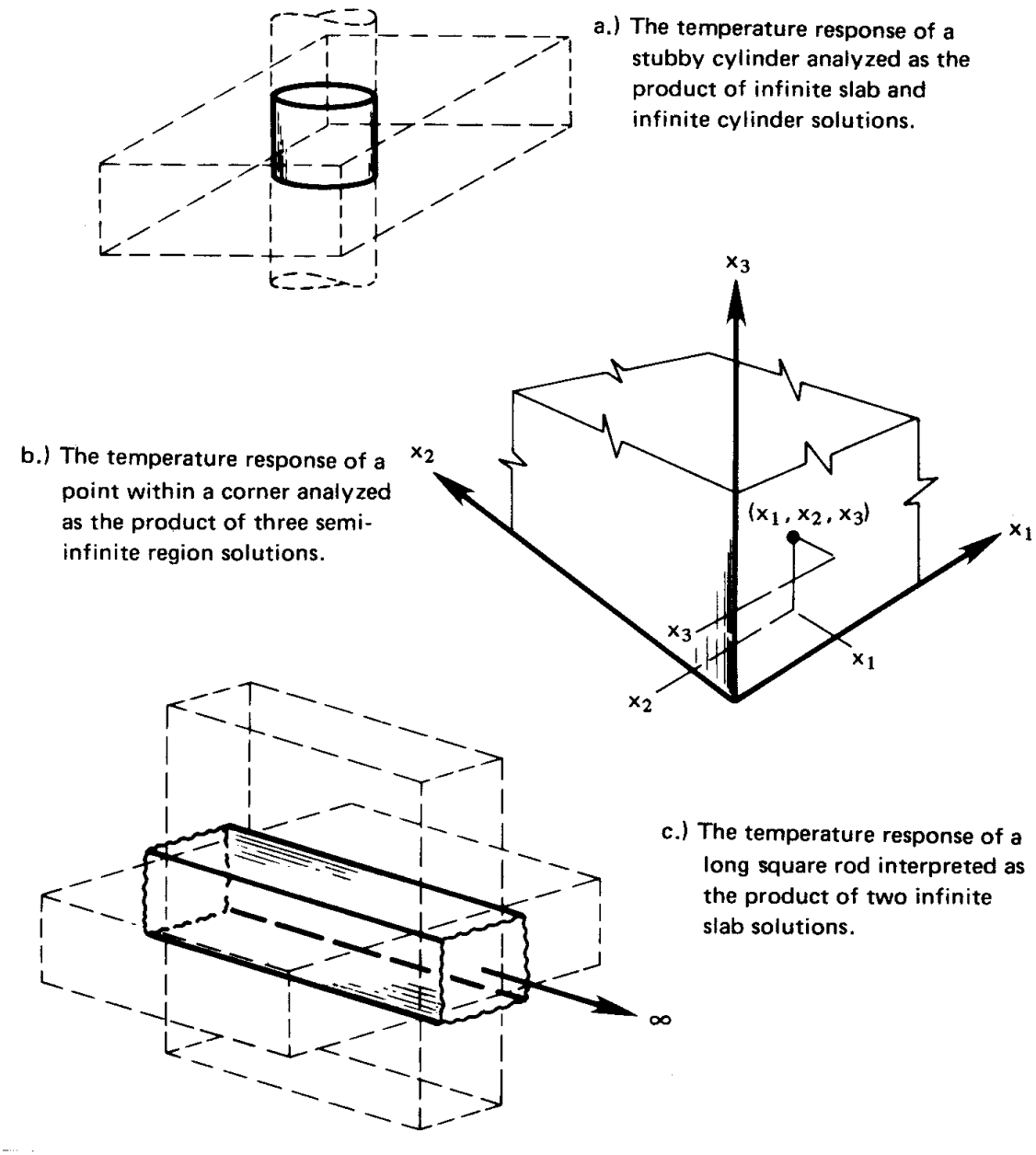
a.) The temperature response of a stubby cylinder analyzed as the product of infinite slab and infinite cylinder solutions.
b.) The temperature response of a point within a corner analyzed as the product of three semi-infinite region solutions.
x3
x2
x1
(x1, x2, x3)
x3
x1
x2
c.) The temperature response of a long square rod interpreted as the product of two infinite slab solutions.
∞

Figure 5.27 Various solid bodies whose transient cooling can be treated as the product of one-dimensional solutions.

in which Θ_{semi} is either the semi-infinite body solution given by eqn. (5.53) when convection is present at the boundary or the solution given by eqn. (5.50) when the boundary temperature itself is changed at time zero.

Several other geometries can also be represented by product solutions. Note that for of these solutions, the value of Θ at $t = 0$ is one for each factor in the product.

Example 5.12

A very long 4 cm square iron rod at $T_i = 100°\text{C}$ is suddenly immersed in a coolant at $T_\infty = 20°\text{C}$ with $\bar{h} = 800\ \text{W/m}^2\text{K}$. What is the temperature on a line 1 cm from one side and 2 cm from the adjoining side, after 10 s?

SOLUTION. With reference to Fig. 5.27c, see that the bar may be treated as the product of two slabs, each 4 cm thick. We first evaluate $\text{Fo}_1 = \text{Fo}_2 = \alpha t/L^2 = (0.0000226\ \text{m}^2/\text{s})(10\ \text{s})/(0.04\ \text{m}/2)^2 = 0.565$, and $\text{Bi}_1 = \text{Bi}_2 = \bar{h}L/k = 800(0.04/2)/76 = 0.2105$, and we then write

$$\Theta\left[\left(\frac{x}{L}\right)_1 = 0,\ \left(\frac{x}{L}\right)_2 = \frac{1}{2},\ \text{Fo}_1, \text{Fo}_2, \text{Bi}_1^{-1}, \text{Bi}_2^{-1}\right]$$

$$= \underbrace{\Theta_1\left[\left(\frac{x}{L}\right)_1 = 0,\ \text{Fo}_1 = 0.565,\ \text{Bi}_1^{-1} = 4.75\right]}_{\substack{= 0.93 \text{ from upper left-hand} \\ \text{side of Fig. 5.7}}}$$

$$\times\ \Theta_2 \underbrace{\left[\left(\frac{x}{L}\right)_2 = \frac{1}{2},\ \text{Fo}_2 = 0.565,\ \text{Bi}_2^{-1} = 4.75\right]}_{\substack{= 0.91 \text{ from interpolation} \\ \text{between lower lefthand side and} \\ \text{upper righthand side of Fig. 5.7}}}$$

Thus, at the axial line of interest,

$$\Theta = (0.93)(0.91) = 0.846$$

so

$$\frac{T - 20}{100 - 20} = 0.846 \quad \text{or} \quad T = 87.7°\text{C}$$

■

Product solutions can also be used to determine the mean temperature, $\overline{\Theta}$, and the total heat removal, Φ, from a multidimensional object. For example, when two or three solutions (Θ_1, Θ_2, and perhaps Θ_3) are multiplied to obtain Θ, the corresponding mean temperature of the multidimensional object is simply the product of the one-dimensional mean temperatures from eqn. (5.40)

$$\overline{\Theta} = \overline{\Theta}_1\,(\mathrm{Fo}_1, \mathrm{Bi}_1) \times \overline{\Theta}_2\,(\mathrm{Fo}_2, \mathrm{Bi}_2) \quad \text{for two factors} \tag{5.72a}$$

$$\overline{\Theta} = \overline{\Theta}_1\,(\mathrm{Fo}_1, \mathrm{Bi}_1) \times \overline{\Theta}_2\,(\mathrm{Fo}_2, \mathrm{Bi}_2) \times \overline{\Theta}_3\,(\mathrm{Fo}_3, \mathrm{Bi}_3) \quad \text{for three factors.} \tag{5.72b}$$

Since $\Phi = 1 - \overline{\Theta}$, a simple calculation shows that Φ can found from Φ_1, Φ_2, and Φ_3 as follows:

$$\Phi = \Phi_1 + \Phi_2\,(1 - \Phi_1) \quad \text{for two factors} \tag{5.73a}$$

$$\Phi = \Phi_1 + \Phi_2\,(1 - \Phi_1) + \Phi_3\,(1 - \Phi_2)\,(1 - \Phi_1) \quad \text{for three factors.} \tag{5.73b}$$

Example 5.13

For the bar described in Example 5.12, what is the mean temperature after 10 s and how much heat has been lost at that time?

SOLUTION. For the Biot and Fourier numbers given in Example 5.12, we find from Fig. 5.10a

$$\Phi_1\,(\mathrm{Fo}_1 = 0.565, \mathrm{Bi}_1 = 0.2105) = 0.10$$
$$\Phi_2\,(\mathrm{Fo}_2 = 0.565, \mathrm{Bi}_2 = 0.2105) = 0.10$$

and, with eqn. (5.73a),

$$\Phi = \Phi_1 + \Phi_2\,(1 - \Phi_1) = 0.19$$

The mean temperature is

$$\overline{\Theta} = \frac{\overline{T} - 20}{100 - 20} = 1 - \Phi = 0.81$$

so

$$\overline{T} = 20 + 80(0.81) = 84.8^{\circ}\mathrm{C}$$ ■

Problems

5.1 Rework Example 5.1, and replot the solution, with one change. This time, insert the thermometer at zero time, at an initial temperature $< (T_i - b\boldsymbol{T})$.

5.2 A body of known volume and surface area and temperature T_i is suddenly immersed in a bath whose temperature is rising as $T_{\text{bath}} = T_i + (T_0 - T_i)e^{t/\tau}$. Let us suppose that $\overline{h}$ is known, that $\tau = 10\rho cV/\overline{h}A$, and that t is measured from the time of immersion. The Biot number of the body is small. Find the temperature response of the body. Plot the response and the bath temperature as a function of time up to $t = 2\tau$. (Do not use Laplace transform methods except, perhaps, as a check.)

5.3 A body of known volume and surface area is immersed in a bath whose temperature is varying sinusoidally with a frequency ω about an average value. The heat transfer coefficient is known and the Biot number is small. Find the temperature variation of the body after a long time has passed, and plot it along with the bath temperature. Comment on any interesting aspects of the solution.

A suggested program for solving this problem:

- Write the differential equation of response.
- To get the particular integral of the complete equation, guess that $T - T_{\text{mean}} = C_1 \cos \omega t + C_2 \sin \omega t$. Substitute this in the differential equation and find C_1 and C_2 values that will make the resulting equation valid.
- Write the general solution of the complete equation. It will have one unknown constant in it.
- Write any initial condition you wish—the simplest one you can think of—and use it to get rid of the constant.
- Let the time be large and note which terms vanish from the solution. Throw them away.
- Combine two trigonometric terms in the solution into a term involving $\sin(\omega t - \beta)$, where $\beta = \text{fn}(\omega\boldsymbol{T})$ is the phase lag of the body temperature.

5.4 A block of copper floats within a large region of well-stirred mercury. The system is initially at a uniform temperature, T_i.

There is a heat transfer coefficient, $\overline{h}_m$, on the inside of the thin metal container of the mercury and another one, $\overline{h}_c$, between the copper block and the mercury. The container is then suddenly subjected to a change in ambient temperature from T_i to $T_s < T_i$. Predict the temperature response of the copper block, neglecting the internal resistance of both the copper and the mercury. Check your result by seeing that it fits both initial conditions and that it gives the expected behavior at $t \to \infty$.

5.5 Sketch the electrical circuit that is analogous to the second-order lumped capacity system treated in the context of Fig. 5.5 and explain it fully.

5.6 A one-inch diameter copper sphere with a thermocouple in its center is mounted as shown in Fig. 5.28 and immersed in water that is saturated at 211°F. The figure shows the thermocouple reading as a function of time during the quenching process. If the Biot number is small, the center temperature can be interpreted as the uniform temperature of the sphere during the quench. First draw tangents to the curve, and graphically differentiate it. Then use the resulting values of dT/dt to construct a graph of the heat transfer coefficient as a function of $(T_{\text{sphere}} - T_{\text{sat}})$. The result will give actual values of $\overline{h}$ during boiling over the range of temperature differences. Check to see whether or not the largest value of the Biot number is too great to permit the use of lumped-capacity methods.

5.7 A butt-welded 36-gage thermocouple is placed in a gas flow whose temperature rises at the rate 20°C/s. The thermocouple steadily records a temperature 2.4°C below the known gas flow temperature. If ρc is 3800 kJ/m^{3}K for the thermocouple material, what is $\overline{h}$ on the thermocouple? [$\overline{h}$ = 1006 W/m^{2}K.]

5.8 Check the point on Fig. 5.7 at Fo = 0.2, Bi = 10, and $x/L = 0$ analytically.

5.9 Prove that when Bi is large, eqn. (5.34) reduces to eqn. (5.33).

5.10 Check the point at Bi = 0.1 and Fo = 2.5 on the slab curve in Fig. 5.10 analytically.

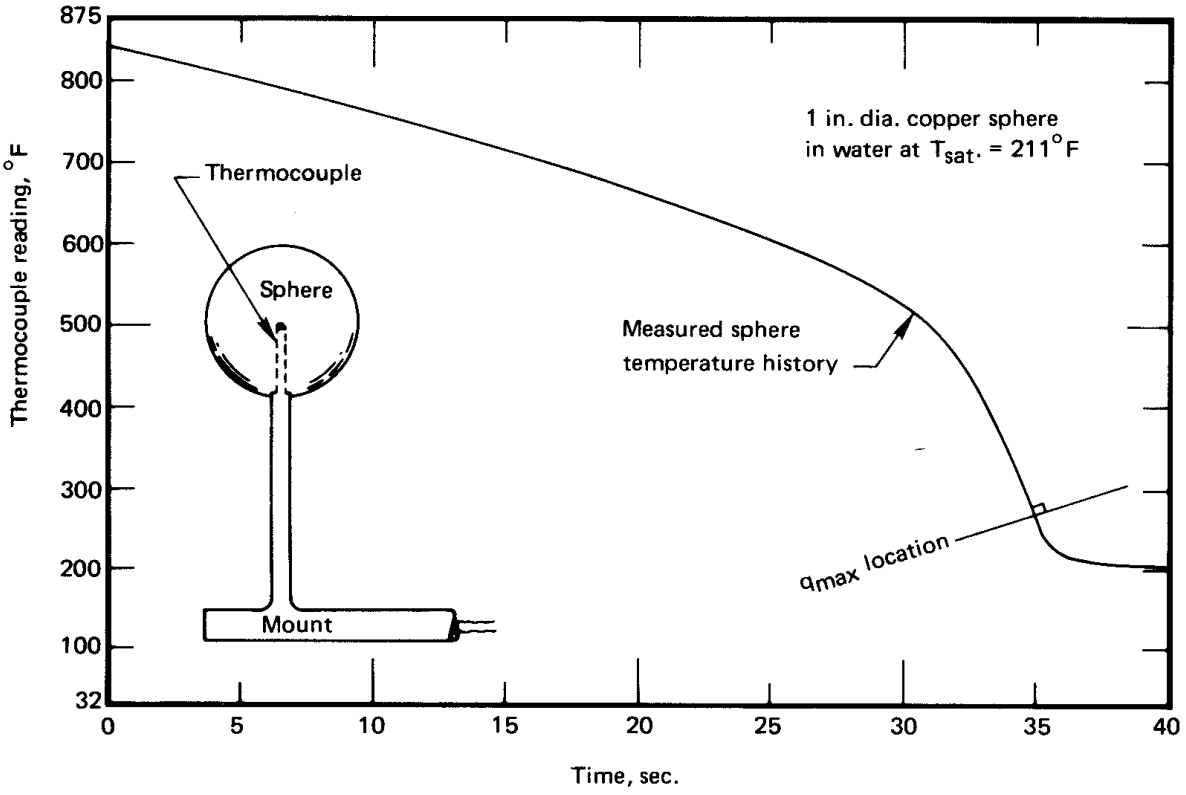

Figure 5.28 Configuration and temperature response for Problem 5.6

5.11 Sketch one of the curves in Fig. 5.7, 5.8, or 5.9 and identify:

- The region in which b.c.'s of the third kind can be replaced with b.c.'s of the first kind.
- The region in which a lumped-capacity response can be assumed.
- The region in which the solid can be viewed as a semi-infinite region.

5.12 Water flows over a flat slab of Nichrome, 0.05 mm thick, which serves as a resistance heater using AC power. The apparent value of $\overline{h}$ is 2000 W/m^{2}K. How much surface temperature fluctuation will there be?

5.13 Put Jakob's bubble growth formula in dimensionless form, identifying a "Jakob number", Ja $\equiv c_p(T_{\text{sup}} - T_{\text{sat}})/h_{\text{fg}}$ as one of the groups. (Ja is the ratio of sensible heat to latent heat.) Be certain that your nondimensionalization is consistent with the Buckingham pi-theorem.

5.14 A 7 cm long vertical glass tube is filled with water that is uniformly at a temperature of $T = 102°\text{C}$. The top is suddenly opened to the air at 1 atm pressure. Plot the decrease of the height of water in the tube by evaporation as a function of time until the bottom of the tube has cooled by 0.05°C.

5.15 A slab is cooled convectively on both sides from a known initial temperature. Compare the variation of surface temperature with time as given in Fig. 5.7 with that given by eqn. (5.53) if Bi = 2. Discuss the meaning of your comparisons.

5.16 To obtain eqn. (5.62), assume a complex solution of the type $\Theta = \text{fn}(\xi)\exp(i\Omega)$, where $i \equiv \sqrt{-1}$. This will assure that the real part of your solution has the required periodicity and, when you substitute it in eqn. (5.60), you will get an easy-to-solve ordinary d.e. in $\text{fn}(\xi)$.

5.17 A certain steel cylinder wall is subjected to a temperature oscillation that we approximate at $T = 650°\text{C} + (300°\text{C})\cos\omega t$, where the piston fires eight times per second. For stress design purposes, plot the amplitude of the temperature variation in the steel as a function of depth. If the cylinder is 1 cm thick, can we view it as having infinite depth?

5.18 A 40 cm diameter pipe at 75°C is buried in a large block of Portland cement. It runs parallel with a 15°C isothermal surface at a depth of 1 m. Plot the temperature distribution along the line normal to the 15°C surface that passes through the center of the pipe. Compute the heat loss from the pipe both graphically and analytically.

5.19 Derive shape factor 4 in Table 5.4.

5.20 Verify shape factor 9 in Table 5.4 with a flux plot. Use $R_1/R_2 = 2$ and $R_1/L = ½$. (Be sure to start out with enough blank paper surrounding the cylinders.)

5.21 A copper block 1 in. thick and 3 in. square is held at 100°F on one 1 in. by 3 in. surface. The opposing 1 in. by 3 in. surface is adiabatic for 2 in. and 90°F for 1 inch. The remaining surfaces are adiabatic. Find the rate of heat transfer. [Q = 36.8 W.]

5.22 Obtain the shape factor for any or all of the situations pictured in Fig. 5.29a through j on pages 246–247. In each case, present a well-drawn flux plot. [$S_b \simeq 1.03$, $S_c \gg S_d$, $S_g = 1$.]

5.23 Two copper slabs, 3 cm thick and insulated on the outside, are suddenly slapped tightly together. The one on the left side is initially at 100°C and the one on the right side at 0°C. Determine the left-hand adiabatic boundary's temperature after 2.3 s have elapsed. [$T_{\text{wall}} \simeq 80.5$°C]

Eggs cook as their proteins denature and coagulate. The time to cook depends on whether a soft or hard cooked egg desired. Eggs may be cooked by placing them (cold or warm) into cold water before heating starts or by placing warm eggs directly into simmering water [5.20].

5.24 Estimate the time required to hard-cook an egg if:

- The minor diameter is 3.8 cm.
- k for the egg is about the same as for water. No significant heat release or change of properties occurs during cooking.
- $\overline{h}$ between the egg and the water is 140 W/m^{2}K.
- The egg is put in boiling water when the egg is at a uniform temperature of 25°C.
- The egg is done when the center reaches 96°C.

5.25 Prove that T_1 in Fig. 5.5 cannot oscillate.

5.26 Show that when isothermal and adiabatic lines are interchanged in a two-dimenisonal body, the new shape factor is the inverse of the original one.

5.27 A 0.5 cm diameter cylinder at 300°C is suddenly immersed in saturated water at 1 atm. If $\overline{h} = 10,000$ W/m^{2}K, find the centerline and surface temperatures after 0.2 s:

a. If the cylinder is copper.

b. If the cylinder is Nichrome V. [$T_{\text{sfc}} \simeq 200$°C.]

c. If the cylinder is Nichrome V, obtain the most accurate value of the temperatures after 0.04 s that you can.

5.28 A large, flat electrical resistance strip heater is fastened to a firebrick wall, unformly at 15°C. When it is suddenly turned on, it releases heat at the uniform rate of 4000 W/m^2. Plot the temperature of the brick immediately under the heater as a function of time if the other side of the heater is insulated. What is the heat flux at a depth of 1 cm when the surface reaches 200°C.

5.29 Do Experiment 5.2 and submit a report on the results.

5.30 An approximately spherical container, 2 cm in diameter, containing electronic equipment is placed in wet mineral soil with its center 2 m below the surface. The soil surface is kept at 0°C. What is the maximum rate at which energy can be released by the equipment if the surface of the sphere is not to exceed 30°C?

5.31 A semi-infinite slab of ice at −10°C is exposed to air at 15°C through a heat transfer coefficient of 10 W/m^{2}K. What is the initial rate of melting of ice in kg/m^{2}s? What is the asymptotic rate of melting? Describe the melting process in physical terms. (The latent heat of fusion of ice, $h_{sf} = 333,300$ J/kg.)

5.32 One side of a firebrick wall, 10 cm thick, initially at 20°C is exposed to 1000°C flame through a heat transfer coefficient of 230 W/m^{2}K. How long will it be before the other side is too hot to touch? (Estimate properties at 500°C, and assume that $\overline{h}$ is quite low on the cool side.)

5.33 A particular lead bullet travels for 0.5 sec within a shock wave that heats the air near the bullet to 300°C. Approximate the bullet as a cylinder 0.8 cm in diameter. What is its surface temperature at impact if $\overline{h} = 600$ W/m^{2}K and if the bullet was initially at 20°C? What is its center temperature?

5.34 A loaf of bread is removed from the oven at 125°C and set on the (insulating) counter to cool. The loaf is 30 cm long, 15 cm high, and 12 cm wide. If $k = 0.05$ W/m·K and $\alpha = 5 \times 10^{-7}$ m^2/s for bread, and $\overline{h} = 10$ W/m^{2}K, when will the hottest part of the loaf have cooled to 60°C? [About 1 h 10 min.]

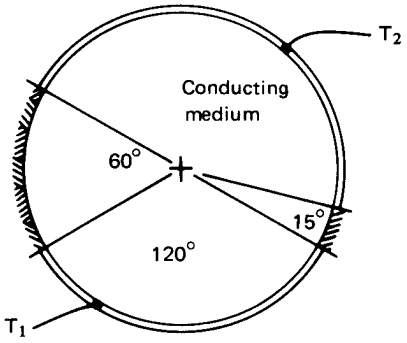

5.22a (Also find T_{center})

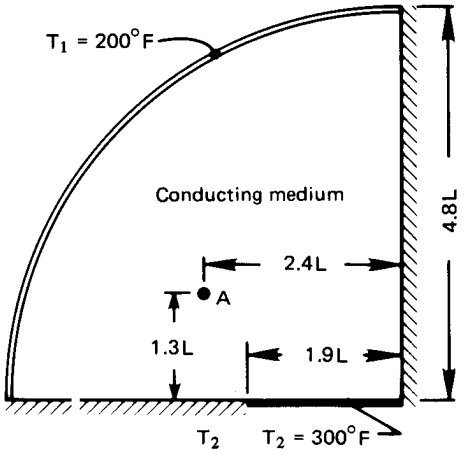

5.22b (Also find T_A)

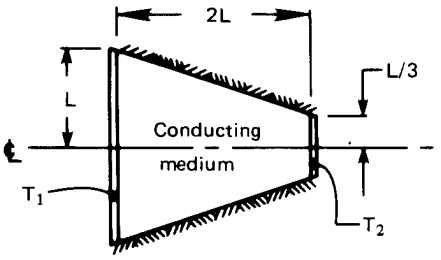

5.22c

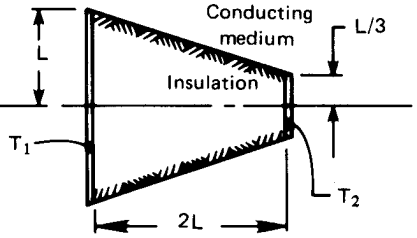

5.22d

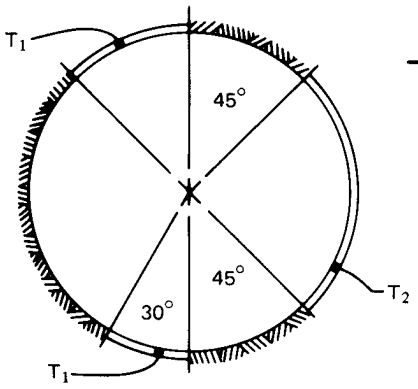

5.22e

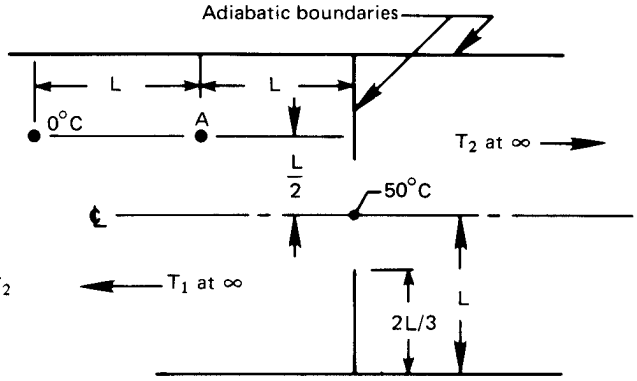

5.22f (Also find T_A)

Figure 5.29 Configurations for Problem 5.22

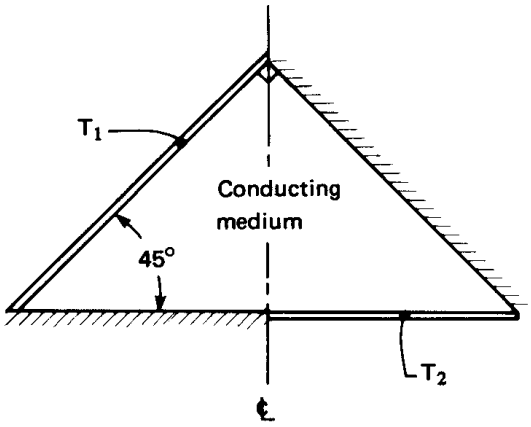

5.22g

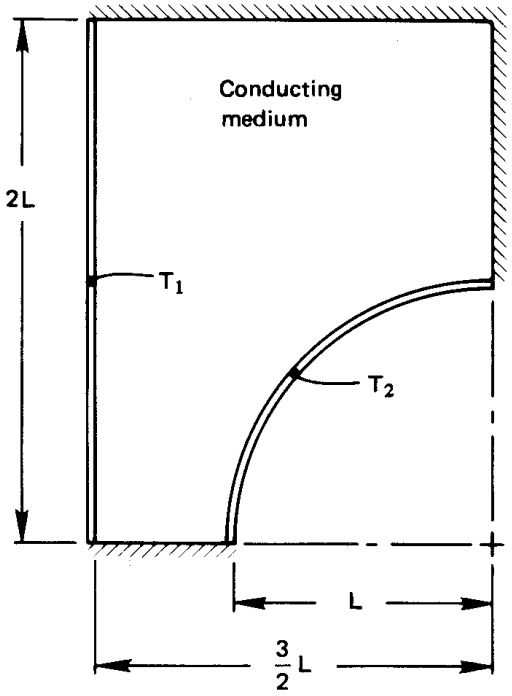

5.22h

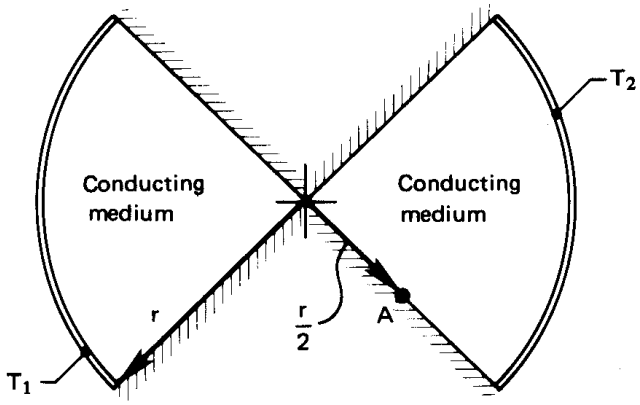

5.22i (Also find T_A)

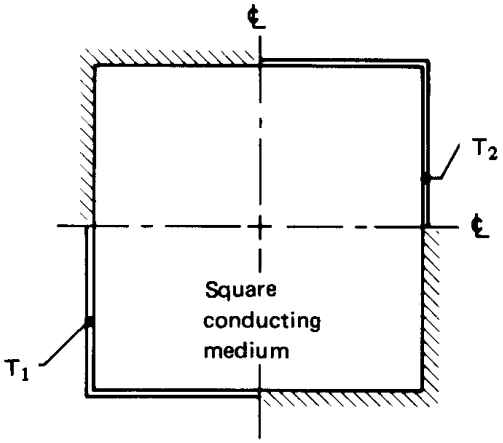

5.22j

Figure 5.29 Configurations for Problem 5.22 *(con't)*

5.35 A lead cube, 50 cm on each side, is initially at 20°C. The surroundings are suddenly raised to 200°C and $\overline{h}$ around the cube is 272 W/m^{2}K. Plot the cube temperature along a line from the center to the middle of one face after 20 minutes have elapsed.

5.36 A jet of clean water superheated to 150°C issues from a 1/16 inch diameter sharp-edged orifice into air at 1 atm, moving at 27 m/s. The coefficient of contraction of the jet is 0.611. Evaporation at $T = T_{\text{sat}}$ begins immediately on the outside of the jet. Plot the centerline temperature of the jet and $T(r/r_o = 0.6)$ as functions of distance from the orifice up to about 5 m. Neglect any axial conduction and any dynamic interactions between the jet and the air.

5.37 A 3 cm thick slab of aluminum (initially at 50°C) is slapped tightly against a 5 cm slab of copper (initially at 20°C). The outsides are both insulated and the contact resistance is neglible. What is the initial interfacial temperature? Estimate how long the interface will keep its initial temperature.

5.38 A cylindrical underground gasoline tank, 2 m in diameter and 4 m long, is embedded in 10°C soil with $k = 0.8$ W/m^{2}K and $\alpha = 1.3 \times 10^{-6}$ m^2/s. water at 27°C is injected into the tank to test it for leaks. It is well-stirred with a submerged ½ kW pump. We observe the water level in a 10 cm I.D. transparent standpipe and measure its rate of rise and fall. What rate of change of height will occur after one hour if there is no leakage? Will the level rise or fall? Neglect thermal expansion and deformation of the tank, which should be complete by the time the tank is filled.

5.39 A 47°C copper cylinder, 3 cm in diameter, is suddenly immersed horizontally in water at 27°C in a reduced gravity environment. Plot T_{cyl} as a function of time if $g = 0.76$ m/s^2 and if $\overline{h} = [2.733 + 10.448(\Delta T°\text{C})^{1/6}]^2$ W/m^{2}K. (Do it numerically if you cannot integrate the resulting equation analytically.)

5.40 The mechanical engineers at the University of Utah end spring semester by roasting a pig and having a picnic. The pig is roughly cylindrical and about 26 cm in diameter. It is roasted

over a propane flame, whose products have properties similar to those of air, at 280°C. The hot gas flows across the pig at about 2 m/s. If the meat is cooked when it reaches 95°C, and if it is to be served at 2:00 pm, what time should cooking commence? Assume Bi to be large, but note Problem 7.40. The pig is initially at 25°C.

5.41 People from cold northern climates know not to grasp metal with their bare hands in subzero weather. A very slightly frosted peice of, say, cast iron will stick to your hand like glue in, say, −20°C weather and might tear off patches of skin. Explain this *quantitatively*.

5.42 A 4 cm diameter rod of type 304 stainless steel has a very small hole down its center. The hole is clogged with wax that has a melting point of 60°C. The rod is at 20°C. In an attempt to free the hole, a workman swirls the end of the rod—and about a meter of its length—in a tank of water at 80°C. If $\overline{h}$ is 688 W/m^{2}K on both the end and the sides of the rod, plot the depth of the melt front as a function of time up to say, 4 cm.

5.43 A cylindrical insulator contains a single, very thin electrical resistor wire that runs along a line halfway between the center and the outside. The wire liberates 480 W/m. The thermal conductivity of the insulation is 3 W/m^{2}K, and the outside perimeter is held at 20°C. Develop a flux plot for the cross section, considering carefully how the field should look in the neighborhood of the point through which the wire passes. Evaluate the temperature at the center of the insulation.

5.44 A long, 10 cm square copper bar is bounded by 260°C gas flows on two opposing sides. These flows impose heat transfer coefficients of 46 W/m^{2}K. The two intervening sides are cooled by natural convection to water at 15°C, with a heat transfer coefficient of 30 W/m^{2}K. What is the heat flow through the block and the temperature at the center of the block? (This could be a pretty complicated problem, but take the trouble to think about Biot numbers before you begin.)

5.45 Lord Kelvin made an interesting estimate of the age of the earth in 1864. He assumed that the earth originated as a mass of

molten rock at 4144 K (7000°F) and that it had been cooled by outer space at 0 K ever since. To do this, he assumed that Bi for the earth is very large and that cooling had thus far penetrated through only a relatively thin (one-dimensional) layer. Using $\alpha_{\text{rock}} = 1.18 \times 10^{-6}$ m/s^2 and the measured surface temperature gradient of the earth, $\frac{1}{27}$°C/m, Find Kelvin's value of Earth's age. (Kelvin's result turns out to be much less than the accepted value of 4 billion years. His calculation fails because internal heat generation by radioactive decay of the material in the surface layer causes the surface temperature gradient to be higher than it would otherwise be.)

5.46 A pure aluminum cylinder, 4 cm diam. by 8 cm long, is initially at 300°C. It is plunged into a liquid bath at 40°C with $\overline{h} = 500$ W/m^{2}K. Calculate the hottest and coldest temperatures in the cylinder after one minute. Compare these results with the lumped capacity calculation, and discuss the comparison.

References

[5.1] H. D. Baehr and K. Stephan. *Heat and Mass Transfer*. Springer-Verlag, Berlin, 1998.

[5.2] A.F. Mills. *Basic Heat and Mass Transfer*. Prentice-Hall, Inc., Upper Saddle River, NJ, 2nd edition, 1999.

[5.3] L. M. K. Boelter, V. H. Cherry, H. A. Johnson, and R. C. Martinelli. *Heat Transfer Notes*. McGraw-Hill Book Company, New York, 1965. Originally issued as class notes at the University of California at Berkeley between 1932 and 1941.

[5.4] M. P. Heisler. Temperature charts for induction and constant temperature heating. *Trans. ASME*, 69:227–236, 1947.

[5.5] P. J. Schneider. *Temperature Response Charts*. John Wiley & Sons, Inc., New York, 1963.

[5.6] H. S. Carslaw and J. C. Jaeger. *Conduction of Heat in Solids*. Oxford University Press, New York, 2nd edition, 1959. Very comprehenisve, but quite dense.

[5.7] F. A. Jeglic. An analytical determination of temperature oscillations in wall heated by alternating current. NASA TN D-1286, July 1962.

[5.8] F. A. Jeglic, K. A. Switzer, and J. H. Lienhard. Surface temperature oscillations of electric resistance heaters supplied with alternating current. *J. Heat Transfer*, 102(2):392–393, 1980.

[5.9] J. Bronowski. *The Ascent of Man*. Chapter 4. Little, Brown and Company, Boston, 1973.

[5.10] N. Zuber. Hydrodynamic aspects of boiling heat transfer. AEC Report AECU-4439, Physics and Mathematics, June 1959.

[5.11] M. S. Plesset and S. A. Zwick. The growth of vapor bubbles in superheated liquids. *J. Appl. Phys.*, 25:493–500, 1954.

[5.12] L. E. Scriven. On the dynamics of phase growth. *Chem. Eng. Sci.*, 10:1–13, 1959.

[5.13] P. Dergarabedian. The rate of growth of bubbles in superheated water. *J. Appl. Mech., Trans. ASME*, 75:537, 1953.

[5.14] E. R. G. Eckert and R. M. Drake, Jr. *Analysis of Heat and Mass Transfer*. Hemisphere Publishing Corp., Washington, D.C., 1987.

[5.15] V. S. Arpaci. *Conduction Heat Transfer*. Ginn Press/Pearson Custom Publishing, Needham Heights, Mass., 1991. Abridgement of the 1966 edition, omitting numerical analysis.

[5.16] E. Hahne and U. Grigull. Formfactor and formwiderstand der stationären mehrdimensionalen wärmeleitung. *Int. J. Heat Mass Transfer*, 18:751–767, 1975.

[5.17] P. M. Morse and H. Feshbach. *Methods of Theoretical Physics*. McGraw-Hill Book Company, New York, 1953.

[5.18] R. Rüdenberg. Die ausbreitung der luft—und erdfelder um hochspannungsleitungen besonders bei erd—und kurzschlüssen. *Electrotech. Z.*, 36:1342–1346, 1925.

[5.19] M. M. Yovanovich. Conduction and thermal contact resistances (conductances). In W. M. Rohsenow, J. P. Hartnett, and Y. I. Cho, editors, *Handbook of Heat Transfer*, chapter 3. McGraw-Hill, New York, 3rd edition, 1998.

[5.20] S. H. Corriher. *Cookwise: the hows and whys of successful cooking*. Wm. Morrow and Company, New York, 1997. Includes excellent desciptions of the physical and chemical processes of cooking. *The* cookbook for those who enjoyed freshman chemistry.

Part III

Convective Heat Transfer

6. Laminar and turbulent boundary layers

In cold weather, if the air is calm, we are not so much chilled as when there is wind along with the cold; for in calm weather, our clothes and the air entangled in them receive heat from our bodies; this heat…brings them nearer than the surrounding air to the temperature of our skin. But in windy weather, this heat is prevented…from accumulating; the cold air, by its impulse…both cools our clothes faster and carries away the warm air that was entangled in them.

notes on "The General Effects of Heat", **Joseph Black, c. 1790s**

6.1 Some introductory ideas

Joseph Black's perception about forced convection (above) represents a very correct understanding of the way forced convective cooling works. When cold air moves past a warm body, it constantly sweeps away warm air that has become, as Black put it, "entangled" with the body and replaces it with cold air. In this chapter we learn to form analytical descriptions of these convective heating (or cooling) processes.

Our aim is to predict h and $\overline{h}$, and it is clear that such predictions must begin in the motion of fluid around the bodies that they heat or cool. It is by predicting such motion that we will be able to find out how much heat is removed during the replacement of hot fluid with cold, and vice versa.

Flow boundary layer

Fluids flowing past solid bodies adhere to them, so a region of variable velocity must be built up between the body and the free fluid stream, as

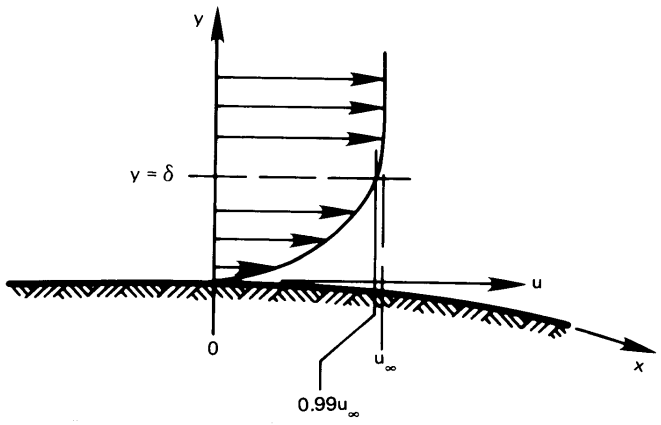

Figure 6.1 A boundary layer of thickness δ.

indicated in Fig. 6.1. This region is called a *boundary layer*, which we will often abbreviate as b.l. The b.l. has a thickness, δ. The boundary layer thickness is arbitrarily defined as the distance from the wall at which the flow velocity approaches to within 1% of u_∞. The boundary layer is normally very thin in comparison with the dimensions of the body immersed in the flow.[1]

The first step that has to be taken before h can be predicted is the mathematical description of the boundary layer. This description was first made by Prandtl[2] (see Fig. 6.2) and his students, starting in 1904, and it depended upon simplifications that followed after he recognized how thin the layer must be.

The dimensional functional equation for the boundary layer thickness on a flat surface is

$$\delta = \text{fn}(u_\infty, \rho, \mu, x)$$

where x is the length along the surface and ρ and μ are the fluid density in kg/m^3 and the dynamic viscosity in kg/m·s. We have five variables in

[1] We qualify this remark when we treat the b.l. quantitatively.

[2] Prandtl was educated at the Technical University in Munich and finished his doctorate there in 1900. He was given a chair in a new fluid mechanics institute at Göttingen University in 1904—the same year that he presented his historic paper explaining the boundary layer. His work at Göttingen, during the period up to Hitler's regime, set the course of modern fluid mechanics and aerodynamics and laid the foundations for the analysis of heat convection.

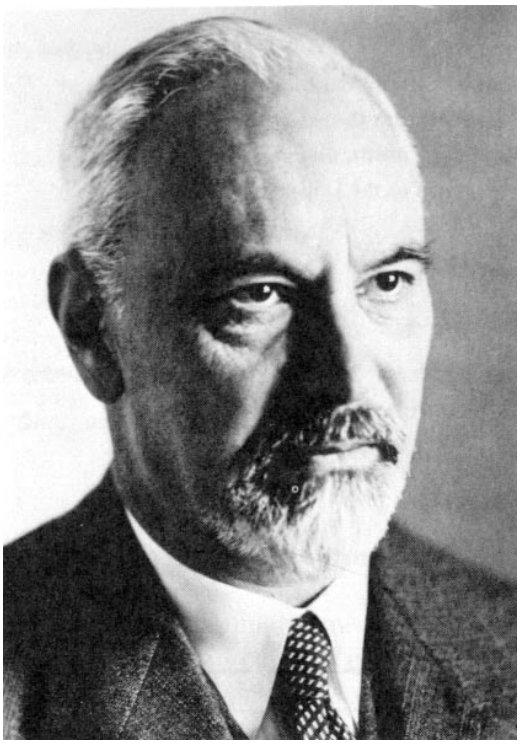

Figure 6.2 Ludwig Prandtl (1875–1953). (Photograph courtesy of *Appl. Mech. Revs.*, vol. 26, Feb. 1973.)

kg, m, and s, so we anticipate two pi-groups:

$$\frac{\delta}{x} = \text{fn}(\text{Re}_x) \qquad \text{Re}_x \equiv \frac{\rho u_\infty x}{\mu} = \frac{u_\infty x}{\nu} \tag{6.1}$$

where ν is the kinematic viscosity μ/ρ and Re_x is called the *Reynolds number*. It characterizes the relative influences of inertial and viscous forces in a fluid problem. The subscript on Re—x in this case—tells what length it is based upon.

We discover shortly that the actual form of eqn. (6.1) for a flat surface, where u_∞ remains constant, is

$$\boxed{\frac{\delta}{x} = \frac{4.92}{\sqrt{\text{Re}_x}}} \tag{6.2}$$

which means that if the velocity is great or the viscosity is low, δ/x will be relatively small. Heat transfer will be relatively high in such cases. If the velocity is low, the b.l. will be relatively thick. A good deal of nearly

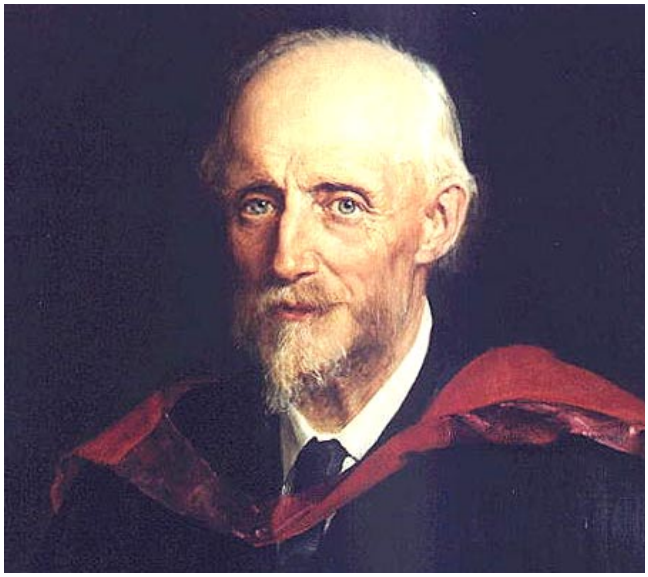

Osborne Reynolds (1842 to 1912)
Reynolds was born in Ireland but he taught at the University of Manchester. He was a significant contributor to the subject of fluid mechanics in the late 19th C. His original laminar-to-turbulent flow transition experiment, pictured below, was still being used as a student experiment at the University of Manchester in the 1970s.

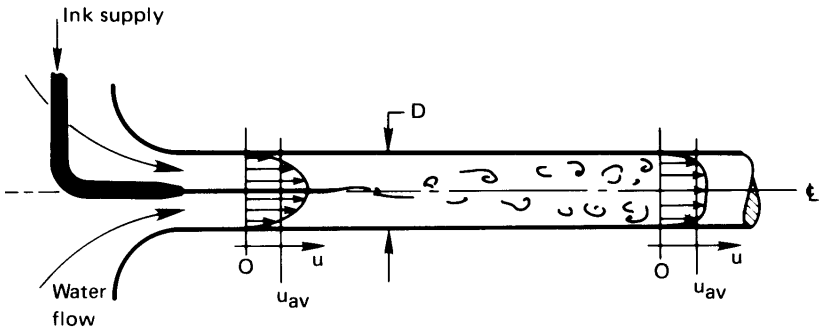

Figure 6.3 Osborne Reynolds and his laminar–turbulent flow transition experiment. (Photograph courtesy of *Appl. Mech. Revs.*, vol. 26, Feb. 1973.)

stagnant fluid will accumulate near the surface and be "entangled" with the body, although in a different way than Black envisioned it to be.

The Reynolds number is named after Osborne Reynolds (see Fig. 6.3), who discovered the laminar–turbulent transition during fluid flow in a tube. He injected ink into a steady and undisturbed flow of water and found that, beyond a certain average velocity, u_{av}, the liquid streamline marked with ink would become wobbly and then break up into increasingly disorderly eddies, and it would finally be completely mixed into the

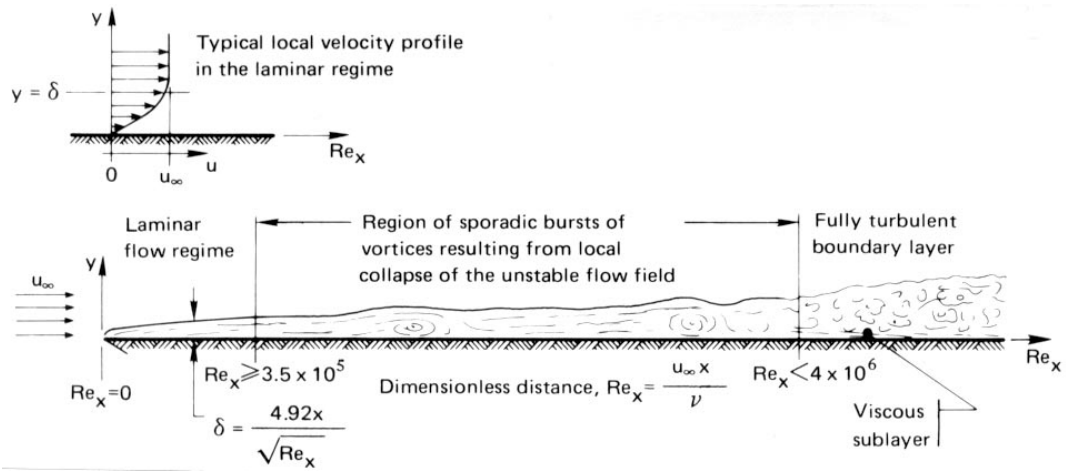

Figure 6.4 Boundary layer on a long, flat surface with a sharp leading edge.

water, as is suggested in the sketch.

To define the transition, we first note that $(u_{\text{av}})_{\text{crit}}$, the transitional value of the average velocity, must depend on the pipe diameter, D, on μ, and on ρ—four variables in kg, m, and s. There is therefore only one pi-group:

$$\text{Re}_{\text{critical}} \equiv \frac{\rho D (u_{\text{av}})_{\text{crit}}}{\mu} \tag{6.3}$$

The maximum Reynolds number for which fully developed laminar flow in a pipe will always be stable, regardless of the level of background noise, is 2100. In a reasonably careful experiment, laminar flow can be made to persist up to Re = 10,000. With enormous care it can be increased still another order of magnitude. But the value below which the flow will *always* be laminar—the critical value of Re—is 2100.

Much the same sort of thing happens in a boundary layer. Figure 6.4 shows fluid flowing over a plate with a sharp leading edge. The flow is laminar up to a transitional Reynolds number based on x:

$$\text{Re}_{x_{\text{critical}}} = \frac{u_\infty x_{\text{crit}}}{\nu} \tag{6.4}$$

At larger values of x the b.l. exhibits sporadic vortexlike instabilities over a fairly long range, and it finally settles into a fully turbulent b.l.

For the boundary layer shown, $\mathrm{Re}_{x_{\text{critical}}} = 3.5 \times 10^5$, but the actual onset of turbulent behavior depends strongly on the amount of turbulence in the flow over the plate, the precise shape of the leading edge, the roughness of the wall, and the presence of acoustic or structural vibrations [6.1, §5.5]. On a flat plate, a boundary layer remains laminar even for very large disturbances when $\mathrm{Re}_x \leq 6 \times 10^4$. With relatively undisturbed conditions, transition occurs for Re_x in the range of 3×10^5 to 5×10^5, and in very careful laboratory experiments, turbulent transition can be delayed until $\mathrm{Re}_x \approx 3 \times 10^6$ or so. Turbulent transition is essentially always complete before $\mathrm{Re}_x = 4 \times 10^6$ and usually much earlier.

These specifications of the critical Re are restricted to flat surfaces. If the surface is curved into the flow, as shown in Fig. 6.1, turbulence might be triggered at greatly lowered values of Re_x.

Thermal boundary layer

If the wall is at a temperature T_w, different from that of the free stream, T_∞, there is a *thermal boundary layer* thickness, δ_t—different from the *flow* b.l. thickness, δ. A thermal b.l. is pictured in Fig. 6.5. Now, with reference to this picture, we equate the heat conducted away from the wall by the fluid to the same heat transfer expressed in terms of a convective heat transfer coefficient:

$$\underbrace{-k_f \left.\frac{\partial T}{\partial y}\right|_{y=0}}_{\substack{\text{conduction} \\ \text{into the fluid}}} = h(T_w - T_\infty) \tag{6.5}$$

where k_f is the conductivity of the fluid. Notice two things about this result. In the first place, it is correct to express heat removal *at the wall* using Fourier's law of conduction, because there is no fluid motion in the direction of q. The other point is that while eqn. (6.5) looks like a b.c. of the third kind, it is not. This condition *defines h within the fluid* instead of specifying it as known information on the boundary. Equation (6.5) can be arranged in the form

$$\left.\frac{\partial\left(\dfrac{T_w - T}{T_w - T_\infty}\right)}{\partial(y/L)}\right|_{y/L=0} = \frac{hL}{k_f} = \mathrm{Nu}_L, \text{ the Nusselt number} \tag{6.5a}$$

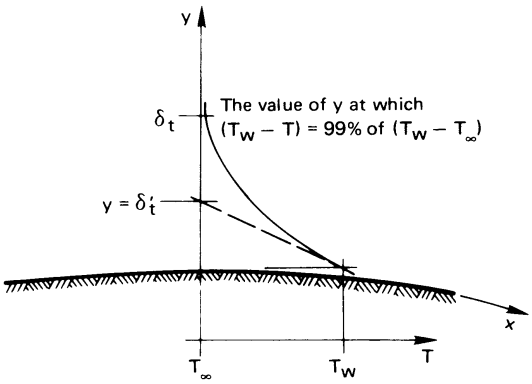

Figure 6.5 The thermal boundary layer during the flow of cool fluid over a warm plate.

where L is a characteristic dimension of the body under consideration—the length of a plate, the diameter of a cylinder, or [if we write eqn. (6.5) at a point of interest along a flat surface] $\mathrm{Nu}_x \equiv hx/k_f$. From Fig. 6.5 we see immediately that the physical significance of Nu is given by

$$\mathrm{Nu}_L = \frac{L}{\delta_t'} \tag{6.6}$$

In other words, the Nusselt number is inversely proportional to the thickness of the thermal b.l.

The Nusselt number is named after Wilhelm Nusselt,[3] whose work on convective heat transfer was as basic as Prandtl's was in analyzing the related fluid dynamics (see Fig. 6.6).

We now turn to the detailed evaluation of h. And, as the preceding remarks make very clear, this evaluation will have to start with a development of the flow field in the boundary layer.

[3]Nusselt finished his doctorate in mechanical engineering at the Technical University in Munich in 1907. During an indefinite teaching appointment at Dresden (1913 to 1917) he made two of his most important contributions: He did the dimensional analysis of heat convection before he had access to Buckingham and Rayleigh's work. In so doing, he showed how to generalize limited data, and he set the pattern of subsequent analysis. He also showed how to predict convective heat transfer during film condensation. After moving about Germany and Switzerland from 1907 until 1925, he was named to the important Chair of Theoretical Mechanics at Munich. During his early years in this post, he made basic contributions to heat exchanger design methodology. He held this position until 1952, during which time his, and Germany's, great influence in heat transfer and fluid mechanics waned. He was succeeded in the chair by another of Germany's heat transfer luminaries, Ernst Schmidt.

Figure 6.6 Ernst Kraft Wilhelm Nusselt (1882–1957). This photograph, provided by his student, G. Lück, shows Nusselt at the Kesselberg waterfall in 1912. He was an avid mountain climber.

6.2 Laminar incompressible boundary layer on a flat surface

We predict the boundary layer flow field by solving the equations that express conservation of mass and momentum in the b.l. Thus, the first order of business is to develop these equations.

Conservation of mass—The continuity equation

A two- or three-dimensional velocity field can be expressed in vectorial form:

$$\vec{u} = \vec{i}u + \vec{j}v + \vec{k}w$$

where u, v, and w are the x, y, and z components of velocity. Figure 6.7 shows a two-dimensional velocity flow field. If the flow is steady, the paths of individual particles appear as steady *streamlines*. The streamlines can be expressed in terms of a *stream function*, $\psi(x, y)$ = constant, where each value of the constant identifies a separate streamline, as shown in the figure.

The velocity, $\vec{u}$, is directed along the streamlines so that no flow can cross them. Any pair of adjacent streamlines thus resembles a heat flow

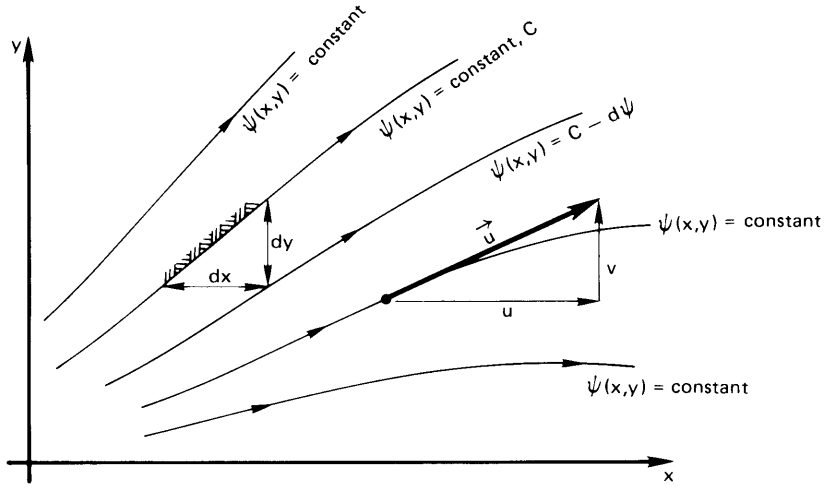

Figure 6.7 A steady, incompressible, two-dimensional flow field represented by streamlines, or lines of constant ψ.

channel in a flux plot (Section 5.7); such channels are adiabatic—no heat flow can cross them. Therefore, we write the equation for the conservation of mass by summing the inflow and outflow of mass on two faces of a triangular element of unit depth, as shown in Fig. 6.7:

$$\rho v\, dx - \rho u\, dy = 0 \tag{6.7}$$

If the fluid is incompressible, so that ρ = constant along each streamline, then

$$-v\, dx + u\, dy = 0 \tag{6.8}$$

But we can also differentiate the stream function along any streamline, $\psi(x, y)$ = constant, in Fig. 6.7:

$$d\psi = \left.\frac{\partial \psi}{\partial x}\right|_y dx + \left.\frac{\partial \psi}{\partial y}\right|_x dy = 0 \tag{6.9}$$

If we compare eqns. (6.8) and (6.9), we immediately see that the coefficients of dx and dy must be the same, so

$$v = -\left.\frac{\partial \psi}{\partial x}\right|_y \quad \text{and} \quad u = \left.\frac{\partial \psi}{\partial y}\right|_x \tag{6.10}$$

Furthermore,

$$\frac{\partial^2 \psi}{\partial y \partial x} = \frac{\partial^2 \psi}{\partial x \partial y}$$

so it follows that

$$\boxed{\frac{\partial u}{\partial x} + \frac{\partial v}{\partial y} = 0} \tag{6.11}$$

This is called the two-dimensional *continuity equation* for incompressible flow, because it expresses mathematically the fact that the flow is *continuous*; it has no breaks in it. In three dimensions, the continuity equation for an incompressible fluid is

$$\boxed{\nabla \cdot \vec{u} = \frac{\partial u}{\partial x} + \frac{\partial v}{\partial y} + \frac{\partial w}{\partial z} = 0}$$

Example 6.1

Fluid moves with a uniform velocity, u_∞, in the x-direction. Find the stream function and see if it gives plausible behavior (see Fig. 6.8).

SOLUTION. $u = u_\infty$ and $v = 0$. Therefore, from eqns. (6.10)

$$u_\infty = \left.\frac{\partial \psi}{\partial y}\right|_x \quad \text{and} \quad 0 = \left.\frac{\partial \psi}{\partial x}\right|_y$$

Integrating these equations, we get

$$\psi = u_\infty y + \text{fn}(x) \quad \text{and} \quad \psi = 0 + \text{fn}(y)$$

Comparing these equations, we get $\text{fn}(x) = \text{constant}$ and $\text{fn}(y) = u_\infty y + \text{constant}$, so

$$\psi = u_\infty y + \text{constant}$$ ■

This gives a series of equally spaced, horizontal streamlines, as we would expect (see Fig. 6.8). We set the arbitrary constant equal to zero in the figure.

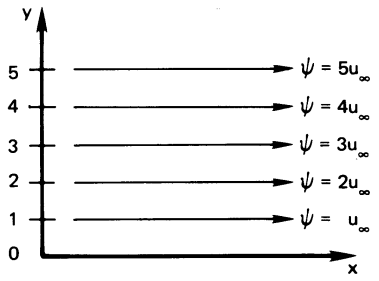

Figure 6.8 Streamlines in a uniform horizontal flow field, $\psi = u_\infty y$.

Conservation of momentum

The momentum equation in a viscous flow is a complicated vectorial expression called the Navier-Stokes equation. Its derivation is carried out in any advanced fluid mechanics text (see, e.g., [6.2, Chap. III]). We shall offer a very restrictive derivation of the equation—one that applies only to a two-dimensional incompressible b.l. flow, as shown in Fig. 6.9.

Here we see that shear stresses act upon any element such as to continuously distort and rotate it. In the lower part of the figure, one such element is enlarged, so we can see the horizontal shear stresses[4] and the pressure forces that act upon it. They are shown as heavy arrows. We also display, as lighter arrows, the momentum fluxes entering and leaving the element.

Notice that both x- and y-directed momentum enters and leaves the element. To understand this, one can envision a boxcar moving down the railroad track with a man standing, facing its open door. A child standing at a crossing throws him a baseball as the car passes. When he catches the ball, its momentum will push him back, but a component of momentum will also jar him toward the rear of the train, because of the relative motion. Particles of fluid entering element A will likewise influence its motion, with their x components of momentum carried into the element by both components of flow.

The velocities must adjust themselves to satisfy the principle of conservation of linear momentum. Thus, we require that the sum of the external forces in the x-direction, which act on the control volume, A, must be balanced by the rate at which the control volume, A, forces x-

[4]The stress, τ, is often given two subscripts. The first one identifies the direction normal to the plane on which it acts, and the second one identifies the line along which it acts. Thus, if both subscripts are the same, the stress must act normal to a surface—it must be a pressure or tension instead of a shear stress.

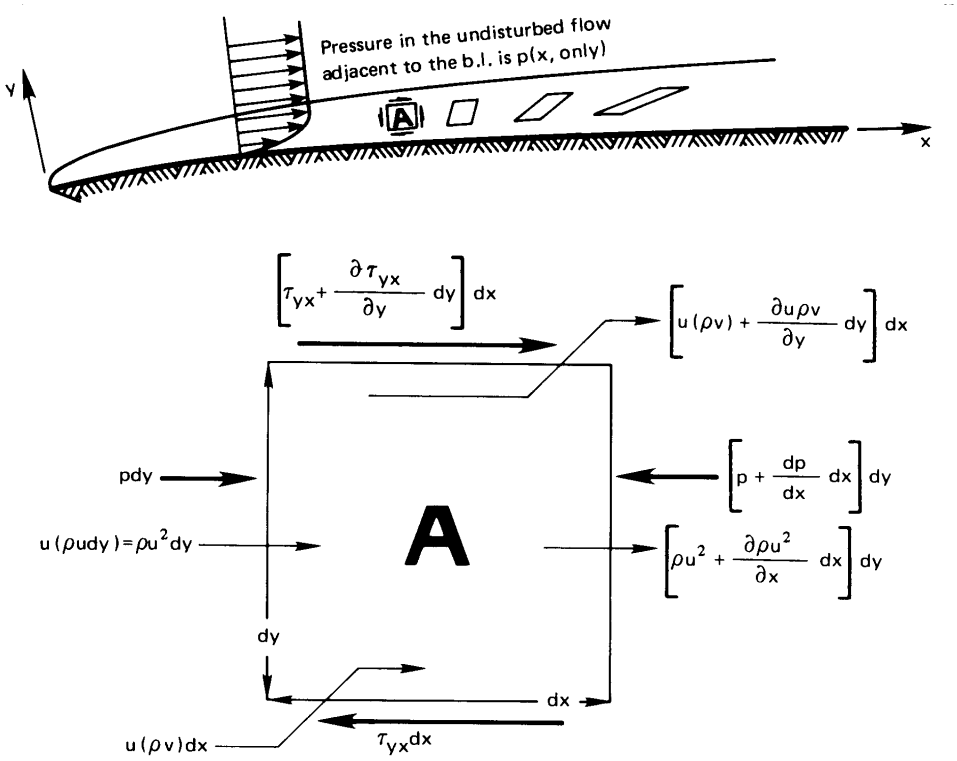
Pressure in the undisturbed flow
adjacent to the b.l. is p(x, only)
y
x
A
$\left[\tau_{yx} + \frac{\partial \tau_{yx}}{\partial y} dy\right] dx$
$\left[u(\rho v) + \frac{\partial u \rho v}{\partial y} dy\right] dx$
pdy
$\left[p + \frac{dp}{dx} dx\right] dy$
$u(\rho u dy) = \rho u^2 dy$
$\left[\rho u^2 + \frac{\partial \rho u^2}{\partial x} dx\right] dy$
dy
dx
$u(\rho v) dx$
$\tau_{yx} dx$

Figure 6.9 Forces acting in a two-dimensional incompressible boundary layer.

directed momentum out. The external forces, shown in Fig. 6.9, are

$$\left(\tau_{yx} + \frac{\partial \tau_{yx}}{\partial y} dy\right) dx - \tau_{yx} dx + p\, dy - \left(p + \frac{\partial p}{\partial x} dx\right) dy = \left(\frac{\partial \tau_{yx}}{\partial y} - \frac{\partial p}{\partial x}\right) dx\, dy$$

The rate at which A loses x-directed momentum to its surroundings is

$$\left(\rho u^2 + \frac{\partial \rho u^2}{\partial x} dx\right) dy - \rho u^2 dy + \left[u(\rho v) + \frac{\partial \rho u v}{\partial y} dy\right] dx - \rho u v\, dx = \left(\frac{\partial \rho u^2}{\partial x} + \frac{\partial \rho u v}{\partial y}\right) dx\, dy$$

We equate these results and obtain the basic statement of conservation of x-directed momentum for the b.l.:

$$\frac{\partial \tau_{yx}}{\partial y}\,dy\,dx - \frac{dp}{dx}\,dx\,dy = \left(\frac{\partial \rho u^2}{\partial x} + \frac{\partial \rho uv}{\partial y}\right) dx\,dy$$

The shear stress in this result can be eliminated with the help of Newton's law of viscous shear:

$$\tau_{yx} = \mu \frac{\partial u}{\partial y}$$

so the momentum equation becomes

$$\frac{\partial}{\partial y}\left(\mu \frac{\partial u}{\partial y}\right) - \frac{dp}{dx} = \left(\frac{\partial \rho u^2}{\partial x} + \frac{\partial \rho uv}{\partial y}\right)$$

Finally, we remember that the analysis is limited to $\rho \simeq$ constant, and we limit use of the equation to temperature ranges in which $\mu \cong$ constant. Then

$$\boxed{\frac{\partial u^2}{\partial x} + \frac{\partial uv}{\partial y} = -\frac{1}{\rho}\frac{dp}{dx} + \nu \frac{\partial^2 u}{\partial y^2}} \tag{6.12}$$

This is one form of the steady, two-dimensional, incompressible boundary layer momentum equation. Although we have taken $\rho \simeq$ constant, a more complete derivation reveals that the result is valid for compressible flow as well. If we multiply eqn. (6.11) by u and subtract the result from the left-hand side of eqn. (6.12), we obtain a second form of the momentum equation:

$$\boxed{u\frac{\partial u}{\partial x} + v\frac{\partial u}{\partial y} = -\frac{1}{\rho}\frac{dp}{dx} + \nu \frac{\partial^2 u}{\partial y^2}} \tag{6.13}$$

Equation (6.13) has a number of so-called *boundary layer approximations* built into it:

- $|\partial u/\partial x|$ is generally $\ll |\partial u/\partial y|$.
- v is generally $\ll u$.
- $p \neq \text{fn}(y)$

The Bernoulli equation for the free stream flow just above the boundary layer where there is no viscous shear,

$$\frac{p}{\rho} + \frac{u_\infty^2}{2} = \text{constant}$$

can be differentiated and used to eliminate the pressure gradient,

$$\frac{1}{\rho}\frac{dp}{dx} = -u_\infty \frac{du_\infty}{dx}$$

so from eqn. (6.12):

$$\frac{\partial u^2}{\partial x} + \frac{\partial (uv)}{\partial y} = u_\infty \frac{du_\infty}{dx} + \nu \frac{\partial^2 u}{\partial y^2} \tag{6.14}$$

And if there is no pressure gradient in the flow—if p and u_∞ are constant as they would be for flow past a flat plate—then eqns. (6.12), (6.13), and (6.14) become

$$\boxed{\frac{\partial u^2}{\partial x} + \frac{\partial (uv)}{\partial y} = u\frac{\partial u}{\partial x} + v\frac{\partial u}{\partial y} = \nu \frac{\partial^2 u}{\partial y^2}} \tag{6.15}$$

Predicting the velocity profile in the laminar boundary layer without a pressure gradient

Exact solution. Two strategies for solving eqn. (6.15) for the velocity profile have long been widely used. The first was developed by Prandtl's student, H. Blasius,[5] before World War I. It is exact, and we shall sketch it only briefly. First we introduce the stream function, ψ, into eqn. (6.15). This reduces the number of dependent variables from two (u and v) to just one—namely, ψ. We do this by substituting eqns. (6.10) in eqn. (6.15):

$$\frac{\partial \psi}{\partial y}\frac{\partial^2 \psi}{\partial y \partial x} - \frac{\partial \psi}{\partial x}\frac{\partial^2 \psi}{\partial y^2} = \nu \frac{\partial^3 \psi}{\partial y^3} \tag{6.16}$$

It turns out that eqn. (6.16) can be converted into an ordinary d.e. with the following change of variables:

$$\psi(x, y) \equiv \sqrt{u_\infty \nu x}\, f(\eta) \quad \text{where} \quad \eta \equiv \sqrt{\frac{u_\infty}{\nu x}}\, y \tag{6.17}$$

[5] Blasius achieved great fame for many accomplishments in fluid mechanics and then gave it up. He is quoted as saying: "I decided that I had no gift for it; all of my ideas came from Prandtl."

where $f(\eta)$ is an as-yet-undertermined function. [This transformation is rather similar to the one that we used to make an ordinary d.e. of the heat conduction equation, between eqns. (5.44) and (5.45).] After some manipulation of partial derivatives, this substitution gives (Problem 6.2)

$$f\frac{d^2f}{d\eta^2} + 2\frac{d^3f}{d\eta^3} = 0 \tag{6.18}$$

and

$$\frac{u}{u_\infty} = \frac{df}{d\eta} \qquad \frac{v}{\sqrt{u_\infty \nu/x}} = \frac{1}{2}\left(\eta\frac{df}{d\eta} - f\right) \tag{6.19}$$

The boundary conditions for this flow are

$$\left.\begin{aligned} u(y=0) &= 0 \quad \text{or} \quad \left.\frac{df}{d\eta}\right|_{\eta=0} = 0 \\ u(y=\infty) &= u_\infty \quad \text{or} \quad \left.\frac{df}{d\eta}\right|_{\eta=\infty} = 1 \\ v(y=0) &= 0 \quad \text{or} \quad f(\eta=0) = 0 \end{aligned}\right\} \tag{6.20}$$

The solution of eqn. (6.18) subject to these b.c.'s must be done numerically. (See Problem 6.3.)

The solution of the Blasius problem is listed in Table 6.1, and the dimensionless velocity components are plotted in Fig. 6.10. The u component increases from zero at the wall ($\eta = 0$) to 99% of u_∞ at $\eta = 4.92$. Thus, the b.l. thickness is given by

$$4.92 = \frac{\delta}{\sqrt{\nu x/u_\infty}}$$

or, as we anticipated earlier [eqn. (6.2)],

$$\frac{\delta}{x} = \frac{4.92}{\sqrt{u_\infty x/\nu}} = \frac{4.92}{\sqrt{\mathrm{Re}_x}}$$

Concept of similarity. The exact solution for $u(x,y)$ reveals a most useful fact—namely, that u can be expressed as a function of a single variable, η:

$$\frac{u}{u_\infty} = f'(\eta) = f'\left(y\sqrt{\frac{u_\infty}{\nu x}}\right)$$

Table 6.1 Exact velocity profile in the boundary layer on a flat surface with no pressure gradient

$y\sqrt{u_\infty/\nu x}$		u/u_∞	$v\sqrt{x/\nu u_\infty}$	
η	$f(\eta)$	$f'(\eta)$	$(\eta f' - f)/2$	$f''(\eta)$
0.00	0.00000	0.00000	0.00000	0.33206
0.20	0.00664	0.06641	0.00332	0.33199
0.40	0.02656	0.13277	0.01322	0.33147
0.60	0.05974	0.19894	0.02981	0.33008
0.80	0.10611	0.26471	0.05283	0.32739
1.00	0.16557	0.32979	0.08211	0.32301
2.00	0.65003	0.62977	0.30476	0.26675
3.00	1.39682	0.84605	0.57067	0.16136
4.00	2.30576	0.95552	0.75816	0.06424
4.918	3.20169	*0.99000*	0.83344	0.01837
6.00	4.27964	0.99898	0.85712	0.00240
8.00	6.27923	1.00000^-	0.86039	0.00001

This is called a *similarity solution*. To see why, we solve eqn. (6.2) for

$$\sqrt{\frac{u_\infty}{\nu x}} = \frac{4.92}{\delta(x)}$$

and substitute this in $f'(y/\sqrt{u_\infty/\nu x})$. The result is

$$f' = \frac{u}{u_\infty} = \text{fn}\left[\frac{y}{\delta(x)}\right] \tag{6.21}$$

The velocity profile thus has the same shape with respect to the b.l. thickness at each x-station. We say, in other words, that the profile is *similar* at each station. This is what we found to be true for conduction into a semi-infinite region. In that case [recall eqn. (5.51)], $x/\sqrt{t}$ always had the same value at the outer limit of the thermally disturbed region.

Boundary layer similarity makes it especially easy to use a simple approximate method for solving other b.l. problems. This method, called the *momentum integral method*, is the subject of the next subsection.

Example 6.2

Air at 27°C blows over a flat surface with a sharp leading edge at

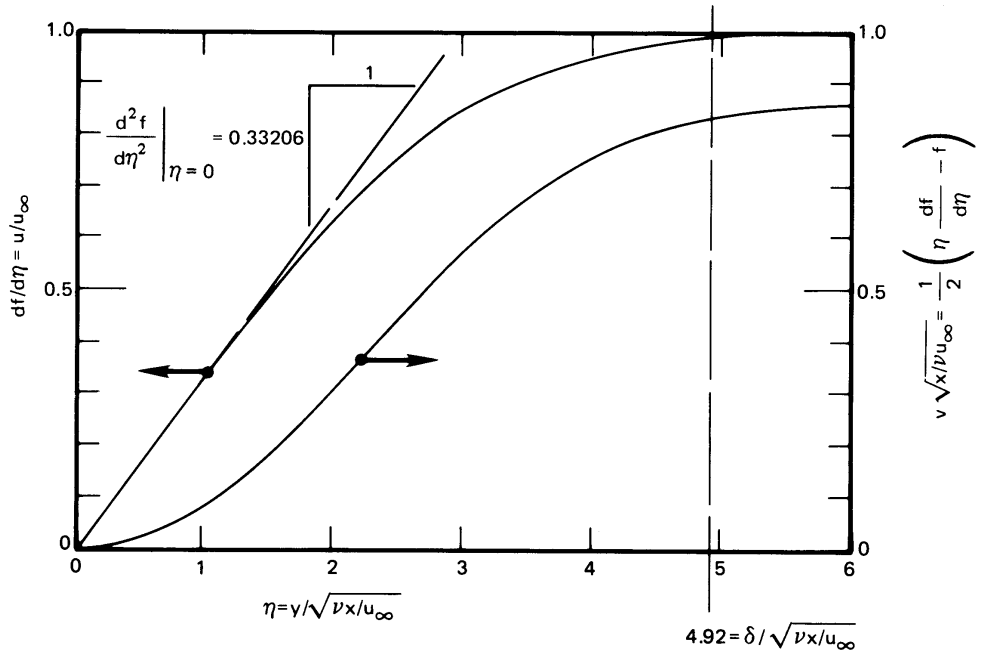

Figure 6.10 The dimensionless velocity components in a laminar boundary layer.

1.5 m/s. Find the b.l. thickness $\frac{1}{2}$ m from the leading edge. Check the b.l. assumption that $u \gg v$ at the trailing edge.

SOLUTION. The dynamic and kinematic viscosities are $\mu = 1.853 \times 10^{-5}$ kg/m·s and $\nu = 1.566 \times 10^{-5}$ m^2/s. Then

$$\mathrm{Re}_x = \frac{u_\infty x}{\nu} = \frac{1.5(0.5)}{1.566 \times 10^{-5}} = 47,893$$

The Reynolds number is low enough to permit the use of a laminar flow analysis. Then

$$\delta = \frac{4.92x}{\sqrt{\mathrm{Re}_x}} = \frac{4.92(0.5)}{\sqrt{47,893}} = 0.01124 = 1.124 \text{ cm}$$

(Remember that the b.l. analysis is only valid if $\delta/x \ll 1$. In this case, $\delta/x = 1.124/50 = 0.0225$.) Finally, according to Fig. 6.10 or Table 6.1,

v at $x = 0.5$ m is

$$v = \frac{0.8604}{\sqrt{x/\nu u_\infty}} = 0.8604\sqrt{\frac{(1.566)(10^{-5})(1.5)}{(0.5)}}$$
$$= 0.00590 \text{ m/s}$$

or

$$\frac{v}{u_\infty} = \frac{0.00590}{1.5} = 0.00393 \qquad \blacksquare$$

Therefore, v is always $\ll u$, at least so long as we are not near the leading edge, where the b.l. assumptions themselves break down. We say more about this breakdown after eqn. (6.34).

Momentum integral method.[6] A second method for solving the b.l. momentum equation is approximate and much easier to apply to a wide range of problems than is any exact method of solution. The idea is this: We are not really interested in the details of the velocity or temperature profiles in the b.l., beyond learning their slopes at the wall. [These slopes give us the shear stress at the wall, $\tau_w = \mu(\partial u/\partial y)_{y=0}$, and the heat flux at the wall, $q_w = -k(\partial T/\partial y)_{y=0}$.] Therefore, we integrate the b.l. equations from the wall, $y = 0$, to the b.l. thickness, $y = \delta$, to make ordinary d.e.'s of them. It turns out that while these much simpler equations do not reveal anything new about the temperature and velocity profiles, they do give quite accurate explicit equations for τ_w and q_w.

Let us see how this procedure works with the b.l. momentum equation. We integrate eqn. (6.15), as follows, for the case in which there is no pressure gradient ($dp/dx = 0$):

$$\int_0^\delta \frac{\partial u^2}{\partial x}\,dy + \int_0^\delta \frac{\partial (uv)}{\partial y}\,dy = \nu \int_0^\delta \frac{\partial^2 u}{\partial y^2}\,dy$$

At $y = \delta$, u can be approximated as the free stream value, u_∞, and other quantities can also be evaluated at $y = \delta$ just as though y were infinite:

$$\int_0^\delta \frac{\partial u^2}{\partial x}\,dy + \Big[\underbrace{(uv)_{y=\delta}}_{=u_\infty v_\infty} - \underbrace{(uv)_{y=0}}_{=0}\Big] = \nu \left[\underbrace{\left(\frac{\partial u}{\partial y}\right)_{y=\delta}}_{\simeq 0} - \left(\frac{\partial u}{\partial y}\right)_{y=0}\right] \tag{6.22}$$

[6] This method was developed by Pohlhausen, von Kármán, and others. See the discussion in [6.2, Chap. XII].

The continuity equation (6.11) can be integrated thus:

$$v_\infty - \underbrace{v_{y=0}}_{=0} = -\int_0^\delta \frac{\partial u}{\partial x}\, dy \tag{6.23}$$

Multiplying this by u_∞ gives

$$u_\infty v_\infty = -\int_0^\delta \frac{\partial u u_\infty}{\partial x}\, dy$$

Using this result in eqn. (6.22), we obtain

$$\int_0^\delta \frac{\partial}{\partial x}[u(u-u_\infty)]\, dy = -\nu \left.\frac{\partial u}{\partial y}\right|_{y=0}$$

Finally, we note that $\mu(\partial u/\partial y)_{y=0}$ is the shear stress on the wall, $\tau_w = \tau_w$ (x only), so this becomes[7]

$$\boxed{\frac{d}{dx}\int_0^{\delta(x)} u(u-u_\infty)\, dy = -\frac{\tau_w}{\rho}} \tag{6.24}$$

Equation (6.24) expresses the conservation of linear momentum in integrated form. It shows that the rate of momentum loss caused by the b.l. is balanced by the shear force on the wall. When we use it in place of eqn. (6.15), we are said to be *using an integral method*. To make use of eqn. (6.24), we first nondimensionalize it as follows:

$$\begin{aligned}\frac{d}{dx}\left[\delta\int_0^1 \frac{u}{u_\infty}\left(\frac{u}{u_\infty}-1\right) d\left(\frac{y}{\delta}\right)\right] &= -\frac{\nu}{u_\infty \delta}\left.\frac{\partial(u/u_\infty)}{\partial(y/\delta)}\right|_{y=0} \\ &= -\frac{\tau_w(x)}{\rho u_\infty^2} \equiv -\frac{1}{2}C_f(x)\end{aligned} \tag{6.25}$$

where $\tau_w/(\rho u_\infty^2/2)$ is defined as the *skin friction coefficient*, C_f.

Equation (6.25) will be satisfied precisely by the exact solution (Problem 6.4) for u/u_∞. However, the point is to use eqn. (6.25) to determine u/u_∞ when we do not already have an exact solution. To do this, we recall that the exact solution exhibits *similarity*. First, we guess the solution in the form of eqn. (6.21): $u/u_\infty = \text{fn}(y/\delta)$. This guess is made

[7] The interchange of integration and differentiation is consistent with Leibnitz's rule for differentiation of an integral (Problem 6.14).

in such a way that it will fit the following four things that are true of the velocity profile:

$$\left.\begin{array}{l} \bullet\ u/u_\infty = 0 \ \text{ at } \ y/\delta = 0 \\ \bullet\ u/u_\infty \cong 1 \ \text{ at } \ y/\delta = 1 \\ \bullet\ d\left(\dfrac{u}{u_\infty}\right) \Big/ d\left(\dfrac{y}{\delta}\right) \cong 0 \ \text{ at } \ y/\delta = 1 \end{array}\right\} \tag{6.26}$$

- and from eqn. (6.15), we know that at $y/\delta = 0$:

$$u \underbrace{\frac{\partial u}{\partial x}}_{=0} + \underbrace{v}_{=0} \frac{\partial u}{\partial y} = \nu \left.\frac{\partial^2 u}{\partial y^2}\right|_{y=0}$$

so

$$\left.\frac{\partial^2 (u/u_\infty)}{\partial (y/\delta)^2}\right|_{y/\delta=0} = 0 \tag{6.27}$$

If fn(y/δ) is written as a polynomial with four constants—a, b, c, and d—in it,

$$\frac{u}{u_\infty} = a + b\frac{y}{\delta} + c\left(\frac{y}{\delta}\right)^2 + d\left(\frac{y}{\delta}\right)^3 \tag{6.28}$$

the four things that are known about the profile give

- $0 = a$, which eliminates a immediately
- $1 = 0 + b + c + d$
- $0 = b + 2c + 3d$
- $0 = 2c$, which eliminates c as well

Solving the middle two equations (above) for b and d, we obtain $d = -\frac{1}{2}$ and $b = +\frac{3}{2}$, so

$$\frac{u}{u_\infty} = \frac{3}{2}\frac{y}{\delta} - \frac{1}{2}\left(\frac{y}{\delta}\right)^3 \tag{6.29}$$

This approximation velocity profile is compared with the exact Blasius profile in Fig. 6.11, and they prove to be equal within a maximum error of 8%. The only remaining problem is then that of calculating $\delta(x)$. To

do this, we substitute eqn. (6.29) in eqn. (6.25) and get, after integration (see Problem 6.5):

$$-\frac{d}{dx}\left[\delta\left(\frac{39}{280}\right)\right] = -\frac{\nu}{u_\infty \delta}\left(\frac{3}{2}\right) \tag{6.30}$$

or

$$-\frac{39}{280}\left(\frac{2}{3}\right)\left(\frac{1}{2}\right)\frac{d\delta^2}{dx} = -\frac{\nu}{u_\infty}$$

We integrate this using the b.c. $\delta^2 = 0$ at $x = 0$:

$$\delta^2 = \frac{280}{13}\frac{\nu x}{u_\infty}$$

or

$$\frac{\delta}{x} = \frac{4.64}{\sqrt{\mathrm{Re}_x}} \tag{6.31}$$

This b.l. thickness is of the correct functional form, and the constant is low by only 5.6%.

The skin friction coefficient

The fact that the function $u/u_\infty = f'(\eta)$ or $\mathrm{fn}(y/\delta)$ gives all information about flow in the b.l. must be stressed. For example, the shear stress can be obtained from it by using Newton's law of viscous shear. Thus,

$$\tau_w = \mu\left.\frac{\partial u}{\partial y}\right|_{y=0} = \mu u_\infty\left(\frac{\partial f'}{\partial \eta}\frac{\partial \eta}{\partial y}\right)_{\eta=0} = \mu u_\infty \frac{\sqrt{u_\infty}}{\sqrt{\nu x}}\left.\frac{d^2 f}{d\eta^2}\right|_{\eta=0}$$

But from Fig. 6.10 and Table 6.1, we see that $(d^2 f/d\eta^2)_{\eta=0} = 0.33206$, so

$$\tau_w = 0.332\,\frac{\mu u_\infty}{x}\sqrt{\mathrm{Re}_x} \tag{6.32}$$

The integral method that we just outlined would have given 0.323 for the constant in eqn. (6.32) instead of 0.332 (Problem 6.6).

The *local skin friction coefficient,* or local skin drag coefficient, is defined as

$$\boxed{C_f \equiv \frac{\tau_w}{\rho u_\infty^2/2} = \frac{0.664}{\sqrt{\mathrm{Re}_x}}} \tag{6.33}$$

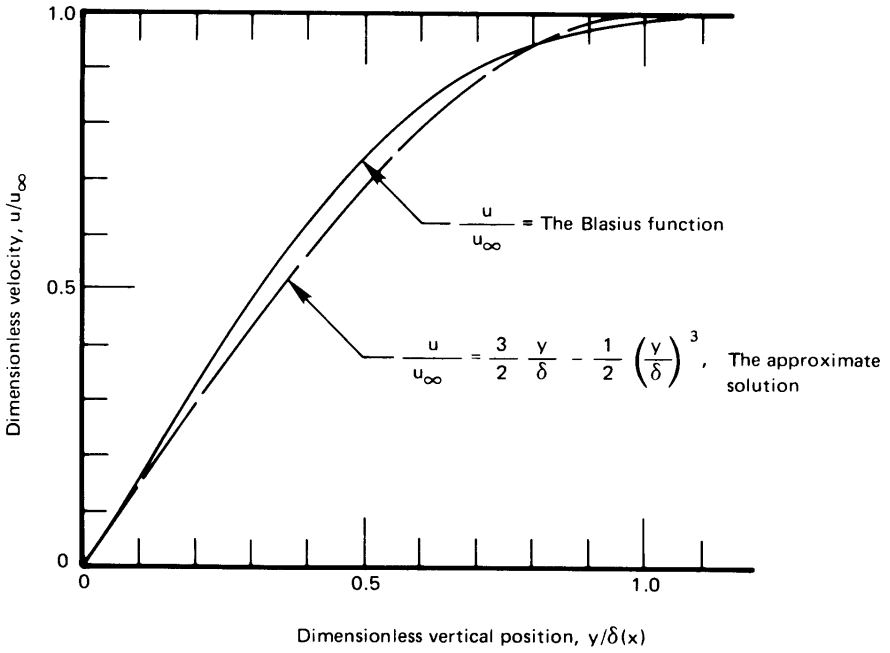

Figure 6.11 Comparison of the third-degree polynomial fit with the exact b.l. velocity profile. (Notice that the approximate result has been forced to $u/u_\infty = 1$ instead of 0.99 at $y = \delta$.)

The *overall skin friction coefficient*, $\overline{C}_f$, is based on the average of the shear stress, τ_w, over the length, L, of the plate

$$\overline{\tau}_w = \frac{1}{L}\int_0^L \tau_w \, dx = \frac{\rho u_\infty^2}{2L}\int_0^L \frac{0.664}{\sqrt{u_\infty x/\nu}}\, dx = 1.328\,\frac{\rho u_\infty^2}{2}\sqrt{\frac{\nu}{u_\infty L}}$$

so

$$\boxed{\overline{C}_f = \frac{1.328}{\sqrt{\mathrm{Re}_L}}} \tag{6.34}$$

As a matter of interest, we note that $C_f(x)$ approaches infinity at the leading edge of the flat surface. This means that to stop the fluid that first touches the front of the plate—dead in its tracks—would require infinite shear stress right at that point. Nature, of course, will not allow such a thing to happen; and it turns out that the boundary layer analysis is not really valid right at the leading edge.

Actually, we must declare that the range $x \lesssim 5\delta$ (in which the b.l. is relatively thick) is too close to the edge to use this analysis with accuracy. This converts to

$$x > 600\,\nu/u_\infty \quad \text{for a boundary layer to exist}$$

In Example 6.2, this condition is satisfied for all x's greater than about 6 mm. This region is usually very small.

Example 6.3

Calculate the average shear stress and the overall friction coefficient for the surface in Example 6.2 if its total length is $L = 0.5$ m. Compare $\overline{\tau}_w$ with τ_w at the trailing edge. At what point on the surface does $\tau_w = \overline{\tau}_w$? Finally, estimate what fraction of the surface can legitimately be analyzed using boundary layer theory.

SOLUTION.

$$\overline{C}_f = \frac{1.328}{\sqrt{\mathrm{Re}_{0.5}}} = \frac{1.328}{\sqrt{47,893}} = 0.00607$$

and

$$\overline{\tau}_w = \frac{\rho u_\infty^2}{2}\,\overline{C}_f = \frac{1.183(1.5)^2}{2}\,0.00607 = 0.00808\ \underbrace{\mathrm{kg/m\cdot s^2}}_{\mathrm{N/m^2}}$$

(This is very little drag. It amounts only to about $1/50$ ounce/m^2.)

At $x = L$,

$$\left.\frac{\tau_w(x)}{\overline{\tau}_w}\right|_{x=L} = \frac{\rho u_\infty^2/2}{\rho u_\infty^2/2}\left[\frac{0.664/\sqrt{\mathrm{Re}_L}}{1.328/\sqrt{\mathrm{Re}_L}}\right] = \frac{1}{2}$$

and

$$\tau_w(x) = \overline{\tau}_w \quad \text{where} \quad \frac{0.664}{\sqrt{x}} = \frac{1.328}{\sqrt{0.5}}$$

so the local shear stress equals the average value, where

$$x = \tfrac{1}{8}\ \mathrm{m} \qquad \text{or} \qquad \frac{x}{L} = \frac{1}{4}$$

Thus, the shear stress, which is initially infinite, plummets to $\overline{\tau}_w$ one-fourth of the way from the leading edge and drops only to one-half of $\overline{\tau}_w$ in the remaining 75% of the plate.

The boundary layer assumptions fail when

$$x < 600\,\frac{\nu}{u_\infty} = 600\,\frac{1.566\times10^{-5}}{1.5} = 0.0063\text{ m}$$

Thus, the preceding analysis should be good over almost 99% of the 0.5 m length of the surface. ■

6.3 The energy equation

Derivation

We now know how fluid moves in the b.l. Next, we must extend the heat conduction equation to allow for the motion of the fluid. This equation can be solved for the temperature field in the b.l., and its solution can be used to calculate h, using Fourier's law:

$$\boxed{h = \frac{q}{T_w - T_\infty} = -\frac{k}{T_w - T_\infty}\left.\frac{\partial T}{\partial y}\right|_{y=0}} \tag{6.35}$$

To predict T, we extend the analysis done in Section 2.1. Figure 2.4 shows an element of a solid body subjected to a temperature field. We allow this volume to contain fluid with a velocity field $\vec{u}(x,y,z)$ in it, as shown in Fig. 6.12. We make the following restrictive approximations:

- The fluid is incompressible. This means that ρ is constant for each tiny parcel of fluid; we shall make the stronger approximation that ρ is constant for *all* parcels of fluid. This approximation is reasonable for most liquid flows and for gas flows moving at speeds less than about 1/3 the speed of sound. We have seen in Sect. 6.2 that $\nabla\cdot\vec{u} = 0$ for incompressible flow.

- Pressure variations in the flow are not large enough to affect thermodynamic properties. From thermodynamics, we know that the specific internal energy, $\hat{u}$, satisfies $d\hat{u} = c_v\,dT + (\partial\hat{u}/\partial p)_T\,dp$ and that the specific enthalpy, $\hat{h} = \hat{u} + p/\rho$, satisfies $d\hat{h} = c_p\,dT + (\partial\hat{h}/\partial p)_T\,dp$. We shall neglect the dp contributions to both energies. We have already neglected the effect of p on ρ.

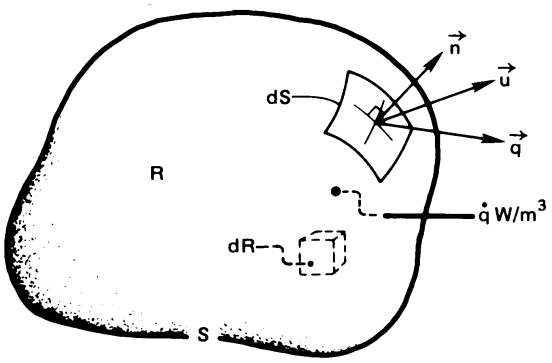

Figure 6.12 Control volume in a heat-flow and fluid-flow field.

- Temperature variations in the flow are not large enough to change k significantly; we have already neglected temperature effects on ρ.
- Potential and kinetic energy changes are negligible in comparison to thermal energy changes. Since the kinetic energy of a fluid can change owing to pressure gradients, this again means that pressure variations may not be too large.
- The viscous stresses do not dissipate enough energy to warm the fluid significantly.

Just as we wrote eqn. (2.7) in Section 2.1, we now write conservation of energy in the form

$$\underbrace{\frac{d}{dt}\int_R \rho\hat{u}\,dR}_{\substack{\text{rate of internal}\\ \text{energy increase}\\ \text{in } R}} = -\underbrace{\int_S (\rho\hat{h})\,\vec{u}\cdot\vec{n}\,dS}_{\substack{\text{rate of internal energy and}\\ \text{flow work out of } R}}$$

$$-\underbrace{\int_S (-k\nabla T)\cdot\vec{n}\,dS}_{\substack{\text{net heat conduction}\\ \text{rate out of } R}} + \underbrace{\int_R \dot{q}\,dR}_{\substack{\text{rate of heat}\\ \text{generation in } R}} \qquad (6.36)$$

In the third integral, $\vec{u}\cdot\vec{n}\,dS$ represents the volume flow rate through an element dS of the control surface. The position of R is not changing in time, so we can bring the time derivative inside the first integral. If we then we call in Gauss's theorem [eqn. (2.8)] to make volume integrals of the surface integrals, eqn. (6.36) becomes

$$\int_R \left(\rho\frac{\partial\hat{u}}{\partial t} + \rho\nabla\cdot(\vec{u}\,\hat{h}) - \nabla\cdot k\nabla T - \dot{q}\right) dR = 0$$

Because the integrand must vanish identically (recall the footnote on pg. 55 in Chap. 2) and because k depends weakly on T,

$$\rho\Big(\frac{\partial \hat{u}}{\partial t} + \underbrace{\nabla \cdot (\vec{u}\hat{h})}_{= \vec{u}\cdot\nabla\hat{h} + \hat{h}\underbrace{\nabla\cdot\vec{u}}_{= 0,\text{ by continuity}}} \Big) - k\nabla^2 T - \dot{q} = 0$$

Since we are neglecting pressure effects and density changes, we can approximate changes in the internal energy by changes in the enthalpy:

$$d\hat{u} = d\hat{h} - d\left(\frac{p}{\rho}\right) \approx d\hat{h}$$

Upon substituting $d\hat{h} \approx c_p\, dT$, it follows that

$$\rho c_p \Big(\underbrace{\frac{\partial T}{\partial t}}_{\substack{\text{energy}\\ \text{storage}}} + \underbrace{\vec{u}\cdot\nabla T}_{\substack{\text{enthalpy}\\ \text{convection}}} \Big) = \underbrace{k\nabla^2 T}_{\substack{\text{heat}\\ \text{conduction}}} + \underbrace{\dot{q}}_{\substack{\text{heat}\\ \text{generation}}} \tag{6.37}$$

This is the energy equation for an incompressible flow field. It is the same as the corresponding equation (2.11) for a solid body, except for the enthalpy transport, or convection, term, $\rho c_p \vec{u}\cdot\nabla T$.

Consider the term in parentheses in eqn. (6.37):

$$\frac{\partial T}{\partial t} + \vec{u}\cdot\nabla T = \frac{\partial T}{\partial t} + u\frac{\partial T}{\partial x} + v\frac{\partial T}{\partial y} + w\frac{\partial T}{\partial z} \equiv \frac{DT}{Dt} \tag{6.38}$$

DT/Dt is exactly the so-called *material derivative*, which is treated in some detail in every fluid mechanics course. DT/Dt is the rate of change of the temperature of a fluid particle as it moves in a flow field.

In a steady two-dimensional flow field without heat sources, eqn. (6.37) takes the form

$$u\frac{\partial T}{\partial x} + v\frac{\partial T}{\partial y} = \alpha\left(\frac{\partial^2 T}{\partial x^2} + \frac{\partial^2 T}{\partial y^2}\right) \tag{6.39}$$

Furthermore, in a b.l., $\partial^2 T/\partial x^2 \ll \partial^2 T/\partial y^2$, so the b.l. energy equation is

$$u\frac{\partial T}{\partial x} + v\frac{\partial T}{\partial y} = \alpha\frac{\partial^2 T}{\partial y^2} \tag{6.40}$$

Heat and momentum transfer analogy

Consider a b.l. in a fluid of bulk temperature T_∞, flowing over a flat surface at temperature T_w. The momentum equation and its b.c.'s can be written as

$$u\frac{\partial}{\partial x}\left(\frac{u}{u_\infty}\right)+v\frac{\partial}{\partial y}\left(\frac{u}{u_\infty}\right)=\nu\frac{\partial^2}{\partial y^2}\left(\frac{u}{u_\infty}\right) \qquad \begin{cases} \left.\dfrac{u}{u_\infty}\right|_{y=0}=0 \\ \left.\dfrac{u}{u_\infty}\right|_{y=\infty}=1 \\ \dfrac{\partial}{\partial y}\left(\dfrac{u}{u_\infty}\right)_{y=\infty}=0 \end{cases} \tag{6.41}$$

And the energy equation (6.40) can be written in terms of a dimensionless temperature, $\Theta=(T-T_w)/(T_\infty-T_w)$, as

$$u\frac{\partial\Theta}{\partial x}+v\frac{\partial\Theta}{\partial y}=\alpha\frac{\partial^2\Theta}{\partial y^2} \qquad \begin{cases} \Theta(y=0)=0 \\ \Theta(y=\infty)=1 \\ \left.\dfrac{\partial\Theta}{\partial y}\right|_{y=\infty}=0 \end{cases} \tag{6.42}$$

Notice that the problems of predicting u/u_∞ and Θ are *identical*, with one exception: eqn. (6.41) has ν in it whereas eqn. (6.42) has α. If ν and α should happen to be equal, the temperature distribution in the b.l. is

$$\text{for } \nu=\alpha: \quad \frac{T-T_w}{T_\infty-T_w}=f'(\eta) \quad \text{derivative of the Blasius function}$$

since the two problems must have the same solution.

In this case, we can immediately calculate the heat transfer coefficient using eqn. (6.5):

$$h=\frac{k}{T_\infty-T_w}\left.\frac{\partial(T-T_w)}{\partial y}\right|_{y=0}=k\left(\frac{\partial f'}{\partial\eta}\frac{\partial\eta}{\partial y}\right)_{\eta=0}$$

but $(\partial^2 f/\partial\eta^2)_{\eta=0}=0.33206$ (see Fig. 6.10) and $\partial\eta/\partial y=\sqrt{u_\infty/\nu x}$, so

$$\frac{hx}{k}=\mathrm{Nu}_x=0.33206\sqrt{\mathrm{Re}_x} \quad \text{for } \nu=\alpha \tag{6.43}$$

Normally, in using eqn. (6.43) or any other forced convection equation, properties should be evaluated at the *film temperature*, $T_{\mathrm{av}}=(T_w+T_\infty)/2$.

Example 6.4

Water flows over a flat heater, 0.06 m in length, under high pressure at 300°C. The free stream velocity is 2 m/s and the heater is held at 315°C. What is the average heat flux?

SOLUTION. At $T_{\text{av}} = (315 + 300)/2 = 307°\text{C}$:

$$\nu = 0.124 \times 10^{-6}\ \text{m}^2/\text{s}$$
$$\alpha = 0.124 \times 10^{-6}\text{m}^2/\text{s}$$

Therefore, $\nu = \alpha$ and we can use eqn. (6.43). First we must calculate the average heat flux, $\overline{q}$. To do this, we call $T_w - T_\infty \equiv \Delta T$ and write

$$\overline{q} = \frac{1}{L}\int_0^L h\Delta T\, dx = \frac{k\Delta T}{L}\int_0^L \frac{1}{x}\text{Nu}_x\, dx = 0.332\frac{k\Delta T}{L}\int_0^L \sqrt{\frac{u_\infty}{\nu x}}\, dx$$

so

$$\overline{q} = 2\Delta T\left(0.332\frac{k}{L}\sqrt{\text{Re}_L}\right) = 2q_{x=L}$$

Thus,

$$\overline{h} = 2h_{x=L} = 0.664\frac{0.520}{0.06}\sqrt{\frac{2(0.06)}{0.124\times 10^{-6}}} = 5661\ \text{W/m}^2\text{K}$$

and

$$\overline{q} = \overline{h}\Delta T = 5661(315 - 300) = 84,915\ \text{W/m}^2 = 84.9\ \text{kW/m}^2$$

Equation (6.43) is clearly a very restrictive heat transfer solution. We now want to find how to evaluate q when ν does not equal α. ■

6.4 The Prandtl number and the boundary layer thicknesses

Dimensional analysis

We must now look more closely at the implications of the similarity between the velocity and thermal boundary layers. We first ask what dimensional analysis reveals about heat transfer in the laminar b.l. We know by now that the dimensional functional equation for the heat transfer coefficient, h, should be

$$h = \text{fn}(k, x, \rho, c_p, \mu, u_\infty)$$

We have excluded $T_w - T_\infty$ on the basis of Newton's original hypothesis, borne out in eqn. (6.43), that $h \neq \text{fn}(\Delta T)$ during forced convection. This gives seven variables in J/°C , m, kg, and s, or $7 - 4 = 3$ pi-groups. Note that, as we indicated at the end of Section 4.3, there is no conversion between heat and work so it we should not regard J as N·m, but rather as a separate unit. The dimensionless groups are then:

$$\Pi_1 = \frac{hx}{k} \equiv \text{Nu}_x \qquad \Pi_2 = \frac{\rho u_\infty x}{\mu} \equiv \text{Re}_x$$

and a new group:

$$\Pi_3 = \frac{\mu c_p}{k} \equiv \frac{\nu}{\alpha} \equiv \text{Pr, Prandtl number}$$

Thus,

$$\text{Nu}_x = \text{fn}(\text{Re}_x, \text{Pr}) \tag{6.44}$$

in forced convection flow situations. Equation (6.43) was developed for the case in which $\nu = \alpha$ or $\text{Pr} = 1$; therefore, it is of the same form as eqn. (6.44), although it does not display the Pr dependence of Nu_x.

To better understand the physical meaning of the Prandtl number, let us briefly consider how to predict its value in a gas.

Kinetic theory of μ and k

Figure 6.13 shows a small neighborhood of a point of interest in a gas in which there exists a velocity or temperature gradient. We identify the *mean free path* of molecules between collisions as ℓ and indicate planes at $y \pm \ell/2$ which bracket the average travel of those molecules found at plane y. (Actually, these planes should be located closer to $y \pm \ell$ for a variety of subtle reasons. This and other fine points of these arguments are explained in detail in [6.3].)

The shear stress, τ_{yx}, can be expressed as the change of momentum of all molecules that pass through the y-plane of interest, per unit area:

$$\tau_{yx} = \begin{pmatrix} \text{mass flux of molecules} \\ \text{from } y - \ell/2 \text{ to } y + \ell/2 \end{pmatrix} \cdot \begin{pmatrix} \text{change in fluid} \\ \text{velocity} \end{pmatrix}$$

The mass flux from top to bottom is proportional to $\rho\overline{C}$, where $\overline{C}$, the mean molecular speed of the stationary fluid, is $\gg u$ or v in incompressible flow. Thus,

$$\tau_{yx} = C_1 \left(\rho\overline{C}\right) \left(\ell \frac{du}{dy}\right) \frac{\text{N}}{\text{m}^2} \text{ and this also equals } \mu \frac{du}{dy} \tag{6.45}$$

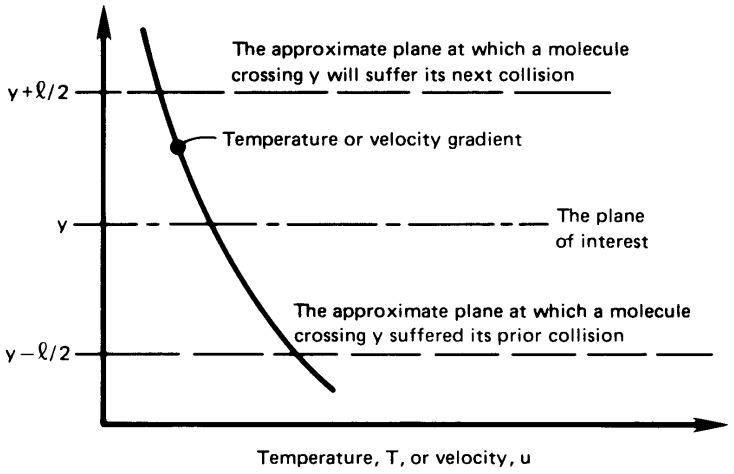
The approximate plane at which a molecule crossing y will suffer its next collision
y+ℓ/2
Temperature or velocity gradient
y
The plane of interest
The approximate plane at which a molecule crossing y suffered its prior collision
y−ℓ/2
Temperature, T, or velocity, u

Figure 6.13 Momentum and energy transfer in a gas with a velocity or temperature gradient.

By the same token,

$$q_y = C_2\left(\rho c_v \overline{C}\right)\left(\ell \frac{dT}{dy}\right) \text{ and this also equals } -k\frac{dT}{dy}$$

where c_v is the specific heat at constant volume. The constants, C_1 and C_2, are on the order of unity. It follows immediately that

$$\mu = C_1\left(\rho \overline{C}\ell\right) \qquad \text{so} \qquad \nu = C_1\left(\overline{C}\ell\right)$$

and

$$k = C_2\left(\rho c_v \overline{C}\ell\right) \qquad \text{so} \qquad \alpha = C_2\frac{\overline{C}\ell}{\gamma}$$

where $\gamma \equiv c_p/c_v$ is approximately a constant on the order of unity for a given gas. Thus, for a gas,

$$\text{Pr} \equiv \frac{\nu}{\alpha} = \text{ a constant on the order of unity}$$

More detailed use of the kinetic theory of gases reveals more specific information as to the value of the Prandtl number, and these points are borne out reasonably well experimentally, as you can determine from Appendix A:

- For simple monatomic gases, $\text{Pr} = \frac{2}{3}$.

- For diatomic gases in which vibration is unexcited (such as N_2 and O_2 at room temperature), $\mathrm{Pr} = \frac{5}{7}$.
- As the complexity of gas molecules increases, Pr approaches an upper value of unity.
- Pr is most insensitive to temperature in gases made up of the simplest molecules because their structure is least responsive to temperature changes.

In a liquid, the physical mechanisms of molecular momentum and energy transport are much more complicated and Pr can be far from unity. For example (cf. Table A.3):

- For liquids composed of fairly simple molecules, excluding metals, Pr is of the order of magnitude of 1 to 10.
- For liquid metals, Pr is of the order of magnitude of 10^{-2} or less.
- If the molecular structure of a liquid is very complex, Pr might reach values on the order of 10^5. This is true of oils made of long-chain hydrocarbons, for example.

Thus, while Pr can vary over almost eight orders of magnitude in common fluids, it is still the result of analogous mechanisms of heat and momentum transfer. The numerical values of Pr, as well as the analogy itself, have their origins in the same basic process of molecular transport.

Boundary layer thicknesses, δ and δ_t, and the Prandtl number

We have seen that the exact solution of the b.l. equations gives $\delta = \delta_t$ for $\mathrm{Pr} = 1$, and it gives dimensionless velocity and temperature profiles that are identical on a flat surface. Two other things should be easy to see:

- When $\mathrm{Pr} > 1$, $\delta > \delta_t$, and when $\mathrm{Pr} < 1$, $\delta < \delta_t$. This is true because high viscosity leads to a thick velocity b.l., and a high thermal diffusivity should give a thick thermal b.l.
- Since the exact governing equations (6.41) and (6.42) are identical for either b.l., except for the appearance of α in one and ν in the other, we expect that

$$\frac{\delta_t}{\delta} = \mathrm{fn}\left(\frac{\nu}{\alpha}\ \text{only}\right)$$

Therefore, we can combine these two observations, defining $\delta_t/\delta \equiv \phi$, and get

$$\phi = \text{ monotonically decreasing function of Pr only} \tag{6.46}$$

The exact solution of the thermal b.l. equations proves this to be precisely true.

The fact that ϕ is independent of x will greatly simplify the use of the integral method. We shall establish the correct form of eqn. (6.46) in the following section.

6.5 Heat transfer coefficient for laminar, incompressible flow over a flat surface

The integral method for solving the energy equation

Integrating the b.l. energy equation in the same way as the momentum equation gives

$$\int_0^{\delta_t} u\frac{\partial T}{\partial x}\,dy + \int_0^{\delta_t} v\frac{\partial T}{\partial y}\,dy = \alpha\int_0^{\delta_t}\frac{\partial^2 T}{\partial y^2}\,dy$$

And the chain rule of differentiation in the form $x\,dy \equiv d(xy) - y\,dx$, reduces this to

$$\int_0^{\delta_t}\frac{\partial uT}{\partial x}\,dy - \int_0^{\delta_t} T\frac{\partial u}{\partial x}\,dy + \int_0^{\delta_t}\frac{\partial vT}{\partial y}\,dy - \int_0^{\delta_t} T\frac{\partial v}{\partial y}\,dy = \alpha\frac{\partial T}{\partial y}\bigg|_0^{\delta_t}$$

or

$$\int_0^{\delta_t}\frac{\partial uT}{\partial x}\,dy + \underbrace{vT\Big|_0^{\delta_t}}_{=T_\infty\, v|_{y=\delta_t} - 0} - \int_0^{\delta_t} T\underbrace{\left(\frac{\partial u}{\partial x} + \frac{\partial v}{\partial y}\right)}_{=0,\ \text{eqn. (6.11)}}dy = \alpha\left[\underbrace{\frac{\partial T}{\partial y}\bigg|_{\delta_t}}_{=0} - \frac{\partial T}{\partial y}\bigg|_0\right]$$

We evaluate v at $y = \delta_t$, using the continuity equation in the form of eqn. (6.23), in the preceeding expression:

$$\int_0^{\delta_t}\frac{\partial}{\partial x}u(T - T_\infty)\,dy = \frac{1}{\rho c_p}\left(-k\,\frac{\partial T}{\partial y}\bigg|_0\right) = \text{fn}(x \text{ only})$$

or

$$\boxed{\frac{d}{dx}\int_0^{\delta_t} u(T-T_\infty)\,dy = \frac{q_w}{\rho c_p}} \tag{6.47}$$

Equation (6.47) expresses the conservation of thermal energy in integrated form. It shows that the rate thermal energy is carried away by the b.l. flow is matched by the rate heat is transferred in at the wall.

Predicting the temperature distribution in the laminar thermal boundary layer

We can continue to paraphrase the development of the velocity profile in the laminar b.l., from the preceding section. We previously guessed the velocity profile in such a way as to make it match what we know to be true. We also know certain things to be true of the temperature profile. The temperatures at the wall and at the outer edge of the b.l. are known. Furthermore, the temperature distribution should be smooth as it blends into T_∞ for $y > \delta_t$. This condition is imposed by setting dT/dy equal to zero at $y = \delta_t$. A fourth condition is obtained by writing eqn. (6.40) at the wall, where $u = v = 0$. This gives $(\partial^2 T/\partial y^2)_{y=0} = 0$. These four conditions take the following dimensionless form:

$$\left.\begin{aligned}
\frac{T-T_\infty}{T_w-T_\infty} &= 1 \quad \text{at } y/\delta_t = 0\\
\frac{T-T_\infty}{T_w-T_\infty} &= 0 \quad \text{at } y/\delta_t = 1\\
\frac{d[(T-T_\infty)/(T_w-T_\infty)]}{d(y/\delta_t)} &= 0 \quad \text{at } y/\delta_t = 1\\
\frac{\partial^2[(T-T_\infty)/(T_w-T_\infty)]}{\partial(y/\delta_t)^2} &= 0 \quad \text{at } y/\delta_t = 0
\end{aligned}\right\} \tag{6.48}$$

Equations (6.48) provide enough information to approximate the temperature profile with a cubic function.

$$\frac{T-T_\infty}{T_w-T_\infty} = a + b\frac{y}{\delta_t} + c\left(\frac{y}{\delta_t}\right)^2 + d\left(\frac{y}{\delta_t}\right)^3 \tag{6.49}$$

Substituting eqn. (6.49) into eqns. (6.48), we get

$$a = 1 \qquad -1 = b + c + d \qquad 0 = b + 2c + 3d \qquad 0 = 2c$$

which gives

$$a = 1 \qquad b = -\tfrac{3}{2} \qquad c = 0 \qquad d = \tfrac{1}{2}$$

so the temperature profile is

$$\boxed{\frac{T - T_\infty}{T_w - T_\infty} = 1 - \frac{3}{2}\frac{y}{\delta_t} + \frac{1}{2}\left(\frac{y}{\delta_t}\right)^3} \tag{6.50}$$

Predicting the heat flux in the laminar boundary layer

Equation (6.47) contains an as-yet-unknown quantity—the thermal b.l. thickness, δ_t. To calculate δ_t, we substitute the temperature profile, eqn. (6.50), and the velocity profile, eqn. (6.29), in the integral form of the energy equation, (6.47), which we first express as

$$u_\infty (T_w - T_\infty)\frac{d}{dx}\left[\delta_t \int_0^1 \frac{u}{u_\infty}\left(\frac{T - T_\infty}{T_w - T_\infty}\right) d\left(\frac{y}{\delta_t}\right)\right] = -\frac{\alpha(T_w - T_\infty)}{\delta_t}\left.\frac{d\left(\dfrac{T - T_\infty}{T_w - T_\infty}\right)}{d(y/\delta_t)}\right|_{y/\delta_t = 0} \tag{6.51}$$

There is no problem in completing this integration if $\delta_t < \delta$. However, if $\delta_t > \delta$, there will be a problem because the equation $u/u_\infty = 1$, instead of eqn. (6.29), defines the velocity beyond $y = \delta$. Let us proceed for the moment in the hope that the requirement that $\delta_t \ll \delta$ will be satisfied. Introducing $\phi \equiv \delta_t/\delta$ in eqn. (6.51) and calling $y/\delta_t \equiv \eta$, we get

$$\delta_t \frac{d\delta_t}{dx}\left[\underbrace{\int_0^1 \left(\frac{3}{2}\eta\phi - \frac{1}{2}\eta^3\phi^3\right)\left(1 - \frac{3}{2}\eta + \frac{1}{2}\eta^3\right) d\eta}_{= \frac{3}{20}\phi - \frac{3}{280}\phi^3}\right] = \frac{3\alpha}{2u_\infty} \tag{6.52}$$

Since ϕ is a constant for any Pr [recall eqn. (6.46)], we separate variables:

$$\frac{d\delta_t^2}{dx} = \frac{3\alpha/u_\infty}{\left(\dfrac{3}{20}\phi - \dfrac{3}{280}\phi^3\right)}$$

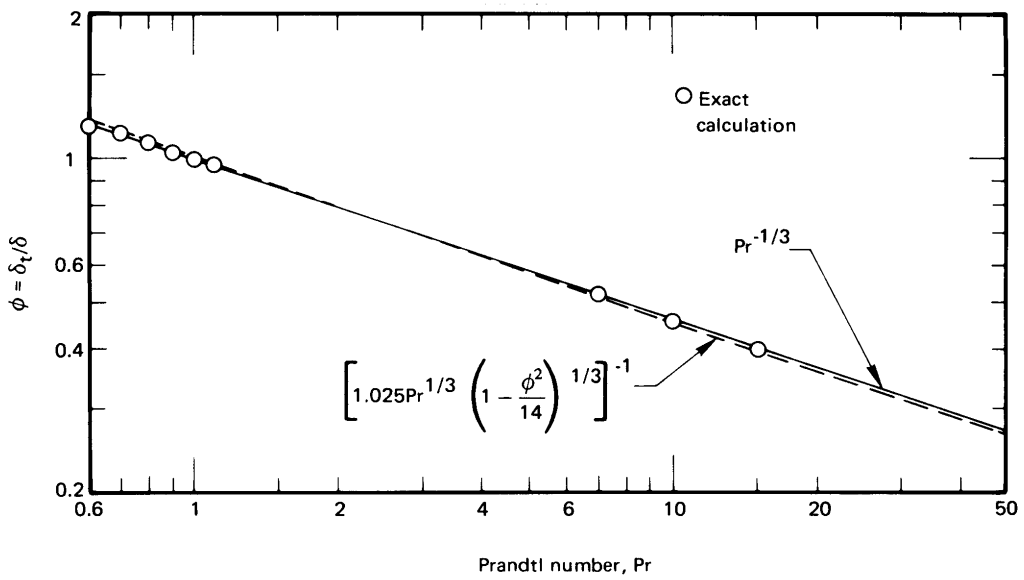

Figure 6.14 The exact and approximate Prandtl number influence on the ratio of b.l. thicknesses.

Integrating this result with respect to x and taking $\delta_t = 0$ at $x = 0$, we get

$$\delta_t = \sqrt{\frac{3\alpha x}{u_\infty}} \Big/ \sqrt{\frac{3}{20}\phi - \frac{3}{280}\phi^3} \tag{6.53}$$

But $\delta = 4.64x/\sqrt{\mathrm{Re}_x}$ in the integral formulation [eqn. (6.31)]. We divide by this value of δ to be consistent and obtain

$$\frac{\delta_t}{\delta} \equiv \phi = 0.9638 \Big/ \sqrt{\mathrm{Pr}\,\phi\,(1 - \phi^2/14)}$$

Rearranging this gives

$$\frac{\delta_t}{\delta} = \frac{1}{1.025\,\mathrm{Pr}^{1/3}\left[1 - (\delta_t^2/14\delta^2)\right]^{1/3}} \simeq \frac{1}{1.025\,\mathrm{Pr}^{1/3}} \tag{6.54}$$

The unapproximated result above is shown in Fig. 6.14, along with the results of Pohlhausen's precise calculation (see Schlichting [6.2, Chap. 14]). It turns out that the exact ratio, δ/δ_t, is represented with great accuracy

by

$$\boxed{\frac{\delta_t}{\delta} = \mathrm{Pr}^{-1/3}} \qquad 0.6 \leqslant \mathrm{Pr} \leqslant 50 \tag{6.55}$$

So the integral method is accurate within 2.5% in the Prandtl number range indicated.

Notice that Fig. 6.14 is terminated for Pr less than 0.6. The reason for doing this is that the lowest Pr for pure gases is 0.67, and the next lower values of Pr are on the order of 10^{-2} for liquid metals. For Pr = 0.67, $\delta_t/\delta = 1.143$, which violates the assumption that $\delta_t \leqslant \delta$, but only by a small margin. For, say, mercury at 100°C, Pr = 0.0162 and $\delta_t/\delta = 3.952$, which violates the condition by an intolerable margin. We therefore have a theory that is acceptable for gases and all liquids except the metallic ones.

The final step in predicting the heat flux is to write Fourier's law:

$$q = -k\left.\frac{\partial T}{\partial y}\right|_{y=0} = -k\,\frac{T_w - T_\infty}{\delta_t}\left.\frac{\partial\left(\dfrac{T - T_\infty}{T_w - T_\infty}\right)}{\partial(y/\delta_t)}\right|_{y/\delta_t=0} \tag{6.56}$$

Using the dimensionless temperature distribution given by eqn. (6.50), we get

$$q = +k\,\frac{T_w - T_\infty}{\delta_t}\,\frac{3}{2}$$

or

$$h \equiv \frac{q}{\Delta T} = \frac{3k}{2\delta_t} = \frac{3}{2}\frac{k}{\delta}\frac{\delta}{\delta_t} \tag{6.57}$$

and substituting eqns. (6.54) and (6.31) for δ/δ_t and δ, we obtain

$$\mathrm{Nu}_x \equiv \frac{hx}{k} = \frac{3}{2}\frac{\sqrt{\mathrm{Re}_x}}{4.64}\,1.025\,\mathrm{Pr}^{1/3} = 0.3314\,\mathrm{Re}_x^{1/2}\,\mathrm{Pr}^{1/3}$$

Considering the various approximations, this is very close to the result of the exact calculation, which turns out to be

$$\boxed{\mathrm{Nu}_x = 0.332\,\mathrm{Re}_x^{1/2}\,\mathrm{Pr}^{1/3}} \qquad 0.6 \leqslant \mathrm{Pr} \leqslant 50 \tag{6.58}$$

This expression gives very accurate results under the assumptions on which it is based: a laminar two-dimensional b.l. on a flat surface, with T_w = constant and $0.6 \leqslant \mathrm{Pr} \leqslant 50$.

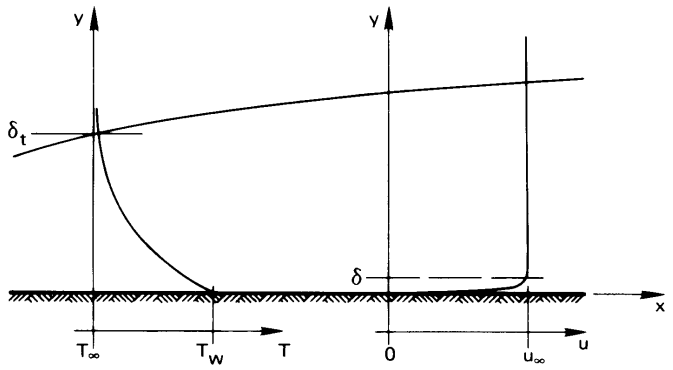

Figure 6.15 A laminar b.l. in a low-Pr liquid. The velocity b.l. is so thin that $u \simeq u_\infty$ in the thermal b.l.

Some other laminar boundary layer heat transfer equations

High Pr. At high Pr, eqn. (6.58) is still close to correct. The exact solution is

$$\mathrm{Nu}_x \longrightarrow 0.339\ \mathrm{Re}_x^{1/2}\,\mathrm{Pr}^{1/3}, \quad \mathrm{Pr} \longrightarrow \infty \tag{6.59}$$

Low Pr. Figure 6.15 shows a low-Pr liquid flowing over a flat plate. In this case $\delta_t \gg \delta$, and for all practical purposes $u = u_\infty$ everywhere within the thermal b.l. It is as though the no-slip condition $[u(y = 0) = 0]$ and the influence of viscosity were removed from the problem. Thus, the dimensional functional equation for h becomes

$$h = \mathrm{fn}\left(x, k, \rho c_p, u_\infty\right) \tag{6.60}$$

There are five variables in J/°C, m, and s, so there are only two pi-groups. They are

$$\mathrm{Nu}_x = \frac{hx}{k} \quad \text{and} \quad \Pi_2 \equiv \mathrm{Re}_x\mathrm{Pr} = \frac{u_\infty x}{\alpha}$$

The new group, Π_2, is called a *Péclét number*, Pe_x, where the subscript identifies the length upon which it is based. It can be interpreted as follows:

$$\mathrm{Pe}_x \equiv \frac{u_\infty x}{\alpha} = \frac{\rho c_p u_\infty \Delta T}{k\Delta T} = \frac{\text{heat capacity rate of fluid in the b.l.}}{\text{axial heat conductance of the b.l.}} \tag{6.61}$$

So long as Pe_x is large, the b.l. assumption that $\partial^2 T/\partial x^2 \ll \partial^2 T/\partial y^2$ will be valid; but for small Pe_x (i.e., $\mathrm{Pe}_x \ll 100$), it will be violated and a boundary layer solution cannot be used.

The exact solution of the b.l. equations gives, in this case:

$$\mathrm{Nu}_x = 0.565\ \mathrm{Pe}_x^{1/2} \qquad \begin{cases} \mathrm{Pe}_x \geq 100 & \text{and} \\ \mathrm{Pr} \lesssim \frac{1}{100} & \text{or} \\ \mathrm{Re}_x \geq 10^4 & \end{cases} \tag{6.62}$$

General relationship. Churchill and Ozoe [6.4] recommend the following empirical correlation for laminar flow on a constant-temperature flat surface for the entire range of Pr:

$$\boxed{\mathrm{Nu}_x = \frac{0.3387\ \mathrm{Re}_x^{1/2}\,\mathrm{Pr}^{1/3}}{\left[1 + (0.0468/\mathrm{Pr})^{2/3}\right]^{1/4}}} \qquad \mathrm{Pe}_x > 100 \tag{6.63}$$

This relationship proves to be quite accurate, and it approximates eqns. (6.59) and (6.62), respectively, in the high- and low-Pr limits. The calculations of an average Nusselt number for the general case is left as an exercise (Problem 6.10).

Boundary layer with an unheated starting length Figure 6.16 shows a b.l. with a heated region that starts at a distance x_0 from the leading edge. The heat transfer in this instance is easily obtained using integral methods (see, e.g., [6.5, Chap. 10]):

$$\mathrm{Nu}_x = \frac{0.332\ \mathrm{Re}_x^{1/2}\,\mathrm{Pr}^{1/3}}{\left[1 - (x_0/x)^{3/4}\right]^{1/3}}, \qquad x > x_0 \tag{6.64}$$

Average heat transfer coefficient, $\overline{h}$. The heat transfer coefficient h, is the ratio of two quantities, q and ΔT, either of which might vary with x. So far, we have only dealt with the *uniform wall temperature problem*. Equations (6.58), (6.59), (6.62), and (6.63), for example, can all be used to calculate $q(x)$ when $(T_w - T_\infty) \equiv \Delta T$ is a specified constant. In the next subsection, we discuss the problem of predicting $[T(x) - T_\infty]$ when q is a specified constant. This is called the *uniform wall heat flux problem*.

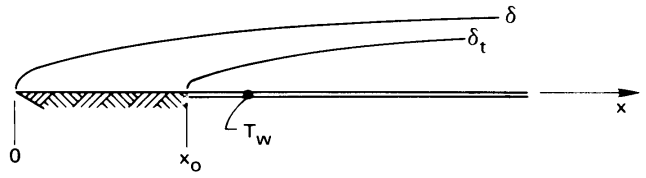

Figure 6.16 A b.l. with an unheated region at the leading edge.

The term $\overline{h}$ is used to designate either $\overline{q}/\Delta T$ in the uniform wall temperature problem or $q/\overline{\Delta T}$ in the uniform wall heat flux problem. Thus,

$$\text{uniform wall temp.:}\quad \overline{h} \equiv \frac{\overline{q}}{\Delta T} = \frac{1}{\Delta T}\left[\frac{1}{L}\int_0^L q\,dx\right] = \frac{1}{L}\int_0^L h(x)\,dx \tag{6.65}$$

$$\text{uniform heat flux:}\quad \overline{h} \equiv \frac{q}{\overline{\Delta T}} = \frac{q}{\dfrac{1}{L}\displaystyle\int_0^L \Delta T(x)\,dx} \tag{6.66}$$

The Nusselt number based on $\overline{h}$ and a characteristic length, L, is designated $\overline{\mathrm{Nu}}_L$. This is not to be construed as an average of Nu_x, which would be meaningless in either of these cases.

Thus, for a flat surface (with $x_0 = 0$), we use eqn. (6.58) in eqn. (6.65) to get

$$\overline{h} = \frac{1}{L}\int_0^L \underbrace{h(x)\,dx}_{\frac{k}{x}\,\mathrm{Nu}_x} = \frac{0.332\,k\,\mathrm{Pr}^{1/3}}{L}\sqrt{\frac{u_\infty}{\nu}}\int_0^L \frac{\sqrt{x}\,dx}{x}$$

$$= 0.664\,\mathrm{Re}_L^{1/2}\,\mathrm{Pr}^{1/3}\left(\frac{k}{L}\right) \tag{6.67}$$

Thus, $\overline{h} = 2h(x = L)$ in a laminar flow, and

$$\boxed{\overline{\mathrm{Nu}}_L = \frac{\overline{h}L}{k} = 0.664\,\mathrm{Re}_L^{1/2}\,\mathrm{Pr}^{1/3}} \tag{6.68}$$

Likewise for liquid metal flows:

$$\overline{\mathrm{Nu}}_L = 1.13\,\mathrm{Pe}_L^{1/2} \tag{6.69}$$

Some final observations. The preceding results are restricted to the two-dimensional, incompressible, laminar b.l. on a flat isothermal wall at velocities that are not too high. These conditions are usually met if:

- Re_x or Re_L is not above the turbulent transition value, which is typically a few hundred thousand.
- The Mach number of the flow, $\mathrm{Ma} \equiv u_\infty/(\text{sound speed})$, is less than about 0.3. (Even gaseous flows behave incompressibly at velocities well below sonic.) A related condition is:
- The *Eckert number*, $\mathrm{Ec} \equiv u_\infty^2/c_p(T_w - T_\infty)$, is substantially less than unity. (This means that heating by viscous dissipation—which we have neglected—does not play any role in the problem. This assumption was included implicitly when we treated J as an independent unit in the dimensional analysis of this problem.)

It is worthwhile to notice how h and Nu depend on their independent variables:

$$\begin{aligned} h \text{ or } \overline{h} &\propto \frac{1}{\sqrt{x}} \text{ or } \frac{1}{\sqrt{L}}, \qquad \sqrt{u_\infty},\ \nu^{-1/6},\ (\rho c_p)^{1/3},\ k^{2/3} \\ \mathrm{Nu}_x \text{ or } \overline{\mathrm{Nu}}_L &\propto \sqrt{x \text{ or } L}, \qquad \sqrt{u_\infty},\ \nu^{-1/6},\ (\rho c_p)^{1/3},\ k^{-1/3} \end{aligned} \tag{6.70}$$

Thus, $h \longrightarrow \infty$ and Nu_x vanishes at the leading edge, $x = 0$. Of course, an infinite value of h, like infinite shear stress, will not really occur at the leading edge because the b.l. description will actually break down in a small neighborhood of $x = 0$.

In all of the preceding considerations, the fluid properties have been assumed constant. Actually, k, ρc_p, and especially μ might all vary noticeably with T within the b.l. It turns out that if properties are all evaluated at the average temperature of the b.l. or film temperature $(T_w + T_\infty)/2$, the results will normally be quite accurate. It is also worth noting that, although properties are given only at one pressure in Appendix A; μ, k, and c_p change very little with pressure, especially in liquids.

Example 6.5

Air at 20°C and moving at 15 m/s is warmed by an isothermal steam-heated plate at 110°C, ½ m in length and ½ m in width. Find the average heat transfer coefficient and the total heat transferred. What are h, δ_t, and δ at the trailing edge?

SOLUTION. We evaluate properties at $T = (110+20)/2 = 65°\text{C}$. Then

$$\text{Pr} = 0.707 \qquad \text{and} \qquad \text{Re}_L = \frac{u_\infty L}{\nu} = \frac{15(0.5)}{0.0000194} = 386,600$$

so the flow ought to be laminar up to the trailing edge. The Nusselt number is then

$$\overline{\text{Nu}}_L = 0.664\ \text{Re}_L^{1/2}\,\text{Pr}^{1/3} = 367.8$$

and

$$\overline{h} = 367.8\frac{k}{L} = \frac{367.8(0.02885)}{0.5} = 21.2\ \text{W/m}^2\text{K}$$

The value is quite low because of the low conductivity of air. The total heat flux is then

$$Q = \overline{h}A\,\Delta T = 21.2(0.5)^2(110-20) = 477\ \text{W}$$

By comparing eqns. (6.58) and (6.68), we see that $h(x=L) = \frac{1}{2}\overline{h}$, so

$$h(\text{trailing edge}) = \tfrac{1}{2}(21.2) = 10.6\ \text{W/m}^2\text{K}$$

And finally,

$$\delta(x=L) = 4.92L/\sqrt{\text{Re}_L} = \frac{4.92(0.5)}{\sqrt{386,600}} = 0.00396\ \text{m}$$
$$= 3.96\ \text{mm}$$

and

$$\delta_t = \frac{\delta}{\sqrt[3]{\text{Pr}}} = \frac{3.96}{\sqrt[3]{0.707}} = 4.44\ \text{mm}$$ ■

The problem of uniform wall heat flux

When the heat flux at the heater wall, q_w, is specified instead of the temperature, it is T_w that we need to know. We leave the problem of finding Nu_x for q_w = constant as an exercise (Problem 6.11). The exact result is

$$\text{Nu}_x = 0.453\ \text{Re}_x^{1/2}\,\text{Pr}^{1/3} \tag{6.71}$$

where $\mathrm{Nu}_x = hx/k = q_w x/k(T_w - T_\infty)$. The integral method gives the same result with a slightly lower constant (0.417).

We must be very careful in discussing *average* results in the constant heat flux case. The problem now might be that of finding an average temperature difference (cf. (6.66)):

$$\overline{T_w - T_\infty} = \frac{1}{L}\int_0^L (T_w - T_\infty)\,dx = \frac{1}{L}\int_0^L \frac{q_w x}{k(0.453\sqrt{u_\infty/\nu}\,\mathrm{Pr}^{1/3})}\frac{dx}{\sqrt{x}}$$

or

$$\overline{T_w - T_\infty} = \frac{q_w L/k}{0.6795\ \mathrm{Re}_L^{1/2}\,\mathrm{Pr}^{1/3}} \tag{6.72}$$

which can be put into the form $\overline{\mathrm{Nu}}_L = 0.6795\ \mathrm{Re}_L^{1/2}\mathrm{Pr}^{1/3}$ (although the Nusselt number yields an awkward nondimensionalization for $\overline{T_w - T_\infty}$). Churchill and Ozoe [6.4] have pointed out that their eqn. (6.63) will describe $(T_w - T_\infty)$ with high accuracy over the full range of Pr if the constants are changed as follows:

- 0.3387 is changed to 0.4637.
- 0.0468 is changed to 0.02052.

Example 6.6

Air at 15°C flows at 1.8 m/s over a 0.6 m-long heating panel. The panel is intended to supply 420 W/m^2 to the air, but the surface can sustain only about 105°C without being damaged. Is it safe? What is the *average* temperature of the plate?

SOLUTION. In accordance with eqn. (6.71),

$$\Delta T_{\max} = \Delta T_{x=L} = \frac{qL}{k\,\mathrm{Nu}_{x=L}} = \frac{qL/k}{0.453\,\mathrm{Re}_x^{1/2}\,\mathrm{Pr}^{1/3}}$$

or if we evaluate properties at $(85 + 15)/2 = 50$°C, for the moment,

$$\Delta T_{\max} = \frac{420(0.6)/0.0278}{0.453\left[0.6(1.8)/1.794\times 10^{-5}\right]^{1/2}(0.709)^{1/3}} = 91.5\text{°C}$$

This will give $T_{w_{\max}} = 15 + 91.5 = 106.5$°C. This is very close to 105°C. If 105°C is at all conservative, $q = 420$ W/m^2 should be safe—particularly since it only occurs over a very small distance at the end of the plate.

From eqn. (6.72) we find that

$$\overline{\Delta T} = \frac{0.453}{0.6795}\,\Delta T_{\max} = 61.0^{\circ}\mathrm{C}$$

so

$$\overline{T_w} = 15 + 61.0 = 76.0^{\circ}\mathrm{C} \qquad \blacksquare$$

6.6 The Reynolds analogy

The analogy between heat and momentum transfer can now be generalized to provide a very useful result. We begin by recalling eqn. (6.25), which is restricted to a flat surface with no pressure gradient:

$$\frac{d}{dx}\left[\delta \int_0^1 \frac{u}{u_\infty}\left(\frac{u}{u_\infty} - 1\right) d\left(\frac{y}{\delta}\right)\right] = -\frac{C_f}{2} \tag{6.25}$$

and by rewriting eqns. (6.47) and (6.51), we obtain for the constant wall temperature case:

$$\frac{d}{dx}\left[\phi\,\delta \int_0^1 \frac{u}{u_\infty}\left(\frac{T - T_\infty}{T_w - T_\infty}\right) d\left(\frac{y}{\delta_t}\right)\right] = \frac{q_w}{\rho c_p u_\infty (T_w - T_\infty)} \tag{6.73}$$

But the similarity of temperature and flow boundary layers to one another [see, e.g., eqns. (6.29) and (6.50)], suggests the following approximation, which becomes exact only when Pr = 1:

$$\frac{T - T_\infty}{T_w - T_\infty}\,\delta = \left(1 - \frac{u}{u_\infty}\right)\delta_t$$

Substituting this result in eqn. (6.73) and comparing it to eqn. (6.25), we get

$$-\frac{d}{dx}\left[\delta \int_0^1 \frac{u}{u_\infty}\left(\frac{u}{u_\infty} - 1\right) d\left(\frac{y}{\delta}\right)\right] = -\frac{C_f}{2} = -\frac{q_w}{\rho c_p u_\infty (T_w - T_\infty)\phi^2} \tag{6.74}$$

Finally, we substitute eqn. (6.55) to eliminate ϕ from eqn. (6.74). The result is one instance of the *Reynolds-Colburn analogy*:[8]

$$\frac{h}{\rho c_p u_\infty}\,\mathrm{Pr}^{2/3} = \frac{C_f}{2} \tag{6.75}$$

[8] Reynolds [6.6] developed the analogy in 1874. Colburn made important use of it in this century. The form given is for flat plates with $0.6 \le \mathrm{Pr} \le 50$. The Prandtl number factor is usually a little different for other flows or other ranges of Pr.

For use in Reynolds' analogy, C_f must be a pure *skin* friction coefficient. The profile drag that results from the variation of pressure around the body is unrelated to heat transfer. The analogy does not apply when profile drag is included in C_f.

The dimensionless group $h/\rho c_p u_\infty$ is called the *Stanton number*. It is defined as follows:

$$\text{St, Stanton number} \equiv \frac{h}{\rho c_p u_\infty} = \frac{\text{Nu}_x}{\text{Re}_x \text{Pr}}$$

The physical significance of the Stanton number is

$$\text{St} = \frac{h\Delta T}{\rho c_p u_\infty \Delta T} = \frac{\text{actual heat flux to the fluid}}{\text{heat flux capacity of the fluid flow}} \tag{6.76}$$

The group $\text{St}\,\text{Pr}^{2/3}$ was dealt with by the chemical engineer Colburn, who gave it a special symbol:

$$j \equiv \text{Colburn } j\text{-factor} = \text{St}\,\text{Pr}^{2/3} = \frac{\text{Nu}_x}{\text{Re}_x \text{Pr}^{1/3}} \tag{6.77}$$

Example 6.7

Does the equation for the Nusselt number on an isothermal flat surface in laminar flow satisfy the Reynolds analogy?

SOLUTION. If we rewrite eqn. (6.58), we obtain

$$\frac{\text{Nu}_x}{\text{Re}_x \text{Pr}^{1/3}} = \text{St}\,\text{Pr}^{2/3} = \frac{0.332}{\sqrt{\text{Re}_x}} \tag{6.78}$$

But comparison with eqn. (6.33) reveals that the left-hand side of eqn. (6.78) is precisely $C_f/2$, so the analogy is satisfied perfectly. Likewise, from eqns. (6.68) and (6.34), we get

$$\frac{\overline{\text{Nu}}_L}{\text{Re}_L \text{Pr}^{1/3}} \equiv \overline{\text{St}}\,\text{Pr}^{2/3} = \frac{0.664}{\sqrt{\text{Re}_L}} = \frac{\overline{C}_f}{2} \tag{6.79}$$

■

The Reynolds-Colburn analogy can be used directly to infer heat transfer data from measurements of the shear stress, or vice versa. It can also be extended to turbulent flow, which is much harder to predict analytically. We shall undertake that problem in the next section.

Example 6.8

How much drag force does the air flow in Example 6.5 exert on the heat transfer surface?

SOLUTION. From eqn. (6.79) in Example 6.7, we obtain

$$\overline{C}_f = \frac{2\,\overline{\mathrm{Nu}}_L}{\mathrm{Re}_L\,\mathrm{Pr}^{1/3}}$$

From Example 6.5 we obtain $\overline{\mathrm{Nu}}_L$, Re_L, and $\mathrm{Pr}^{1/3}$:

$$\overline{C}_f = \frac{2(367.8)}{(386,600)(0.707)^{1/3}} = 0.002135$$

so

$$\overline{\tau_{yx}} = (0.002135)\,\frac{1}{2}\rho u_\infty^2 = \frac{(0.002135)(1.05)(15)^2}{2} = 0.2522\ \mathrm{kg/m{\cdot}s^2}$$

and the force is

$$\overline{\tau_{yx}}A = 0.2522(0.5)^2 = 0.06305\ \mathrm{kg{\cdot}m/s^2} = 0.06305\ \mathrm{N} = 0.23\ \mathrm{oz}$$ ■

6.7 Turbulent boundary layers

Turbulence

> Big whirls have little whirls,
> That feed on their velocity.
> Little whirls have littler whirls,
> And so on, to viscosity.

This bit of doggerel by the English fluid mechanic, L. F. Richardson, tells us a great deal about the nature of turbulence. Turbulence in a fluid can be viewed as a spectrum of coexisting vortices of different sizes that dissipate energy from the larger ones to the smaller ones until we no longer see macroscopic vortices (or "whirls"). Then we identify the process as viscous dissipation.

The next time the weatherman shows a satellite photograph of North America on the 10:00 P.M. news, notice the cloud patterns. There will be

one or two enormous vortices of continental proportions. These huge vortices, in turn, feed smaller "weather-making" vortices on the order of hundreds of miles in diameter. These further dissipate into vortices of cyclone and tornado proportions—sometimes with that level of violence but more often not. These dissipate into still smaller whirls as they interact with the ground and its various protrusions. The next time the wind blows, stand behind any tree and *feel* the vortices. In the great plains, where there are not many ground vortex generators, you will see small cyclonic eddies called "dust devils." The process continues right on down to molecular dimensions. There, momentum exchange is no longer identifiable as turbulence but appears as viscosity.

The same kind of process exists within, say, a turbulent pipe flow at high Reynolds number. Such a flow is shown in Fig. 6.17. Turbulence in such a case consists of coexisting vortices which vary in size from a substantial fraction of the pipe radius down to molecular dimensions. The spectrum of sizes varies with location in the pipe. The size and intensity of vortices at the wall must clearly approach zero, since the fluid velocity approaches zero at the wall.

Figure 6.17 shows the fluctuation of a typical flow variable—namely, velocity—both with location in the pipe and with time. This fluctuation arises because of the turbulent motions that are superposed on the average local flow. Other flow variables, such as T or ρ, can also vary in the same manner. For any variable we can write a local time-average value as

$$\overline{u} \equiv \frac{1}{\mathbf{T}} \int_0^{\mathbf{T}} u \, dt \tag{6.80}$$

where $\mathbf{T}$ is a time that is much longer than the period of typical fluctuations.[9] Equation (6.80) can only be written for so-called *stationary processes*—ones for which $\overline{u}$ is nearly time-independent.

If we substitute $u = \overline{u} + u'$ in eqn. (6.80), where u is the actual local velocity and u' is the instantaneous magnitude of the fluctuation, we obtain

$$\overline{u} = \underbrace{\frac{1}{\mathbf{T}} \int_0^{\mathbf{T}} \overline{u} \, dt}_{\overline{u}} + \underbrace{\frac{1}{\mathbf{T}} \int_0^{\mathbf{T}} u' \, dt}_{\overline{u'}} \tag{6.81}$$

[9] Take care not to interpret this $\mathbf{T}$ as a time constant; time constants are denoted as $\boldsymbol{T}$.

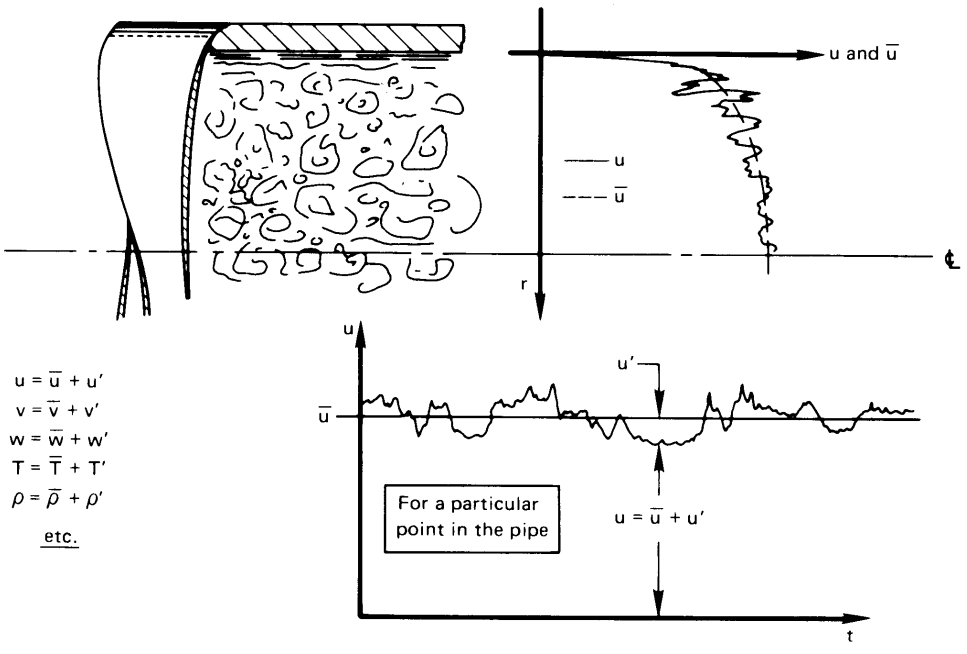

Figure 6.17 Fluctuation of u and other quantities in a turbulent pipe flow.

This is consistent with the fact that

$$\overline{u'} \text{ or any other average fluctuation} = 0 \tag{6.82}$$

We now want to create a measure of the size, or *lengthscale*, of turbulent fluctuations. This might be done experimentally by placing two velocity-measuring devices very close to one another in a turbulent flow field. There will then be a very high correlation between the two measurements. Then, suppose that the two velocity probes are moved apart until the measurements first become unrelated to one another. That spacing gives an indication of the average size of the turbulent motions.

Prandtl invented a slightly different (although related) measure of the lengthscale of turbulence, called the *mixing length*, ℓ. He saw ℓ as an average distance that a parcel of fluid moves between interactions. It has a physical significance similar to that of the molecular mean free path. It is harder to devise a clean experimental measure of ℓ than of the lengthscale of turbulence. But we can use ℓ to examine the notion of turbulent shear stress.

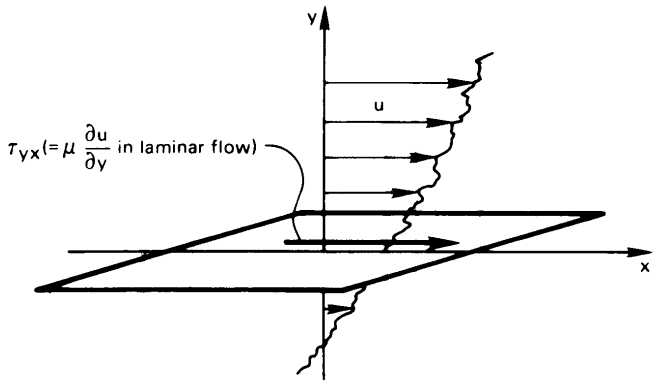

Figure 6.18 The shear stress, τ_{yx}, in a laminar or turbulent flow.

The contribution of turbulence to the shear stress arises from the same kind of momentum exchange process that gives rise to the molecular viscosity. Recall that, in the latter case, a kinetic calculation gave eqn. (6.45)

$$\tau_{yx} = C_1 \left(\rho \overline{C}\right) \left(\ell \frac{du}{dy}\right) = \mu \frac{du}{dy} \tag{6.45}$$

where ℓ was the molecular mean free path. In the turbulent flow case, pictured in Fig. 6.18, we can think of Prandtl's parcels of fluid as carrying the x-momentum, rather than molecules. We rewrite eqn. (6.45) in the following way:

- ℓ changes from the mean free path to the mixing length.
- $\overline{C}$ is replaced by $v = \overline{v} + v'$, the vertical speed of fluid parcels
- The derivative du/dy is approximated as u'/ℓ.

Then

$$\tau'_{yx} = C_1 \rho \left(\overline{v} + v'\right) u' \tag{6.83}$$

Equation (6.83) can also be derived formally and precisely with the help of the Navier-Stokes equation. When this is done, C_1 comes out

equal to −1. Then

$$\overline{\tau'_{yx}} = -\frac{\rho}{\mathbf{T}} \int_0^{\mathbf{T}} (\overline{v}u' + v'u')\, dt = -\rho\overline{v}\underbrace{\overline{u'}}_{=0} - \rho\overline{v'u'} \tag{6.84}$$

Notice that, while $\overline{u'} = \overline{v'} = 0$, averages of cross products of fluctuations (such as $\overline{u'v'}$ or $\overline{u'^2}$) do not generally vanish. Thus, the time average of the turbulence component of shear stress is

$$\overline{\tau'_{yx}} = -\rho\overline{v'u'} = \overline{\tau'_{yx}} \tag{6.85}$$

In addition to the turbulent shear stress, the flow will have a mean shear stress associated with the mean velocity gradient, $\partial\overline{u}/\partial y$.

It is not obvious how to calculate $\overline{v'u'}$ (although it can be measured), so we shall not make direct use of eqn. (6.85). Still, the essential similarity of the mechanisms giving rise to laminar and turbulent shear stresses suggests that the total time-average shear stress, τ_{yx}, might be expressed as a combination of mean flow and turbulence contributions that are each proportional to the mean velocity gradient:

$$\tau_{yx} = \mu\frac{\partial\overline{u}}{\partial y} + \underbrace{\left(\begin{array}{c}\text{some other factor, which}\\ \text{reflects turbulent mixing}\end{array}\right)}_{\equiv\,\rho\cdot\varepsilon_m}\frac{\partial\overline{u}}{\partial y} \tag{6.86}$$

or

$$\tau_{yx} = \rho\,(\nu + \varepsilon_m)\frac{\partial\overline{u}}{\partial y} \tag{6.87}$$

where ε_m is called the *eddy diffusivity for momentum*. We shall use this characterization in calculating the heat transfer.

The Reynolds-Colburn analogy for turbulent flow

The eddy diffusivity was actually introduced by Boussinesq [6.7] in 1877. It was subsequently proposed that Fourier's law might likewise be modified to

$$q = -k\frac{\partial\overline{T}}{\partial y} - \underbrace{\left(\begin{array}{c}\text{another constant, which}\\ \text{reflects turbulent mixing}\end{array}\right)}_{\equiv\,\rho c_p\cdot\varepsilon_h}\frac{\partial\overline{T}}{\partial y}$$

where $\overline{T}$ is the average of the fluctuating temperature. Therefore,

$$q = -\rho c_p \left(\alpha + \varepsilon_h\right) \frac{\partial \overline{T}}{\partial y} \tag{6.88}$$

where ε_h is called the *eddy diffusivity of heat.* This immediately suggests yet another definition:

$$\text{turbulent Prandtl number, } \mathrm{Pr}_t \equiv \frac{\varepsilon_m}{\varepsilon_h} \tag{6.89}$$

Equation (6.88) can be written in terms of ν and ε_m by introducing Pr and Pr_t into it. Thus,

$$\frac{q}{\rho c_p} = -\left(\frac{\nu}{\mathrm{Pr}} + \frac{\varepsilon_m}{\mathrm{Pr}_t}\right) \frac{d\overline{T}}{dy} \tag{6.90}$$

which looks a little like eqn. (6.87) when the latter is written in the form

$$\frac{\tau_{yx}}{\rho} = \left(\nu + \varepsilon_m\right) \frac{d\overline{u}}{dy} \tag{6.91}$$

Notice that the derivatives have been changed from partial to total. This restricts the use of eqns. (6.90) and (6.91), in which $\overline{u}$ and $\overline{T}$ are predominantly y-dependent. This is strictly true only in the so-called *parallel flows*—ones in which all streamlines and isotherms are parallel. Parallel flow exists in pipes, but it is only an approximation in boundary layers.

Before trying to build a form of the Reynolds analogy for turbulent flow, we must note the behavior of Pr and Pr_t:

- Pr is a physical property of the fluid. It is both theoretically and actually near unity for ideal gases, but for liquids it may differ from unity by orders of magnitude.
- Pr_t is a property of the flow field more than of the fluid. The numerical value of Pr_t is normally well within a factor of 2 of unity. It varies with location in the b.l., but it is often near 0.85.

Let us first consider what will happen if $\mathrm{Pr} = \mathrm{Pr}_t = 1$. Then

$$\frac{q}{\rho c} = -\left(\nu + \varepsilon_m\right) \frac{d\overline{T}}{dy} = -\frac{\tau_{yx}}{\rho} \frac{dy}{d\overline{u}} \frac{d\overline{T}}{dy} = -\frac{\tau_{yx}}{\rho} \frac{d\overline{T}}{d\overline{u}}$$

So, at the wall,

$$q_w(x) = -c_p \tau_w(x) \frac{d(\overline{T} - T_w)}{d\overline{u}} \tag{6.92}$$

In laminar flow, for $\mathrm{Pr} = 1$, $(T - T_w)/(T_\infty - T_w) = u/u_\infty$. Therefore, we presume this same fact to be true for turbulent flow when $\mathrm{Pr} = \mathrm{Pr}_t = 1$. Equation (6.92) then becomes

$$q_w(x) = -c_p \tau_w(x) \frac{d}{d\overline{u}} \left[(T_\infty - T_w) \frac{\overline{u}}{u_\infty} \right]$$

or

$$q_w(x) = \frac{k}{\mu} \frac{T_w - T_\infty}{u_\infty} \tau_w(x) \tag{6.93}$$

since $\mathrm{Pr} = \mu c_p/k = 1$. We define $(T_w - T_\infty) \equiv \Delta T$ and rearrange eqn. (6.93) to obtain

$$\frac{q_w(x)}{k\,\Delta T} x = \frac{1}{2} \frac{u_\infty x}{\nu} \frac{\tau_w(x)}{\rho u_\infty^2/2}$$

or

$$\mathrm{Nu}_x = \tfrac{1}{2} \mathrm{Re}_x C_f(x) \tag{6.94}$$

Equation (6.94) is based upon the assumption that $\mathrm{Pr} = \mathrm{Pr}_t = 1$ and upon the notion that the flow is parallel. It is also identical with the corresponding laminar flow equation for heat transfer in a b.l. with $\mathrm{Pr} = 1$. Recall eqns. (6.75) and (6.77), which can be written as

$$\boxed{j = \mathrm{St}_x \mathrm{Pr}^{2/3} = \frac{C_f}{2}} \qquad 0.5 \le \mathrm{Pr} \tag{6.95}$$

This suggests that the same result might also apply to the turbulent b.l. on an isothermal plate when $\mathrm{Pr} \neq 1$. In fact, the result is a bit more complicated for turbulent boundary layers [6.1, §6.10]:

$$\boxed{\mathrm{St}_x = \frac{C_f/2}{1 + 13\left(\mathrm{Pr}^{2/3} - 1\right)\sqrt{C_f/2}}} \qquad 0.7 \le \mathrm{Pr} \tag{6.96}$$

The above formula can be approximated by the Stanton number from eqn. (6.95) for Prandtl numbers not too far from unity. We have noted already that eqn. (6.95) is called the Reynolds-Colburn analogy. Both results are only for smooth walls with little or no pressure gradient.

Predictions of heat transfer in the turbulent boundary layer

The skin friction coefficient, C_f, in this case is no longer the laminar value, $0.664/\sqrt{\mathrm{Re}_x}$. It is, instead, the value appropriate to the turbulent flow in question. For example, Schlichting ([6.2, Chap. XXI]) shows that on a smooth flat plate in the low-Re turbulent b.l. range:

$$C_f = \frac{0.0592}{\mathrm{Re}_x^{1/5}}, \qquad 5 \times 10^5 \leqslant \mathrm{Re}_x \leqslant 10^7 \tag{6.97}$$

In this case eqn. (6.95) becomes

$$\mathrm{St}_x \mathrm{Pr}^{2/3} = \frac{0.0296}{\mathrm{Re}_x^{1/5}}$$

or

$$\mathrm{Nu}_x = 0.0296\, \mathrm{Re}_x^{0.8}\, \mathrm{Pr}^{1/3} \tag{6.98}$$

The Nusselt number based on $\overline{h}$ is obtained from eqn. (6.98) as follows:

$$\overline{\mathrm{Nu}}_L = \frac{L}{k}\overline{h} = \frac{0.0296\ \mathrm{Pr}^{1/3} L}{k}\left[\frac{k}{L}\int_0^L \left(\frac{1}{x}\mathrm{Re}_x^{0.8}\right) dx\right]$$

where we ignore the fact that there is a laminar region at the front of the plate. Thus,

$$\overline{\mathrm{Nu}}_L = 0.0370\, \mathrm{Re}_L^{0.8}\, \mathrm{Pr}^{1/3} \tag{6.99}$$

A flat heater with a turbulent b.l. on it actually has a laminar b.l. between $x = 0$ and $x = x_{\text{transition}}$, as is indicated in Fig. 6.4. The obvious way to calculate $\overline{h}$ in this case is to write

$$\begin{aligned} \overline{h} &= \frac{1}{L\Delta T}\int_0^L q\, dx \\ &= \frac{1}{L}\left[\int_0^{x_{\text{transition}}} h_{\text{laminar}}\, dx + \int_{x_{\text{transition}}}^L h_{\text{turbulent}}\, dx\right] \end{aligned} \tag{6.100}$$

where $x_{\text{transition}} = (\nu/u_\infty)\mathrm{Re}_{\text{transition}}$. Thus, we substitute eqns. (6.58) and (6.98) in eqn. (6.100) and obtain, for $0.6 \leqslant \mathrm{Pr} \leqslant 50$,

$$\boxed{\overline{\mathrm{Nu}}_L = 0.037\ \mathrm{Pr}^{1/3}\left\{\mathrm{Re}_L^{0.8} - \left[\mathrm{Re}_{\text{transition}}^{0.8} - 17.95\ (\mathrm{Re}_{\text{transition}})^{1/2}\right]\right\}} \tag{6.101}$$

If $\mathrm{Re}_L \gg \mathrm{Re}_{\text{transition}}$, this result reduces to eqn. (6.99).

Whitaker [6.8] offers the following correlation for $\overline{\mathrm{Nu}_L}$, which is similar in form to eqn. (6.101):

$$\boxed{\overline{\mathrm{Nu}}_L = 0.036\,\mathrm{Pr}^{0.43}\left(\mathrm{Re}_L^{0.8} - 9200\right)\left(\frac{\mu_\infty}{\mu_w}\right)^{1/4}} \qquad 0.7 \le \mathrm{Pr} \le 400 \tag{6.102}$$

This expression has been corrected to account for the variability of liquid viscosity with the factor $(\mu_\infty/\mu_w)^{1/4}$, where μ_∞ is evaluated at the free stream temperature, T_∞, and μ_w is evaluated at the wall temperature, T_w. If eqn. (6.102) is used to predict heat transfer to a gaseous flow, the viscosity-ratio correction term should not be used. This is because the viscosity of a gas rises with temperature instead of dropping, and the correction will be incorrect. Notice, too, that eqn. (6.102) compares very well with eqn. (6.101) when Pr is on the order of unity, if $\mathrm{Re}_{\text{transition}}$ is only about 200,000.

Finally, it is important to remember that eqns. (6.101) and (6.102) should be used only when Re_L is substantially above the transitional value.

A problem with the preceding relations is that they do not really deal with the question of heat transfer in the rather lengthy transition region. Both eqns. (6.101) and (6.102) are based on the assumption that flow abruptly passes from laminar to turbulent at a critical value of x, and we have noted in the context of Fig. 6.4 that this is not what occurs. The location of the transition depends upon such variables as surface roughness and the turbulence, or lack of it, in the stream approaching the heater. Churchill [6.9] suggests correlating any *particular set* of data with

$$\boxed{\frac{\overline{\mathrm{Nu}}_L - 0.45}{0.6774\,\phi^{1/2}} = \left\{1 + \frac{(\phi/12,500)^{3/5}}{\left[1 + (\phi_{\mathrm{um}}/\phi)^{7/2}\right]^{2/5}}\right\}^{1/2}} \tag{6.103}$$

where

$$\phi \equiv \mathrm{Re}_L \mathrm{Pr}^{2/3}\left[1 + \left(\frac{0.0468}{\mathrm{Pr}}\right)^{2/3}\right]^{-1/2}$$

and ϕ_{um} is a number between about 10^5 and 10^7. The actual value of ϕ_{um} must be fit to the particular set of data. In a very "clean" system, ϕ_{um} will be larger; in a very "noisy" one, it will be smaller.

The advantage of eqn. (6.103) is that, once ϕ_{um} is known, it will predict q_w *through* the transition regime.

Example 6.9

Ammonia at 100°C flows at 15 m/s over a flat surface 1.6 m in length at 200°C. Evaluate $\overline{h}$.

SOLUTION. The properties of NH_3 at $(100 + 200)/2 = 150$°C are $\nu = 2.97 \times 10^{-5}$ m^2/s, $k = 0.0391$ W/m·K, and Pr $= 0.87$. $\text{Re}_L = 1.6(15)/2.97(10)^{-5} = 808,000$, so the flow is turbulent over a part of the surface. Then if we take $\text{Re}_{\text{transition}}$ as 400,000 in eqn. (6.101), we get

$$\begin{aligned}\overline{\text{Nu}}_L &= 0.037(0.87)^{1/3}\left\{(808,000)^{0.8}\right. \\ &\quad \left. - \left[400,000^{0.8} - 17.95(400,000)^{1/2}\right]\right\} = 1209\end{aligned}$$

so

$$\overline{h} = \frac{1209\,k}{L} = \frac{1209(0.0391)}{1.6} = 29.5 \text{ W/m}^2\text{K}$$

Whitaker's eqn. (6.102), on the other hand, gives

$$\overline{\text{Nu}}_L = 0.036(0.87)^{0.43}\left[(808,000)^{0.8} - 9200\right] = 1492$$

where we have deleted the viscosity correction since the NH_3 is gaseous. This gives a 19% higher value of $\overline{h}$.

$$\overline{h} = \frac{1492(0.0391)}{1.6} = 36.5 \text{ W/m}^2\text{K}$$

Finally, using Churchill's formulation, we get $\phi = 7.87 \times 10^5$, so eqn. (6.103) gives $\overline{\text{Nu}}_L = 697$ if ϕ_{um} is 10^7 and 2168 if it is 10^5. These values spread over a factor of three and they embrace the values above. This serves to show how minor system variations can introduce a great deal of uncertainty into a combined laminar–turbulent system. ■

Example 6.10

Compare eqns. (6.101) and (6.102) at high Re_L—say, $\mathrm{Re}_L \geqslant 10^7$.

SOLUTION. Neglecting the viscosity ratio,

$$\frac{\overline{\mathrm{Nu}}_{L_{7.100}}}{\overline{\mathrm{Nu}}_{L_{7.101}}} = \frac{1.03}{\mathrm{Pr}^{0.13}} \left[\frac{1 - \left(\mathrm{Re}_{\mathrm{trans}}^{0.8} - 17.95\sqrt{\mathrm{Re}_{\mathrm{trans}}} \right) \Big/ \mathrm{Re}_L^{0.8}}{1 - 9200/\mathrm{Re}_L^{0.8}} \right]$$

In the worst case, $\mathrm{Re}_{\mathrm{transition}} = 500,000$ and $\mathrm{Re}_L = 10^7$, this reduces to

$$\frac{\overline{\mathrm{Nu}}_{L_{7.100}}}{\overline{\mathrm{Nu}}_{L_{7.101}}} = \frac{1.066}{\mathrm{Pr}^{0.13}}$$

Up to $\mathrm{Pr} \simeq 3$, the disagreement is within $\pm 7\%$. For higher Pr, we should use Whitaker's relation, eqn. (6.102), with its broader Pr dependence. ■

Example 6.11

What is $\overline{\tau}_w$ in Example 6.9?

SOLUTION. From Reynolds's analogy, we obtain

$$\overline{C}_f = 2\overline{\mathrm{St}}_L \, \mathrm{Pr}^{2/3} = \frac{2\overline{\mathrm{Nu}}_L}{\mathrm{Re}_L \, \mathrm{Pr}^{1/3}} = \frac{2(1492)}{808,000(0.87)^{1/3}} = 0.00387$$

Therefore,

$$\overline{\tau_w} = \frac{1}{2}\rho u_\infty^2 \, \overline{C}_f = \frac{0.4934(15)^2}{2}(0.00387) = 0.215 \ \mathrm{N/m^2}$$

(If the plate were 1 m wide, this would be a drag force of 0.344 N, or 1.2 oz.) ■

A word about the analysis of turbulent boundary layers

The preceding discussion has circumvented serious *analysis* of heat transfer in turbulent flows. Sophisticated methods of analysis are beyond the scope of this book. In the past, boundary layer heat transfer has been analyzed in many flows (with and without pressure gradients, dp/dx) using integral methods. However, in recent decades, computational techniques have largely supplanted these techniques. In boundary layer situations,

various methods based on turbulent kinetic energy and dissipation, so-called k-ε methods, are widely-used and have been implemented in a variety of commercial fluid-dynamics codes. These methods are described in the technical literature and in monographs on turbulence [6.10, 6.11].

We have found our way around analysis by presenting some correlations for common situations. In the next chapter, we deal with more complicated configurations than the simple plane surface. A few of these configurations will be amenable to a level of analysis appropriate to a first course, but for others we shall only be able to present the best data correlations available.

Problems

6.1 Verify that eqn. (6.13) follows from eqns. (6.11) and (6.12).

6.2 The student with some analytical ability (or some assistance from the instructor) should complete the algebra between eqns. (6.16) and (6.20).

6.3 Use a computer to solve eqn. (6.18) subject to b.c.'s (6.20). To do this you need all three b.c.'s at $\eta = 0$, but one is presently at $\eta = \infty$. There are three ways to get around this:

- Start out by guessing a value of $\partial f'/\partial\eta$ at $\eta = 0$—say, $\partial f'/\partial\eta = 1$. When η is large—say, 6 or 10—$\partial f'/\partial\eta$ will asymptotically approach a constant. If the constant > 1, go back and guess a lower value of $\partial f'/\partial\eta$, or vice versa, until the constant converges on unity. (There are many ways to automate the successive guesses.)
- The correct value of $df'/d\eta$ is approximately 0.33206 at $\eta = 0$. You might cheat and begin with it.
- There exists a clever way to map $df/d\eta = 1$ at $\eta = \infty$ back into the origin. (Consult your instructor.)

6.4 Verify that the Blasius solution (Table 6.1) satisfies eqn. (6.25). To do this, carry out the required integration.

6.5 Verify eqn. (6.30).

6.6 Obtain the counterpart of eqn. (6.32) based on the velocity profile given by the integral method.

6.7 Assume a laminar b.l. velocity profile of the simple form $u/u_\infty = y/\delta$ and calculate δ and C_f on the basis of this very rough estimate, using the momentum integral method. How accurate is each? [C_f is about 13% low.]

6.8 In a certain flow of water at 40°C over a flat plate $\delta = 0.005\sqrt{x}$, for δ and x measured in meters. Plot *to scale* on a common graph (with an appropriately expanded y-scale):

- δ and δ_t for the water.
- δ and δ_t for air at the same temperature and velocity.

6.9 A thin film of liquid with a constant thickness, δ_0, falls down a vertical plate. It has reached its terminal velocity so that viscous shear and weight are in balance and the flow is steady. The b.l. equation for such a flow is the same as eqn. (6.13), except that it has a gravity force in it. Thus,

$$u\frac{\partial u}{\partial x} + v\frac{\partial u}{\partial y} = -\frac{1}{\rho}\frac{dp}{dx} + g + \nu\frac{\partial^2 u}{\partial y^2}$$

where x increases in the downward direction and y is normal to the wall. Assume that the surrounding air density $\simeq 0$, so there is no hydrostatic pressure gradient in the surrounding air. Then:

- Simplify the equation to describe this situation.
- Write the b.c.'s for the equation, neglecting any air drag on the film.
- Solve for the velocity distribution in the film, assuming that you know δ_0 (cf. Chap. 8).

(This solution is the starting point in the study of many process heat and mass transfer problems.)

6.10 Develop an equation for $\overline{\mathrm{Nu}}_L$ that is valid over the entire range of Pr for a laminar b.l. over a flat, isothermal surface.

6.11 Use an integral method to develop a prediction of Nu_x for a laminar b.l. over a uniform heat flux surface. Compare your result with eqn. (6.71). What is the temperature difference at the leading edge of the surface?

6.12 Verify eqn. (6.101).

6.13 It is known from flow measurements that the transition to turbulence occurs when the Reynolds number based on mean velocity and diameter exceeds 4000 in a certain pipe. Use the fact that the laminar boundary layer on a flat plate grows according to the relation

$$\frac{\delta}{x} = 4.92\sqrt{\frac{\nu}{u_{\max} x}}$$

to find an equivalent value for the Reynolds number of transition based on distance from the leading edge of the plate and $u_{\max}$. (Note that $u_{\max} = 2\overline{u}_{\text{av}}$ during laminar flow in a pipe.)

6.14 Execute the differentiation in eqn. (6.24) with the help of Leibnitz's rule for the differentiation of an integral and show that the equation preceding it results.

6.15 Liquid at 23°C flows at 2 m/s over a smooth, sharp-edged, flat surface 12 cm in length which is kept at 57°C. Calculate h at the trailing edge (a) if the fluid is water; (b) if the fluid is glycerin ($h = 346$ W/m^{2}K). (c) Compare the drag forces in the two cases. [There is 23.4 times as much drag in the glycerin.]

6.16 Air at −10°C flows over a smooth, sharp-edged, almost-flat, aerodynamic surface at 240 km/hr. The surface is at 10°C. Find (a) the approximate location of the laminar turbulent transition; (b) the overall $\overline{h}$ for a 2 m chord; (c) h at the trailing edge for a 2 m chord; (d) δ and h at the beginning of the transition region. [$\delta_{x_t} = 0.54$ mm.]

6.17 Find $\overline{h}$ in Example 6.9 using eqn. (6.103) with $\phi_{\text{um}} = 10^7$ and 10^6. Discuss the result.

6.18 Suppose that you had one data point with which to fix ϕ_{um} in Churchill's equation for $\overline{\text{Nu}}_L$ on a flat plate. This value is $\overline{h} = 32$ W/m^{2}K in the system in Example 6.9. Evaluate ϕ_{um} and then use eqn. (6.103) to predict $\overline{h}$ if u_∞ is increased to 21 m/s.

6.19 Mercury at 25°C flows at 0.7 m/s over a 4 cm-long flat heater at 60°C. Find $\overline{h}$, $\overline{\tau}_w$, $h(x = 0.04\text{ m})$, and $\delta(x = 0.04\text{ m})$.

6.20 A large plate is at rest in water at 15°C. The plate is suddenly translated parallel to itself, at 1.5 m/s. The resulting fluid movement is not exactly like that in a b.l. because the velocity profile builds up uniformly, all over, instead of from an edge. The governing transient momentum equation, $Du/Dt = \nu(\partial^2 u/\partial y^2)$, takes the form

$$\frac{1}{\nu}\frac{\partial u}{\partial t} = \frac{\partial^2 u}{\partial y^2}$$

Determine u at 0.015 m from the plate for $t = 1$, 10, and 1000 s. Do this by first posing the problem fully and then comparing it with the solution in Section 5.6. [$u \simeq 0.003$ m/s after 10 s.]

6.21 Notice that, when Pr is large, the velocity b.l. on an isothermal, flat heater is much larger than δ_t. The small part of the velocity b.l. inside the thermal b.l. is approximately $u/u_\infty = \frac{3}{2}y/\delta = \frac{3}{2}\phi(y/\delta_t)$. Derive Nu_x for this case based on this velocity profile.

6.22 Plot the ratio of $h(x)_{\text{laminar}}$ to $h(x)_{\text{turbulent}}$ against Re_x in the range of Re_x that might be either laminar or turbulent. What does the plot suggest about heat transfer design?

6.23 Water at 7°C flows at 0.38 m/s across the top of a 0.207 m-long, thin copper plate. Methanol at 87°C flows across the bottom of the same plate, at the same speed but in the opposite direction. Make the obvious first guess as to the temperature at which to evaluate physical properties. Then plot the plate temperature as a function of position. (Do not bother to correct the physical properties in this problem, but note Problem 6.24.)

6.24 Work Problem 6.23 taking full account of property variations.

6.25 If the wall temperature in Example 6.6 (with a uniform $q_w = 420$ W/m^2) were instead fixed at its average value of 76°C, what would the *average* wall heat flux be?

6.26 A cold, 20 mph westerly wind at 20°F cools a rectangular building, 35 ft by 35 ft by 22 ft high, with a flat roof. The outer walls are at 27°F. Find the heat loss, conservatively assuming that the east and west faces have the same $\overline{h}$ as the north, south, and top faces. Estimate U for the walls.

6.27 A 2 ft-square slab of mild steel leaves a forging operation 0.25 in. thick at 1000°C. It is laid flat on an insulating bed and 27°C air is blown over it at 30 m/s. How long will it take to cool to 200°C. (State your assumptions about property evaluation.)

6.28 Do Problem 6.27 numerically, recalculating properties at successive points. If you did Problem 6.27, compare results.

6.29 Plot q against x for the situation described in Example 6.9.

6.30 Consider the plate in Example 6.9. Suppose that instead of specifying $T_w = 200°C$, we specified $q_w = 3650\ \text{W/m}^2$. Plot T_w against x for this case.

6.31 A thin metal sheet separates air at 44°C, flowing at 48 m/s, from water at 4°C, flowing at 0.2 m/s. Both fluids start at a leading edge and move in the same direction. Plot T_{plate} and q as a function of x up to $x = 0.1$ m.

6.32 A mixture of 60% glycerin and 40% water flows over a 1-m-long flat plate. The glycerin is at 20°C and the plate is at 40°. A thermocouple 1 mm above the trailing edge records 35°C. What is u_∞, and what is u at the thermocouple?

6.33 What is the maximum $\overline{h}$ that can be achieved in laminar flow over a 5 m plate, based on data from Table A.3? What physical circumstances give this result?

6.34 A 17°C sheet of water, Δ_1 m thick and moving at a constant speed u_∞ m/s, impacts a horizontal plate at 45°, turns, and flows along it. Develop a dimensionless equation for the thickness Δ_2 at a distance L from the point of impact. Assume that $\delta \ll \Delta_2$. Evaluate the result for $u_\infty = 1$ m/s, $\Delta_1 = 0.01$ m, and $L = 0.1$ m, in water at 27°C.

6.35 A good approximation to the temperature dependence of μ in gases is given by the Sutherland formula:

$$\frac{\mu}{\mu_{\text{ref}}} = \left(\frac{T}{T_{\text{ref}}}\right)^{1.5} \frac{T_{\text{ref}} + S}{T + S},$$

where the reference state can be chosen anywhere. Use data for air at two points to evaluate S for air. Use this value to predict a third point. (T and T_{ref} are expressed in °K.)

6.36 We have derived a steady-state continuity equation in Section 6.3. Now derive the time-dependent, compressible, three-dimensional version of the equation:

$$\frac{\partial \rho}{\partial t} + \nabla \cdot (\rho \vec{u}) = 0$$

To do this, paraphrase the development of equation (2.10), requiring that mass be conserved instead of energy.

6.37 Various considerations show that the smallest-scale motions in a turbulent flow have no preferred spatial orientation at large enough values of Re. Moreover, these small eddies are responsible for most of the viscous dissipation of kinetic energy. The dissipation rate, ε(W/kg), may be regarded as given information about the small-scale motion, since it is set by the larger-scale motion. Both ε and ν are governing parameters of the small-scale motion.

a. Find the characteristic length and velocity scales of the small-scale motion. These are called the *Kolmogorov scales* of the flow.

b. Compute Re for the small-scale motion and interpret the result.

c. The Kolmogorov length scale characterizes the smallest motions found in a turbulent flow. If ε is 10 W/kg and the mean free path is 7×10^{-8} m, show that turbulent motion is a continuum phenomenon and thus is properly governed by the equations of this chapter.

d. The temperature outside is 35°F, but with the wind chill it's −15°F. And you forgot your hat. If you go outdoors for long, are you in danger of freezing your ears?

References

[6.1] F.M. White. *Viscous Fluid Flow*. McGraw-Hill, Inc., New York, 2nd edition, 1991. Excellent development of fundamental results for boundary layers and internal flows.

[6.2] H. Schlichting. *Boundary-Layer Theory*. (trans. J. Kestin). McGraw-Hill Book Company, New York, 6th edition, 1968.

[6.3] C. L. Tien and J. H. Lienhard. *Statistical Thermodynamics*. Hemisphere Publishing Corp., Washington, D.C., rev. edition, 1978.

[6.4] S. W. Churchill and H. Ozoe. Correlations for laminar forced convection in flow over an isothermal flat plate and in developing and fully developed flow in an isothermal tube. *J. Heat Trans., Trans. ASME, Ser. C*, 95:78, 1973.

[6.5] W. M. Kays and M. E. Crawford. *Convective Heat and Mass Transfer*. McGraw-Hill Book Company, New York, 3rd edition, 1993. Coverage is mainly of boundary layers and internal flows.

[6.6] O. Reynolds. On the extent and action of the heating surface for steam boilers. *Proc. Manchester Lit. Phil. Soc.*, 14:7–12, 1874.

[6.7] J. Boussinesq. Théorie de l'écoulement tourbillant. *Mem. Pres. Acad. Sci.,* (Paris), 23:46, 1877.

[6.8] S. Whitaker. Forced convection heat transfer correlation for flow in pipes past flat plates, single cylinders, single spheres, and for flow in packed beds and tube bundles. *AIChE J.*, 18:361, 1972.

[6.9] S. W. Churchill. A comprehensive correlating equation for forced convection from flat plates. *AIChE J.*, 22:264–268, 1976.

[6.10] S. B. Pope. *Turbulent Flows*. Cambridge University Press, Cambridge, 2000.

[6.11] P. A. Libby. *Introduction to Turbulence*. Taylor & Francis, Washington D.C., 1996.

7. Forced convection in a variety of configurations

The bed was soft enough to suit me...But I soon found that there came such a draught of cold air over me from the sill of the window that this plan would never do at all, especially as another current from the rickety door met the one from the window and both together formed a series of small whirlwinds in the immediate vicinity of the spot where I had thought to spend the night. ***Moby Dick*, H. Melville**

7.1 Introduction

Consider for a moment the fluid flow pattern within a shell-and-tube heat exchanger, such as that shown in Fig. 3.5. The shell-pass flow moves up and down across the tube bundle from one baffle to the next. The flow around each pipe is determined by the complexities of the one before it, and the direction of the mean flow relative to each pipe can vary. Yet the problem of determining the heat transfer in this situation, however difficult it appears to be, is a task that must be undertaken.

The flow within the tubes of the exchanger is somewhat more tractable, but it, too, brings with it several problems that do not arise in the flow of fluids over a flat surface. Heat exchangers thus present a kind of microcosm of internal and external forced convection problems. Other such problems arise everywhere that energy is delivered, controlled, utilized, or produced. They arise in the complex flow of water through nuclear heating elements or in the liquid heating tubes of a solar collector—in the flow of a cryogenic liquid coolant in certain digital computers or in the circulation of refrigerant in the spacesuit of a lunar astronaut.

We dealt with the simple configuration of flow over a flat surface in

Chapter 6. This situation has considerable importance in its own right, and it also reveals a number of analytical methods that apply to other configurations. Now we wish to undertake a sequence of progressively harder problems of forced convection heat transfer in more complicated flow configurations.

Incompressible forced convection heat transfer problems normally admit an extremely important simplification: the fluid flow problem can be solved without reference to the temperature distribution in the fluid. Thus, we can first find the velocity distribution and then put it in the energy equation as known information and solve for the temperature distribution. Two things can impede this procedure, however:

- If the fluid properties (especially μ and ρ) vary significantly with temperature, we cannot predict the velocity without knowing the temperature, and vice versa. The problems of predicting velocity and temperature become intertwined and harder to solve. We encounter such a situation later in the study of natural convection, where the fluid is driven by thermally induced density changes.

- Either the fluid flow solution or the temperature solution can, itself, become prohibitively hard to find. When that happens, we resort to the correlation of experimental data with the help of dimensional analysis.

Our aim in this chapter is to present the analysis of a few simple problems and to show the progression toward increasingly empirical solutions as the problems become progressively more unwieldy. We begin this undertaking with one of the simplest problems: that of predicting laminar convection in a pipe.

7.2 Heat transfer to and from laminar flows in pipes

Not many industrial pipe flows are laminar, but laminar heating and cooling does occur in an increasing variety of modern instruments and equipment: micro-electro-mechanical systems (MEMS), laser coolant lines, and many compact heat exchangers, for example. As in any forced convection problem, we first describe the flow field. This description will include a number of ideas that apply to turbulent as well as laminar flow.

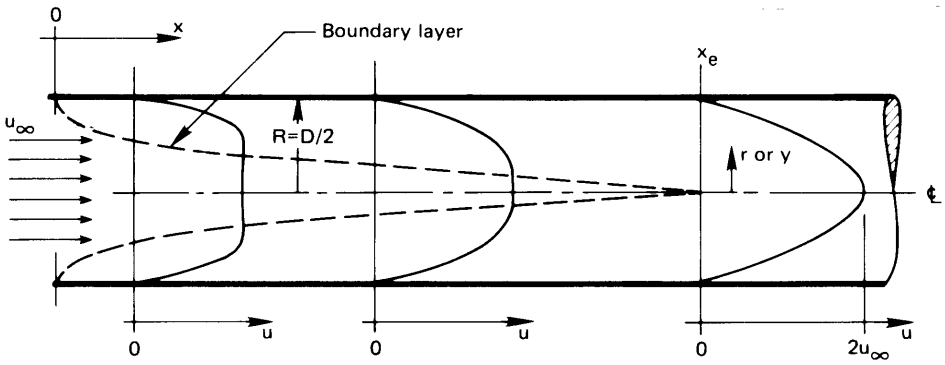

Figure 7.1 The development of a laminar velocity profile in a pipe.

Development of a laminar flow

Figure 7.1 shows the evolution of a laminar velocity profile from the entrance of a pipe. Throughout the length of the pipe, the mass flow rate, $\dot{m}$ (kg/s), is constant, of course, and the *average*, or *bulk*, velocity u_{av} is also constant:

$$\dot{m} = \int_{A_c} \rho u \, dA_c = \rho u_{\text{av}} A_c \tag{7.1}$$

where A_c is the cross-sectional area of the pipe. The velocity profile, on the other hand, changes greatly near the inlet to the pipe. A b.l. builds up from the front, generally accelerating the otherwise undisturbed core. The b.l. eventually occupies the entire flow area and defines a velocity profile that changes very little thereafter. We call such a flow *fully developed*. A flow is fully developed from the hydrodynamic standpoint when

$$\frac{\partial u}{\partial x} = 0 \quad \text{or} \quad v = 0 \tag{7.2}$$

at each radial location in the cross section. An attribute of a dynamically fully developed flow is that the streamlines are all parallel to one another.

The concept of a fully developed flow, from the thermal standpoint, is a little more complicated. We must first understand the notion of the *mixing-cup*, or *bulk*, enthalpy and temperature, $\hat{h}_b$ and T_b. The enthalpy is of interest because we use it in writing the First Law of Thermodynamics when calculating the inflow of thermal energy and flow work to open control volumes. The bulk enthalpy is an average enthalpy for the fluid

flowing through a cross section of the pipe:

$$\dot{m}\,\hat{h}_b \equiv \int_{A_c} \rho u \hat{h}\, dA_c \tag{7.3}$$

If we assume that fluid pressure variations in the pipe are too small to affect the thermodynamic state much (see Sect. 6.3) and if we assume a constant value of c_p, then $\hat{h} = c_p(T - T_{\text{ref}})$ and

$$\dot{m}\, c_p\, (T_b - T_{\text{ref}}) = \int_{A_c} \rho c_p u\, (T - T_{\text{ref}})\; dA_c \tag{7.4}$$

or simply

$$T_b = \frac{\displaystyle\int_{A_c} \rho c_p u T\, dA_c}{\dot{m} c_p} \tag{7.5}$$

In words, then,

$$T_b \equiv \frac{\text{rate of flow of enthalpy through a cross section}}{\text{rate of flow of heat capacity through a cross section}}$$

Thus, if the pipe were broken at any x-station and allowed to discharge into a mixing cup, the enthalpy of the mixed fluid in the cup would equal the average enthalpy of the fluid flowing through the cross section, and the temperature of the fluid in the cup would be T_b. This definition of T_b is perfectly general and applies to either laminar or turbulent flow. For a circular pipe, with $dA_c = 2\pi r\, dr$, eqn. (7.5) becomes

$$T_b = \frac{\displaystyle\int_0^R \rho c_p u T\, 2\pi r\, dr}{\displaystyle\int_0^R \rho c_p u\, 2\pi r\, dr} \tag{7.6}$$

A fully developed flow, from the thermal standpoint, is one for which the relative shape of the temperature profile does not change with x. We state this mathematically as

$$\frac{\partial}{\partial x}\left(\frac{T_w - T}{T_w - T_b}\right) = 0 \tag{7.7}$$

where T generally depends on x and r. This means that the profile can be scaled up or down with $T_w - T_b$. Of course, a flow must be hydrodynamically developed if it is to be thermally developed.

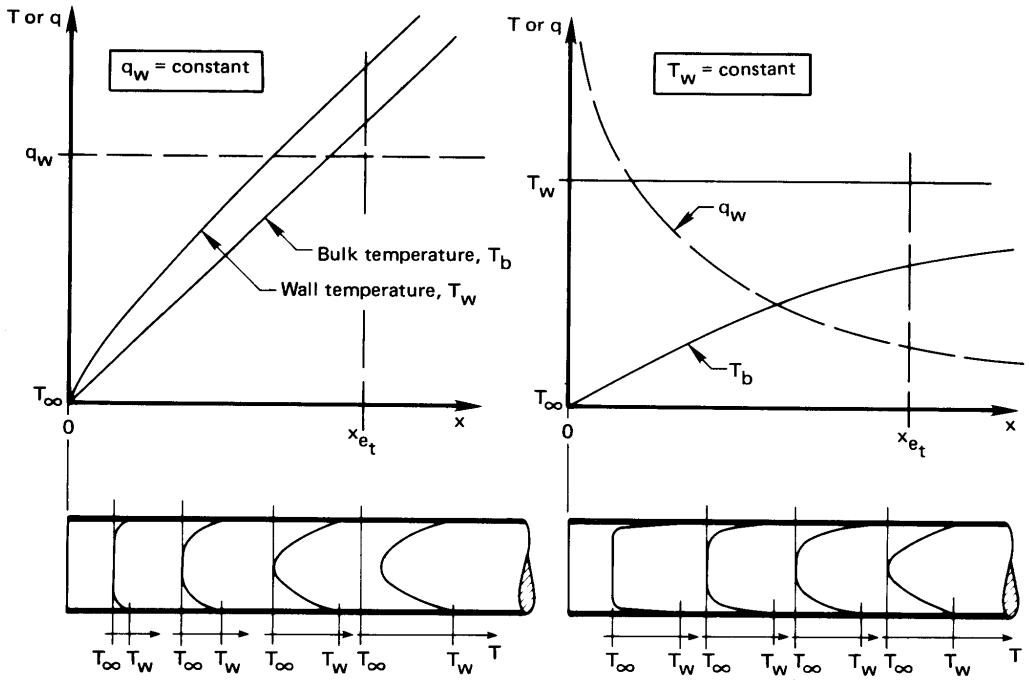

Figure 7.2 The thermal development of flows in tubes with a uniform wall heat flux and with a uniform wall temperature (the *entrance region*).

Figures 7.2 and 7.3 show the development of two flows and their subsequent behavior. The two flows are subjected to either a uniform wall heat flux or a uniform wall temperature. In Fig. 7.2 we see each flow develop until its temperature profile achieves a shape which, except for a linear stretching, it will retain thereafter. If we consider a small length of pipe, dx long with perimeter P, then its surface area is $P\,dx$ (e.g., $2\pi R\,dx$ for a circular pipe) and an energy balance on it is[1]

$$dQ = q_w P dx = \dot{m} d\hat{h}_b \tag{7.8}$$

$$= \dot{m} c_p\, dT_b \tag{7.9}$$

so that

$$\frac{dT_b}{dx} = \frac{q_w P}{\dot{m} c_p} \tag{7.10}$$

[1]Here we make the same approximations as were made in deriving the energy equation in Sect. 6.3.

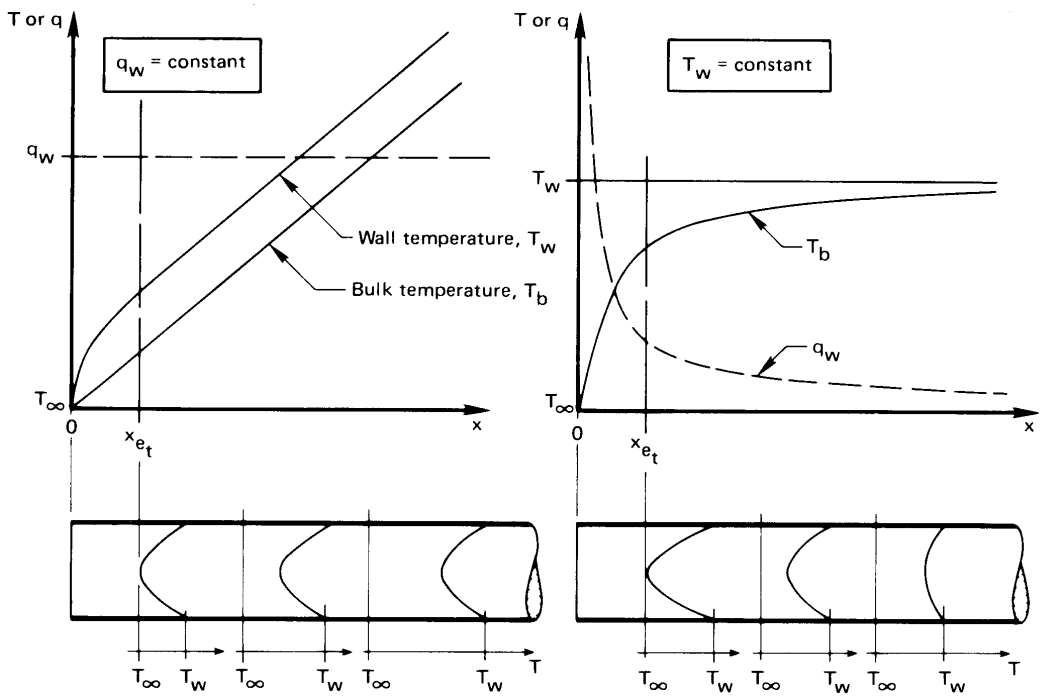

Figure 7.3 The thermal behavior of flows in tubes with a uniform wall heat flux and with a uniform temperature (the *thermally developed region*).

This result is also valid for the bulk temperature in a turbulent flow.

In Fig. 7.3 we see the fully developed variation of the temperature profile. If the flow is fully developed, the boundary layers are no longer growing thicker, and we expect that h will become constant. When q_w is constant, then $T_w - T_b$ will be constant in fully developed flow, so that the temperature profile will retain the same shape while the temperature rises at a constant rate at all values of r. Thus, at any radial position,

$$\frac{\partial T}{\partial x} = \frac{dT_b}{dx} = \frac{q_w P}{\dot{m} c_p} = \text{constant} \tag{7.11}$$

In the uniform wall temperature case, the temperature profile keeps the same shape, but its amplitude decreases with x, as does q_w. The lower right-hand corner of Fig. 7.3 has been drawn to conform with this requirement, as expressed in eqn. (7.7).

The velocity profile in laminar tube flows

The Buckingham pi-theorem tells us that if the hydrodynamic *entry length*, x_e, required to establish a fully developed velocity profile depends on u_{av}, μ, ρ, and D in three dimensions (kg, m, and s), then we expect to find two pi-groups:

$$\frac{x_e}{D} = \text{fn}\,(\text{Re}_D)$$

where $\text{Re}_D \equiv u_{\text{av}} D/\nu$. The matter of entry length is discussed by White [7.1, Chap. 4], who quotes

$$\frac{x_e}{D} \simeq 0.03\ \text{Re}_D \tag{7.12}$$

The constant, 0.03, guarantees that the laminar shear stress on the pipe wall will be within 5% of the value for fully developed flow when $x > x_e$. The number 0.05 can be used, instead, if a deviation of just 1.4% is desired. The thermal entry length, x_{e_t}, turns out to be different from x_e. We deal with it shortly.

The hydrodynamic entry length for a pipe carrying fluid at speeds near the transitional Reynolds number (2100) will extend beyond 100 diameters. Since heat transfer in pipes shorter than this is very often important, we will eventually have to deal with the entry region.

The velocity profile for a fully developed laminar incompressible pipe flow can be derived from the momentum equation for an axisymmetric flow. It turns out that the b.l. assumptions all happen to be valid for a fully developed pipe flow:

- The pressure is constant across any section.
- $\partial^2 u/\partial x^2$ is exactly zero.
- The radial velocity is not just small, but it is zero.
- The term $\partial u/\partial x$ is not just small, but it is zero.

The boundary layer equation for cylindrically symmetrical flows is quite similar to that for a flat surface, eqn. (6.13):

$$u\frac{\partial u}{\partial x} + v\frac{\partial u}{\partial r} = -\frac{1}{\rho}\frac{dp}{dx} + \frac{\nu}{r}\frac{\partial}{\partial r}\left(r\frac{\partial u}{\partial r}\right) \tag{7.13}$$

For fully developed flows, we go beyond the b.l. assumptions and set v and $\partial u/\partial x$ equal to zero as well, so eqn. (7.13) becomes

$$\frac{1}{r}\frac{d}{dr}\left(r\frac{du}{dr}\right) = \frac{1}{\mu}\frac{dp}{dx}$$

We integrate this twice and get

$$u = \left(\frac{1}{4\mu}\frac{dp}{dx}\right)r^2 + C_1 \ln r + C_2$$

The two b.c.'s on u express the no-slip (or zero-velocity) condition at the wall and the fact that u must be symmetrical in r:

$$u(r = R) = 0 \quad \text{and} \quad \left.\frac{du}{dr}\right|_{r=0} = 0$$

They give $C_1 = 0$ and $C_2 = (-dp/dx)R^2/4\mu$, so

$$u = \frac{R^2}{4\mu}\left(-\frac{dp}{dx}\right)\left[1 - \left(\frac{r}{R}\right)^2\right] \tag{7.14}$$

This is the familiar Hagen-Poiseuille[2] parabolic velocity profile. We can identify the lead constant $(-dp/dx)R^2/4\mu$ as the maximum centerline velocity, $u_{\max}$. In accordance with the conservation of mass (see Problem 7.1), $2u_{\text{av}} = u_{\max}$, so

$$\frac{u}{u_{\text{av}}} = 2\left[1 - \left(\frac{r}{R}\right)^2\right] \tag{7.15}$$

Thermal behavior of a flow with a uniform heat flux at the wall

The b.l. energy equation for a fully developed laminar incompressible flow, eqn. (6.40), takes the following simple form in a pipe flow where the radial velocity is equal to zero:

$$u\frac{\partial T}{\partial x} = \alpha\frac{1}{r}\frac{\partial}{\partial r}\left(r\frac{\partial T}{\partial r}\right) \tag{7.16}$$

[2]The German scientist G. Hagen showed experimentally how u varied with r, dp/dx, μ, and R, in 1839. J. Poiseuille (pronounced Pwa-zói or, more precisely, Pwä-zóē) did the same thing, almost simultaneously (1840), in France. Poiseuille was a physician interested in blood flow, and we find today that if medical students know nothing else about fluid flow, they know "Poiseuille's law."

For a fully developed flow with q_w = constant, T_w and T_b increase linearly with x. In particular, by integrating eqn. (7.10), we find

$$T_b(x) - T_{b_{\text{in}}} = \int_0^x \frac{q_w P}{\dot{m} c_p}\, dx = \frac{q_w P x}{\dot{m} c_p} \tag{7.17}$$

Then, from eqns. (7.11) and (7.1), we get

$$\frac{\partial T}{\partial x} = \frac{dT_b}{dx} = \frac{q_w P}{\dot{m} c_p} = \frac{q_w (2\pi R)}{\rho c_p u_{\text{av}} (\pi R^2)} = \frac{2 q_w \alpha}{u_{\text{av}} R k}$$

Using this result and eqn. (7.15) in eqn. (7.16), we obtain

$$4\left[1 - \left(\frac{r}{R}\right)^2\right] \frac{q_w}{Rk} = \frac{1}{r}\frac{d}{dr}\left(r\frac{dT}{dr}\right) \tag{7.18}$$

This ordinary d.e. in r can be integrated twice to obtain

$$T = \frac{4 q_w}{Rk}\left(\frac{r^2}{4} - \frac{r^4}{16R^2}\right) + C_1 \ln r + C_2 \tag{7.19}$$

The first b.c. on this equation is the symmetry condition, $\partial T/\partial r = 0$ at $r = 0$, and it gives $C_1 = 0$. The second b.c. is the definition of the mixing-cup temperature, eqn. (7.6). Substituting eqn. (7.19) with $C_1 = 0$ into eqn. (7.6) and carrying out the indicated integrations, we get

$$C_2 = T_b - \frac{7}{24}\frac{q_w R}{k}$$

so

$$T - T_b = \frac{q_w R}{k}\left[\left(\frac{r}{R}\right)^2 - \frac{1}{4}\left(\frac{r}{R}\right)^4 - \frac{7}{24}\right] \tag{7.20}$$

and at $r = R$, eqn. (7.20) gives

$$T_w - T_b = \frac{11}{24}\frac{q_w R}{k} = \frac{11}{48}\frac{q_w D}{k} \tag{7.21}$$

so the local Nu_D for fully developed flow, based on $h(x) = q_w/[T_w(x) - T_b(x)]$, is

$$\text{Nu}_D \equiv \frac{q_w D}{(T_w - T_b)k} = \frac{48}{11} = 4.364 \tag{7.22}$$

Equation (7.22) is surprisingly simple. Indeed, the fact that there is only one dimensionless group in it is predictable by dimensional analysis. In this case the dimensional functional equation is merely

$$h = \text{fn}\,(D, k)$$

We exclude ΔT, because h should be independent of ΔT in forced convection; μ, because the flow is parallel regardless of the viscosity; and ρu_{av}^2, because there is no influence of momentum in a laminar incompressible flow that never changes direction. This gives three variables, effectively in only two dimensions, W/K and m, resulting in just one dimensionless group, Nu_D, which must therefore be a constant.

Example 7.1

Water at 20°C flows through a small-bore tube 1 mm in diameter at a uniform speed of 0.2 m/s. The flow is fully developed at a point beyond which a constant heat flux of 6000 W/m^2 is imposed. How much farther down the tube will the water reach 74°C at its hottest point?

Solution. As a fairly rough approximation, we evaluate properties at $(74 + 20)/2 = 47$°C: $k = 0.6367$ W/m·K, $\alpha = 1.541 \times 10^{-7}$, and $\nu = 0.556 \times 10^{-6}$ m^2/s. Therefore, $\text{Re}_D = (0.001\text{ m})(0.2\text{ m/s})/0.556 \times 10^{-6}$ m^2/s $= 360$, and the flow is laminar. Then, noting that T is greatest at the wall and setting $x = L$ at the point where $T_{\text{wall}} = 74$°C, eqn. (7.17) gives:

$$T_b(x = L) = 20 + \frac{q_w P}{\dot{m} c_p} L = 20 + \frac{4 q_w \alpha}{u_{\text{av}} D k} L$$

And eqn. (7.21) gives

$$74 = T_b(x = L) + \frac{11}{48}\frac{q_w D}{k} = 20 + \frac{4 q_w \alpha}{u_{\text{av}} D k} L + \frac{11}{48}\frac{q_w D}{k}$$

so

$$\frac{L}{D} = \left(54 - \frac{11}{48}\frac{q_w D}{k}\right)\frac{u_{\text{av}} k}{4 q_w \alpha}$$

or

$$\frac{L}{D} = \left[54 - \frac{11}{48}\frac{6000(0.001)}{0.6367}\right]\frac{0.2(0.6367)}{4(6000)1.541(10)^{-7}} = 1785$$

so the wall temperature reaches the limiting temperature of 74°C at

$$L = 1785(0.001 \text{ m}) = 1.785 \text{ m}$$

While we did not evaluate the thermal entry length here, it may be shown to be much, much less than 1785 diameters. ■

In the preceding example, the heat transfer coefficient is actually rather large

$$h = \text{Nu}_D \frac{k}{D} = 4.364 \frac{0.6367}{0.001} = 2,778 \text{ W/m}^2\text{K}$$

The high h is a direct result of the small tube diameter, which limits the thermal boundary layer to a small thickness and keeps the thermal resistance low. This trend leads directly to the notion of a *microchannel heat exchanger*. Using small scale fabrication technologies, such as have been developed in the semiconductor industry, it is possible to create channels whose characteristic diameter is in the range of 100 μm, resulting in heat transfer coefficients in the range of 10^4 W/m^{2}Kfor water. If, instead, liquid sodium ($k \approx 80$ W/m·K) is used as the working fluid, the laminar flow heat transfer coefficient is on the order of 10^6 W/m^{2}K— a range that is usually associated with boiling processes!

Thermal behavior of the flow in an isothermal pipe

The dimensional analysis that showed Nu_D = constant for flow with a uniform heat flux at the wall is unchanged when the pipe wall is isothermal. Thus, Nu_D should still be constant. But this time (see, e.g., [7.2, Chap. 8]) the constant changes to

$$\text{Nu}_D = 3.657, \qquad T_w = \text{constant} \tag{7.23}$$

for fully developed flow. The behavior of the bulk temperature is discussed in Sect. 7.4.

The thermal entrance region

The thermal entrance region is of great importance in laminar flow because the thermally undeveloped region becomes extremely long for higher-Pr fluids. The entry-length equation (7.12) takes the following form for

the thermal entry region[3], where the velocity profile is assumed to be fully developed before heat transfer starts at $x = 0$:

$$\frac{x_{e_t}}{D} \simeq 0.034\ \mathrm{Re}_D \mathrm{Pr} \tag{7.24}$$

Thus, the thermal entry length for the flow of cold water ($\mathrm{Pr} \simeq 10$) can be over 600 diameters in length near the transitional Reynolds number, and oil flows (Pr on the order of 10^4) practically never achieve fully developed temperature profiles.

A complete analysis of the heat transfer rate in the thermal entry region becomes quite complicated. The reader interested in details should look at [7.2, Chap. 8]. Dimensional analysis of the entry problem shows that the local value of h depends on u_{av}, μ, ρ, D, c_p, k, and x—eight variables in m, s, kg, and J/K. This means that we should anticipate four pi-groups:

$$\mathrm{Nu}_D = \mathrm{fn}\,(\mathrm{Re}_D, \mathrm{Pr}, x/D) \tag{7.25}$$

In other words, to the already familiar Nu_D, Re_D, and Pr, we add a new length parameter, x/D. The solution of the constant wall temperature problem, originally formulated by Graetz in 1885 [7.5] and solved in convenient form by Sellars, Tribus, and Klein in 1956 [7.6], includes an arrangement of these dimensionless groups, called the Graetz number:

$$\text{Graetz number, Gz} \equiv \frac{\mathrm{Re}_D \mathrm{Pr}\, D}{x} \tag{7.26}$$

Figure 7.4 shows values of $\mathrm{Nu}_D \equiv hD/k$ for both the uniform wall temperature and uniform wall heat flux cases. The independent variable in the figure is a dimensionless length equal to $2/\mathrm{Gz}$. The figure also presents an average Nusselt number, $\overline{\mathrm{Nu}}_D$ for the isothermal wall case:

$$\overline{\mathrm{Nu}}_D \equiv \frac{\overline{h}D}{k} = \frac{D}{k}\left(\frac{1}{L}\int_0^L h\,dx\right) = \frac{1}{L}\int_0^L \mathrm{Nu}_D\,dx \tag{7.27}$$

[3]The Nusselt number will be within 5% of the fully developed value if $x_{e_t} \geqslant 0.034\ \mathrm{Re}_D \mathrm{Pr} D$ for T_w = constant. The error decreases to 1.4% if the coefficient is raised from 0.034 to 0.05 [Compare this with eqn. (7.12) and its context.]. For other situations, the coefficient changes. With q_w = constant, it is 0.043 at a 5% error level; when the velocity and temperature profiles develop simultaneously, the coefficient ranges between about 0.028 and 0.053 depending upon the Prandtl number and the wall boundary condition [7.3, 7.4].

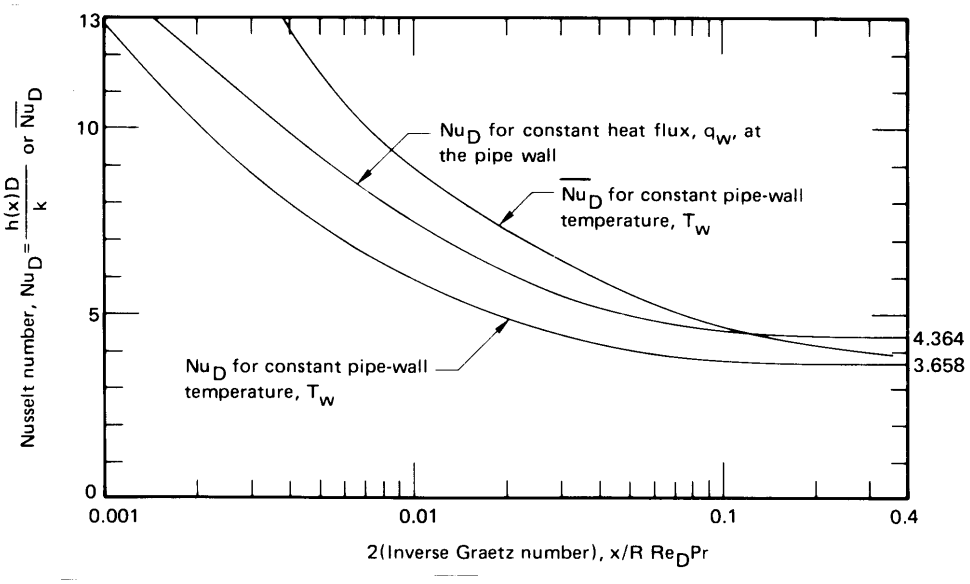

Figure 7.4 Local and average Nusselt numbers for the thermal entry region in a hydrodynamically developed laminar pipe flow.

where, since $h = q(x)/[T_w - T_b(x)]$, it is not possible to average just q or ΔT. We show how to find the change in T_b using $\overline{h}$ for an isothermal wall in Sect. 7.4. For a fixed heat flux, the change in T_b is given by eqn. (7.17), and a value of $\overline{h}$ is not needed.

For an isothermal wall, the following curve fits are available for the Nusselt number in thermally developing flow [7.3]:

$$\mathrm{Nu}_D = 3.657 + \frac{0.0018\ \mathrm{Gz}^{1/3}}{(0.04 + \mathrm{Gz}^{-2/3})^2} \tag{7.28}$$

$$\overline{\mathrm{Nu}}_D = 3.657 + \frac{0.0668\ \mathrm{Gz}^{1/3}}{0.04 + \mathrm{Gz}^{-2/3}} \tag{7.29}$$

The error is less than 14% for $\mathrm{Gz} > 1000$ and less than 7% for $\mathrm{Gz} < 1000$. For fixed q_w, a more complicated formula reproduces the exact result for local Nusselt number to within 1%:

$$\mathrm{Nu}_D = \begin{cases} 1.302\,\mathrm{Gz}^{1/3} - 1 & \text{for } 2 \times 10^4 \le \mathrm{Gz} \\ 1.302\,\mathrm{Gz}^{1/3} - 0.5 & \text{for } 667 \le \mathrm{Gz} \le 2 \times 10^4 \\ 4.364 + 0.263\,\mathrm{Gz}^{0.506}\,e^{-41/\mathrm{Gz}} & \text{for } 0 \le \mathrm{Gz} \le 667 \end{cases} \tag{7.30}$$

Example 7.2

A fully developed flow of air at 27°C moves at 2 m/s in a 1 cm I.D. pipe. An electric resistance heater surrounds the last 20 cm of the pipe and supplies a constant heat flux to bring the air out at $T_b = 40°\text{C}$. What power input is needed to do this? What will be the wall temperature at the exit?

SOLUTION. This is a case in which the wall heat flux is uniform along the pipe. We first must compute $\text{Gz}_{20\text{ cm}}$, evaluating properties at $(27 + 40)/2 \simeq 34°\text{C}$.

$$\text{Gz}_{20\text{ cm}} = \frac{\text{Re}_D \text{Pr}\, D}{x} = \frac{\dfrac{(2\text{ m/s})(0.01\text{ m})}{16.4 \times 10^{-6}\text{ m}^2/\text{s}}(0.711)(0.01\text{ m})}{0.2\text{ m}} = 43.38$$

From eqn. 7.30, we compute $\text{Nu}_D = 5.05$, so

$$T_{w_{\text{exit}}} - T_b = \frac{q_w D}{5.05\, k}$$

Notice that we still have two unknowns, q_w and T_w. The bulk temperature is specified as 40°C, and q_w is obtained from this number by a simple energy balance:

$$q_w(2\pi R x) = \rho c_p u_{\text{av}}(T_b - T_{\text{entry}})\pi R^2$$

so

$$q_w = 1.159\frac{\text{kg}}{\text{m}^3} \cdot 1004\frac{\text{J}}{\text{kg·K}} \cdot 2\frac{\text{m}}{\text{s}} \cdot (40 - 27)°\text{C} \cdot \underbrace{\frac{R}{2x}}_{1/80} = 378\text{ W/m}^2$$

Then

$$T_{w_{\text{exit}}} = 40°\text{C} + \frac{(378\text{ W/m}^2)(0.01\text{ m})}{5.05(0.0266\text{ W/m·K})} = 68.1°\text{C}$$ ■

7.3 Turbulent pipe flow

Turbulent entry length

The entry lengths x_e and x_{e_t} are generally shorter in turbulent flow than they are in laminar flow. However, x_{e_t} depends on both Re and Pr in a

Table 7.1 Thermal entry lengths for which Nu_D will be no more than 10% above its fully developed value in turbulent flow

Pr	Re_D	x_{e_t}/D
0.01	200,000	28
0.01	100,000	20
0.01	50,000	12
0.7	200,000	7
0.7	100,000	7
0.7	50,000	7
10.0	100,000	$\mathcal{O}(1)$

complicated way. Table 7.1 gives the thermal entry length for various values of Pr and Re_D, based on a maximum of 10% error in Nu_D.

Here we see that x_{e_t} is very strongly dependent on Pr and influenced rather less by Re_D. Notice, too, that x_{e_t} decreases with Pr in turbulent flow while it increases in laminar flow.

Only liquid metal flows give fairly long thermal entry regimes, and they require a separate discussion because of certain problems that emerge at low Pr's.

The discussion that follows deals almost entirely with fully developed turbulent pipe flows.

Illustrative experiment

Figure 7.5 shows average heat transfer data given by Kreith [7.7, Chap. 8] for air flowing in a 1 in. I.D. isothermal pipe 60 in. in length. Let us see how these data compare with what we know about pipe flows thus far.

The data are plotted for a single Prandtl number on $\overline{\mathrm{Nu}}_D$ vs. Re_D coordinates. This format is consistent with eqn. (7.25) in the fully developed range, but the actual pipe incorporates a significant entry region. Therefore, the data will reflect entry behavior.

For laminar flow, $\overline{\mathrm{Nu}}_D \simeq 3.66$ at $\mathrm{Re}_D = 750$. This is the correct value for an isothermal pipe. However, the pipe is too short for flow to be fully developed over much, if any, of its length. Therefore $\overline{\mathrm{Nu}}_D$ is not constant in the laminar range. The rate of rise of $\overline{\mathrm{Nu}}_D$ with Re_D becomes very great in the transitional range, which lies between $\mathrm{Re}_D = 2100$ and about 5000 in this case. Above $\mathrm{Re}_D \simeq 5000$, the flow is turbulent and it turns out

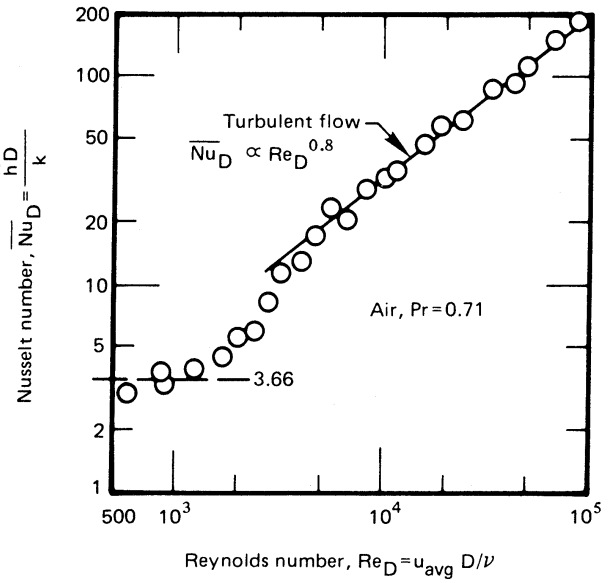

Figure 7.5 Heat transfer to air flowing in a 1 in. I.D., 60 in. long pipe (after Kreith [7.7]).

that $\overline{\mathrm{Nu}}_D \simeq \mathrm{Re}_D^{0.8}$.

The Reynolds analogy and heat transfer

The form of the Reynolds analogy appropriate to fully developed turbulent flow in a pipe can be derived from eqn. (6.96) in the form

$$\mathrm{St}_x = \frac{h}{\rho c_p u_\infty} = \frac{C_f(x)/2}{1 + 13\left(\mathrm{Pr}^{2/3} - 1\right)\sqrt{C_f(x)/2}} \tag{6.96}$$

where h, in a pipe flow, is defined as $q_w/(T_w - T_b)$. We merely replace u_∞ with u_{av} and $C_f(x)$ with a constant value of the friction coefficient, C_f, for fully developed pipe flow to get

$$\mathrm{St} = \frac{h}{\rho c_p u_{\mathrm{av}}} = \frac{C_f/2}{1 + 13\left(\mathrm{Pr}^{2/3} - 1\right)\sqrt{C_f/2}} \tag{7.31}$$

This should not be used at very low Pr's, but it can be used in either uniform q_w or uniform T_w situations. It applies only to smooth walls.

The frictional resistance to flow in a pipe is normally expressed in terms of the Darcy-Weisbach friction factor, f [recall eqn. (3.24)]:

$$f \equiv \frac{\text{head loss}}{\dfrac{\text{pipe length}}{D}\dfrac{u_{\mathrm{av}}^2}{2}} = \frac{\Delta p}{\dfrac{L}{D}\dfrac{\rho u_{\mathrm{av}}^2}{2}} \tag{7.32}$$

where Δp is the pressure drop in a pipe of length L. However,

$$\tau_w = \frac{\text{frictional force on liquid}}{\text{surface area of pipe}} = \frac{\Delta p\left[(\pi/4)D^2\right]}{\pi DL} = \frac{\Delta pD}{4L}$$

so

$$f = \frac{\tau_w}{\rho u_{\text{av}}^2/8} = 4C_f \tag{7.33}$$

Substituting eqn. (7.33) in eqn. (7.31) and rearranging the result, we obtain, for fully developed flow,

$$\text{Nu}_D = \frac{(f/8)\text{Re}_D\,\text{Pr}}{1 + 13\left(\text{Pr}^{2/3} - 1\right)\sqrt{f/8}} \tag{7.34}$$

The friction factor is given graphically in Fig. 7.6 as a function of Re_D and the relative roughness, ε/D, where ε is the root-mean-square roughness of the pipe wall. Equation (7.34) can be used directly along with Fig. 7.6 to calculate the Nusselt number, but only for smooth-walled pipes.

Historical formulations. A number of early formulations for the Nusselt number in turbulent pipe flow were based on Reynolds analogy in the form of eqn. (6.95), which for a pipe flow becomes

$$\text{St}\,\text{Pr}^{2/3} = \frac{C_f}{2} = \frac{f}{8} \tag{7.35}$$

or

$$\text{Nu}_D = \text{Re}_D\,\text{Pr}^{1/3}\,(f/8) \tag{7.36}$$

For smooth pipes, the curve $\varepsilon/D = 0$ in Fig. 7.6 is approximately given by this equation:

$$\frac{f}{4} = C_f = \frac{0.046}{\text{Re}_D^{0.2}} \tag{7.37}$$

in the range $20,000 < \text{Re}_D < 300,000$, so eqn. (7.36) becomes

$$\text{Nu}_D = 0.023\,\text{Pr}^{1/3}\,\text{Re}_D^{0.8}$$

for smooth pipes. This result was given by Colburn [7.8] in 1933. Actually, it is quite similar to an earlier result developed by Dittus and Boelter in 1930 (see [7.9, pg. 552]) for smooth pipes.

$$\text{Nu}_D = 0.0243\,\text{Pr}^{0.4}\,\text{Re}_D^{0.8} \tag{7.38}$$

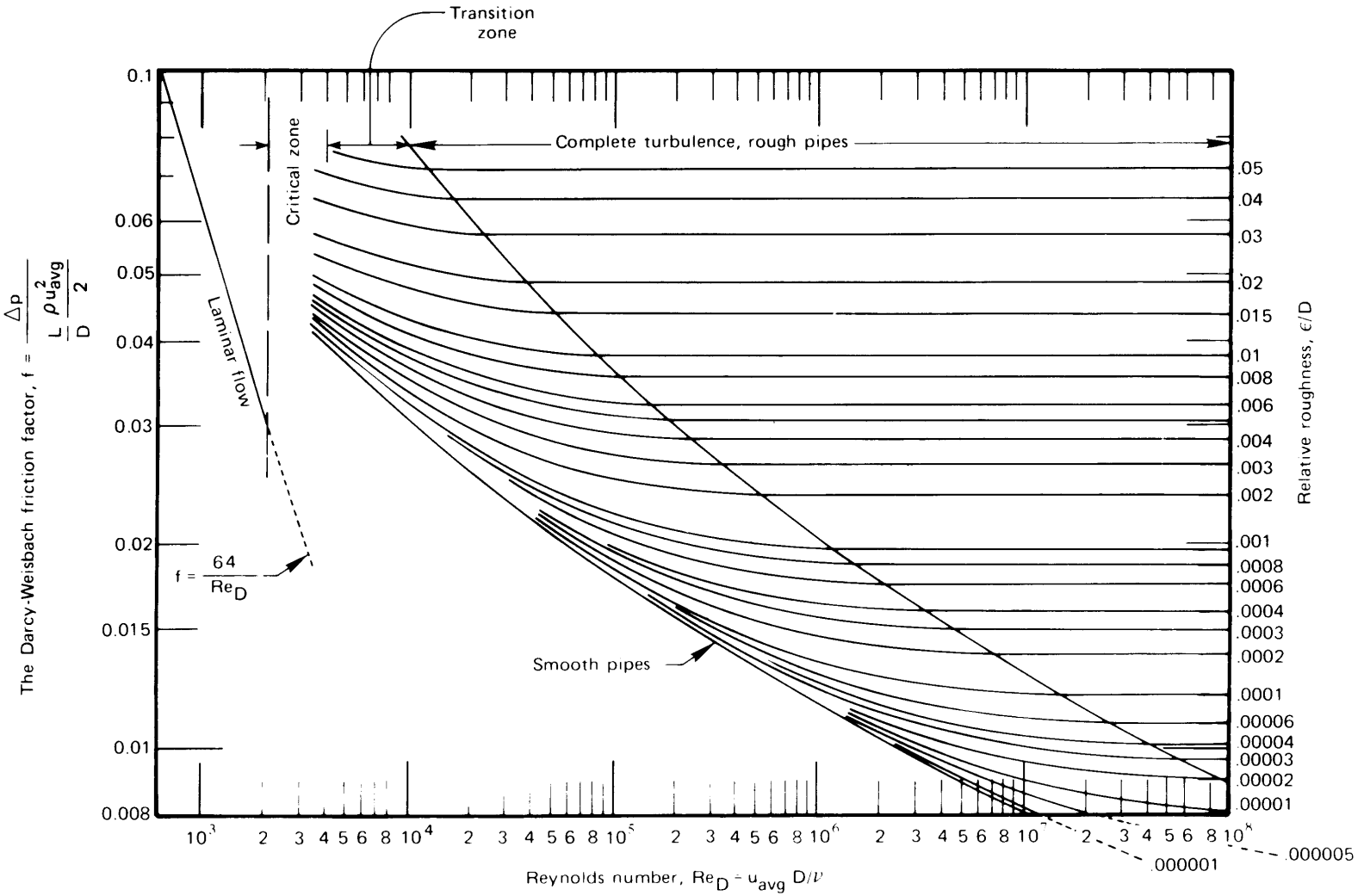

Figure 7.6 Pipefriction factors.

These equations are intended for reasonably low temperature differences under which properties can be evaluated at a mean temperature $(T_b + T_w)/2$. In 1936, Sieder and Tate [7.10] provided a correlation that suggests that when $|T_w - T_b|$ is large enough to cause serious changes of μ, the Colburn equation can be modified in the following way for liquids:

$$\mathrm{Nu}_D = 0.023\ \mathrm{Re}_D^{0.8}\,\mathrm{Pr}^{1/3}\left(\frac{\mu_b}{\mu_w}\right)^{0.14} \tag{7.39}$$

where all properties are evaluated at the local bulk temperature except μ_w, which is the viscosity evaluated at the wall temperature.

These early relations proved to be reasonably accurate. They gave maximum errors of +25% and −40% in the range $0.67 \leqslant \mathrm{Pr} < 100$ and usually were considerably more accurate than this. However, subsequent research has provided a great many more data, and better theoretical and physical understanding of how to represent them accurately. During the 1950s and 1960s, B. S. Petukhov and his co-workers at the Moscow Institute for High Temperature developed a vastly improved description of forced convection heat transfer in pipes. Much of this work is described in a 1970 survey article by Petukhov [7.11].

Modern formulations. Petukhov recommends the following equation, which is built from eqn. (7.34), for the local Nusselt number in fully developed flow in smooth pipes where all properties are evaluated at T_b.

$$\boxed{\mathrm{Nu}_D = \frac{(f/8)\ \mathrm{Re}_D\,\mathrm{Pr}}{1.07 + 12.7\sqrt{f/8}\left(\mathrm{Pr}^{2/3} - 1\right)}} \tag{7.40}$$

where

$$\begin{aligned} &10^4 < \mathrm{Re}_D < 5 \times 10^6 && \\ &0.5 < \mathrm{Pr} < 200 && \text{for 6\% accuracy} \\ &200 \leqslant \mathrm{Pr} < 2000 && \text{for 10\% accuracy} \end{aligned}$$

and where the friction factor for smooth pipes is given by

$$f = \frac{1}{\left(1.82\log_{10}\mathrm{Re}_D - 1.64\right)^2} \tag{7.41}$$

Gnielinski [7.12] later showed that the range of validity could be extended down to the transition Reynolds number by making a small adjustment to eqn. (7.40):

$$\boxed{\mathrm{Nu}_D = \frac{(f/8)\,(\mathrm{Re}_D - 1000)\,\mathrm{Pr}}{1 + 12.7\sqrt{f/8}\left(\mathrm{Pr}^{2/3} - 1\right)}} \tag{7.42}$$

for $2300 \le \mathrm{Re}_D \le 5 \times 10^6$.

Variations in physical properties. The effect of variable physical properties is dealt with differently for liquids and gases. In both cases, the Nusselt number is first calculated with all properties evaluated at T_b. For liquids, one then corrects by multiplying with a viscosity ratio, $0.025 \le (\mu_b/\mu_w) \le 12.5$ [7.11],

$$\mathrm{Nu}_D = \mathrm{Nu}_D\Big|_{T_b} \left(\frac{\mu_b}{\mu_w}\right)^n \qquad \text{where } n = \begin{cases} 0.11 & \text{for } T_w > T_b \\ 0.25 & \text{for } T_w < T_b \end{cases} \tag{7.43}$$

For gases a ratio of temperatures *in kelvins* is used, with $0.27 \le (T_b/T_w) \le 2.7$,

$$\mathrm{Nu}_D = \mathrm{Nu}_D\Big|_{T_b} \left(\frac{T_b}{T_w}\right)^n \qquad \text{where } n = \begin{cases} 0.47 & \text{for } T_w > T_b \\ 0.36 & \text{for } T_w < T_b \end{cases} \tag{7.44}$$

After eqn. (7.41) is used to calculate Nu_D, it should also be corrected for the effect of variable viscosity. For liquids, with $0.5 \le (\mu_b/\mu_w) \le 3$

$$f = f\Big|_{T_b} \times K \qquad \text{where } K = \begin{cases} (7 - \mu_b/\mu_w)/6 & \text{for } T_w > T_b \\ (\mu_b/\mu_w)^{-0.24} & \text{for } T_w < T_b \end{cases} \tag{7.45}$$

For gases, with $0.27 \le (T_b/T_w) \le 2.7$

$$f = f\Big|_{T_b} \left(\frac{T_b}{T_w}\right)^m \qquad \text{where } m = \begin{cases} 0.52 & \text{for } T_w > T_b \\ 0.38 & \text{for } T_w < T_b \end{cases} \tag{7.46}$$

Example 7.3

A 21.5 kg/s flow of water is dynamically and thermally developed in

a 12 cm I.D. pipe. The pipe is held at 90°C and $\varepsilon/D = 0$. Find h and f where the bulk temperature of the fluid has reached 50°C.

SOLUTION.

$$u_{\text{av}} = \frac{\dot{m}}{\rho A_c} = \frac{21.5}{977\pi(0.06)^2} = 1.946 \text{ m/s}$$

so

$$\text{Re}_D = \frac{u_{\text{av}} D}{\nu} = \frac{1.946(0.12)}{4.07 \times 10^{-7}} = 573,700$$

and

$$\text{Pr} = 2.47, \qquad \frac{\mu_b}{\mu_w} = \frac{5.38 \times 10^{-4}}{3.10 \times 10^{-4}} = 1.74$$

From eqn. (7.41), $f = 0.0128$ at T_b, and since $T_w > T_b$, $n = 0.11$ in eqn. (7.43). Thus, with eqn. (7.40) we have

$$\text{Nu}_D = \frac{(0.0128/8)(5.74 \times 10^5)(2.47)}{1.07 + 12.7\sqrt{0.0128/8}\ (2.47^{2/3} - 1)}(1.74)^{0.11} = 1617$$

or

$$h = 1831 \frac{k}{D} = 1617 \frac{0.661}{0.12} = 8,907 \text{ W/m}^2\text{K}$$

The corrected friction factor, with eqn. (7.45), is

$$f = (0.0128)\,(7 - 1.74)/6 = 0.0122$$ ■

Heat transfer to fully developed liquid-metal flows in tubes

A dimensional analysis of the forced convection flow of a liquid metal over a flat surface [recall eqn. (6.60) et seq.] showed that

$$\text{Nu} = \text{fn}(\text{Pe}) \tag{7.47}$$

because viscous influences were confined to a region very close to the wall. Thus, the thermal b.l., which extends far beyond δ, is hardly influenced by the dynamic b.l. or by viscosity. During heat transfer to liquid metals in pipes, the same thing occurs as is illustrated in Fig. 7.7. The region of thermal influence extends far beyond the laminar sublayer, when $\text{Pr} \ll 1$, and the temperature profile is not influenced by the sublayer.

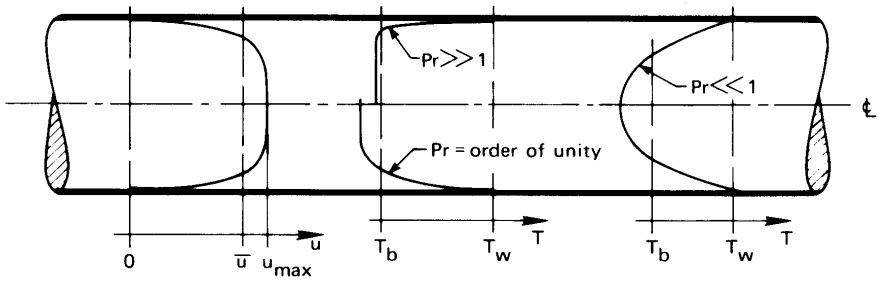

Figure 7.7 Velocity and temperature profiles during fully developed turbulent flow in a pipe.

Conversely, if Pr $\gg$ 1, the temperature profile is largely shaped within the laminar sublayer. At high or even moderate Pr's, ν is therefore very important, but at low Pr's it vanishes from the functional equation. Equation (7.47) thus applies to pipe flows as well as to flow over a flat surface.

Numerous measured values of Nu_D for liquid metals flowing in pipes with a constant wall heat flux, q_w, were assembled by Lubarsky and Kaufman [7.13]. They are included in Fig. 7.8. It is clear that while most of the data correlate fairly well on Nu_D vs. Pe coordinates, certain sets of data are badly scattered. This occurs in part because liquid metal experiments are hard to carry out. Temperature differences are small and must often be measured at high temperatures. Some of the very low data might possibly result from a failure of the metals to wet the inner surface of the pipe.

Another problem that besets liquid metal heat transfer measurements is the very great difficulty involved in keeping such liquids pure. Most impurities tend to result in lower values of h. Thus, most of the Nusselt numbers in Fig. 7.8 have probably been lowered by impurities in the liquids; the few high values are probably the more correct ones for pure liquids.

There is a body of theory for turbulent liquid metal heat transfer that yields a prediction of the form

$$\mathrm{Nu}_D = C_1 + C_2\,\mathrm{Pe}_D^{0.8} \tag{7.48}$$

where the Péclét number is defined as $\mathrm{Pe}_D = u_{\mathrm{av}}D/\alpha$. The constants are normally in the ranges $2 \leqslant C_1 \leqslant 7$ and $0.0185 \leqslant C_2 \leqslant 0.386$ according to the test circumstances. Using the few reliable data sets available for

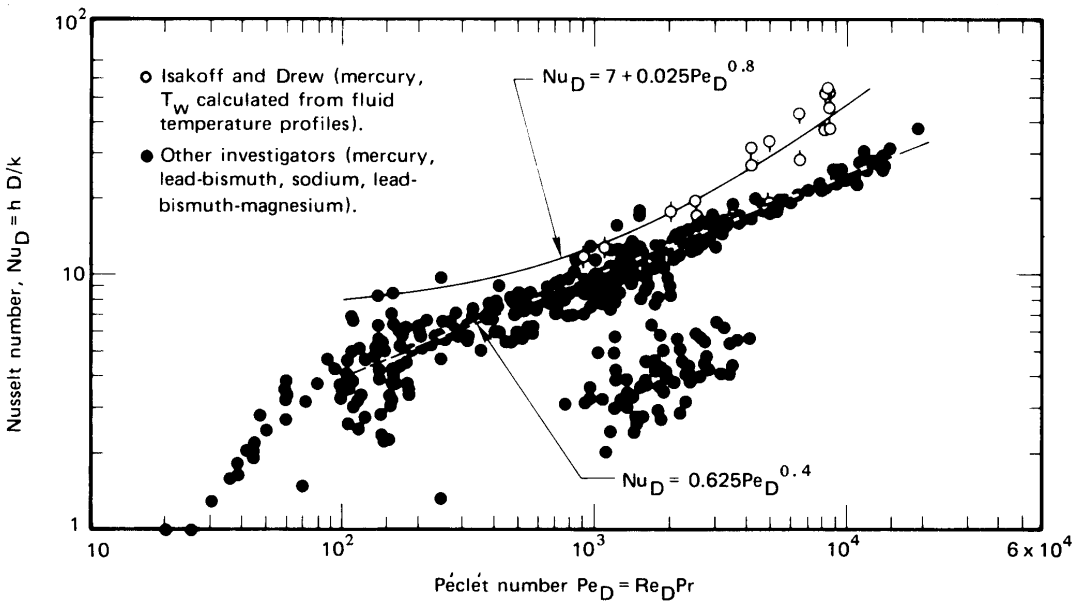

Figure 7.8 Comparison of measured and predicted Nusselt numbers for liquid metals heated in long tubes with uniform wall heat flux, q_w. (See NACA TN 336, 1955, for details and data source references.)

uniform wall temperature conditions, Reed [7.14] recommends

$$\mathrm{Nu}_D = 3.3 + 0.02\ \mathrm{Pe}_D^{0.8} \tag{7.49}$$

(Earlier work by Seban and Shimazaki [7.15] had suggested $C_1 = 4.8$ and $C_2 = 0.025$.) For uniform wall heat flux, many more data are available, and Lyon [7.16] recommends the following equation, shown in Fig. 7.8:

$$\mathrm{Nu}_D = 7 + 0.025\ \mathrm{Pe}_D^{0.8} \tag{7.50}$$

In both these equations, properties should be evaluated at the average of the inlet and outlet bulk temperatures and the pipe flow should have $L/D > 60$ and $\mathrm{Pe}_D > 100$. For lower Pe_D, axial heat conduction in the liquid metal may become significant.

Although eqns. (7.49) and (7.50) are probably correct for pure liquids, we cannot overlook the fact that the liquid metals in actual use are seldom pure. Lubarsky and Kaufman [7.13] put the following line through the bulk of the data in Fig. 7.8:

$$\mathrm{Nu}_D = 0.625\ \mathrm{Pe}_D^{0.4} \tag{7.51}$$

The use of eqn. (7.51) for q_w = constant is far less optimistic than the use of eqn. (7.50). It should probably be used if it is safer to err on the low side.

7.4 Heat transfer surface viewed as a heat exchanger

Let us reconsider the problem of a fluid flowing through a pipe with a uniform wall temperature. By now we can predict $\overline{h}$ for a pretty wide range of conditions. Suppose that we need to know the net heat transfer to a pipe of known length once $\overline{h}$ is known. This problem is complicated by the fact that the bulk temperature, T_b, is varying along its length.

However, we need only recognize that such a section of pipe is a heat exchanger whose overall heat transfer coefficient, U (between the wall and the bulk), is just $\overline{h}$. Thus, if we wish to know how much pipe surface area is needed to raise the bulk temperature from $T_{b_{\text{in}}}$ to $T_{b_{\text{out}}}$, we can calculate it as follows:

$$Q = (\dot{m}c_p)_b \left(T_{b_{\text{out}}} - T_{b_{\text{in}}}\right) = \overline{h}A(\text{LMTD})$$

or

$$A = \frac{(\dot{m}c_p)_b \left(T_{b_{\text{out}}} - T_{b_{\text{in}}}\right)}{\overline{h}} \frac{\ln\left(\dfrac{T_{b_{\text{out}}} - T_w}{T_{b_{\text{in}}} - T_w}\right)}{(T_{b_{\text{out}}} - T_w) - (T_{b_{\text{in}}} - T_w)} \tag{7.52}$$

By the same token, heat transfer in a duct can be analyzed with the effectiveness method (Sect. 3.3) if the existing fluid temperature is unknown. Suppose that we do not know $T_{b_{\text{out}}}$ in the example above. Then we can write an energy balance at any cross section, as we did in eqn. (7.8):

$$dQ = q_w P\, dx = hP\left(T_w - T_b\right)\, dx = \dot{m}c_P\, dT_b$$

Integration can be done from $T_b(x = 0) = T_{b_{\text{in}}}$ to $T_b(x = L) = T_{b_{\text{out}}}$

$$\int_0^L \frac{hP}{\dot{m}c_p}\, dx = -\int_{T_{b_{\text{in}}}}^{T_{b_{\text{out}}}} \frac{d(T_w - T_b)}{(T_w - T_b)}$$

$$\frac{P}{\dot{m}c_p}\int_0^L h\, dx = -\ln\left(\frac{T_w - T_{b_{\text{out}}}}{T_w - T_{b_{\text{in}}}}\right)$$

We recognize in this the definition of $\overline{h}$ from eqn. (7.27). Hence,

$$\frac{\overline{h}PL}{\dot{m}c_p} = -\ln\left(\frac{T_w - T_{b_{\text{out}}}}{T_w - T_{b_{\text{in}}}}\right)$$

which can be rearranged as

$$\frac{T_{b_{\text{out}}} - T_{b_{\text{in}}}}{T_w - T_{b_{\text{in}}}} = 1 - \exp\left(-\frac{\overline{h}PL}{\dot{m}c_p}\right) \tag{7.53}$$

This equation can be used in either laminar or turbulent flow to compute the variation of bulk temperature if $T_{b_{\text{out}}}$ is replaced by $T_b(x)$, L is replaced by x, and $\overline{h}$ is adjusted accordingly.

The left-hand side of eqn. (7.53) is the heat exchanger effectiveness. On the right-hand side we replace U with $\overline{h}$; we note that $PL = A$, the exchanger surface area; and we write $C_{\min} = \dot{m}c_p$. Since T_w is uniform, the stream that it represents must have a very large capacity rate, so that $C_{\min}/C_{\max} = 0$. Under these substitutions, we identify the argument of the exponential as NTU $= UA/C_{\min}$, and eqn. (7.53) becomes

$$\varepsilon = 1 - \exp(-\text{NTU}) \tag{7.54}$$

which we could have obtained directly, from either eqn. (3.20) or (3.21), by setting $C_{\min}/C_{\max} = 0$. A heat exchanger for which one stream is isothermal, so that $C_{\min}/C_{\max} = 0$, is sometimes called a *single-stream* heat exchanger.

Equation 7.53 applies to ducts of any cross-sectional shape. We can cast it in terms of the *hydraulic diameter*, $D_h = 4A_c/P$, by substituting $\dot{m} = \rho u_{\text{av}} A_c$:

$$\begin{aligned}\frac{T_{b_{\text{out}}} - T_{b_{\text{in}}}}{T_w - T_{b_{\text{in}}}} &= 1 - \exp\left(-\frac{\overline{h}PL}{\rho u_{\text{av}} c_p A_c}\right) \\ &= 1 - \exp\left(-\frac{\overline{h}}{\rho u_{\text{av}} c_p}\frac{4L}{D_h}\right)\end{aligned} \tag{7.55}$$

For a circular tube, $D_h = 4(\pi/4)D^2/(\pi D) = D$. To use eqn. 7.55 for a non-circular duct, of course, we will need the value of $\overline{h}$ for a noncircular duct. We consider this issue in the next section.

Example 7.4

Air at 20°C is fully thermally developed as it flows in a 1 cm I.D. pipe.

The average velocity is 0.7 m/s. If the pipe wall is at 60°C , what is the temperature 0.25 m farther downstream?

SOLUTION.

$$\mathrm{Re}_D = \frac{u_{\mathrm{av}} D}{\nu} = \frac{(0.7)(0.01)}{1.70 \times 10^{-5}} = 412$$

The flow is therefore laminar, so

$$\mathrm{Nu}_D = \frac{\overline{h} D}{k} = 3.658$$

Thus,

$$\overline{h} = \frac{3.658(0.0271)}{0.01} = 9.91 \text{ W/m}^2\text{K}$$

Then

$$\varepsilon = 1 - \exp\left(-\frac{\overline{h}}{\rho c_p u_{\mathrm{av}}} \frac{4L}{D}\right) = 1 - \exp\left[-\frac{9.91}{1.14(1004)(0.7)} \frac{4(0.25)}{0.01}\right]$$

so that

$$\frac{T_b - 20}{60 - 20} = 0.698 \qquad \text{or} \qquad T_b = 47.9°\text{C}$$ ■

7.5 Heat transfer coefficients for noncircular ducts

To appear.

7.6 Heat transfer during cross flow over cylinders

Fluid flow pattern

It will help us to understand the complexity of heat transfer from bodies in a cross flow if we first look in detail at the fluid flow patterns that occur in one cross-flow configuration—a cylinder with fluid flowing normal to it. Figure 7.9 shows how the flow develops as $\mathrm{Re} \equiv u_\infty D/\nu$ is increased from below 5 to near 10^7. An interesting feature of this evolving flow pattern is the fairly continuous way in which one flow transition follows another. The flow field degenerates to greater and greater degrees of

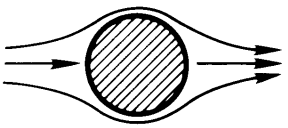

$Re_D < 5$ Regime of unseparated flow.

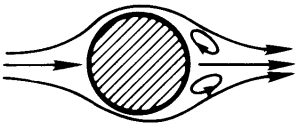

$5 \text{ to } 15 \leqslant Re_D < 40$ A fixed pair of Föppl vortices in the wake

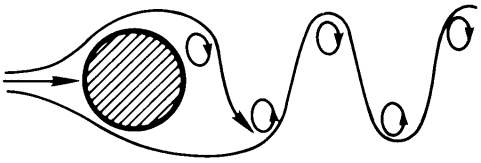

$40 \leqslant Re_D < 90$ and $90 \leqslant Re_D < 150$

Two regimes in which vortex street is laminar:

Periodicity governed in low Re_D range by wake instability

Periodicity governed in high Re_D range by vortex shedding.

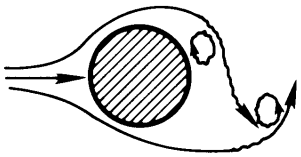

$150 \leqslant Re_D < 300$ Transition range to turbulence in vortex.

$300 \leqslant Re_D \lesssim 3 \times 10^5$ Vortex street is fully turbulent, and the flow field is increasingly 3-dimensional.

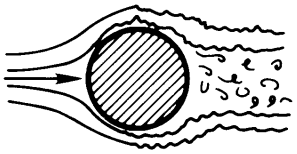

$3 \times 10^5 \lesssim Re_D < 3.5 \times 10^6$

Laminar boundary layer has undergone turbulent transition. The wake is narrower and disorganized. No vortex street is apparent.

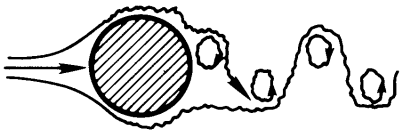

$3.5 \times 10^6 \leqslant Re_D < \infty$ (?)

Re-establishment of the turbulent vortex street that was evident in $300 \leqslant Re_D \lesssim 3 \times 10^5$. This time the boundary layer is turbulent and the wake is thinner.

Figure 7.9 Regimes of fluid flow across circular cylinders [7.17].

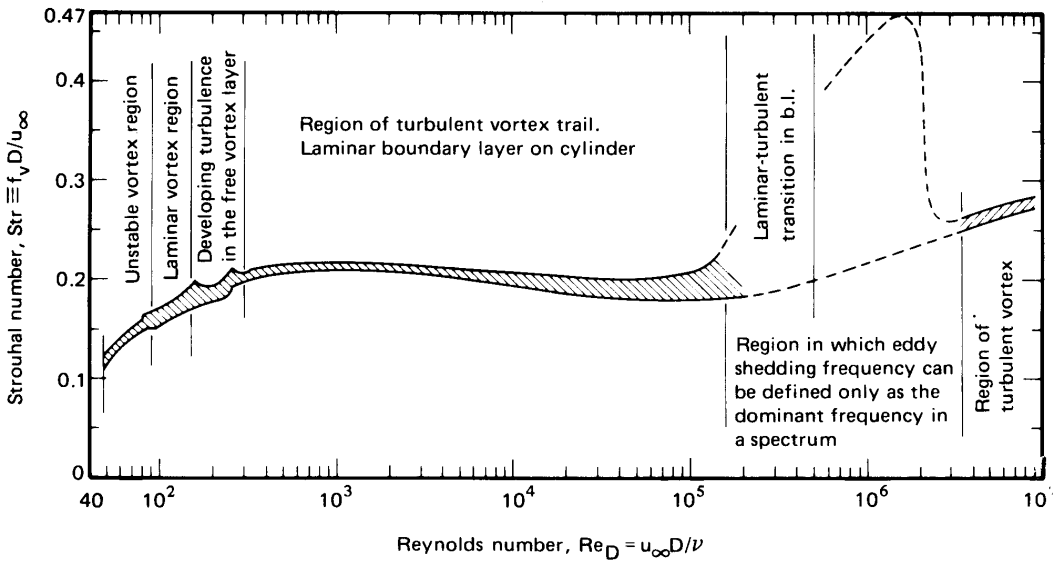

Figure 7.10 The Strouhal–Reynolds number relationship for circular cylinders, as defined by existing data [7.17].

disorder with each successive transition until, rather strangely, it regains order at the highest values of Re_D.

An important reflection of the complexity of the flow field is the vortex-shedding frequency, f_v. Dimensional analysis shows that a dimensionless frequency called the Strouhal number, Str, depends on the Reynolds number of the flow:

$$\mathrm{Str} \equiv \frac{f_v D}{u_\infty} = \mathrm{fn}\,(\mathrm{Re}_D) \tag{7.56}$$

Figure 7.10 defines this relationship experimentally on the basis of about 550 of the best data available (see [7.17]). The Strouhal numbers stay a little over 0.2 over most of the range of Re_D. This means that behind a given object, the vortex-shedding frequency rises almost linearly with velocity.

Experiment 7.1

When there is a gentle breeze blowing outdoors, go out and locate a large tree with a straight trunk or the shaft of a water tower. Wet your finger and place it in the wake a couple of diameters downstream and

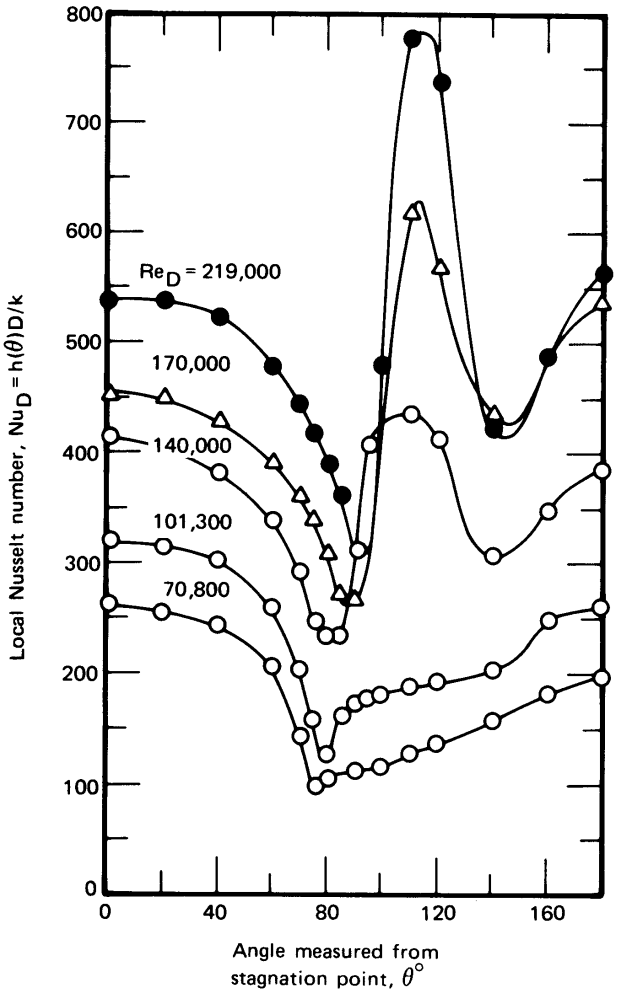

Figure 7.11 Giedt's local measurements of heat transfer around a cylinder in a normal cross flow of air.

about one radius off center. Estimate the vortex-shedding frequency and use Str $\simeq 0.21$ to estimate u_∞. Is your value of u_∞ reasonable?

Heat transfer

The action of vortex shedding greatly complicates the heat removal process. Giedt's data [7.18] in Fig. 7.11 show how the heat removal changes as the constantly fluctuating motion of the fluid to the rear of the cylinder changes with Re_D. Notice, for example, that Nu_D is near its minimum

at 110° when $\mathrm{Re}_D = 71,000$, but it maximizes at the same place when $\mathrm{Re}_D = 140,000$. Direct prediction by the sort of b.l. methods that we discussed in Chapter 6 is out of the question. However, a great deal can be done with the data using relations of the form

$$\overline{\mathrm{Nu}}_D = \mathrm{fn}\,(\mathrm{Re}_D, \mathrm{Pr})$$

The broad study of Churchill and Bernstein [7.19] probably brings the correlation of heat transfer data from cylinders about as far as it is possible. For the entire range of the available data, they offer

$$\boxed{\overline{\mathrm{Nu}}_D = 0.3 + \frac{0.62\ \mathrm{Re}_D^{1/2}\,\mathrm{Pr}^{1/3}}{\left[1 + (0.4/\mathrm{Pr})^{2/3}\right]^{1/4}}\left[1 + \left(\frac{\mathrm{Re}_D}{282,000}\right)^{5/8}\right]^{4/5}} \tag{7.57}$$

This expression underpredicts most of the data by about 20% in the range $20,000 < \mathrm{Re}_D < 400,000$ but is quite good at other Reynolds numbers above $\mathrm{Pe}_D \equiv \mathrm{Re}_D\mathrm{Pr} = 0.2$. This is evident in Fig. 7.12, where eqn. (7.57) is compared with data.

Greater accuracy and, in most cases, greater convenience results from breaking the correlation into component equations:

- Below $\mathrm{Re}_D = 4000$, the bracketed term $[1 + (\mathrm{Re}_D/282,000)^{5/8}]^{4/5}$ is $\simeq 1$, so

$$\overline{\mathrm{Nu}}_D = 0.3 + \frac{0.62\ \mathrm{Re}_D^{1/2}\mathrm{Pr}^{1/3}}{\left[1 + (0.4/\mathrm{Pr})^{2/3}\right]^{1/4}} \tag{7.58}$$

- Below $\mathrm{Pe} = 0.2$, the Nakai-Okazaki [7.20] relation

$$\overline{\mathrm{Nu}}_D = \frac{1}{0.8237 - \ln(\mathrm{Pe}^{1/2})} \tag{7.59}$$

  should be used.

- In the range $20,000 < \mathrm{Re}_D < 400,000$, somewhat better results are given by

$$\overline{\mathrm{Nu}}_D = 0.3 + \frac{0.62\ \mathrm{Re}_D^{1/2}\,\mathrm{Pr}^{1/3}}{\left[1 + (0.4/\mathrm{Pr})^{2/3}\right]^{1/4}}\left[1 + \left(\frac{\mathrm{Re}_D}{282,000}\right)^{1/2}\right] \tag{7.60}$$

  than by eqn. (7.57).

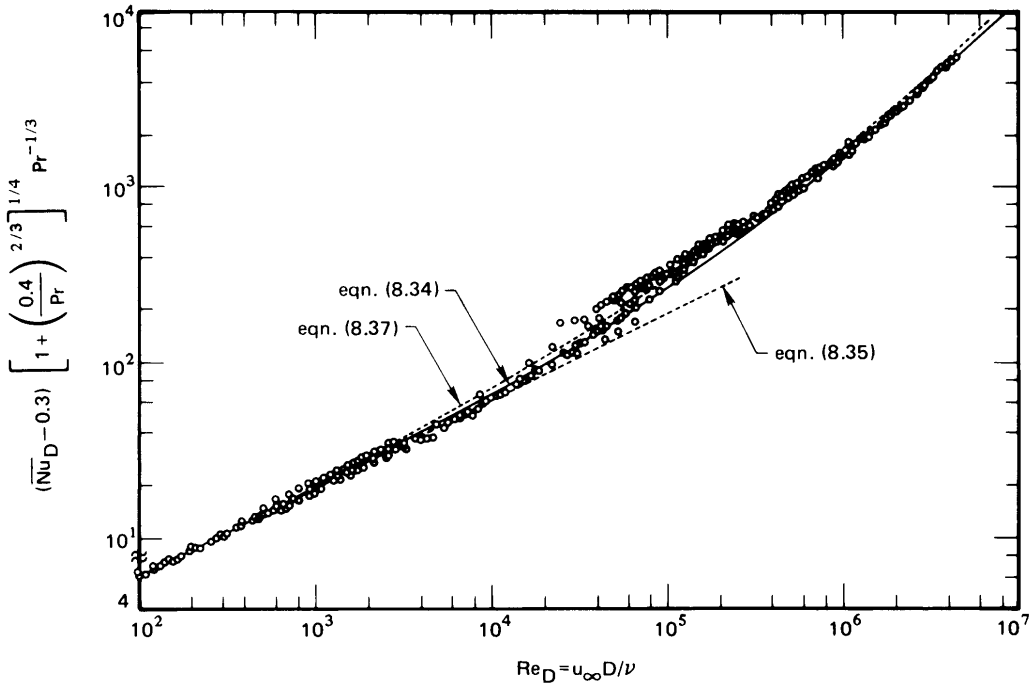

Figure 7.12 Comparison of Churchill and Bernstein's correlation with data by many workers from several countries for heat transfer during cross flow over a cylinder. (See [7.19] for data sources.) Fluids include air, water, and sodium, with both q_w and T_w constant.

All properties in eqns. (7.57) to (7.60) are to be evaluated at a film temperature $T_f = (T_w + T_\infty)/2$.

Example 7.5

An electric resistance wire heater 0.0001 m in diameter is placed perpendicular to an air flow. It holds a temperature of 40°C in a 20°C air flow while it dissipates 17.8 W/m of heat to the flow. How fast is the air flowing?

SOLUTION. $\overline{h} = (17.8\ \text{W/m})/[\pi(0.0001\ \text{m})(40 - 20)\ K] = 2833\ \text{W/m}^2\text{K}$. Therefore, $\overline{\text{Nu}}_D = 2833(0.0001)/0.0264 = 10.75$, where we have evaluated $k = 0.0264$ at $T = 30°\text{C}$. We now want to find the Re_D for which $\overline{\text{Nu}}_D$ is 10.75. From Fig. 7.12 we see that Re_D is around 300

when the ordinate is on the order of 10. This means that we can solve eqn. (7.58) to get an accurate value of Re_D:

$$\mathrm{Re}_D = \left\{ (\overline{\mathrm{Nu}}_D - 0.3) \left[1 + \left(\frac{0.4}{\mathrm{Pr}} \right)^{2/3} \right]^{1/4} \Big/ 0.62\ \mathrm{Pr}^{1/3} \right\}^2$$

but Pr = 0.71, so

$$\mathrm{Re}_D = \left\{ (10.75 - 0.3) \left[1 + \left(\frac{0.40}{0.71} \right)^{2/3} \right]^{1/4} \Big/ 0.62(0.71)^{1/3} \right\}^2 = 463$$

Then

$$u_\infty = \frac{\nu}{D} \mathrm{Re}_D = \left(\frac{1.596 \times 10^{-5}}{10^{-4}} \right) 463 = 73.9 \text{ m/s}$$

The data scatter in Re_D is quite small—less than 10%, it would appear—in Fig. 7.12. Therefore, this method can be used to measure local velocities with good accuracy. If the device is calibrated, its accuracy can be improved further. Such an air speed indicator is called a *hot-wire anemometer*. ■

Heat transfer during flow across tube bundles

A rod or tube bundle is an arrangement of parallel cylinders that heat, or are being heated by, a fluid that might flow normal to them, parallel with them, or at some angle in between. The flow of coolant through the fuel elements of all nuclear reactors being used in this country is parallel to the heating rods. The flow on the shell side of most shell-and-tube heat exchangers is generally normal to the tube bundles.

Figure 7.13 shows the two basic configurations of a tube bundle in a cross flow. In one, the tubes are in a line with the flow; in the other, the tubes are staggered in alternating rows. For either of these configurations, heat transfer data can be correlated reasonably well with power-law relations of the form

$$\overline{\mathrm{Nu}}_D = C\ \mathrm{Re}_D^n\ \mathrm{Pr}^{1/3} \tag{7.61}$$

but in which the Reynolds number is based on the maximum velocity,

$u_{\max} = \overline{u}_{\mathrm{av}}$ in the narrowest transverse area of the passage

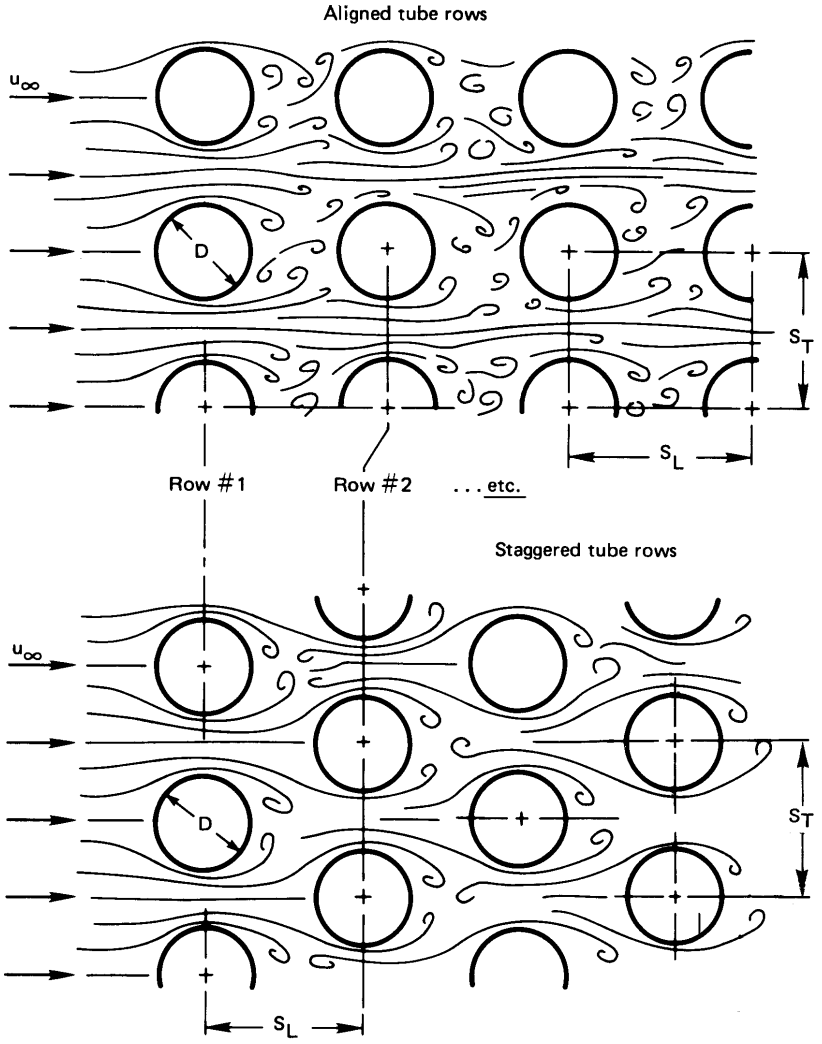

Figure 7.13 Aligned and staggered tube rows in tube bundles.

Thus, the Nusselt number based on the average heat transfer coefficient over any particular isothermal tube is

$$\overline{\mathrm{Nu}}_D = \frac{\overline{h}D}{k} \quad \text{and} \quad \mathrm{Re}_D = \frac{u_{\max}D}{\nu}$$

Žukauskas at the Lithuanian Academy of Sciences Institute in Vilnius has written a comprehensive review article on tube-bundle heat trans-

fer [7.21]. In it he summarizes his work and that of other Soviet workers, together with earlier work from the West. He was able to correlate data over very large ranges of Pr, Re_D, S_T/D, and S_L/D (see Fig. 7.13) with an expression of the form

$$\overline{\mathrm{Nu}}_D = \mathrm{Pr}^{0.36}\,(\mathrm{Pr}/\mathrm{Pr}_w)^n\ \mathrm{fn}\,(\mathrm{Re}_D) \quad \text{with } n = \begin{cases} 0 & \text{for gases} \\ \frac{1}{4} & \text{for liquids} \end{cases} \tag{7.62}$$

where properties are to be evaluated at the local fluid bulk temperature, except for Pr_w, which is evaluated at the uniform tube wall temperature, T_w.

The function $\mathrm{fn}(\mathrm{Re}_D)$ takes the following form for the various circumstances of flow and tube configuration:

$10 \leqslant \mathrm{Re}_D \leqslant 100$:

aligned rows: $\mathrm{fn}\,(\mathrm{Re}_D) = 0.8\,\mathrm{Re}_D^{0.4}$ (7.63)

staggered rows: $\mathrm{fn}\,(\mathrm{Re}_D) = 0.9\,\mathrm{Re}_D^{0.4}$ (7.64)

$100 < \mathrm{Re}_D < 10^3$: treat tubes as though they were isolated

$10^3 \leqslant \mathrm{Re}_D \leqslant 2\times 10^5$:

aligned rows: $\mathrm{fn}\,(\mathrm{Re}_D) = 0.27\,\mathrm{Re}_D^{0.63}$, $S_T/S_L < 0.7$ (7.65)

For $S_T/S_L \geqslant 0.7$, heat exchange is much less effective. Therefore, aligned tube bundles are not designed in this range and no correlation is given.

staggered rows: $\mathrm{fn}\,(\mathrm{Re}_D) = 0.35\,(S_T/S_L)^{0.2}\,\mathrm{Re}_D^{0.6}$, $S_T/S_L \leqslant 2$ (7.66)

$\mathrm{fn}\,(\mathrm{Re}_D) = 0.40\,\mathrm{Re}_D^{0.6}$, $S_T/S_L > 2$ (7.67)

$\mathrm{Re}_D > 2\times 10^5$:

aligned rows: $\mathrm{fn}\,(\mathrm{Re}_D) = 0.021\,\mathrm{Re}_D^{0.84}$ (7.68)

staggered rows: $\mathrm{fn}\,(\mathrm{Re}_D) = 0.022\,\mathrm{Re}_D^{0.84}$, $\mathrm{Pr} > 1$ (7.69)

$\overline{\mathrm{Nu}}_D = 0.019\,\mathrm{Re}_D^{0.84}$, $\mathrm{Pr} = 0.7$ (7.70)

All of the preceding relations apply to the inner rows of tube bundles. The heat transfer coefficient is smaller in the rows at the front of a bundle, facing the oncoming flow. The heat transfer coefficient can be corrected so that it will apply to any of the front rows using Fig. 7.14.

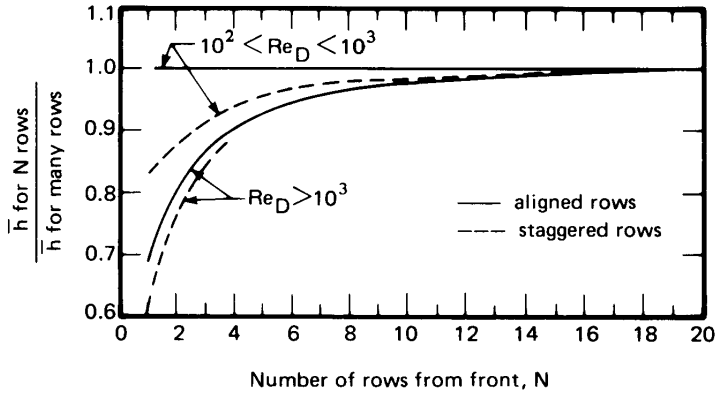

Figure 7.14 Correction for the heat transfer coefficients in the front rows of a tube bundle [7.21].

Early in this chapter we alluded to the problem of predicting the heat transfer coefficient during the flow of a fluid at an angle other than 90° to the axes of the tubes in a bundle. Žukauskas provides the empirical corrections in Fig. 7.15 to account for this problem.

The work of Žukauskas does not extend to liquid metals. However, Kalish and Dwyer [7.22] present the results of an experimental study of heat transfer to the liquid eutectic mixture of 77.2% potassium and 22.8% sodium (called NaK). NaK is a fairly popular low-melting-point metallic coolant which has received a good deal of attention for its potential use in certain kinds of nuclear reactors. For isothermal tubes in an equilateral triangular array, as shown in Fig. 7.16, Kalish and Dwyer give

$$\mathrm{Nu}_D = \left(5.44 + 0.228\ \mathrm{Pe}^{0.614}\right)\sqrt{C\,\frac{P-D}{P}\left(\frac{\sin\phi + \sin^2\phi}{1+\sin^2\phi}\right)} \qquad (7.71)$$

where

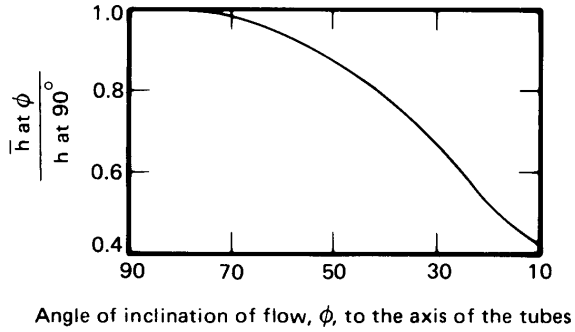

Figure 7.15 Correction for the heat transfer coefficient in flows that are not perfectly perpendicular to heat exchanger tubes [7.21].

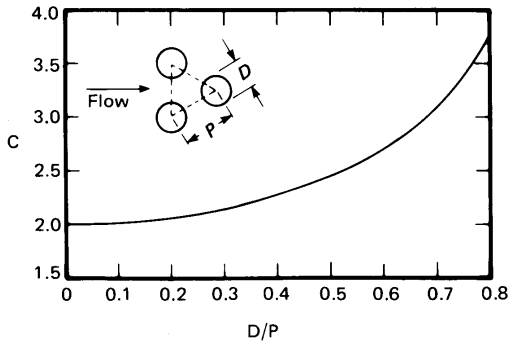

Figure 7.16 Geometric correction for the Kalish-Dwyer equation (7.71).

- ϕ is the angle between the flow direction and the rod axis.
- P is the "pitch" of the tube array, as shown in Fig. 7.16, and D is the tube diameter.
- C is the constant given in Fig. 7.16.
- Pe_D is the Péclét number based on the mean flow velocity through the narrowest opening between the tubes.
- For the same uniform heat flux around each tube, the constants in eqn. (7.71) change as follows: 5.44 becomes 4.60; 0.228 becomes 0.193.

7.7 Other configurations

At the outset, we noted that this chapter would move further and further beyond the reach of analysis in the heat convection problems that it dealt with. However, we must not forget that even the most completely empirical relations in Section 7.6 were devised by people who were keenly aware of the theoretical framework into which these relations had to fit. Notice, for example, that eqn. (7.58) reduces to $\mathrm{Nu}_D \propto \sqrt{\mathrm{Pe}_D}$ as Pr becomes small. That sort of theoretical requirement did not just pop out of a data plot. Instead, it was a consideration that led the authors to select an empirical equation that agreed with theory at low Pr.

Thus, the theoretical considerations in Chapter 6 guide us in correlating limited data in situations that cannot be analyzed. Such correlations can be found for all kinds of situations, but all must be viewed critically.

Many are based on limited data, and many incorporate systematic errors of one kind or another.

In the face of a heat transfer situation that has to be predicted, one can often find a correlation of data from similar systems. This might involve flow in or across noncircular ducts; axial flow through tube or rod bundles; flow over such bluff bodies as spheres, cubes, or cones; or flow in circular and noncircular annuli. The *Handbook of Heat Transfer* [7.23], the shelf of heat transfer texts in your library, or the journals referred to by the *Engineering Index* are among the first places to look for a correlation curve or equation. When you find a correlation, there are many questions that you should ask yourself:

- Is my case included within the range of dimensionless parameters upon which the correlation is based, or must I extrapolate to reach my case?
- What geometric differences exist between the situation represented in the correlation and the one I am dealing with? (Such elements as these might differ:
  (a) inlet flow conditions;
  (b) small but important differences in hardware, mounting brackets, and so on;
  (c) minor aspect ratio or other geometric nonsimilarities
- Does the form of the correlating equation that represents the data, if there is one, have any basis in theory? (If it is only a curve fit to the existing data, one might be unjustified in using it for more than interpolation of those data.)
- What nuisance variables might make our systems different? For example:
  (a) surface roughness;
  (b) fluid purity;
  (c) problems of surface wetting
- To what extend do the data scatter around the correlation line? Are error limits reported? Can I actually see the data points? (In this regard, you must notice whether you are looking at a correlation on linear or logarithmic coordinates. Errors usually appear smaller

than they really are on logarithmic coordinates. Compare, for example, the data of Figs. 8.3 and 8.10.)

- Are the ranges of physical variables large enough to guarantee that I can rely on the correlation for the full range of dimensionless groups that it purports to embrace?
- Am I looking at a primary or secondary source (i.e., is this the author's original presentation or someone's report of the original)? If it is a secondary source, have I been given enough information to question it?
- Has the correlation been signed by the persons who formulated it? (If not, why *haven't* the authors taken responsibility for the work?) Has it been subjected to critical review by independent experts in the field?

Problems

7.1 Prove that in fully developed laminar pipe flow, $(-dp/dx)R^2/4\mu$ is twice the average velocity in the pipe. To do this, set the mass flow rate through the pipe equal to (ρu_{av})(area).

7.2 A flow of air at 27°C and 1 atm is hydrodynamically fully developed in a 1 cm I.D. pipe with $u_{\text{av}} = 2$ m/s. Plot (to scale) T_w, q_w, and T_b as a function of the distance x after T_w is changed or q_w is imposed:

a. In the case for which $T_w = 68.4$°C = constant.

b. In the case for which $q_w = 378$ W/m^2 = constant.

Indicate x_{e_t} on your graphs.

7.3 Prove that C_f is $16/\text{Re}_D$ in fully developed laminar pipe flow.

7.4 Air at 200°C flows at 4 m/s over a 3 cm O.D. pipe that is kept at 240°C. (a) Find $\overline{h}$. (b) If the flow were pressurized water at 200°C, what velocities would give the same $\overline{h}$, the same $\overline{\text{Nu}}_D$, and the same Re_D? (c) If someone asked if you could model the water flow with an air experiment, how would you answer? [$u_\infty = 0.0156$ m/s for same $\overline{\text{Nu}}_D$.]

7.5 Compare the h value calculated in Example 7.3 with those calculated from the Dittus-Boelter, Colburn, and Sieder-Tate equations. Comment on the comparison.

7.6 Water at $T_{b_{\text{local}}} = 10°\text{C}$ flows in a 3 cm I.D. pipe at 1 m/s. The pipe walls are kept at 70°C and the flow is fully developed. Evaluate h and the local value of dT_b/dx at the point of interest. The relative roughness is 0.001.

7.7 Water at 10°C flows over a 3 cm O.D. cylinder at 70°C. The velocity is 1 m/s. Evaluate $\overline{h}$.

7.8 Consider the hot wire anemometer in Example 7.5. Suppose that 17.8 W/m is the constant heat input, and plot u_∞ vs. T_{wire} over a reasonable range of variables. Must you deal with any changes in the flow regime over the range of interest?

7.9 Water at 20°C flows at 2 m/s over a 2 m length of pipe, 10 cm in diameter, at 60°C. Compare $\overline{h}$ for flow normal to the pipe with that for flow parallel to the pipe. What does the comparison suggest about baffling in a heat exchanger?

7.10 A thermally fully developed flow of NaK in a 5 cm I.D. pipe moves at $u_{\text{av}} = 8$ m/s. If $T_b = 395°\text{C}$ and T_w is constant at 403°C, what is the local heat transfer coefficient? Is the flow laminar or turbulent?

7.11 Water enters a 7 cm I.D. pipe at 5°C and moves through it at an average speed of 0.86 m/s. The pipe wall is kept at 73°C. Plot T_b against the position in the pipe until $(T_w - T_b)/68 = 0.01$. Neglect the entry problem and consider property variations.

7.12 Air at 20°C flows over a very large bank of 2 cm O.D. tubes that are kept at 100°C. The air approaches at an angle 15° off normal to the tubes. The tube array is staggered, with $S_L = 3.5$ cm and $S_T = 2.8$ cm. Find $\overline{h}$ on the first tubes and on the tubes deep in the array if the air velocity is 4.3 m/s before it enters the array. [$\overline{h}_{\text{deep}} = 118$ W/m^{2}K.]

7.13 Rework Problem 7.11 using a single value of $\overline{h}$ evaluated at $3(73 - 5)/4 = 51°\text{C}$ and treating the pipe as a heat exchanger. At what length would you judge that the pipe is no longer efficient as an exchanger? Explain.

7.14 Go to the periodical engineering literature in your library. Find a correlation of heat transfer data. Evaluate the applicability of the correlation according to the criteria outlined in Section 7.7.

7.15 Water at 24°C flows at 0.8 m/s in a smooth, 1.5 cm I.D. tube that is kept at 27°C. The system is extremely clean and quiet, and the flow stays laminar until a noisy air compressor is turned on in the laboratory. Then it suddenly goes turbulent. Calculate the ratio of the turbulent h to the laminar h. [$h_{\text{turb}} = 4429\ \text{W/m}^2\text{K}$.]

7.16 Laboratory observations of heat transfer during the forced flow of air at 27°C over a bluff body, 12 cm wide, kept at 77°C yield $q = 646\ \text{W/m}^2$ when the air moves 2 m/s and $q = 3590\ \text{W/m}^2$ when it moves 18 m/s. In another test, everything else is the same, but now 17°C water flowing 0.4 m/s yields 131,000 W/m^2. The correlations in Chapter 7 suggest that, with such limited data, we can probably create a fairly good correlation in the form: $\overline{\text{Nu}}_L = C\text{Re}^a\text{Pr}^b$. Estimate the constants C, a, and b by cross-plotting the data on log-log paper.

7.17 Air at 200 psia flows at 12 m/s in an 11 cm I.D. duct. Its bulk temperature is 40°C and the pipe wall is at 268°C. Evaluate h if $\varepsilon/D = 0.00006$.

7.18 How does $\overline{h}$ during cross flow over a cylindrical heat vary with the diameter when Re_D is very large?

7.19 Air enters a 0.8 cm I.D. tube at 20°C with an average velocity of 0.8 m/s. The tube wall is kept at 40°C. Plot $T_b(x)$ until it reaches 39°C. Use properties evaluated at $[(20 + 40)/2]$°C for the whole problem, but report the local error in h at the end to get a sense of the error incurred by the simplification.

7.20 Write Re_D in terms of $\dot{m}$ in pipe flow and explain why this representation could be particularly useful in dealing with compressible pipe flows.

7.21 NaK at 394°C flows at 0.57 m/s across a 1.82 m length of 0.036 m O.D. tube. The tube is kept at 404°C. Find $\overline{h}$ and the heat removal rate from the tube.

7.22 Verify the value of h specified in Problem 3.22.

7.23 Check the value of h given in Example 7.3 by using Reynolds's analogy *directly* to calculate it. Which h do you deem to be in error, and by what percent?

7.24 A homemade heat exchanger consists of a copper plate, 0.5 m square, with 201.5 cm I.D. copper tubes soldered to it. The ten tubes on top are evenly spaced across the top and parallel with two sides. The ten on the bottom are also evenly spaced, but they run at 90° to the top tubes. The exchanger is used to cool methanol flowing at 0.48 m/s in the tubes from an initial temperature of 73°C, using water flowing at 0.91 m/s and entering at 7°C. What is the temperature of the methanol when it is mixed in a header on the outlet side? Make a judgement of the heat exchanger.

7.25 Given that $\overline{\text{Nu}}_D = 12.7$ at $(2/\text{Gz}) = 0.004$, evaluate $\overline{\text{Nu}}_D$ at $(2/\text{Gz}) = 0.02$ numerically, using Fig. 7.4. Compare the result with the value you read from the figure.

7.26 Report the maximum percent scatter of data in Fig. 7.12. What is happening in the fluid flow when the scatter is worst?

7.27 Water at 27°C flows at 2.2 m/s in a 0.04 m I.D. thin-walled pipe. Air at 227°C flows across it at 7.6 m/s. Find the pipe wall temperature.

7.28 Freshly painted aluminum rods, 0.02 m in diameter, are withdrawn from a drying oven at 150°C and cooled in a 3 m/s cross flow of air at 23°C. How long will it take to cool them to 50°C so that they can be handled?

7.29 At what speed, u_∞, must 20°C air flow across an insulated tube before the insulation on it will do any good? The tube is at 60°C and is 6 mm in diameter. The insulation is 12 mm in diameter, with $k = 0.08$ W/m·K. (Notice that we do *not* ask for the u_∞ for which the insulation will do the most harm.)

7.30 Water at 37°C flows at 3 m/s across at 6 cm O.D. tube that is held at 97°C. In a second configuration, 37°C water flows at an average velocity of 3 m/s through a bundle of 6 cm O.D. tubes that are held at 97°C. The bundle is staggered, with $S_T/S_L = 2$. Compare the heat transfer coefficients for the two situations.

7.31 It is proposed to cool 64°C air as it flows, fully developed, in a 1 m length of 8 cm I.D. smooth, thin-walled tubing. The coolant is Freon 12 flowing, fully developed, in the opposite direction, in eight smooth 1 cm I.D. tubes equally spaced around the periphery of the large tube. The Freon enters at −15°C and is fully developed over almost the entire length. The average speeds are 30 m/s for the air and 0.5 m/s for the Freon. Determine the exiting air temperature, assuming that soldering provides perfect thermal contact between the entire surface of the small tubes and the surface of the large tube. Criticize the heat exchanger design and propose some design improvement.

7.32 Evaluate $\overline{\mathrm{Nu}}_D$ using Giedt's data for air flowing over a cylinder at $\mathrm{Re}_D = 140,000$. Compare your result with the appropriate correlation and with Fig. 7.12.

7.33 A 25 mph wind blows across a 0.25 in. telephone line. What is the pitch of the hum that it emits?

7.34 A large Nichrome V slab, 0.2 m thick, has two parallel 1 cm I.D. holes drilled through it. Their centers are 8 cm apart. One carries liquid CO_2 at 1.2 m/s from a −13°C reservoir below. The other carries methanol at 1.9 m/s from a 47°C reservoir above. Take account of the intervening Nichrome and compute the heat transfer. Need we worry about the CO_2 being warmed up by the methanol?

7.35 Consider the situation described in Problem 4.38 but suppose that you do not know $\overline{h}$. Suppose, instead, that you know there is a 10 m/s cross flow of 27°C air over the rod. Then rework the problem.

7.36 A liquid whose properties are not known flows across a 40 cm O.D. tube at 20 m/s. The measured heat transfer coefficient is 8000 W/m^{2}K. We can be fairly confident that Re_D is very large indeed. What would $\overline{h}$ be if D were 53 cm? What would $\overline{h}$ be if u_∞ were 28 m/s?

7.37 Water flows at 4 m/s, at a temperature of 100°C, in a 6 cm I.D. thin-walled tube with a 2 cm layer of 85% magnesia insulation on it. The outside heat transfer coefficient is 6 W/m^{2}K, and the outside temperature is 20°C. Find: (a) U based on the inside

area, (b) Q W/m, and (c) the temperature on either side of the insulation.

7.38 Glycerin is added to water in a mixing tank at 20°C. The mixture discharges through a 4 m length of 0.04 m I.D. tubing under a constant 3 m head. Plot the discharge rate in m^3/hr as a function of composition.

7.39 Plot $\overline{h}$ as a function of composition for the discharge pipe in Problem 7.38. Assume a small temperature difference.

7.40 Rework Problem 5.40 without assuming the Bi number to be very large.

7.41 Water enters a 0.5 cm I.D. pipe at 24°C. The pipe walls are held at 30°C. Plot T_b against distance from entry if u_{av} is 0.27 m/s, neglecting entry behavior in your calculation. (Indicate the entry region on your graph, however.)

7.42 Devise a numerical method to find the velocity distribution and friction factor for laminar flow in a square duct of side length a. Set up a square grid of size N by N and solve the difference equations by hand for $N = 2$, 3, and 4. *Hint*: First show that the velocity distribution is given by the solution to the equation

$$\frac{\partial^2 \overline{u}}{\partial \overline{x}^2} + \frac{\partial^2 \overline{u}}{\partial \overline{y}^2} = 1$$

where $u = 0$ on the sides of the square and we define $\overline{u} = u/[(a^2/\mu)(dp/dz)]$, $\overline{x} = (x/a)$, and $\overline{y} = (y/a)$. Then show that the friction factor, f [eqn. (7.33)], is given by

$$f = \frac{-2}{\dfrac{\rho u_{av} a}{\mu} \iint \overline{u}\, d\overline{x} d\overline{y}}$$

Note that the area integral can be evaluated as $\sum \overline{u}/N^2$.

References

[7.1] F. M. White. *Viscous Fluid Flow*. McGraw-Hill Book Company, New York, 1974.

[7.2] W. M. Kays and M. E. Crawford. *Convective Heat and Mass Transfer*. McGraw-Hill Book Company, New York, 3rd edition, 1993. Coverage is mainly of boundary layers and internal flows.

[7.3] R. K. Shah and M. S. Bhatti. Laminar convective heat transfer in ducts. In S. Kakaç, R. K. Shah, and W. Aung, editors, *Handbook of Single-Phase Convective Heat Transfer*, chapter 3. Wiley-Interscience, New York, 1987.

[7.4] R. K. Shah and A. L. London. *Laminar Flow Forced Convection in Ducts*. Academic Press, Inc., New York, 1978. Supplement 1 to the series *Advances in Heat Transfer*.

[7.5] L. Graetz. Über die wärmeleitfähigkeit von flüssigkeiten. *Ann. Phys.*, 25:337, 1885.

[7.6] S. R. Sellars, M. Tribus, and J. S. Klein. Heat transfer to laminar flow in a round tube or a flat plate—the Graetz problem extended. *Trans. ASME*, 78:441–448, 1956.

[7.7] F. Kreith. *Principles of Heat Transfer*. Intext Press, inc., New York, 3rd edition, 1973.

[7.8] A. P. Colburn. A method of correlating forced convection heat transfer data and a comparison with fluid friction. *Trans. AIChE*, 29:174, 1933.

[7.9] L. M. K. Boelter, V. H. Cherry, H. A. Johnson, and R. C. Martinelli. *Heat Transfer Notes*. McGraw-Hill Book Company, New York, 1965. Originally issued as class notes at the University of California at Berkeley between 1932 and 1941.

[7.10] E. N. Sieder and G. E. Tate. Heat transfer and pressure drop of liquids in tubes. *Ind. Eng. Chem.*, 28:1429, 1936.

[7.11] B. S. Petukhov. Heat transfer and friction in turbulent pipe flow with variable physical properties. In T.F. Irvine, Jr. and J. P. Hartnett, editors, *Advances in Heat Transfer*, volume 6, pages 504–564. Academic Press, Inc., New York, 1970.

[7.12] V. Gnielinski. New equations for heat and mass transfer in turbulent pipe and channel flow. *Int. Chemical Engineering*, 16:359–368, 1976.

[7.13] B. Lubarsky and S. J. Kaufman. Review of experimental investigations of liquid-metal heat transfer. NACA Tech. Note 3336, 1955.

[7.14] C. B. Reed. Convective heat transfer in liquid metals. In S. Kakaç, R. K. Shah, and W. Aung, editors, *Handbook of Single-Phase Convective Heat Transfer*, chapter 8. Wiley-Interscience, New York, 1987.

[7.15] R. A. Seban and T. T. Shimazaki. Heat transfer to a fluid flowing turbulently in a smooth pipe with walls at a constant temperature. *Trans. ASME*, 73:803, 1951.

[7.16] R. N. Lyon, editor. *Liquid Metals Handbook*. A.E.C. and Dept. of the Navy, Washington, D.C., 3rd edition, 1952.

[7.17] J. H. Lienhard. Synopsis of lift, drag, and vortex frequency data for rigid circular cylinders. Bull. 300. Wash. State Univ., Pullman, 1966.

[7.18] W. H. Giedt. Investigation of variation of point unit-heat-transfer coefficient around a cylinder normal to an air stream. *Trans. ASME*, 71:375–381, 1949.

[7.19] S. W. Churchill and M. Bernstein. A correlating equation for forced convection from gases and liquids to a circular cylinder in crossflow. *J. Heat Transfer, Trans. ASME, Ser. C*, 99:300–306, 1977.

[7.20] S. Nakai and T. Okazaki. Heat transfer from a horizontal circular wire at small Reynolds and Grashof numbers—1 pure convection. *Int. J. Heat Mass Transfer*, 18:387–396, 1975.

[7.21] A. Žukauskas. Heat transfer from tubes in crossflow. In T.F. Irvine, Jr. and J. P. Hartnett, editors, *Advances in Heat Transfer*, volume 8, pages 93–160. Academic Press, Inc., New York, 1972.

[7.22] S. Kalish and O. E. Dwyer. Heat transfer to NaK flowing through unbaffled rod bundles. *Int. J. Heat Mass Transfer*, 10:1533–1558, 1967.

[7.23] W. M. Rohsenow, J. P. Hartnett, and Y. I. Cho, editors. *Handbook of Heat Transfer*. McGraw-Hill, New York, 3rd edition, 1998.

8. Natural convection in single-phase fluids and during film condensation

There is a natural place for everything to seek, as:
Heavy things go downward, fire upward, and rivers to the sea.
The Anatomy of Melancholy, **R. Burton, 1621**

8.1 Scope

The remaining convection mechanisms that we deal with are to a large degree gravity-driven. Unlike forced convection, in which the driving force is external to the fluid, these so-called natural convection processes are driven by body forces exerted directly within the fluid as the result of heating or cooling. Two such mechanisms that are rather alike are:

- *Natural convection.* When we speak of natural convection without any qualifying words, we mean natural convection in a single-phase fluid.

- *Film condensation.* This natural convection process has much in common with single-phase natural convection.

We therefore deal with both mechanisms in this chapter. The governing equations are developed side by side in two brief opening sections. Then each mechanism is developed independently in Sections 8.3 and 8.4 and in Section 8.5, respectively.

Chapter 9 deals with other natural convection heat transfer processes that involve phase change—for example:

- *Nucleate boiling.* This heat transfer process is highly disordered as opposed to the processes described in Chapter 8.
- *Film boiling.* This is so similar to film condensation that it is usually treated by simply modifying film condensation predictions.
- *Dropwise condensation.* This bears some similarity to nucleate boiling.

8.2 The nature of the problems of film condensation and of natural convection

Description

The natural convection problem is sketched in its simplest form on the left-hand side of Fig. 8.1. Here we see a vertical isothermal plate that cools the fluid adjacent to it. The cooled fluid sinks downward to form a b.l. The figure would be inverted if the plate were warmer than the fluid next to it. Then the fluid would buoy upward.

On the right-hand side of Fig. 8.1 is the corresponding film condensation problem in its simplest form. An isothermal vertical plate cools an adjacent vapor, which condenses and forms a liquid film on the wall.[1] The film is normally very thin and it flows off, rather like a b.l., as the figure suggests. While natural convection can carry fluid either upward or downward, a condensate film can only move downward. The temperature in the film rises from T_w at the cool wall to T_{sat} at the outer edge of the film.

In both problems, but particularly in film condensation, the b.l. and the film are normally thin enough to accommodate the b.l. assumptions [recall the discussion following eqn. (6.13)]. A second idiosyncrasy of both problems is that δ and δ_t are closely related. In the condensing film they are equal, since the edge of the condensate film forms the edge of both b.l.'s. In natural convection, δ and δ_t are approximately equal when Pr is on the order of unity or less, because all cooled (or heated) fluid must buoy downward (or upward). When Pr is large, the cooled (or heated) fluid will fall (or rise) and, although it is all very close to the wall, this fluid, with its high viscosity, will also drag unheated liquid with it.

[1] It might instead condense into individual droplets, which roll of without forming into a film. This process, called *dropwise condensation*, is dealt with in Section 9.10.

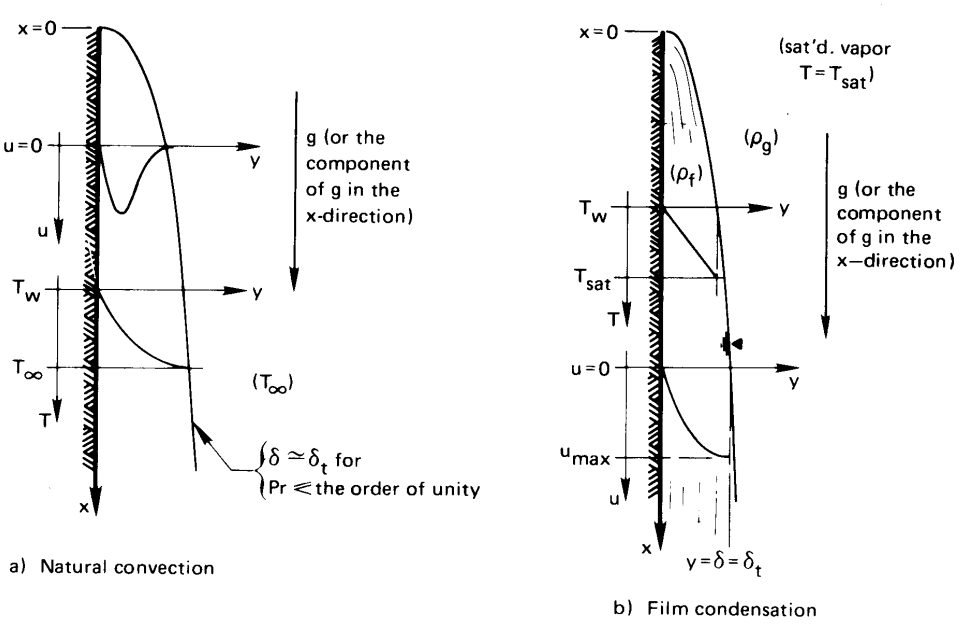

Figure 8.1 The convective boundary layers for natural convection and film condensation. In both sketches, but particularly in that for film condensation, the y-coordinate has been stretched.

In this case, δ can exceed δ_t. We deal with cases for which $\delta \cong \delta_t$ in the subsequent analysis.

Governing equations

To describe laminar film condensation and laminar natural convection, we must add a gravity term to the momentum equation. The dimensions of the terms in the momentum equation should be examined before we do this. Equation (6.13) can be written as

$$\left(u\frac{\partial u}{\partial x}+v\frac{\partial u}{\partial y}\right)\underbrace{\frac{\mathrm{m}}{\mathrm{s}^2}}_{=\frac{\mathrm{kg}\cdot\mathrm{m}}{\mathrm{kg}\cdot\mathrm{s}^2}=\frac{\mathrm{N}}{\mathrm{kg}}}=-\frac{1}{\rho}\frac{dp}{dx}\underbrace{\frac{\mathrm{m}^3}{\mathrm{kg}}\frac{\mathrm{N}}{\mathrm{m}^2\cdot\mathrm{m}}}_{=\frac{\mathrm{N}}{\mathrm{kg}}}+\nu\frac{\partial^2 u}{\partial y^2}\underbrace{\frac{\mathrm{m}^2}{\mathrm{s}}\frac{\mathrm{m}}{\mathrm{s}\cdot\mathrm{m}^2}}_{=\frac{\mathrm{m}}{\mathrm{s}^2}=\frac{\mathrm{N}}{\mathrm{kg}}}$$

where $\partial p/\partial x \simeq dp/dx$ in the b.l. and where $\mu \simeq$ constant. Thus, every term in the equation has units of acceleration or (equivalently) force per unit mass. The component of gravity in the x-direction therefore enters

the momentum balance as $(+g)$. This is because x and g point in the same direction. Gravity would enter as $-g$ if it acted opposite the x-direction.

$$u\frac{\partial u}{\partial x} + v\frac{\partial u}{\partial y} = -\frac{1}{\rho}\frac{dp}{dx} + g + \nu\frac{\partial^2 u}{\partial y^2} \tag{8.1}$$

In the two problems at hand, the pressure gradient is the hydrostatic gradient outside the b.l. Thus,

$$\underbrace{\frac{dp}{dx} = \rho_\infty g}_{\substack{\text{natural}\\ \text{convection}}} \qquad \underbrace{\frac{dp}{dx} = \rho_g g}_{\substack{\text{film}\\ \text{condensation}}} \tag{8.2}$$

where ρ_∞ is the density of the undisturbed fluid and ρ_g (and ρ_f below) are the saturated vapor and liquid densities. Equation (8.1) then becomes

$$u\frac{\partial u}{\partial x} + v\frac{\partial u}{\partial y} = \left(1 - \frac{\rho_\infty}{\rho}\right) g + \nu\frac{\partial^2 u}{\partial y^2} \qquad \text{for natural convection} \tag{8.3}$$

$$u\frac{\partial u}{\partial x} + v\frac{\partial u}{\partial y} = \left(1 - \frac{\rho_g}{\rho_f}\right) g + \nu\frac{\partial^2 u}{\partial y^2} \qquad \text{for film condensation} \tag{8.4}$$

Two boundary conditions, which apply to *both* problems, are

$$\left.\begin{aligned} u\,(y=0) &= 0 \quad \text{the no-slip condition}\\ v\,(y=0) &= 0 \quad \text{no flow into the wall}\end{aligned}\right\} \tag{8.5a}$$

The third b.c. is different for the film condensation and natural convection problems:

$$\left.\begin{aligned} \left.\frac{\partial u}{\partial y}\right|_{y=\delta} &= 0 \quad \begin{array}{l}\text{condensation:}\\ \text{no shear at the edge of the film}\end{array}\\ u\,(y=\delta) &= 0 \quad \begin{array}{l}\text{natural convection:}\\ \text{undisturbed fluid outside the b.l.}\end{array}\end{aligned}\right\} \tag{8.5b}$$

The energy equation for either of the two cases is eqn. (6.40):

$$u\frac{\partial T}{\partial x} + v\frac{\partial T}{\partial y} = \alpha\frac{\partial^2 T}{\partial y^2}$$

We leave the identification of the b.c.'s for temperature until later.

The crucial thing we must recognize about the momentum equation at the moment is that it is coupled to the energy equation. Let us consider how that occurs:

In natural convection: The velocity, u, is driven by buoyancy, which is reflected in the term $(1 - \rho_\infty/\rho)g$ in the momentum equation. The density, $\rho = \rho(T)$, varies with T, so it is impossible to solve the momentum and energy equations independently of one another.

In film condensation: The third boundary condition (8.5b) for the momentum equation involves the film thickness, δ. But to calculate δ we must make an energy balance on the film to find out how much latent heat—and thus how much condensate—it has absorbed. This will bring $(T_{\text{sat}} - T_w)$ into the solution of the momentum equation.

Recall that the boundary layer on a flat surface, during forced convection, was easy to analyze because the momentum equation could be solved completely before any consideration of the energy equation was attempted. We do not have that advantage in predicting natural convection or film condensation.

8.3 Laminar natural convection on a vertical isothermal surface

Dimensional analysis and experimental data

Before we attempt a dimensional analysis of the natural convection problem, let us simplify the buoyancy term, $(\rho - \rho_\infty)g/\rho$, in the momentum equation (8.3). The equation was derived for incompressible flow, but we modified it by admitting a small variation of density with temperature in this term only. Now we wish to eliminate $(\rho - \rho_\infty)$ in favor of $(T - T_\infty)$ with the help of the coefficient of thermal expansion, β:

$$\beta \equiv \frac{1}{v}\left.\frac{\partial v}{\partial T}\right|_p = -\frac{1}{\rho}\left.\frac{\partial \rho}{\partial T}\right|_p \simeq -\frac{1}{\rho}\frac{\rho - \rho_\infty}{T - T_\infty} = -\frac{(1 - \rho_\infty/\rho)}{T - T_\infty} \tag{8.6}$$

where v designates the specific volume here, not a velocity component.

Figure 8.2 shows natural convection from a vertical surface that is hotter than its surroundings. In either this case or on the cold plate shown in Fig. 8.1, we replace $(1 - \rho_\infty/\rho)g$ with $-g\beta(T - T_\infty)$. The sign (see Fig. 8.2) is the same in either case. Then

$$u\frac{\partial u}{\partial x} + v\frac{\partial u}{\partial y} = -g\beta(T - T_\infty) + \nu\frac{\partial^2 u}{\partial y^2} \tag{8.7}$$

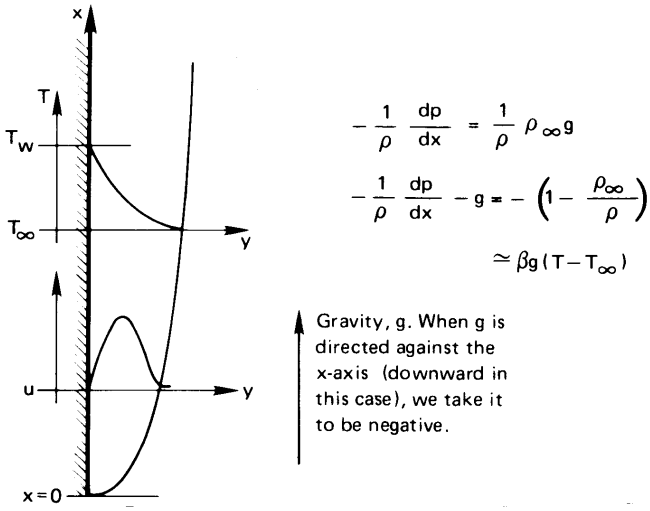

Figure 8.2 Natural convection from a vertical heated plate.

where the minus sign corresponds to plate orientation in Fig. 8.1a. This conveniently removes ρ from the equation and makes the coupling of the momentum and energy equations very clear.

The functional equation for the heat transfer coefficient, h, in natural convection is therefore (cf. Section 6.4)

$$h \text{ or } \overline{h} = \text{fn}\,(k, |T_w - T_\infty|, x \text{ or } L, \nu, \alpha, g, \beta)$$

where L is a length that must be specified for a given problem. Notice that while h was assumed to be independent of ΔT in the forced convection problem (Section 6.4), the explicit appearance of $(T - T_\infty)$ in eqn. (8.7) suggests that we cannot make that assumption here. There are thus eight variables in W, m, s, and °C (where we again regard J as a unit independent of N and m); so we look for $8-4 = 4$ pi-groups. For $\overline{h}$ and a characteristic length, L, the groups may be chosen as

$$\overline{\text{Nu}}_L \equiv \frac{\overline{h}L}{k}, \qquad \text{Pr} \equiv \frac{\nu}{\alpha}, \qquad \Pi_3 \equiv \frac{L^3}{\nu^2}\,|g|\,, \qquad \Pi_4 \equiv \beta\,|T_w - T_\infty| = \beta\,\Delta T$$

where we set $\Delta T \equiv |T_w - T_\infty|$. Two of these groups are new to us:

- $\Pi_3 \equiv gL^3/\nu^2$: This characterizes the importance of buoyant forces relative to viscous forces.[2]

[2]Note that gL is dimensionally the same as a velocity squared—say, u^2. Then $\sqrt{\Pi_3}$ can be interpreted as a Reynolds number: uL/ν. In a laminar b.l. we recall that $\text{Nu} \propto \text{Re}^{1/2}$; so here we expect that $\text{Nu} \propto \Pi_3^{1/4}$.

- $\Pi_4 \equiv \beta\Delta T$: This characterizes the thermal expansion of the fluid. For an ideal gas,

$$\beta = \frac{1}{v}\frac{\partial}{\partial T}\left(\frac{RT}{p}\right)_p = \frac{1}{T_\infty}$$

where R is the gas constant. Therefore, for ideal gases

$$\beta\,\Delta T = \frac{\Delta T}{T_\infty} \tag{8.8}$$

It turns out that Π_3 and Π_4 (which do not bear the names of famous people) usually appear as a product. This product is called the Grashof (pronounced Gráhs-hoff) number,[3] Gr_L, where the subscript designates the length on which it is based:

$$\Pi_3\Pi_4 \equiv \mathrm{Gr}_L = \frac{g\beta\Delta T L^3}{\nu^2} \tag{8.9}$$

Two exceptions in which Π_3 and Π_4 appear independently are rotating systems (where Coriolis forces are part of the body force) and situations in which $\beta\Delta T$ is no longer $\ll 1$ but instead approaches unity. We therefore expect to correlate data in most other situations with functional equations of the form

$$\mathrm{Nu} = \mathrm{fn}(\mathrm{Gr}, \mathrm{Pr}) \tag{8.10}$$

Another attribute of the dimensionless functional equation is that the primary independent variable is usually the product of Gr and Pr. This is called the Rayleigh number, Ra_L, where the subscript designates the length on which it is based:

$$\mathrm{Ra}_L \equiv \mathrm{Gr}_L\mathrm{Pr} = \frac{g\beta\Delta T L^3}{\alpha\nu} \tag{8.11}$$

[3] Nu, Pr, Π_3, Π_4, and Gr were all suggested by Nusselt in his pioneering paper on convective heat transfer [8.1]. Grashof was a notable nineteenth-century mechanical engineering professor who was simply given the honor of having a dimensionless group named after him posthumously (see, e.g., [8.2]). He did not work with natural convection.

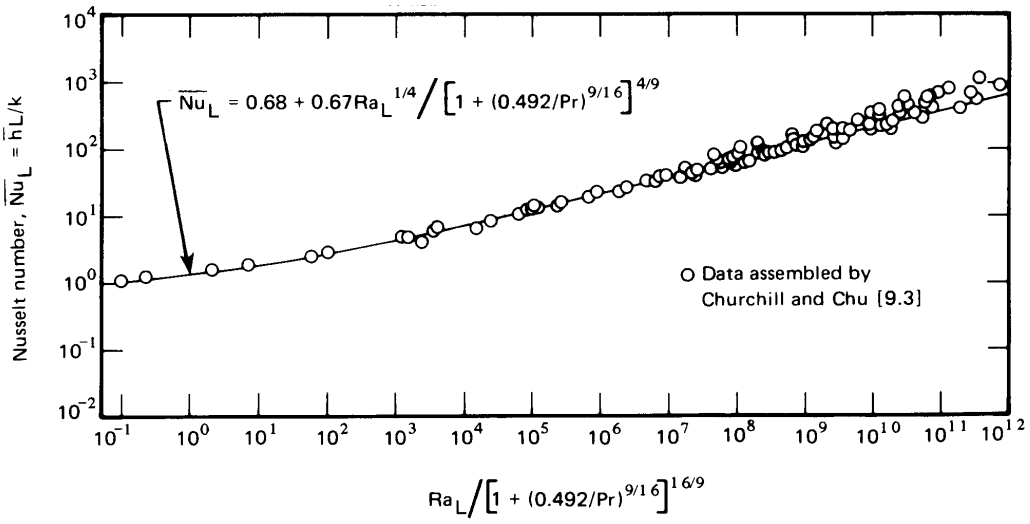
$\overline{Nu}_L = 0.68 + 0.67Ra_L^{1/4} / \left[1 + (0.492/Pr)^{9/16}\right]^{4/9}$
O Data assembled by Churchill and Chu [9.3]
Nusselt number, $\overline{Nu}_L = \bar{h}L/k$
$Ra_L / \left[1 + (0.492/Pr)^{9/16}\right]^{16/9}$

Figure 8.3 The correlation of $\bar{h}$ data for vertical isothermal surfaces by Churchill and Chu [8.3], using $\mathrm{Nu}_L = \mathrm{fn}(\mathrm{Ra}_L, \mathrm{Pr})$. (Applies to full range of Pr.)

Thus, most (but not all) analyses and correlations of natural convection yield

$$\mathrm{Nu} = \mathrm{fn}(\underbrace{\mathrm{Ra}}_{\text{primary (or most important) independent variable}}, \underbrace{\mathrm{Pr}}_{\text{secondary parameter}}) \tag{8.12}$$

Figure 8.3 is a careful selection of the best data available for natural convection from vertical isothermal surfaces. These data were organized by Churchill and Chu [8.3] and they span 13 orders of magnitude of the Rayleigh number. The correlation of these data in the coordinates of Fig. 8.2 is exactly in the form of eqn. (8.12), and it brings to light the dominant influence of Ra_L, while any influence of Pr is small.

The data correlate on these coordinates within a few percent up to $\mathrm{Ra}_L/[1+(0.492/\mathrm{Pr}^{9/16})]^{16/9} \simeq 10^8$. That is about where the b.l. starts exhibiting turbulent behavior. Beyond that point, the overall Nusselt number, Nu_L, rises more sharply, and the data scatter increases somewhat because the heat transfer mechanisms change.

Prediction of h in natural convection on a vertical surface

The analysis of natural convection using an integral method was done independently by Squire (see [8.4]) and by Eckert [8.5] in the 1930s. We shall refer to this important development as the Squire-Eckert formulation.

The analysis begins with the integrated momentum and energy equations. We assume $\delta = \delta_t$ and integrate both equations to the same value of δ:

$$\frac{d}{dx}\int_0^\delta \Big(u^2 - \underbrace{uu_\infty}_{\substack{=0,\ \text{since}\\ u_\infty = 0}}\Big)dy = -\nu \left.\frac{\partial u}{\partial y}\right|_{y=0} + g\beta \int_0^\delta (T - T_\infty)\, dy \qquad (8.13)$$

and [eqn. (6.47)]

$$\frac{d}{dx}\int_0^\delta u\,(T - T_\infty)\, dy = \frac{q_w}{\rho c_p} = -\alpha \left.\frac{\partial T}{\partial y}\right|_{y=0}$$

The integrated momentum equation is the same as eqn. (6.24) except that it includes the buoyancy term, which was added to the differential momentum equation in eqn. (8.7).

We now must estimate the temperature and velocity profiles for use in eqns. (8.13) and (6.47). This is done here in much the same way as it was done in Sections 6.2 and 6.3 for forced convection. We write down a set of known facts about the profiles and then use these things to evaluate the constants in power-series expressions for u and T.

Since the temperature profile has a fairly simple shape, a simple quadratic expression can be used:

$$\frac{T - T_\infty}{T_w - T_\infty} = a + b\left(\frac{y}{\delta}\right) + c\left(\frac{y}{\delta}\right)^2 \qquad (8.14)$$

Notice that the thermal boundary layer thickness, δ_t, is assumed equal to δ in eqn. (8.14). This would seemingly limit the results to Prandtl numbers not too much larger than unity. Actually, the analysis will also prove useful for large Pr's because the velocity profile exerts diminishing influence on the temperature profile as Pr increases. We require the following

things to be true of this profile:

- $T(y=0) = T_w$ or $\left.\dfrac{T-T_\infty}{T_w-T_\infty}\right|_{y/\delta=0} = 1 = a$
- $T(y=\delta) = T_\infty$ or $\left.\dfrac{T-T_\infty}{T_w-T_\infty}\right|_{y/\delta=1} = 0 = 1+b+c$
- $\left.\dfrac{\partial T}{\partial y}\right|_{y=\delta} = 0$ or $\dfrac{d}{d(y/\delta)}\left(\dfrac{T-T_\infty}{T_w-T_\infty}\right)_{y/\delta=1} = 0 = b+2c$

so $a = 1$, $b = -2$, and $c = 1$. This gives the following dimensionless temperature profile:

$$\frac{T-T_\infty}{T_w-T_\infty} = 1 - 2\left(\frac{y}{\delta}\right) + \left(\frac{y}{\delta}\right)^2 = \left(1-\frac{y}{\delta}\right)^2 \tag{8.15}$$

We anticipate a somewhat complicated velocity profile (recall Fig. 8.1) and seek to represent it with a cubic function:

$$u = u_c(x)\left[\left(\frac{y}{\delta}\right) + c\left(\frac{y}{\delta}\right)^2 + d\left(\frac{y}{\delta}\right)^3\right] \tag{8.16}$$

where, since there is no obvious characteristic velocity in the problem, we write u_c as an as-yet-unknown function. (u_c will have to increase with x, since u must increase with x.) We know three things about u:

- $u(y=0) = 0$ { we have already satisfied this condition by writing eqn. (8.16) with no lead constant
- $u(y=\delta) = 0$ or $\dfrac{u}{u_c} = 0 = (1+c+d)$
- $\left.\dfrac{\partial u}{\partial y}\right|_{y=\delta} = 0$ or $\left.\dfrac{\partial u}{\partial(y/\delta)}\right|_{y/\delta=1} = 0 = (1+2c+3d)\,u_c$

These give $c = -2$ and $d = 1$, so

$$\frac{u}{u_c(x)} = \frac{y}{\delta}\left(1-\frac{y}{\delta}\right)^2 \tag{8.17}$$

We could also have written the momentum equation (8.7) at the wall, where $u = v = 0$, and created a fourth condition:

$$\left.\frac{\partial^2 u}{\partial y^2}\right|_{y=0} = -\frac{g\beta\,(T_w-T_\infty)}{\nu}$$

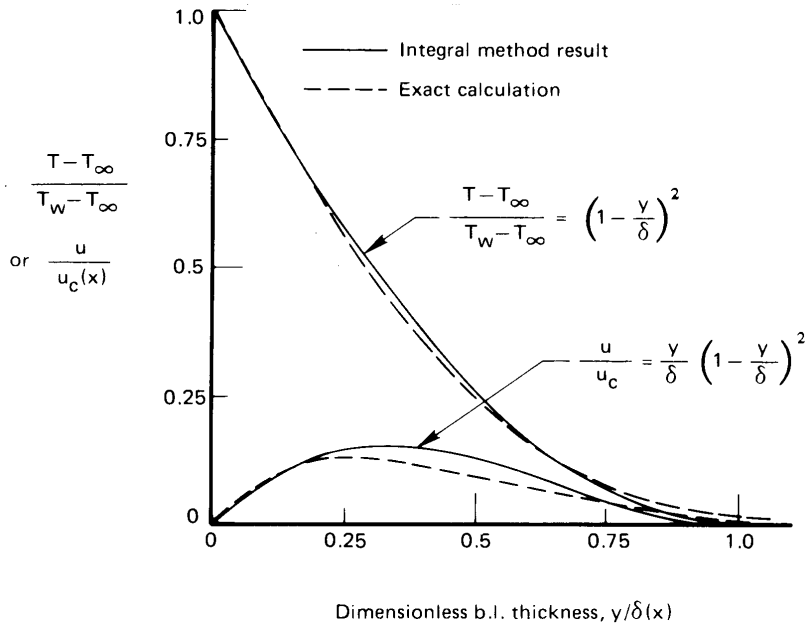

Figure 8.4 The temperature and velocity profiles for air (Pr = 0.7) in a laminar convection b.l.

and then we could have evaluated $u_c(x)$ as $\beta g|T_w - T_\infty|\delta^2/4\nu$. A correct expression for u_c will eventually depend upon these variables, but we will not attempt to make u_c fit this particular condition. Doing so would yield two equations, (8.13) and (6.47), in a single unknown, $\delta(x)$. It would be impossible to satisfy both of them. Instead, we shall allow the velocity profile to violate this condition slightly and write

$$u_c(x) = C_1 \frac{\beta g\,|T_w - T_\infty|}{\nu}\,\delta^2(x) \tag{8.18}$$

Then we shall solve the *two* integrated conservation equations for the two unknowns, C_1 (which should $\simeq$¼) and $\delta(x)$.

The dimensionless temperature and velocity profiles are plotted in Fig. 8.4. With them are included Schmidt and Beckmann's exact calculation for air (Pr = 0.7), as presented in [8.4]. Notice that the integral approximation to the temperature profile is better than the approximation to the velocity profile. That is fortunate, since the temperature profile exerts the major influence in the heat transfer solution.

When we substitute eqns. (8.15) and (8.17) in the momentum equa-

tion (8.13), using eqn. (8.18) for $u_c(x)$, we get

$$C_1^2\left(\frac{g\beta\,|T_w-T_\infty|}{\nu}\right)^2\frac{d}{dx}\left[\delta^5\underbrace{\int_0^1\left(\frac{y}{\delta}\right)^2\left(1-\frac{y}{\delta}\right)^4 d\left(\frac{y}{\delta}\right)}_{=\frac{1}{105}}\right]$$
$$= g\beta\,|T_w-T_\infty|\,\delta\underbrace{\int_0^1\left(1-\frac{y}{\delta}\right)^2 d\left(\frac{y}{\delta}\right)}_{=\frac{1}{3}}$$
$$-C_1 g\beta\,|T_w-T_\infty|\,\delta(x)\underbrace{\frac{\partial}{\partial\,(y/\delta)}\left[\frac{y}{\delta}\left(1-\frac{y}{\delta}\right)^2\right]_{\frac{y}{\delta}=0}}_{=1} \tag{8.19}$$

where we change the sign of the terms on the left by replacing $(T_w - T_\infty)$ with its absolute value. Equation (8.19) then becomes

$$\left(\frac{1}{21}C_1^2\frac{g\beta\,|T_w-T_\infty|}{\nu^2}\right)\delta^3\frac{d\delta}{dx}=\frac{1}{3}-C_1$$

or

$$\frac{d\delta^4}{dx}=\frac{84\left(\frac{1}{3}-C_1\right)}{C_1^2\frac{g\beta\,|T_w-T_\infty|}{\nu^2}}$$

Integrating this with the b.c., $\delta(x=0)=0$, gives

$$\delta^4=\frac{84\left(\frac{1}{3}-C_1\right)}{C_1^2\frac{g\beta\,|T_w-T_\infty|}{\nu^2}x} \tag{8.20}$$

Substituting eqns. (8.15), (8.17), and (8.18) in eqn. (6.47) likewise gives

$$(T_w-T_\infty)\,C_1\frac{g\beta\,|T_w-T_\infty|}{\nu}\frac{d}{dx}\left[\delta^3\underbrace{\int_0^1\frac{y}{\delta}\left(1-\frac{y}{\delta}\right)^4 d\left(\frac{y}{\delta}\right)}_{=\frac{1}{30}}\right]$$
$$=-\alpha\frac{T_w-T_\infty}{\delta}\underbrace{\frac{d}{d(y/\delta)}\left[\left(1-\frac{y}{\delta}\right)^2\right]_{y/\delta=0}}_{=-2}$$

or

$$3\,\frac{C_1}{30}\,\delta^3\frac{d\delta}{dx} = \frac{C_1}{40}\,\frac{d\delta^4}{dx} = \frac{2}{\mathrm{Pr}\,\dfrac{g\beta\,|T_w - T_\infty|}{\nu^2}}$$

Integrating this with the b.c., $\delta(x=0)=0$, we get

$$\delta^4 = \frac{80}{C_1\mathrm{Pr}\,\dfrac{g\beta|T_w - T_\infty|}{\nu^2}}\,x \tag{8.21}$$

Equating eqns. (8.20) and (8.21) for δ^4, we then obtain

$$\frac{21}{20}\,\frac{\dfrac{1}{3} - C_1}{C_1\,\dfrac{g\beta\,|T_w - T_\infty|}{\nu^2}}\,x = \frac{1}{\mathrm{Pr}\,\dfrac{g\beta\,|T_w - T_\infty|}{\nu^2}}\,x$$

or

$$C_1 = \frac{\mathrm{Pr}}{3\left(\dfrac{20}{21} + \mathrm{Pr}\right)} \tag{8.22}$$

Then, from eqn. (8.21):

$$\delta^4 = \frac{240\left(\dfrac{20}{21} + \mathrm{Pr}\right)}{\mathrm{Pr}^2\,\dfrac{g\beta\,|T_w - T_\infty|}{\nu^2}}\,x$$

or

$$\frac{\delta}{x} = 3.936\left(\frac{0.952 + \mathrm{Pr}}{\mathrm{Pr}^2}\right)^{1/4}\frac{1}{\mathrm{Gr}_x^{1/4}} \tag{8.23}$$

Equation (8.23) can be combined with the known temperature profile, eqn. (8.15), and substituted in Fourier's law to find q:

$$q = -k\,\frac{\partial T}{\partial y}\bigg|_{y=0} = -\frac{k(T_w - T_\infty)}{\delta}\underbrace{\left.\frac{d\left(\dfrac{T - T_\infty}{T_w - T_\infty}\right)}{d\left(\dfrac{y}{\delta}\right)}\right|_{y/\delta=0}}_{=-2} = 2\,\frac{k\Delta T}{\delta} \tag{8.24}$$

so, writing $h = q/|T_w - T_\infty| \equiv q/\Delta T$, we obtain[4]

$$\mathrm{Nu}_x \equiv \frac{qx}{\Delta T k} = 2\,\frac{x}{\delta} = \frac{2}{3.936}\,(\mathrm{PrGr}_x)^{1/4}\left(\frac{\mathrm{Pr}}{0.952+\mathrm{Pr}}\right)^{1/4}$$

or

$$\mathrm{Nu}_x = 0.508\,\mathrm{Ra}_x^{1/4}\left(\frac{\mathrm{Pr}}{0.952+\mathrm{Pr}}\right)^{1/4} \tag{8.25}$$

This is the Squire-Eckert result for the local heat transfer from a vertical isothermal wall during laminar natural convection. It applies for either $T_w > T_\infty$ or $T_w < T_\infty$.

The average heat transfer coefficient can be obtained from

$$\overline{h} = \frac{\int_0^L q(x)\,dx}{L\Delta T} = \frac{\int_0^L h(x)\,dx}{L}$$

Thus,

$$\overline{\mathrm{Nu}}_L = \frac{\overline{h}L}{k} = \frac{1}{k}\int_0^L \frac{k}{x}\,\mathrm{Nu}_x\,dx = \frac{4}{3}\,\mathrm{Nu}_x\Big|_{x=L}$$

or

$$\boxed{\overline{\mathrm{Nu}}_L = 0.678\,\mathrm{Ra}_L^{1/4}\left(\frac{\mathrm{Pr}}{0.952+\mathrm{Pr}}\right)^{1/4}} \tag{8.26}$$

All properties in eqn. (8.26) and the preceding equations should be evaluated at $T = (T_w + T_\infty)/2$ except in gases, where β should be evaluated at T_∞.

Example 8.1

A thin-walled metal tank containing fluid at 40°C cools in air at 14°C; $\overline{h}$ is very large inside the tank. If the sides are 0.4 m high, compute $\overline{h}$, $\overline{q}$, and δ at the top. Are the b.l. assumptions reasonable?

SOLUTION.

$\beta_{\mathrm{air}} = 1/T_\infty = 1/(273+14) = 0.00348\ \mathrm{K}^{-1}$. Then

$$\mathrm{Ra}_L = \frac{g\beta\Delta T L^3}{\nu\alpha} = \frac{9.8(0.00348)(40-14)(0.4)^3}{(1.566\times10^{-5})\,(2.203\times10^{-5})} = 1.645\times10^8$$

[4]Recall that, in footnote 2, we anticipated that Nu would vary as $\mathrm{Gr}^{1/4}$. We now see that this is the case.

and Pr = 0.711, where the properties are evaluated at 300 K = 27°C. Then, from eqn. (8.26),

$$\overline{\mathrm{Nu}}_L = 0.678\left(1.645\times 10^8\right)^{1/4}\left(\frac{0.711}{0.952+0.711}\right)^{1/4} = 62.1$$

so

$$\overline{h} = \frac{62.1k}{L} = \frac{62.1(0.02614)}{0.4} = 4.06\ \mathrm{W/m^2K}$$

and

$$\overline{q} = \overline{h}\,\Delta T = 4.06(40-14) = 105.5\ \mathrm{W/m^2}$$

The b.l. thickness at the top of the tank is given by eqn. (8.23) at $x = L$:

$$\frac{\delta}{L} = 3.936\left(\frac{0.952+0.711}{0.711^2}\right)^{1/4}\frac{1}{(\mathrm{Ra}_L/\mathrm{Pr})^{1/4}} = 0.0430$$

Thus, the b.l. thickness at the end of the plate is only 4% of the height, or 1.72 cm thick. This is thicker than typical forced convection b.l.'s, but it is still reasonably thin. ■

Example 8.2

Large thin metal sheets of length L are dipped in an electroplating bath in the vertical position. Their average temperature is initially cooler than the liquid in the bath. How rapidly will they come up to bath temperature?

SOLUTION. We can probably take Bi $\ll 1$ and use the lumped-capacity response equation (1.20). We obtain $\overline{h}$ for use in eqn. (1.20) from eqn. (8.26):

$$\overline{h} = \underbrace{0.678\,\frac{k}{L}\left(\frac{\mathrm{Pr}}{0.952+\mathrm{Pr}}\right)^{1/4}\left(\frac{g\beta L^3}{\alpha\nu}\right)^{1/4}}_{\text{call this } B}\Delta T^{1/4}$$

Since $\overline{h}\propto\Delta T^{1/4}$, eqn. (1.20) becomes

$$\frac{d(T-T_b)}{dt} = -\frac{BA}{\rho cV}(T-T_b)^{5/4}$$

where V/A = the half-thickness of the plate, w. Integrating this between the initial temperature of the plate, T_i, and the temperature at time t, we get

$$\int_{T_i}^{T} \frac{d(T - T_b)}{(T - T_b)^{5/4}} = -\int_0^t \frac{B}{\rho c w}\, dt$$

so

$$T - T_b = \left[\frac{1}{(T_i - T_b)^{1/4}} + \frac{B}{4\rho c w}\, t \right]^{-4}$$

(Before we use this result, we should check $\mathrm{Bi} = Bw\Delta T^{1/4}/k$ to be certain that it is, in fact, less than unity.) The temperature can be put in dimensionless form as

$$\frac{T - T_b}{T_i - T_b} = \left[1 + \frac{B\,(T_i - T_b)^{1/4}}{4\rho c w}\, t \right]^{-4}$$

where the coefficient of t is a kind of inverse time constant of the response. Thus, the temperature dependence of $\overline{h}$ in natural convection leads to a solution quite different from the exponential response that resulted from a constant $\overline{h}$ [eqn. (1.22)]. ■

Comparison of analysis and correlations with experimental data

Churchill and Chu have proposed two equations for the data correlated in Fig. 8.3. The simpler of the two is shown in the figure. It is

$$\overline{\mathrm{Nu}}_L = 0.68 + 0.67\,\mathrm{Ra}_L^{1/4} \left[1 + \left(\frac{0.492}{\mathrm{Pr}} \right)^{9/16} \right]^{-4/9} \tag{8.27}$$

This approaches to within 1.2% of the Squire-Eckert prediction as Pr and Ra_L are increased, and it differs from the prediction by only 5.5% if the fluid is a gas and $\mathrm{Ra}_L > 10^5$. Typical Rayleigh numbers usually exceed 10^5, so we conclude that the Squire–Eckert prediction is remarkably accurate in the range of practical interest, despite the approximations upon which it is built. The additive constant of 0.68 in eqn. (8.27) is required to correct eqn. (8.27) at low Ra_L, where the b.l. assumptions are invalid and $\overline{\mathrm{Nu}}_L$ is no longer proportional to $\mathrm{Ra}_L^{1/4}$.

At low Prandtl numbers, the Squire-Eckert prediction fails and eqn. (8.27) has to be used. In the turbulent regime, $\mathrm{Gr} \gtrsim 10^9$ [8.6], eqn. (8.27)

predicts a lower bound on the data (see Fig. 8.3). It thus gives a conservative estimate in this range, although it is really intended only for laminar boundary layers. In this correlation, as in eqn. (8.26), the thermal properties should all be evaluated at a mean b.l. temperature, except for β, which is to be evaluated at T_∞ if the fluid is a gas.

Example 8.3

Verify the first heat transfer coefficient in Table 1.1. This is for air at 20°C next to a 0.3 m high wall at 50°C.

SOLUTION. At $T = 35°\text{C} = 308$ K, we find Pr $= 0.71$, $\nu = 16.45 \times 10^{-6}\,\text{m}^2/\text{s}$, $\alpha = 0.2318\times10^{-4}\,\text{m}^2/\text{s}$, and $\beta = 1/(273+20) = 0.00341\,\text{K}^{-1}$. Then

$$\text{Ra}_L = \frac{g\beta\Delta T L^3}{\alpha\nu} = \frac{9.8(0.00341)(30)(0.3)^3}{(16.45)(0.2318)10^{-10}} = 7.10\times10^7$$

The Squire-Eckert prediction gives

$$\overline{\text{Nu}_L} = 0.678\left(7.10\times10^7\right)^{1/4}\left(\frac{0.71}{0.952+0.71}\right)^{1/4} = 50.3$$

so

$$\overline{h} = 50.3\,\frac{k}{L} = 50.3\left(\frac{0.0267}{0.3}\right) = 4.48\ \text{W/m}^2\text{K}$$

And the Churchill-Chu correlation gives

$$\overline{\text{Nu}_L} = 0.68 + 0.67\,\frac{(7.10\times10^7)^{1/4}}{\left[1+(0.492/0.71)^{9/16}\right]^{4/9}} = 47.88$$

so

$$\overline{h} = 47.88\left(\frac{0.0267}{0.3}\right) = 4.26\ \text{W/m}^2\text{K}$$

The prediction is therefore within 5% of the correlation. We should use the latter result in preference to the theoretical one, although the difference is slight. ■

Variable-properties problem

Sparrow and Gregg [8.7] provide an extended discussion of the influence of physical property variations on predicted values of Nu. They found that while β for gases should be evaluated at T_∞, all other properties should be evaluated at T_r, where

$$T_r = T_w - C\,(T_w - T_\infty) \tag{8.28}$$

and where $C = 0.38$ for gases. Most books recommend that a simple mean between T_w and T_∞ (or $C = 0.50$) be used. A simple mean seldom differs much from the more precise result above, of course.

It has also been shown by Barrow and Sitharamarao [8.8] that when $\beta\Delta T$ is no longer $\ll 1$, the Squire-Eckert formula should be corrected as follows:

$$\mathrm{Nu} = \mathrm{Nu}_{\mathrm{sq-Ek}}\left[1 + \tfrac{3}{5}\beta\Delta T + \mathcal{O}(\beta\Delta T)^2\right]^{1/4} \tag{8.29}$$

This same correction can be applied to the Churchill-Chu correlation or to other expressions for Nu. Since $\beta = 1/T_\infty$ for an ideal gas, eqn. (8.29) gives only about a 1.5% correction for a 330 K plate heating 300 K air.

Note on the validity of the boundary layer approximations

The boundary layer approximations are sometimes put to a rather severe test in natural convection problems. Thermal b.l. thicknesses are often fairly large, and the usual analyses that take the b.l. to be thin can be significantly in error. This is particularly true as Gr becomes small. Figure 8.5 includes three pictures that illustrate this. These pictures are interferograms (or in the case of Fig. 8.5c, data deduced from interferograms). An interferogram is a photograph made in a kind of lighting that causes regions of uniform density to appear as alternating light and dark bands.

Figure 8.5a was made at the University of Kentucky by G.S. Wang and R. Eichhorn. The Grashof number based on the radius of the leading edge is 2250 in this case. This is low enough to result in a b.l. that is larger than the radius near the leading edge. Figure 8.5b and c are from Kraus's classic study of natural convection visualization methods [8.9]. Figure 8.5c shows that, at Gr = 585, the b.l. assumptions are quite unreasonable since the cylinder is small in comparison with the large region of thermal disturbance.

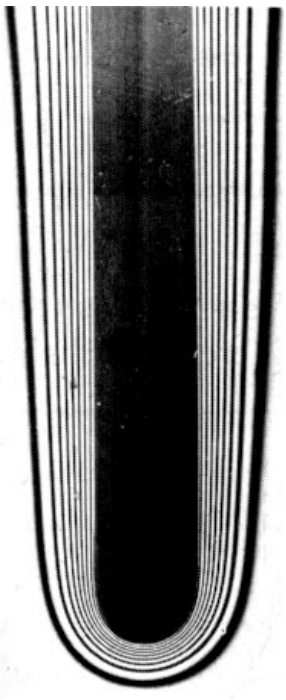

a. A 1.34 cm wide flat plate with a rounded leading edge in air. T_w = 46.5°C, ΔT = 17.0°C, $\mathrm{Gr}_{\mathrm{radius}} \simeq 2250$

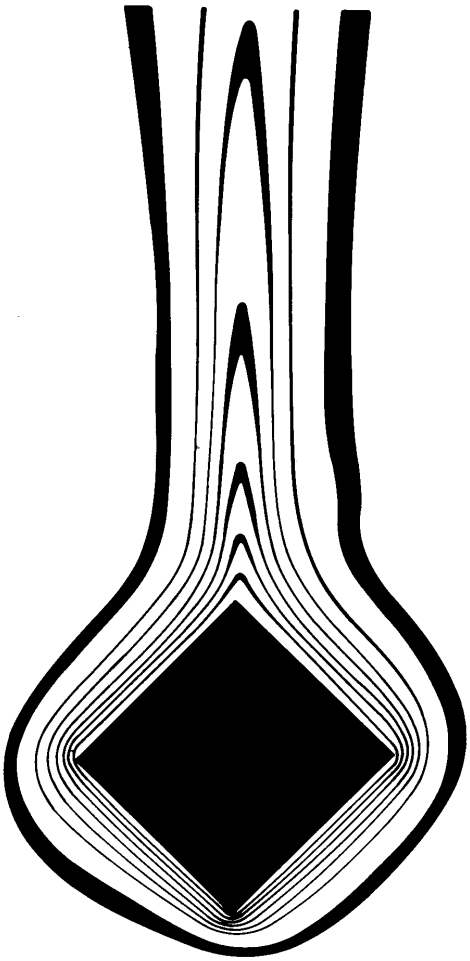

b. A square cylinder with a fairly low value of Gr. (Rendering of an interferogram shown in [8.9].)

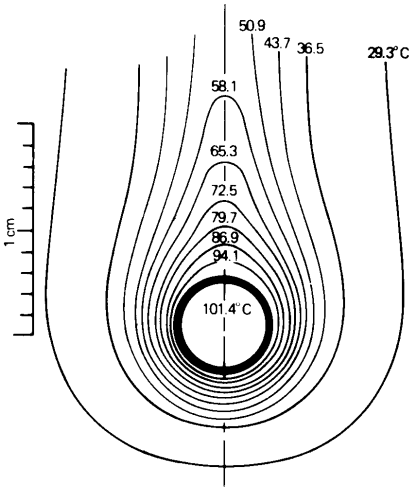

c. Measured isotherms around a cylinder in airwhen $\mathrm{Gr}_D \approx 585$ (from [8.9]).

Figure 8.5 The thickening of the b.l. during natural convection at low Gr, as illustrated by interferograms made on two-dimensional bodies. (The dark lines in the pictures are isotherms.)

The analysis of free convection becomes a far more complicated problem at low Gr's, since the b.l. equations can no longer be used. We shall not discuss any of the numerical solutions of the full Navier-Stokes equations that have been carried out in this regime. We shall instead note that correlations of data using functional equations of the form

$$\mathrm{Nu} = \mathrm{fn}(\mathrm{Ra}, \mathrm{Pr})$$

will be the first thing that we resort to in such cases. Indeed, Fig. 8.3 reveals that Churchill and Chu's equation (8.27) already serves this purpose in the case of the vertical isothermal plate, at low values of $\mathrm{Ra} \equiv \mathrm{Gr}\,\mathrm{Pr}$.

8.4 Natural convection in other situations

Natural convection from horizontal isothermal cylinders

Churchill and Chu [8.10] provide yet another comprehensive correlation of existing data. For horizontal isothermal cylinders, they find that an equation with the same form as eqn. (8.27) correlates the data for horizontal cylinders as well. Horizontal cylinder data from a variety of sources, over about 24 orders of magnitude of the Rayleigh number based on the diameter, Ra_D, are shown in Fig. 8.6. The equation that correlates them is

$$\boxed{\overline{\mathrm{Nu}}_D = 0.36 + \frac{0.518\,\mathrm{Ra}_D^{1/4}}{\left[1 + (0.559/\mathrm{Pr})^{9/16}\right]^{4/9}}} \tag{8.30}$$

They recommend that eqn. (8.30) be used in the range $10^{-6} \leqslant \mathrm{Ra}_D \leqslant 10^9$.

When Ra_D is greater than 10^9, the flow becomes turbulent. The following equation is a little more complex, but it gives comparable accuracy over a larger range:

$$\boxed{\overline{\mathrm{Nu}}_D = \left\{0.60 + 0.387\left[\frac{\mathrm{Ra}_D}{\left[1 + (0.559/\mathrm{Pr})^{9/16}\right]^{16/9}}\right]^{1/6}\right\}^2} \tag{8.31}$$

The recommended range of applicability of eqn. (8.31) is

$$10^{-6} \leqslant \mathrm{Ra}_D$$

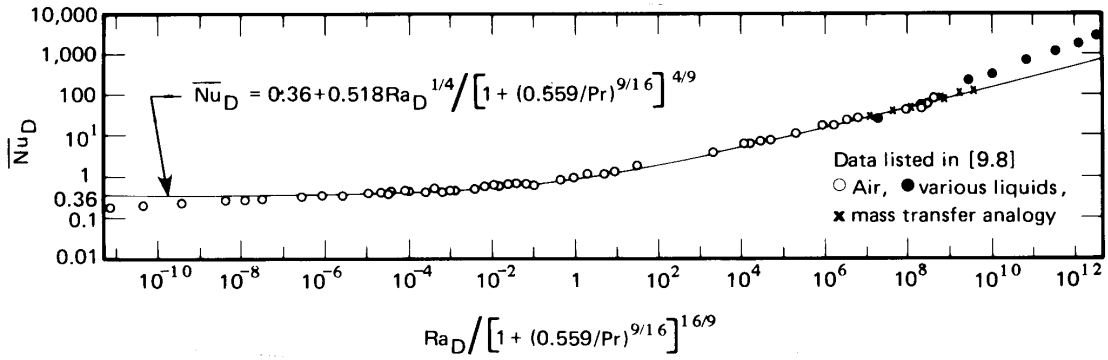

Figure 8.6 The data of many investigators for heat transfer from isothermal horizontal cylinders during natural convection, as correlated by Churchill and Chu [8.10].

Example 8.4

Space vehicles are subject to a "g-jitter," or background variation of acceleration, on the order of 10^{-6} or 10^{-5} earth gravities. Brief periods of gravity up to 10^{-4} or 10^{-2} earth gravities can be exerted by accelerating the whole vehicle. A certain line carrying hot oil is ½ cm in diameter and it is at 127°C. How does Q vary with g-level if $T_\infty = 27$°C in the air around the tube?

SOLUTION. The average b.l. temperature is 350 K. We evaluate properties at this temperature and write g as $g_e \times$ (g-level), where g_e is g at the earth's surface and the g-level is the fraction of g_e in the space vehicle.

$$\mathrm{Ra}_D = \frac{g\,(\Delta T/T_\infty)\,D^3}{\nu\alpha} = \frac{9.8\left(\dfrac{400-300}{300}\right)(0.005)^3}{2.062(10)^{-5}2.92(10)^{-5}}\,(g\text{-level})$$

$$= (678.2)\,(g\text{-level})$$

From eqn. (8.31), with Pr = 0.706, we compute

$$\overline{\mathrm{Nu}}_D = \left\{0.6 + \underbrace{0.387\left[\frac{678.2}{\left[1+(0.559/0.706)^{9/16}\right]^{16/9}}\right]^{1/6}}_{=0.952}(g\text{-level})^{1/6}\right\}^2$$

so

g-level	$\overline{\mathrm{Nu}}_D$	$\overline{h} = \overline{\mathrm{Nu}}_D \left(\frac{0.0297}{0.005}\right)$	$Q = \pi D \overline{h} \Delta T$
10^{-6}	0.483	2.87 W/m^{2}K	4.51 W/m of tube
10^{-5}	0.547	3.25 W/m^{2}K	5.10 W/m of tube
10^{-4}	0.648	3.85 W/m^{2}K	6.05 W/m of tube
10^{-2}	1.086	6.45 W/m^{2}K	10.1 W/m of tube

The numbers in the rightmost column are quite low. Cooling is clearly inefficient at these low gravities. ■

Natural convection from vertical cylinders

The heat transfer from the wall of a cylinder with its axis running vertically is the same as that from a vertical plate, so long as the thermal b.l. is thin. However, if the b.l. is thick, as is indicated in Fig. 8.7, heat transfer will be enhanced by the curvature of the thermal b.l. This correction was first considered some years ago by Sparrow and Gregg, and the analysis was subsequently extended with the help of more powerful numerical methods by Cebeci [8.11].

Figure 8.7 includes the corrections to the vertical plate results that were calculated for many Pr's by Cebeci. The left-hand graph gives a correction that must be multiplied by the local flat-plate Nusselt number to get the vertical cylinder result. Notice that the correction increases when the Grashof number decreases. The right-hand curve gives a similar correction for the overall Nusselt number on a cylinder of height L. Notice that in either situation, the correction for all but liquid metals is less than 1% if $D/(x \text{ or } L) < 0.02\ \mathrm{Gr}^{1/4}_{x \text{ or } L}$.

Heat transfer from general submerged bodies

Spheres. The sphere is an interesting case because it has a clearly specifiable value of Nu_D as $\mathrm{Ra}_D \to 0$. We look first at this limit. When the buoyancy forces approach zero by virtue of:

- low gravity,
- small diameter,
- very high viscosity,
- a very small value of β,

then heated fluid will no longer be buoyed away convectively. In that case, only conduction will serve to remove heat. Using shape factor number 4

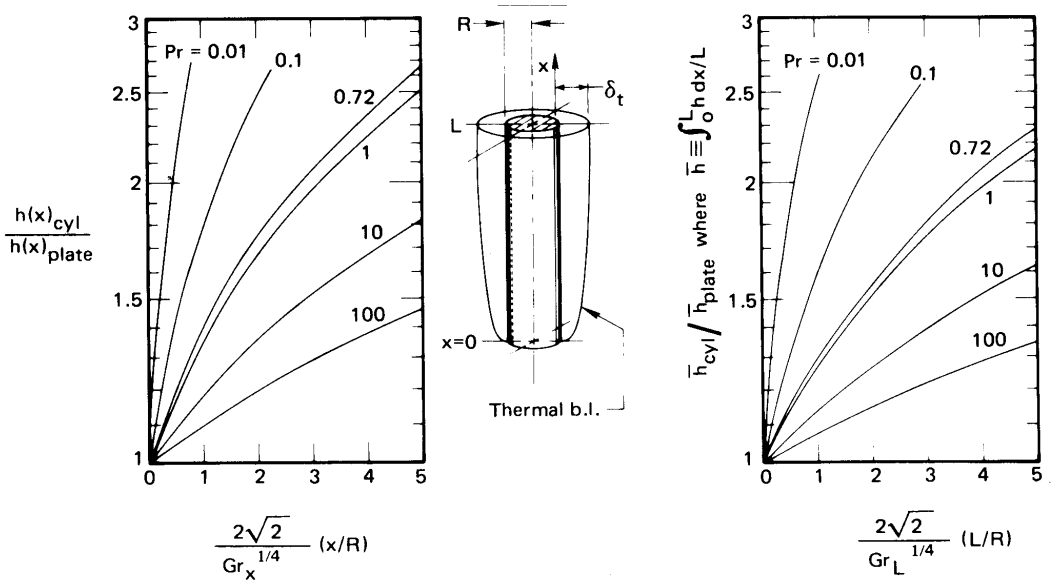

Figure 8.7 Corrections for h and $\overline{h}$ on vertical isothermal plates to make them apply to vertical isothermal cylinders [8.11].

in Table 5.4, we compute in this case

$$\lim_{\mathrm{Ra}_D \to 0} \mathrm{Nu}_D = \frac{Q}{A\Delta T}\frac{D}{k} = \frac{k\Delta T(S)D}{4\pi(D/2)^2\Delta T k} = \frac{4\pi(D/2)}{4\pi(D/4)} = 2 \tag{8.32}$$

Every proper correlation of data for heat transfer from spheres therefore has the lead constant, 2, in it.[5] A typical example is that of Yuge [8.12] for spheres immersed in gases:

$$\overline{\mathrm{Nu}}_D = 2 + 0.43\ \mathrm{Ra}_D^{1/4}, \quad \mathrm{Ra}_D < 10^5 \tag{8.33}$$

A more complex expression [8.13] encompasses other Prandtl numbers:

$$\boxed{\overline{\mathrm{Nu}}_D = 2 + \frac{0.589\ \mathrm{Ra}_D^{1/4}}{\left[1 + (0.492/\mathrm{Pr})^{9/16}\right]^{4/9}}} \quad \mathrm{Ra}_D < 10^{12} \tag{8.34}$$

This result has an estimated uncertainty of 5% in air and an rms error of about 10% at higher Prandtl numbers.

[5] It is important to note that while Nu_D for spheres approaches a limiting value at small Ra_D, no such limit exists for cylinders or vertical surfaces. The constants in eqns. (8.27) and (8.30) are not valid at extremely low values of Ra_D.

Rough estimate of Nu for other bodies. In 1973 Lienhard [8.14] noted that, for laminar convection in which the b.l. does not separate, the expression

$$\boxed{\overline{\mathrm{Nu}}_\tau \simeq 0.52\ \mathrm{Ra}_\tau^{1/4}} \tag{8.35}$$

would predict heat transfer from any submerged body within about 10% if Pr is not $\ll 1$. The characteristic dimension in eqn. (8.35) is the length of travel, τ, of fluid in the unseparated b.l.

In the case of spheres without separation, for example, $\tau = \pi D/2$, the distance from the bottom to the top around the circumference. Thus, for spheres, eqn. (8.35) becomes

$$\frac{\overline{h}\pi D}{2k} = 0.52\left[\frac{g\beta\Delta T(\pi D/2)^3}{\nu\alpha}\right]^{1/4}$$

or

$$\frac{\overline{h}D}{k} = 0.52\left(\frac{2}{\pi}\right)\left(\frac{\pi}{2}\right)^{3/4}\left[\frac{g\beta\Delta T D^3}{\nu\alpha}\right]^{1/4}$$

or

$$\overline{\mathrm{Nu}}_D = 0.465\ \mathrm{Ra}_D^{1/4}$$

This is within 8% of Yuge's correlation if Ra_D remains fairly large.

Laminar heat transfer from inclined and horizontal plates

In 1953, Rich [8.15] showed that heat transfer from inclined plates could be predicted by vertical plate formulas if the component of the gravity vector along the surface of the plate was used in the calculation of the Grashof number. Thus, the heat transfer rate decreases as $(\cos\theta)^{1/4}$, where θ is the angle of inclination measured from the vertical, as shown in Fig. 8.8.

Subsequent studies have shown that Rich's result is substantially correct for the lower surface of a heated plate or the upper surface of a cooled plate. For the upper surface of a heated plate or the lower surface of a cooled plate, the boundary layer becomes unstable and separates at a relatively low value of Gr. Experimental observations of such instability have been reported by Fujii and Imura [8.16], Vliet [8.17], Pera and Gebhart [8.18], and Al-Arabi and El-Riedy [8.19], among others.

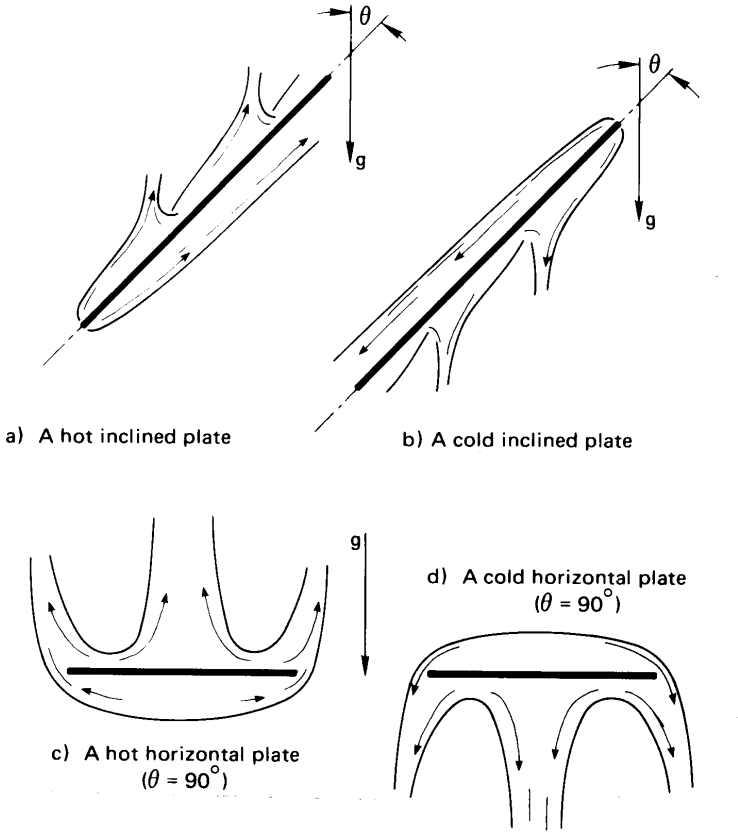

Figure 8.8 Natural convection b.l.'s on some inclined and horizontal surfaces. The b.l. separation, shown here for the unstable cases in (a) and (b), occurs only at sufficiently large values of Gr.

In the limit $\theta = 90°$ — a horizontal plate — the fluid flow above a hot plate or below a cold plate must form one or more plumes, as shown in Fig. 8.8c and d. In such cases, the b.l. is unstable for all but small Rayleigh numbers, and even then a plume must leave the center of the plate. The unstable cases can only be represented with empirical correlations.

Theoretical considerations, and experiments, show that the Nusselt number for laminar b.l.s on horizontal and slightly inclined plates varies as $\mathrm{Ra}^{1/5}$ [8.20, 8.21]. For the unstable cases, when the Rayleigh number exceeds 10^4 or so, the experimental variation is as $\mathrm{Ra}^{1/4}$, and once the flow is fully turbulent, for Rayleigh numbers above about 10^7, experi-

ments show a $\mathrm{Ra}^{1/3}$ variation of the Nusselt number [8.22, 8.23]. In the latter case, both Nu_L and $\mathrm{Ra}_L^{1/3}$ are proportional to L, so that the heat transfer coefficient is *independent* of L. Moreover, the flow field in these situations is driven mainly by the component of gravity normal to the plate.

Unstable Cases: For the lower side of cold plates and the upper side of hot plates, the boundary layer becomes increasingly unstable as Ra is increased.

- For inclinations $\theta \lesssim 45°$ and $10^5 \leqslant \mathrm{Ra}_L \leqslant 10^9$, replace g with $g\cos\theta$ in eqn. (8.27).
- For horizontal plates with Rayleigh numbers above 10^7, nearly identical results have been obtained by many investigators. From these results, Raithby and Hollands propose [8.13]:

$$\overline{\mathrm{Nu}}_L = 0.14\,\mathrm{Ra}_L^{1/3}\left(\frac{1+0.0107\,\mathrm{Pr}}{1+0.01\,\mathrm{Pr}}\right), \quad 0.024 \leqslant \mathrm{Pr} \leqslant 2000 \tag{8.36}$$

  This formula is consistent with available data up to $\mathrm{Ra}_L = 2\times10^{11}$, and probably goes higher. As noted before, the choice of length-scale L is immaterial. Fujii and Imura's results support using the above for $60° \leqslant \theta \leqslant 90°$ with g in the Rayleigh number.

  For high Ra in gases, temperature differences and variable properties effects can be large. From experiments on upward facing plates, Clausing and Berton [8.23] suggest evaluating all gas properties at a reference temperature, in kelvin, of

$$T_{\mathrm{ref}} = T_w - 0.83\,(T_w - T_\infty) \quad \text{for} \quad 1 \leqslant T_w/T_\infty \leqslant 3.$$

- For horizontal plates of area A and perimeter P at lower Rayleigh numbers, Raithby and Hollands suggest [8.13]

$$\overline{\mathrm{Nu}}_{L^*} = \frac{0.560\,\mathrm{Ra}_{L^*}^{1/4}}{\left[1+(0.492/\mathrm{Pr})^{9/16}\right]^{4/9}} \tag{8.37a}$$

  where, following Lloyd and Moran [8.22], a characteristic length-scale $L^* = A/P$, is used in the Rayleigh and Nusselt numbers. If

$\overline{\mathrm{Nu}}_{L^*} \lesssim 10$, the b.l.s will be thick, and they suggest correcting the result to

$$\overline{\mathrm{Nu}}_{\text{corrected}} = \frac{1.4}{\ln\left(1 + 1.4/\overline{\mathrm{Nu}}_{L^*}\right)} \tag{8.37b}$$

These equations are recommended[6] for $1 < \mathrm{Ra}_{L^*} < 10^7$.

- In general, for inclined plates in the unstable cases, Raithby and Hollands [8.13] recommend that the heat flow be computed first using the formula for a vertical plate with $g \cos\theta$ and then using the formula for a horizontal plate with $g \sin\theta$ (i.e., the component of gravity normal to the plate) and that the larger value of the heat flow be taken.

Stable Cases: For the upper side of cold plates and the lower side of hot plates, the flow is generally stable. The following results assume that the flow is not obstructed at the edges of the plate; a surrounding adiabatic surface, for example, will lower $\overline{h}$ [8.24, 8.25].

- For $\theta < 88°$ and $10^5 \leqslant \mathrm{Ra}_L \leqslant 10^{11}$, eqn. (8.27) is still valid for the upper side of cold plates and the lower side of hot plates when g is replaced with $g \cos\theta$ in the Rayleigh number [8.16].

- For downward-facing hot plates and upward-facing cold plates of width L with very slight inclinations, Fujii and Imura give:

$$\overline{\mathrm{Nu}}_L = 0.58\ \mathrm{Ra}_L^{1/5} \tag{8.38}$$

This is valid for $10^6 < \mathrm{Ra}_L < 10^9$ if $87° \leqslant \theta \leqslant 90°$ and for $10^9 \leqslant \mathrm{Ra}_L < 10^{11}$ if $89° \leqslant \theta \leqslant 90°$. Ra_L is based on g (*not* $g \cos\theta$). Fujii and Imura's results are for two-dimensional plates—ones in which infinite breadth has been approximated by suppression of end effects.

For circular plates of diameter D in the stable horizontal configurations, the data of Kadambi and Drake [8.26] suggest that

$$\overline{\mathrm{Nu}}_D = 0.82\ \mathrm{Ra}_D^{1/5}\ \mathrm{Pr}^{0.034} \tag{8.39}$$

[6] Raithby and Hollands also suggest using a blending formula for $1 < \mathrm{Ra}_{L^*} < 10^{10}$

$$\overline{\mathrm{Nu}}_{\text{blended},L^*} = \left[\left(\overline{\mathrm{Nu}}_{\text{corrected}}\right)^{10} + \left(\overline{\mathrm{Nu}}_{\text{turb}}\right)^{10}\right]^{1/10} \tag{8.37c}$$

in which $\overline{\mathrm{Nu}}_{\text{turb}}$ is calculated from eqn. (8.36) using L^*. The formula is useful for numerical progamming, but its effect on $\overline{h}$ is usually small.

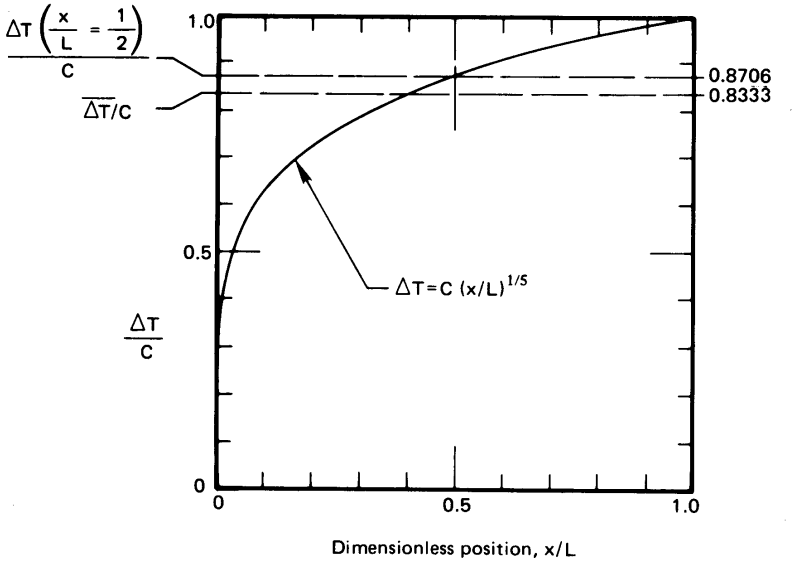

Figure 8.9 The mean value of $\Delta T \equiv T_w - T_\infty$ during natural convection.

Natural convection with uniform heat flux

When q_w is specified instead of $\Delta T \equiv (T_w - T_\infty)$ in natural convection, there is a problem that did not arise in forced convection. That problem is that ΔT, which appears both in Nu on the left and in Ra on the right, is now the unknown dependent variable. Since Nu usually varies as $\mathrm{Ra}^{1/4}$, we can write

$$\mathrm{Nu}_x = \frac{q_w}{\Delta T}\frac{x}{k} \propto \mathrm{Ra}_x^{1/4} \propto \Delta T^{1/4} x^{3/4}$$

This can be solved for ΔT in the following way:

$$\Delta T = C\left(\frac{x}{L}\right)^{1/5} \tag{8.40}$$

where C involves q_w, L, and the relevant physical properties. Then the average of ΔT over the length of the heater is given by

$$\frac{\overline{\Delta T}}{C} = \int_0^1 \left(\frac{x}{L}\right)^{1/5} d\left(\frac{x}{L}\right) = \frac{5}{6} \tag{8.41}$$

We plot ΔT against x/L in Fig. 8.9. Here, $\overline{\Delta T}$ and $\Delta T\,(x/L = ½)$ are within 4% of each other. This suggests the first of two strategies for

eliminating the dependent variable ΔT from the right-hand side of an equation for the Nusselt number:

1. If we are interested in *average* values of ΔT, we can use ΔT evaluated at the midpoint of the plate on the right-hand side.

2. If we want to form an equation for $\mathrm{Nu}_x \equiv q_w x/k\Delta T(x)$, we can use a Rayleigh number, Ra^*, defined as

$$\mathrm{Ra}_x^* \equiv \mathrm{Ra}_x \mathrm{Nu}_x \equiv \frac{g\beta\Delta T x^3}{\nu\alpha}\,\frac{q_w x}{\Delta T k} = \frac{g\beta q_w x^4}{k\nu\alpha} \tag{8.42}$$

Churchill and Chu, for example, show that their vertical plate correlation formula, eqn. (8.27), will correlate q_w = constant data exceptionally well in the range $\mathrm{Ra}_L > 1$ when Ra_L is based on ΔT at the middle of the plate. For design purposes, however, we wish to eliminate ΔT from the right-hand side, so we replace Ra_L with $\mathrm{Ra}_L^*/\overline{\mathrm{Nu}_L}$. The result is

$$\overline{\mathrm{Nu}_L} = 0.68 + 0.67\,(\mathrm{Ra}_L^*)^{1/4} \Big/ \overline{\mathrm{Nu}_L}^{1/4}\left[1 + \left(\frac{0.492}{\mathrm{Pr}}\right)^{9/16}\right]^{4/9}$$

where $\overline{\mathrm{Nu}_L} = q_w L/k\overline{\Delta T}$. This can be written in the form

$$\boxed{\overline{\mathrm{Nu}_L}^{5/4} - 0.68\,\overline{\mathrm{Nu}_L}^{1/4} = \frac{0.67\,(\mathrm{Ra}_L^*)^{1/4}}{\left[1 + (0.492/\mathrm{Pr})^{9/16}\right]^{4/9}}} \tag{8.43}$$

for laminar natural convection from vertical plates with a uniform wall heat flux.

The same thing can be done with eqn. (8.30) for horizontal cylinders, although the result has not been verified experimentally for very small values of Ra_L.

Some other natural convection problems

There are many natural convection situations that are beyond the scope of this book but which arise in practice.

Natural convection in enclosures. When a natural convection process occurs within a confined space, the heated fluid buoys up and then follows the contours of the container, releasing heat and in some way returning to the heater. This recirculation process normally enhances heat

transfer beyond that which would occur by conduction through the stationary fluid. These processes are of importance to energy conservation processes in buildings (as in multiply glazed windows, uninsulated walls, and attics), to crystal growth and solidification processes, to hot or cold liquid storage systems, and to countless other configurations. Survey articles on natural convection in enclosures have been written by Yang [8.27], Raithby and Hollands [8.13], and Catton [8.28].

Combined natural and forced convection. When forced convection along, say, a vertical wall occurs at a relatively low velocity but at a relatively high heating rate, the resulting density changes can give rise to a superimposed natural convection process. We saw in footnote 2 on page 368 that $\mathrm{Gr}_L^{1/2}$ plays the role of of a natural convection Reynolds number, it follows that we can estimate of the relative importance of natural and forced convection can be gained by considering the ratio

$$\frac{\mathrm{Gr}_L}{\mathrm{Re}_L^2} = \frac{\text{strength of natural convection flow}}{\text{strength of forced convection flow}} \tag{8.44}$$

where Re_L is for the forced convection along the wall. If this ratio is small compared to one, the flow is essentially that due to forced convection, whereas if it is large compared to one, we have natural convection. When $\mathrm{Gr}_L/\mathrm{Re}_L^2$ is on the order of one, we have a *mixed convection* process.

It should be clear that the relative orientation of the forced flow and the natural convection flow matters. For example, compare cool air flowing downward past a hot wall to cool air flowing upward along a hot wall. The former situation is called *opposing flow* and the latter is called *assisting flow*. Opposing flow may lead to boundary layer separation and degraded heat transfer.

Churchill [8.29] has provided an extensive discussion of both the conditions that give rise to mixed convection and the prediction of heat transfer for it. Review articles on the subject have been written by Chen and Armaly [8.30] and by Aung [8.31].

Example 8.5

A horizontal circular disk heater of diameter 0.17 m faces downward in air at 27°C. If it delivers 15 W, estimate its average surface temperature.

SOLUTION. We have no formula for this situation, so the problem calls for some judicious guesswork. Following the lead of Churchill and Chu, we replace Ra_D with $\mathrm{Ra}_D^*/\overline{\mathrm{Nu}}_D$ in eqn. (8.39):

$$\left(\overline{\mathrm{Nu}}_D\right)^{6/5} = \left(\frac{q_w D}{\overline{\Delta T} k}\right)^{6/5} = 0.82\,(\mathrm{Ra}_D^*)^{1/5}\,\mathrm{Pr}^{0.034}$$

so

$$\begin{aligned}\overline{\Delta T} &= 1.18\,\frac{q_w D/k}{\left(\dfrac{g\beta q_w D^4}{k\nu\alpha}\right)^{1/6}\mathrm{Pr}^{0.028}} \\ &= 1.18\,\frac{\left(\dfrac{15}{\pi(0.085)^2}\right)\dfrac{0.17}{0.02614}}{\left[\dfrac{9.8[15/\pi(0.085)^2]0.17^4}{300(0.02164)(1.566)(2.203)10^{-10}}\right]^{1/6}(0.711)^{0.028}} \\ &= 140\ \mathrm{K}\end{aligned}$$

In the preceding computation, all properties were evaluated at T_∞. Now we must return the calculation, reevaluating all properties except β at $27 + (140/2) = 97$°C:

$$\begin{aligned}\overline{\Delta T}_{\text{corrected}} &= 1.18\,\frac{661(0.17)/0.03104}{\left[\dfrac{9.8[15/\pi(0.085)^2]0.17^4}{300(0.03104)(3.231)(2.277)10^{-10}}\right]^{1/6}(0.99)} \\ &= 142\ \mathrm{K}\end{aligned}$$

so the surface temperature is $27 + 142 = 169$°C.

That is rather hot. Obviously, the cooling process is quite ineffective in this case. ■

8.5 Film condensation

Dimensional analysis and experimental data

The dimensional functional equation for h (or $\overline{h}$) during film condensation is[7]

$$\overline{h} \text{ or } h = \text{fn}\left[c_p, \rho_f, h_{fg}, g(\rho_f - \rho_g), k, \mu, (T_{\text{sat}} - T_w), L \text{ or } x\right]$$

where h_{fg} is the latent heat of vaporization. It does not appear in the differential equations (8.4) and (6.40); however, it is used in the calculation of δ [which enters in the b.c.'s (8.5)]. The film thickness, δ, depends heavily on the latent heat and slightly on the sensible heat, $c_p \Delta T$, which the film must absorb to condense. Notice, too, that $g(\rho_f - \rho_g)$ is included as a product, because gravity only enters the problem as it acts upon the density difference [cf. eqn. (8.4)].

The problem is therefore expressed nine variables in J, kg, m, s, and °C (where we once more avoid resolving J into N · m since heat is not being converted into work in this situation). It follows that we look for $9 - 5 = 4$ pi-groups. The ones we choose are

$$\Pi_1 = \overline{\text{Nu}}_L \equiv \frac{\overline{h}L}{k} \qquad \Pi_2 = \text{Pr} \equiv \frac{\nu}{\alpha}$$

$$\Pi_3 = \text{Ja} \equiv \frac{c_p(T_{\text{sat}} - T_w)}{h_{fg}} \qquad \Pi_4 \equiv \frac{\rho_f(\rho_f - \rho_g)g h_{fg} L^3}{\mu k (T_{\text{sat}} - T_w)}$$

Two of these groups are new to us. The group Π_3 is called the *Jakob number*, Ja, to honor Max Jakob's important pioneering work during the 1930s on problems of phase change. It compares the maximum sensible heat absorbed by the liquid to the latent heat absorbed. The group Π_4 does not normally bear anyone's name, but, if it is multiplied by Ja, it may be regarded as a Rayleigh number for the condensate film.

Notice that if we condensed water at 1 atm on a wall 10°C below T_{sat}, then Ja would equal $4.174(10/2257) = 0.0185$. Although 10°C is a fairly large temperature difference in a condensation process, it gives a maximum sensible heat that is less than 2% of the latent heat. The Jakob number is accordingly small in most cases of practical interest, and it turns out that sensible heat can often be neglected. (There are important exceptions to this.) The same is true of the role of the Prandtl number. Therefore, during film condensation

[7] Note that, throughout this section, k, μ, c_p, and Pr refer to properties of the liquid, rather than the vapor.

$$\overline{\mathrm{Nu}}_L = \mathrm{fn}\left(\underbrace{\frac{\rho_f(\rho_f - \rho_g) g h_{fg} L^3}{\mu k (T_{\mathrm{sat}} - T_w)}}, \underbrace{\mathrm{Pr}, \mathrm{Ja}} \right) \tag{8.45}$$

secondary independent variables

primary independent variable, Π_4

Equation (8.45) is not restricted to any geometrical configuration, since the same variables govern h during film condensation on any body. Figure 8.10, for example, shows laminar film condensation data given for spheres by Dhir[8] [8.32]. They have been correlated according to eqn. (8.12). The data are for only one value of Pr but for a range of Π_4 and Ja. They generally correlate well within ±10%, despite a broad variation of the not-very-influential variable, Ja. A predictive curve [8.32] is included in Fig. 8.10 for future reference.

Laminar film condensation on a vertical plate

Consider the following feature of film condensation. The latent heat of a liquid is normally a very large number. Therefore, even a high rate of heat transfer will typically result in only very thin films. These films move relatively slowly, so it is safe to ignore the inertia terms in the momentum equation (8.4):

$$\underbrace{u\frac{\partial u}{\partial x} + v\frac{\partial v}{\partial y}}_{\simeq 0} = \left(1 - \frac{\rho_g}{\rho_f}\right) g + \nu \underbrace{\frac{\partial^2 u}{\partial y^2}}_{\simeq \frac{d^2 u}{dy^2}}$$

This result will give $u = u(y, \delta)$ (where δ is the local b.l. thickness) when it is integrated. We recognize that $\delta = \delta(x)$, so that u is not strictly dependent on y alone. However, the y-dependence is predominant, and it is reasonable to use the approximate momentum equation

$$\frac{d^2 u}{dy^2} = -\frac{\rho_f - \rho_g}{\rho_f}\frac{g}{\nu} \tag{8.46}$$

[8] Professor Dhir very kindly recalculated his data into the form shown in Fig. 8.10 for use here.

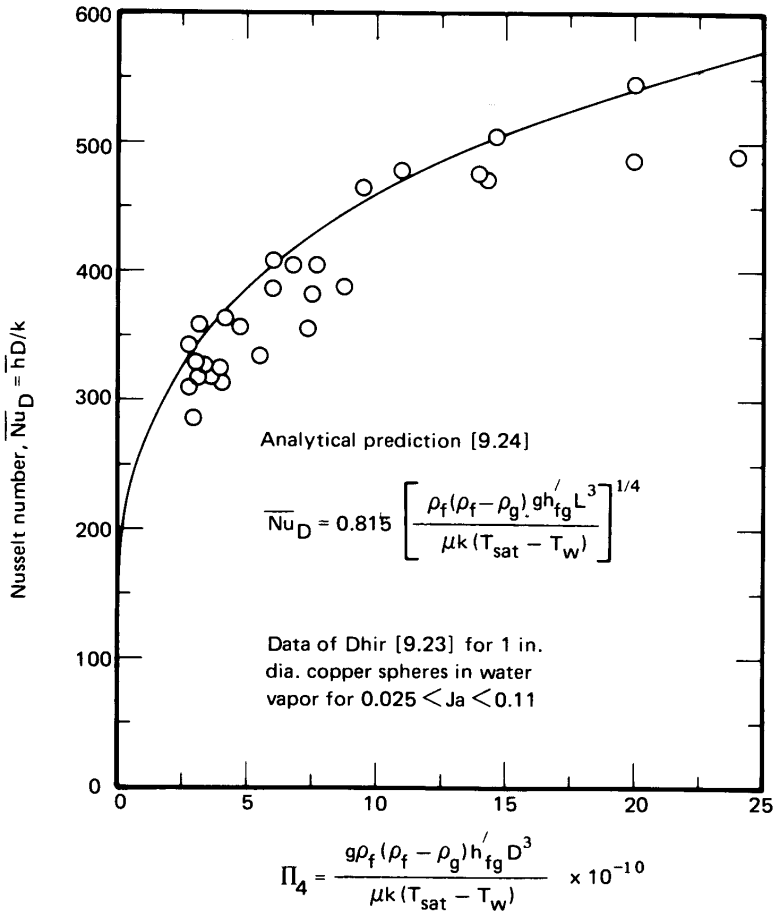

Figure 8.10 Correlation of the data of Dhir [8.32] for laminar film condensation on spheres at one value of Pr and for a range of Π_4 and Ja. [Properties were evaluated at $(T_{sat} + T_w)/2$.]

This simplification was made by Nusselt in 1916 when he set down the original analysis of film condensation [8.33]. He also eliminated the convective terms from the energy equation (6.40):

$$\underbrace{u\frac{\partial T}{\partial x} + v\frac{\partial T}{\partial y}}_{\simeq 0} = \alpha \frac{\partial^2 T}{\partial y^2}$$

on the same basis. The integration of eqn. (8.46) subject to the b.c.'s

$$u\,(y=0)=0 \qquad \text{and} \qquad \left.\frac{\partial u}{\partial y}\right|_{y=\delta}=0$$

gives the parabolic velocity profile:

$$u=\frac{(\rho_f-\rho_g)g\delta^2}{2\mu}\left[2\left(\frac{y}{\delta}\right)-\left(\frac{y}{\delta}\right)^2\right] \tag{8.47}$$

And integration of the energy equation subject to the b.c.'s

$$T\,(y=0)=T_w \qquad \text{and} \qquad T\,(y=\delta)=T_{\text{sat}}$$

gives the linear temperature profile:

$$T=T_w+(T_{\text{sat}}-T_w)\,\frac{y}{\delta} \tag{8.48}$$

To complete the analysis, we must calculate δ. This can be done in two steps. First, we express the mass flow rate in the film, $\dot{m}$, in terms of δ, with the help of eqn. (8.47):

$$\dot{m}=\int_0^\delta \rho_f u\,dy=\frac{\rho_f(\rho_f-\rho_g)}{3\mu}\,g\delta^3 \tag{8.49}$$

Second, we neglect the sensible heat absorbed by that part of the film cooled below T_{sat} and express the local heat flux in terms of the rate of change of $\dot{m}$ (see Fig. 8.11):

$$|q|=k\left.\frac{\partial T}{\partial y}\right|_{y=0}=k\,\frac{T_{\text{sat}}-T_w}{\delta}=h_{fg}\,\frac{d\dot{m}}{dx} \tag{8.50}$$

Substituting eqn. (8.49) in eqn. (8.50), we obtain a first-order differential equation for δ:

$$k\,\frac{T_{\text{sat}}-T_w}{\delta}=\frac{h_{fg}\rho_f(\rho_f-\rho_g)}{\mu}\,g\delta^2\frac{d\delta}{dx} \tag{8.51}$$

This can be integrated directly, subject to the b.c., $\delta(x=0)=0$. The result is

$$\delta=\left[\frac{4k(T_{\text{sat}}-T_w)\mu x}{\rho_f(\rho_f-\rho_g)gh_{fg}}\right]^{1/4} \tag{8.52}$$

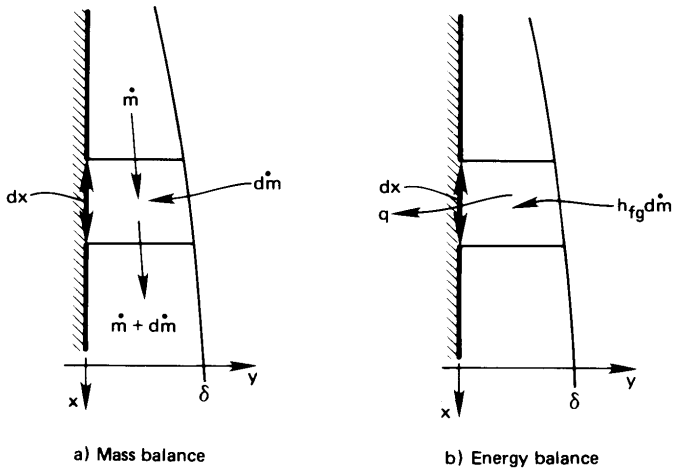

Figure 8.11 Heat and mass flow in an element of a condensing film.

Both Nusselt and, subsequently, Rohsenow [8.34] showed how to correct the film thickness calculation for the sensible heat that is needed to cool the inner parts of the film below T_{sat}. Rohsenow's calculation was, in part, an assessment of Nusselt's linear-temperature-profile assumption, and it led to a corrected latent heat—designated h'_{fg}—which accounted for subcooling in the liquid film when Pr is large. Rohsenow's result, which we show below to be strictly true only for large Pr, was

$$h'_{fg} = h_{fg}\left[\,1 + 0.68\,\underbrace{\frac{c_p(T_{\text{sat}} - T_w)}{h_{fg}}}_{\equiv \text{ Ja, Jakob number}}\,\right] \tag{8.53}$$

Thus, we simply replace h_{fg} with h'_{fg} wherever it appears explicitly in the analysis, beginning with eqn. (8.50).

Finally, the heat transfer coefficient is obtained from

$$h \equiv \frac{q}{T_{\text{sat}} - T_w} = \frac{1}{T_{\text{sat}} - T_w}\left[\frac{k(T_{\text{sat}} - T_w)}{\delta}\right] = \frac{k}{\delta} \tag{8.54}$$

so

$$\text{Nu}_x = \frac{hx}{k} = \frac{x}{\delta} \tag{8.55}$$

Thus, with the help of eqn. (8.53), we substitute eqn. (8.52) in eqn. (8.55) and get

$$\boxed{\mathrm{Nu}_x = 0.707 \left[\frac{\rho_f(\rho_f - \rho_g) g h'_{fg} x^3}{\mu k (T_{\mathrm{sat}} - T_w)} \right]^{1/4}} \tag{8.56}$$

This equation carries out the functional dependence that we anticipated in eqn. (8.45):

$$\mathrm{Nu}_x = \mathrm{fn}\left(\underbrace{\Pi_4}, \underbrace{\mathrm{Ja}}, \underbrace{\mathrm{Pr}} \right)$$

- Π_4: this is clearly the dominant variable
- Ja: this is carried implicitly in h'_{fg}
- Pr: eliminated in so far as we neglected convective terms in the energy equation

The physical properties in Π_4, Ja, and Pr (with the exception of h_{fg}) are to be evaluated at the mean film temperature. However, if $T_{\mathrm{sat}} - T_w$ is small—and it often is—one might approximate them at T_{sat}.

At this point we should ask just how great the missing influence of Pr is and what degree of approximation is involved in representing the influence of Ja with the use of h'_{fg}. Sparrow and Gregg [8.35] answered these questions with a complete b.l. analysis of film condensation. They did not introduce Ja in a corrected latent heat but instead showed its influence directly.

Figure 8.12 displays two figures from the Sparrow and Gregg paper. The first shows heat transfer results plotted in the form

$$\frac{\mathrm{Nu}_x}{\sqrt[4]{\Pi_4}} = \mathrm{fn}\,(\mathrm{Ja}, \mathrm{Pr}) \longrightarrow \text{constant, as Ja} \longrightarrow 0 \tag{8.57}$$

Notice that the calculation approaches Nusselt's simple result for all Pr as Ja $\to$ 0. It also approaches Nusselt's result, even for fairly large values of Ja, if Pr is not small. The second figure shows how the temperature deviates from the linear profile that we assumed to exist in the film in developing eqn. (8.48). If we remember that a Jakob number of 0.02 is about as large as we normally find in laminar condensation, it is clear that the linear temperature profile is a very sound assumption for nonmetallic liquids.

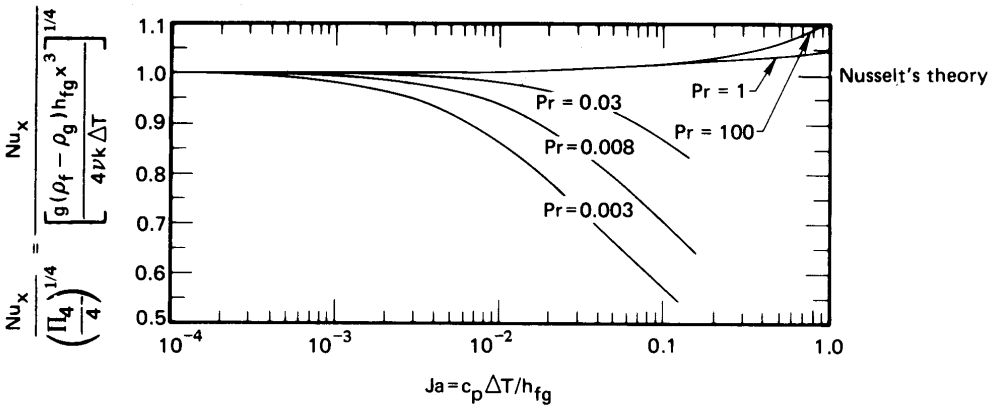

Predicted heat transfer results

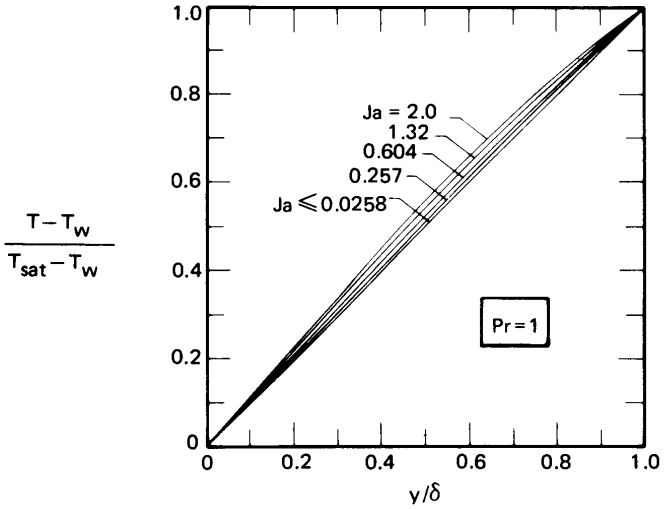

Predicted temperature profiles in condensing films

Figure 8.12 Results of the exact b.l. analysis of laminar film condensation on a vertical plate [8.35].

Sadasivan and Lienhard [8.36] have shown that the Sparrow-Gregg formulation can be expressed with high accuracy, for Pr ⩾ 0.6, by including Pr in the latent heat correction. Thus they wrote

$$h'_{fg} = h_{fg}\,[1 + (0.683 - 0.228/\mathrm{Pr})\,\mathrm{Ja}] \tag{8.58}$$

which includes eqn. (8.53) for Pr → ∞ as we anticipated.

The Sparrow and Gregg analysis proves that Nusselt's analysis is quite accurate for all Prandtl numbers above the liquid-metal range. The very high Ja flows, for which Nusselt's theory requires some correction, usually result in thicker films, which become turbulent so the exact analysis no longer applies.

The average heat transfer coefficient is calculated in the usual way for T_{wall} = constant:

$$\overline{h} = \frac{1}{L}\int_0^L h(x)\,dx = \tfrac{4}{3}\,h(L)$$

so

$$\boxed{\overline{\text{Nu}_L} = 0.9428\left[\frac{\rho_f(\rho_f-\rho_g)gh'_{fg}L^3}{\mu k(T_{\text{sat}}-T_w)}\right]^{1/4}} \tag{8.59}$$

Example 8.6

Water at atmospheric pressure condenses on a strip 30 cm in height that is held at 90°C. Calculate the overall heat transfer per meter, the film thickness at the bottom, and the mass rate of condensation per meter.

SOLUTION.

$$\delta = \left[\frac{4k(T_{\text{sat}}-T_w)\nu x}{(\rho_f-\rho_g)gh'_{fg}}\right]^{1/4}$$

where we have replaced h_{fg} with h'_{fg}:

$$h'_{fg} = 2257\left[1+\left(0.683-\frac{0.228}{1.72}\right)\frac{4.216(10)}{2257}\right] = 2280\ \text{kJ/kg}$$

so

$$\delta = \left[\frac{4(0.681)(10)(0.290)10^{-6}x}{(957.2-0.6)(9.8)(2280)(10)^3}\right]^{1/4} = 0.000138\,x^{1/4}$$

Then

$$\delta(L) = 0.000102\ \text{m} = 0.102\ \text{mm}$$

Notice how thin the film is. Finally, we use eqns. (8.55) and (8.58) to compute

$$\overline{\mathrm{Nu}}_L = \frac{4}{3}\frac{L}{\delta} = \frac{4(0.3)}{3(0.000102)} = 3903$$

so

$$q = \frac{\mathrm{Nu}_L\, k\Delta T}{L} = \frac{3903(0.681)(10)}{0.3} = 88,602 \text{ W/m}^2$$

(This is a heat flow of over 88.6 kW on an area about half the size of a desk top. That is very high for such a small temperature difference.) Then

$$Q = 88,602(0.3) = 26,581 \text{ W/m} = 26.5 \text{ kW/m}$$

The rate of condensate flow, $\dot{m}$ is

$$\dot{m} = \frac{Q}{h'_{fg}} = \frac{26.5}{2291} = 0.0116 \text{ kg/m·s}$$ ■

Condensation on other bodies

Nusselt himself extended his prediction to certain other bodies but was restricted by the lack of a digital computer from evaluating as many cases as he might have. In 1971 Dhir and Lienhard [8.37] showed how Nusselt's method could be readily extended to a large class of problems. They showed that one need only to replace the gravity, g, with an effective gravity, g_{eff}:

$$g_{\text{eff}} \equiv \frac{x\,(gR)^{4/3}}{\displaystyle\int_0^x g^{1/3}R^{4/3}\,dx} \tag{8.60}$$

in eqns. (8.52) and (8.56), to predict δ and Nu_x for a variety of bodies. The terms in eqn. (8.60) are (see Fig. 8.13):

- x is the distance along the liquid film measured from the upper stagnation point.
- $g = g(x)$, the component of gravity (or other body force) along x; g can vary from point to point as it does in Fig. 8.13b and c.

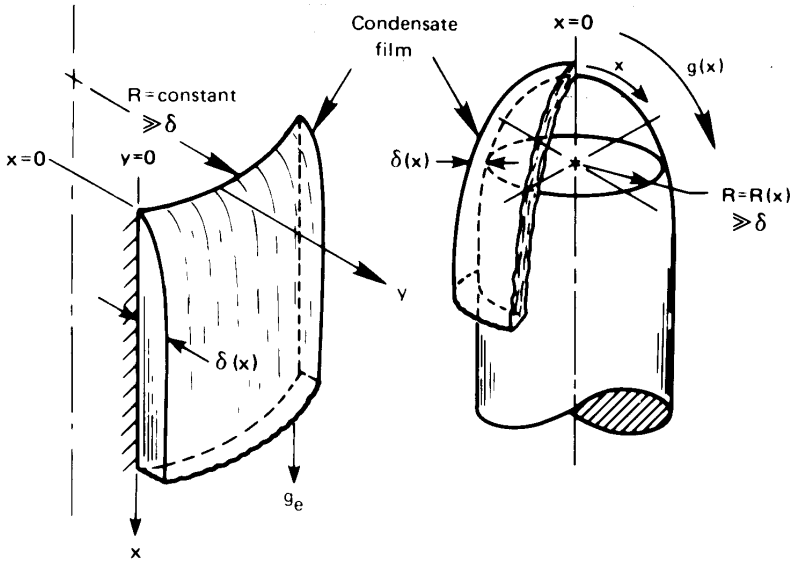

a) Vertical plate or vertical cylinder

b) Axi-symmetric body

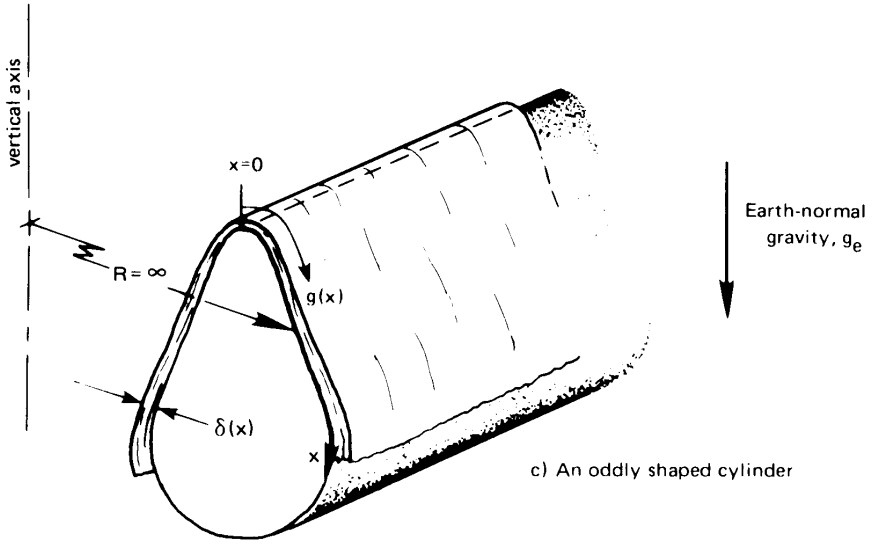

c) An oddly shaped cylinder

Figure 8.13 Condensation on various bodies. $g(x)$ is the component of gravity or other body force in the x-direction.

- $R(x)$ is a radius of curvature about the vertical axis. In Fig. 8.13a, it is a constant that factors out of eqn. (8.60). In Fig. 8.13c, R is infinite. Since it appear to the same ower in both the numerator and the denominator, it again can be factored out of eqn. (8.60). Only in axisymmetric bodies, where R varies with x, need it be included. When it can be factored out,

$$g_{\text{eff}} \text{ reduces to } \frac{x g^{4/3}}{\int_0^x g^{1/3}\, dx} \tag{8.61}$$

- g_e is earth-normal gravity. We introduce g_e at this point to distinguish it from $g(x)$.

Example 8.7

Find Nu_x for laminar film condensation on the top of a flat surface sloping at $\theta°$ from the vertical plane.

Solution. In this case $g = g_e \cos\theta$ and $R = \infty$. Therefore, eqn. (8.60) or (8.61) reduces to

$$g_{\text{eff}} = \frac{x g_e^{4/3} (\cos\theta)^{4/3}}{g_e^{1/3} (\cos\theta)^{1/3} \int_0^x dx} = g_e \cos\theta$$

as we might expect. Then, for a slanting plate,

$$\text{Nu}_x = 0.707 \left[\frac{\rho_f (\rho_f - \rho_g)(g_e \cos\theta) h'_{fg} x^3}{\mu k (T_{\text{sat}} - T_w)} \right]^{1/4} \tag{8.62}$$

■

Example 8.8

Find the overall Nusselt number for a horizontal cylinder.

Solution. There is an important conceptual hurdle here. The radius $R(x)$ is infinity, as shown in Fig. 8.13c—it is not the radius of the cylinder. It is also very easy to show that $g(x)$ is equal to $g_e \sin(2x/D)$, where D is the diameter of the cylinder. Then

$$g_{\text{eff}} = \frac{x g_e^{4/3} (\sin 2x/D)^{4/3}}{g_e^{1/3} \int_0^x (\sin 2x/D)^{1/3}\, dx}$$

and, with $h(x)$ from eqn. (8.56),

$$\overline{h} = \frac{2}{\pi D}\int_0^{\pi D/2} \frac{1}{\sqrt{2}}\frac{k}{x}\left[\frac{\rho_f(\rho_f-\rho_g)h'_{fg}x^3}{\mu k\,(T_{\text{sat}}-T_w)}\,\frac{x g_e(\sin 2x/D)^{4/3}}{\int_0^x(\sin 2x/D)^{1/3}\,dx}\right]^{1/4} dx$$

This integral can be evaulated in terms of gamma functions. The result, when it is put back in the form of a Nusselt number, is

$$\overline{\text{Nu}}_D = 0.728\left[\frac{\rho_f(\rho_f-\rho_g)g_e h'_{fg}D^3}{\mu k\,(T_{\text{sat}}-T_w)}\right]^{1/4} \tag{8.63}$$

for a horizontal cylinder. (Nusselt got 0.725 for the lead constant, but he had to approximate the integral with a hand calculation.) ■

Some other results of this calculation include the following cases.

Sphere of diameter D:

$$\overline{\text{Nu}}_D = 0.828\left[\frac{\rho_f(\rho_f-\rho_g)g_e h'_{fg}D^3}{\mu k\,(T_{\text{sat}}-T_w)}\right]^{1/4} \tag{8.64}$$

This result[9] has already been compared with the experimental data in Fig. 8.10.

Vertical cone with the apex on top, the bottom insulated, and a cone angle of $\alpha°$:

$$\text{Nu}_x = 0.874\,[\cos(\alpha/2)]^{1/4}\left[\frac{\rho_f(\rho_f-\rho_g)g_e h'_{fg}x^3}{\mu k\,(T_{\text{sat}}-T_w)}\right]^{1/4} \tag{8.65}$$

Rotating horizontal disk[10]: In this case, $g = \omega^2 x$, where x is the distance from the center and ω is the speed of rotation. The Nusselt number, based on $L = (\mu/\rho_f\omega)^{1/2}$, is

$$\overline{\text{Nu}} = 0.9034\left[\frac{\mu(\rho_f-\rho_g)h'_{fg}}{\rho_f k\,(T_{\text{sat}}-T_w)}\right]^{1/4} = \text{constant} \tag{8.66}$$

[9]There is an error in [8.37]: the constant given there is 0.785. The value of 0.828 given here is correct.

[10]This problem was originally solved by Sparrow and Gregg [8.38].

This result might seem strange at first glance. It says that Nu ≠ fn(x or ω). The reason is that δ just happens to be independent of x in this configuration.

The Nusselt solution can thus be bent to fit many complicated geometric figures. One of the most complicated ones that have been dealt with is the reflux condenser shown in Fig. 8.14. In such a configuration, cooling water flows through a helically wound tube and vapor condenses on the outside, running downward along the tube. As the condensate flows, centripetal forces sling the liquid outward at a downward angle. This complicated flow was analyzed by Karimi [8.39], who found that

$$\overline{\mathrm{Nu}} \equiv \frac{\overline{h} d \cos\alpha}{k} = \left[\frac{(\rho_f - \rho_g)\rho_f h'_{fg} g (d\cos\alpha)^3}{\mu k \Delta T} \right]^{1/4} \mathrm{fn}\left(\frac{d}{D}, B\right) \tag{8.67}$$

where B is a centripetal parameter:

$$B \equiv \frac{\rho_f - \rho_g}{\rho_f} \frac{c_p \Delta T}{h'_{fg}} \frac{\tan^2\alpha}{\mathrm{Pr}}$$

and α is the helix angle (see Fig. 8.14). The function on the righthand side of eqn. (8.67) was a complicated one that must be evaluated numerically. Karimi's result is plotted in Fig. 8.14.

Laminar–turbulent transition

The mass flow rate of condensate in the film, $\dot{m}$, is more commonly designated as Γ_c kg/m · s. Its calculation in eqn. (8.49) involved substituting eqn. (8.47) in

$$\dot{m} \text{ or } \Gamma_c = \rho_f \int_0^\delta u \, dy$$

Equation (8.47) gives $u(y)$ independently of any geometric features. [The geometry is characterized by $\delta(x)$.] Thus, the resulting equation for the mass flow rate is still

$$\Gamma_c = \frac{\rho_f(\rho_f - \rho_g) g \delta^3}{3\mu} \tag{8.49a}$$

This expression is valid for any location along any film, regardless of the geometry of the body. The configuration will lead to variations of $g(x)$ and $\delta(x)$, but eqn. (8.49a) still applies.

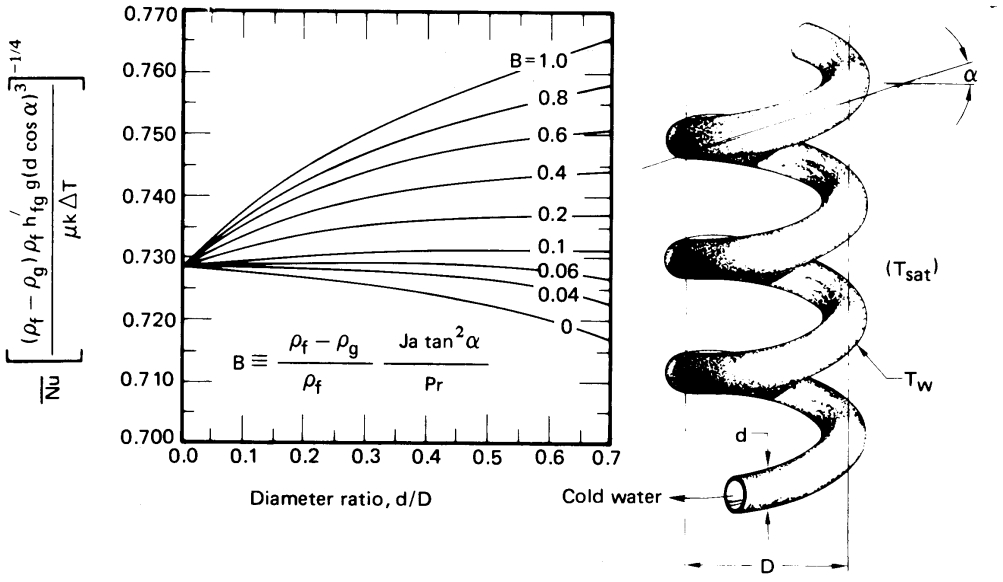

Figure 8.14 Fully developed film condensation heat transfer on a helical reflux condenser [8.39].

It is useful to define a Reynolds number in terms of Γ_c. This is easy to do, because Γ_c is equal to $\rho u_{\text{av}}\delta$.

$$\text{Re}_c = \frac{\Gamma_c}{\mu} = \frac{\rho_f(\rho_f - \rho_g)g\delta^3}{3\mu^2} \tag{8.68}$$

It turns out that the Reynolds number dictates the onset of film instability, just as it dictates the instability of a b.l. or of a pipe flow.[11] When $\text{Re}_c \cong 7$, scallop-shaped ripples become visible on the condensate film. When Re_c reaches about 400, a full-scale laminar-to-turbulent transition occurs.

Gregorig, Kern, and Turek [8.40] reviewed many data for the film condensation of water and added their own measurements. Figure 8.15 shows these data in comparison with Nusselt's theory, eqn. (8.59). The comparison is almost perfect up to $\text{Re}_c \cong 7$. Then the data start yielding somewhat higher heat transfer rates than the prediction. This is because

[11] Two Reynolds numbers are defined for film condensation: Γ_c/μ and $4\Gamma_c/\mu$. The latter one, which is simply four times as large as the one we use, is more common in the American literature.

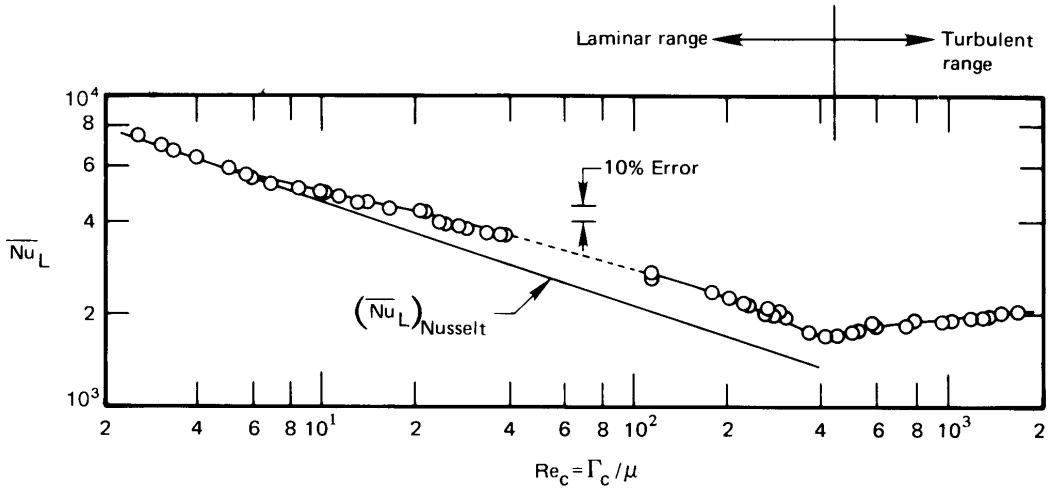

Figure 8.15 Film condensation on vertical plates. Data are for water [8.40].

the ripples improve heat transfer—just a little at first and by about 20% when the full laminar-to-turbulent transition occurs at $\mathrm{Re}_c = 400$.

Above $\mathrm{Re}_c = 400$, $\overline{\mathrm{Nu}}_L$ begins to rise with Re_c. The Nusselt number begins to exhibit an increasingly strong dependence on the Prandtl number in this turbulent regime. Therefore, one can use Fig. 8.15, directly as a data correlation, to predict the heat transfer coefficient for steam condensating at 1 atm. But for other fluids with different Prandtl numbers, one should consult [8.41] or [8.42].

Two final issues in natural convection film condensation

- *Condensation in tube bundles.* Nusselt showed that if n horizontal tubes are arrayed over one another, and if the condensate leaves each one and flows directly onto the one below it without splashing, then

$$\mathrm{Nu}_{D\text{for } n \text{ tubes}} = \frac{\mathrm{Nu}_{D_1 \text{ tube}}}{n^{1/4}} \tag{8.69}$$

  This is a fairly optimistic extension of the theory, of course. In addition, the effects of vapor shear stress on the condensate and of pressure losses on the saturation temperature are often important in tube bundles. These effects are discussed by Rose et al. [8.42] and Marto [8.41].

- *Condensation in the presence of noncondensable gases.* When the condensing vapor is mixed with noncondensable air, uncondensed air must constantly diffuse away from the condensing film and vapor must diffuse inward toward the film. This coupled diffusion process can considerably slow condensation. The resulting h can easily be cut by a factor of five if there is as little as 5% by mass of air mixed into the steam. This effect was first analyzed in detail by Sparrow and Lin [8.43]. More recent studies of this problem are reviewed in [8.41, 8.42].

Problems

8.1 Show that Π_4 in the film condensation problem can properly be interpreted as $\mathrm{Pr}\,\mathrm{Re}^2/\mathrm{Ja}$.

8.2 A 20 cm high vertical plate is kept at 34°C in a 20°C room. Plot (*to scale*) δ and h vs. height and the actual temperature and velocity vs. y at the top.

8.3 Redo the Squire-Eckert analysis, neglecting inertia, to get a high-Pr approximation to Nu_x. Compare your result with the Squire-Eckert formula.

8.4 Assume a linear temperature profile and a simple triangular velocity profile, as shown in Fig. 8.16, for natural convection on a vertical isothermal plate. Derive $\mathrm{Nu}_x = \mathrm{fn}(\mathrm{Pr}, \mathrm{Gr}_x)$, compare your result with the Squire-Eckert result, and discuss the comparison.

8.5 A horizontal cylindrical duct of diamond-shaped cross section (Fig. 8.17) carries air at 35°C. Since almost all thermal resistance is in the natural convection b.l. on the outside, take T_w to be approximately 35°C. $T_\infty = 25$°C. Estimate the heat loss per meter of duct if the duct is uninsulated. [$Q = 24.0$ W/m.]

8.6 The heat flux from a 3 m high electrically heated panel in a wall is 75 W/m^2 in an 18°C room. What is the average temperature of the panel? What is the temperature at the top? at the bottom?

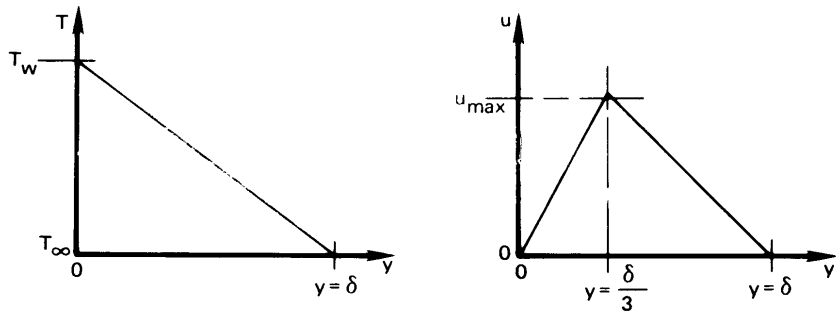

Figure 8.16 Configuration for Problem 8.4.

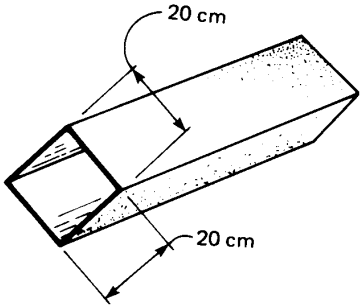

Figure 8.17 Configuration for Problem 8.5.

8.7 Find pipe diameters and wall temperatures for which the film condensation heat transfer coefficients given in Table 1.1 are valid.

8.8 Consider Example 8.6. What value of wall temperature (if any), or what height of the plate, would result in a laminar-to-turbulent transition at the bottom in this example?

8.9 A plate spins, as shown in Fig. 8.18, in a vapor that rotates synchronously with it. Neglect earth-normal gravity and calculate Nu_L as a result of film condensation.

8.10 A laminar liquid film of temperature T_{sat} flows down a vertical wall that is also at T_{sat}. Flow is fully developed and the film thickness is δ_o. Along a particular horizontal line, the wall temperature has a lower value, T_w, and it is kept at that temperature everywhere below that position. Call the line where the wall temperature changes $x = 0$. If the whole system is

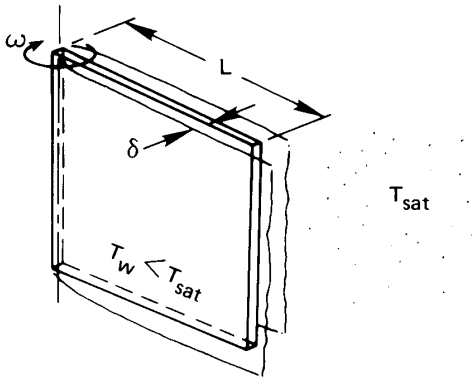

Figure 8.18 Configuration for Problem 8.9.

immersed in saturated vapor of the flowing liquid, calculate $\delta(x)$, Nu_x, and Nu_L, where $x = L$ is the bottom edge of the wall. (Neglect any transition behavior in the neighborhood of $x = 0$.)

8.11 Prepare a table of formulas of the form

$$\overline{h}\,(\mathrm{W/m^2K}) = C\,[\Delta T^\circ\mathrm{C}/L\ \mathrm{m}]^{1/4}$$

for natural convection at normal gravity in air and in water at $T_\infty = 27^\circ$C. Assume that T_w is close to 27°C. Your table should include results for vertical plates, horizontal cylinders, spheres, and possibly additional geometries. Do not include your calculations.

8.12 For what value of Pr is the condition

$$\left.\frac{\partial^2 u}{\partial y^2}\right|_{y=0} = \frac{g\beta(T_w - T_\infty)}{\nu}$$

satisfied exactly in the Squire-Eckert b.l. solution? [Pr = 2.86.]

8.13 The overall heat transfer coefficient on the side of a particular house 10 m in height is 2.5 W/m^{2}K, excluding exterior convection. It is a cold, still winter night with $T_{\text{outside}} = -30^\circ$C and $T_{\text{inside air}} = 25^\circ$C. What is $\overline{h}$ on the outside of the house? Is external convection laminar or turbulent?

8.14 Consider Example 8.2. The sheets are mild steel, 2 m long and 6 mm thick. The bath is basically water at 60°C, and the sheets

are put in it at 18°C. (a) Plot the sheet temperature as a function of time. (b) Approximate $\overline{h}$ at $\Delta T = [(60 + 18)/2 - 18]$°C and plot the conventional exponential response on the same graph.

8.15 A vertical heater 0.15 m in height is immersed in water at 7°C. Plot $\overline{h}$ against $(T_w - T_\infty)^{1/4}$, where T_w is the heater temperature, in the range $0 < (T_w - T_\infty) < 100$°C. Comment on the result. should the line be straight?

8.16 A 77°C vertical wall heats 27°C air. Evaluate $\delta_{\text{top}}/L, \text{Ra}_L$, and L where the line in Fig. 8.3 ceases to be straight. Comment on the implications of your results. [$\delta_{\text{top}}/L \simeq 0.6$.]

8.17 A horizontal 8 cm O.D. pipe carries steam at 150°C through a room at 17°C. The pipe has a 1.5 cm layer of 85% magnesia insulation on it. Evaluate the heat loss per meter of pipe. [$Q = 97.3$ W/m.]

8.18 What heat rate (in W/m) must be supplied to a 0.01 mm horizontal wire to keep it 30°C above the 10°C water around it?

8.19 A vertical run of copper tubing, 5 mm in diameter and 20 cm long, carries condensation vapor at 60°C through 27°C air. What is the total heat loss?

8.20 A body consists of two cones joined at their bases. The diameter is 10 cm and the overall length of the joined cones is 25 cm. The axis of the body is vertical, and the body is kept at 27°C in 7°C air. What is the rate of heat removal from the body? [$Q = 3.38$ W.]

8.21 Consider the plate dealt with in Example 8.3. Plot $\overline{h}$ as a function of the angle of inclination of the plate as the hot side is tilted both upward and downward. Note that you must make do with discontinuous formulas in different ranges of θ.

8.22 You have been asked to design a vertical wall panel heater, 1.5 m high, for a dwelling. What should the heat flux be if no part of the wall should exceed 33°C? How much heat will be added to the room if the panel is 7 m in width?

8.23 A 14 cm high vertical surface is heated by condensing steam at 1 atm. If the wall is kept at 30°C, how would the average

heat transfer coefficient change if methanol, CCl_4, or acetone were used instead of steam to heat it? How would the heat flux change? (This problem requires that certain information be obtained from sources outside this book.)

8.24 A 1 cm diameter tube extends 27 cm horizontally through a region of saturated steam at 1 atm. The outside of the tube can be maintained at any temperature between 50°C and 150°C. Plot the total heat transfer as a function of tube temperature.

8.25 A 2 m high vertical plate condenses steam at 1 atm. Below what temperature will Nusselt's prediction of $\overline{h}$ be in error? Below what temperature will the condensing film be turbulent?

8.26 A reflux condenser is made of copper tubing 0.8 cm in diameter with a wall temperature of 30°C. It condenses steam at 1 atm. Find $\overline{h}$ if $\alpha = 18°$ and the coil diameter is 7 cm.

8.27 The coil diameter of a helical condenser is 5 cm and the tube diameter is 5 mm. The condenser carries water at 15°C and is in a bath of saturated steam at 1 atm. Specify the number of coils and a reasonable helix angle if 6 kg/hr of steam is to be condensed. $h_{\text{inside}} = 600$ W/m^{2}K.

8.28 A schedule 40 type 304 stainless steam pipe with a 4 in. nominal diameter carries saturated steam at 150 psia in a processing plant. Calculate the heat loss per unit length of pipe if it is bare and the surrounding air is still at 68°F. How much would this heat loss be reduced if the pipe were insulated with a 1 in. layer of 85% magnesia insulation? [$Q_{\text{saved}} \simeq 127$ W/m.]

8.29 What is the maximum speed of air in the natural convection b.l. in Example 8.1?

8.30 All of the uniform-T_w, natural convection formulas for $\overline{\text{Nu}}$ take the same form, within a constant, at high Pr and Ra. What is that form? (Exclude any equation that includes turbulence.)

8.31 A large industrial process requires that water be heated by a large horizontal cylinder using natural convection. The water is at 27°C. The diameter of the cylinder is 5 m, and it is kept at 67°C. First, find $\overline{h}$. Then suppose that D is increased to 10 m.

What is the new $\overline{h}$? Explain the similarity of these answers in the turbulent natural convection regime.

8.32 A vertical jet of liquid of diameter d and moving at velocity u_∞ impinges on a horizontal disk rotating ω rad/s. There is no heat transfer in the system. Develop an expression for $\delta(r)$, where r is the radial coordinate on the disk. Contrast the r dependence of δ with that of a condensing film on a rotating disk and explain the difference qualitatively.

8.33 We have seen that if properties are constant, $h \propto \Delta T^{1/4}$ in natural convection. If we consider the variation of properties as T_w is increased over T_∞, will h depend more or less strongly on ΔT in air? in water?

8.34 A film of liquid falls along a vertical plate. It is initially saturated and it is surrounded by saturated vapor. The film thickness is δ_o. If the wall temperature below a certain point on the wall (call it $x = 0$) is raised to a value of T_w, slightly above T_{sat}, derive expressions for $\delta(x)$, Nu_x, and x_f—the distance at which the plate becomes dry. Calculate x_f if the fluid is water at 1 atm, if $T_w = 105°\text{C}$ and $\delta_o = 0.1$ mm.

8.35 In a particular solar collector, dyed water runs down a vertical plate in a laminar film with thickness δ_o at the top. The sun's rays pass through parallel glass plates (see Section 10.6) and deposit q_s W/m^2 in the film. Assume the water to be saturated at the inlet and the plate behind it to be insulated. Develop an expression for $\delta(x)$ as the water evaporates. Develop an expression for the maximum length of wetted plate, and provide a criterion for the laminar solution to be valid.

8.36 What heat removal flux can be achieved at the surface of a horizontal 0.01 mm diameter electrical resistance wire in still 27°C air if its melting point is 927°C? Neglect radiation.

8.37 A 0.03 m O.D. vertical pipe, 3 m in length, carries refrigerant through a 24°C room. How much heat does it absorb from the room if the pipe wall is at 10°C?

8.38 A 1 cm O.D. tube at 50°C runs horizontally in 20°C air. What is the critical radius of 85% magnesium insulation on the tube?

8.39 A 1 in. cube of ice is suspended in 20°C air. Estimate the drip rate in gm/min. (Neglect ΔT through the departing water film. $h_{sf} = 333,300$ J/kg.)

8.40 A horizontal electrical resistance heater, 1 mm in diameter, releases 100 W/m in water at 17°C. What is the wire temperature?

8.41 Solve Problem 5.39 using the correct formula for the heat transfer coefficient.

8.42 A red-hot vertical rod, 0.02 m in length and 0.005 m in diameter, is used to shunt an electrical current in air at room temperature. How much power can it dissipate if it melts at 1200°C? Note all assumptions and corrections. Include radiation using $\mathcal{F}_{\text{rod-room}} = 0.064$.

8.43 A 0.25 mm diameter platinum wire, 0.2 m long, is to be held horizontally at 1035°C. It is black. How much electric power is needed? Is it legitimate to treat it as a constant-wall-temperature heater in calculating the convective part of the heat transfer? The surroundings are at 20°C and the surrounding room is virtually black.

8.44 A vertical plate, 11.6 m long, condenses saturated steam at 1 atm. We want to be sure that the film stays laminar. What is the lowest allowable plate temperature, and what is $\overline{q}$ at this temperature?

8.45 A straight horizontal fin exchanges heat by laminar natural convection with the surrounding air.

a. Show that

$$\frac{d^2\theta}{d\xi^2} = m^2 L^2 \theta^{5/4}$$

where m is based on $\overline{h}_o \equiv \overline{h}(T = T_o)$.

b. Develop an iterative numerical method to solve this equation for $T(x = 0) = T_o$ and an insulated tip. (*Hint*: linearize the right side by writing it as $(m^2 L^2 \theta^{1/4})\theta$, and evaluate the term in parenthesis at the previous iteration step.)

c. Solve the resulting difference equations for m^2L^2 values ranging from 10^{-3} to 10^3. Use Gauss elimination or the tridiagonal algorithm. Express the results as η/η_o where η is the fin efficiency and η_o is the efficiency that would result if $\overline{h}_o$ were the uniform heat transfer coefficient over the entire fin.

8.46 A 2.5 cm black sphere ($\mathcal{F} = 1$) is in radiation-convection equilibrium with air at 20°C. The surroundings are at 1000 K. What is the temperature of the sphere?

8.47 Develop expressions for $\overline{h}(D)$ and $\overline{\mathrm{Nu}}_D$ during condensation on a vertical circular plate.

8.48 A cold copper plate is surrounded by a 5 mm high ridge which forms a shallow container. It is surrounded by saturated water vapor at 100°C. Estimate the steady heat flux and the rate of condensation.

a. When the plate is perfectly horizontal and filled to overflowing with condensate.

b. When the plate is in the vertical position.

c. Did you have to make any idealizations? Would they result in under- or over-estimation of the condensation?

References

[8.1] W. Nusselt. Das grundgesetz des wärmeüberganges. *Gesund. Ing.*, 38:872, 1915.

[8.2] C. J. Sanders and J. P. Holman. Franz Grashof and the Grashof Number. *Int. J. Heat Mass Transfer*, 15:562–563, 1972.

[8.3] S. W. Churchill and H. H. S. Chu. Correlating equations for laminar and turbulent free convection from a vertical plate. *Int. J. Heat Mass Transfer*, 18:1323–1329, 1975.

[8.4] S. Goldstein, editor. *Modern Developments in Fluid Mechanics*, volume 2, chapter 14. Oxford University Press, New York, 1938.

[8.5] E. R. G. Eckert and R. M. Drake, Jr. *Analysis of Heat and Mass Transfer*. Hemisphere Publishing Corp., Washington, D.C., 1987.

[8.6] A. Bejan and J. L. Lage. The Prandtl number effect on the transition in natural convection along a vertical surface. *J. Heat Transfer, Trans. ASME*, 112:787–790, 1990.

[8.7] E. M. Sparrow and J. L. Gregg. The variable fluid-property problem in free convection. In J. P. Hartnett, editor, *Recent Advances in Heat and Mass Transfer*, pages 353–371. McGraw-Hill Book Company, New York, 1961.

[8.8] H. Barrow and T. L. Sitharamarao. The effect of variable β on free convection. *Brit. Chem. Eng.*, 16(8):704, 1971.

[8.9] W. Kraus. *Messungen des Temperatur- und Geschwindigskeitsfeldes bei freier Konvection.* Verlag G. Braun, Karlsruhe, 1955. Chapter F.

[8.10] S. W. Churchill and H. H. S. Chu. Correlating equations for laminar and turbulent free convection from a horizontal cylinder. *Int. J. Heat Mass Transfer*, 18:1049–1053, 1975.

[8.11] T. Cebeci. Laminar-free-convective-heat transfer from the outer surface of a vertical slender circular cylinder. *Proc. Fifth Int. Heat Transfer Conf., Tokyo*, (NC 1.4):15–19, September 1974.

[8.12] T. Yuge. Experiments on heat transfer from spheres including combined forced and natural convection. *J. Heat Transfer, Trans. ASME, Ser. C*, 82(1):214, 1960.

[8.13] G. D. Raithby and K. G. T. Hollands. Natural convection. In W. M. Rohsenow, J. P. Hartnett, and Y. I. Cho, editors, *Handbook of Heat Transfer*, chapter 4. McGraw-Hill, New York, 3rd edition, 1998.

[8.14] J. H. Lienhard. On the commonality of equations for natural convection from immersed bodies. *Int. J. Heat Mass Transfer*, 16:2121, 1973.

[8.15] B. R. Rich. An investigation of heat transfer from an inclined flat plate in free convection. *Trans. ASME*, 75:489–499, 1953.

[8.16] T. Fujii and H. Imura. Natural convection heat transfer from a plate with arbitrary inclination. *Int. J. Heat Mass Transfer*, 15(4): 755–767, 1972.

[8.17] G. C. Vliet. Natural convection local heat transfer on constant heat transfer inclined surface. *J. Heat Transfer, Trans. ASME, Ser. C*, 91:511–516, 1969.

[8.18] L. Pera and B. Gebhart. On the stability of natural convection boundary layer flow over horizontal and slightly inclined surfaces. *Int. J. Heat Mass Transfer*, 16(6):1147–1163, 1973.

[8.19] M. Al-Arabi and M. K. El-Riedy. Natural convection heat transfer from isothermal horizontal plates of different shapes. *Int. J. Heat Mass Transfer*, 19:1399–1404, 1976.

[8.20] L. Pera and B. Gebhart. Natural convection boundary layer flow over horizontal and slightly inclined surfaces. *Int. J. Heat Mass Transfer*, 16(6):1131–1147, 1973.

[8.21] B. Gebhart, Y. Jaluria, R. L. Mahajan, and B. Sammakia. *Buoyancy-Induced Flows and Transport*. Hemisphere Publishing Corp., Washington, 1988.

[8.22] J. R. Lloyd and W. R. Moran. Natural convection adjacent to horizontal surface of various planforms. *J. Heat Transfer, Trans. ASME, Ser. C*, 96(4):443–447, 1974.

[8.23] A. M. Clausing and J. J. Berton. An experimental investigation of natural convection from an isothermal horizontal plate. *J. Heat Transfer, Trans. ASME*, 111(4):904–908, 1989.

[8.24] F. Restrepo and L. R. Glicksman. The effect of edge conditions on natural convection heat transfer from a horizontal plates. *Int. J. Heat Mass Transfer*, 17(1):135–142, 1974.

[8.25] D. W. Hatfield and D. K. Edwards. Edge and aspect ratio effects on natural convection from the horizontal heated plate facing downwards. *Int. J. Heat Mass Transfer*, 24(6):1019–1024, 1981.

[8.26] V. Kadambi and R. M. Drake, Jr. Free convection heat transfer from horizontal surfaces for prescribed variations in surface temperature and mass flow through the surface. Tech. Rept. Mech. Eng. HT-1, Princeton Univ., June 30 1959.

[8.27] K. T. Yang. Natural convection in enclosures. In S. Kakaç, R. K. Shah, and W. Aung, editors, *Handbook of Single-Phase Convective Heat Transfer*, chapter 13. Wiley-Interscience, New York, 1987.

[8.28] I. Catton. Natural convection in enclosures. In *Proc. Sixth Intl. Heat Transfer Conf.*, volume 6, pages 13–31. Toronto, Aug. 7–11 1978.

[8.29] S. W. Churchill. A comprehensive correlating equation for laminar, assisting, forced and free convection. *AIChE J.*, 23(1):10–16, 1977.

[8.30] T. S. Chen and B. F. Armaly. Mixed convection in external flow. In S. Kakaç, R. K. Shah, and W. Aung, editors, *Handbook of Single-Phase Convective Heat Transfer*, chapter 14. Wiley-Interscience, New York, 1987.

[8.31] W. Aung. Mixed convection in internal flow. In S. Kakaç, R. K. Shah, and W. Aung, editors, *Handbook of Single-Phase Convective Heat Transfer*, chapter 15. Wiley-Interscience, New York, 1987.

[8.32] V. K. Dhir. Quasi-steady laminar film condensation of steam on copper spheres. *J. Heat Transfer, Trans. ASME, Ser. C*, 97(3):347–351, 1975.

[8.33] W. Nusselt. Die oberflächenkondensation des wasserdampfes. *Z. Ver. Dtsch. Ing.*, 60:541 and 569, 1916.

[8.34] W. M. Rohsenow. Heat transfer and temperature distribution in laminar-film condensation. *Trans. ASME*, 78:1645–1648, 1956.

[8.35] E. M. Sparrow and J. L. Gregg. A boundary-layer treatment of laminar-film condensation. *J. Heat Transfer, Trans. ASME, Ser. C*, 81:13–18, 1959.

[8.36] P. Sadasivan and J. H. Lienhard. Sensible heat correction in laminar film boiling and condensation. *J. Heat Transfer, Trans. ASME*, 109: 545–547, 1987.

[8.37] V. K. Dhir and J. H. Lienhard. Laminar film condensation on plane and axi-symmetric bodies in non-uniform gravity. *J. Heat Transfer, Trans. ASME, Ser. C*, 93(1):97–100, 1971.

[8.38] E. M. Sparrow and J. L. Gregg. A theory of rotating condensation. *J. Heat Transfer, Trans. ASME, Ser. C*, 81:113–120, 1959.

[8.39] A. Karimi. Laminar film condensation on helical reflux condensers and related configurations. *Int. J. Heat Mass Transfer*, 20:1137–1144, 1977.

[8.40] R. Gregorig, J. Kern, and K. Turek. Improved correlation of film condensation data based on a more rigorous application of similarity parameters. *Wärme- und Stoffübertragung*, 7:1–13, 1974.

[8.41] P. J. Marto. Condensation. In W. M. Rohsenow, J. P. Hartnett, and Y. I. Cho, editors, *Handbook of Heat Transfer*, chapter 14. McGraw-Hill, New York, 3rd edition, 1998.

[8.42] J. Rose, H. Uehara, S. Koyama, and T. Fujii. Film condensation. In S. G. Kandlikar, M. Shoji, and V. K. Dhir, editors, *Handbook of Phase Change: Boiling and Condensation*, chapter 19. Taylor & Francis, Philadelphia, 1999.

[8.43] E. M. Sparrow and S. H. Lin. Condensation in the presence of a non-condensible gas. *J. Heat Transfer, Trans. ASME, Ser. C*, 86: 430, 1963.

9. Heat transfer in boiling and other phase-change configurations

For a charm of powerful trouble,
like a Hell-broth boil and bubble...
...Cool it with a baboon's blood,
then the charm is firm and good.
***Macbeth*, Wm. Shakespeare**

"A watched pot never boils"—the water in a teakettle takes a long time to get hot enough to boil because natural convection initially warms it rather slowly. Once boiling begins, the water is heated the rest of the way to the saturation point very quickly. Boiling is of interest to us because it is remarkably effective in carrying heat from a heater into a liquid. The heater in question might be a red-hot horseshoe quenched in a bucket or the core of a nuclear reactor with coolant flowing through it. Our aim is to learn enough about the boiling process to design systems that use boiling for cooling. We begin by considering pool boiling—the boiling that occurs when a stationary heater transfers heat to an otherwise stationary liquid.

9.1 Nukiyama's experiment and the pool boiling curve

Hysteresis in the q vs. ΔT relation for pool boiling

In 1934, Nukiyama [9.1] did the experiment described in Fig. 9.1. He boiled saturated water on a horizontal wire that functioned both as an electric resistance heater and as a resistance thermometer. By calibrating

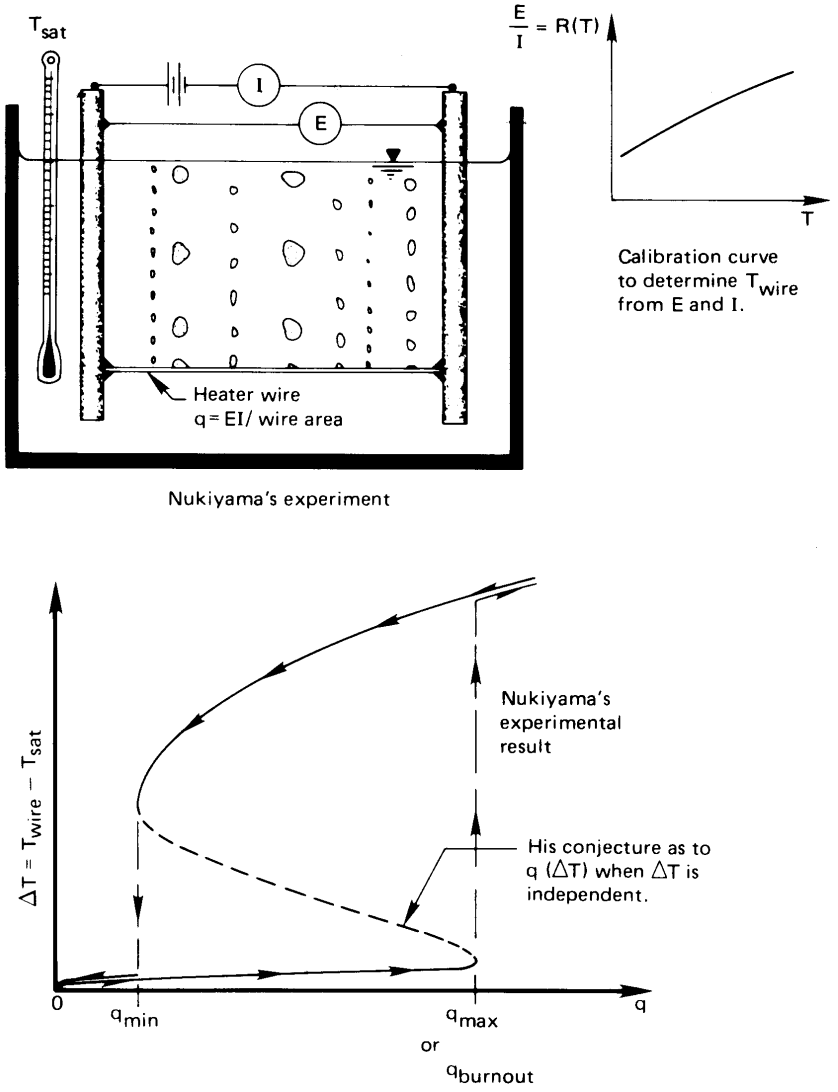

Figure 9.1 Nukiyama's boiling hysteresis loop.

the resistance of a Nichrome wire as a function of temperature before the experiment, he was able to obtain both the heat flux and the temperature using the observed current and voltage. He found that, as he increased the power input to the wire, the temperature of the wire rose sharply but the heat flux increased relatively little. Suddenly, at a particular high value of the heat flux, the wire abruptly melted. Nukiyama then obtained a platinum wire and tried again. This time the wire reached the same

limiting heat flux, but then it turned almost white-hot without melting.

As he reduced the power input to the white-hot wire, the temperature dropped in a continuous way, as shown in Fig. 9.1, until the heat flux was far below the value where the first temperature jump occurred. Then the temperature dropped abruptly to the original q vs. $\Delta T = (T_{\text{wire}} - T_{\text{sat}})$ curve, as shown. Nukiyama suspected that the hysteresis would not occur if ΔT could be specified as the independent controlled variable. He conjectured that such an experiment would result in the connecting line shown between the points where the temperatures jumped.

In 1937, Drew and Mueller [9.2] succeeded in making ΔT the independent variable by boiling organic liquids outside a tube. Steam was allowed to condense inside the tube at an elevated pressure. The steam saturation temperature—and hence the tube-wall temperature—was varied by controlling the steam pressure. This permitted them to obtain a few scattered data that seemed to bear out Nukiyama's conjecture. Measurements of this kind are inherently hard to make accurately. For the next forty years, the relatively few nucleate boiling data that people obtained were usually—and sometimes imaginatively—interpreted as verifying Nukiyama's suggestion that this part of the boiling curve is continuous.

Figure 9.2 is a completed boiling curve for saturated water at atmospheric pressure on a particular flat horizontal heater. It displays the behavior shown in Fig. 9.1, but it has been rotated to place the independent variable, ΔT, on the abscissa. (We represent Nukiyama's connecting region as two unconnected extensions of the neighboring regions for reasons that we explain subsequently.)

Modes of pool boiling

The boiling curve in Fig. 9.2 has been divided into five regimes of behavior. These regimes, and the transitions that divide them, are discussed next.

Natural convection. Water that is not in contact with its own vapor does not boil at the so-called normal boiling point,[1] T_{sat}. Instead, it continues to rise in temperature until bubbles finally to begin to form. On conventional machined metal surfaces, this occurs when the surface is a few degrees above T_{sat}. Below the bubble inception point, heat is removed by natural convection, and it can be predicted by the methods laid out in Chapter 8.

[1] This notion might be new to some readers. It is explained in Section 9.2.

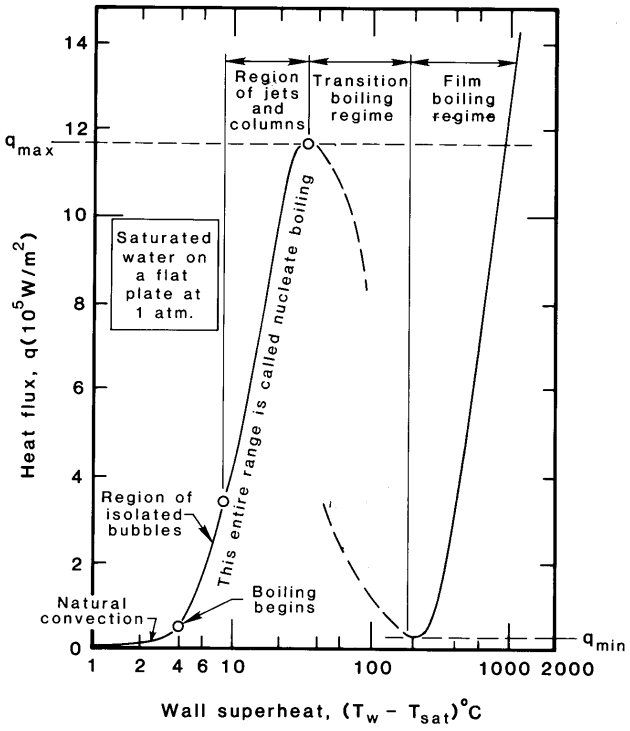

Figure 9.2 Typical boiling curve and regimes of boiling for an unspecified heater surface.

Nucleate boiling. The nucleate boiling regime embraces the two distinct regimes that lie between bubble inception and Nukiyama's first transition point:

1. *The region of isolated bubbles.* In this range, bubbles rise from isolated nucleation sites, more or less as they are sketched in Fig. 9.1. As q and ΔT increase, more and more sites are activated. Figure 9.3a is a photograph of this regime as it appears on a horizontal plate.

2. *The region of slugs and columns.* When the active sites become very numerous, the bubbles start to merge into one another, and an entirely different kind of vapor escape path comes into play. Vapor formed at the surface merges immediately into jets that feed into large overhead bubbles or "slugs" of vapor. This process is shown as it occurs on a horizontal cylinder in Fig. 9.3b.

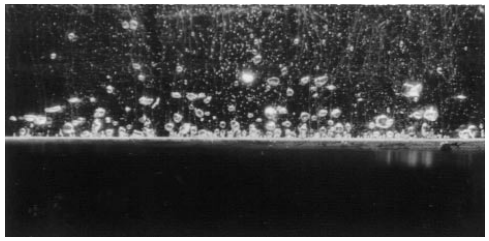

a. Isolated bubble regime—water.

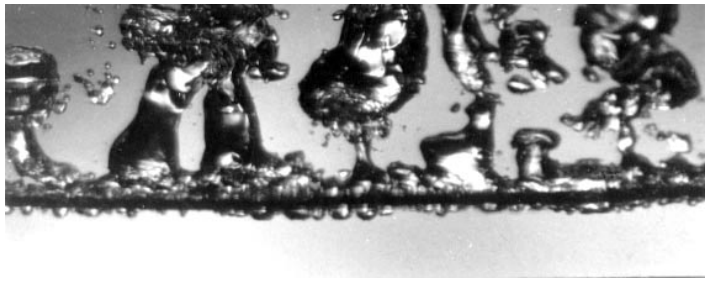

3.45 cm length of 0.0322 cm diam. wire in methanol at 10 earth-normal gravities. q=1.04×10^6 W/m^2

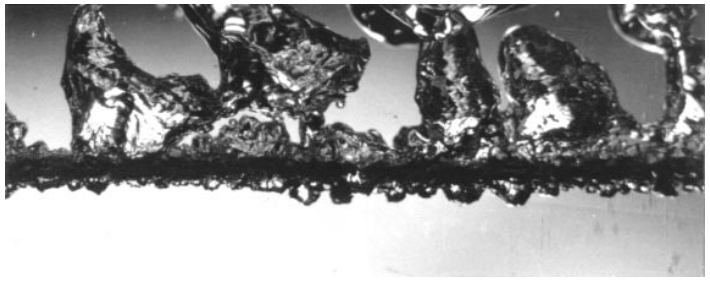

3.75 cm length of 0.164 cm diam. wire in benzene at earth-normal gravity. q=0.35×10^6 W/m^2

c. Two views of the regime of slugs and columns.

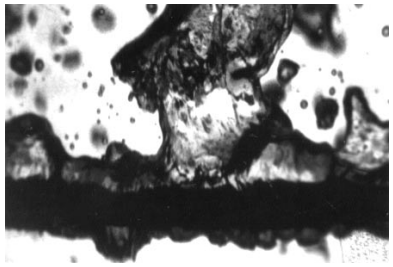

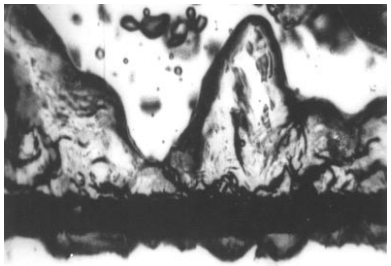

b. Two views of transitional boiling in acetone on a 0.32 cm diam. tube.

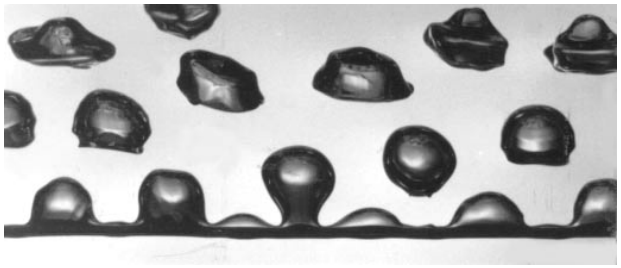

d. Film boiling of acetone on a 22 gage wire at earth-normal gravity. The true width of this image is 3.48 cm.

Figure 9.3 Typical photographs of boiling in the four regimes identified in Fig. 9.2.

Peak heat flux. Clearly, it is very desirable to be able to operate heat exchange equipment at the upper end of the region of slugs and columns. Here the temperature difference is low while the heat flux is very high. Heat transfer coefficients in this range are enormous. However, it is very dangerous to run equipment near $q_{\max}$ in systems for which q is the independent variable (as in nuclear reactors). If q is raised beyond the upper limit of the nucleate boiling regime, such a system will suffer a sudden and damaging increase of temperature. This transition[2] is known by a variety of names: the *burnout* point (although a complete burning up or melting away does not always accompany it); the *peak heat flux* (a modest descriptive term); the *boiling crisis* (a Russian term); the *DNB*, or *departure from nucleate boiling*, and the *CHF*, or *critical heat flux* (terms more often used in flow boiling); and the *first boiling transition* (which term ignores previous transitions). We designate the peak heat flux as $q_{\max}$.

Transitional boiling regime. It is a curious fact that the heat flux actually diminishes with ΔT after $q_{\max}$ is reached. In this regime the effectiveness of the vapor escape process becomes worse and worse. Furthermore, the hot surface becomes completely blanketed in vapor and q reaches a minimum heat flux which we call $q_{\min}$. Figure 9.3c shows two typical instances of transitional boiling just beyond the peak heat flux.

Film boiling. Once a stable vapor blanket is established, q again increases with increasing ΔT. The mechanics of the heat removal process during film boiling, and the regular removal of bubbles, has a great deal in common with film condensation, but the heat transfer coefficients are much lower because heat must be conducted through a vapor film instead of through a liquid film. We see an instance of film boiling in Fig. 9.3d.

Experiment 9.1

Set an open pan of cold tap water on your stove to boil. Observe the following stages as you watch:

- At first nothing appears to happen; then you notice that numerous small, stationary bubbles have formed over the bottom of the pan. These bubbles have nothing to do with boiling—they contain air that was driven out of solution as the temperature rose.

[2] We defer a proper physical explanation of the transition to Section 9.3.

- Suddenly the pan will begin to "sing." There will be a somewhat high-pitched buzzing-humming sound as the first vapor bubbles are triggered. They grow at the heated surface and condense very suddenly when their tops encounter the still-cold water above them. This *cavitation* collapse is accompanied by a small "ping" or "click," over and over, as the process is repeated at a fairly high frequency.

- As the temperature of the liquid bulk rises, the singing is increasingly muted. You may then look in the pan and see a number of points on the bottom where a feathery blur appears to be affixed. These blurred images are bubble columns emanating scores of bubbles per second. The bubbles in these columns condense completely at some distance above the surface. Notice that the air bubbles are all gradually being swept away.

- The "singing" finally gives way to a full rolling boil, accompanied by a gentle burbling sound. Bubbles no longer condense but now reach the surface, where they break.

- A full rolling-boil process, in which the liquid bulk is saturated, is a kind of isolated-bubble process, as plotted in Fig. 9.2. No kitchen stove supplies energy fast enough to boil water in the slugs-and-columns regime. You might, therefore, reflect on the relative intensity of the slugs-and-columns process.

Experiment 9.2

Repeat Experiment 54 with a glass beaker instead of a kitchen pan. Place a strobe light, blinking about 6 to 10 times per second, behind the beaker with a piece of frosted glass or tissue paper between it and the beaker. You can now see the evolution of bubble columns from the first singing mode up to the rolling boil. You will also be able to see natural convection in the refraction of the light before boiling begins.

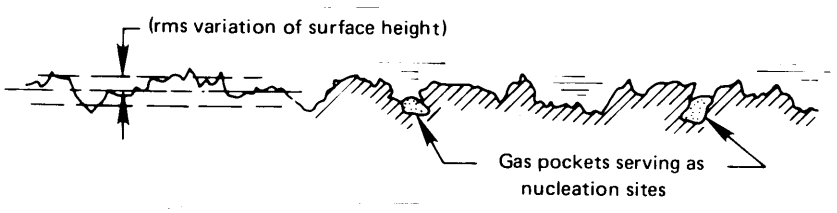

Figure 9.4 Enlarged sketch of a typical metal surface.

9.2 Nucleate boiling

Inception of boiling

Figure 9.4 shows a highly enlarged sketch of a heater surface. Most metal-finishing operations score tiny grooves on the surface, but they also typically involve some *chattering* or bouncing action, which hammers small holes into the surface. When a surface is wetted, liquid is prevented by surface tension from entering these holes, so small gas or vapor pockets are formed. These little pockets are the sites at which bubble nucleation occurs.

To see why vapor pockets serve as nucleation sites, consider Fig. 9.5. Here we see the problem in highly idealized form. Suppose that a spherical bubble of pure saturated steam is at equilibrium with an infinite superheated liquid. To determine the size of such a bubble, we impose the conditions of mechanical and thermal equilibrium.

The bubble will be in *mechanical* equilibrium when the pressure difference between the inside and the outside of the bubble is balanced by the forces of surface tension, σ, as indicated in the cutaway sketch in Fig. 9.5. Since *thermal* equilibrium requires that the temperature must be the same inside and outside the bubble, and since the vapor inside must be saturated at T_{sup} because it is in contact with its liquid, the force balance takes the form

$$R_b = \frac{2\sigma}{(p_{\text{sat}} \text{ at } T_{\text{sup}}) - p_{\text{ambient}}} \tag{9.1}$$

The p–v diagram in Fig. 9.5 shows the state points of the internal vapor and external liquid for a bubble at equilibrium. Notice that the external liquid is superheated to $(T_{\text{sup}} - T_{\text{sat}})$ K above its boiling point at the ambient pressure; but the vapor inside, being held at just the right elevated pressure by surface tension, is just saturated.

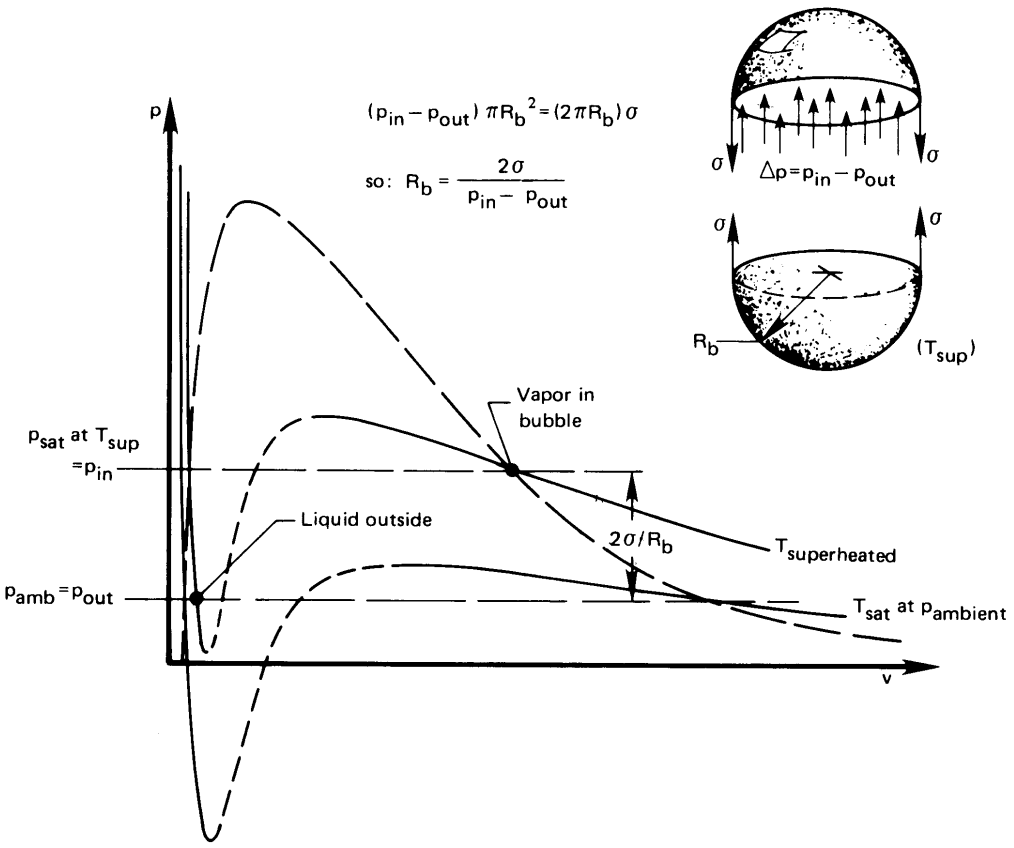

Figure 9.5 The conditions required for simultaneous mechanical and thermal equilibrium of a vapor bubble.

Physical Digression 9.1

The surface tension of water in contact with its vapor is given with great accuracy by [9.3]:

$$\sigma_{\text{water}} = 235.8\left(1 - \frac{T_{\text{sat}}}{T_c}\right)^{1.256}\left[1 - 0.625\left(1 - \frac{T_{\text{sat}}}{T_c}\right)\right]\frac{\text{mN}}{\text{m}} \qquad (9.2a)$$

where both T_{sat} and the thermodynamical critical temperature, T_c = 647.096 K, are expressed in K. The units of σ are millinewtons (mN) per meter. Table 9.1 gives additional values of σ for several substances.

Equation 9.2a is a specialized refinement of a simple, but quite accurate and widely-used, semi-empirical equation for correlating surface

Table 9.1 Surface tension for various substances from the collection of Jasper [9.4][a]

Substance	*Temperature Range* (°C)	σ (mN/m)	$\sigma = a - bT$ (°C)	
			a (mN/m)	b (mN/m·°C)
Acetone	25 to 50		26.26	0.112
Ammonia	−70	42.39		
	−60	40.25		
	−50	37.91		
	−40	35.38		
Aniline	15 to 90		44.83	0.1085
Benzene	10	30.21		
	30	27.56		
	50	24.96		
	70	22.40		
Butyl alcohol	10 to 100		27.18	0.08983
Carbon dioxide	−30	10.08		
	−10	6.14		
	10	2.67		
	30	0.07		
Carbon tetrachloride	15 to 105		29.49	0.1224
Cyclohexanol	20 to 100		35.33	0.0966
Ethyl alcohol	10 to 100		24.05	0.0832
Ethylene glycol	20 to 140		50.21	0.089
Hydrogen	−258	2.80		
	−255	2.29		
	−253	1.95		
Isopropyl alcohol	10 to 100		22.90	0.0789
Mercury	5 to 200		490.6	0.2049
Methane	90	18.877		
	100	16.328		
	115	12.371		
Methyl alcohol	10 to 60		24.00	0.0773
Naphthalene	100 to 200		42.84	0.1107
Nicotine	−40 to 90		41.07	0.1112
Nitrogen	−195 to −183		26.42	0.2265
Octane	10 to 120		23.52	0.09509
Oxygen	−202 to −184		−33.72	−0.2561
Pentane	10 to 30		18.25	0.11021
Toluene	10 to 100		30.90	0.1189
Water	10 to 100		75.83	0.1477
Carbon dioxide	−56 to 31	$\sigma = 75.00\,[1 - (T\,(\mathrm{K})/304.26)]^{1.25}$		
CFC-12 (R12) [9.5]	−148 to 112	$\sigma = 56.52\,[1 - (T\,(\mathrm{K})/385.01)]^{1.27}$		
HCFC-22 (R22) [9.5]	−158 to 96	$\sigma = 61.23\,[1 - (T\,(\mathrm{K})/369.32)]^{1.23}$		

[a] The function $\sigma = \sigma(T)$ is not really linear, but Jasper was able to linearize it over modest ranges of temperature [e.g., compare the water equation above with eqn. (9.2a)].

tension:

$$\sigma = \sigma_o \left(1 - T_{\text{sat}}/T_c\right)^{11/9} \tag{9.2b}$$

We include correlating equations of this form for CO_2, R12, and R22 at the bottom of Table 9.1. Equations of this general form are discussed in Reference [9.6].

It is easy to see that the equilibrium bubble, whose radius is described by eqn. (9.1), is unstable. If its radius is less than this value, surface tension will overbalance $[p_{\text{sat}}(T_{\text{sup}}) - p_{\text{ambient}}]$. Thus, vapor inside will condense at this higher pressure and the bubble will collapse. If the bubble radius is slightly larger than the equation specifies, liquid at the interface will evaporate and the bubble will begin to grow.

Thus, as the heater surface temperature is increased, higher and higher values of $[p_{\text{sat}}(T_{\text{sup}}) - p_{\text{ambient}}]$ will result and the equilibrium radius, R_b, will decrease in accordance with eqn. (9.1). It follows that smaller and smaller vapor pockets will be triggered into active bubble growth as the temperature is increased. As an approximation, we can use eqn. (9.1) to specify the radius of those vapor pockets that become active nucleation sites. More accurate estimates can be made using Hsu's [9.7] bubble inception theory, the subsequent work by Rohsenow and his coworkers (see, e.g., [9.8, Chap. 13]), or the still more recent technical literature.

Example 9.1

Estimate the approximate size of active nucleation sites in water at 1 atm on a wall superheated by 8 K and by 16 K. This is roughly in the regime of isolated bubbles indicated in Fig. 9.2.

SOLUTION. $p_{\text{sat}} = 1.203 \times 10^5$ N/m^2 at 108°C and 1.769×10^5 N/m^2 at 116°C, and σ is given as 57.36 mN/m at $T_{\text{sat}} = 108$°C and as 55.78 mN/m at $T_{\text{sat}} = 116$°C by eqn. (9.2a). Then, at 108°C, R_b from eqn. (9.1) is

$$R_b = \frac{2(57.36 \times 10^{-3})\ \text{N/m}}{(1.203 \times 10^5 - 1.013 \times 10^5)\ \text{N/m}^2}$$

and similarly for 116°C, so the radius of active nucleation sites is on the order of

$$R_b = 0.0060 \text{ mm at } T = 108°\text{C} \quad \text{or} \quad 0.0015 \text{ mm at } 116°\text{C}$$

This means that active nucleation sites would be holes with diameters very roughly on the order of magnitude of 0.005 mm or 5μm—at least on the heater represented by Fig. 9.2. That is within the range of roughness of commercially finished surfaces. ■

Region of isolated bubbles

The mechanism of heat transfer enhancement in the isolated bubble regime was hotly argued in the years following World War II. A few conclusions have emerged from that debate, and we shall attempt to identify them. There is little doubt that bubbles act in some way as small pumps that keep replacing liquid heated at the wall with cool liquid. The question is that of specifying the correct mechanism. Figure 9.6 shows the way bubbles probably act to remove hot liquid from the wall and introduce cold liquid to be heated.

It is apparent that the number of active nucleation sites generating bubbles will strongly influence q. On the basis of his experiments, Yamagata showed in 1955 (see, e.g., [9.9]) that

$$q \propto \Delta T^a n^b \tag{9.3}$$

where $\Delta T \equiv T_w - T_{\text{sat}}$ and n is the site density or number of active sites per square meter. A great deal of subsequent work has been done to fix the constant of proportionality and the constant exponents, a and b. The exponents turn out to be approximately $a = 1.2$ and $b = \frac{1}{3}$.

The problem with eqn. (9.3) is that it introduces what engineers call a *nuisance variable*. A nuisance variable is one that varies from system to system and cannot easily be evaluated—the site density, n, in this case. Normally, n increases with ΔT in some way, but how? If all sites were identical in size, all sites would be activated simultaneously, and q would be a discontinuous function of ΔT. When the sites have a typical distribution of sizes, n (and hence q) can increase very strongly with ΔT.

It is a lucky fact that for a large class of factory-finished materials, n varies approximately as $\Delta T^{5 \text{ or } 6}$, so q varies roughly as ΔT^3. This has made it possible for various authors to correlate q approximately for a large variety of materials. One of the first and most useful correlations for nucleate boiling was that of Rohsenow [9.10] in 1952. It is

$$\frac{c_p\,(T_w - T_{\text{sat}})}{h_{fg}\,\text{Pr}^s} = C_{\text{sf}} \left[\frac{q}{\mu h_{fg}} \sqrt{\frac{\sigma}{g(\rho_f - \rho_g)}} \right]^{0.33} \tag{9.4}$$

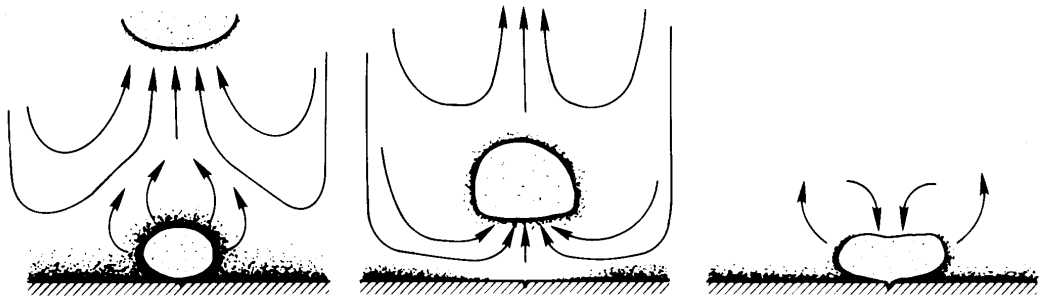

A bubble growing and departing in saturated liquid. The bubble grows, absorbing heat from the superheated liquid on its periphery. As it leaves, it entrains cold liquid onto the plate which then warms up until nucleation occurs and the cycle repeats.

A bubble growing in subcooled liquid. When the bubble protrudes into cold liquid, steam can condense on the top while evaporation continues on the bottom. This provides a short-circuit for cooling the wall. Then, when the bubble caves in, cold liquid is brought to the wall.

Figure 9.6 Heat removal by bubble action during boiling. Dark regions denote locally superheated liquid.

where all properties, unless otherwise noted, are for liquid at T_{sat}. The constant C_{sf} is an empirical correction for typical surface conditions. Table 9.2 includes a set of values of C_{sf} for common surfaces (taken from [9.10]) as well as the Prandtl number exponent, s. A more extensive compilation of these constants was published by Pioro in 1999 [9.11].

We noted, initially, that there are two nucleate boiling regimes, and the Yamagata equation (9.3) applies only to the first of them. Rohsenow's equation is frankly empirical and does not depend on the rational analysis of either nucleate boiling process. It turns out that it represents $q(\Delta T)$ in both regimes, but it is not terribly accurate in either one. Figure 9.7 shows Rohsenow's original comparison of eqn. (9.4) with data for water over a large range of conditions. It shows typical errors in heat flux of 100% and typical errors in ΔT of about 25%.

Thus, our ability to predict the nucleate pool boiling heat flux is poor. Our ability to predict ΔT is better because, with $q \propto \Delta T^3$, a large error in q gives a much smaller error in ΔT. It appears that any substantial improvement in this situation will have to wait until someone has managed to deal realistically with the nuisance variable, n. Current research efforts are dealing with this matter, and we can simply hope that such work will eventually produce a method for achieving reliable heat transfer design relationships for nucleate boiling.

Table 9.2 Selected values of the surface correction factor for use with eqn. (9.4) [9.10]

Surface–Fluid Combination	C_{sf}	s
Water–nickel	0.006	1.0
Water–platinum	0.013	1.0
Water–copper	0.013	1.0
Water–brass	0.006	1.0
CCl_4–copper	0.013	1.7
Benzene–chromium	0.010	1.7
n-Pentane–chromium	0.015	1.7
Ethyl alcohol–chromium	0.0027	1.7
Isopropyl alcohol–copper	0.0025	1.7
35% K_2CO_3–copper	0.0054	1.7
50% K_2CO_3–copper	0.0027	1.7
n-Butyl alcohol–copper	0.0030	1.7

It is indeed fortunate that we do not often have to calculate q, given ΔT, in the nucleate boiling regime. More often, the major problem is to avoid exceeding q_{max}. We turn our attention in the next section to predicting this limit.

Example 9.2

What is C_{sf} for the heater surface in Fig. 9.2?

SOLUTION. From eqn. (9.4) we obtain

$$\frac{q}{\Delta T^3} C_{sf}^3 = \frac{\mu c_p^3}{h_{fg}^2 \mathrm{Pr}^3} \sqrt{\frac{g(\rho_f - \rho_g)}{\sigma}}$$

where, since the liquid is water, we take s to be 1.0. Then, for water at $T_{sat} = 100°C$: $c_p = 4.22$ kJ/kg·K, Pr = 1.75, $(\rho_f - \rho_g) = 958$ kg/m^3, $\sigma = 0.0589$ N/m or kg/s^2, $h_{fg} = 2257$ kJ/kg, $\mu = 0.000282$ kg/m·s.

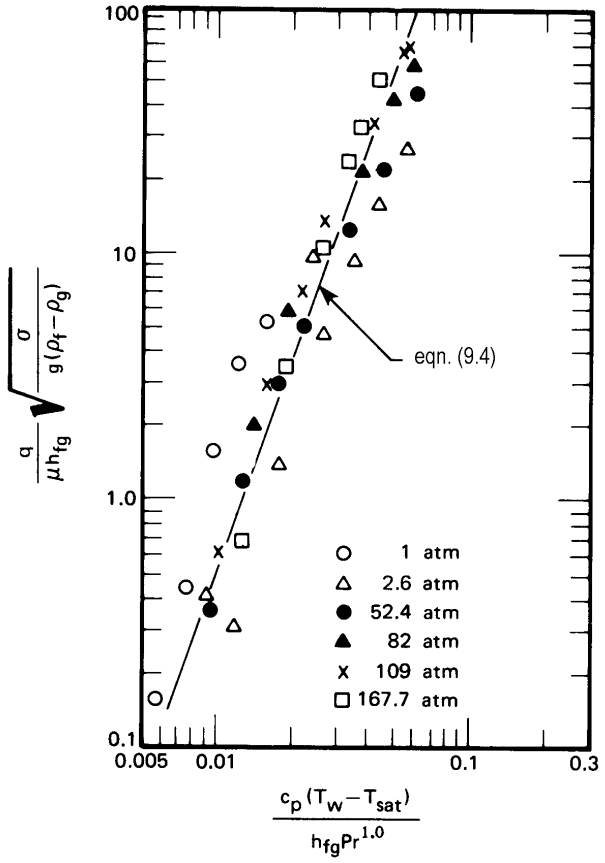

Figure 9.7 Illustration of Rohsenow's [9.10] correlation applied to data for water boiling on 0.61 mm diameter platinum wire.

Thus,

$$\frac{q}{\Delta T^3}\,C_{\text{sf}}^3 = 3.10\times 10^{-7}\,\frac{\text{kW}}{\text{m}^2\text{K}^3}$$

At $q = 800$ kW/m^2, we read $\Delta T = 22$ K from Fig. 9.2. This gives

$$C_{\text{sf}} = \left[\frac{3.10\times 10^{-7}(22)^3}{800}\right]^{1/3} = 0.016$$

This value compares favorably with C_{sf} for a platinum or copper surface under water. ■

9.3 Peak pool boiling heat flux

Transitional boiling regime and Taylor instability

It will help us to understand the peak heat flux if we first consider the process that connects the peak and the minimum heat fluxes. During high heat flux transitional boiling, a large amount of vapor is glutted about the heater. It wants to buoy upward, but it has no clearly defined escape route. The jets that carry vapor away from the heater in the region of slugs and columns are unstable and cannot serve that function in this regime. Therefore, vapor buoys up in big slugs—then liquid falls in, touches the surface briefly, and a new slug begins to form. Figure 9.3c shows part of this process.

The high and low heat flux transitional boiling regimes are different in character. The low heat flux region does not look like Fig. 9.2c but is almost indistinguishable from the film boiling shown in Fig. 9.2d. However, both processes display a common conceptual key: In both, the heater is almost completely blanketed with vapor. In both, we must contend with the unstable configuration of a liquid on top of a vapor.

Figure 9.8 shows two commonplace examples of such behavior. In either an inverted honey jar or the water condensing from a cold water pipe, we have seen how a heavy fluid falls into a light one (water or honey, in this case, collapses into air). The heavy phase falls down at one node of a wave and the light fluid rises into the other node.

The collapse process is called *Taylor instability* after G. I. Taylor, who first predicted it. The so-called Taylor wavelength, λ_d, is the length of the wave that grows fastest and therefore predominates during the collapse of an infinite plane horizontal interface. It can be predicted using dimensional analysis. The dimensional functional equation for λ_d is

$$\lambda_d = \text{fn}\left[\sigma, g(\rho_f - \rho_g)\right] \tag{9.5}$$

since the wave is formed as a result of the balancing forces of surface tension against inertia and gravity. There are three variables involving m and kg/s^2, so we look for just one dimensionless group:

$$\lambda_d \sqrt{\frac{g(\rho_f - \rho_g)}{\sigma}} = \text{constant}$$

This relationship was derived analytically by Bellman and Pennington [9.12] for one-dimensional waves and by Sernas [9.13] for the two-dimensional

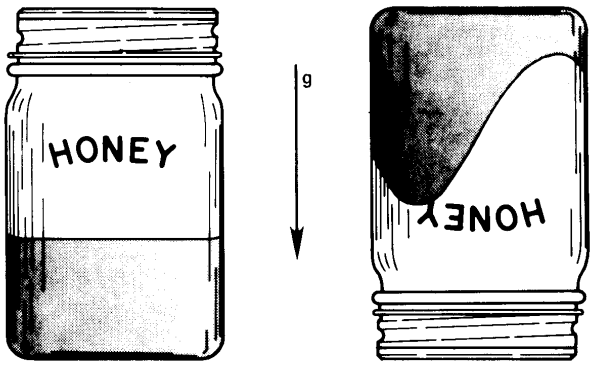

a. Taylor instability in the surface of the honey in an inverted honey jar

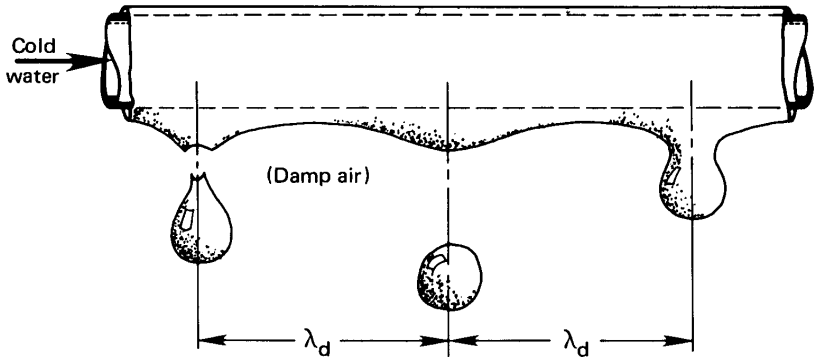

b. Taylor instability in the interface of the water condensing on the underside of a small cold water pipe.

Figure 9.8 Two examples of Taylor instabilities that one might commonly experience.

waves that actually occur in a plane horizontal interface. The results were

$$\lambda_d \sqrt{\frac{g(\rho_f - \rho_g)}{\sigma}} = \begin{cases} 2\pi\sqrt{3} & \text{for one-dimensional waves} \\ 2\pi\sqrt{6} & \text{for two-dimensional waves} \end{cases} \tag{9.6}$$

Experiment 9.3

Hang a metal rod in the horizontal position by threads at both ends. The rod should be about 30 cm in length and perhaps 1 to 2 cm in diameter. Pour motor oil or glycerin in a narrow cake pan and lift the pan up under the rod until it is submerged. Then lower the pan and watch the liquid drain into it. Take note of the wave action on the underside of the rod. The same thing can be done in an even more satisfactory way by running cold water through a horizontal copper tube above a beaker of boiling water. The condensing liquid will also come off in a Taylor wave such as is shown in Fig. 9.8. In either case, the waves will approximate λ_{d_1} (the length of a one-dimensional wave, since they are arrayed on a line), but the wavelength will be influenced by the curvature of the rod.

Throughout the transitional boiling regime, vapor rises into liquid on the nodes of Taylor waves, and at $q_{\max}$ this rising vapor forms into jets. These jets arrange themselves on a staggered square grid, as shown in Fig. 9.9. The basic spacing of the grid is λ_{d_2} (the two-dimensional Taylor wavelength). Since

$$\lambda_{d_2} = \sqrt{2}\,\lambda_{d_1} \tag{9.7}$$

[recall eqn. (9.6)], the spacing of the most basic module of jets is actually λ_{d_1}, as shown in Fig. 9.9.

Next we must consider how the jets become unstable at the peak, to bring about burnout.

Helmholtz instability of vapor jets

Figure 9.10 shows a commonplace example of what is called *Helmholtz instability*. This is the phenomenon that causes the vapor jets to cave in when the vapor velocity in them reaches a critical value. Any flag in a breeze will constantly be in a state of collapse as the result of relatively high pressures where the velocity is low and relatively low pressures where the velocity is high, as is indicated in the top view.

This same instability is shown as it occurs in a vapor jet wall in Fig. 9.11. This situation differs from the flag in one important particular. There is surface tension in the jet walls, which tends to balance the flow-induced pressure forces that bring about collapse. Thus, while the flag is unstable in *any* breeze, the vapor velocity in the jet must reach a limiting value, u_g, before the jet becomes unstable.

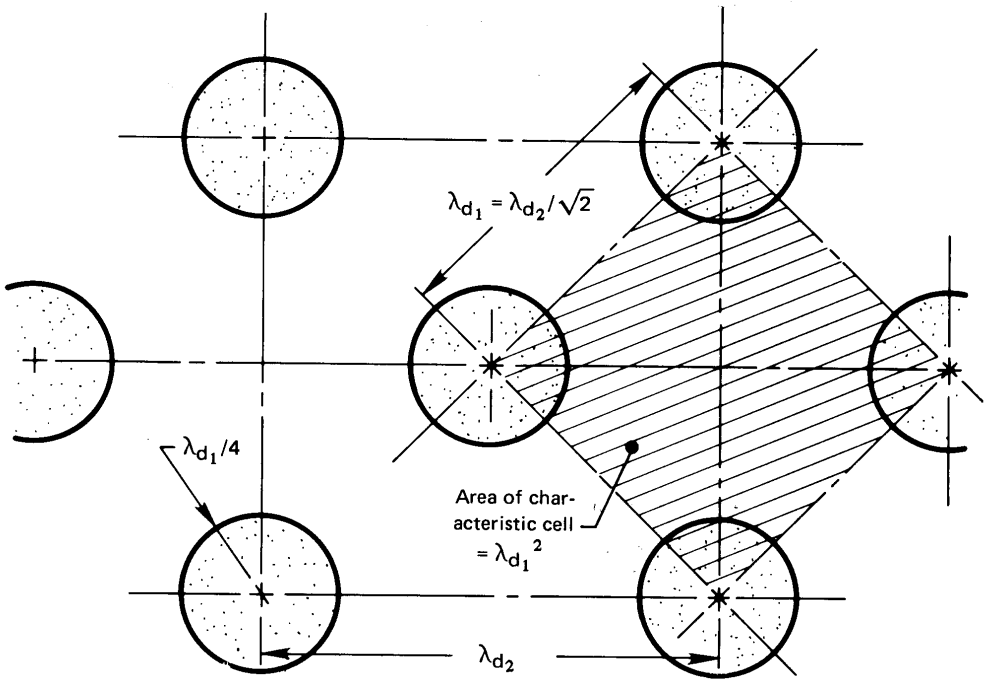

a. Plan view of bubbles rising from surface

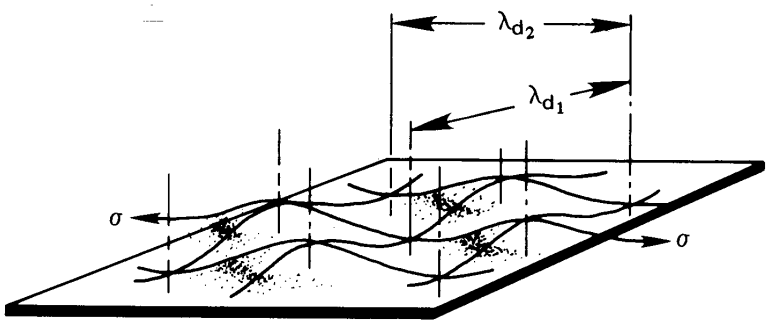

b. Waveform underneath the bubbles shown in **a.**

Figure 9.9 The array of vapor jets as seen on an infinite horizontal heater surface.

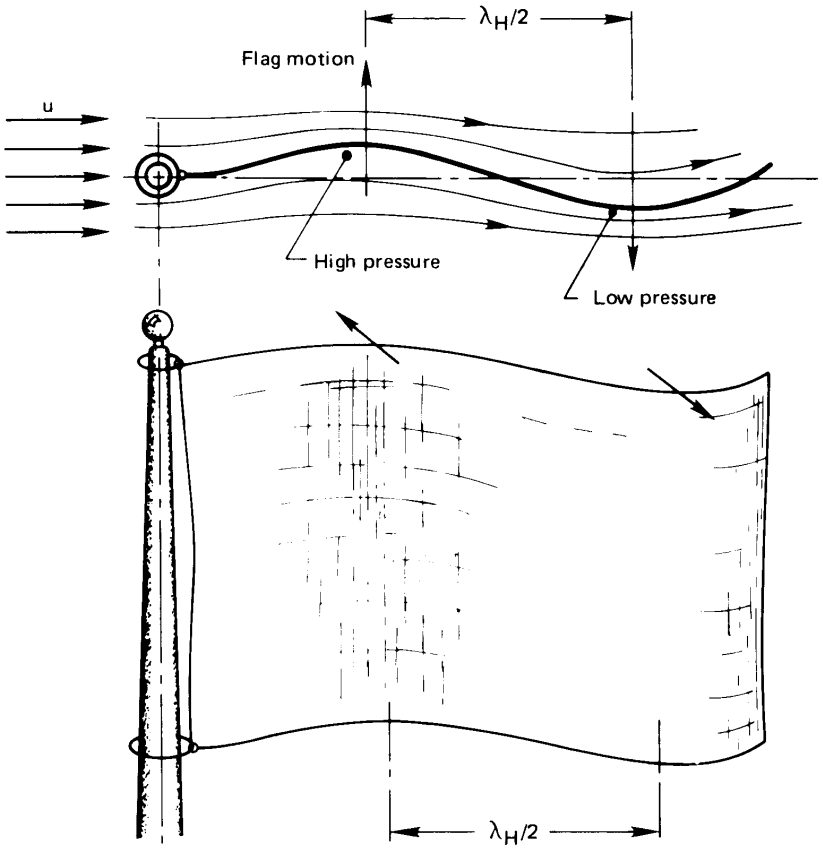

Figure 9.10 The flapping of a flag due to Helmholtz instability.

Lamb [9.14] gives the following relation between the vapor flow u_g, shown in Fig. 9.11, and the wavelength of a disturbance in the jet wall, λ_H:

$$u_g = \sqrt{\frac{2\pi\sigma}{\rho_g \lambda_H}} \tag{9.8}$$

[This result, like eqn. (9.6), can be predicted within a constant using dimensional analysis. See Problem 9.19.] A real liquid–vapor interface will usually be irregular, and therefore it can be viewed as containing all possible sinusoidal wavelengths superposed on one another. One problem we face is that of guessing whether or not one of those wavelengths

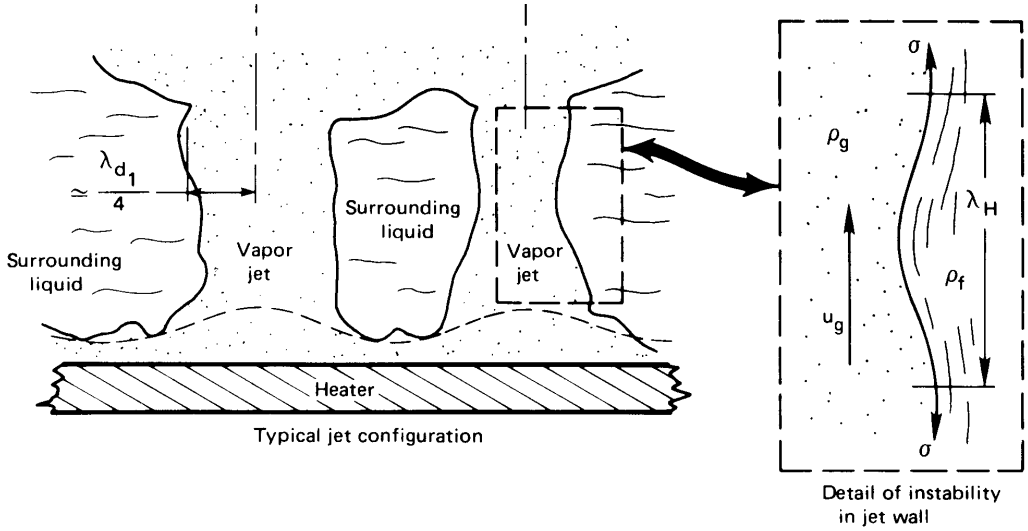

Figure 9.11 Helmholtz instability of vapor jets.

will be better developed than the others and therefore more liable to collapse.

Example 9.3

Saturated water at 1 atm flows down the periphery of the inside of a 10 cm I.D. vertical tube. Steam flows upward in the center. The wall of the pipe has circumferential corrugations in it, with a 4 cm wavelength in the axial direction. Neglect problems raised by curvature and the finite thickness of the liquid, and estimate the steam velocity required to destabilize the liquid flow over these corrugations, assuming that the liquid moves slowly.

SOLUTION. The flow will be Helmholtz-stable until the steam velocity reaches the value given by eqn. (9.8):

$$u_g = \sqrt{\frac{2\pi(0.0589)}{0.577(0.04\text{ m})}}$$

Thus, the maximum stable steam velocity would be $u_g = 4$ m/s. Beyond that, the liquid will form whitecaps and be blown back upward. ■

Example 9.4

Capillary forces hold mercury in place between two parallel steel plates with a lid across the top. The plates are slowly pulled apart until the mercury interface collapses. Approximately what is the maximum spacing?

SOLUTION. The mercury is most susceptible to Taylor instability when the spacing reaches the wavelength given by eqn. (9.6):

$$\lambda_{d_1} = 2\pi\sqrt{3}\sqrt{\frac{\sigma}{g(\rho_f - \rho_g)}} = 2\pi\sqrt{3}\sqrt{\frac{0.487}{9.8(13600)}} = 0.021 \text{ m} = 2.1 \text{ cm}$$

(Actually, this spacing would give the maximum *rate* of collapse. It can be shown that collapse would begin at $1/\sqrt{3}$ times this value, or at 1.2 cm.) ■

Prediction of $q_{\max}$

General expression for $q_{\max}$ The heat flux must be balanced by the latent heat carried away in the jets when the liquid is saturated. Thus, we can write immediately

$$q_{\max} = \rho_g h_{fg} u_g \left(\frac{A_j}{A_h}\right) \tag{9.9}$$

where A_j is the cross-sectional area of a jet and A_h is the heater area that supplies each jet.

For any heater configuration, two things must be determined. One is the length of the particular disturbance in the jet wall, λ_H, which will trigger Helmholtz instability and fix u_g in eqn. (9.8) for use in eqn. (9.9). The other is the ratio A_j/A_h. The prediction of $q_{\max}$ in any pool boiling configuration always comes down to these two problems.

$q_{\max}$ on an infinite horizontal plate. The original analysis of this type was done by Zuber in his doctoral dissertation at UCLA in 1958 (see [9.15]). He first guessed that the jet radius was $\lambda_{d_1}/4$. This guess has received corroboration by subsequent investigators, and (with reference to Fig. 9.9)

it gives

$$\frac{A_j}{A_h} = \frac{\text{cross-sectional area of circular jet}}{\text{area of the square portion of the heater that feeds the jet}} = \frac{\pi(\lambda_{d_1}/4)^2}{(\lambda_{d_1})^2} = \frac{\pi}{16} \tag{9.10}$$

Lienhard and Dhir ([9.16, 9.17, 9.18]) guessed that the Helmholtz-unstable wavelength might be equal to λ_{d_1}, so eqn. (9.9) became

$$q_{\max} = \rho_g h_{fg} \sqrt{\frac{2\pi\sigma}{\rho_g}} \frac{1}{2\pi\sqrt{3}} \sqrt{\frac{g(\rho_f - \rho_g)}{\sigma}} \times \frac{\pi}{16}$$

or[3]

$$\boxed{q_{\max} = 0.149\ \rho_g^{1/2} h_{fg}\ \sqrt[4]{g(\rho_f - \rho_g)\sigma}} \tag{9.11}$$

Equation (9.11) is compared with available data for large flat heaters, with vertical sidewalls to prevent any liquid sideflow, in Fig. 9.12. So long as the diameter or width of the heater is more than about $3\lambda_{d_1}$, the prediction is quite accurate. When the width or diameter is less than this, there is a small integral number of jets on a plate which may be larger or smaller in area than $16/\pi$ per jet. When this is the case, the actual $q_{\max}$ may be larger or smaller than that predicted by eqn. (9.11) (see Problem 9.13).

The form of the preceding prediction is usually credited to Kutateladze [9.19] and Zuber [9.15]. Kutateladze (then working in Leningrad and later director of the Heat Transfer Laboratory near Novosibirsk, Siberia) recognized that burnout resembled the flooding of a distillation column. At any level in a distillation column, alcohol-rich vapor (for example) rises while water-rich liquid flows downward in counterflow. If the process is driven too far, the flows become Helmholtz-unstable and the process collapses. The liquid then cannot move downward and the column is said to "flood."

Kutateladze did the dimensional analysis of $q_{\max}$ based on the flooding mechanism and obtained the following relationship, which, lacking a characteristic length and being of the same form as eqn. (9.11), is really valid only for an infinite horizontal plate:

$$q_{\max} = C\ \rho_g^{1/2} h_{fg}\ \sqrt[4]{g(\rho_f - \rho_g)\sigma}$$

[3] Readers are reminded that $\sqrt[n]{x} \equiv x^{1/n}$.

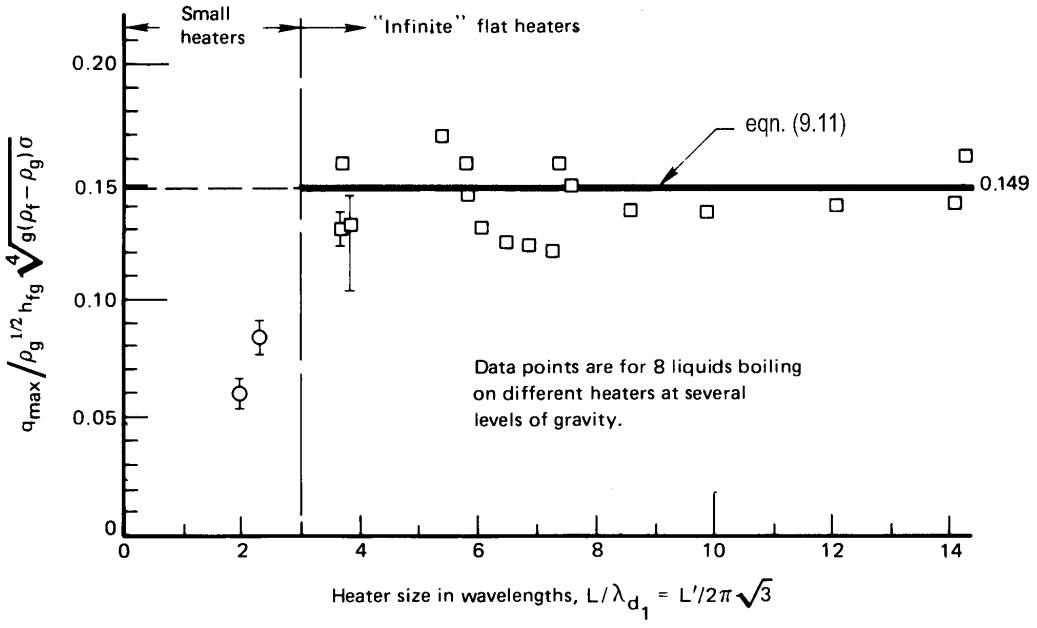

Figure 9.12 Comparison of the $q_{\max}$ prediction for infinite horizontal heaters with data reported in [9.16].

He then suggested that C was equal to 0.131 on the basis of data from configurations other than infinite flat plates (horizontal cylinders, for example). Zuber's analysis yielded $C = \pi/24 = 0.1309$, which was quite close to Kutateladze's value but lower by 14% than eqn. (9.11). We therefore designate the Zuber-Kutateladze prediction as $q_{\max_z}$. However, we shall not use it directly, since it does not predict any actual physical configuration.

$$q_{\max_z} \equiv 0.131\, \rho_g^{1/2} h_{fg} \sqrt[4]{g(\rho_f - \rho_g)\sigma} \tag{9.12}$$

It is very interesting that C. F. Bonilla, whose $q_{\max}$ experiments in the early 1940s are included in Fig. 9.12, also suggested that $q_{\max}$ should be compared with the column-flooding mechanism. He presented these ideas in a paper, but A. P. Colburn wrote to him: "A correlation [of the flooding velocity plots with] boiling data would not serve any great purpose and would perhaps be very misleading." And T. H. Chilton—another eminent chemical engineer of that period—wrote to him: "I venture to suggest that you delete from the manuscript…the relationship between boiling rates and loading velocities in packed towers." Thus, the technical conservativism of the period prevented the idea from gaining acceptance for another decade.

Example 9.5

Predict the peak heat flux for Fig. 9.2.

SOLUTION. We use eqn. (9.11) to evaluate $q_{\max}$ for water at 100°C on an infinite flat plate:

$$\begin{aligned} q_{\max} &= 0.149\, \rho_g^{1/2} h_{fg} \sqrt[4]{g(\rho_f - \rho_g)\sigma} \\ &= 0.149(0.597)^{1/2}(2,257,000) \sqrt[4]{9.8(958.2 - 0.6)(0.0589)} \\ &= 1.260 \times 10^6 \text{ W/m}^2 \\ &= 1.260 \text{ MW/m}^2 \end{aligned}$$

Figure 9.2 shows $q_{\max} \simeq 1.160$ MW/m^2, which is less by only about 8%. ■

Example 9.6

What is $q_{\max}$ in mercury on a large flat plate at 1 atm?

SOLUTION. The normal boiling point of mercury is 355°C. At this temperature, $h_{fg} = 292,500$ J/kg, $\rho_f = 13,400$ kg/m^3, $\rho_g = 4.0$ kg/m^3, and $\sigma \simeq 0.418$ kg/s^2, so

$$\begin{aligned} q_{\max} &= 0.149(4.0)^{1/2}(292,500) \sqrt[4]{9.8(13,400 - 4)(0.418)} \\ &= 1.334 \text{ MW/m}^2 \end{aligned}$$

The result is very close to that for water. The increases in density and surface tension have been compensated by a much lower latent heat. ■

Peak heat flux in other pool boiling configurations

The prediction of $q_{\max}$ in configurations other than an infinite flat heater will involve a characteristic length, L. Thus, the dimensional functional equation for $q_{\max}$ becomes

$$q_{\max} = \text{fn}\left[\rho_g, h_{fg}, \sigma, g(\rho_f - \rho_g), L\right]$$

which involves six variables and four dimensions: J, m, s, and kg, and kg, where, once more in accordance with Section 4.3, we note that no significant conversion from work to heat is occurring so that J must be retained as a separate unit. There are thus two pi-groups. The first group

can arbitrarily be multiplied by $24/\pi$ to give

$$\Pi_1 = \frac{q_{\max}}{(\pi/24)\,\rho_g^{1/2} h_{fg}\,\sqrt[4]{\sigma g(\rho_f - \rho_g)}} = \frac{q_{\max}}{q_{\max_z}} \tag{9.13}$$

Notice that the factor of $24/\pi$ has served to make the denominator equal to $q_{\max_z}$ (Zuber's expression for $q_{\max}$). Thus, for $q_{\max}$ on a flat plate, Π_1 equals 0.149/0.131, or 1.14. The second pi-group is

$$\Pi_2 = \frac{L}{\sqrt{\sigma/g(\rho_f - \rho_g)}} = 2\pi\sqrt{3}\frac{L}{\lambda_{d_1}} \equiv L' \tag{9.14}$$

The latter group, Π_2, is the square root of the *Bond number*, Bo, which is used to compare buoyant force with capillary forces.

Predictions and correlations of $q_{\max}$ have been made for several finite geometries in the form

$$\frac{q_{\max}}{q_{\max_z}} = \text{fn}\,(L') \tag{9.15}$$

The dimensionless characteristic length in eqn. (9.15) might be a dimensionless radius (R'), a dimensionless diameter (D'), or a dimensionless height (H'). The graphs in Fig. 9.13 are comparisons of several of the existing predictions and correlations with experimental data. These predictions and others are listed in Table 9.3. Notice that the last three items in Table 9.3 (10, 11, and 12) are general expressions from which several of the preceding expressions in the table can be obtained.

The equations in Table 9.3 are all valid within ±15% or 20%, which is very little more than the inherent scatter of $q_{\max}$ data. However, they are subject to the following conditions:

- The bulk liquid is saturated.
- There are no pathological surface imperfections.
- There is no forced convection.

Another limitation on all the equations in Table 9.3 is that neither the size of the heater nor the relative force of gravity can be too small. When $L' < 0.15$ in most configurations, the Bond number is

$$\text{Bo} \equiv L'^2 = \frac{g(\rho_f - \rho_g)L^3}{\sigma L} = \frac{\text{buoyant force}}{\text{capillary force}} < \frac{1}{44}$$

In this case, the process becomes completely dominated by surface tension and the Taylor-Helmholtz wave mechanisms no longer operate. As L' is reduced, the peak and minimum heat fluxes cease to occur and the

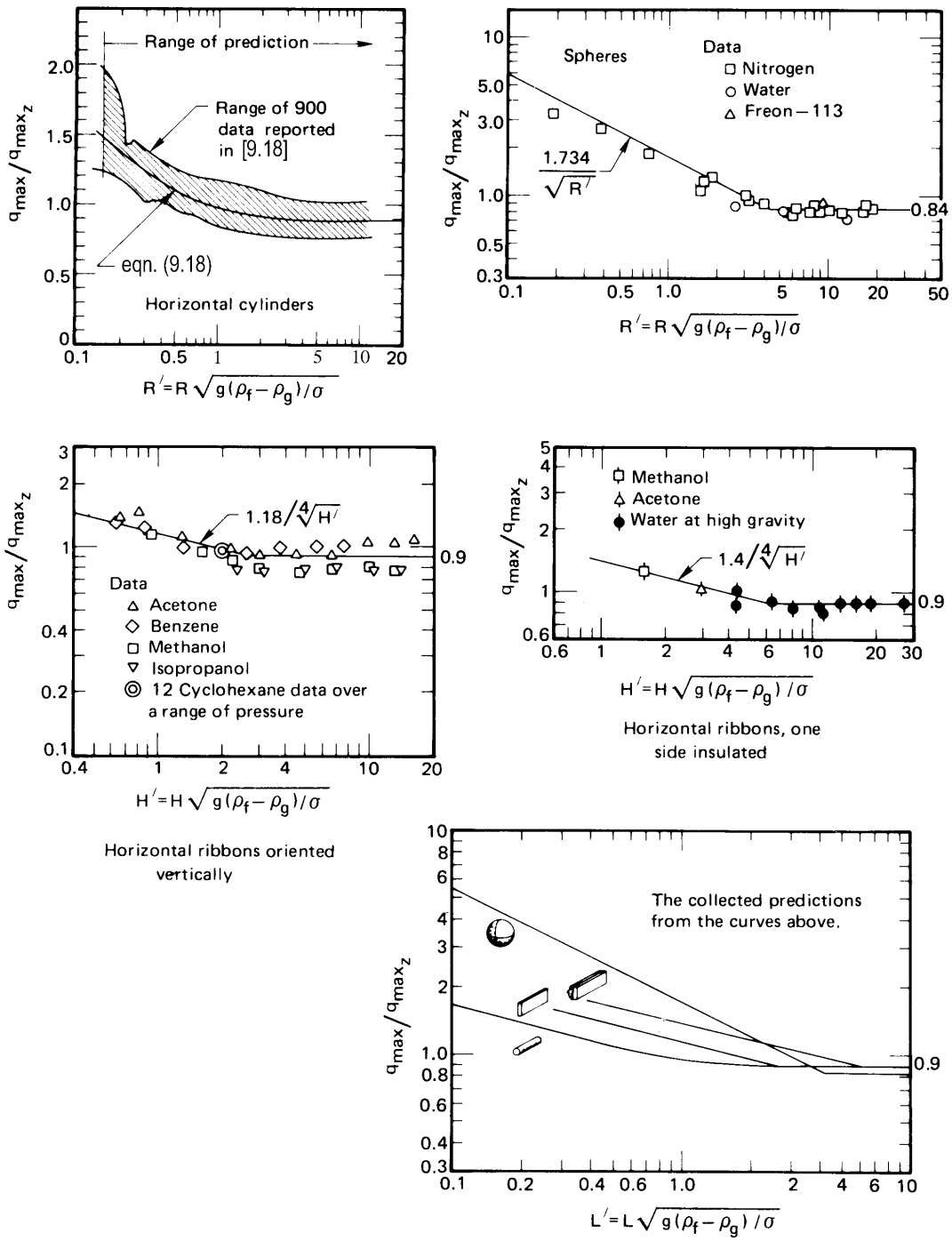

Figure 9.13 The peak pool boiling heat flux on several heaters.

Table 9.3 Predictions of the peak pool boiling heat flux

Situation	$q_{\max}/q_{\max_z}$	*Basis for* L'	*Range of* L'	*Source*	*Eqn. No.*
1. Infinite flat heater	1.14	Heater width or diameter	$L' \geq 27$	[9.17]	(9.16)
2. Small flat heater	$1.14(\lambda_{d_1}/A_{\text{heater}})$	Heater width or diameter	$9 < L' < 20$	[9.17]	(9.17)
3. Horizontal cylinder	$0.89 + 2.27e^{-3.44\sqrt{R'}}$	Cylinder radius, R	$R' \geq 0.15$	[9.20]	(9.18)
4. Large horizontal cylinder	0.90	Cylinder radius, R	$R' \geq 1.2$	[9.18]	(9.19)
5. Small horizontal cylinder	$0.94/(R')^{1/4}$	Cylinder radius, R	$0.15 \leq R' \leq 1.2$	[9.18]	(9.20)
6. Large sphere	0.84	Sphere radius, R	$R' \geq 4.26$	[9.21]	(9.21)
7. Small sphere	$1.734/(R')^{1/2}$	Sphere radius, R	$0.15 \leq R' \leq 4.26$	[9.21]	(9.22)
Small horizontal ribbon oriented vertically					
8. plain	$1.18/(H')^{1/4}$	Height of side, H	$0.15 \leq H' \leq 2.96$	[9.18]	(9.23)
9. 1 side insulated	$1.4/(H')^{1/4}$	Height of side, H	$0.15 \leq H' \leq 5.86$	[9.18]	(9.24)
10. Any large finite body	~ 0.90	Characteristic length, L	cannot specify generally; $L' \gtrsim 4$	[9.18]	(9.25)
11. Small slender cylinder of any cross section	$1.4/(P')^{1/4}$	Transverse perimeter, P	$0.15 \leq P' \leq 5.86$	[9.18]	(9.26)
12. Small bluff body	$\text{Constant}/(L')^{1/2}$	Characteristic length, L	cannot specify generally; $L' \lesssim 4$	[9.18]	(9.27)

boiling curve becomes monotonic. When nucleation occurs on a very small wire, the wire is immediately enveloped in vapor and the mechanism of heat removal passes directly from natural convection to film boiling.

Example 9.7

A spheroidal metallic body of surface area 400 cm^2 and volume 600 cm^3 is quenched in saturated water at 1 atm. What is the most rapid rate of heat removal during the quench?

SOLUTION. As the cooling process progresses, it goes through the boiling curve from film boiling, through $q_{\min}$, up the transitional boiling regime, through $q_{\max}$, and down the nucleate boiling curve. Cooling is finally completed by natural convection. One who has watched the quenching of a red-hot horseshoe will recall the great gush of bubbling that occurs as $q_{\max}$ is reached. We therefore calculate the required heat flow as $Q = q_{\max} A_{\text{spheroid}}$, where $q_{\max}$ is given by eqn. (9.25) in Table 9.3:

$$q_{\max} = 0.9\, q_{\max_z} = 0.9(0.131)\rho_g^{1/2} h_{fg} \sqrt[4]{g\sigma(\rho_f - \rho_g)}$$

so

$$Q = \left[0.9(0.131)(0.597)^{1/2}(2,257,000)\sqrt[4]{9.8(0.0589)(958)}\ \text{W/m}^2\right] \times \left(400 \times 10^{-4}\ \text{m}^2\right)$$

or

$$Q = 39,900\ \text{W} \quad \text{or} \quad 39.9\ \text{kW}$$

This is a startingly large rate of energy removal for such a small object.

To complete the calculation, it is necessary to check whether or not R' is large enough to justify the use of eqn. (9.25):

$$R' = \frac{V/A}{\sqrt{\sigma/g(\rho_f - \rho_g)}} = \frac{0.0006}{0.04}\sqrt{\frac{9.8(958)}{0.0589}} = 6.0$$

This is larger than the specified lower bound of about 4. ■

9.4 Film boiling

Film boiling bears an uncanny similarity to film condensation. The similarity is so great that in 1950, Bromley [9.22] was able to use the eqn. (8.63) for condensation on cylinders—almost directly—to predict film boiling from cylinders. He observed that the boundary condition $(\partial u/\partial y)_{y=\delta} = 0$ at the liquid–vapor interface in film condensation would have to change to something in between $(\partial u/\partial y)_{y=\delta} = 0$ and $u(y = \delta) = 0$ during film boiling. The reason is that the external liquid is not so easily set into motion. He then redid the film condensation analysis, merely changing k and ν from liquid to vapor properties. The change of boundary conditions gave eqn. (8.63) with the constant changed from 0.729 to 0.512 and with k and ν changed to vapor values. By comparing the equation with experimental data, he fixed the constant at the intermediate value of 0.62. Thus, $\overline{\mathrm{Nu}}_D$ based on k_g became

$$\boxed{\overline{\mathrm{Nu}}_D = 0.62 \left[\frac{(\rho_f - \rho_g) g h'_{fg} D^3}{\nu_g k_g (T_w - T_{\mathrm{sat}})} \right]^{1/4}} \tag{9.28}$$

where vapor and liquid properties should be evaluated at $T_{\mathrm{sat}} + \Delta T/2$ and at T_{sat}, respectively. The latent heat correction in this case is similar in form to that for film condensation, but with different constants in it. Sadasivan and Lienhard [9.23] have shown it to be

$$h'_{fg} = h_{fg} \left[1 + (0.968 - 0.163/\mathrm{Pr})\, \mathrm{Ja} \right] \tag{9.29}$$

Dhir and Lienhard [9.24] did the same thing for *spheres*, as Bromley did for *cylinders*, 20 years later. Their result [cf. eqn. (8.64)] was

$$\boxed{\overline{\mathrm{Nu}}_D = 0.67 \left[\frac{(\rho_f - \rho_g) g h'_{fg} D^3}{\nu_g k_g (T_w - T_{\mathrm{sat}})} \right]^{1/4}} \tag{9.30}$$

The preceding expressions are based on heat transfer by convection through the vapor film, alone. However, when film boiling occurs much beyond $q_{\min}$ in water, the heater glows dull cherry-red to white-hot. Radiation in such cases can be enormous. One's first temptation might be simply to add a radiation heat transfer coefficient, $\overline{h}_{\mathrm{rad}}$ to $\overline{h}_{\mathrm{boiling}}$ as

obtained from eqn. (9.28) or (9.30), where

$$\overline{h}_{\text{rad}} = \frac{q_{\text{rad}}}{T_w - T_{\text{sat}}} = \frac{\varepsilon\sigma\left(T_w^4 - T_{\text{sat}}^4\right)}{T_w - T_{\text{sat}}}$$

and where ε is a surface radiation property called the emittance (see Section 10.1).

Unfortunately, such addition is not correct, because the additional radiative heat transfer will increase the vapor blanket thickness, reducing the convective contribution. Bromley [9.22] suggested for cylinders the approximate relation

$$\overline{h}_{\text{total}} = \overline{h}_{\text{boiling}} + \tfrac{3}{4}\,\overline{h}_{\text{rad}}, \qquad \overline{h}_{\text{rad}} < \overline{h}_{\text{boiling}} \tag{9.31}$$

An accurate correction would be considerably more complex than this. Other suggested forms have subsequently been offered for the radiation correction. One of the most comprehensive is that of Pitschmann and Grigull [9.25]. Their correlation, which is fairly intricate, brings together an enormous range of heat transfer data for cylinders, within 20%. It is worth noting that radiation is seldom important when the heater temperature is less than 300°C.

The use of the analogy between film condensation and film boiling is somewhat questionable during film boiling on a vertical surface. In this case, the liquid–vapor interface becomes Helmholtz-unstable at a short distance from the leading edge. However, Leonard, Sun, and Dix [9.26] have shown that by using $\lambda_{d_1}/\sqrt{3}$ in place of D in eqn. (9.28), one obtains a very satisfactory prediction of $\overline{h}$ for rather tall vertical plates.

The analogy between film condensation and film boiling also deteriorates when it is applied to small curved bodies. The reason is that the thickness of the vapor film in boiling is far greater than the liquid film during condensation. Consequently, a curvature correction, which could be ignored in film condensation, must be included during film boiling from small cylinders, spheres, and other curved bodies. The first curvature correction to be made was an empirical one given by Westwater and Breen [9.27] in 1962. They showed that the equation

$$\boxed{\overline{\text{Nu}}_D = \left[\left(0.715 + \frac{0.263}{R'}\right)(R')^{1/4}\right]\overline{\text{Nu}}_{D_{\text{Bromley}}}} \tag{9.32}$$

applies when $R' < 1.86$. Otherwise, Bromley's equation should be used directly.

9.5 Minimum heat flux

Zuber [9.15] also provided a prediction of the minimum heat flux, $q_{\min}$, along with his prediction of $q_{\max}$. He assumed that as $T_w - T_{\text{sat}}$ is reduced in the film boiling regime, the rate of vapor generation eventually becomes too small to sustain the Taylor wave action that characterizes film boiling. Zuber's $q_{\min}$ prediction, based on this assumption, has to include an arbitrary constant. The result for flat horizontal heaters is

$$q_{\min} = C\ \rho_g h_{fg} \sqrt[4]{\frac{\sigma g(\rho_f - \rho_g)}{(\rho_f + \rho_g)^2}} \tag{9.33}$$

Zuber guessed a value of C which Berenson [9.28] subsequently corrected on the basis of experimental data. Berenson used measured values of $q_{\min}$ on horizontal heaters to get

$$\boxed{q_{\min_{\text{Berenson}}} = 0.09\ \rho_g h_{fg} \sqrt[4]{\frac{\sigma g(\rho_f - \rho_g)}{(\rho_f + \rho_g)^2}}} \tag{9.34}$$

Lienhard and Wong [9.29] did the parallel prediction for horizontal wires and found that

$$\boxed{q_{\min} = 0.515 \left[\frac{18}{R'^2(2R'^2 + 1)}\right]^{1/4} q_{\min\ \text{Berenson}}} \tag{9.35}$$

The problem with all of these expressions is that some contact frequently occurs between the liquid and the heater wall at film boiling heat fluxes higher than the minimum. When this happens, the boiling curve deviates above the film boiling curve and finds a higher minimum than those reported above. The values of the constants shown above should therefore be viewed as practical lower limits of $q_{\min}$. We return to this matter subsequently.

Example 9.8

Check the value of $q_{\min}$ shown in Fig. 9.2.

SOLUTION. The heater is a flat surface, so we use eqn. (9.34) and the physical properties given in Example 9.5.

$$q_{\min} = 0.09(0.597)(2,257,000) \sqrt[4]{\frac{9.8(0.0589)(958)}{(959)^2}}$$

or

$$q_{\min} = 18,990 \text{ W/m}^2$$

From Fig. 9.2 we read 20,000 W/m^2, which is the same, within the accuracy of the graph. ■

9.6 Transition boiling and system influences

Many system features influence the pool boiling behavior we have discussed thus far. These include forced convection, subcooling, gravity, surface roughness and surface chemistry, and the heater configuration, among others. To understand one of the most serious of these—the influence of surface roughness and surface chemistry—we begin by thinking about transition boiling, which is extremely sensitive to both.

Surface condition and transition boiling

Less is known about transition boiling than about any other mode of boiling. Data are limited, and there is no comprehensive body of theory. The first systematic sets of accurate measurements of transition boiling were reported by Berenson [9.28] in 1960. Figure 9.14 shows two sets of his data.

The upper set of curves shows the typical influence of surface chemistry on transition boiling. It makes it clear that a change in the surface chemistry has little effect on the boiling curve except in the transition boiling region and the low heat flux film boiling region. The oxidation of the surface has the effect of changing the *contact angle* dramatically—making it far easier for the liquid to wet the surface when it touches it. Transition boiling is more susceptible than any other mode to such a change.

The bottom set of curves shows the influence of surface roughness on boiling. In this case, nucleate boiling is far more susceptible to roughness than any other mode of boiling except, perhaps, the very lowest end of the film boiling range. That is because as roughness increases the number of active nucleation sites, the heat transfer rises in accordance with the Yamagata relation, eqn. (9.3).

It is important to recognize that neither roughness nor surface chemistry affects film boiling, because the liquid does not touch the heater.

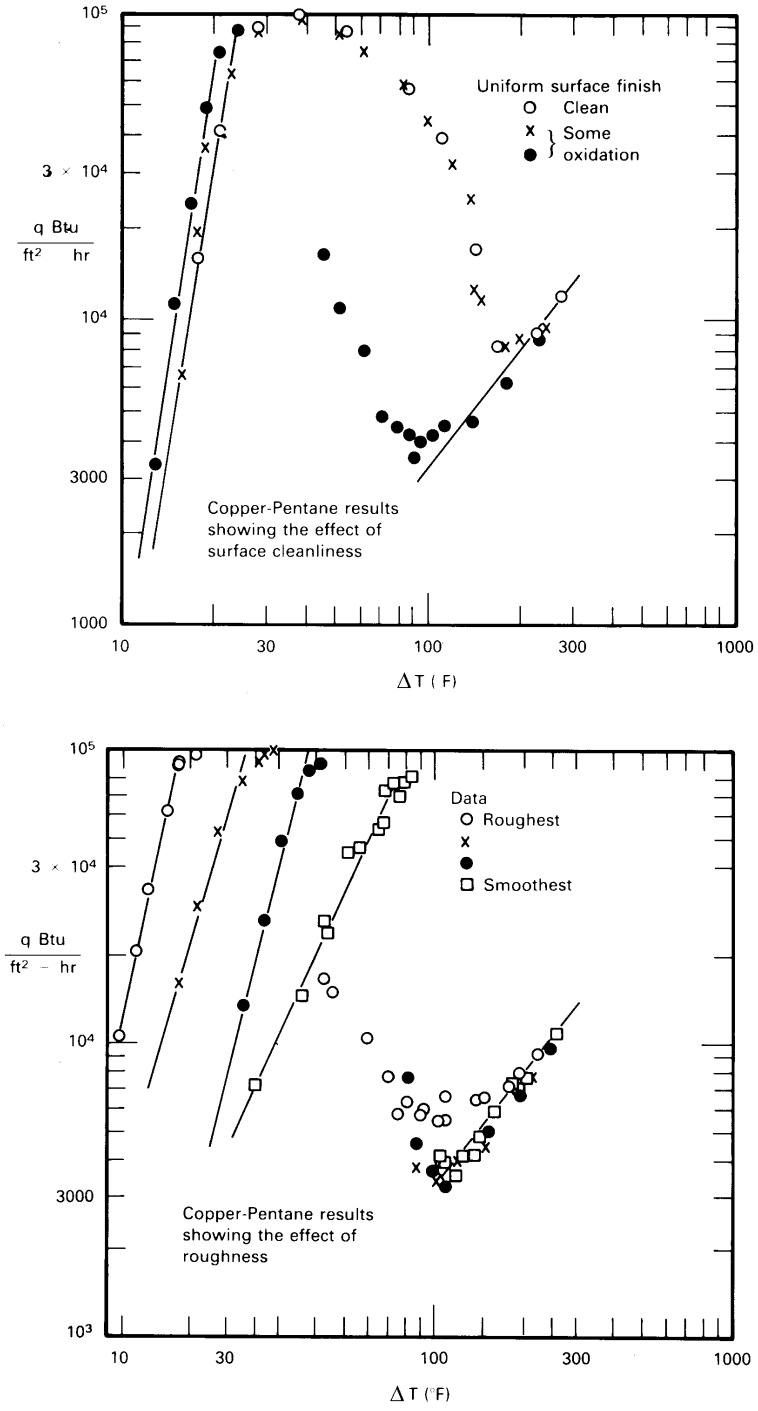

Figure 9.14 Typical data from Berenson's [9.28] study of the influence of surface condition on the boiling curve.

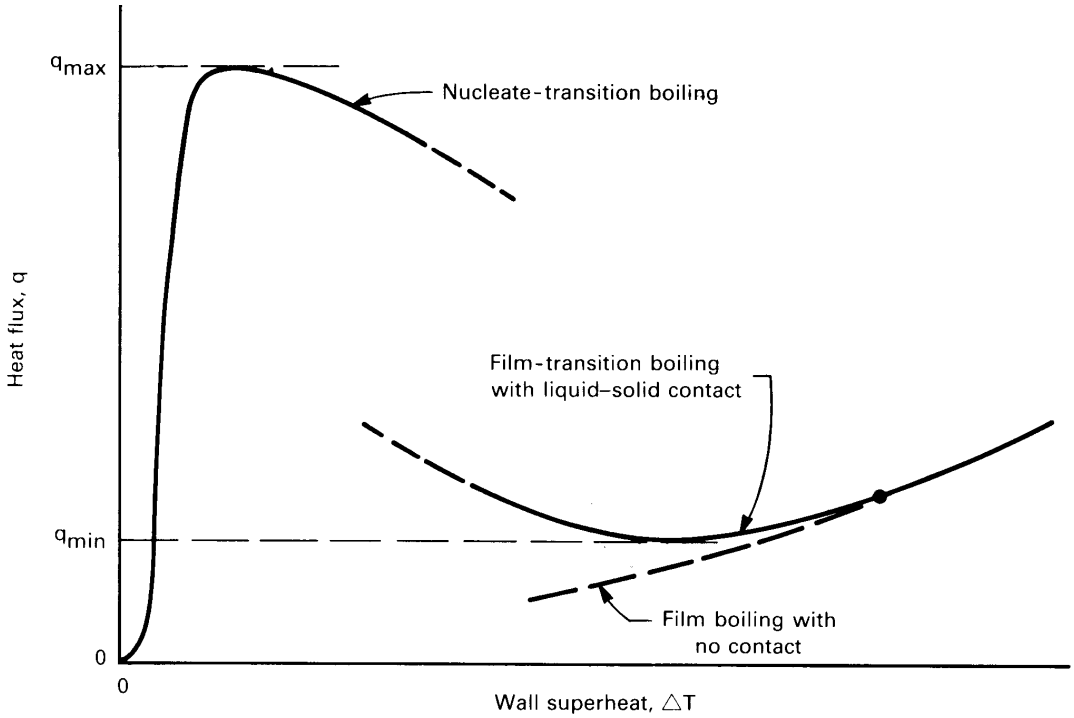

Figure 9.15 The transition boiling regime.

The fact that both effects appear to influence the lower film boiling range means that they actually cause film boiling to break down by initiating liquid–solid contact at low heat fluxes.

Figure 9.15 shows what an actual boiling curve looks like under the influence of a wetting (or even slightly wetting) contact angle. This figure is based on the work of Witte and Lienhard ([9.30] and [9.31]). On it are identified a *nucleate-transition* and a *film-transition* boiling region. These are continuations of nucleate boiling behavior with decreasing liquid–solid contact (as shown in Fig. 9.3c) and of film boiling behavior with increasing liquid–solid contact, respectively.

These two regions of transition boiling are often connected by abrupt jumps. However, no one has yet seen how to predict where such jumps take place. Reference [9.31] is a full discussion of the hydrodynamic theory of boiling, which includes an extended discussion of the transition boiling problem and a recent correlation for the transition-film boiling heat flux by Ramilison and Lienhard [9.32].

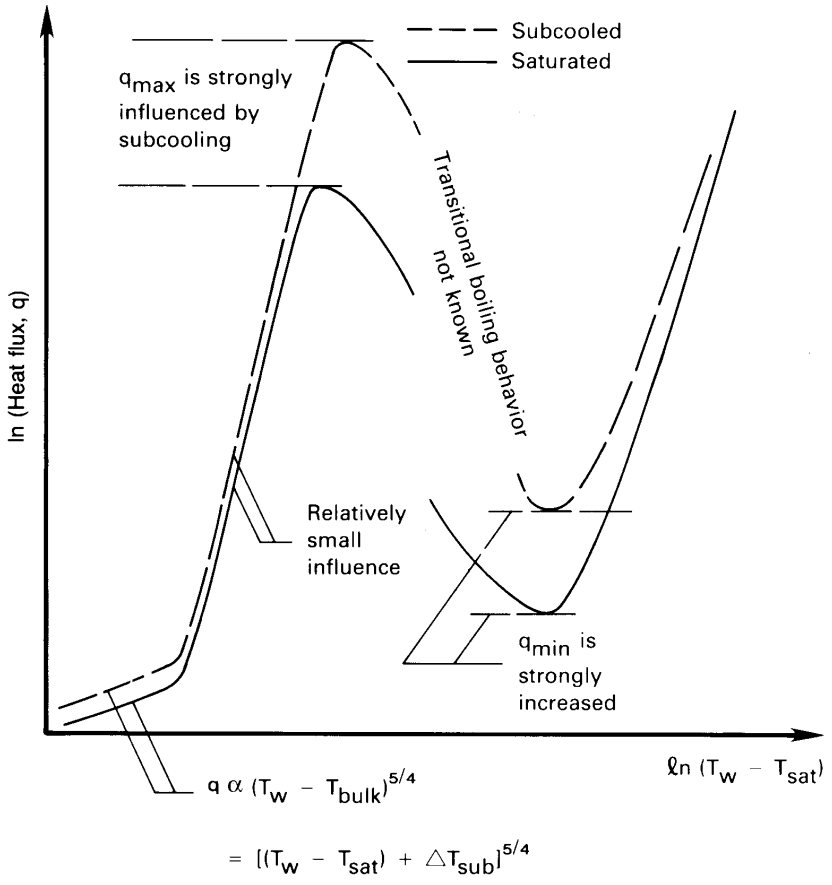

Figure 9.16 The influence of subcooling on the boiling curve.

Figure 9.14 also indicates fairly accurately the influence of roughness and surface chemistry on $q_{\max}$. It suggests that these influences normally can cause, at the very least, a ±10% variation in $q_{\max}$ that is not predicted in the hydrodynamic theory.

Subcooling

A stationary pool will normally not remain below its saturation temperature over an extended period of time. When heat is transferred to the pool, the liquid soon becomes saturated—as it does in a teakettle (recall Experiment 54). However, before a liquid comes up to temperature, or if

a very small rate of forced convection continuously replaces warm liquid with cool liquid, we can justly ask what the effect of a cool liquid bulk might be.

Figure 9.16 shows how a typical boiling curve might be changed if $T_{\text{bulk}} < T_{\text{sat}}$: We know, for example, that in *laminar natural convection*, q will increase as $(T_w - T_{\text{bulk}})^{5/4}$ or as $[(T_w - T_{\text{sat}}) + \Delta T_{\text{sub}}]^{5/4}$, where $\Delta T_{\text{sub}} \equiv T_{\text{sat}} - T_{\text{bulk}}$. During *nucleate boiling*, the influence of subcooling on q is known to be small. The *peak and minimum heat fluxes* are known to increase linearly with ΔT_{sub}. These increases are quite significant. The *film boiling* heat flux increases rather strongly, especially at lower heat fluxes. The influence of ΔT_{sub} on transitional boiling is not well documented.

Gravity

The influence of gravity (or any other such body force) is of concern because boiling processes frequently take place in rotating or accelerating systems. The reduction of gravity is a serious concern in boiling processes on-board space vehicles. Since g appears explicitly in the equations for $q_{\max}$, $q_{\min}$, and $q_{\text{film boiling}}$, we know what its influence is. Both $q_{\max}$ and $q_{\min}$ increase directly as $g^{1/4}$ in finite bodies, and there is a secondary gravitational influence which enters through the parameter L'. However, when gravity is small enough to reduce R' below about 0.15, the hydrodynamic transitions deteriorate and eventually vanish altogether. Although Rohsenow's equation suggests that q is proportional to $g^{1/2}$ in the nucleate boiling regime, other evidence suggests that the influence of gravity is very slight in this range.

Forced convection

The influence of superposed flow on the pool boiling curve for a given heater (e.g., Fig. 9.2) is generally to improve heat transfer everywhere. But flow is particularly effective in raising $q_{\max}$. Let us look at the influence of flow on the different regimes of boiling.

Influences of forced convection on nucleate boiling. Figure 9.17 shows nucleate boiling during the forced convection of water over a flat plate. Bergles and Rohsenow (see, e.g., [9.8, Chap. 13]) offer an empirical strategy for predicting the heat flux during nucleate flow boiling when the net vapor generation is still relatively small. (The photograph in Fig. 9.17

shows how a substantial buildup of vapor can radically alter flow boiling behavior.) They suggest that

$$q = q_{\text{FC}}\sqrt{1 + \frac{q_B}{q_{\text{FC}}}\left(1 - \frac{q_i}{q_B}\right)^2} \tag{9.36}$$

where

- q_{FC} is the single-phase forced convection heat transfer for the heater, as one might calculate using the methods of Chapters 6 and 7.
- q_B is the *pool* boiling heat flux for that liquid and that heater.
- q_i is the heat flux from the pool boiling curve evaluated at the value of $(T_w - T_{\text{sat}})$ where boiling begins during flow boiling (see Fig. 9.17).

Notice that as q_B increases, eqn. (9.36) suggests that

$$q \longrightarrow \sqrt{q_{\text{FC}} q_B} = \text{ a geometric mean } q$$

Equation (9.36) will provide a first approximation in most boiling configurations, but it is restricted to subcooled flows or other situations in which vapor generation is not too great.

Peak heat flux in external flows. The peak heat flux on a submerged body is strongly augmented by an external flow around it. Although knowledge of this area is in a state of flux, we do know from dimensional analysis that

$$\frac{q_{\max}}{\rho_g h_{fg} u_\infty} = \text{fn}\left(\text{We}_D, \rho_f/\rho_g\right) \tag{9.37}$$

where the Weber number, We, is

$$\text{We}_L \equiv \frac{\rho_g u_\infty^2 L}{\sigma} = \frac{\text{inertia force}/L}{\text{surface force}/L}$$

and where L is any characteristic length.

Kheyrandish and Lienhard [9.33] suggest fairly complex expressions of this form for $q_{\max}$ on horizontal cylinders in cross flows. For a cylindrical jet impinging on a heated disk of diameter D, Sharan and Lienhard [9.34] obtained

$$\frac{q_{\max}}{\rho_g h_{fg} u_{\text{jet}}} = \left(0.21 + 0.0017\rho_f/\rho_g\right)\left(\frac{d_{\text{jet}}}{D}\right)^{1/3}\left(\frac{1000\rho_g/\rho_f}{\text{We}_D}\right)A \tag{9.38}$$

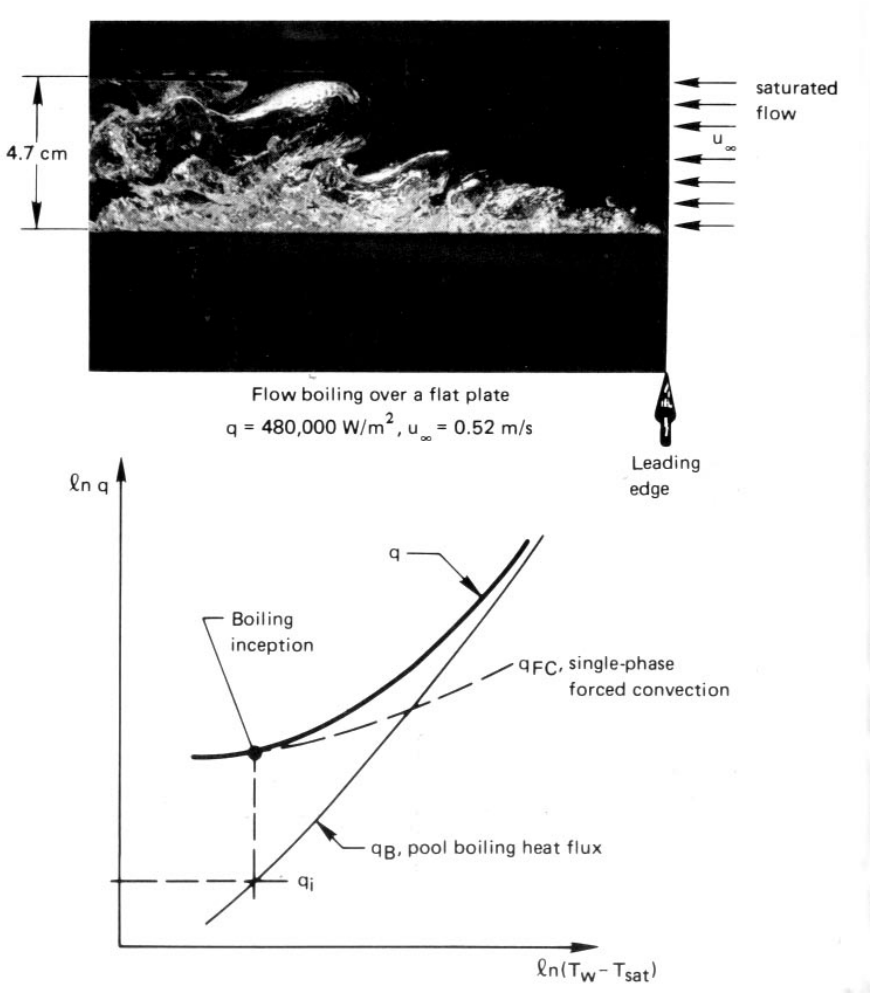

Figure 9.17 Forced convection boiling on an external surface.

where, if we call $\rho_f/\rho_g \equiv r$,

$$A = 0.486 + 0.06052 \ln r - 0.0378 (\ln r)^2 + 0.00362 (\ln r)^3 \qquad (9.39)$$

This correlation represents all the existing data within ±20% over the full range of the data.

The influence of fluid flow on film boiling. The work of Bromley, LeRoy, and Robbers [9.35] shows that the film boiling heat flux during forced

flow normal to a cylinder should take the form

$$q = \text{constant}\left(\frac{k\Delta T\rho_g h'_{fg} u_\infty}{D}\right)^{1/2} \tag{9.40}$$

where their data fixed the constant at 2.70. Witte [9.36] obtained the same relationship for flow over a sphere and recommended a value of 2.98 for the constant.

Additional work in the literature deals with forced film boiling on plane surfaces and combined forced and subcooled film boiling in a variety of geometries. Although these studies are beyond our present scope, it is worth noting that one may attain very high cooling rates using film boiling with both forced convection and subcooling.

9.7 Forced convection boiling in tubes

Relationship between heat transfer and temperature difference

Forced convection boiling in a tube or duct is a process that becomes very hard to delineate because it takes so many forms. In addition to the usual system variables that must be considered in pool boiling, the formation of many regimes of boiling requires that we understand several boiling mechanisms and the transitions between them, as well.

Collier and Thome's excellent book, *Convective Boiling and Condensation* [9.37], provides a comprehensive discussion of the issues involved in forced convection boiling. Figure 9.18 is their representation of the fairly simple case of flow of liquid in a *uniform wall heat flux* tube in which body forces can be neglected. This situation is representative of a fairly low heat flux at the wall. The vapor fraction, or *quality*, of the flow increases steadily until the wall "dries out." Then the wall temperature rises rapidly. With a very high wall heat flux, the pipe could burn out before dryout occurs.

Figure 9.19, also provided by Collier, shows how the regimes shown in Fig. 9.18 are distributed in heat flux and in position along the tube. Notice that at high enough heat fluxes, burnout can be made to occur at any station in the pipe. In the nucleate boiling regimes the heat transfer can be predicted fairly well using the method described in Section 9.6. But in the annular flow regimes (*E* and *F* in Fig. 9.18) the heat transfer mechanism is radically altered, and one of the best methods for predicting q is that of Chen [9.38].

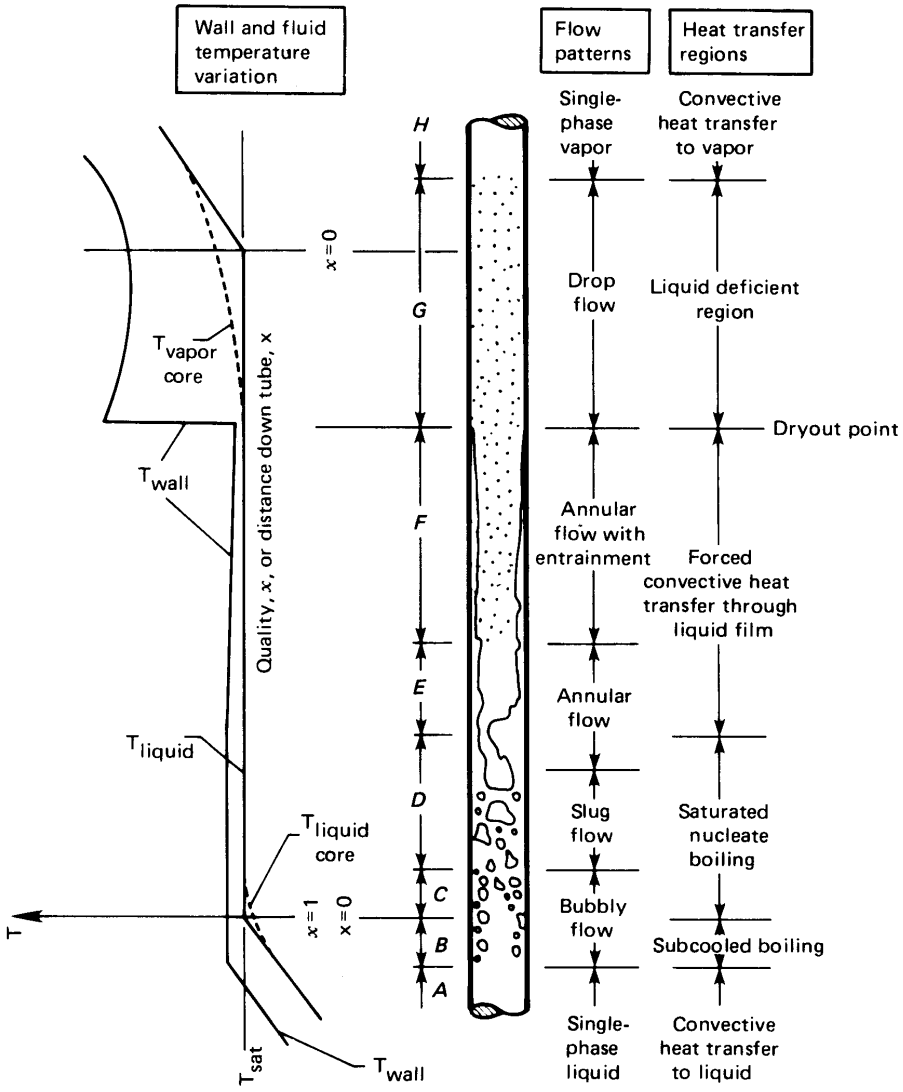

Figure 9.18 The development of a two-phase flow in a tube with a uniform wall heat flux (not to scale).

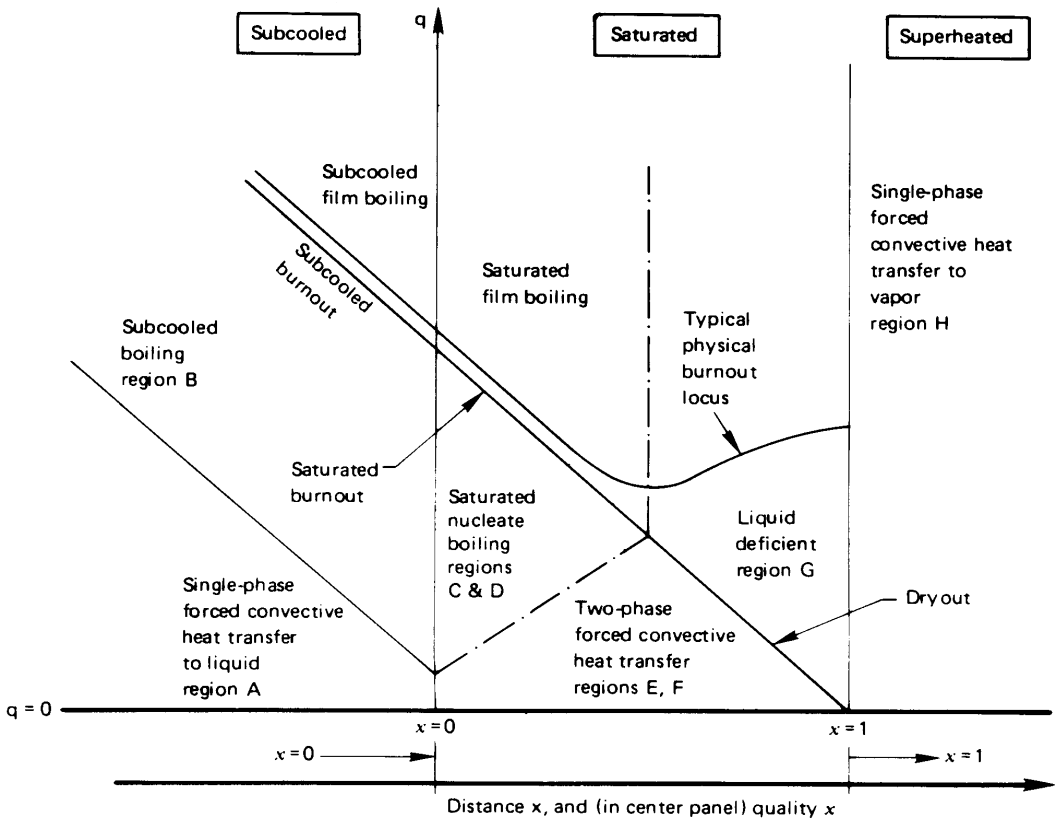

Figure 9.19 The influence of heat flux on two-phase flow behavior.

Chen developed a complex—but fairly accurate—method for computing h for water in an annular pipe flow. It is best explained in the form of a recipe:

- Compute the Martinelli parameter,[4] X_{tt}, for the flow:

$$X_{tt} \cong \left(\frac{1-x}{x}\right)^{0.9} \left(\frac{\rho_g}{\rho_f}\right)^{0.5} \left(\frac{\mu_f}{\mu_g}\right)^{0.1} \tag{9.41}$$

where x is the quality of the flow at the point of interest. The

[4] R. C. Martinelli was an important figure in American heat transfer for a few brief years in the 1940s, before he died of leukemia at an early age. He contributed to the famous Berkeley *Heat Transfer Notes* [9.39], and he set down the foundations for predicting heat transfer in two-phase flows, among other accomplishments.

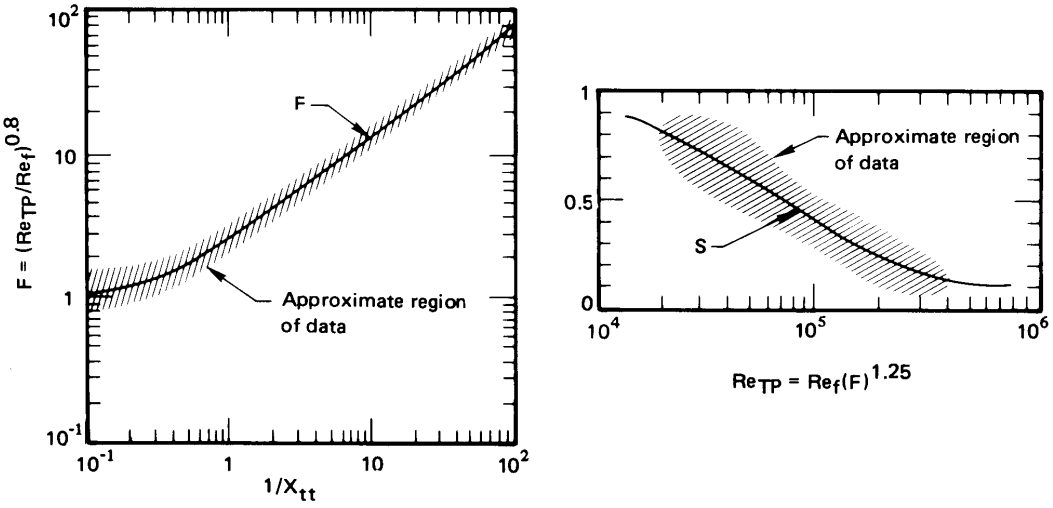

Figure 9.20 Chen's [9.38] two-phase flow parameters.

Martinelli parameter is defined as

$$X_{tt} = \sqrt{\left(\frac{dp}{dx}\right)_f \Big/ \left(\frac{dp}{dx}\right)_g} \tag{9.42}$$

and eqn. (9.41) is a correlation that approximates X_{tt} as it is defined by eqn. (9.42). Thus, X_{tt}^2 is the ratio of the frictional pressure gradient for a single-phase turbulent liquid flow at the mass flow rate of the *liquid component* of the two-phase flow to a similarly-defined pressure gradient for the vapor component.

- Obtain the empirical function, F, at this X_{tt} from Fig. 9.20. $F^{1/0.8}$ is the ratio of the *two-phase Reynolds number*, Re_{TP} (defined below) to the conventional liquid-phase Reynolds number, Re_f.
- Calculate the superficial mass flux, G, through the pipe:

$$G \equiv \frac{\dot{m}}{A_{\text{pipe}}}$$

- Calculate the single-phase heat transfer coefficient, h_c, from the Dittus-Boelter equation, eqn. (7.38), using saturated liquid properties and the Reynolds number, Re_{TP}:

$$\mathrm{Re}_{TP} \equiv F^{1.25}\left[G(1-x)D/\mu_f\right] \equiv F^{1.25}\mathrm{Re}_f \tag{9.43}$$

- Obtain the empirical factor, S, from Fig. 9.20 at the known value of Re_{TP}.
- Calculate a *nucleate boiling heat transfer coefficient*, h_{NB}, from

$$h_{NB} = 0.00122 \left[\frac{k_f^{0.79} c_{P_f}^{0.45} \rho_f^{0.49}}{\sigma^{0.5} \mu_f^{0.29} h_{fg}^{0.24} \rho_g^{0.24}} \right] (\Delta T_{\text{sat}})^{0.24} (\Delta p_{\text{sat}})^{0.75} \tag{9.44}$$

  where Δp_{sat} is p_{sat} at T_w minus p_{sat} at T_{sat}, ΔT_{sat} is $(T_w - T_{\text{sat}})$, and any consistent units may be used.

- Calculate h_{TP} from

$$h_{TP} = S h_{NB} + h_c \tag{9.45}$$

  for a range of values of ΔT_{sat}.

- Plot $q = h_{TP} \Delta T_{\text{sat}}$ against ΔT_{sat} and read ΔT_{sat}, for the case of interest, where this curve intersects q_w; or solve eqn. (9.45) for ΔT_{sat} by trial and error, using the steam tables to get Δp_{sat}.

Example 9.9

0.6 kg/s of H_2O at 200°C flows in a 5 cm diameter tube heated by 184,000 W/m^2. Find the wall temperature at a point where the quality x is 20%.

SOLUTION.

$$X_{tt} = \left(\frac{1 - 0.20}{0.2} \right)^{0.9} 5.23 \times 10^{-4} \left(\frac{0.000139}{0.00001607} \right)^{0.1} = 0.411,$$

so from Fig. 9.20 we read $F = 5.1$. Then, since

$$G = \frac{\dot{m}}{A_{\text{pipe}}} = \frac{0.6}{0.00196} = 306 \text{ kg/m}^2 \cdot \text{s}$$

we calculate

$$\mathrm{Re}_{TP} = F^{1.25} \left[G(1 - x) \frac{D}{\mu_f} \right] = \frac{7.66(306)(1 - 0.2)(0.05)}{0.00139}$$
$$= 67,500$$

Then, from eqn. (7.38),

$$\begin{aligned} h_c &= 0.0246 \frac{k}{D} \mathrm{Pr}^{0.4} \mathrm{Re}_{TP}^{0.8} \\ &= 0.0246 \frac{0.658}{0.05} (0.915)^{0.4} (67,500)^{0.8} \\ &= 2281 \text{ W/m}^2\text{K} \end{aligned}$$

and from Fig. 9.20, we read $S = 0.51$. Finally, we calculate

$$\begin{aligned} h_{NB} &= 0.00122 \left[\frac{(0.658)^{0.79}(4505)^{0.45}(865)^{0.49}}{(0.0377)^{0.5}(0.000139)^{0.29}(1,941,000)^{0.24}(0.597)^{0.24}} \right] \\ &\quad \times \Delta T_{\text{sat}}^{0.24} \Delta p_{\text{sat}}^{0.75} \\ &= 2.52 \ \Delta T_{\text{sat}}^{0.24} \Delta p_{\text{sat}}^{0.75} \end{aligned}$$

so

$$h_{TP} = S h_{NB} + h_c = 1.284 \ \Delta T_{\text{sat}}^{0.24} \Delta p_{\text{sat}}^{0.75} + 2281$$

and

$$q_w = 25,000 = 1.284 \ \Delta T_{\text{sat}}^{1.24} \Delta p_{\text{sat}}^{0.75} + 2281 \ \Delta T_{\text{sat}}$$

Then, using a steam table to evaluate Δp_{sat}, we solve for ΔT_{sat} by trial and error. The first trial goes like this: first guess,

$$\Delta T_{\text{sat}} = 10 \text{ K} \qquad \text{so} \qquad T_w = 210^\circ\text{C}$$

then

$$\Delta p_{\text{sat}} = p_{\text{sat}}(210^\circ\text{C}) - p_{\text{sat}}(200^\circ\text{C}) = 352,900 \text{ N/m}^2$$

and

$$184,000 \neq 323,075 + 22,810 = 345,885$$

so we try a lower ΔT. After a few more tries, we get

$$\Delta T \simeq 7.3 \text{ K} \quad \text{so} \quad T_w \simeq 207.3^\circ\text{C}$$

This is a very low temperature difference because the heat transfer process is very efficient. In this case,

$$h \simeq \frac{184,000}{7.3} = 25,200 \text{ W/m}^2\text{K} \qquad \blacksquare$$

Peak heat flux

We have seen that there are two limiting heat fluxes in flow boiling in a tube: dryout and burnout. The latter is the more dangerous of the two since it occurs at higher heat fluxes and gives rise to more catastrophic temperature rises. A great deal of work continues to be done on this problem, but the matter is far from resolved. Collier and Thome provide an extensive discussion of this subject [9.37]. Hsu and Graham [9.40] include a useful catalog of restrictive empirical burnout formulas.

A promising development in the prediction of the burnout heat flux has recently been given by Katto [9.41]. Katto used dimensional analysis to show that

$$\frac{q_{\max}}{Gh_{fg}} = \text{fn}\left(\frac{\rho_g}{\rho_f}, \frac{\sigma\rho_f}{G^2L}, \frac{L}{D}\right)$$

where L is the length of the tube and D its diameter. Since $G^2L/\sigma\rho_f$ is a Weber number, we can see that this equation is of the same form as eqn. (9.37). Katto identifies several regimes of flow boiling with both saturated and subcooled liquid entering the pipe. For each of these regions, he fits a successful correlation of this form to existing data.

9.8 Two-phase flow in horizontal tubes

The preceding discussion of flow boiling in tubes is restricted to vertical tubes. Several of the flow regimes in Fig. 9.18 will be altered as shown in Fig. 9.21 if the tube is oriented horizontally. The reason is that, especially at low quality, liquid will tend to flow along the bottom of the pipe and vapor along the top. The pattern shown in Fig. 9.21, by the way, will be observed during boiling during the reverse process—condensation—or during adiabatic two-phase flow.

Many methods have been suggested to predict what flow patterns will result for a given set of conditions in the pipe. Figure 9.22 shows a so-called *modified Baker plot*, given by Bell, Taborek, and Fenoglio [9.42]. This graph gives the approximate flow regime as a function of the liquid and vapor flow rates in the tube. The precision of such a representation is not high, since transitions themselves are not sharply defined. The coordinates, which involve other variables as well as the flow rates, are in mixed English and metric units.

In the upper right-hand corner of the flow regime plot (Fig. 9.22) is

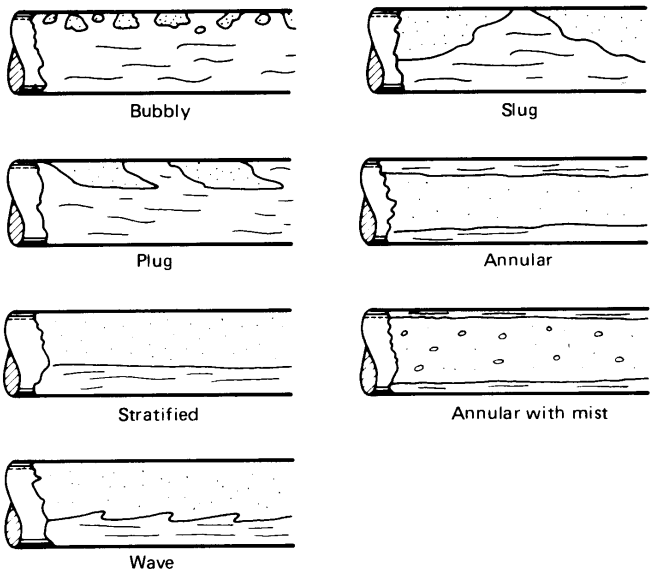

Figure 9.21 The discernible flow regimes during boiling, condensation, or adiabatic flow from left to right in horizontal tubes.

shown a quality overlay curve. By translating this dashed curve so that it overlays one point of known quality on Fig. 9.22, it is possible to read off any other quality directly with no additional computation. We illustrate its use with an example.

Example 9.10

Water vapor is condensing in a 4 cm I.D. horizontal tube at 1 atm. The total mass flow rate is 0.2 kg/s. Estimate how much heat transfer will occur in the annular flow regime.

SOLUTION. We first identify the point of—say—50% quality. This will be the point at which $\dot{m}_{\text{vapor}} = \dot{m}_{\text{liquid}} = 0.1$ kg/s.

$$\frac{\dot{m}_{\text{vapor}}}{A_{\text{tube}}\sqrt{\rho_f \rho_g}} = \frac{0.1}{(\pi/4)(0.04)^2\sqrt{958(0.597)}}$$
$$= 3.33 \text{ m/s} = 39,331 \text{ ft/hr}$$

and

$$\frac{\dot{m}_{\text{liquid}}}{A_{\text{tube}}}\left(\frac{\mu_f^{1/3}}{\sigma \rho_f^{2/3}}\right) = \frac{0.1}{(\pi/4)(0.04)^2}\left(\frac{0.000277^{1/3}}{0.0589(958)^{2/3}}\right)$$

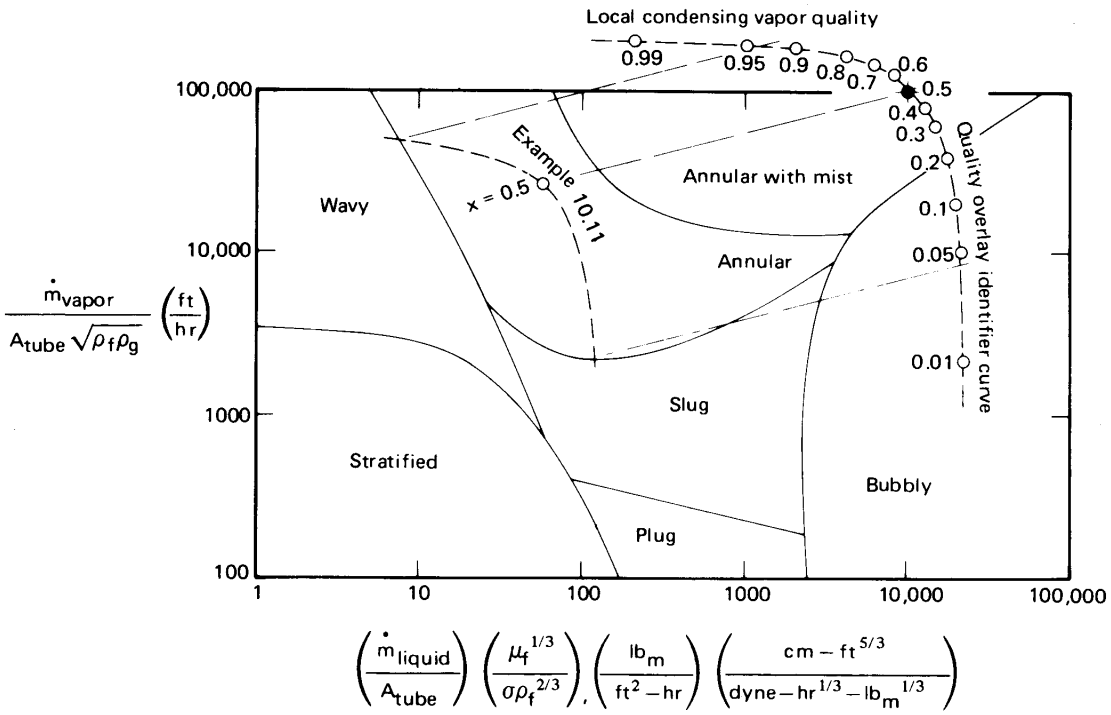

Figure 9.22 Modified Baker plot for identifying two-phase flow regimes (after [9.42]).

$$= 0.906\ \frac{kg}{m^2\cdot s}\ \frac{m^{8/3}}{N\cdot s^{1/3}\cdot kg^{1/3}}$$

$$= 0.906\ \frac{kg}{m^2\cdot s}\ \frac{m^{8/3}}{N\cdot s^{1/3}\cdot kg^{1/3}}\left(\frac{N/m}{10^3\ dyn/cm}\right)$$

$$\times\left(2.205\frac{lb_m}{kg}\right)^{2/3}\left(0.3048\frac{m}{ft}\right)^{1/3}\left(3600\frac{s}{hr}\right)^{4/3}$$

$$= 57.0\ \frac{lb_m}{ft^2\cdot hr}\ \frac{cm\cdot hr^{5/3}}{dyn\cdot hr^{1/3}\cdot lb_m^{1/3}}$$

Now we identify the point with these coordinates on Fig. 9.22 and slide the dashed curve over so that the point at which $x = 0.5$ lies on top of it. Then we note where the curve crosses the boundaries of the annular flow regime. This can easily be done by connecting the calculated point with the $x = 0.5$ point on the dashed line and by locating the parallel line segments of equal length that connect

the dashed line to the annular flow region boundaries. These line segments intersect the overlay line at $x = 0.94$ and 0.043.

The heat transfer required to change the quality of 0.2 kg/s of steam/water from 0.94 to 0.043 is $\dot{m}_{\text{total}} h_{fg} (x_{\text{initial}} - x_{\text{final}})$, or

$$Q = \left(0.2 \frac{\text{kg}}{\text{s}}\right) \left(2257 \frac{\text{kJ}}{\text{kg}}\right) (0.94 - 0.043) = 405 \text{ kW} \quad \blacksquare$$

The Baker plot is somewhat limited by the restrictive data on which it is based. It is therefore most accurate when applied to air–water flows in small horizontal tubes. Dukler, Taitel, and many co-workers have developed more comprehensive and accurate methods for predicting two-phase flow regimes. Their work is summarized in [9.43].

9.9 Forced convective condensation heat transfer

When vapor is blown or forced past a cool wall, it exerts a shear stress on the condensate film. If the direction of forced flow is downward, it will drag the condensate film along, thinning it out and enhancing heat transfer. It is not hard to show (see Problem 9.22) that

$$\frac{4\mu k (T_{\text{sat}} - T_w) x}{g h'_{fg} \rho_f (\rho_f - \rho_g)} = \delta^4 + \frac{4}{3} \left[\frac{\tau_\delta \delta^3}{(\rho_f - \rho_g) g} \right] \tag{9.46}$$

where τ_δ is the shear stress exerted by the vapor flow on the condensate film.

Equation (9.46) is the starting point for any analysis of forced convection condensation on an external surface. Notice that if τ_δ is negative—if the shear opposes the direction of gravity—then it will have the effect of thickening δ and reducing heat transfer. Indeed, if for any value of δ,

$$\tau_\delta = -\frac{3g(\rho_f - \rho_g)}{4} \delta \tag{9.47}$$

the shear stress will have the effect of halting the flow of condensate completely for a moment until δ grows to a larger value.

Heat transfer solutions based on eqn. (9.46) are complex because they require that one solve the boundary layer problem in the vapor in order to evaluate τ_δ; and this solution must be matched with the velocity at the outside surface of the condensate film. Collier [9.37, §10.5] discussed such solutions in some detail. One explicit result has been obtained

in this way for condensation on the outside of a horizontal cylinder by Shekriladze and Gomelauri [9.44]:

$$\overline{\mathrm{Nu}}_D = 0.64 \left\{ \frac{\rho_f u_\infty D}{\mu_f} \left[1 + \left(1 + 1.69 \frac{g h'_{fg} \mu_f D}{u_\infty^2 k_f (T_{\mathrm{sat}} - T_w)} \right)^{1/2} \right] \right\}^{1/2} \tag{9.48}$$

where u_∞ is the free stream velocity and $\overline{\mathrm{Nu}}_D$ is based on the liquid conductivity. Equation (9.48) is valid up to $\mathrm{Re}_D \equiv \rho_f u_\infty D/\mu_f = 10^6$. Notice, too, that under appropriate flow conditions (large values of u_∞, for example), gravity becomes unimportant and

$$\overline{\mathrm{Nu}}_D \longrightarrow 0.64 \sqrt{2\mathrm{Re}_D} \tag{9.49}$$

The prediction of heat transfer during forced convective condensation in tubes becomes a different problem for each of the many possible flow regimes. The reader is referred to [9.37, §10.5] or [9.42] for details.

9.10 Dropwise condensation

An automobile windshield normally is covered with droplets during a light rainfall. They are hard to see through, and one must keep the windshield wiper moving constantly to achieve any kind of visibility. A glass windshield is normally quite clean and is free of any natural oxides, so the water forms a contact angle on it and any film will be unstable. The water tends to pull into droplets, which intersect the surface at the contact angle. Visibility can be improved by mixing a surfactant chemical into the window-washing water to reduce surface tension. It can also be improved by preparing the surface with a "wetting agent" to reduce the contact angle.[5]

Such behavior can also occur on a metallic condensing surface, but there is an important difference: Such surfaces are generally wetting. Wetting can be temporarily suppressed, and dropwise condensation can be encouraged, by treating an otherwise clean surface (or the vapor) with oil, kerosene, or a fatty acid. But these contaminates wash away fairly quickly, and the liquid condensed in a heat exchanger almost always forms a film.

[5] A way in which one can accomplish these ends is by wiping the wet window with a cigarette. It is hard to tell which of the two effects the many nasty chemicals in the cigarette achieve.

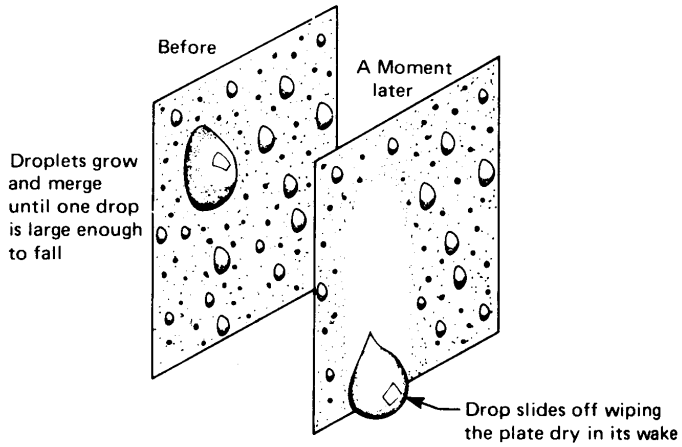
Before
A Moment later
Droplets grow and merge until one drop is large enough to fall
Drop slides off wiping the plate dry in its wake

a. The process of liquid removal during dropwise condensation.

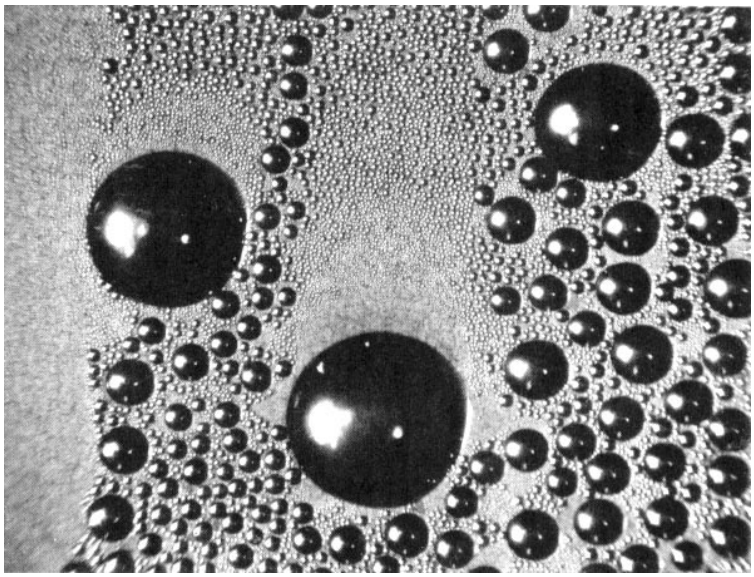

b. Typical photograph of dropwise condensation provided by Professor Borivoje B. Mikić. Notice the dry paths on the left and in the wake of the middle droplet.

Figure 9.23 Dropwise condensation.

It is regrettable that this is the case, because what is called *dropwise* condensation is an extremely effective heat removal mechanism. Figure 9.23 shows how it works. Droplets grow from active nucleation sites on the surface, and in this sense there is a great similarity between nucleate boiling and dropwise condensation. The similarity persists as the droplets grow, touch, and merge with one another until one is large enough to be pulled away from its position by gravity. It then slides off, wiping away the smaller droplets in its path and leaving a dry swathe in its wake. New droplets immediately begin to grow at the nucleation sites in the path.

The repeated re-creation of the early droplet growth cycle creates a very efficient heat removal mechanism. It is typically ten times more effective than film condensation under the same temperature difference. Indeed, condensing heat transfer coefficients as high as 200,000 $W/m^2 \cdot °C$ can be obtained with water at 1 atm. Were it possible to sustain dropwise condensation, we would certainly design equipment in such a way as to make use of it. Unfortunately, laboratory experiments on dropwise condensation are almost always done on surfaces that have been prepared with oleic, stearic, or other fatty acids, or, more recently, with dioctadecyl disulphide. These nonwetting agents, or *promoters* as they are called, are discussed in [9.45, 9.46]. While promoters are normally impractical for industrial use, since they either wash away or oxidize, experienced plant engineers have sometimes added rancid butter through the cup valves of commercial condensers to get at least temporary dropwise condensation.

Finally, we note that the obvious tactic of coating the surface with a thin, nonwetting, polymer film (such as PTFE, or Teflon) adds just enough conduction resistance to reduce the overall heat transfer coefficient to a value similar to film condensation, fully defeating its purpose! (Sufficiently thin polymer layers have not been found to be durable.) Noble metals, such as gold, platinum, and palladium, can also be used as nonwetting coating, and they have sufficiently high thermal conductivity to avoid the problem encountered with polymeric coatings. For gold, however, the minimum effective coating thickness is about 0.2 μm, or about 1/8 Troy ounce per square meter [9.47]. Such coatings are far too expensive for the vast majority of technical applications.

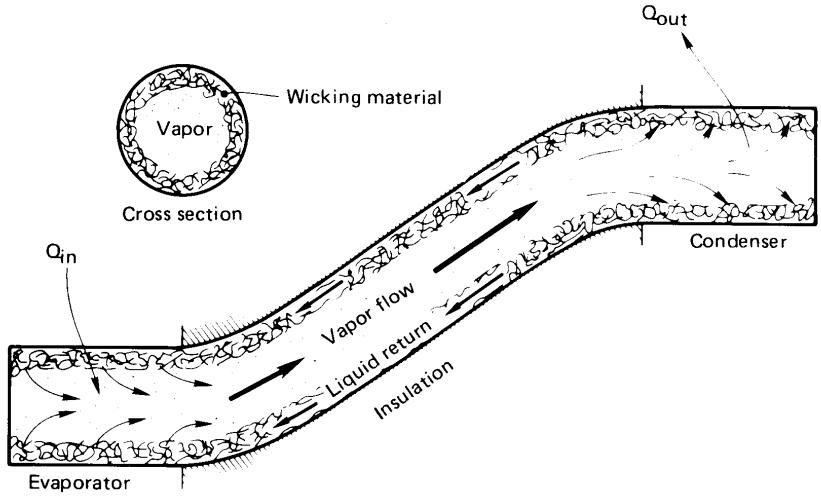

Figure 9.24 A typical heat pipe configuration.

9.11 The heat pipe

One significant application of phase change heat transfer is a device that combines the high efficiencies of boiling and condensation. The device, called a *heat pipe*, is aptly named because it literally pipes heat from a hot region to a cold one.

The operation of the heat pipe is shown in Fig. 9.24. The pipe is a tube that can be bent or turned in any way that is convenient. The inside of the tube is lined with a layer of wicking material. The wick is wetted with an appropriate liquid. One end of the tube is exposed to a heat source that evaporates the liquid, drying out the wick. Capillary action quickly replenishes the evaporated fluid and moves liquid axially along the wick. Vapor likewise flows from the hot end of the tube to the cold end, where it is condensed.

Placing a heat pipe between a hot region and a cold one is thus similar to connecting the regions with a material of extremely high thermal conductivity—orders of magnitude higher than any known substance (other than helium II). Such devices are used not only for achieving high heat transfer between a source and a sink but for a variety of less obvious purposes. They are used, for example, to level out temperature hot spots in systems, since they function almost isothermally and require enormous heat transfer to sustain any temperature difference.

Design considerations in the specification of a given heat pipe for a given application center on the following issues:

- *Selection and installation of the wick.* The wick is normally made of stainless steel, copper, or another metallic mesh. Many ingenious schemes have been created for bonding it to the inside of the pipe and keeping it at optimum density.
- *Selection of the right liquid.* The liquid can be a cryogen, water, liquid metal, or almost any substance, depending on the operating temperature of the device. The following physical property characteristics make a fluid desirable for heat pipe application:

  (a) High latent heat.
  (b) High thermal conductivity.
  (c) High surface tension.
  (d) Low viscosity.
  (e) It should wet the wick material.
  (f) It should have a suitable boiling point.

  Two liquids that meet the first four criteria admirably are water and mercury.
- *Operating limits of the heat pipe.* The heat flux through a heat pipe is restricted by

  (a) Viscous drag in the wick at low temperature.
  (b) Ability of the wick to move the liquid through the required head.
  (c) Drag of the vapor on the returning liquid.
  (d) The sonic or choking speed of the vapor.
  (e) The burnout heat flux during boiling in the evaporation section.
- *Control of the pipe performance.* Often a given heat pipe will be called upon to function over a range of conditions—under varying evaporator temperatures, for example, or under varying heat loads. One way to vary its performance is to "spike" its effectiveness by injecting more-or-less noncondensable gas into the pipe with an automatic control system.

Heat pipes have proven useful in cooling high power-density electronic devices. The evaporator is located on a small electronic component to be cooled, perhaps a microprocessor, and the condenser is finned and cooled by a forced air flow (in a desktop or mainframe computer) or is unfinned and cooled by conduction into the exterior casing or structural frame (in a laptop computer). These applications rely on having a heat pipe with much larger condenser area than evaporator area. Thus, the heat fluxes on the condenser are kept relatively low. This facilitates such uncomplicated means for the ultimate heat disposal as using a small fan to blow air over the condenser.

The reader interested in designing or selecting a heat pipe will find a broad discussion of such devices in the book by Dunn and Reay [9.48] or the review by Winter and Barsch [9.49]. Tien [9.50] has provided a useful review of the fluid mechanics problems involved in heat pipes.

Problems

9.1 A large square tank with insulated sides has a copper base 1.27 cm thick. The base is heated to 650°C and saturated water is suddenly poured in the tank. Plot the temperature of the base as a function of time on the basis of Fig. 9.2 if the bottom of the base is insulated. In your graph, indicate the regimes of boiling and note the temperature at which cooling is most rapid.

9.2 Predict $q_{\max}$ for the two heaters in Fig. 9.3b. At what percentage of $q_{\max}$ is each one operating?

9.3 A very clean glass container of water at 70°C is depressurized until it is subcooled 30°C. Then it suddenly and explosively "flashes" (or boils). What is the pressure at which this happens? Approximately what diameter of gas bubble, or other disturbance in the liquid, caused it to flash?

9.4 Plot the unstable bubble radius as a function of liquid superheat for water at 1 atm. Comment on the significance of your curve.

9.5 In chemistry class you have probably witnessed the phenomenon of "bumping" in a test tube (the explosive boiling that blows the

contents of the tube all over the ceiling). Yet you have never seen this happen in a kitchen pot. Explain why not.

9.6 Use van der Waal's equation of state to approximate the highest reduced temperature to which water can be superheated at low pressure. How many degrees of superheat does this suggest that water can sustain at the low pressure of 1 atm? (It turns out that this calculation is accurate within about 10%.) What would R_b be at this superheat?

9.7 Use Yamagata's equation to determine how nucleation site density increases with ΔT for Berenson's curves in Fig. 9.14. (That is, find c in the relation $n = \text{constant}\ \Delta T^c$.)

9.8 Suppose that C_{sf} for a given surface is high by 50%. What will be the percentage error in q calculated for a given value of ΔT? [Low by 70%.]

9.9 Water at 100 atm boils on a nickel heater whose temperature is 6°C above T_{sat}. Find h and q.

9.10 Water boils on a large flat plate at 1 atm. Calculate q_{max} if the plate is operated on the surface of the moon (at $\frac{1}{6}$ of $g_{earth-normal}$). What would q_{max} be in a space vehicle experiencing 10^{-4} of $g_{earth-normal}$?

9.11 Water boils on a 0.002 m diameter horizontal copper wire. Plot, to scale, as much of the boiling curve on $\log q$ vs. $\log \Delta T$ coordinates as you can. The system is at 1 atm.

9.12 Redo Problem 9.11 for a 0.03 m diameter sphere in water at 10 atm.

9.13 Verify eqn. (9.17).

9.14 Make a sketch of the q vs. $(T_w - T_{sat})$ relation for a pool boiling process, and invent a graphical method for locating the points where h is maximum and minimum.

9.15 A 2 mm diameter jet of methanol is directed normal to the center of a 1.5 cm diameter disk heater at 1 m/s. How many watts can safely be supplied by the heater?

9.16 Saturated water at 1 atm boils on a ½ cm diameter platinum rod. Estimate the temperature of the rod at burnout.

9.17 Plot $(T_w - T_{sat})$ and the quality x as a function of position for the conditions in Example 9.6. Set $x = 0$ where $x = 0$.

9.18 Plot $(T_w - T_{sat})$ and the quality x as a function of position in an 8 cm I.D. pipe if 0.3 kg/s of water at 100°C passes through it and $q_w = 200,000$ W/m^2. Explain how you would use Fig. 9.19 to set the range of the calculation if it were plotted to scale.

9.19 Use dimensional analysis to verify the form of eqn. (9.8).

9.20 Compare the peak heat flux calculated from the data given in Problem 5.6 with the appropriate prediction. [The prediction is within 11%.]

9.21 Find the highest and lowest mass flow rates for which the annular flow region would not occur (except at extremely high qualitites) in Example 9.9.

9.22 Verify eqn. (9.46) by repeating the analysis following eqn. (8.46) but using the b.c. $(\partial u/\partial y)_{y=\delta} = \tau_\delta/\mu$ in place of $(\partial u/\partial y)_{y=\delta} = 0$. Verify the statement involving eqn. (9.47).

9.23 A cool-water-carrying pipe 7 cm in outside diameter has an outside temperature of 40°C. Saturated steam at 80°C flows across it. Plot $\overline{h}_{condensation}$ over the range of Reynolds numbers $0 \leqslant \mathrm{Re}_D \leqslant 10^6$. Do you get the value at $\mathrm{Re}_D = 0$ that you would anticipate from Chapter 8?

9.24 (a) Suppose that you have pits of roughly 0.002 mm diameter in a metallic heater surface. At about what temperature might you expect water to boil on that surface if the pressure is 20 atm. (b) Measurements have shown that water at atmospheric pressure can be superheated about 200°C above its normal boiling point. Roughly how large an embryonic bubble would be needed to trigger nucleation in water in such a state.

9.25 Obtain the dimensionless functional form of the pool boiling q_{max} equation and the q_{max} equation for flow boiling on external surfaces, using dimensional analysis.

9.26 A chemist produces a nondegradable additive that will increase σ by a factor of ten for water at 1 atm. By what factor will the additive improve $q_{\max}$ during pool boiling on (a) infinite flat plates and (b) small horizontal cylinders? By what factor will it improve burnout in the flow of jet on a disk?

9.27 Steam at 1 atm is blown at 26 m/s over a 1 cm O.D. cylinder at 90°C. What is $\overline{h}$? Can you suggest any physical process within the cylinder that could sustain this temperature in this flow?

9.28 The water shown in Fig. 9.17 is at 1 atm, and the Nichrome heater can be approximated as nickel. What is $T_w - T_{\text{sat}}$?

9.29 For film boiling on horizontal cylinders, eqn. (9.6) is modified to

$$\lambda_d = 2\pi\sqrt{3}\left[\frac{g(\rho_f - \rho_g)}{\sigma} + \frac{2}{(\text{diam.})^2}\right]^{-1/2}.$$

If ρ_f is 748 kg/m^3 for saturated acetone, compare this λ_d, and the flat plate value, with Fig. 9.3d.

9.30 Water at 47°C flows through a 13 cm diameter thin-walled tube at 8 m/s. Saturated water vapor, at 1 atm, flows across the tube at 50 m/s. Evaluate T_{tube}, U, and q.

9.31 A 1 cm diameter thin-walled tube carries liquid metal through saturated water at 1 atm. The throughflow of metal is increased until burnout occurs. At that point the metal temperature is 250°C and h inside the tube is 9600 W/m^2·°C. What is the wall temperature at burnout?

9.32 At about what velocity of liquid metal flow does burnout occur in Problem 9.31 if the metal is mercury?

9.33 Explain, in physical terms, why eqns. (9.23) and (9.24), instead of differing by a factor of two, are almost equal. How do these equations change when H' is large?

References

[9.1] S. Nukiyama. The maximum and minimum values of the heat q transmitted from metal to boiling water under atmospheric pres-

sure. *J. Jap. Soc. Mech. Eng.*, 37:367–374, 1934. (transl.: *Int. J. Heat Mass Transfer*, vol. 9, 1966, pp. 1419–1433).

[9.2] T. B. Drew and C. Mueller. Boiling. *Trans. AIChE*, 33:449, 1937.

[9.3] International Association for the Properties of Water and Steam. Release on surface tension of ordinary water substance. Technical report, September 1994. Available from the Executive Secretary of IAPWS or on the internet: http://www.iapws.org/.

[9.4] J. J. Jasper. The surface tension of pure liquid compounds. *J. Phys. Chem. Ref. Data*, 1(4):841–1010, 1972.

[9.5] M. Okado and K. Watanabe. Surface tension correlations for several fluorocarbon refrigerants. *Heat Transfer: Japanese Research*, 17 (1):35–52, 1988.

[9.6] P.O. Binney, W.-G. Dong, and J. H. Lienhard. Use of a cubic equation to predict surface tension and spinodal limits. *J. Heat Transfer*, 108(2):405–410, 1986.

[9.7] Y. Y. Hsu. On the size range of active nucleation cavities on a heating surface. *J. Heat Transfer, Trans. ASME, Ser. C*, 84:207–216, 1962.

[9.8] W. M. Rohsenow and J. P. Hartnett, editors. *Handbook of Heat Transfer*. McGraw-Hill Book Company, New York, 1973.

[9.9] K. Yamagata, F. Hirano, K. Nishiwaka, and H. Matsuoka. Nucleate boiling of water on the horizontal heating surface. *Mem. Fac. Eng. Kyushu*, 15:98, 1955.

[9.10] W. M. Rohsenow. A method of correlating heat transfer data for surface boiling of liquids. *Trans. ASME*, 74:969, 1952.

[9.11] I. L. Pioro. Experimental evaluation of constants for the Rohsenow pool boiling correlation. *Int. J. Heat. Mass Transfer*, 42:2003–2013, 1999.

[9.12] R. Bellman and R. H. Pennington. Effects of surface tension and viscosity on Taylor instability. *Quart. Appl. Math.*, 12:151, 1954.

[9.13] V. Sernas. Minimum heat flux in film boiling—a three dimensional model. In *Proc. 2nd Can. Cong. Appl. Mech.*, pages 425–426, Canada, 1969.

[9.14] H. Lamb. *Hydrodynamics*. Dover Publications, Inc., New York, 6th edition, 1945.

[9.15] N. Zuber. Hydrodynamic aspects of boiling heat transfer. AEC Report AECU-4439, Physics and Mathematics, 1959.

[9.16] J. H. Lienhard and V. K. Dhir. Extended hydrodynamic theory of the peak and minimum pool boiling heat fluxes. NASA CR-2270, July 1973.

[9.17] J. H. Lienhard, V. K. Dhir, and D. M. Riherd. Peak pool boiling heat-flux measurements on finite horizontal flat plates. *J. Heat Transfer, Trans. ASME, Ser. C*, 95:477–482, 1973.

[9.18] J. H. Lienhard and V. K. Dhir. Hydrodynamic prediction of peak pool-boiling heat fluxes from finite bodies. *J. Heat Transfer, Trans. ASME, Ser. C*, 95:152–158, 1973.

[9.19] S. S. Kutateladze. On the transition to film boiling under natural convection. *Kotloturbostroenie*, (3):10, 1948.

[9.20] K. H. Sun and J. H. Lienhard. The peak pool boiling heat flux on horizontal cylinders. *Int. J. Heat Mass Transfer*, 13:1425–1439, 1970.

[9.21] J. S. Ded and J. H. Lienhard. The peak pool boiling heat flux from a sphere. *AIChE J.*, 18(2):337–342, 1972.

[9.22] A. L. Bromley. Heat transfer in stable film boiling. *Chem. Eng. Progr.*, 46:221–227, 1950.

[9.23] P. Sadasivan and J. H. Lienhard. Sensible heat correction in laminar film boiling and condensation. *J. Heat Transfer, Trans. ASME*, 109: 545–547, 1987.

[9.24] V. K. Dhir and J. H. Lienhard. Laminar film condensation on plane and axi-symmetric bodies in non-uniform gravity. *J. Heat Transfer, Trans. ASME, Ser. C*, 93(1):97–100, 1971.

[9.25] P. Pitschmann and U. Grigull. Filmverdampfung an waagerechten zylindern. *Wärme- und Stoffübertragung*, 3:75–84, 1970.

[9.26] J. E. Leonard, K. H. Sun, and G. E. Dix. Low flow film boiling heat transfer on vertical surfaces: Part II: Empirical formulations and

application to BWR-LOCA analysis. ASME-AIChE Nat. Heat Transfer Conf. St. Louis, August 1976.

[9.27] J. W. Westwater and B. P. Breen. Effect of diameter of horizontal tubes on film boiling heat transfer. *Chem. Eng. Progr.*, 58:67–72, 1962.

[9.28] P. J. Berenson. Transition boiling heat transfer from a horizontal surface. M.I.T. Heat Transfer Lab. Tech. Rep. 17, 1960.

[9.29] J. H. Lienhard and P. T. Y. Wong. The dominant unstable wavelength and minimum heat flux during film boiling on a horizontal cylinder. *J. Heat Transfer, Trans. ASME, Ser. C*, 86:220–226, 1964.

[9.30] L. C. Witte and J. H. Lienhard. On the existence of two transition boiling curves. *Int. J. Heat Mass Transfer*, 25:771–779, 1982.

[9.31] J. H. Lienhard and L. C. Witte. An historical review of the hydrodynamic theory of boiling. *Revs. in Chem. Engr.*, 3(3):187–280, 1985.

[9.32] J. R. Ramilison and J. H. Lienhard. Transition boiling heat transfer and the film transition region. *J. Heat Transfer*, 109, 1987.

[9.33] K. Kheyrandish and J. H. Lienhard. Mechanisms of burnout in saturated and subcooled flow boiling over a horizontal cylinder. ASME–AIChE Nat. Heat Transfer Conf. Denver, Aug. 4–7 1985.

[9.34] A. Sharan and J. H. Lienhard. On predicting burnout in the jet-disk configuration. *J. Heat Transfer*, 107:398–401, 1985.

[9.35] A. L. Bromley, N. R. LeRoy, and J. A. Robbers. Heat transfer in forced convection film boiling. *Ind. Eng. Chem.*, 45(12):2639–2646, 1953.

[9.36] L. C. Witte. Film boiling from a sphere. *Ind. Eng. Chem. Fundamentals*, 7(3):517–518, 1968.

[9.37] J. G. Collier and J. R. Thome. *Convective Boiling and Condensation*. Oxford University Press, Oxford, 3rd edition, 1994.

[9.38] J. C. Chen. A correlation for boiling heat transfer to saturated fluids in convective flow. ASME Prepr. 63-HT-34, 5th ASME-AIChE Heat Transfer Conf. Boston, August 1963.

[9.39] L. M. K. Boelter, V. H. Cherry, H. A. Johnson, and R. C. Martinelli. *Heat Transfer Notes*. McGraw-Hill Book Company, New York, 1965. Originally issued as class notes at the University of California at Berkeley between 1932 and 1941.

[9.40] Y. Y. Hsu and R. W. Graham. *Transport Processes in Boiling and Two-Phase Systems Including Near-Critical Systems*. American Nuclear Society, LaGrange Park, IL, 1986.

[9.41] Y. Katto. A generalized correlation of critical heat flux for the forced convection boiling in vertical uniformly heated round tubes. *Int. J. Heat Mass Transfer*, 21:1527–1542, 1978.

[9.42] K. J. Bell, J. Taborek, and F. Fenoglio. Interpretation of horizontal in-tube condensation heat transfer correlations with a two-phase flow regime map. *Chem. Eng. Symp. Ser.*, 66(102):150–163, 1970.

[9.43] A. E. Dukler and Y. Taitel. Flow pattern transitions in gas–liquid systems measurement and modelling. In J. M. Delhaye, N. Zuber, and G. F. Hewitt, editors, *Advances in Multi-Phase Flow*, volume II. Hemisphere/McGraw-Hill, New York, 1985.

[9.44] I. G. Shekriladze and V. I. Gomelauri. Theoretical study of laminar film condensation of flowing vapour. *Int. J. Heat. Mass Transfer*, 9:581–591, 1966.

[9.45] J. Rose, Y. Utaka, and I. Tanasawa. Dropwise condensation. In S. G. Kandlikar, M. Shoji, and V. K. Dhir, editors, *Handbook of Phase Change: Boiling and Condensation*, chapter 20. Taylor & Francis, Philadelphia, 1999.

[9.46] P. J. Marto. Condensation. In W. M. Rohsenow, J. P. Hartnett, and Y. I. Cho, editors, *Handbook of Heat Transfer*, chapter 14. McGraw-Hill, New York, 3rd edition, 1998.

[9.47] D. W. Woodruff and J. W. Westwater. Steam condensation on electroplated gold: effect of plating thickness. *Int. J. Heat. Mass Transfer*, 22:629–632, 1979.

[9.48] P. D. Dunn and D. A. Reay. *Heat Pipes*. Pergamon Press Ltd., Oxford, UK, 3rd edition, 1982.

[9.49] E. R. F. Winter and W. O. Barsch. The heat pipe. In T. F. Irvine, Jr. and J. P. Hartnett, editors, *Advances in Heat Transfer*, volume 7, pages 219–320e. Academic Press, Inc., New York, 1971.

[9.50] C. L. Tien. Fluid mechanics of heat pipes. *Ann. Rev. Fluid Mech.*, 7: 167–185, 1975.

Part IV

Thermal Radiation Heat Transfer

10. Radiative heat transfer

The sun that shines from Heaven shines but warm,
And, lo, I lie between that sun and thee:
The heat I have from thence doth little harm,
Thine eye darts forth the fire that burneth me:
And were I not immortal, life were done
Between this heavenly and earthly sun.
***Venus and Adonis*, Wm. Shakespeare**

10.1 The problem of radiative exchange

Chapter 1 described the elementary mechanisms of heat radiation. Before we proceed, you should reflect upon what you remember about the following key ideas from Chapter 1:

- Electromagnetic wave spectrum
- Black body
- Hohlraum
- Infrared (and other) radiation
- Heat radiation
- Transmittance
- Reflectance
- Absorptance
- $\alpha + \rho + \tau = 1$
- The Stefan-Boltzmann law
- The Stefan-Boltzmann constant
- $e(T)$ and $e_\lambda(T)$ for black bodies
- Planck's law
- F_{1-2} and $\mathcal{F}_{1-2}$
- Radiation shielding

We presume that these concepts are understood.

The heat exchange problem

Figure 10.1 shows two arbitrary surfaces radiating energy to one another. The net heat exchange, Q_{net}, from the hotter surface (1) to the cooler surface (2) depends on the following influences:

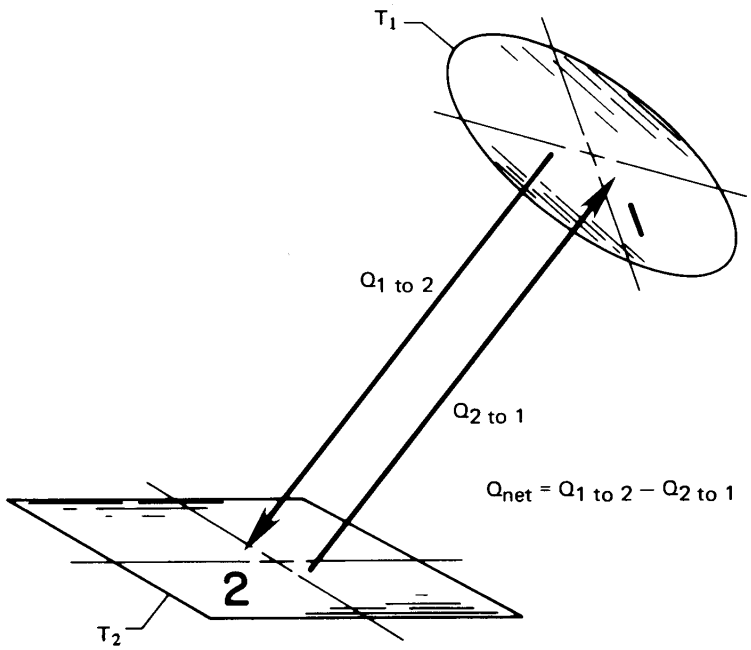

Figure 10.1 Thermal radiation between two arbitrary surfaces.

- T_1 and T_2.
- The areas of (1) and (2).
- The configurations of (1) and (2) and the spacing between them.
- The radiative characteristics of the surfaces.
- Additional surfaces in the environment.
- The medium between (1) and (2). (If the medium is air, we can usually neglect its influence.)

If surfaces (1) and (2) are black, if they are surrounded by air, if the surfaces in the environment are black, and if no heat flows between (1) and (2) by conduction or convection, then only the first three considerations are involved in determining Q_{net}. We saw some elementary examples of how this could be done in Chapter 1. In this case

$$Q_{\text{net}} = F_{1-2} A_1 \sigma \left(T_1^4 - T_2^4 \right) \tag{10.1}$$

The last three considerations lead to great complications of the problem. In Chapter 1 we saw that these nonideal factors are sometimes included in a "real body view factor," or *transfer factor* $\mathcal{F}_{1-2}$, such that

$$Q_{\text{net}} = \mathcal{F}_{1-2} A_1 \sigma \left(T_1^4 - T_2^4\right) \tag{10.2}$$

Before we undertake the problem of evaluating heat exchange among real bodies, we need several definitions.

Some definitions

Emittance. A real body at temperature T does not emit with the black body emissive power $e_b = \sigma T^4$ but rather with some fraction, ε, of e_b. Thus, we define either the monochromatic emittance, ε_λ:

$$\varepsilon_\lambda \equiv \frac{e_\lambda(\lambda, T)}{e_{\lambda_b}(\lambda, T)} \tag{10.3}$$

or the total emittance, ε:

$$\varepsilon \equiv \frac{e(T)}{e_b(T)} = \frac{\int_0^\infty e_\lambda(\lambda, T)\, d\lambda}{\sigma T^4} \tag{10.4}$$

The emittance is determined entirely by the properties of the surface of the particular body and its temperature. It is independent of the environment of the body.

Table 10.1 lists typical values of the total emittance for a variety of real substances. (These were summarized from [10.1].) Notice that most metals have quite low emittances, unless they are oxidized. Most nonmetals have emittances that are quite high—approaching the black body limit of unity. Notice that among the "blackest" surfaces in the table are white paint, paper, and ice.

One particular kind of surface behavior is that for which ε_λ is independent of λ. We call such a surface a *gray body*. The emissive power, $e(T)$, for a gray body is a constant fraction, ε, of $e_b(T)$, as indicated in the inset of Fig. 10.2. No real body is gray, but many exhibit approximately gray behavior. We see in Fig. 10.2, for example, that the sun appears to us on earth as an approximately gray body with an emittance of approximately 0.6. We shall often use the gray body simplification in this chapter to avoid the formidable difficulties of considering the variation of ε_λ with λ.

Yet the emittance of most, but far from all, common materials and coatings tends to decrease with wavelength in the thermal range. Some

Table 10.1 Total emittances for a variety of surfaces

Metals			*Nonmetals*		
Surface	*Temp.* (°C)	ε	*Surface*	*Temp.* (°C)	ε
Aluminum			Asbestos	40	0.93–0.97
Polished, 98% pure	200–600	0.04–0.06	Brick		
Commercial sheet	90	0.09	Red, rough	40	0.93
Heavily oxidized	90–540	0.20–0.33	Silica	980	0.80–0.85
Brass			Fireclay	980	0.75
Highly polished	260	0.03	Ordinary refractory	1090	0.59
Dull plate	40–260	0.22	Magnesite refractory	980	0.38
Oxidized	40–260	0.46–0.56	White refractory	1090	0.29
Copper			Carbon		
Highly polished electrolytic	90	0.02	Filament	1040–1430	0.53
Slightly polished to dull	40	0.12–0.15	Lampsoot	40	0.95
Black oxidized	40	0.76	Concrete, rough	40	0.94
Gold: pure, polished	90–600	0.02–0.035	Glass		
Iron and steel			Smooth	40	0.94
Mild steel, polished	150–480	0.14–0.32	Quartz glass (2 mm)	260–540	0.96–0.66
Steel, polished	40–260	0.07–0.10	Pyrex	260–540	0.94–0.74
Sheet steel, rolled	40	0.66	Gypsum	40	0.80–0.90
Sheet steel, strong rough oxide	40	0.80	Ice	0	0.97–0.98
Cast iron, oxidized	40–260	0.57–0.66	Limestone	400–260	0.95–0.83
Iron, rusted	40	0.61–0.85	Marble	40	0.93–0.95
Wrought iron, smooth	40	0.35	Mica	40	0.75
Wrought iron, dull oxidized	20–360	0.94	Paints		
Stainless, polished	40	0.07–0.17	Black gloss	40	0.90
Stainless, after repeated heating	230–900	0.50–0.70	White paint	40	0.89–0.97
			Lacquer	40	0.80–0.95
Lead			Various oil paints	40	0.92–0.96
Polished	40–260	0.05–0.08	Red lead	90	0.93
Oxidized	40–200	0.63	Paper		
Mercury: pure, clean	40–90	0.10–0.12	White	40	0.95–0.98
Platinum			Other colors	40	0.92–0.94
Pure, polished plate	200–590	0.05–0.10	Roofing	40	0.91
Oxidized at 590°C	260–590	0.07–0.11	Plaster, rough lime	40–260	0.92
Drawn wire and strips	40–1370	0.04–0.19	Quartz	100–1000	0.89–0.58
Silver	200	0.01–0.04	Rubber	40	0.86–0.94
Tin	40–90	0.05	Snow	10–20	0.82
Tungsten			Water, thickness ≥0.1 mm	40	0.96
Filament	540–1090	0.11–0.16	Wood	40	0.80–0.90
Filament	2760	0.39	Oak, planed	20	0.90

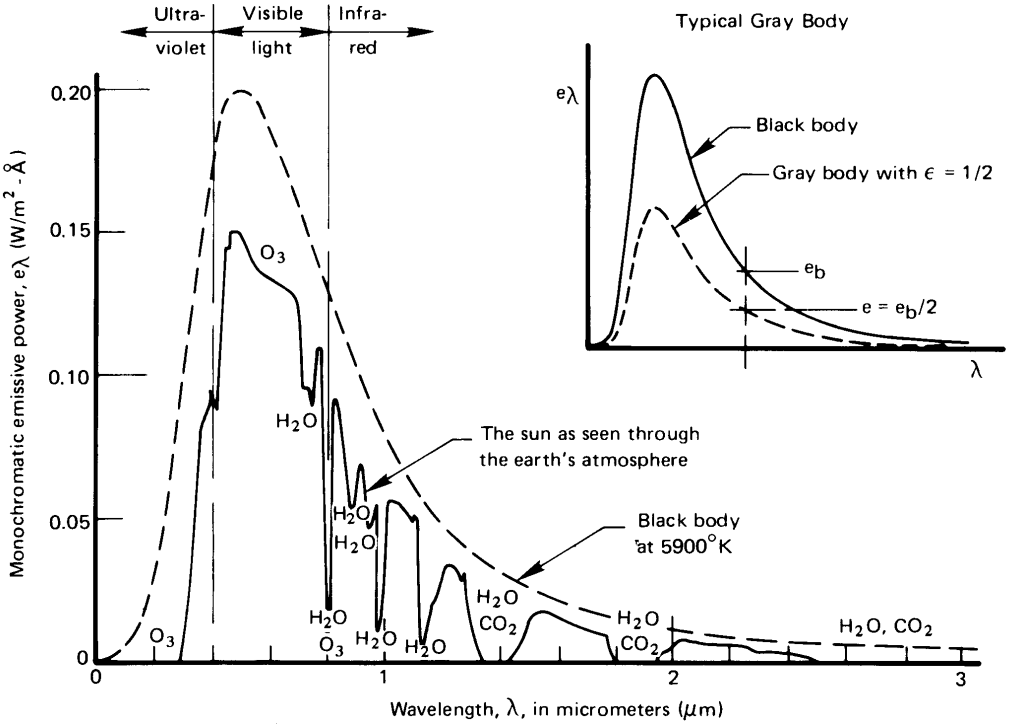

Figure 10.2 Comparison of the energy emitted by the sun (as viewed through the earth's atmosphere) with a black body at the same mean temperature. (Notice that the effective e_{λ_b}, just outside the earth's atmosphere, is far less than it is on the surface of the sun because the radiation has spread out.)

materials—for example, copper, aluminum oxide, and certain paints—are actually pretty close to being gray surfaces at normal temperatures.

The *selective surface* presents an important example of nongray behavior. Such a surface has a very high emittance above or below a certain wavelength and a very low value in the other range. Window glass, for example, is quite selective. Its emissivity is quite low below $\lambda \cong 2.7$ μm, and it abruptly jumps to a high value above 2.7 μm. In accordance with Kirchhoff's law, the absorptance behaves similarly. However, the fact that glass admits short-wavelength energy from the sun to a room, but does not let the long-wavelength energy from the room escape, is the result of its transmissivity, which is selectively high in the visible range and close to zero at longer wavelengths.

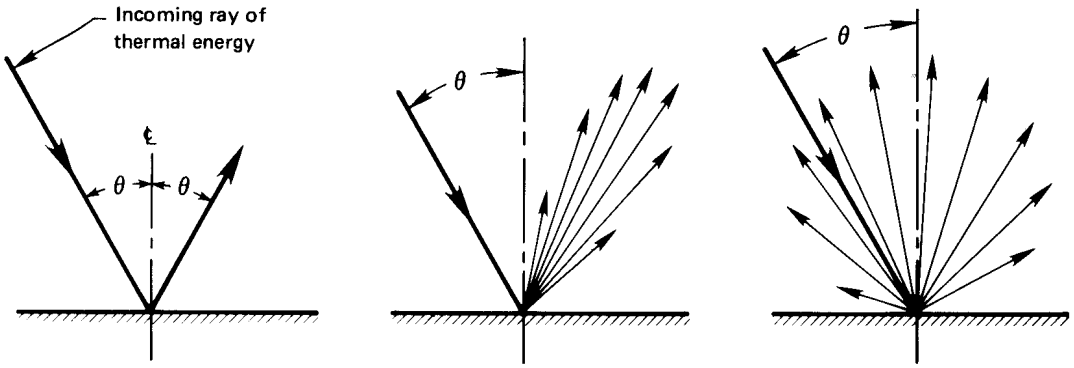

Specular or mirror-like reflection of incoming ray.

Reflection which is between diffuse and specular (a real surface).

Diffuse radiation in which directions of departure are uninfluenced by incoming ray angle, θ.

Figure 10.3 Specular and diffuse reflection of radiation. (Arrows indicate magnitude of the heat flux in the directions indicated.)

The emittance can also exhibit a strong surface temperature dependence, either increasing or decreasing with temperature. Certain metals—for example, clean or oxidized copper or stainless steel—are relatively insensitive to temperature over large ranges. Whether or not the emittance can be assumed temperature-independent in a given problem often depends on how large a temperature range is being considered.

Diffuse and specular emittance and reflection. The energy emitted by a surface, together with that portion of an incoming ray of energy that is reflected from another non-black surface, may leave the body *diffusely* or *specularly*. That energy may also be emitted or reflected in a way that lies between these limits. Figure 10.3 shows how radiation might be reflected in these various ways. A mirror reflects visible radiation in an almost perfectly *specular* fashion. (The "reflection" of a billiard ball from the side of a table is also specular.) When reflection or emission is diffuse, there is no preferred direction for outgoing rays.

The character of the emittance or reflectance of a surface will normally change with the wavelength of the radiation. We shall often assume diffuse behavior on the part of the surface, but this will be strictly true only if the surface is black.

Experiment 10.1

Obtain a flashlight with as narrow a spot focus as you can find. Direct it at an angle onto a mirror, onto the surface of a bowl filled with sugar, and onto a variety of other surfaces, all in a darkened room. In each case, move the palm of your hand around the surface of an imaginary hemisphere centered on the point where the spot touches the surface. Notice how your palm is illuminated, and categorize the kind of reflectance of each surface—at least in the range of visible wavelengths.

Intensity of radiation. Consider radiation from a circular surface element, dA, as shown at the top of Fig. 10.4. If the element is black, the radiation that it emits is indistinguishable from the radiation that would be emitted from a black cavity at the same temperature, and it is the same in all directions. (For diffusely radiating nonblack bodies, the considerations below apply equally to the radiant energy leaving the surface.) Thus, the rate at which energy is emitted in any direction is proportional to the projected area of dA normal to the direction of view, as shown in the upper right side of Fig. 10.4.

If an aperture of area dA_a is placed at a radius r from dA and normal to the radius, it will intercept a fraction of the energy emitted by dA. The magnitude of that fraction is equal to the ratio of the solid angle,[1] ω, subtended by dA_a to the solid angle subtended by the entire hemisphere. We define a quantity called the *intensity of radiation*, i (W/m$^2\cdot$steradian), which is defined by an energy balance statement:

$$dq_{\text{outgoing}} = i\,d\omega\cos\theta = \begin{cases}\text{fraction of radiant heat transfer}\\ \text{from } dA \text{ that is intercepted by } dA_a\end{cases} \tag{10.5}$$

Notice that while the heat flux from dA decreases with θ (as indicated on the right side of Fig. 10.3), the intensity of energy from a diffuse surface is uniform in all directions.

Finally, we compute i in terms of q by integrating $i\,d\omega$ over the entire unit hemisphere and noting (see Fig. 10.4) that $d\omega = \sin\theta\,d\theta d\phi$.

$$q_{\text{outgoing}} = \int_{\phi=0}^{2\pi}\int_{\theta=0}^{\pi/2} i\cos\theta\,(\sin\theta\,d\theta d\phi) = \pi i \tag{10.6a}$$

[1] The unit of solid angle is the *steradian*. One steradian is the solid angle subtended by a spherical segment whose area equals the square of its radius. A full sphere therefore subtends $4\pi r^2/r^2 = 4\pi$ steradians.

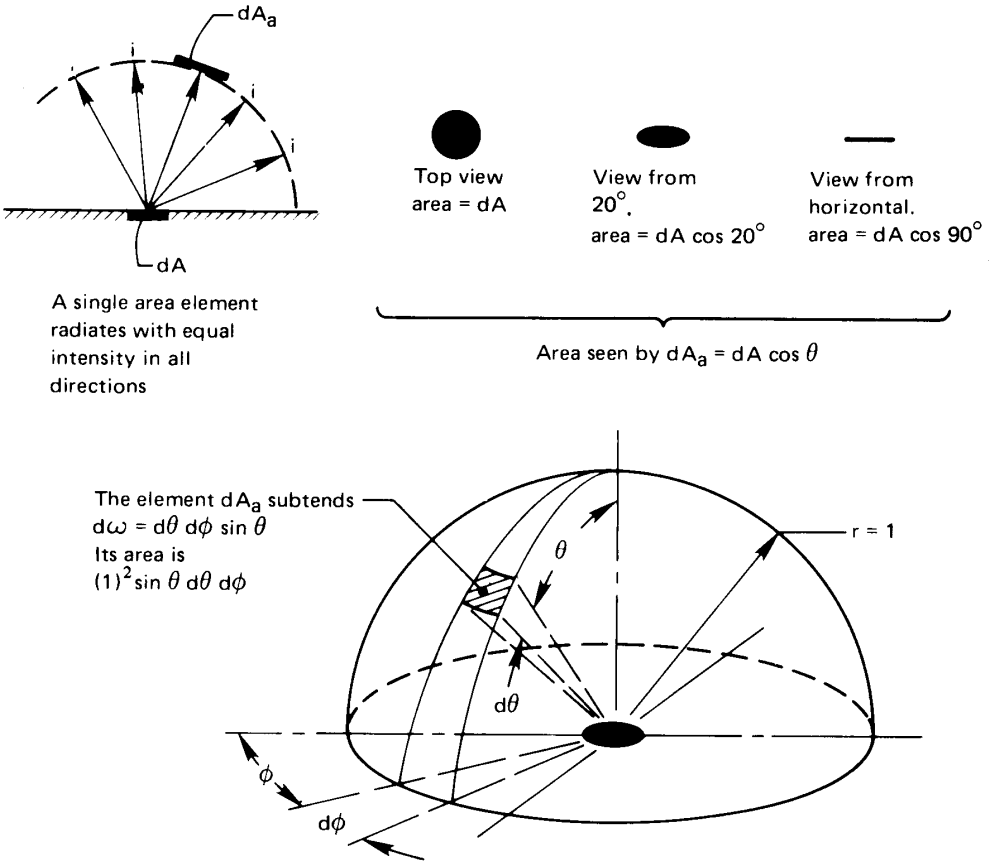

Figure 10.4 Radiation intensity through a unit sphere.

Thus, for a black body,

$$i_b = \frac{\sigma T^4}{\pi} = \frac{e_b}{\pi} = \text{fn}\,(T \text{ only}) \tag{10.6b}$$

and for any particular wavelength, we define the monochromatic intensity

$$i_\lambda = \frac{e_\lambda}{\pi} = \text{fn}\,(T, \lambda) \tag{10.6c}$$

10.2 Kirchhoff's law

The problem of predicting α

The total emittance, ε, of a surface is uniquely determined by the characteristics of the surface. But the absorptance, α, while it is surface-dependent, is also influenced by the environment from which the surface receives energy. The reason is that α depends on the way in which incoming energy is distributed in wavelength. That distribution is determined by the characteristics of the surfaces from which the surface of interest receives radiation. Furthermore, if the temperatures of those bodies from which radiation is received are changed, the energy distribution in wavelength will change as well.

We are thus faced with the problem that α depends on the surface characteristics and the temperatures of *all* bodies involved in a given heat exchange process. Kirchhoff's law[2] is a theoretical relation that can be used to predict α under certain restrictions. Next, we shall develop the law and state the restrictions on it.

Simple heat exchange problem

Figure 10.5 shows two surfaces that exchange heat by radiation. We want to sum the energy exchanges between the two bodies to get the net heat transfer from plane (1) to plane (2). The outward heat flux, q_1, from plane (1) is the sum of two parts: the fraction of the heat from plane (2) that is reflected away from it (and not absorbed) and the heat that is emitted by it. Thus,

$$q_1 = (1 - \alpha_1)\, q_2 + \varepsilon_1 e_{b_1} \tag{10.7a}$$

The outward heat flux, q_2, from plane (2) is likewise

$$q_2 = (1 - \alpha_2)\, q_1 + \varepsilon_2 e_{b_2} \tag{10.7b}$$

Solving this pair of simultaneous equations and noting that $\varepsilon_1 e_{b_1} = e_1$ and $\varepsilon_2 e_{b_2} = e_2$, we get

$$q_1 = \frac{e_1 + e_2 - \alpha_1 e_2}{\alpha_1 + \alpha_2 - \alpha_1 \alpha_2} \quad \text{and} \quad q_2 = \frac{e_1 + e_2 - \alpha_2 e_1}{\alpha_1 + \alpha_2 - \alpha_1 \alpha_2}$$

[2] Gustav Robert Kirchhoff (1824–1887) was a very important German physicist of the nineteenth century. He presented this "Kirchhoff's law" when he was only 25 years old. But he is also known for a great deal of basic work in the thermodynamics of phase change and in electric theory.

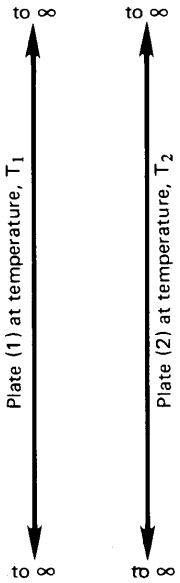

Figure 10.5 Heat transfer between two infinite parallel plates.

The net heat flux from plane (1) to plane (2) is then the difference between these two heat fluxes:

$$q_{1\text{ to }2} = \frac{\alpha_2 e_1 - \alpha_1 e_2}{\alpha_1 + \alpha_2 - \alpha_1 \alpha_2} = \frac{\dfrac{e_1}{\alpha_1} - \dfrac{e_2}{\alpha_2}}{\left(\dfrac{1}{\alpha_1} + \dfrac{1}{\alpha_2} - 1\right)} \tag{10.8}$$

Finally, we note that if $T_1 = T_2$, $q_{1\text{ to }2}$ must equal zero. Furthermore, all the quantities here depend on the common temperature $T_1 = T_2 = T$. Thus, we obtain from eqn. (10.8)

$$\boxed{\frac{e_1}{\alpha_1} = \frac{e_2}{\alpha_2} = \text{fn}(T)} \tag{10.9}$$

This result is *Kirchhoff's law*. The most important consequence of Kirchhoff's law is obtained by allowing, say, body (2) to be black. Then $\alpha_2 = 1$, $e_2 = \sigma T^4$ and eqn. (10.9) becomes

$$\frac{\varepsilon_1 \sigma T^4}{\alpha_1} = \frac{\sigma T^4}{1}$$

so $\varepsilon_1 = \alpha_1$. The subscripts are then superfluous and we can write

$$\boxed{\varepsilon = \alpha} \qquad \text{approximate form of Kirchhoff's law} \tag{10.10a}$$

Equation (10.10a) is a somewhat dangerous result in that it is only strictly true under very restrictive circumstances. We have noted that when radiation from a hot surface falls on a cooler one, the wavelength distribution of the incoming energy will differ from that of the re-emitted energy. A more precise derivation (see, e.g. [10.2], Chapter 3) reveals that Kirchhoff's law is exactly true only for a specific temperature, T, wavelength, λ, and direction of radiation, (θ, ϕ):

$$\boxed{\varepsilon_\lambda(T,\theta,\phi) = \alpha_\lambda(T,\theta,\phi)} \qquad \begin{matrix}\text{exact form of}\\ \text{Kirchhoff's law}\end{matrix} \qquad (10.10b)$$

Of course, the use of eqn. (10.10a) is a great convenience when it is legitimate. It turns out that it is valid under the following conditions:

- The body is gray. Then $\alpha = \varepsilon \neq \text{fn}(\lambda)$.
- The surroundings are black, so that $\alpha_\lambda = \varepsilon_\lambda \neq \text{fn}(T)$.
- The trivial case in which the body and its surroundings are at the same temperature.

It can also be shown for metallic surfaces that if the surroundings are black or gray, $\alpha = \varepsilon(\overline{T})$, where

$$\overline{T} \equiv \sqrt{(T_{\text{surroundings}})(T_{\text{surface}})}$$

As a typical example of the failure of eqn. (10.10a), consider solar radiation incident on a roof, painted black. From Table 10.1, we see that ε is on the order of 0.94. It turns out that α is just about the same. If we repaint the roof white, ε will not change noticeably. However, much of the energy arriving from the sun is carried in visible wavelengths. Our eyes tell us that white paint reflects sunlight very strongly in these wavelengths, and indeed this is the case. The absorptance of white paint to energy from the sun is only on the order of 0.10—much less than ε for the energy it receives.

10.3 Simple radiant heat exchange between two surfaces

One body enclosed by another

Parallel plates. Equation (10.8) is not a useful design equation in its present form. But when we substitute $e_1 = \varepsilon_1 \sigma T_1^4$ and $e_2 = \varepsilon_2 \sigma T_2^4$ and

use $\varepsilon = \alpha$, we get

$$q_{1 \text{ to } 2} = \sigma \frac{\varepsilon_1 \varepsilon_2 T_1^4 - \varepsilon_2 \varepsilon_1 T_2^4}{\varepsilon_1 + \varepsilon_2 - \varepsilon_1 \varepsilon_2}$$

or

$$\boxed{q_{1 \text{ to } 2} = \frac{1}{\left(\frac{1}{\varepsilon_1} + \frac{1}{\varepsilon_2} - 1\right)} \sigma \left(T_1^4 - T_2^4\right)} \tag{10.11}$$

Comparing eqn. (10.11) with eqn. (10.2), we may identify

$$\mathcal{F}_{1 \text{ to } 2} = \frac{1}{\left(\frac{1}{\varepsilon_1} + \frac{1}{\varepsilon_2} - 1\right)} \tag{10.12}$$

for infinite parallel plates. Notice, too, that if the surfaces are both black, $\varepsilon_1 = \varepsilon_2 = 1$ and

$$\mathcal{F}_{1 \text{ to } 2} = 1 = F_{1 \text{ to } 2} \tag{10.13}$$

which, of course, is what we would expect.

Example 10.1

A stainless steel plate at 100°C faces a firebrick wall at 500°C. Estimate the heat flux and *radiation heat transfer coefficient*, h_r.

SOLUTION. From Table 10.1, we read the emittances of stainless steel and firebrick as approximately 0.6 and 0.75. Thus,

$$q_{1 \text{ to } 2} = \frac{1}{\left(\frac{1}{0.75} + \frac{1}{0.6} - 1\right)} 5.67 \times 10^{-8} \left[(773 \text{ K})^4 - (373 \text{ K})^4\right]$$

$$= 9573 \text{ W/m}^2$$

This can be put in the form of a *radiation heat transfer coefficient*:

$$h_r = \frac{q_{1 \text{ to } 2}}{T_1 - T_2} = \frac{9573}{500 - 100} = 24 \text{ W/m}^2\text{·°C}$$

This heat transfer coefficient is rather low. If we had done the calculation for a brick wall at 1500°C, we would have found that $q = 280,000$ W/m^2 and $h_r = 200$ W/m^2·°C. Thus, we see that h_r rises in a fairly dramatic nonlinear way with T_1. ■

General case in which one body surrounds another

A pair of parallel plates is a special case of the general situation in which one body surrounds another. The general situation is suggested in Fig. 10.6, and it includes such configurations as concentric cylinders or a sphere within a sphere. As long as both surfaces emit diffusely, the factor $\mathcal{F}_{1\text{ to }2}$ in this case takes either of two limiting forms, which we state, for the moment, without proof.

$$\mathcal{F}_{1\text{ to }2} = \begin{cases} \dfrac{1}{\left[\dfrac{1}{\varepsilon_1} + \dfrac{A_1}{A_2}\left(\dfrac{1}{\varepsilon_2} - 1\right)\right]} & \text{for diffusely reflecting bodies} \\ \dfrac{1}{\left[\dfrac{1}{\varepsilon_1} + \dfrac{1}{\varepsilon_2} - 1\right]} & \text{for specularly reflecting bodies} \end{cases} \tag{10.14}$$

The latter result is interestingly identical to eqn. (10.12), even though that result was true for either specular or diffuse radiation.

Radiant heat exchange between two finite black bodies

Some evident results. Let us now return to the purely geometric problem of evaluating the view factor, F_{1-2}. Although the evaluation of F_{1-2} is also used in the calculation of heat exchange among nonblack bodies, it is the *only* correction of the Stefan-Boltzmann law that we need for black bodies.

Figure 10.7 shows three elementary situations in which the value of F_{1-2} is evident under the definition:

F_{1-2} = fraction of energy emitted by (1) that reaches (2)

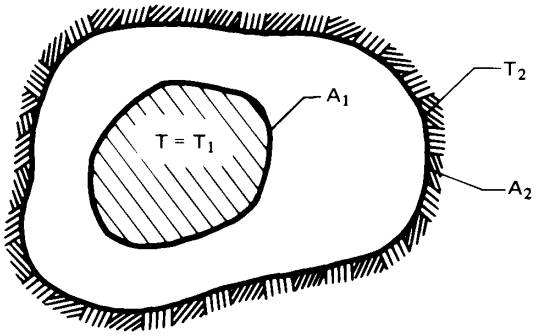

Figure 10.6 Heat transfer between an enclosed body and the body surrounding it.

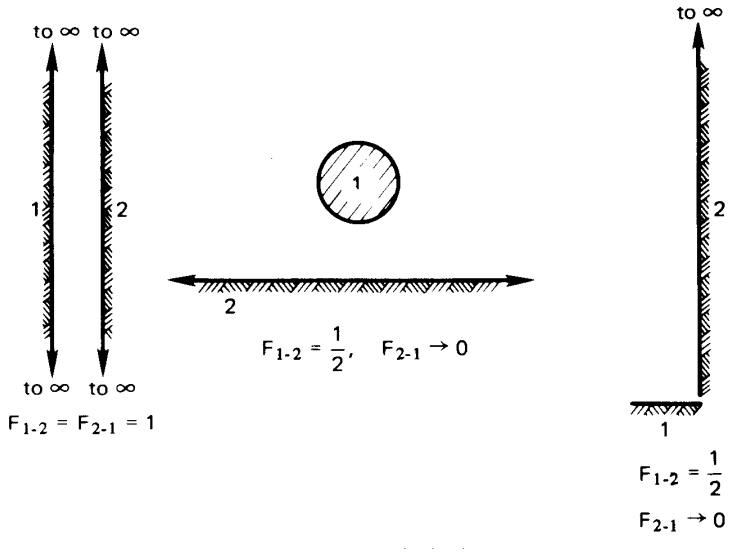

Figure 10.7 Some configurations for which the value of the view factor is immediately apparent.

A second apparent result in regard to the view factor is that all the energy leaving a body (1) reaches something else. Thus, conservation of energy requires

$$1 = F_{1-1} + F_{1-2} + F_{1-3} + \cdots + F_{1-n} \tag{10.15}$$

where (2), (3),...,(n) are all of the bodies in the neighborhood of (1). Figure 10.8 shows a representative situation in which a body (1) is surrounded by three other bodies. It sees all three bodies, but it also views itself, in part. This accounts for the inclusion of the view factor, F_{1-1} in eqn. (10.15).

By the same token, it should also be apparent from Fig. 10.8 that the kind of sum expressed by eqn. (10.15) would also be true for just a portion of what is seen by surface 1. Thus,

$$F_{1-(2+3)} = F_{1-2} + F_{1-3}$$

Of course, such a sum makes sense only when all the view factors are based on the same viewing surface (surface 1 in this case). One might be tempted to write this sort of sum in the opposite direction, but it would clearly be untrue:

$$F_{(2+3)-1} \neq F_{2-1} + F_{3-1}$$

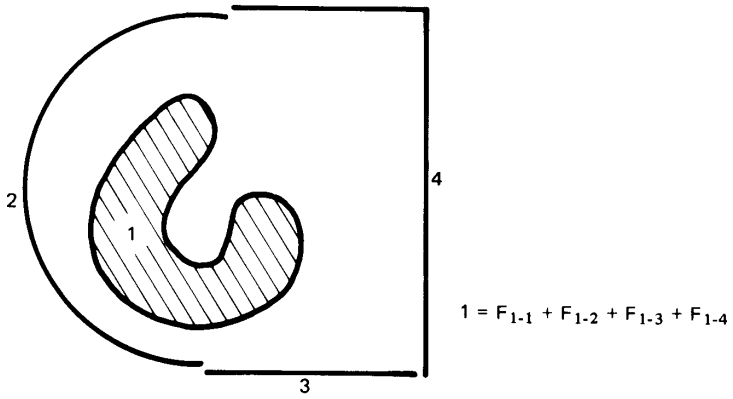

Figure 10.8 A body (1) that views three other bodies and itself as well.

since each view factor is for a different viewing surface—(2 + 3), 2, and 3 in this case.

Example 10.2

A jet of liquid metal at 2000°C pours from a crucible. It is 3 mm in diameter. A 5 cm diameter cylindrical radiation shield surrounds the jet through an angle of 330°, but there is a 30° slit in it. The jet is otherwise surrounded by a large cubic room at 30°C. How much radiant energy reaches the room per meter of length of the shield if it is legitimate to assume that the jet and the shield are both black under these conditions?

SOLUTION. There are two paths by which radiant energy can reach the room: directly through the slit, and from the shield to the room. Clearly, $F_{\text{jet-room}} = 30/360 = 0.0833$ and $F_{\text{jet-shield}} = 330/360 = 0.9167$. Then

$$\begin{aligned} Q_{\text{jet-room}} &= F_{\text{jet-room}} A_{\text{jet}} \sigma \left(T_{\text{jet}}^4 - T_{\text{room}}^4 \right) \\ &= 0.0833 \left[\frac{\pi (0.003)\ \text{m}^2}{\text{m length}} \right] \left(5.67 \times 10^{-8} \right) \left(2273^4 - 303^4 \right) \\ &= 1188\ \text{W/m} \end{aligned}$$

The shield temperature is obtained by balancing the heat it re-

ceives with the heat it emits:

$$F_{\text{jet-shield}} A_{\text{jet}} \sigma \left(T_{\text{jet}}^4 - T_{\text{shield}}^4 \right) = F_{\text{shield-room}} A_{\text{shield}} \sigma \left(T_{\text{shield}}^4 - T_{\text{room}}^4 \right)$$

The view factor $F_{\text{shield-room}}$ can be approximated as unity. (Notice that we neglect heat transfer from the *inside* of the shield to the room.) Then

$$\frac{0.9167(0.003)}{1(0.050)} \left(2273^4 - T_{\text{shield}}^4 \right) = T_{\text{shield}}^4 - 303^4$$

or

$$T_{\text{shield}} = \left[\frac{303^4 + \dfrac{0.9167(0.003)}{1(0.050)} (2273)^4}{1 + \dfrac{0.9167(0.003)}{1(0.050)}} \right]^{1/4} = 1088 \text{ K}$$

It is now possible to calculate $Q_{\text{shield-room}}$:

$$\begin{aligned} Q_{\text{shield-room}} &= F_{\text{shield-room}} A_{\text{shield}} \sigma \left(T_{\text{shield}}^4 - T_{\text{room}}^4 \right) \\ &= 1 \left[\frac{\pi (0.05) \text{ m}^2}{\text{m length}} \right] \left(5.67 \times 10^{-8} \right) \left(1088^4 - 303^4 \right) \\ &= 12,400 \text{ W/m} \end{aligned}$$

so the total heat transfer is

$$Q_{\text{shield-room}} + Q_{\text{jet-room}} = 13,590 \text{ W/m}$$

most of which is re-emitted by the shield.

Notice that the unshielded jet would have transferred

$$\frac{1}{0.0833} (1188) = 14,260 \text{ W/m}$$

to the room. Therefore, this particular shield has accomplished only a 4.7% reduction of heat transfer. To be effective, the shield would have to have a low emittance. ■

Calculation of the black-body view factor, F_{1-2}. Consider two elements, dA_1 and dA_2, of larger black bodies (1) and (2), as shown in Fig. 10.9. The entire body (1) and the entire body (2) are isothermal. Since element dA_2 subtends a solid angle $d\omega_1$, we use eqn. (10.5) to write

$$dQ_{1 \text{ to } 2} = (i_1 d\omega_1)(dA_1 \cos \beta_1)$$

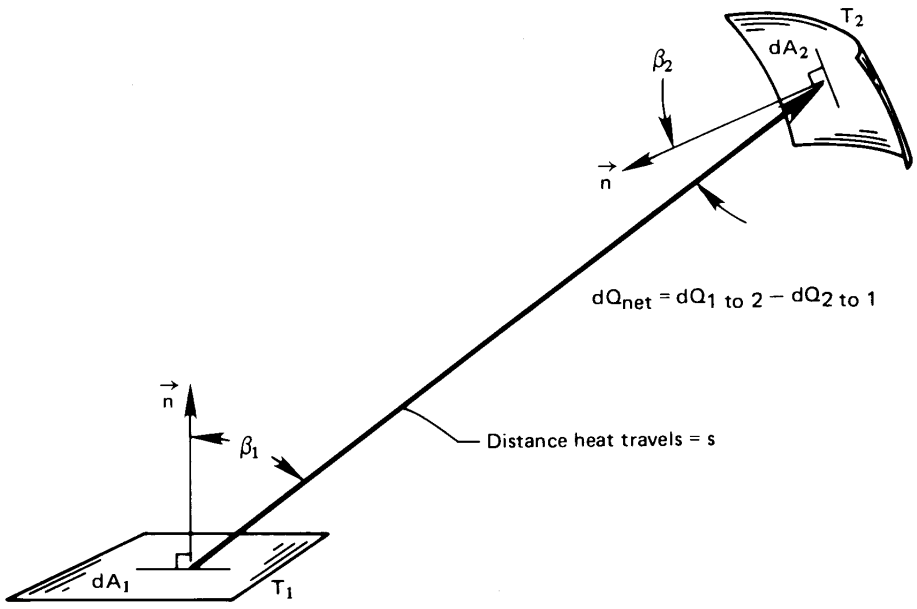

Figure 10.9 Radiant exchange between two black elements that are part of the bodies (1) and (2).

But from eqn. (10.6b),

$$i_1 = \frac{\sigma T_1^4}{\pi}$$

Furthermore,

$$d\omega_1 = \frac{dA_2 \cos\beta_2}{s^2}$$

where s is the distance from (1) to (2). Thus,

$$dQ_{1 \text{ to } 2} = \frac{\sigma T_1^4}{\pi}\left(\frac{\cos\beta_1 \cos\beta_2 \, dA_1 dA_2}{s^2}\right)$$

By the same token,

$$dQ_{2 \text{ to } 1} = \frac{\sigma T_2^4}{\pi}\left(\frac{\cos\beta_2 \cos\beta_1 \, dA_2 dA_1}{s^2}\right)$$

Then

$$\boxed{Q_{\text{net}} = \sigma\left(T_1^4 - T_2^4\right)\int_{A_1}\int_{A_2}\frac{\cos\beta_1 \cos\beta_2}{\pi s^2}\, dA_1 dA_2} \qquad (10.16)$$

The view factors F_{1-2} and F_{2-1} are immediately obtainable from eqn. (10.16). If we compare this result with $Q_{\text{net}} = F_{1-2}A_1\sigma(T_1^4 - T_2^4)$, we get

$$\boxed{F_{1-2} = \frac{1}{A_1}\int_{A_1}\int_{A_2}\frac{\cos\beta_1\cos\beta_2}{\pi s^2}\,dA_1 dA_2} \tag{10.17a}$$

From the inherent symmetry of the problem, we can also write

$$\boxed{F_{2-1} = \frac{1}{A_2}\int_{A_2}\int_{A_1}\frac{\cos\beta_2\cos\beta_1}{\pi s^2}\,dA_2 dA_1} \tag{10.17b}$$

It follows from eqns. (10.17a) and (10.17b) that

$$\int_{A_1}\int_{A_2}\frac{\cos\beta_1\cos\beta_2}{\pi s^2}\,dA_1 dA_2 = \boxed{A_1F_{1-2} = A_2F_{2-1}} \tag{10.18}$$

This reciprocity relation will prove to be very useful in subsequent work.

The direct evaluation of F_{1-2} from eqn. (10.17a) becomes fairly involved, even for the simplest configurations. Siegel and Howell [10.2] provide an unusually comprehensive discussion of such calculations and a large catalog of their results. We shall not actually use eqns. (10.17a) and (10.17b) directly but shall instead refer the interested reader to Siegel and Howell for the results of such calculations. Siegel and Howell use a contour integral technique to evaluate F_{1-2} and F_{2-1} in place of eqns. (10.17a) and (10.17b). The method is more sophisticated, but if one actually has to perform the integration, that formulation can simplify the task.

We list some typical results of the calculation in Tables 10.2 and 10.3. Table 10.2 gives calculated values of F_{1-2} for two-dimensional bodies—various configurations of cylinders and strips that approach being infinite in length. Table 10.3 gives F_{1-2} for some three-dimensional configurations.

Many of these and other results have been evaluated numerically and presented in graphical form for easy reference. Figure 10.10, for example, includes the solutions for configurations 1, 2, and 3 from Table 10.3. The reader should study these results and be sure that the tendencies they show make sense. Is it clear, for example, that $F_{1-2} \longrightarrow$ constant, which is < 1 in each case, as the abscissa becomes large? Can you locate the right-hand element of Fig. 10.7 in Fig. 10.10? And so forth.

Table 10.2 View factors for a variety of two-dimensional configurations (infinite in extent normal to the paper)

Configuration	*Equation*
1. 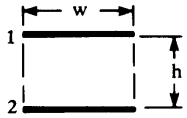	$F_{1-2} = F_{2-1} = \sqrt{1 + \left(\frac{h}{w}\right)^2} - \left(\frac{h}{w}\right)$
2. 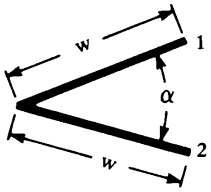	$F_{1-2} = F_{2-1} = 1 - \sin(\alpha/2)$
3. 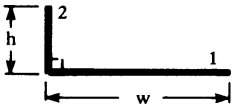	$F_{1-2} = \frac{1}{2}\left[1 + \frac{h}{w} - \sqrt{1 + \left(\frac{h}{w}\right)^2}\right]$
4. 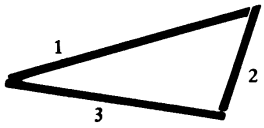	$F_{1-2} = (A_1 + A_2 - A_3)/2A_1$
5. 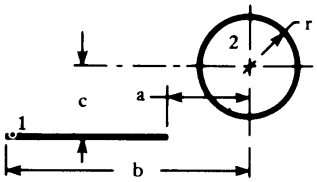	$F_{1-2} = \frac{r}{b-a}\left[\tan^{-1}\frac{b}{c} - \tan^{-1}\frac{a}{c}\right]$
6. 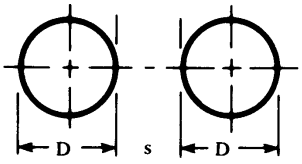	Let $X = 1 + s/D$. Then: $F_{1-2} = F_{2-1} = \frac{1}{\pi}\left[\sqrt{X^2 - 1} + \sin^{-1}\frac{1}{X} - X\right]$
7. 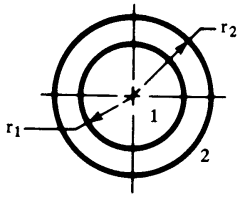	$F_{1-2} = 1, \quad F_{2-1} = \frac{r_1}{r_2}$, and $F_{2-2} = 1 - F_{2-1} = 1 - \frac{r_1}{r_2}$

Table 10.3 View factors for some three-dimensional configurations

Configuration	*Equation*
1. 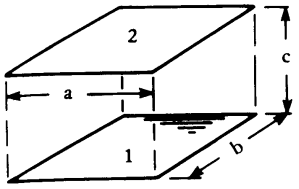	Let $X = a/c$ and $Y = b/c$. Then: $F_{1-2} = \frac{2}{\pi XY}\left\{\ln\left[\frac{(1+X^2)(1+Y^2)}{1+X^2+Y^2}\right]^{1/2} - X\tan^{-1}X - Y\tan^{-1}Y + X\sqrt{1+Y^2}\tan^{-1}\frac{X}{\sqrt{1+Y^2}} + Y\sqrt{1+X^2}\tan^{-1}\frac{Y}{\sqrt{1+X^2}}\right\}$
2. 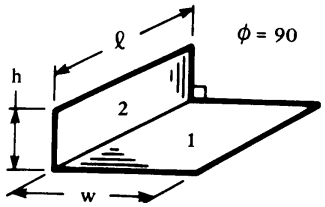	Let $H = h/\ell$ and $W = w/\ell$. Then: $F_{1-2} = \frac{1}{\pi W}\left\{W\tan^{-1}\frac{1}{W} - \sqrt{H^2+W^2}\tan^{-1}\left(H^2+W^2\right)^{-1/2} + H\tan^{-1}\frac{1}{H} + \frac{1}{4}\ln\left\{\left[\frac{(1+W^2)(1+H^2)}{1+W^2+H^2}\right] \times \left[\frac{W^2(1+W^2+H^2)}{(1+W^2)(W^2+H^2)}\right]^{W^2}\left[\frac{H^2(1+H^2+W^2)}{(1+H^2)(H^2+W^2)}\right]^{H^2}\right\}\right\}$
3. 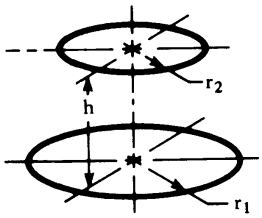	Let $R_1 = r_1/h$, $R_2 = r_2/h$, and $X = 1 + \left(1+R_2^2\right)/R_1^2$. Then: $F_{1-2} = \frac{1}{2}\left[X - \sqrt{X^2 - 4(R_2/R_1)^2}\right]$
4. 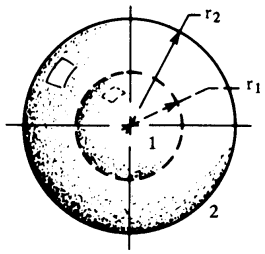	Concentric spheres: $F_{1-2} = 1, \quad F_{2-1} = (r_1/r_2)^2, \quad F_{2-2} = 1 - (r_1/r_2)^2$

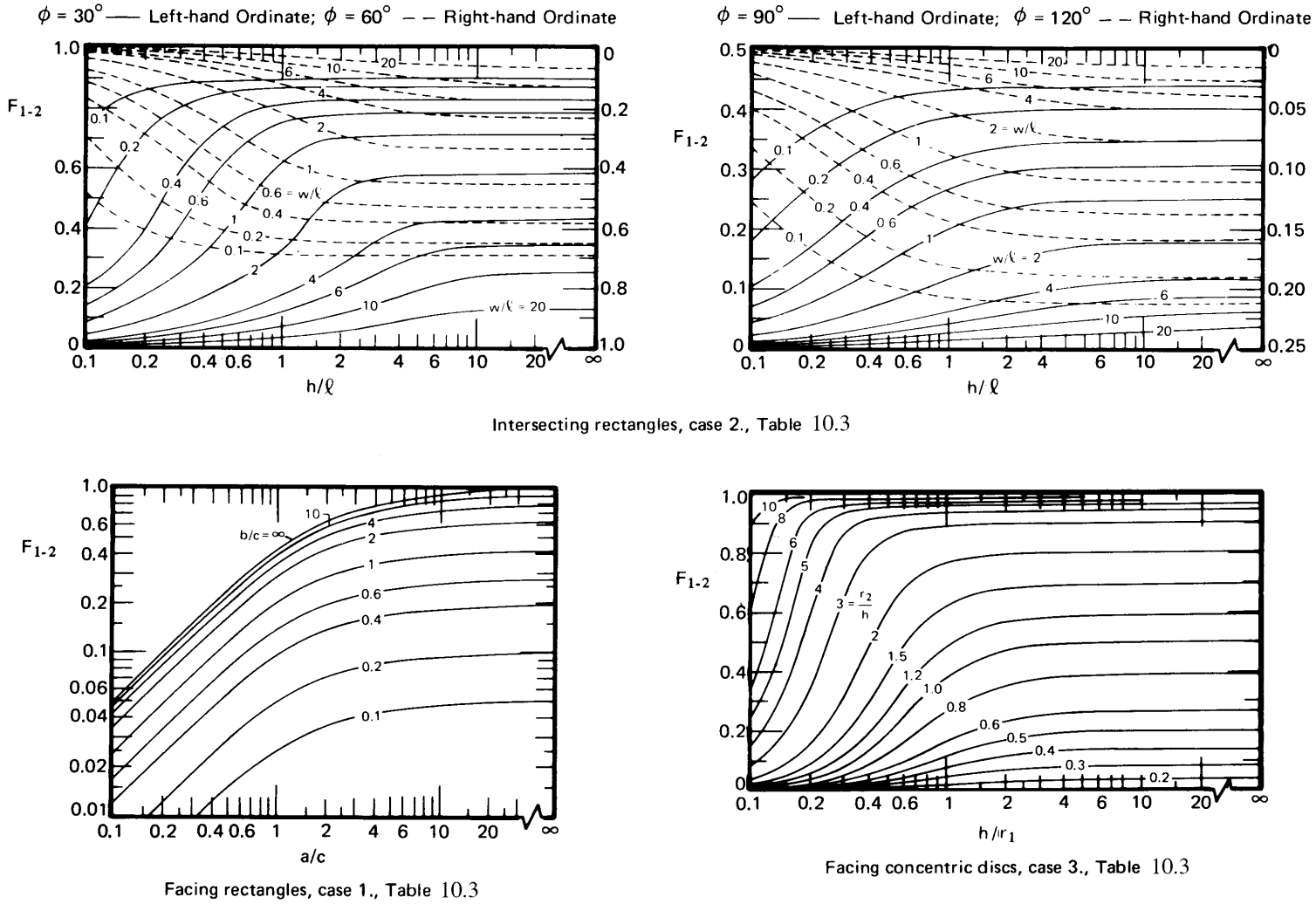

Figure 10.10 The view factors for configurations shown in Table 10.3

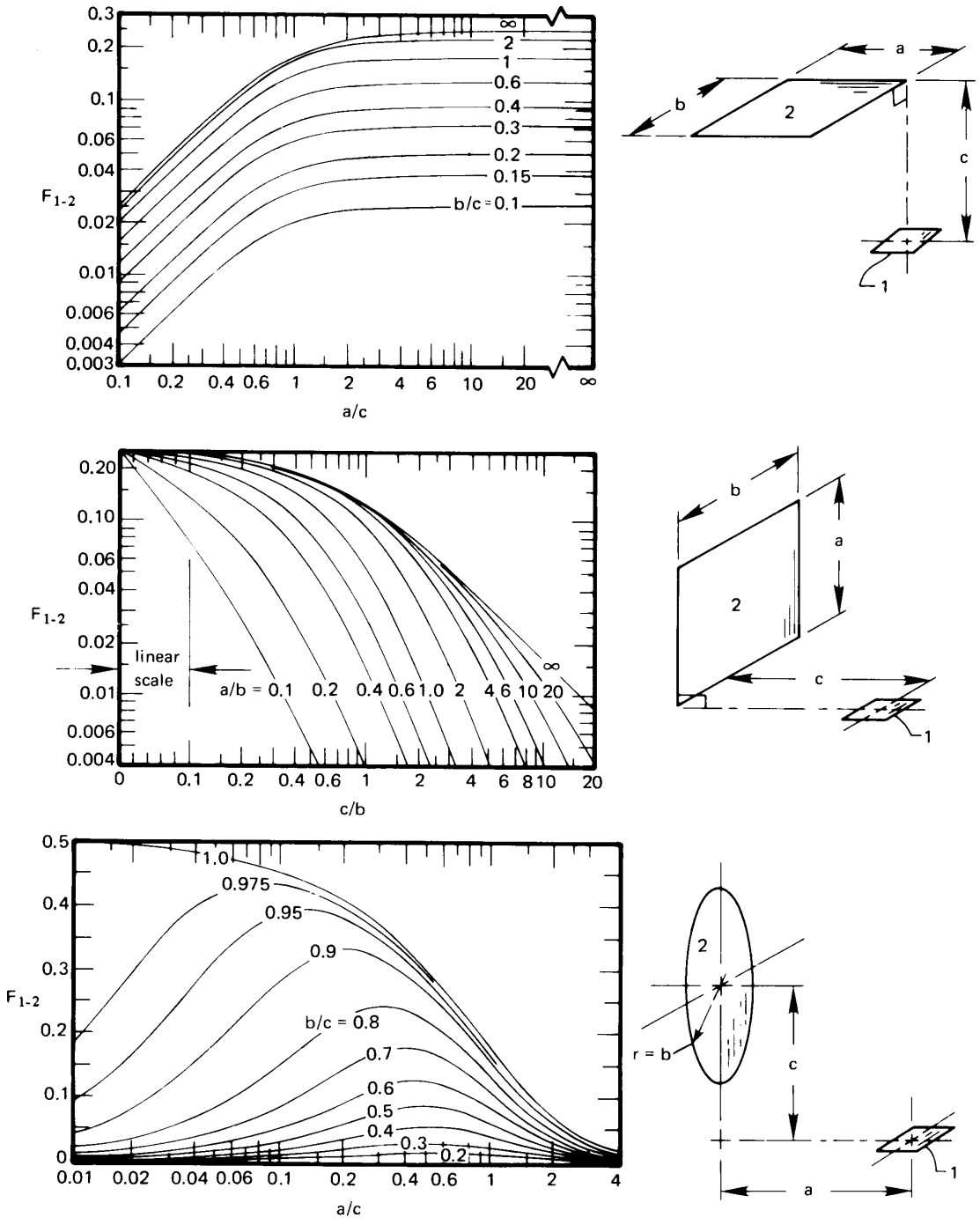

Figure 10.11 The view factor for three very small surfaces "looking at" three large surfaces ($A_1 \ll A_2$).

Figure 10.11 shows view factors for another kind of configuration—one in which one area is very small in comparison with the other one. Many such solutions exist because they are somewhat less difficult to calculate, and they can often be very useful in practice.

Example 10.3

A heater (h) as shown in Fig. 10.12 radiates to the partially conical shield (s) that surrounds it. If the heater and shield are black, calculate the net heat transfer from the heater to the shield.

SOLUTION. First imagine a plane (i) laid across the open top of the shield:

$$F_{h-s} + F_{h-i} = 1$$

But F_{h-i} can be obtained from Fig. 10.10 or the equation in case 3 of Table 10.3, for $R_1 = r_1/h = 5/20 = 0.25$ and $R_2 = r_2/h = 10/20 = 0.5$. The result is $F_{h-i} = 0.192$. Then

$$F_{h-s} = 1 - 0.192 = 0.808$$

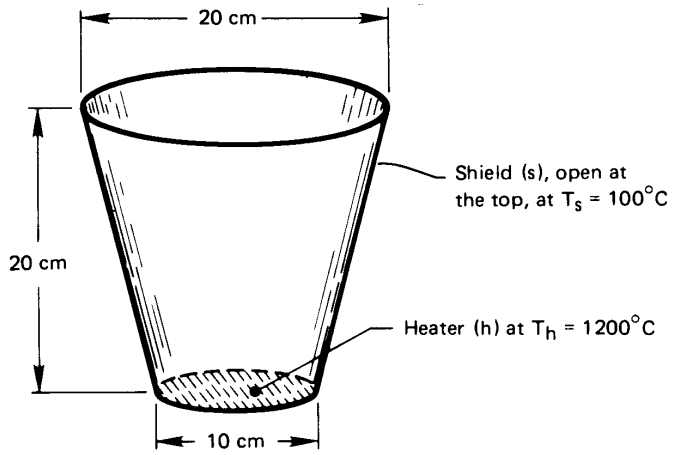

Figure 10.12 Heat transfer from a disc heater to its radiation shield.

Thus,

$$\begin{aligned} Q_{\text{net}} &= F_{h-s} A_h \sigma \left(T_h^4 - T_s^4\right) \\ &= 0.808 \left(\frac{\pi}{4} 0.1^2\right) 5.67 \times 10^{-8} \left[(1200 + 273)^4 - 373^4\right] \\ &= 1687 \text{ W} \end{aligned}$$

■

Example 10.4

Suppose that the shield in Example 10.3 is heating the region where the heater is presently located. What would F_{s-h} be?

SOLUTION. From eqn. (10.18) we have

$$A_s F_{s-h} = A_h F_{h-s}$$

But the frustrum-shaped shield has an area of

$$A_s = \frac{\pi}{2}(0.2 + 0.1)\sqrt{0.05^2 + 0.20^2} = 0.0971 \text{ m}^2$$

and

$$A_h = \frac{\pi}{4}(0.1)^2 = 0.007854 \text{ m}^2$$

so

$$F_{s-h} = \frac{0.007854}{0.0971}(0.808) = 0.0654$$

■

Example 10.5

Verify F_{1-2} for case 4 in Table 10.2.

SOLUTION. Multiply $F_{1-2} + F_{1-3} = 1$ by A_1:

$$A_1 F_{1-2} + A_1 F_{1-3} = A_1$$

Likewise,

$$A_2 F_{2-1} + A_2 F_{2-3} = A_2$$

and

$$A_3 F_{3-1} + A_3 F_{3-2} = A_3$$

Then use $A_2F_{2-1} = A_1F_{1-2}$, $A_3F_{3-1} = A_1F_{1-3}$, and $A_3F_{3-2} = A_2F_{2-3}$ to get

$$\begin{aligned} A_1F_{1-2} + A_1F_{1-3} &= A_1 \\ A_1F_{1-2} + A_2F_{2-3} &= A_2 \\ A_1F_{1-3} + A_2F_{2-3} &= A_3 \end{aligned}$$

This is easily solved for F_{1-2}:

$$F_{1-2} = \frac{A_1 + A_2 - A_3}{2A_1} \qquad \blacksquare$$

Example 10.6

Find F_{1-2} for the configuration of two offset squares of area A, as shown in Fig. 10.13.

SOLUTION.

$$\begin{aligned} 2AF_{(1+3)-(4+2)} &= AF_{1-4} + AF_{1-2} + AF_{3-4} + AF_{3-2} \\ 2F_{(1+3)-(4+2)} &= 2F_{1-4} + 2F_{1-2} \end{aligned}$$

And $F_{(1+3)-(4+2)}$ can be read from Fig. 10.10 (at $\phi = 90$, $w/\ell = \frac{1}{2}$, and $h/\ell = \frac{1}{2}$) as 0.245 and F_{1-4} as 0.20. Thus,

$$F_{1-2} = (0.245 - 0.20) = 0.045 \qquad \blacksquare$$

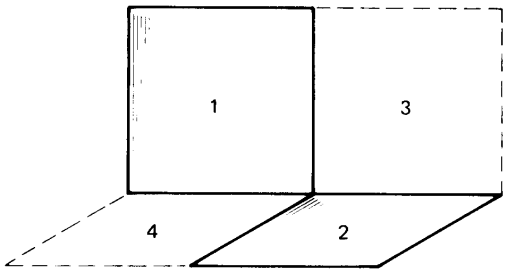

Figure 10.13 Radiation between two offset perpendicular squares.

10.4 Heat transfer among gray bodies

Electrical analogy for gray body heat exchange

A rather clever adaptation of the electric analogy for calculating heat exchange among gray bodies was developed by Oppenheim [10.3] in 1956. It requires the definition of two new quantities:

$$H \ \text{W/m}^2 \equiv \textit{irradiance} = \begin{cases}\text{flux of energy that irradiates} \\ \text{the surface}\end{cases}$$

and

$$B \ \text{W/m}^2 \equiv \textit{radiosity} = \begin{cases}\text{total flux of radiative energy} \\ \text{away from the surface}\end{cases}$$

The radiosity can be expressed as the sum of the irradiated energy that reflects away from the surface and the radiation emitted from it. Thus,

$$B = \rho H + \varepsilon e_b \tag{10.19}$$

We can immediately write the net heat flux from any particular surface as the difference between B and H for that surface. Then, with the help of eqn. (10.19), we get

$$q_{\text{net}} = B - H = B - \frac{B - \varepsilon e_b}{\rho} \tag{10.20}$$

This can be rearranged as

$$q_{\text{net}} = \frac{\varepsilon}{\rho} e_b - \frac{1-\rho}{\rho} B \tag{10.21}$$

As long as the surface is opaque ($\tau = 0$), $\varepsilon = \alpha = 1 - \rho$, eqn. (10.21) gives

$$q_{\text{net}} A = Q_{\text{net}} = \frac{e_b - B}{\rho/\varepsilon A} = \frac{e_b - B}{(1-\varepsilon)/\varepsilon A} \tag{10.22}$$

Equation (10.22) is a form of Ohm's law, which tells us that $(e_b - B)$ can be viewed as a driving potential for transferring heat away from a surface through an effective surface resistance, $(1-\varepsilon)/\varepsilon A$.

Now consider heat transfer from one infinite gray plane to another parallel with it, in these terms. Radiant energy flows past an imaginary surface, parallel with the first infinite plate in Fig. 10.14 but quite close to it. There is no way of telling whether this energy comes from a real

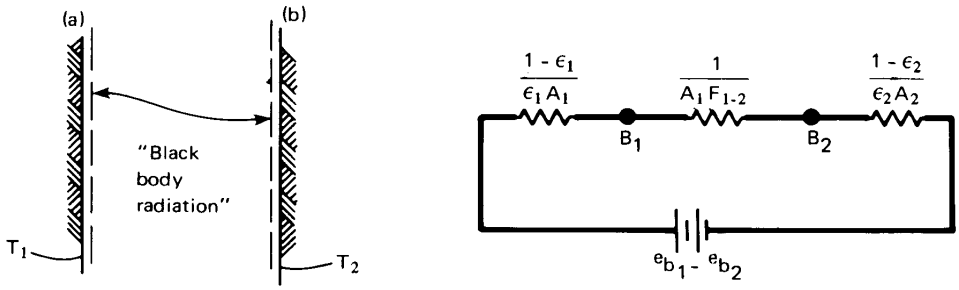

Figure 10.14 The electrical circuit analogy for radiation between two gray infinite plates.

surface or a black body. Therefore, we can isolate radiation at the surface and treat radiation from just above the surface as though it were from a black body. Thus,

$$Q_{\text{net}} = A_1 F_{1-2}\,(B_1 - B_2) = \frac{B_1 - B_2}{\left(\dfrac{1}{A_1 F_{1-2}}\right)} \tag{10.23}$$

which is again a form of Ohm's law. The radiosity difference $(B_1 - B_2)$, can be imagined to drive heat through the geometrical resistance $1/A_1F_{1-2}$ that describes the field of view between the two surfaces.

When two grey surfaces exchange heat by thermal radiation, we have a surface resistance for each surface and a geometric resistance due to their configuration. The electrical circuit shown in Fig. 10.14 expresses the analogy and gives us means for calculating Q_{net} in accordance with Ohm's law. Recalling that $e_b = \sigma T^4$, we obtain

$$Q_{\text{net}} = \frac{e_{b_1} - e_{b_2}}{\sum \text{ resistances}} = \frac{\sigma\,(T_1^4 - T_2^4)}{\left(\dfrac{1-\varepsilon}{\varepsilon A}\right)_1 + \dfrac{1}{A_1 F_{1-2}} + \left(\dfrac{1-\varepsilon}{\varepsilon A}\right)_2} \tag{10.24}$$

or, if we remember that $F_{1-2} = 1$ and $A_1 = A_2$ for infinite parallel plates,

$$q_{1-2} = \frac{1}{\left(\dfrac{1}{\varepsilon_1} + \dfrac{1}{\varepsilon_2} - 1\right)} \sigma \left(T_1^4 - T_2^4\right) \tag{10.11}$$

This result is one that we arrived at during the derivation of Kirchhoff's law. But the method we have used to develop it here can quickly be extended to develop other results as well.

Example 10.7

Evaluate the heat transfer between one gray body and another enclosing it, as shown in Fig. 10.6.

SOLUTION. The electrical circuit analogy is exactly the same as that shown in Fig. 10.14, and F_{1-2} is still unity. Therefore,

$$Q_{\text{net}} = q_{\text{net}} A_1 = \frac{\sigma (T_1^4 - T_2^4)}{\left(\dfrac{1-\varepsilon_1}{\varepsilon_1 A_1} + \dfrac{1}{A_1} + \dfrac{1-\varepsilon_2}{\varepsilon_2 A_2} \right)} \tag{10.25}$$

Therefore,

$$q_{\text{net}} = \underbrace{\frac{1}{\dfrac{1}{\varepsilon_1} + \dfrac{A_1}{A_2}\left(\dfrac{1}{\varepsilon_2} - 1\right)}}_{\mathcal{F}_{1-2}} \sigma \left(T_1^4 - T_2^4 \right)$$

which is the result we anticipated in eqn. (10.14) for diffusely reflecting bodies. ■

Example 10.8

Derive $\mathcal{F}_{2-1}$ for the enclosed bodies shown in Fig. 10.6.

SOLUTION. By the same rationale used in Example 10.7, but replacing the center resistance with $1/A_2 F_{2-1}$, we get

$$\mathcal{F}_{2-1} = \frac{1}{\dfrac{1}{\varepsilon_2} + \dfrac{A_2}{A_1}\left(\dfrac{1}{\varepsilon_1} - 1\right) + \left(\dfrac{1}{F_{2-1}} - 1\right)}$$

To eliminate the unknown view factor, F_{2-1}, from this result, we use the reciprocity relation, eqn. (10.18):

$$F_{2-1} = \frac{A_1}{A_2} \underbrace{F_{1-2}}_{=1} = \frac{A_1}{A_2}$$

so

$$\mathcal{F}_{2-1} = \frac{1}{\dfrac{1}{\varepsilon_1}\dfrac{A_2}{A_1} + \left(\dfrac{1}{\varepsilon_2} - 1\right)} \tag{10.26}$$

■

Use of the electrical circuit analogy when more than one gray body is involved in heat exchange

Let us first consider a three-body transaction, as pictured in Fig. 10.15. Body (3) either might be insulated or might exchange a net amount of heat with bodies (1) and (2), but in either case it absorbs and reemits energy. If it is insulated, there is no net surface heat transfer and we can eliminate one leg of the circuit, as shown in Fig. 10.15.

The circuit for such an exchange is not so easy to analyze as the in-line circuits we have previously analyzed. In this case, one must sum the energy exchanges at each of the interior nodes:

$$\text{node } B_1: \qquad \frac{e_{b_1} - B_1}{\dfrac{1-\varepsilon_1}{\varepsilon_1 A_1}} = \frac{B_1 - B_2}{\dfrac{1}{A_1 F_{1-2}}} + \frac{B_1 - B_3}{\dfrac{1}{A_1 F_{1-3}}} \tag{10.27}$$

$$\text{node } B_2: \qquad \frac{e_{b_2} - B_2}{\dfrac{1-\varepsilon_2}{\varepsilon_2 A_2}} = \frac{B_2 - B_1}{\dfrac{1}{A_1 F_{1-2}}} + \frac{B_2 - B_3}{\dfrac{1}{A_2 F_{2-3}}} \tag{10.28}$$

$$\text{node } B_3: \qquad \frac{e_{b_3} - B_3}{\dfrac{1-\varepsilon_3}{\varepsilon_3 A_3}} \text{ or } 0 = \frac{B_3 - B_1}{\dfrac{1}{A_1 F_{1-3}}} + \frac{B_3 - B_2}{\dfrac{1}{A_2 F_{2-3}}} \tag{10.29}$$

These equations must be solved simultaneously for the three unknowns, B_1, B_2, and B_3. When they are solved, one can compute the net heat transfer to or from any body (a) as a result of all surrounding bodies (i) as

$$Q_{\text{net}} = \sum_i \left(\frac{B_i - B_a}{1/(A_a F_{a-i})} \right) \tag{10.30}$$

Thus far, we have considered only the specified wall temperature boundary condition on each of the bodies involved in heat exchange. Consider two other possibilities.

The insulated wall. If $q = 0$ at a wall, then the nodal sum at that wall vanishes. Thus, when the third body in Fig. 10.15 is insulated, $e_{b_3} = B_3$ in eqn. (10.29). This means that the insulated body participates in the transaction as though it were black. In this case, the right-hand circuit in Fig. 10.15 can be treated as a series-parallel circuit, since all the heat

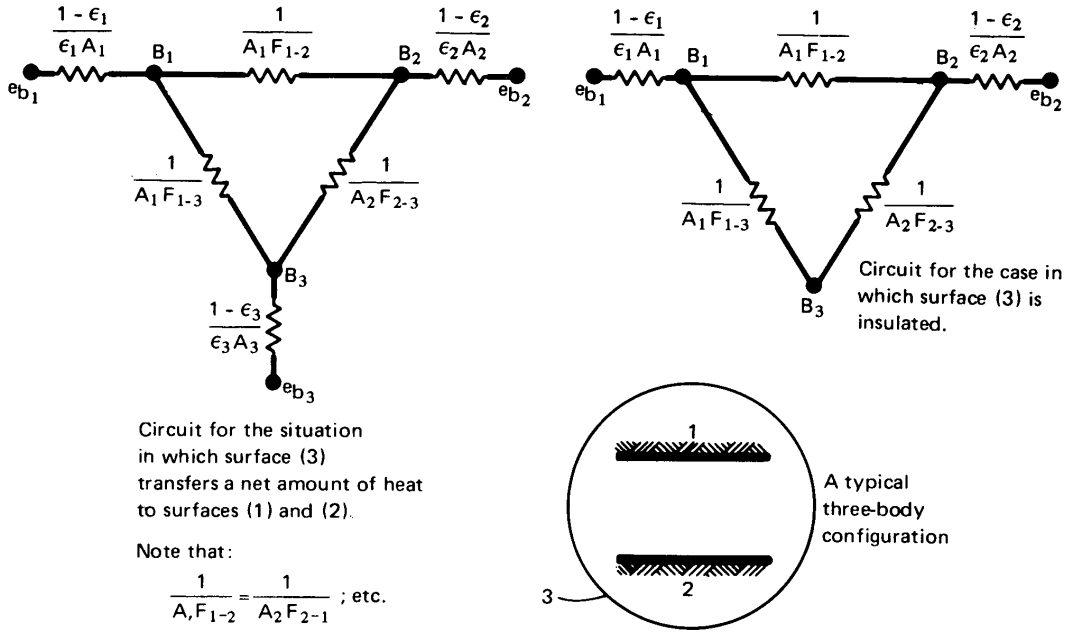

Figure 10.15 The electrical circuit analogy for radiation among three gray surfaces.

from body (1) flows to body (2). Then

$$Q_{\text{net}} = \frac{e_{b_1} - e_{b_2}}{\dfrac{1-\varepsilon_1}{\varepsilon_1 A_1} + \dfrac{1}{\dfrac{1}{1/(A_1F_{1-3}) + 1/(A_2F_{2-3})} + \dfrac{1}{1/(A_1F_{1-2})}} + \dfrac{1-\varepsilon_2}{\varepsilon_2 A_2}} \tag{10.31}$$

However when the third body is heated or cooled, the three equations (10.27), (10.28), and (10.29) have to be used and this simplification does not apply.

The specified wall heat flux case. When the heat flux leaving the surface is known, eqn. (10.22) requires that $(e_b - B)$ be known for that surface. This, too, can greatly simplify the solution of sets of equations such as (10.27), (10.28), and (10.29).

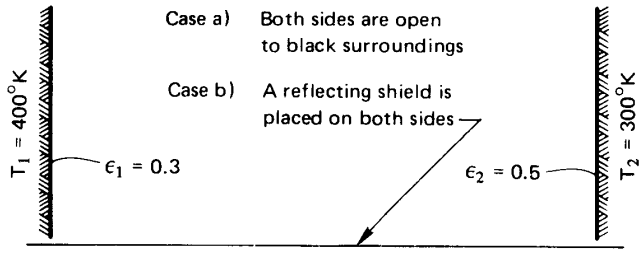
Case a) Both sides are open to black surroundings
Case b) A reflecting shield is placed on both sides
T1 = 400°K
T2 = 300°K
ε1 = 0.3
ε2 = 0.5

Figure 10.16 Illustration for Example 10.9.

Example 10.9

Two very long strips 1 m wide and 2.33 m apart face each other, as shown in Fig. 10.16. (a) Find Q_{net} W/m from one to the other if the surroundings are cold and black. (b) Find Q_{net} W/m if they are connected by an insulated diffuse reflector between the edges on both sides. (c) Evaluate the temperature of the reflector in part (b). Assume $(T_{\text{surroundings}})^4 \ll T_1^4$ or T_2^4.

SOLUTION. From Fig. 10.10, we read $F_{1-2} = 0.2 = F_{2-1}$. Then the three nodal equations (10.27), (10.28), and (10.29) become

$$\frac{1451 - B_1}{2.333} = \frac{B_1 - B_2}{5} + \frac{B_1 - B_3}{\dfrac{1}{1 - 0.2}}$$

$$\frac{459.3 - B_2}{1} = \frac{B_2 - B_1}{5} + \frac{B_2 - B_3}{\dfrac{1}{1 - 0.2}}$$

$$0 = \frac{B_3 - B_1}{\dfrac{1}{1 - 0.2}} + \frac{B_3 - B_2}{\dfrac{1}{1 - 0.2}}$$

where the latter does not apply in case (a). Thus,

$$\begin{aligned} B_1 - 0.14B_2 - 0.56B_3 &= 435 \\ -B_1 + 10B_2 - 4B_3 &= 2296.5 \\ -B_1 - B_2 + 2B_3 &= 0 \end{aligned}$$

Without the reflecting shield, we delete the third equation and neglect B_3, since the surroundings are very cold and black. Then the first two

equations reduce to

$$\left.\begin{aligned} B_1 - 0.14B_2 &= 435 \\ -B_1 + 10B_2 &= 2296.5 \end{aligned}\right\} \quad \text{so} \quad \begin{cases} B_1 = 473.78 \text{ W/m} \\ B_2 = 277.03 \text{ W/m} \end{cases}$$

Thus, the net flow from (1) to (2) is quite small:

$$Q_{1-2_{\text{no shield}}} = \frac{B_1 - B_2}{1/(A_1 F_{1-2})} = 39.35 \text{ W/m}$$

When the shield is in place, we must solve the full set of nodal equations. This can be done manually, by the use of determinants, or with matrix algebra methods that have been packaged as computer subroutines. The result is

$$B_1 = 987.7 \qquad B_2 = 657.4 \qquad B_3 = 822.6$$

Then, from eqn. (10.30), we get

$$Q_{\text{net}} = 1\frac{\text{m}^2}{\text{m}}\left(\frac{987.7 - 657.4}{1/0.2} + \frac{822.6 - 657.4}{1/0.8}\right)\frac{\text{W}}{\text{m}^2} = 198.5 \text{ W/m}$$

Notice that because node (3) is insulated, we could also have used eqn. (10.31) to get Q_{net}:

$$Q_{\text{net}} = \frac{5.67 \times 10^{-8}(400^4 - 300^4)}{\dfrac{0.7}{0.3} + \dfrac{1}{\dfrac{1}{1/0.8 + 1/0.8} + 0.2} + \dfrac{0.5}{0.5}} = 198.5 \text{ W/m}$$

The result, of course, is the same. We note that the presence of the reflector increases the net heat flow from (1) to (2).

The temperature of the reflector (3) is obtained from

$$Q_{3 \text{ to (1 or 2)}} = 0 = e_{b_3} - B_3 = 5.67 \times 10^{-8} T_3^4 - 822.6$$

so

$$T_3 = 347.06 \text{ K}$$ ■

Holman [10.4] presents a very nice discussion of the application of the electrical circuit analog to more complicated problems, and he provides a number of useful examples. However, the digital computer now makes it more feasible to approach complicated problems directly with numerical methods. Sparrow and Cess [10.1] provide an excellent discussion of these methods. Although they generally lie beyond the scope of this text, it is instructive to treat one important class of such solutions.

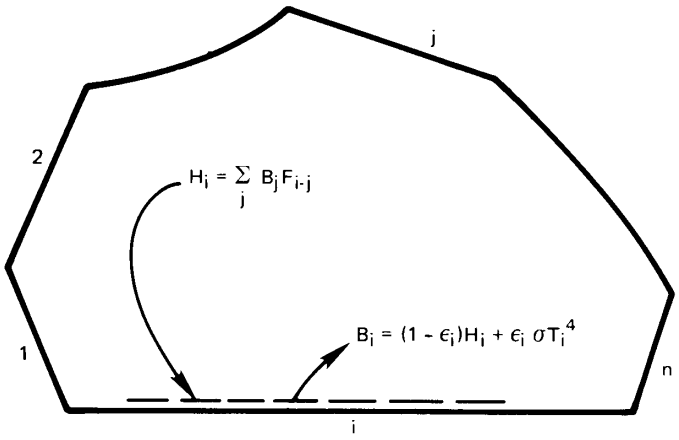

Figure 10.17 An enclosure surrounded by gray and diffuse, isothermal and constant-heat-flux segments.

Algebraic solution of compound radiation problems

Radiant heat exchange in gray, diffuse enclosures. An enclosure can consist of any number of surfaces participating in radiant energy exchange. For example, the case shown in Fig. 10.16 could have been treated as a rectangular enclosure if, in addition to the two walls and the shield, we had assumed a fictitious surface of 0 K to make up the fourth side.

An enclosure formed by n surfaces is shown in Fig. 10.17. We assume that

- Each surface emits or reflects diffusely and it is gray and opaque ($\varepsilon = \alpha$, $\rho = 1 - \varepsilon$).
- Either each surface is at a uniform temperature or its heat flux is a uniform known value and its emittance is known.
- The view factor, F_{i-j}, between any two surfaces i and j is known.
- Conduction and convection within the enclosure can be neglected.

We are interested in determining the heat fluxes at the surfaces where temperatures are specified, and vice versa.

The rate of heat loss from the ith surface of the enclosure can conveniently be written in terms of the radiosity, B_i, and the incident surface

heat flux, H_i [see eqn. (10.22)].

$$q_i = B_i - H_i = \frac{\varepsilon_i}{1-\varepsilon_i}\left(\sigma T_i^4 - B_i\right) \tag{10.32}$$

where

$$B_i = \rho_i H_i + \varepsilon_i e_{b_i} = (1-\varepsilon_i)\, H_i + \varepsilon_i\, \sigma T_i^4 \tag{10.33}$$

However, $A_i H_i$, the incident radiant heat transfer rate to the surface i, is the sum of energies reaching i from all other surfaces, including itself:

$$A_i H_i = \sum_{j=1}^{n} A_j B_j F_{j-i} = \sum_{j=1}^{n} B_j A_i F_{i-j}$$

where we have used the reciprocity rule, $A_j F_{j-i} = A_i F_{i-j}$. Then

$$H_i = \sum_{j=1}^{n} B_j F_{i-j} \tag{10.34}$$

It follows from eqns. (10.33) and (10.34) that

$$B_i = (1-\varepsilon_i) \sum_{j=1}^{n} B_j F_{i-j} + \varepsilon_i\, \sigma T_i^4 \tag{10.35}$$

When all the surface temperatures are specified, eqn. (10.35) can be written for each surface. This yields n algebraic equations that can be solved for the n unknown B's. The rate of heat loss, Q_i, from the ith surface ($i = 1, 2, \ldots, n$) can then be obtained from eqn. (10.32).

For those surfaces where heat fluxes are prescribed, we can eliminate the $\varepsilon_i \sigma T_i^4$ term in eqn. (10.35) using eqn. (10.32). We can still solve for the B's, and eqn. (10.32) can be solved for the unknown temperature of that particular surface.

Example 10.10

Two sides of a long triangular duct, as shown in Fig. 10.18, are made of stainless steel ($\varepsilon = 0.5$) and are maintained at 500°C. The third side is of copper ($\varepsilon = 0.15$) and is at a uniform temperature of 100°C. Calculate the rate of heat transferred to the copper base per meter of length of the duct.

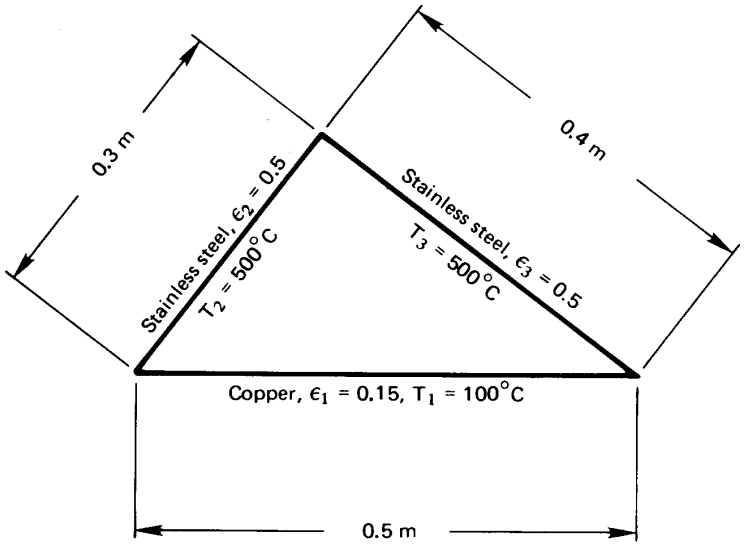

Figure 10.18 Illustration for Example 10.10.

SOLUTION. Assume the duct walls to be gray and diffuse, the fluid in the duct to be radiatively inactive, and convection to be negligible. The view factors can be calculated from configuration (4) of Table 10.2 or Example 10.5:

$$F_{1-2} = \frac{A_1 + A_2 - A_3}{2A_1} = \frac{5 + 3 - 4}{10} = 0.4$$

Similarly, $F_{2-1} = 0.67$, $F_{1-3} = 0.6$, $F_{3-1} = 0.75$, $F_{2-3} = 0.33$, and $F_{3-2} = 0.25$. The surfaces cannot "see" themselves, so $F_{1-1} = F_{2-2} = F_{3-3} = 0$. We therefore use eqn. (10.35) to write the three algebraic equations for the three unknowns, B_1, B_2, and B_3.

$$B_1 = \underbrace{(1-\varepsilon_1)}_{0.85}\left(\underbrace{F_{1-1}}_{0}B_1 + \underbrace{F_{1-2}}_{0.4}B_2 + \underbrace{F_{1-3}}_{0.6}B_3\right) + \underbrace{\varepsilon_1}_{0.15}\sigma T_1^4$$

$$B_2 = \underbrace{(1-\varepsilon_2)}_{0.5}\left(\underbrace{F_{2-1}}_{0.67}B_1 + \underbrace{F_{2-2}}_{0}B_2 + \underbrace{F_{2-3}}_{0.33}B_3\right) + \underbrace{\varepsilon_2}_{0.5}\sigma T_2^4$$

$$B_3 = \underbrace{(1-\varepsilon_3)}_{0.5}\left(\underbrace{F_{3-1}}_{0.75}B_1 + \underbrace{F_{3-2}}_{0.25}B_2 + \underbrace{F_{3-3}}_{0}B_3\right) + \underbrace{\varepsilon_3}_{0.5}\sigma T_3^4$$

If there were more surfaces, it would be easy to solve this system numerically using matrix methods. In this case we can obtain B_1

algebraically:

$$B_1 = 0.232\,\sigma T_1^4 - 0.319\,\sigma T_2^4 + 0.447\,\sigma T_3^4$$

Equation (10.32) gives the rate of heat lost by surface 1 as

$$\begin{aligned} Q_1 &= A_1 \frac{\varepsilon_1}{1-\varepsilon_1}\left(\sigma T_1^4 - B_1\right) \\ &= A_1 \frac{\varepsilon_1}{1-\varepsilon_1}\,\sigma\left(T_1^4 - 0.232T_1^4 + 0.319T_2^4 - 0.447T_3^4\right) \\ &= (0.5)\left(\frac{0.15}{0.85}\right)(5.67\times 10^{-8}) \\ &\quad \times\left[(373)^4 - 0.232(373)^4 + 0.319(773)^4 - 0.447(773)^4\right]\ \text{W/m} \\ &= -154.3\ \text{W/m} \end{aligned}$$

■

The negative sign indicates that the copper base is gaining heat.

10.5 Gaseous radiation

Absorptance, transmittance, and emittance

We have treated every radiation problem thus far as though heat flow in the space separating the surfaces of interest were completely unobstructed. However, all gases and liquids affect the radiation of heat through them to some extent. We have ignored this effect in air because it is generally quite minor. We now turn our attention briefly to problems in which we must consider the role of gases (or liquids, for that matter) as participants in the heat exchange process.

The photons of radiant energy passing through a gaseous region can be impeded in two ways. Some can be "scattered," or deflected, in various directions, and some can be absorbed into the molecules. Scattering is a fairly minor influence in most gases unless they contain foreign particles, such as dust or fog. In cloudless air, for example, we are aware of the scattering of sunlight only when it passes through many miles of the atmosphere. Then the shorter wavelengths of sunlight are scattered (short wavelengths, as it happens, are far more susceptible to scattering by gas molecules than longer wavelengths, through a process known as *Rayleigh scattering*). That scattered light gives the sky its blue hues.

At sunset, sunlight passes through the atmosphere at a shallow angle for hundreds of miles. Radiation in the blue wavelengths has all been

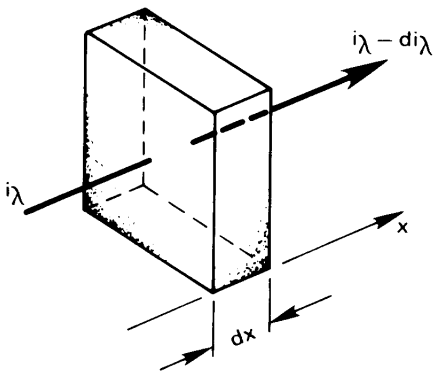

Figure 10.19 The attenuation of radiation through an absorbing (and/or scattering) gas.

scattered out before it can be seen. Thus, we see only the unscattered red hues, just before dark.

Radiant energy can be absorbed by molecules only if the appropriate quantum mechanical conditions prevail. For all practical purposes, monatomic and symmetrical diatomic molecules are transparent to thermal radiation. Thus, the major components of air—N_2 and O_2—are nonabsorbing; so, too, are H_2 and such monatomic gases as argon. Two particularly important absorbing molecules are CO_2 and H_2O, which are usually present in air. Other absorbing gases include ammonia, O_3 (ozone), CO, and SO_2.

Figure 10.19 shows radiant energy passing through an absorbing gas with a monochromatic intensity i_λ. As it passes through an element of thickness dx, the intensity will be reduced by an amount di_λ:

$$di_\lambda = -\kappa_\lambda i_\lambda \, dx \tag{10.36}$$

where κ_λ is called the *monochromatic absorption coefficient*. If the gas scatters radiation, we replace κ_λ with γ_λ, the *monochromatic scattering coefficient*. If it both absorbs and scatters radiation, we replace κ_λ with $\beta_\lambda \equiv \kappa_\lambda + \gamma_\lambda$, the *monochromatic extinction coefficient*.[3] The dimensions of κ_λ, β_λ, and γ_λ are all m^{-1}.

Equation (10.36) can be integrated between $i_\lambda(x = 0) = i_{\lambda_0}$ and $i_\lambda(x) = i_\lambda$. The result is

$$\frac{i_\lambda}{i_{\lambda_0}} = e^{-\kappa_\lambda x} \tag{10.37}$$

[3] All three coefficients, κ_λ, γ_λ, and β_λ, are expressed on a volumetric basis. They could, alternatively, have been expressed on a mass basis.

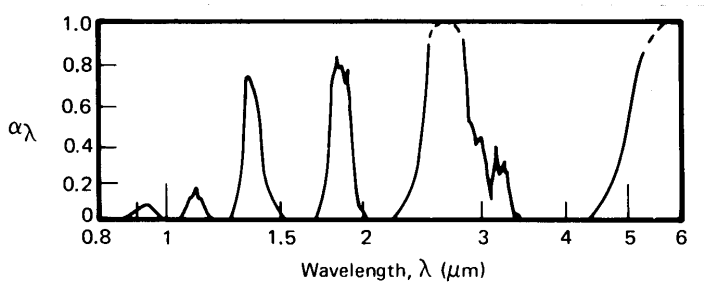

Figure 10.20 The monochromatic absorptance of a 1.09 m thick layer of steam at 127°C.

This result is called Beer's (pronounced Bayr's) law. The ratio

$$\frac{i_\lambda}{i_{\lambda_0}} \equiv \text{monochromatic transmittance, } \tau_\lambda, \text{ of the gas}$$

as we saw in Chapter 1. Since gases do not normally reflect radiant energy, $\tau_\lambda + \alpha_\lambda = 1$. Thus, eqn. (10.37) gives the monochromatic absorptance, α_λ, as

$$\alpha_\lambda = 1 - e^{-\kappa_\lambda x} \tag{10.38}$$

The dependence of α_λ on λ is normally very strong. It arises from the fact that in certain narrow bands of wavelength, radiation will interact with certain molecules and be absorbed, while radiation with somewhat higher or lower wavelengths might pass almost unhindered. Figure 10.20 shows the absorptance of steam as a function of wavelength for a vapor layer of a particular depth.

A comparison of Fig. 10.20 with Fig. 10.2 readily shows why the apparent emittance of the sun, as viewed from the earth's surface, shows a number of spiked indentations at certain wavelengths. Several of these indentations occur at those wavelengths at which water vapor in the air absorbs the incoming radiation of the sun, in accordance with Fig. 10.20. The other indentations in Fig. 10.2 occur where ozone and CO_2 absorb radiation. The sun does not exhibit these regions of low emittance; it is just that much of the radiation in certain wavelength ranges is blocked from our view and trapped in the upper atmosphere.

Just as α and ε are equal to one another for a given surface, under certain restrictions, the monochromatic absorption coefficient, κ_λ, and the monochromatic emittance of a gas, ε_{g_λ}, are also related. However,

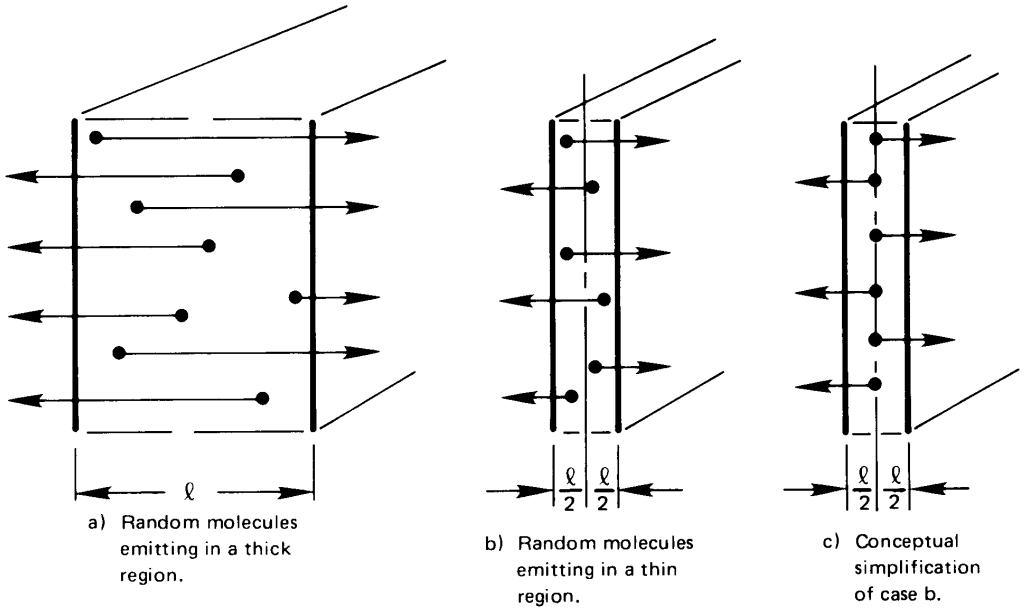

Figure 10.21 One-dimensional emission of radiant energy from within a gas.

while ε_{g_λ} is dimensionless, κ_λ has the dimensions of inverse length. To better see why that should be, consider Fig. 10.21. Figure 10.21a shows a slab of thickness ℓ in which molecules at various depths are emitting energy. If the gas is isothermal and at steady state, the emittance will be balanced uniformly by absorption. Thus, if we consider a sufficiently thin slice, as shown in Fig. 10.21b, it will be accurate to conceive of all of the absorbing and emitting molecules being located in its center, as shown in Fig. 10.21c. Then an energy balance gives, for $\ell \longrightarrow 0$:

$$q_{\text{in}} = 2\left(\kappa_\lambda \frac{1}{\text{m}}\right)\left(\frac{\ell}{2}\frac{\text{m}^3}{\text{m}^2}\right)\left(e_b \frac{\text{W}}{\text{m}^2}\right) = 2\varepsilon_{g_\lambda} e_b = q_{\text{out}}$$

or

$$\kappa_\lambda = \lim_{\ell \to 0} \frac{\varepsilon_{g_\lambda}}{\ell/2} \tag{10.39}$$

For a gas that is kept at a temperature different from the surroundings

to or from which it radiates, Hottel and Sarofim [10.5] quote the result:

$$\alpha_g = \left(\frac{T_{\text{gas}}}{T_{\text{surroundings}}} \right)^b \varepsilon_g \tag{10.40}$$

where b is 0.65 for CO_2 and 0.45 for H_2O and where ε_g is the total emittance, evaluated as

$$\varepsilon_g = \varepsilon_g \left(T_{\text{surroundings}}, pL_e T_{\text{surr.}}/T_g \right) \tag{10.41}$$

Notice that for a thin slice of gas of thickness $\ell/2$ in equilibrium with its surroundings, $\alpha_g = \varepsilon_g$, and eqn. (10.38) gives

$$\alpha_g = 1 - e^{-\kappa(\ell/2)} \simeq 1 - 1 + \ell\kappa/2 = \varepsilon_g$$

which is consistent with eqn. (10.39).

It is therefore clear that ε_g for an emitting gas depends on the thickness of the emitting layer. Notice, too, that ε_g also increases if the molecules are packed more closely by virtue of an increase in pressure. Thus, ε_g is a fairly complicated function of temperature, pressure, size, and configuration of a gaseous region.

Hottel and Sarofim provide empirical correlations of ε_g, using a single parameter, $L_e \equiv$ *mean beam length*, to represent both the size and the configuration of a gaseous region. The mean beam length is defined as

$$L_e \equiv \frac{4\,(\text{volume of gas})}{\text{boundary area that is irradiated}} \tag{10.42}$$

Thus, for two infinite parallel plates a distance ℓ apart, $L_e = 4A\ell/2A = 2\ell$. Some other values of L_e for volumes radiating to all points on their boundaries (unless otherwise noted) are

- For a sphere of diameter D, $L_e = 2D/3$
- For an infinite cylinder of diameter D, $L_e = D$
- For a cube of side L, radiating to one face, $L_e = 2L/3$
- For a cylinder with height $= D$, $L_e = 2D/3$

(Siegel and Howell [10.2] suggest that practical accuracy will be improved if these values are reduced by between 0% and 20%, depending on the configuration.)

We then provide empirical correlations of the form

$$\varepsilon_g = f_1\,[\text{total pressure}, L \cdot (\text{partial pressure of absorbing component})] \cdot f_2\,[T, L \cdot (\text{partial pressure})] \quad (10.43)$$

where the experimental functions f_1 and f_2 are plotted in Figs. 10.22 and 10.23 for CO_2 and H_2O, respectively.

Radiative heat transfer among gases

Consider the problem of a hot gas—say, the products of combustion—in a black container. We are now in a position to calculate the net heat flow from the gas to the container in such circumstances.

Example 10.11

A long cylindrical combustor 40 cm in diameter contains a gas at 1200°C consisting of 80% N_2 and 20% CO_2 at 1 atm. How much heat must we remove from the walls to keep them at 300°C?

SOLUTION. First calculate $q_{\text{gas to wall}}$. To do this, we note that $L_e = D = 0.4$ m and $p_{CO_2} = 0.2$ atm. Then Fig. 10.23a gives f_1 as 0.098 and Fig. 10.23b gives f_2 as 1, so $\varepsilon_g = 0.098$. The view factor is unity, so

$$\begin{aligned} q_{\text{gas to wall}} &= \sigma F_{g-w} \varepsilon_g T_g^4 = 5.67 \times 10^{-8}(0.098)(1200 + 273)^4 \\ &= 26,160 \text{ W/m}^2 \end{aligned}$$

Next we need α_g to calculate $q_{\text{wall to gas}}$. Using eqns. (10.40) and (10.41), we get

$$\alpha_g = \left(\frac{1200 + 273}{300 + 273}\right)^{0.65}(0.091) = 0.168$$

so, since the wall "sees" itself *through* gas with this absorptance, we use $F_{w-g} = 1$ and obtain

$$\begin{aligned} q_{\text{wall to gas}} &= \sigma F_{w-g} \alpha_g T_w^4 = 5.67 \times 10^{-8}(0.168)(573)^4 \\ &= 1027 \text{ W/m}^2 \end{aligned}$$

Thus,

$$q_{\text{net}} = 25,133 \text{ W/m}^2$$

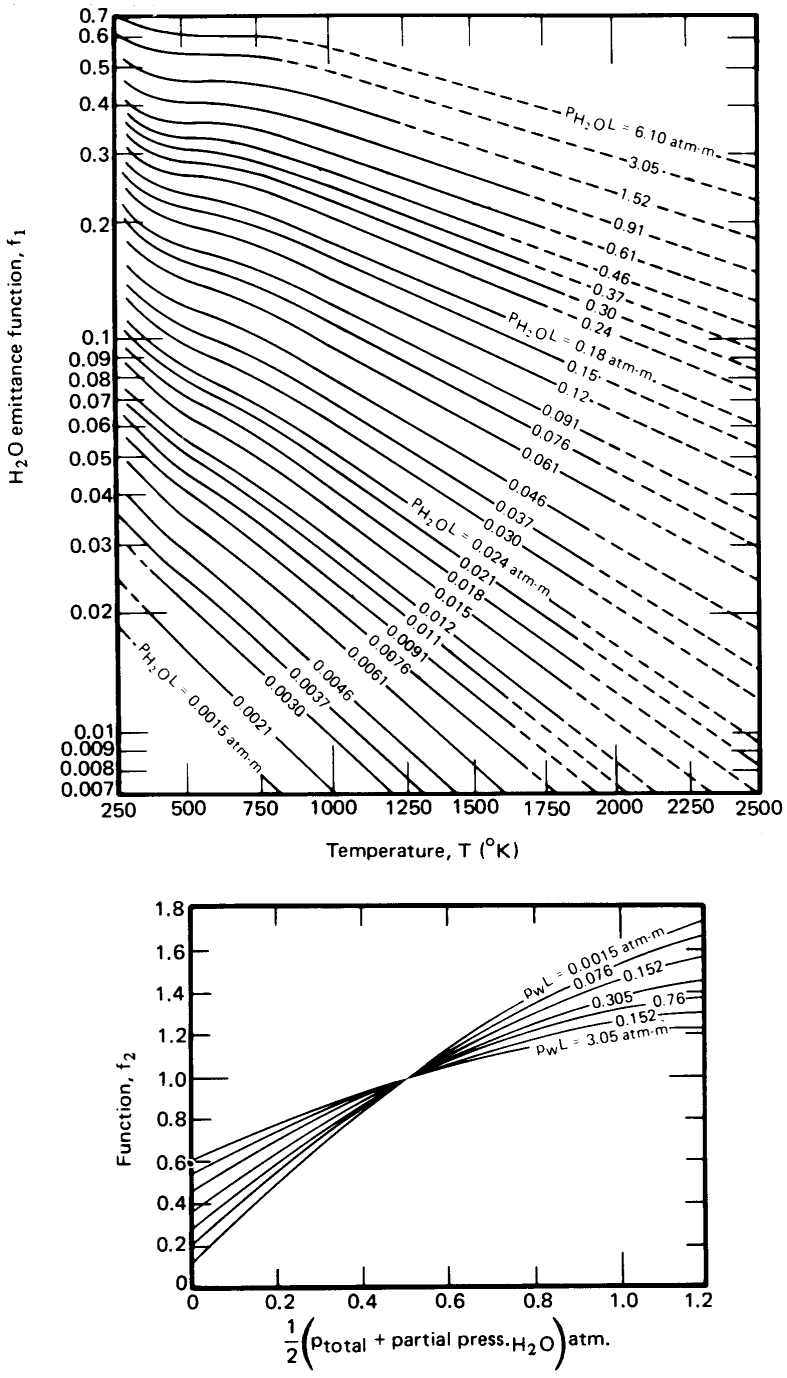

Figure 10.22 Functions used to predict $\varepsilon_g = f_1 f_2$ for water vapor in air.

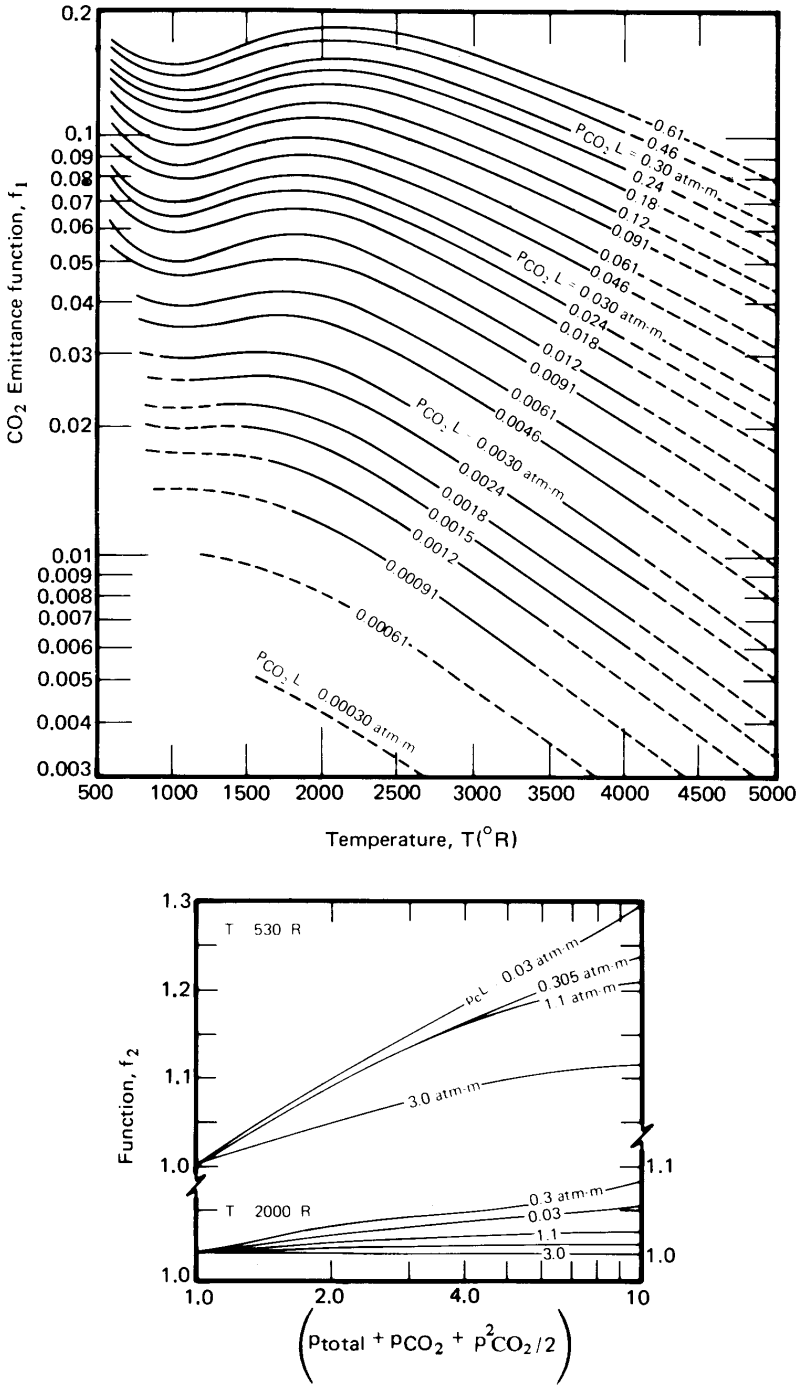

Figure 10.23 Functions used to predict $\varepsilon_g = f_1 f_2$ for CO_2 in air.

or

$$Q_{\text{net/m length}} = \pi(0.4)(25,133) = 31,583 \text{ W/m} \quad \blacksquare$$

The problem of heat transfer among gases and gray bodies is beyond the scope of this book. Sparrow and Cess [10.1] provide a more advanced treatment of analytical methods for treating the problem. Holman's undergraduate text [10.4] shows how to apply the electrical analogy to problems of gaseous radiation.

Finally, it is worth noting that gaseous radiation is frequently less important than one might imagine. Consider, for example, two flames: a bright orange candle flame and a "cold-blue" hydrogen flame. Both have a great deal of water vapor in them, as a result of oxidizing H_2. But the candle will warm your hands if you place them near it and the hydrogen flame will not. Yet the temperature in the hydrogen flame is *higher*. It turns out that what is radiating both heat and light from the candle are small solid particles of almost thermally black carbon. The CO_2 and H_2O in the flame actually contribute relatively little to radiation.

10.6 Solar energy

The sun as an energy source

The sun bestows energy on the earth at a rate[4] just over 1.7×10^{14} kW. We absorb most of it by day, and that which is absorbed is radiated away by night. If the world population is 6 billion people, each of us has a renewable energy birthright of about 28,000 kW. Of course, we can use very little of this. Most of it must go to sustaining those processes that make the earth a fit place to live—to creating weather and to supplying the flora and fauna we live with.

In the United States alone, we consume energy at the rate of about 3×10^9 kW. The interesting thing about this enormous consumption is that almost none of it comes from our renewable energy birthright. Instead, we are burning up the planet to get it. It is interesting to notice that if we price electrical energy at 9 cents/kWh, and thermal energy at 3, the average American could steadily buy about 40 kW by investing all earnings in nothing but energy. This is only four times our per capita rate of energy consumption in this country—a fact that reflects the intimate

[4]This and other numbers were originally derived from [10.6].

connection between energy and money.

There is little doubt that our short-term needs—during the next century or so—can be met by our dwindling fossil fuels and, perhaps, nuclear power, combined with a less wasteful attitude than most of us have been raised with. But our long-term hope for an adequate energy supply probably lies in the sun.[5] Solar energy can be made useful in many different forms; some possibilities include:

- Hydroelectric power. (There is no hope for a dramatic increase in this source because much of the available rainfall runoff has already been harnessed.)
- The combustion of renewable organic matter. (Wood has been used in this way for years, and we now recognize at least the possibility of replacing gasoline with methanol.)
- Offshore thermal energy conversion (OTEC). (This involves the potential use of large floating heat engines operating offshore in tropical ocean waters.)
- Direct solar heating.
- Beaming of energy collected in space to the earth's surface by microwave transmission.
- Photovoltaic collection.
- The energy of ocean waves.

Notice that some of these sources lend themselves to heat production and some lend themselves to work production. Any time we turn thermal energy to electricity or any other form of work, the Second Law of Thermodynamics exacts a severe tax on the energy. Usually, we can only recover about one-third of the total thermal energy as work. Electrical heating, for example, is inherently wasteful because we first sacrifice two-thirds of the energy present in the fuel, or even more from the sun, in producing electricity. Then we degrade the electricity back to heat.

[5] Nuclear fusion—the process by which we might manage to create mini-suns upon the earth—might also be a hope of the future.

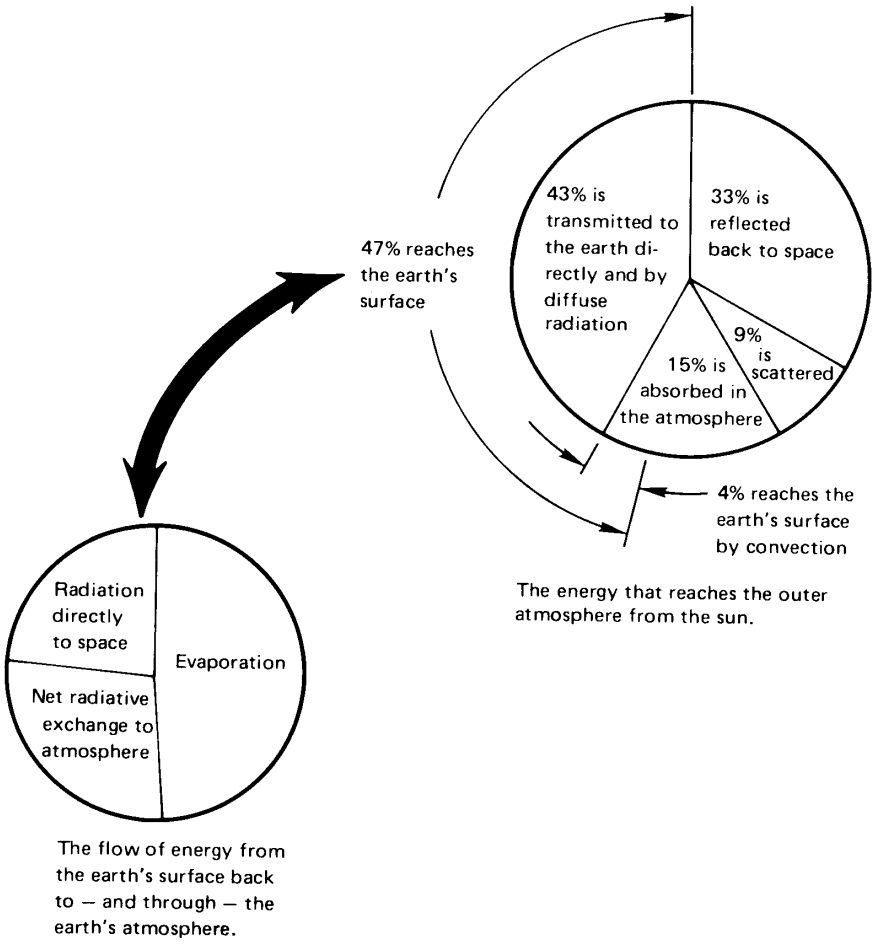
43% is transmitted to the earth directly and by diffuse radiation
33% is reflected back to space
9% is scattered
15% is absorbed in the atmosphere
47% reaches the earth's surface
4% reaches the earth's surface by convection
The energy that reaches the outer atmosphere from the sun.
Radiation directly to space
Evaporation
Net radiative exchange to atmosphere
The flow of energy from the earth's surface back to – and through – the earth's atmosphere.

Figure 10.24 The approximate distribution of the flow of the sun's energy to and from the earth's surface.

Distribution of the sun's energy

Figure 10.24 shows what becomes of the solar energy that impinges on the earth if we average it over the year and the globe, and we consider all kinds of weather. Only 47% of it actually reaches the earth's surface. The lower left-hand portion of the figure shows how this energy is, in turn, returned to the atmosphere and to space.

The heat flux from the sun to the outer edge of the atmosphere is 1367 W/m^2 when the sun is at a mean distance from the earth. We have

seen that 47% of this, or 642 W/m^2, reaches the earth's surface. The solar radiation that is felt at the earth's surface includes direct radiation that has passed through the atmosphere; diffuse radiation from the sky; and reflected radiation from snow, water, or other features on the surface. These arriving and departing flows of solar energy present some interesting problems.

A substantial fraction of the sun's energy arrives at the earth's surface in the ultraviolet and visible wavelengths. However, it is reradiated from the relatively cool surface of the earth in wavelengths that are generally far longer. We have already noted that α and ε for objects that are subject to solar radiation might differ greatly as a consequence of this.

Another important consequence of the difference between incoming and outgoing radiation wavelengths is called the *greenhouse effect*. We have noted that a glass in a greenhouse admits shortwave energy from the sun selectively. This energy is absorbed and reradiated at a much lower temperature—a temperature at which the major heat radiation is accomplished in wavelengths above 3 or 4 μm. But this, in turn, is the wavelength range where glass becomes virtually *opaque*. The heat is therefore trapped inside.

If we look again at Fig. 10.2, we see that our own sky creates a partial greenhouse effect if it is heavily loaded with CO_2, H_2O, and, to a lesser extent, ozone. The escape of long-wavelength reradiated energy from the earth's surface will be reduced in the neighborhood of λ = 1.4, 1.9, and 2.7 μm. But it will be even more strongly impeded at certain higher-wavelength bands not shown in Fig. 10.2. Water, of course, will condense out in rain or snow, but CO_2 must be removed by photosynthesis, and it can build up without limit.

A major objection to the continued use of fossil fuels, or renewable organic fuels, is that we are loading the atmosphere with CO_2 faster than our flora can remove it. The long-range effect of this buildup could be a significant rise in the average temperature of the earth's atmosphere, with accompanying climatic changes. These changes are hard to predict accurately but remain potentially dangerous.

The potential for solar power

With so much solar energy falling upon all parts of the world, and with the apparent safety, reliability, and cleanliness of most—but not all—schemes for utilizing solar energy, one might ask why we do not generally use solar power already. The reason is that solar power involves many

serious heat transfer and thermodynamics design problems. We shall discuss the problems qualitatively and refer the reader to [10.7], [10.8], or [10.9] for detailed discussions of the design of solar energy systems.

Solar energy reaches the earth with very low intensity. We began this discussion in Chapter 1 by noting that human beings can interface with only a few hundred watts of energy. We could not live on earth if the sun were not very gentle. It follows that any large solar power source must concentrate the energy that falls on a very large area. By way of illustration, suppose that we sought to convert 636 W/m^2 of solar energy into electric power with a 10% thermal efficiency (which is not pessimistic) during 8 hr of each day. This would correspond with less than 6 W/ft^2, on the average, and we would need 5 square miles of collector area to match the steady output of an 800 MW power plant.

Hydroelectric power also requires a large collector area, in the form of the watershed and reservoir behind it. The burning of organic matter requires a large forest to be fed by the sun, and so forth. Any energy supply that is served by the sun must draw from a large area of the earth's surface. This, in turn, means that solar power systems inherently involve very high capital investments, and they introduce their own kinds of environmental complications.

A second problem stems from the intermittent nature of solar devices. To provide steady power—day and night, rain or shine—requires thermal storage systems, which are often complex and expensive.

These problems are minimal when one uses solar energy merely to heat air or water to moderate temperatures (50 to 90°C). In this case the efficiency will improve from just a few percent to as high as 70%. Such heating can be used for industrial processes such as crop drying, or it can be used on a small scale for domestic heating of air or water.

Figure 10.25 shows a typical configuration of a domestic solar collector of the flat-plate type. Solar radiation passes through one or more glass plates and impinges on a plate that absorbs the solar wavelengths. The absorber plate might be copper painted with a high-absorptance paint. The glass plates, of course, are almost transparent in the visible range, and each one admits about 90% of the solar energy that reaches it. Once the energy is absorbed, it is reemitted as long-wavelength infrared radiation. Glass is almost opaque in this range, and energy is retained in the collector by a greenhouse effect.

Water flowing through tubes, which are held in close contact with the absorbing plate, carries the energy away for use. The flow rate is adjusted to give an appropriate temperature rise.

When the working fluid is to be brought to a fairly high temperature,

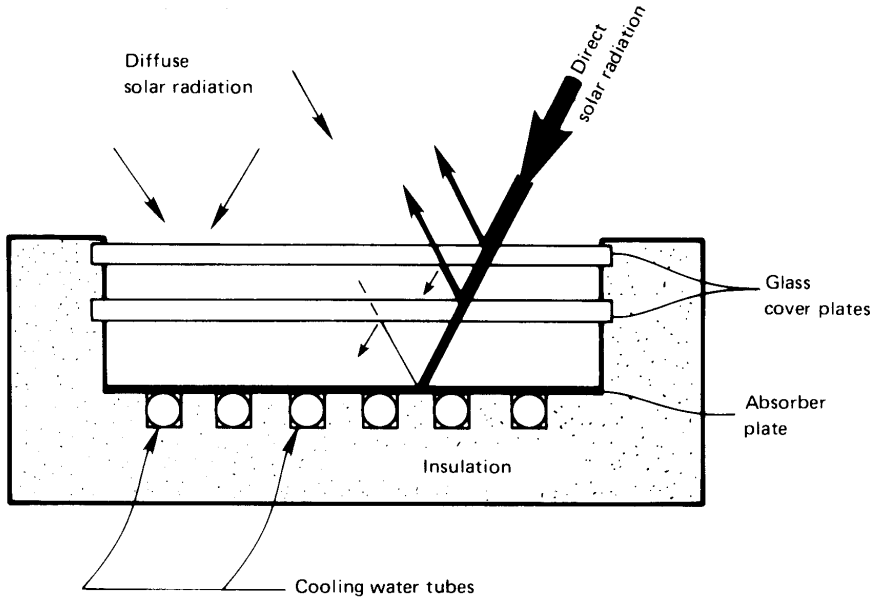

Figure 10.25 A typical flat-plate solar collector.

it is necessary to focus the direct radiation from the sun from a large area down to a very small region, using reflecting mirrors. Collectors equipped with a small parabolic reflector, focused on a water or air pipe, can raise the fluid to between 100 and 200°C. Any scheme intended to produce electrical power with a conventional thermal cycle needs to focus energy in an area ratio on the order of 1000 : 1 if it is to achieve a practical efficiency.

Problems

10.1 What will ε_λ of the sun appear to be to an observer on the earth's surface at $\lambda = 0.2$ μm and 0.65 μm? How do these emittances compare with the real emittances of the sun? [At 0.65 μm, $\varepsilon_\lambda \simeq 0.77$.]

10.2 Plot e_{λ_b} against λ for $T = 300$ K and 10,000 K with the help of eqn. (1.30). About what fraction of energy from each black body is visible?

10.3 A 0.6 mm diameter wire is drawn out through a mandril at 950°C. Its emittance is 0.85. It then passes through a long

cylindrical shield of commercial aluminum sheet, 7 cm in diameter. The shield is horizontal in still air at 25°C. What is the temperature of the shield? Is it reasonable to neglect natural convection inside and radiation outside? [$T_{\text{shield}} = 153$°C.]

10.4 A 1 ft^2 shallow pan with adiabatic sides is filled to the brim with water at 32°F. It radiates to a night sky whose temperature is 360°R, while a 50°F breeze blows over it at 1.5 ft/s. Will the water freeze or warm up?

10.5 A thermometer is held vertically in a room with air at 10°C and walls at 27°C. What temperature will the thermometer read if everything can be considered black? State your assumptions.

10.6 Rework Problem 10.5, taking the room to be wall-papered and considering the thermometer to be nonblack.

10.7 Two thin aluminum plates, the first polished and the second painted black, are placed horizontally outdoors, where they are cooled by air at 10°C. The heat transfer coefficient is 5 W/m^2·°C on both the top and the bottom. The top is irradiated with 750 W/m^2 and it radiates to the sky at 170 K. The earth below the plates is black at 10°C. Find the equilibrium temperature of each plate.

10.8 A sample holder of 99% pure aluminum, 1 cm in diameter and 16 cm in length, protrudes from a small housing on an orbital space vehicle. The holder "sees" almost nothing but outer space at an effective temperature of 30 K. The base of the holders is 0°C and you must find the temperature of the sample at its tip. It will help if you note that aluminum is used, so that the temperature of the tip stays quite close to that of the root. [$T_{\text{end}} = -0.7$°C.]

10.9 There is a radiant heater in the bottom of the box shown in Fig. 10.26. What percentage of the heat goes out the top? What fraction impinges on each of the four sides? (Remember that the percentages must add up to 100.)

10.10 With reference to Fig. 10.13, find $F_{1-2,4}$ and $F_{2,4-1}$.

10.11 Find F_{2-4} for the surfaces shown in Fig. 10.27. [0.315.]

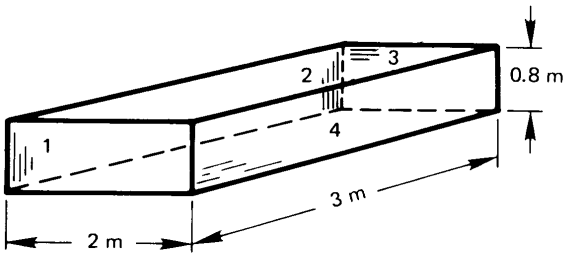

Figure 10.26 Configuration for Prob. 10.9.

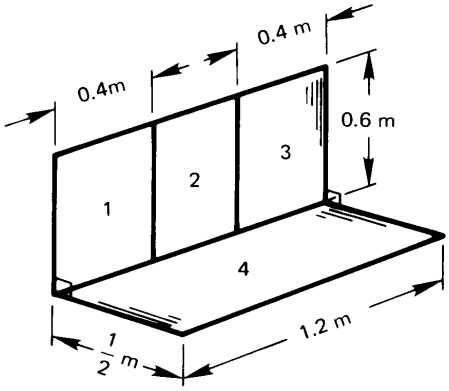

Figure 10.27 Configuration for Prob. 10.11.

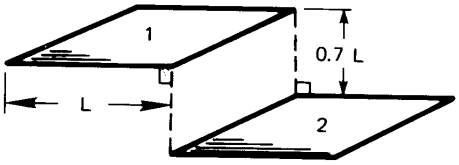

Figure 10.28 Configuration for Prob. 10.12.

10.12 What is F_{1-2} for the squares shown in Fig. 10.28?

10.13 A particular internal combustion engine has an exhaust manifold at 600°C running parallel to a water cooling line at 20°C. If both the manifold and the cooling line are 4 cm in diameter, their centers are 7 cm apart, and both are approximately black, how much heat will be transferred to the cooling line by radiation? [383 W/m.]

10.14 Prove that F_{1-2} for any pair of two-dimensional plane surfaces, as shown in Fig. 10.29, is equal to $[(a + b) - (c + d)]/2L_1$. This is called the *string rule* because we can imagine that the numerator equals the difference between the lengths of a set of crossed strings (a and b) and a set of uncrossed strings (c

and d).

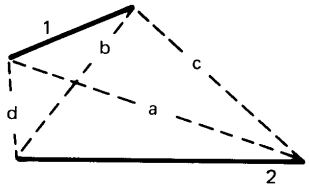

Figure 10.29 Configuration for Prob. 10.14.

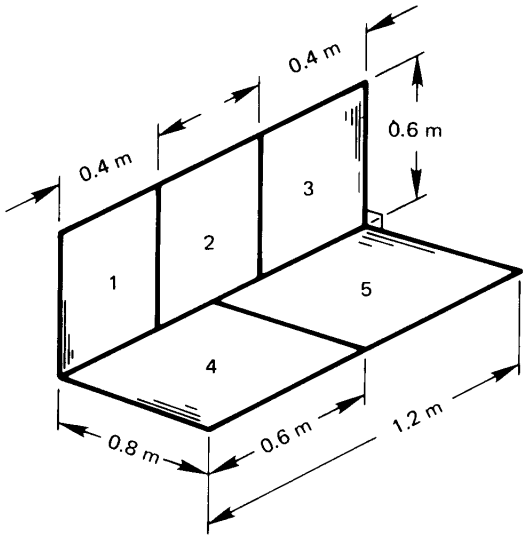

Figure 10.30 Configuration for Prob. 10.15.

10.15 Find F_{1-5} for the surfaces shown in Fig. 10.30.

10.16 Find $F_{1-2,3,4}$ for the surfaces shown in Fig. 10.31.

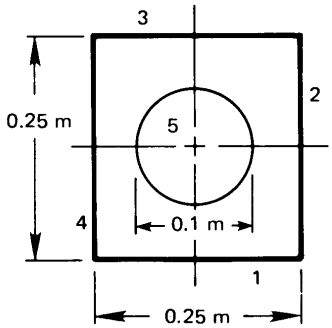

Figure 10.31 Configuration for Prob. 10.16.

10.17 A cubic box 1 m on the side is black except for one side, which has an emittance of 0.2 and is kept at 300°C. An adjacent side is kept at 500°C. The other sides are insulated. Find Q_{net} inside the box. [2494 W.]

10.18 Rework Problem 10.17, but this time set the emittance of the insulated walls equal to 0.6. Compare the insulated wall temperature with the value you would get if the walls were black.

10.19 An insulated black cylinder, 10 cm in length and with an inside diameter of 5 cm, has a black cap on one end and a cap with an emittance of 0.1 on the other. The black end is kept at 100°C and the reflecting end is kept at 0°C. Find Q_{net} inside the cylinder and T_{cylinder}.

10.20 Rework Example 10.3 if the shield has an inside emittance of 0.34 and the room is at 20°C. How much cooling must be provided to keep the shield at 100°C?

10.21 A 0.8 m long cylindrical burning chamber is 0.2 m in diameter. The hot gases within it are at a temperature of 1500°C and a pressure of 1 atm, and the absorbing components consist of 12% by volume of CO_2 and 18% H_2O. Neglect end effects and determine how much cooling must be provided the walls to hold them at 750°C if they are black.

10.22 A 30 ft by 40 ft house has a conventional 30° sloping roof with a peak running in the 40 ft direction. Calculate the temperature of the roof in 20°C still air when the sun is overhead (a) if the roofing is of wooden shingles and (b) if it is commercial aluminum sheet. The incident solar energy is 670W/m^2, Kirchhoff's law applies for both roofs, and T_{eff} for the sky is 22°C.

10.23 Calculate the radiant heat transfer from a 0.2 m diameter stainless steel hemisphere ($\varepsilon_{\text{ss}} = 0.4$) to a copper floor ($\varepsilon_{\text{Cu}} = 0.15$) that forms its base. The hemisphere is kept at 300°C and the base at 100°C. Use the algebraic method. [21.24 W.]

10.24 A hemispherical indentation in a smooth wrought-iron plate has an 0.008 m radius. How much heat radiates from the 40°C dent to the −20°C surroundings?

10.25 A conical hole in a block of metal for which $\varepsilon = 0.5$ is 5 cm in diameter at the surface and 5 cm deep. By what factor will the radiation from the area of the hole be changed by the presence of the hole? (This problem can be done to a close approximation using the methods in this chapter if the cone does not become very deep and slender. If it does, then the fact that the apex is receiving far less radiation makes it incorrect to use the network analogy.)

10.26 A single-pane window in a large room is 4 ft wide and 6 ft high. The room is kept at 70°F, but the pane is at 67°F owing to heat loss to the colder outdoor air. Find (a) the heat transfer by radiation to the window; (b) the heat transfer by natural convection to the window; and (c) the fraction of heat transferred to the window by radiation.

10.27 Suppose that the windowpane temperature is unknown in Problem 10.26. The outdoor air is at 40°F and $\overline{h}$ is 62 W/m^2·°C on the outside of the window. It is nighttime and the effective temperature of the sky is 15°F. Assume $F_{\text{window}-\text{sky}} = 0.5$. Take the rest of the surroundings to be at 40°F. Find T_{window} and draw the analogous electrical circuit, giving numerical values for all thermal resistances. Discuss the circuit. (It will simplify your calculation to note that the window is opaque to infrared radiation but that it offers very little resistance to conduction. Thus, the window temperature is almost uniform.)

10.28 A very effective low-temperature insulation is made by evacuating the space between parallel metal sheets. Convection is eliminated, conduction occurs only at spacers, and radiation is responsible for what little heat transfer occurs. Calculate q between 150 K and 100 K for three cases: (a) two sheets of *highly* polished aluminum, (b) three sheets of highly polished aluminum, and (c) three sheets of rolled sheet steel.

10.29 Three parallel black walls, 1 m wide, form an equilateral triangle. One wall is held at 400 K, one is at 300 K, and the third is insulated. Find Q W/m and the temperature of the third wall.

10.30 Two 1 cm diameter rods run parallel, with centers 4 cm apart. One is at 1500 K and black. The other is unheated, and $\varepsilon = 0.66$. They are both encircled by a cylindrical black radiation shield

at 400 K. Evaluate Q W/m and the temperature of the unheated rod.

10.31 A small-diameter heater is centered in a large cylindrical radiation shield. Discuss the relative importance of the emittance of the shield during specular and diffuse radiation.

10.32 Two 1 m wide commercial aluminum sheets are joined at a 120° angle along one edge. The back (or 240° angle) side is insulated. The plates are both held at 120°C. The 20°C surroundings are distant. What is the net radiant heat transfer from the left-hand plate: to the right-hand side, and to the surroundings?

10.33 Two parallel discs of 0.5 m diameter are separated by an infinite parallel plate, midway between them, with a 0.2 m diameter hole in it. The discs are centered on the hole. What is the view factor between the two discs if they are 0.6 m apart?

10.34 An evacuated spherical cavity, 0.3 m in diameter in a zero-gravity environment, is kept at 300°C. Saturated steam at 1 atm is then placed in the cavity. (a) What is the initial flux of radiant heat transfer to the steam? (b) Determine how long it will take for $q_{\text{conduction}}$ to become less than $q_{\text{radiation}}$. (Correct for the rising steam temperature if it is necessary to do so.)

10.35 Verify cases (1), (2), and (3) in Table 10.2 using the string method described in Problem 10.14.

10.36 Two long parallel heaters consist of 120° segments of 10 cm diameter parallel cylinders whose centers are 20 cm apart. The segments are those nearest each other, symmetrically placed on the plane connecting their centers. Find F_{1-2} using the string method described in Problem 10.14.)

10.37 Two long parallel strips of rolled sheet steel lie along sides of an imaginary 1 m equilateral triangular cylinder. One piece is 1 m wide and kept at 20°C. The other is $\frac{1}{2}$ m wide, centered in an adjacent leg, and kept at 400°C. The surroundings are distant and they are insulated. Find Q. (You will need a shape factor; it can be found using the method described in Problem 10.14.)

10.38 Find the shape factor from the hot to the cold strip in Problem 10.37 using Table 10.2, not the string method. If your instructor asks you to do so, complete Problem 10.37 when you have F_{1-2}.

10.39 Prove that, as the figure becomes very long, the view factor for the second case in Table 10.3 reduces to that given for the third case in Table 10.2.

10.40 Show that F_{1-2} for the first case in Table 10.3 reduces to the expected result when plates 1 and 2 are extended to infinity.

10.41 In Problem 2.26 you were asked to neglect radiation in showing that q was equal to 8227 W/m^2 as the result of conduction alone. Discuss the validity of the assumption quantitatively.

10.42 A 100°C sphere with $\varepsilon = 0.86$ is centered within a second sphere at 300°C with $\varepsilon = 0.47$. The outer diameter is 0.3 m and the inner diameter is 0.1 m. What is the radiant heat flux?

References

[10.1] E. M. Sparrow and R. D. Cess. *Radiation Heat Transfer*. Hemisphere Publishing Corp./McGraw-Hill Book Company, Washington, D.C., 1978.

[10.2] R. Siegel and J. R. Howell. *Thermal Radiative Heat Transfer*. Hemisphere Publishing Corp., Washington, D.C., 3rd edition, 1992.

[10.3] A. K. Oppenheim. Radiation analysis by the network method. *Trans. ASME*, 78:725–735, 1956.

[10.4] J. P. Holman. *Heat Transfer*. McGraw-Hill Book Company, New York, 5th edition, 1981.

[10.5] H. C. Hottel and A. F. Sarofim. *Radiative Transfer*. McGraw-Hill Book Company, New York, 1967.

[10.6] M. K. Hubbert. The energy resources of the earth. *Scientific American*, 224(3):60–70, September 1971. The entire issue, titled "Energy and Power," is of interest.

[10.7] J. A. Duffie and W. A. Beckman. *Solar Engineering of Thermal Processes*. John Wiley & Sons, Inc., New York, 2nd edition, 1991.

[10.8] F. Kreith and J. F. Kreider. *Principles of Solar Engineering*. Hemisphere Publishing Corp./McGraw-Hill Book Company, Washington, D.C., 1978.

[10.9] U.S. Department of Commerce. *Solar Heating and Cooling of Residential Buildings*, volume 1 and 2. Washington, D.C., October 1977.

Part V

Mass Transfer

11. An Introduction to Mass Transfer

The edge of a colossal jungle, so dark-green as to be almost black, fringed with white surf, ran straight, like a ruled line, far, far away along a blue sea whose glitter was blurred by a creeping mist. The sun was fierce, the land seemed to glisten and drip with steam.

Heart of Darkness, **Joseph Conrad, 1902**

11.1 Introduction

The preceding chapters of this book deal with heat transfer by convection and by the *diffusion* of heat, which we have been calling heat conduction. We have only discussed situations in which the medium transferring heat is composed of a single substance—convective processes in which pure fluids transfer heat by convection to adjacent solid walls, phase-change processes in which pure vapors condense on cold surfaces, and so on. Many heat transfer processes, however, involve mixtures of more than one substance. A wall exposed to a hot air stream may be cooled evaporatively by bleeding water through its surface. Water vapor may condense out of damp air onto cool surfaces. Heat will flow through an air-water mixture in these situations, but water vapor will diffuse or convect through air as well.

This sort of transport of one substance relative to another is called *mass transfer*; it did not occur in the single-component processes of the preceding chapters. In this chapter, we study mass transfer phenomena with an eye toward predicting heat and mass transfer rates in situations like those just mentioned.

During mass transfer processes, an individual chemical species trav-

els from regions of high concentration of that species to regions of low concentration. When liquid water is exposed to a dry air stream, its vapor pressure may produce a comparatively high concentration of water vapor in the air near the water surface. The concentration difference between the water vapor near the surface and that in the air stream will drive the diffusion of vapor into the air stream, causing evaporation.

In this and other respects, mass transfer is analogous to heat transfer. In heat transfer, thermal energy diffuses from regions of high concentration (that is, of high temperature) to regions of low concentration (of low temperature), following gradients in the concentration (temperature gradients). In mass transfer, each species in a mixture diffuses along gradients in its concentration. Just as the diffusional (or conductive) heat flux is directly proportional to a temperature gradient, so the diffusional mass flux of a species is often directly proportional to its concentration gradient; this is called Fick's law of diffusion. Just as conservation of energy and Fourier's law lead to equations for the convection and diffusion of heat, conservation of mass and Fick's law lead to equations for the convection and diffusion of species in a mixture. The great similarity of the equations of heat convection and diffusion to those of mass convection and diffusion extends to the definition and use of convective mass transfer coefficients, which, like heat transfer coefficients, relate convective fluxes to concentration differences. Moreover, with simple modifications, the heat transfer coefficients of previous chapters may often be applied to mass transfer calculations.

Mass transfer, by its very nature, is intimately involved with mixtures of chemical species. This chapter begins with a section defining various measures of the concentration of species in a mixture and of the velocities at which individual species move. We make frequent reference to an arbitrary "species i," the ith component of a mixture of N different species. These definitions may remind you of your first course in chemistry. We also spend some time, in Section 11.4, discussing how to calculate transport properties of mixtures, such as diffusion coefficients and viscosities.

The natural-draft cooling tower shown in Fig. 11.1 is a common example of a mass transfer technology. These huge towers are used to cool the circulating water leaving power plant condensers or other large heat exchangers. They are essentially empty shells, at the bottom of which are arrays of cement boards or plastic louvres over which is sprayed the hot water to be cooled. The hot water runs over this packing, and a portion of it evaporates into the cool air that enters from below. The remaining

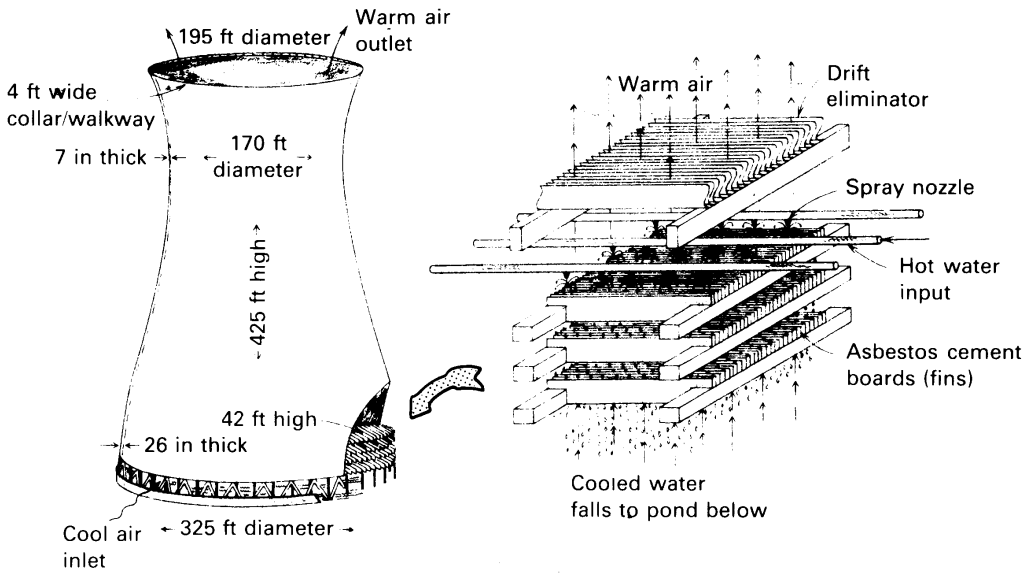

Figure 11.1 Schematic diagram of a cooling tower at the Rancho Seco nuclear power plant. (From [11.1], courtesy of W. C. Reynolds.)

water, having been cooled by evaporation, falls to the bottom, where it is collected and recirculated.

The temperature of the air rises as it absorbs the warm vapor and, in the *natural-draft* form of cooling tower, the upper portion of the tower acts as an enormous chimney through which the warm, moist air buoys, drawing cool air in from below. In a *mechanical-draft* cooling tower, fans are used to pull air through the packing.

The working mass transfer process in a cooling tower is the evaporation of water into air. The rate of evaporation depends on the temperature and humidity of the incoming air, the feed water temperature, and the air-flow characteristics of the tower and the packing. When the air flow is buoyancy-driven, the flow rates are directly coupled. Thus, the complete design of a cooling tower is clearly a complex task. In this chapter, we study only the key issue in such design—the issue of *mass transfer*.

11.2 Mixture compositions and species fluxes

The composition of mixtures

A mixture is made up of various proportions of its constituent chemical species, but it displays its own density, molecular weight, and other overall thermodynamic properties. These properties depend on the types and relative amounts of the component substances. Moreover, the proportions of each substance vary from point to point in the nonuniform mixtures that give rise to mass diffusion. To describe the composition of a mixture, we must introduce measures of the local proportion of each component and the resultant properties of the mixture.

A given volume element of a mixture contains a certain mass of each of its components. Dividing that mass by the volume of the element, we obtain the *partial density*, ρ_i, for each component i of the mixture, in kg of i per m^3. We may then describe the composition of the mixture by stating the partial density of each of its components. The mass density of the mixture itself, ρ, is the total mass in this element divided by the volume of the element; therefore,

$$\rho = \sum_i \rho_i \tag{11.1}$$

The concentration of species i in the mixture may be described by the ratio ρ_i/ρ, which is the mass of i per unit mass of the mixture. This ratio is called the *mass fraction*, m_i:

$$m_i = \frac{\rho_i}{\rho} = \frac{\text{mass of species } i}{\text{mass of mixture}} \tag{11.2}$$

It follows that

$$\sum_i m_i = \sum_i \rho_i/\rho = 1 \quad \text{and} \quad 0 \leqslant m_i \leqslant 1 \tag{11.3}$$

The *molar concentration* of species i in kmol/m^3, c_i, expresses concentration in terms of moles rather than mass. If M_i is the molecular weight of species i in kg/kmol, then

$$c_i = \frac{\rho_i}{M_i} = \frac{\text{moles of } i}{\text{volume}}. \tag{11.4}$$

The molar concentration of the mixture, c, is the total number of moles for all species per unit volume; thus,

$$c = \sum_i c_i. \tag{11.5}$$

The *mole fraction* of species i, x_i, is the number of moles of i per mole of mixture:

$$x_i = \frac{c_i}{c} = \frac{\text{moles of } i}{\text{mole of mixture}}. \tag{11.6}$$

Equations (11.5) and (11.6) lead to

$$\sum_i x_i = 1 \quad \text{and} \quad 0 \leqslant x_i \leqslant 1 \tag{11.7}$$

The molecular weight of the mixture, $M \equiv \rho/c$, may be written as

$$M = \sum_i x_i M_i \quad \text{or} \quad \frac{1}{M} = \sum_i \frac{m_i}{M_i} \tag{11.8}$$

using eqns. (11.1,11.4, and 11.6) and (11.5,11.4, and 11.2), respectively. From these expressions, one may develop the following relations (Problem 11.1):

$$m_i = \frac{x_i M_i}{\sum x_k M_k} \qquad x_i = \frac{m_i/M_i}{\sum m_k/M_k} \tag{11.9}$$

In some circumstances, such as kinetic theory calculations, one works directly with the number of molecules of i per unit volume. This *number density*, $\mathcal{N}_i$, is given by

$$\mathcal{N}_i = N_A c_i \tag{11.10}$$

where N_A is Avogadro's number, 6.02214×10^{26} molecules/kmol.

Ideal gases

The relations we have developed so far involve densities and concentrations that vary in as yet unknown ways with temperature or pressure. They must be combined with equation-of-state information before they can be used in actual processes. To get a more useful, though more restrictive, set of results, we now combine the preceding relations with the ideal gas law, as applied to each individual component:

$$p_i = \rho_i R_i T \tag{11.11}$$

In eqn. (11.11), p_i is the*partial pressure* exerted by component i and R_i is the ideal gas constant for that component:

$$R_i = \frac{R^\circ}{M_i} \tag{11.12a}$$

$$= \frac{N_A k_B}{M_i} \tag{11.12b}$$

where R° is the universal gas constant, 8314.472 J/kmol· K, and Boltzmann's constant, k_B, is equal to R°/N_A. Equation (11.11) may then be rewritten as

$$p_i = \rho_i R_i T = M_i c_i \left(\frac{R^\circ}{M_i}\right) T \tag{11.13a}$$

$$= c_i R^\circ T \tag{11.13b}$$

Equation (11.5) then becomes

$$c = \sum_i c_i = \sum_i \frac{p_i}{R^\circ T} = \frac{p}{R^\circ T} \tag{11.14}$$

Multiplying the last part of eqn. (11.14) by $R^\circ T$ yields Dalton's law of partial pressures,[1]

$$p = \sum_i p_i \tag{11.15}$$

Finally, we combine eqns. (11.6), (11.13b), and (11.15) to obtain the useful result:

$$x_i = \frac{c_i}{c} = \frac{p_i}{c\,R^\circ T} = \frac{p_i}{p} \tag{11.16}$$

in which the last two equalities are restricted to ideal gases.

Example 11.1

The most important mixture that we deal with is air. It has the following composition:

Species	*Mass Fraction*
N_2	0.7556
O_2	0.2315
Ar	0.01289
trace gases	< 0.01

[1] Dalton's law (1801) is an empirical principle (not a deduced result) in classical thermodynamics. It can be deduced from molecular principles, however. We built the appropriate molecular principles into our development when we assumed eqn. (11.11) to be true. The reason that eqn. (11.11) is true is that ideal gas molecules occupy a mixture without influencing one another.

Determine x_{O_2}, p_{O_2}, c_{O_2}, and ρ_{O_2} for air at 1 atm.

SOLUTION. Equation (11.8) and data from Table 11.1 on page 565 yield M_{air} as follows:

$$M_{\text{air}} = \left(\frac{0.7556}{28.02 \text{ kg/kmol}} + \frac{0.2315}{32.00 \text{ kg/kmol}} + \frac{0.01289}{39.95 \text{ kg/kmol}} \right)^{-1}$$
$$= 28.97 \text{ kg/kmol}$$

Using eqn. (11.9), we get

$$x_{O_2} = \frac{(0.2315)(28.97 \text{ kg/kmol})}{32.00 \text{ kg/kmol}} = 0.2095$$

The partial pressure of oxygen in air at 1 atm is [eqn. (11.16)]

$$p_{O_2} = (0.2095)(101,325 \text{ Pa}) = 2.123 \times 10^4 \text{ Pa}$$

We obtain c_{O_2} from eqn. (11.13b):

$$c_{O_2} = (2.123 \times 10^4 \text{ Pa})/(300 \text{ K})(8314.5 \text{ J/kmol·K})$$
$$= 0.008510 \text{ kmol/m}^3$$

and eqn. (11.4) is then used to get the partial density

$$\rho_{O_2} = c_{O_2} M_{O_2}$$
$$= (0.008510 \text{ kmol/m}^3)(32.00 \text{ kg/kmol})$$
$$= 0.2723 \text{ kg/m}^3$$ ■

Velocities and fluxes

Each species in a mixture undergoing a mass transfer process will have an *species-average velocity*, $\vec{v}_i$, which is generally different for each species in the mixture, as suggested by Fig. 11.2. We may obtain the *mass-average velocity*,[2] $\vec{v}$, from the species average velocities using the formula

$$\rho \vec{v} = \sum_i \rho_i \vec{v}_i. \tag{11.17}$$

[2]The mass average velocity, $\vec{v}$, given by eqn. (11.17) is identical to the fluid velocity, $\vec{u}$, used in previous chapters. This is apparent if one applies eqn. (11.17) to a "mixture" composed of only one species. We use the symbol $\vec{v}$ here because $\vec{v}$ is the more common notation in the mass transfer literature.

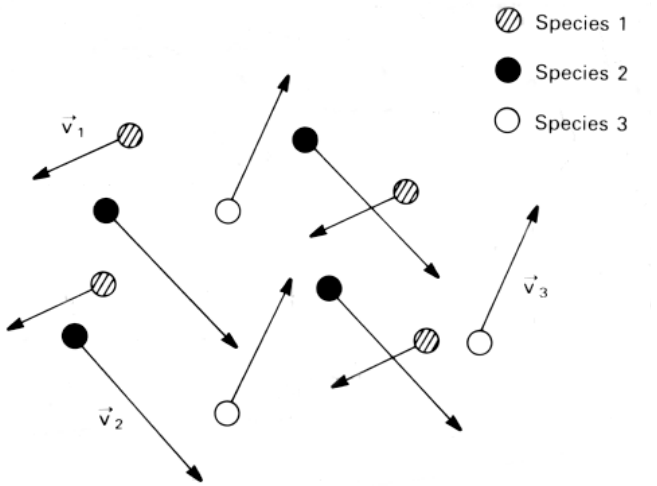

Figure 11.2 Molecules of different species in a mixture moving with different average velocities. The velocity $\vec{v}_i$ is the average over all molecules of species i.

This equation is essentially a local calculation of the mixture's net momentum per unit volume. We refer to $\rho\vec{v}$ as the mixture's *mass flux*, $\vec{n}$, and we call its scalar magnitude $\dot{m}''$; each has units of kg/m$^2\cdot$s. Likewise, the mass flux of species i is

$$\vec{n}_i = \rho_i \vec{v}_i \tag{11.18}$$

and, from eqn. (11.17), we see that the mixture's mass flux equals the sum of all species' mass fluxes

$$\vec{n} = \sum_i \vec{n}_i \tag{11.19}$$

Since each species diffusing through a mixture has some velocity relative to the mixture's mass-average velocity, the *diffusional mass flux*, $\vec{j}_i$, of a species relative to the mixture's mean flow may be identified:

$$\vec{j}_i = \rho_i \left(\vec{v}_i - \vec{v}\right). \tag{11.20}$$

The total mass flux of the ith species, $\vec{n}_i$, includes both this diffusional mass flux and bulk convection by the mean flow, as is easily shown:

$$\boxed{\begin{aligned}\vec{n}_i &= \rho_i\vec{v}_i = \rho_i\vec{v} + \rho_i\left(\vec{v}_i - \vec{v}\right)\\ &= \rho_i\vec{v} + \vec{j}_i\\ &= \underbrace{m_i\vec{n}}_{\text{convection}} + \underbrace{\vec{j}_i}_{\text{diffusion}}\end{aligned}} \tag{11.21}$$

Although the convective transport contribution is fully determined as soon as we know the velocity field and partial densities, the causes of diffusion need further discussion, which we defer to Section 11.3.

Combining eqns. (11.19) and (11.21), we find that

$$\vec{n} = \sum_i \vec{n}_i = \sum_i \rho_i \vec{v} + \sum_i \vec{j}_i = \rho \vec{v} + \sum_i \vec{j}_i = \vec{n} + \sum_i \vec{j}_i$$

so

$$\sum_i \vec{j}_i = 0 \tag{11.22}$$

Diffusional mass fluxes must sum to zero because they are each defined relative to the mean mass flux.

We also uses the mixture's *mole flux*, $\vec{N}$, defined together with the *mole-average velocity*, $\vec{v}^*$, as:

$$\vec{N} = c\vec{v}^* = \sum_i c_i \vec{v}_i. \tag{11.23}$$

The mole flux of the ith species, $\vec{N}_i$, is $c_i \vec{v}_i$. Hence,

$$\sum_i \vec{N}_i = \sum_i c_i \vec{v}_i = c\vec{v}^* = \vec{N}. \tag{11.24}$$

The last flux we define is the *diffusional mole flux*, $\vec{J}_i^*$:

$$\vec{J}_i^* = c_i \left(\vec{v}_i - \vec{v}^*\right) \tag{11.25}$$

It may be shown, using these definitions, that

$$\boxed{\vec{N}_i = x_i \vec{N} + \vec{J}_i^*} \tag{11.26}$$

Substitution of eqn. (11.26) into eqn. (11.24) gives

$$\vec{N} = \sum_i \vec{N}_i = \vec{N} \sum_i x_i + \sum_i \vec{J}_i^* = \vec{N} + \sum_i \vec{J}_i^*$$

so

$$\sum_i \vec{J}_i^* = 0. \tag{11.27}$$

Thus, *both* the $\vec{J}_i^*$'s and the $\vec{j}_i$'s add up to zero.

Example 11.2

At low temperatures, carbon oxidizes (burns) in air through the surface reaction: $C + O_2 \longrightarrow CO_2$. Figure 11.3 shows the carbon-air interface in a coordinate system that moves into the stationary carbon at the same speed that the carbon burns away—as though the observer were seated on the moving interface. Oxygen flows toward the carbon surface and carbon dioxide flows away, with a net flow of carbon through the interface. If the system is at steady state and, if a separate analysis shows that carbon is consumed at the rate of 0.00241 kg/m^2·s, find the mass and mole fluxes through an imaginary surface, s, that stays close to the gas side of the interface. For this case, concentrations at the s-surface turn out to be $m_{O_2,s} = 0.20$, $m_{CO_2,s} = 0.052$, and $\rho_s = 0.29$ kg/m^3.

SOLUTION. The mass balance for the reaction is

$$12.0 \text{ kg C} + 32.0 \text{ kg } O_2 \longrightarrow 44.0 \text{ kg } CO_2$$

Since carbon flows through a second imaginary surface, u, moving through the stationary carbon just below the interface, the mass fluxes are related by

$$n_{C,u} = -\frac{12}{32} n_{O_2,s} = \frac{12}{44} n_{CO_2,s}$$

The minus sign arises because the O_2 flow is opposite the C and CO_2 flows, as shown in Figure 11.3. In steady state, if we apply mass conservation to the control volume between the u and s surfaces, we find that the total mass flow entering the u-surface equals that leaving the s-surface

$$n_{C,u} = n_{CO_2,s} + n_{O_2,s} = \dot{m}''$$

We call the total mass flow $\dot{m}''$. Hence,

$$n_{O_2,s} = -\frac{32}{12}(0.00241 \text{ kg/m}^2\cdot\text{s}) = -0.00643 \text{ kg/m}^2\cdot\text{s}$$
$$n_{CO_2,s} = \frac{44}{12}(0.00241 \text{ kg/m}^2\cdot\text{s}) = 0.00884 \text{ kg/m}^2\cdot\text{s}$$

To get the diffusional mass flux, we need species and mass average

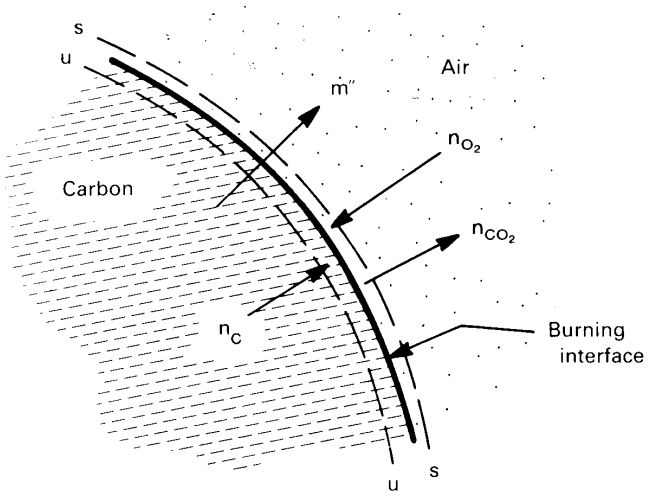

Figure 11.3 Low-temperature carbon oxidation.

speeds:

$$v_{O_2,s} = \frac{n_{O_2,s}}{\rho_{O_2,s}} = \frac{-0.00643 \text{ kg/m}^2\cdot\text{s}}{0.2\,(0.29 \text{ kg/m}^3)} = -0.111 \text{ m/s}$$

$$v_{CO_2,s} = \frac{n_{CO_2,s}}{\rho_{CO_2,s}} = \frac{0.00884 \text{ kg/m}^2\cdot\text{s}}{0.052\,(0.29 \text{ kg/m}^3)} = 0.586 \text{ m/s}$$

$$v_s = \frac{1}{\rho_s}\sum_i n_i = \frac{(0.00884 - 0.00643) \text{ kg/m}^2\cdot\text{s}}{0.29 \text{ kg/m}^3} = 0.00831 \text{ m/s}$$

Thus,

$$j_{i,s} = \rho_{i,s}\,(v_{i,s} - v_s) = \begin{cases} -0.00691 \text{ kg/m}^2\cdot\text{s for } O_2 \\ 0.00876 \text{ kg/m}^2\cdot\text{s for } CO_2 \end{cases}$$

The diffusional mass fluxes, $j_{i,s}$, are very nearly equal to the species mass fluxes, $n_{i,s}$. That is because the mass-average speed, v_s, is here so much less than the species speeds, $v_{i,s}$, that the convective contribution to $n_{i,s}$ is much smaller than the diffusive contribution. Thus, mass transfer occurs primarily by diffusion. Note that $j_{O_2,s}$ and $j_{CO_2,s}$ do *not* sum to zero because the other, nonreacting species in air must diffuse against the small convective velocity, v_s (see Section 11.6).

One mole of carbon surface reacts with one mole of O_2 to form one mole of CO_2. Thus, the mole fluxes of each species have the same

magnitude at the interface:

$$N_{CO_2,s} = -N_{O_2,s} = N_{C,u} = \frac{n_{C,u}}{M_C} = 0.000112 \text{ kmol/m}^2\cdot\text{s}$$

and the mole average velocity at the s-surface is identically zero (since $N_{CO_2,s} + N_{O_2,s} = 0$). The diffusional mole fluxes are

$$J^*_{i,s} = c_{i,s}(v_{i,s} - \underbrace{v^*_s}_{=0}) = \frac{\rho_{i,s}}{m_i} v_{i,s} = \begin{cases} -0.000201 \text{ kmol/m}^2\cdot\text{s for } O_2 \\ 0.000201 \text{ kmol/m}^2\cdot\text{s for } CO_2 \end{cases}$$

These diffusional mole fluxes *do* sum to zero because there is *no* convective mole flux for other species to diffuse against.

The reader may calculate the velocity of the interface from $n_{c,u}$. That calculation would show the interface to be receding so slowly that the velocities calculated here are almost equal to those that would be seen by a stationary observer. ■

11.3 Diffusion fluxes and Fick's Law

When the composition of a mixture is spatially nonuniform, concentration gradients exist in the various species of the mixture. These gradients provide a driving potential for the diffusion of a given species, i, from regions of high concentration of i to regions of low concentration of i—similar to the diffusion of heat from regions of high temperature to regions of low temperature. We have already noted in Section 2.1 that mass diffusion obeys Fick's law

$$\boxed{\vec{j}_i = -\rho \mathcal{D}_{im} \nabla m_i} \tag{11.28}$$

which is analogous to Fourier's law.

The constant of proportionality, $\rho\mathcal{D}_{im}$, between the local diffusive mass flux of species i and the local gradient of the concentration of i involves a physical property called the *diffusion coefficient*, $\mathcal{D}_{im}$, for species i diffusing in the mixture m. Like the thermal diffusivity, α, or the kinematic viscosity (momentum diffusivity), ν, the mass diffusivity $\mathcal{D}_{im}$ has the units of m^2/s. These three diffusivities can form three dimensionless

groups, among which is the Prandtl number:

$$\begin{aligned} \text{The Prandtl number,} \quad & \mathrm{Pr} \equiv \nu/\alpha \\ \text{The Schmidt number,}^{3} \quad & \mathrm{Sc} \equiv \nu/\mathcal{D}_{im} \\ \text{The Lewis number,}^{4} \quad & \mathrm{Le} \equiv \alpha/\mathcal{D}_{im} = \mathrm{Sc}/\mathrm{Pr} \end{aligned} \tag{11.29}$$

Each of these groups compares the relative strength of two different diffusive processes. We make considerable use of the Schmidt number in this chapter.

When diffusion occurs in mixtures of only two species, so-called *binary mixtures*, $\mathcal{D}_{im}$ reduces to the *binary diffusion coefficient*, $\mathcal{D}_{12}$. In fact, the best-known kinetic models are for binary diffusion.[5] In binary diffusion, species 1 has the same diffusivity through species 2 as does species 2 through species 1 (see Problem 11.5); in other words,

$$\mathcal{D}_{12} = \mathcal{D}_{21} \tag{11.30}$$

A Kinetic Model of Diffusion

Diffusion coefficients depend upon composition, temperature, and pressure. We take up the calculation of $\mathcal{D}_{12}$ and $\mathcal{D}_{im}$ in detail in the next section. First, let us see how Fick's law can be obtained from the same sort of elementary molecular kinetics that gave Fourier's and Newton's laws in Section 6.4.

We consider a two-component *dilute* gas (one with a low density) in which the molecules A of one species are very similar to the molecules A'

[3] Ernst Schmidt (1892–1975) served successively as the professor of thermodynamics at the Technical Universities of Danzig, Braunschweig, and Munich (Chapter 6, footnote 3). His many contributions to heat and mass transfer include the introduction of aluminum foil as radiation shielding, the first measurements of velocity and temperature fields in a natural convection boundary layer, and a once widely-used graphical procedure for solving unsteady heat conduction problems. He was among the first to develop the analogy between heat and mass transfer.

[4] Warren K. Lewis (1882–1975) was a professor of chemical engineering at M.I.T. from 1910 to 1975 and headed the department throughout the 1920s. He defined the original paradigm of chemical engineering, that of "unit operations", and, through his textbook with Walker and McAdams, *Principles of Chemical Engineering*, he laid the foundations of the discipline. He was a prolific inventor in the area of industrial chemistry, holding more than 80 patents. He also did important early work on simultaneous heat and mass transfer in connection with evaporation problems.

[5] Actually, Fick's Law is strictly valid only for binary mixtures. It can, however, often be applied to multicomponent mixtures by an appropriate choice of $\mathcal{D}_{im}$. This issue is discussed in Section 11.4.

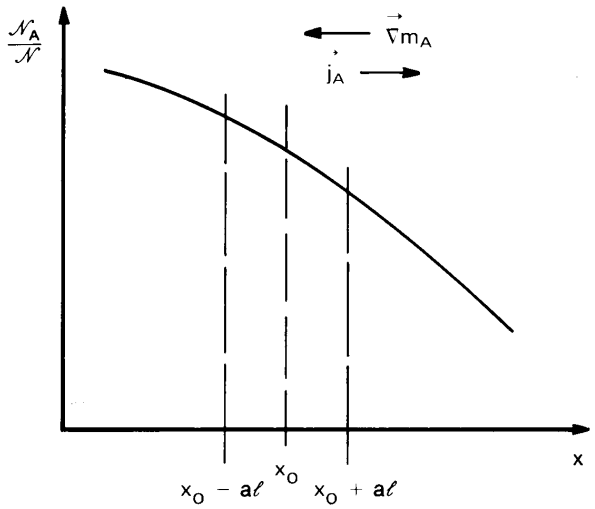

Figure 11.4 One-dimensional diffusion.

of a second species (as though some of the molecules of a pure gas had merely been labeled without changing their properties.) The resulting process is called *self-diffusion*.

If we have a one-dimensional concentration distribution, as shown in Fig. 11.4, molecules of A diffuse down their concentration gradient in the x-direction. This process is entirely analogous to the transport of energy and momentum shown in Fig. 6.13. We take the temperature and pressure of the mixture (and thus its number density) to be uniform and the mass-average velocity to be zero.

Individual molecules have thermal motion at a speed C, which varies randomly from molecule to molecule and is called the *thermal* or *peculiar* speed. The average speed of the molecules is $\overline{C}$. The average rate at which molecules cross the plane $x = x_0$ in either direction is proportional to $\mathcal{N}\overline{C}$. Prior to crossing the x_0-plane, the molecules travel a distance close to one mean free path, ℓ—call it $a\ell$, where a is a number on the order of unity.

The molecular flux travelling rightward across x_0, from its plane of origin at $x_0 - a\ell$, then has a composition equal to the value of $\mathcal{N}_A/\mathcal{N}$ at $x_0 - a\ell$, and the situation is similar for the leftward flux from $x_0 + a\ell$. The magnitude of the net mass flux in the x-direction is then

$$j_A\Big|_{x_0} = \eta\left(\mathcal{N}\overline{C}\right)\left(\frac{M_A}{N_A}\right)\left(\frac{\mathcal{N}_A}{\mathcal{N}}\Big|_{x_0-a\ell} - \frac{\mathcal{N}_A}{\mathcal{N}}\Big|_{x_0+a\ell}\right) \tag{11.31}$$

where η is a constant of proportionality. Since $\mathcal{N}_A/\mathcal{N}$ changes little in a distance of two mean free paths (in most real situations), we can expand the right side of eqn. (11.31) in a two-term Taylor series expansion about x_0 and obtain Fick's law:

$$\begin{aligned} j_A\Big|_{x_0} &= -2\eta a\left(\mathcal{N}\overline{C}\ell\right)\left(\frac{M_A}{N_A}\right)\frac{d(\mathcal{N}_A/\mathcal{N})}{dx}\Big|_{x_0} \\ &= -2\eta a(\overline{C}\ell)\rho\frac{dm_A}{dx}\Big|_{x_0} \end{aligned} \tag{11.32}$$

(see also Problem 11.6.) Thus, we identify

$$\mathcal{D}_{AA'} = (2\eta a)\overline{C}\ell \tag{11.33}$$

and Fick's law takes the form

$$j_A = -\rho\mathcal{D}_{AA'}\frac{dm_A}{dx} \tag{11.34}$$

The constant, ηa, in eqn. (11.33) can be fixed only with the help of a more detailed kinetic theory calculation [11.2], the result of which is given in Section 11.4.

Other Aspects of Diffusion

Fick's law has been verified experimentally low density gases and in dilute liquid solutions, but for liquids the diffusion coefficient is found to depend significantly on the concentration of the diffusing species. In part, the concentration dependence of liquid diffusion coefficients reflects the inadequacy of the concentration gradient in representing the driving force for diffusion in nondilute solutions. Gradients in the chemical potential actually drive diffusion. In concentrated liquid solutions, those gradients are not equivalent to concentration gradients [11.3, 11.4].

The choice of j_i and m_i for the description of diffusion is really somewhat arbitrary. The molar diffusion flux, J_i^*, and the mole fraction, x_i, are often used instead, in which case Fick's law reads

$$\boxed{\vec{J}_i^{\,*} = -c\mathcal{D}_{im}\nabla x_i} \tag{11.35}$$

Obtaining eqn. (11.35) from eqn. (11.28) for a binary mixture is left as an exercise (Problem 11.4).

Mass diffusion need not always arise from concentration gradients, although they are of primary importance. For example, temperature gradients can induce mass diffusion in a process known as *thermal diffusion* or the *Soret effect*. The diffusional mass flux resulting from both temperature and concentration gradients in a binary mixture is then [11.2]

$$\vec{j}_i = -\rho \mathcal{D}_{12} \left[\nabla m_1 + \frac{M_1 M_2}{M^2} k_T \nabla \ln(T) \right] \tag{11.36}$$

where k_T is called the *thermal diffusion ratio* and is generally quite small. Thermal diffusion is occasionally used in chemical separation processes. Pressure gradients and body forces acting unequally on the different species can also cause diffusion; again, these effects are normally small. A related phenomenon is the generation of a heat flux by concentration gradients (as distinct from heat convected by diffusing mass), called the *diffusion-thermo* or *Dufour effect*.

In this chapter, we deal only with mass transfer produced by concentration gradients.

11.4 Transport properties of mixtures

The diffusion coefficient is clearly the key transport property in a mass transfer problem. The analysis of mass transfer, however, is seldom done in isolation from the analysis of concurrent fluid-flow and heat transfer processes. Since mass transfer always involves mixtures, we must therefore be able to obtain not only a mixture's diffusion coefficient, but also its viscosity and thermal conductivity. These three transport properties generally depend upon the mixture's local temperature and pressure *and* its local composition.

Direct experimental measurements of the transport properties are preferable to predicted values, but such data are often unavailable. Thus, we usually use theoretical predictions or experimental correlations to calculate mixture properties. Effective theories exist for the transport properties of dilute gases, but the theoretical framework for calculating liquid properties is weaker. In this section, we discuss methods for computing $\mathcal{D}_{im}$, k, and ν in gas mixtures using equations from kinetic theory—particularly the Chapman-Enskog theory (treated in greater detail in [11.2], [11.3], and [11.5]). We also consider some methods for computing $\mathcal{D}_{12}$ in dilute liquid solutions.

The diffusion coefficient for binary gas mixtures

As a starting point, we return to the self-diffusion coefficient obtained from the simple model of a dilute gas, eqn. (11.33). This result involves an average molecular speed, which can be approximated by Maxwell's equilibrium formula (see, e.g., [11.5]):

$$\overline{C} = \left(\frac{8k_{\mathrm{B}}N_A T}{\pi M}\right)^{1/2} \tag{11.37}$$

If we also assume rigid spherical molecules, then the mean free path takes the form

$$\ell = \frac{1}{\pi\sqrt{2}\mathcal{N}d^2} = \frac{k_{\mathrm{B}}T}{\pi\sqrt{2}d^2 p} \tag{11.38}$$

where d is the effective molecular diameter. Substituting these values of $\overline{C}$ and ℓ in eqn. (11.33) and applying a kinetic theory calculation that shows $2\eta a = 1/2$, we find

$$\begin{aligned}\mathcal{D}_{AA'} &= (2\eta a)\overline{C}\ell \\ &= \frac{(k_{\mathrm{B}}/\pi)^{3/2}}{d^2}\left(\frac{N_A}{M}\right)^{1/2}\frac{T^{3/2}}{p}\end{aligned} \tag{11.39}$$

The diffusion coefficient varies as p^{-1} and $T^{3/2}$, based on the simple model for self-diffusion.

Actual molecules are not hard spheres, nor do molecules of all species have the same size. Moreover, the mixture itself may not be of uniform temperature and pressure. The Chapman-Enskog kinetic theory, taking all these factors into account [11.3], gives the following result for non-polar molecules:

$$\mathcal{D}_{AB} = \frac{(1.8583\times 10^{-7})T^{3/2}}{p\Omega_D^{AB}(T)}\sqrt{\frac{1}{M_A}+\frac{1}{M_B}}$$

where the units of p, T, and $\mathcal{D}_{AB}$ are atm, K, and m^2/s, respectively. The function $\Omega_D^{AB}(T)$ describes the collisions between molecules of A and B. It depends, in general, on the specific type of molecules involved and the temperature.

The type of molecule matters because of the intermolecular forces of attraction and repulsion that arise when molecules collide. A good approximation to those forces is given by the Lennard-Jones intermolecular potential (see Fig. 11.5.) This potential is based on two parameters, a

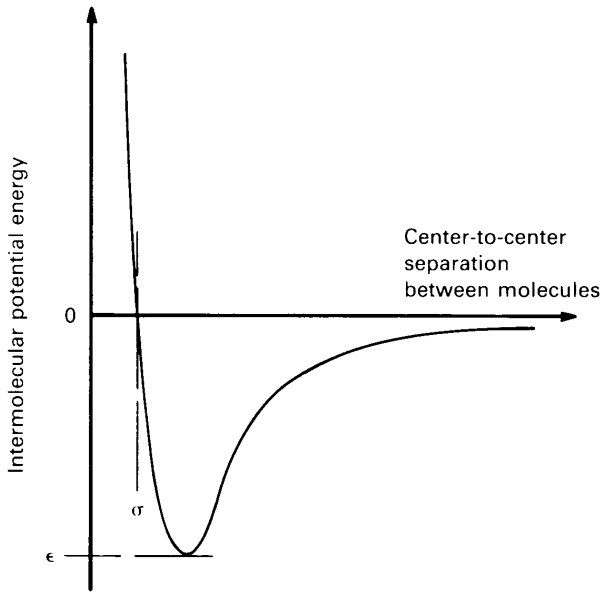

Figure 11.5 The Lennard-Jones potential.

molecular diameter, σ, and the *potential well depth*, ε. The potential well depth is the energy required to separate two molecules from one another. Both constants can be inferred from physical property data. Some values are given in Table 11.1 together with the associated molecular weights (from [11.6], with values for calculating the diffusion coefficients of water from [11.7]).

An accurate approximation to $\Omega_D^{AB}(T)$ can be obtained using the Lennard-Jones potential function. The result is

$$\Omega_D^{AB}(T) = \sigma_{AB}^2 \, \Omega_D(k_b T/\varepsilon_{AB})$$

where, the *collision cross section*, σ_{AB}, may be viewed as an effective molecular diameter for collisions of A and B. If σ_A and σ_B are the cross-sectional diameters of A and B, in Å, then

$$\sigma_{AB} = (\sigma_A + \sigma_B)/2 \tag{11.40}$$

The *collision integral*, Ω_D is a result of kinetic theory calculations calculations based on the Lennard-Jones potential. Table 11.2 gives values of Ω_D from [11.8]. The effective potential well depth for collisions of A and B is

$$\varepsilon_{AB} = \sqrt{\varepsilon_A \varepsilon_B} \tag{11.41}$$

Table 11.1 Lennard-Jones constants and molecular weights of selected species

Species	σ (Å)	ε/k_B (K)	$M\left(\frac{\text{kg}}{\text{kmol}}\right)$	*Species*	σ (Å)	ε/k_B (K)	$M\left(\frac{\text{kg}}{\text{kmol}}\right)$
Al	2.655	2750	26.98	H_2	2.827	59.7	2.016
Air	3.711	78.6	28.96	H_2O	2.655[a]	363[a]	18.02
Ar	3.542	93.3	39.95	H_2O	2.641[b]	809.1[b]	
Br_2	4.296	507.9	159.8	H_2O_2	4.196	289.3	34.01
C	3.385	30.6	12.01	H_2S	3.623	301.1	34.08
CCl_2F_2	5.25	253	120.9	He	2.551	10.22	4.003
CCl_4	5.947	322.7	153.8	Hg	2.969	750	200.6
CH_3OH	3.626	481.8	32.04	I_2	5.160	474.2	253.8
CH_4	3.758	148.6	16.04	Kr	3.655	178.9	83.80
CN	3.856	75.0	26.02	Mg	2.926	1614	24.31
CO	3.690	91.7	28.01	NH_3	2.900	558.3	17.03
CO_2	3.941	195.2	44.01	N_2	3.798	71.4	28.01
C_2H_6	4.443	215.7	30.07	N_2O	3.828	232.4	44.01
C_2H_5OH	4.530	362.6	46.07	Ne	2.820	32.8	20.18
CH_3COCH_3	4.600	560.2	58.08	O_2	3.467	106.7	32.00
C_6H_6	5.349	412.3	78.11	SO_2	4.112	335.4	64.06
Cl_2	4.217	316.0	70.91	Xe	4.047	231.0	131.3
F_2	3.357	112.6	38.00				

[a] Based on mass diffusion data.
[b] Based on viscosity and thermal conductivity data.

Hence, we may calculate the binary diffusion coefficient from

$$\boxed{\mathcal{D}_{AB} = \frac{(1.8583 \times 10^{-7}) T^{3/2}}{p \sigma_{AB}^2 \Omega_D} \sqrt{\frac{1}{M_A} + \frac{1}{M_B}}} \qquad (11.42)$$

where, again, the units of p, T, and $\mathcal{D}_{AB}$ are atm, K, and m^2/s, respectively, and σ_{AB} is in Å.

Equation (11.42) indicates that the diffusivity varies as p^{-1} and is independent of mixture composition, just as the simple model indicated that it should. The temperature dependence of Ω_D, however, increases the overall temperature dependence of $\mathcal{D}_{AB}$ from $T^{3/2}$, as suggested by eqn. (11.39), to approximately $T^{7/4}$.

Table 11.2 Collision integrals for diffusivity, viscosity, and thermal conductivity based on the Lennard-Jones potential

$k_B T/\varepsilon$	Ω_D	$\Omega_\mu = \Omega_k$	$k_B T/\varepsilon$	Ω_D	$\Omega_\mu = \Omega_k$
0.30	2.662	2.785	2.70	0.9770	1.069
0.35	2.476	2.628	2.80	0.9672	1.058
0.40	2.318	2.492	2.90	0.9576	1.048
0.45	2.184	2.368	3.00	0.9490	1.039
0.50	2.066	2.257	3.10	0.9406	1.030
0.55	1.966	2.156	3.20	0.9328	1.022
0.60	1.877	2.065	3.30	0.9256	1.014
0.65	1.798	1.982	3.40	0.9186	1.007
0.70	1.729	1.908	3.50	0.9120	0.9999
0.75	1.667	1.841	3.60	0.9058	0.9932
0.80	1.612	1.780	3.70	0.8998	0.9870
0.85	1.562	1.725	3.80	0.8942	0.9811
0.90	1.517	1.675	3.90	0.8888	0.9755
0.95	1.476	1.629	4.00	0.8836	0.9700
1.00	1.439	1.587	4.10	0.8788	0.9649
1.05	1.406	1.549	4.20	0.8740	0.9600
1.10	1.375	1.514	4.30	0.8694	0.9553
1.15	1.346	1.482	4.40	0.8652	0.9507
1.20	1.320	1.452	4.50	0.8610	0.9464
1.25	1.296	1.424	4.60	0.8568	0.9422
1.30	1.273	1.399	4.70	0.8530	0.9382
1.35	1.253	1.375	4.80	0.8492	0.9343
1.40	1.233	1.353	4.90	0.8456	0.9305
1.45	1.215	1.333	5.00	0.8422	0.9269
1.50	1.198	1.314	6.00	0.8124	0.8963
1.55	1.182	1.296	7.0	0.7896	0.8727
1.60	1.167	1.279	8.0	0.7712	0.8538
1.65	1.153	1.264	9.0	0.7556	0.8379
1.70	1.140	1.248	10.0	0.7424	0.8242
1.75	1.128	1.234	20.0	0.6640	0.7432
1.80	1.116	1.221	30.0	0.6232	0.7005
1.85	1.105	1.209	40.0	0.5960	0.6718
1.90	1.094	1.197	50.0	0.5756	0.6504
1.95	1.084	1.186	60.0	0.5596	0.6335
2.00	1.075	1.175	70.0	0.5464	0.6194
2.10	1.057	1.156	80.0	0.5352	0.6076
2.20	1.041	1.138	90.0	0.5256	0.5973
2.30	1.026	1.122	100.0	0.5170	0.5882
2.40	1.012	1.107	200.0	0.4644	0.5320
2.50	0.9996	1.093	300.0	0.4360	0.5016
2.60	0.9878	1.081	400.0	0.4172	0.4811

Air, by the way, can be treated as a single substance in Table 11.1 owing to the similarity of its two main constituents, N_2 and O_2.

Example 11.3

Compute $\mathcal{D}_{AB}$ for the diffusion of hydrogen in air at 0°C and 1 atm.

SOLUTION. Let air be species A and H_2 be species B. Then we read from Table 11.1

$$\sigma_A = 3.711 \text{ Å}, \quad \sigma_B = 2.827 \text{ Å}, \quad \frac{\varepsilon_A}{k_B} = 79 \text{ K}, \quad \frac{\varepsilon_B}{k_B} = 60 \text{ K}$$

and calculate these values

$$\sigma_{AB} = (3.711 + 2.827)/2 = 3.269 \text{ Å}$$
$$\varepsilon_{AB}/k_B = \sqrt{79(60)} = 68.9 \text{ K}$$

Hence, $k_B T/\varepsilon_{AB} = 3.967$, and $\Omega_D = 0.8853$ from Table 11.2. Then

$$\mathcal{D}_{AB} = \frac{(1.8583 \times 10^{-7})(273.15)^{3/2}}{(1)(3.269)^2(0.8853)} \sqrt{\frac{1}{2.016} + \frac{1}{28.97}} \text{ m}^2/\text{s}$$
$$= 6.46 \times 10^{-5} \text{ m}^2/\text{s}$$

An experimental value [11.9] is 6.34×10^{-5} m^2/s, so the prediction is high by only 2%. ■

Limitations of the diffusion coefficient prediction. Equation (11.42) is not valid for all gas mixtures. We have already noted that concentration gradients cannot be too steep; thus, it cannot be applied in, say, the interior of a shock wave when the Mach number is significantly greater than unity. Furthermore, the gas must be dilute, and its molecules should be, in theory, nonpolar, approximately spherically symmetric, and monatomic.

Figure 11.6 compares values of $\mathcal{D}_{12}$ calculated using eqn. (11.42) with data from [11.10]. It includes data for binary mixtures of monatomic, polyatomic, nonpolar, and polar gases of the sort appearing in Table 11.1. In most cases, eqn. (11.42) represents the data within about 7 percent. Better results can be obtained by using values of σ_{AB} and ε_{AB} that have been fit specifically to the pair of gases involved [11.11, Chap. 11], rather than using eqns. (11.40) and (11.41), or by constructing a mixture-specific equation for $\Omega_D^{AB}(T)$.

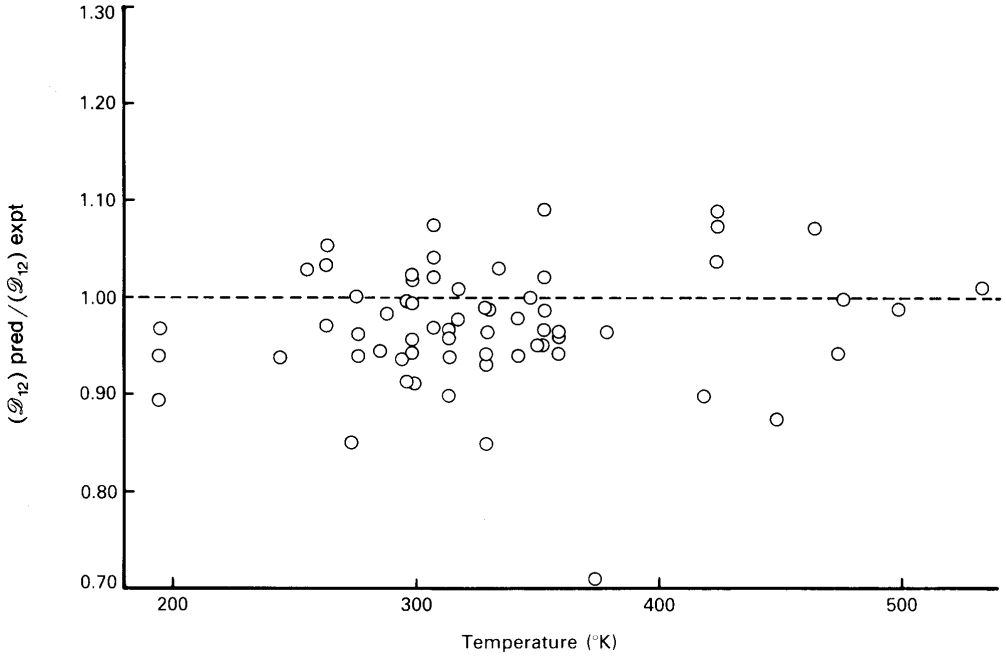

Figure 11.6 Kinetic theory prediction of diffusion coefficients compared with experimental data from [11.10].

A gas is called dilute if its molecules interact with one another only during brief collisions and if collisions of more than two molecules are so infrequent that they can be ignored. Such gases are of course those having a low density. Childs and Hanley [11.12] suggested that the transport properties of gases are within 1% of the dilute values if the gas densities do not exceed the following limiting value

$$\rho_{\max} = 22.93M/\sigma^3\Omega_\mu \tag{11.43}$$

Here, σ (the collision cross section of the gas) and ρ are expressed in Å and kg/m^3, and Ω_μ—a second collision integral for viscosity—is included in Table 11.2. Equation (11.43) normally gives $\rho_{\max}$ values that correspond to pressures substantially above 1 atm.

At higher densities, the transport properties can be estimated by a variety of techniques, such as corresponding states theories, absolute reaction-rate theories, or modified Enskog theories [11.11, Chap. 6] (also see [11.3, 11.10, 11.13]). Conversely, if the gas density is so very *low* that

the a mean free path is on the order of the dimensions of the system, we have what is called *free molecule flow* and the present kinetic models are invalid (see, e.g., [11.14]).

Diffusion coefficients for multicomponent gases

Thus far, we have indicated that the effective binary diffusivity, $\mathcal{D}_{im}$, can be used to represent the diffusion of species i into a mixture m. The preceding analyses, however, are strictly applicable only to the prediction of the diffusion of one pure substance through another. Different equations are needed when there are three or more species present.

If a low concentration of species i diffuses into a homogeneous mixture of n species, then $\vec{J}_j^{\,*} \cong 0$ for $j \neq i$, and one may show (Problem 11.14) that

$$\mathcal{D}_{im}^{-1} = \sum_{\substack{j=1 \\ j \neq i}}^{n} \frac{x_j}{\mathcal{D}_{ij}} \tag{11.44}$$

where $\mathcal{D}_{ij}$ is the binary diffusion coefficient for species i and j alone. This rule is sometimes called *Blanc's law* [11.10].

If a mixture includes several trace gases and one dominant species, A, then the diffusion coefficients of the trace species are approximately the same as they would be if the other traces were not present. In other words, for any particular trace species i,

$$\mathcal{D}_{im} \cong \mathcal{D}_{iA} \tag{11.45}$$

Finally, if the binary diffusion coefficient has the same value for each pair of species in a mixture, then one may show (Problem 11.14) that $\mathcal{D}_{im} = \mathcal{D}_{ij}$.

Diffusion coefficients for binary liquid mixtures

Each molecule in a liquid is always in contact with several neighboring molecules, and a kinetic theory like that used in gases, which relies on detailed descriptions of two-molecule collisions, is no longer feasible. Most of the available predictions of liquid phase diffusion coefficients involve correlations of experimental measurements within a semitheoretical framework.

For a dilute solution of substance A in liquid B, the so-called *hydrodynamic model* has met some success. It begins with the result

$$\mathcal{D}_{AB} = k_B T \, (v_A / F_A) \tag{11.46}$$

where v_A is the steady average velocity of molecules of A relative to the liquid B, and F_A is the force acting on a molecule of A. Equation (11.46) represents diffusion caused by random molecular motions, so-called *Brownian motion*. It can be derived from kinetic and thermodynamic arguments such as those given by Einstein [11.15] and Sutherland [11.16] and is usually called the *Nernst-Einstein equation*. The ratio v_A/F_A is called the *mobility* of A.

To evaluate the mobility of a molecular (or a particulate) solute, we may apply *Stokes' law* [11.17], which gives the drag on a sphere at low Reynolds numbers ($\mathrm{Re_D} < 1$) as

$$F_A = 6\pi\mu_B v_A R_A \left(\frac{1 + 2\mu_B/\beta R_A}{1 + 3\mu_B/\beta R_A} \right) \tag{11.47}$$

Here, R_A is the radius of sphere A and β is a coefficient of "sliding" friction, for a friction force proportional to the velocity. Substituting eqn. (11.47) in eqn. (11.46), we get

$$\frac{\mathcal{D}_{AB}\mu_B}{T} = \frac{k_B}{6\pi R_A} \left(\frac{1 + 3\mu_B/\beta R_A}{1 + 2\mu_B/\beta R_A} \right) \tag{11.48}$$

This model is valid if the concentration of solute A is so low that the molecules of A do not interact with one another.

For viscous liquids one usually assumes that no slip occurs between the liquid and a solid surface that it touches; but, for particles whose size is on the order of the molecular spacing of the solvent molecules, some slip may well occur. This is the reason for the unfamiliar factor in parentheses on the right side of eqn. (11.47). For large solute particles, no slip should occur, so $\beta \longrightarrow \infty$ and the factor in parentheses tends to one, as expected. Equation (11.48) then reduces to[6]

$$\frac{\mathcal{D}_{AB}\mu_B}{T} = \frac{k_B}{6\pi R_A} \tag{11.49a}$$

[6]Equation (11.49a) was first presented by Einstein in May 1905. The more general form, eqn. (11.48), was presented independently by Sutherland in June 1905. Equations (11.48) and (11.49a) are commonly called the *Stokes-Einstein* equation, although Stokes had no hand in applying eqn. (11.47) to diffusion. It might therefore be argued that eqn. (11.48) should be called the *Sutherland-Einstein* equation.

For smaller molecules—close in size to those of the solvent—we expect that $\beta \longrightarrow 0$, leading to [11.18]

$$\frac{\mathcal{D}_{AB}\mu_B}{T} = \frac{k_\mathrm{B}}{4\pi R_A} \tag{11.49b}$$

The most important feature of eqns. (11.48), (11.49a), and (11.49b) is that so long as the solute is dilute, the primary determinant of the group $\mathcal{D}\mu/T$ is the size of the diffusing species, with a secondary dependence on intermolecular forces (e.g., on β.) More complex theories, such as the absolute reaction-rate theory of Eyring [11.19], lead to the same dependence. Moreover, experimental studies of dilute solutions verify that the group $\mathcal{D}\mu/T$ is essentially temperature-independent for a given solute-solvent pair, wiht the only exception occuring in very high viscosity solutions. Thus, most correlations of experimental data have used some form of eqn. (11.48) as a starting point.

Many such correlations have been developed. One fairly successful correlation is due to King, Hsueh, and Mao [11.20]. They expressed the molecular size in terms of molal volumes at the normal boiling point, $V_{m,A}$ and $V_{m,B}$, and accounted for intermolecular association forces using the latent heats of vaporization at the normal boiling point, $h_{fg,A}$ and $h_{fg,B}$. They obtained

$$\frac{\mathcal{D}_{AB}\mu_B}{T} = (4.4\times10^{-15})\left(\frac{V_{m,B}}{V_{m,A}}\right)^{1/6}\left(\frac{h_{fg,B}}{h_{fg,A}}\right)^{1/2} \tag{11.50}$$

which is accurate within an rms error of 19.5% and where the units of $\mathcal{D}_{AB}\mu_B/T$ are kg·m/ K·s^2. Values of h_{fg} and V_m are given for various substances in Table 11.3. Equation (11.50) is valid for nonelectrolytes at high dilution, and it appears to be satisfactory for both polar and nonpolar substances. The difficulties the authors encountered with polar solvents of high viscosity led them to limit eqn. (11.50) to values of $\mathcal{D}\mu/T < 1.5\times10^{-14}$ kg·m/ K·s^2. The predictions of eqn. (11.50) are compared with experimental data from [11.10] in Fig. 11.7. Reid, Prausnitz, and Poling [11.10] review several other liquid-phase correlations and provide an assessment of their accuracies.

The thermal conductivity and viscosity of dilute gases

In any convective mass transfer problem, we must know the viscosity of the fluid and, if heat is also being transferred, we must also know its

Table 11.3 Molal specific volumes and latent heats of vaporization for selected substances at their normal boiling points

Substance	V_m (m^3/kmol)	h_{fg}(MJ/kmol)
Methanol	0.042	35.53
Ethanol	0.064	39.33
n-Propanol	0.081	41.97
Isopropanol	0.072	40.71
n-Butanol	0.103	43.76
tert-Butanol	0.103	40.63
n-Pentane	0.118	25.61
Cyclopentane	0.100	27.32
Isopentane	0.118	24.73
Neopentane	0.118	22.72
n-Hexane	0.141	28.85
Cyclohexane	0.117	33.03
n-Heptane	0.163	31.69
n-Octane	0.185	34.14
n-Nonane	0.207	36.53
n-Decane	0.229	39.33
Carbon tetrachloride	0.102	29.93
Nitromethane	0.056	25.44
Ethyl bromide	0.075	27.41
Acetone	0.074	28.90
Benzene	0.096	30.76
Water	0.0187	40.62

thermal conductivity. Accordingly, we now consider the calculation of μ and k for mixtures of gases.

Two of the most important results of the kinetic theory of gases are the predictions of μ and k for a pure, monatomic gas of species A:

$$\mu_A = \left(2.6693 \times 10^{-6}\right) \frac{\sqrt{M_A T}}{\sigma_A^2 \Omega_\mu} \tag{11.51}$$

and

$$k_A = \frac{0.083228}{\sigma_A^2 \Omega_k} \sqrt{T/M_A} \tag{11.52}$$

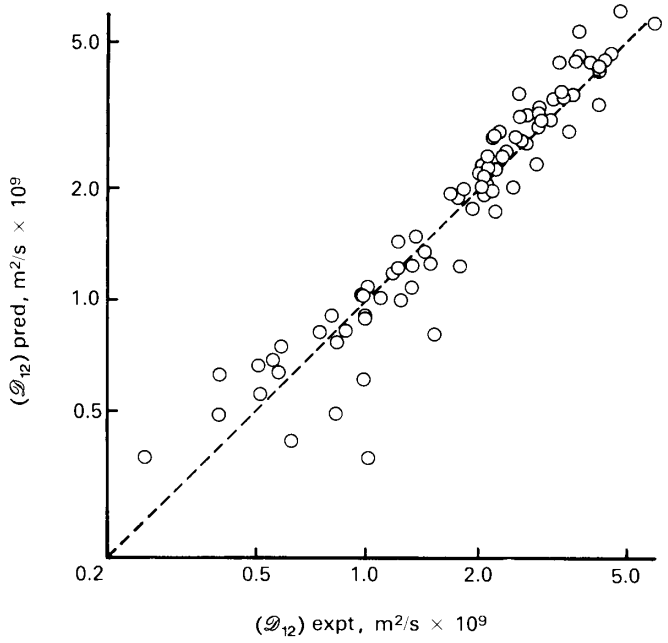

Figure 11.7 Comparison of liquid diffusion coefficients predicted by eqn. (11.50) with experimental values for assorted substances from [11.10].

where Ω_μ and Ω_k are collision integrals for the viscosity and thermal conductivity. In fact, Ω_μ and Ω_k are equal to one another, but they are different from Ω_D. In these equations μ is in kg/m·s, k is in W/m·K, T is in kelvin, and σ_A, has units of Å.

The equation for μ_A applies equally well to polyatomic gases, but k_A must be corrected to account for internal modes of energy storage—chiefly molecular rotation and vibration. Eucken (see, e.g., [11.5]) gave a simple analysis showing that this correction was

$$k = \left(\frac{9\gamma - 5}{4\gamma}\right)\mu c_p \tag{11.53}$$

for an ideal gas, where $\gamma \equiv c_p/c_v$. You may recall from your thermodynamics courses that γ is 5/3 for monatomic gases, 7/5 for diatomic gases at modest temperatures, and approaches unity for very complex molecules. Equation (11.53) should be used with tabulated data for c_p; on average, it will underpredict k by perhaps 10 to 20% [11.10].

An approximate formula for μ for multicomponent gas mixtures was developed by Wilke [11.21], based on the kinetic theory of gases. He introduced certain simplifying assumptions and obtained, for the mixture viscosity,

$$\boxed{\mu_m = \sum_{i=1}^{n} \frac{x_i \mu_i}{\sum_{j=1}^{n} x_j \phi_{ij}}} \tag{11.54}$$

where

$$\phi_{ij} = \frac{\left[1 + (\mu_i/\mu_j)^{1/2} (M_j/M_i)^{1/4}\right]^2}{2\sqrt{2}\left[1 + (M_i/M_j)\right]^{1/2}}$$

The analogous equation for the thermal conductivity of mixtures was developed by Mason and Saxena [11.22]:

$$\boxed{k_m = \sum_{i=1}^{n} \frac{x_i k_i}{\sum_{j=1}^{n} x_j \phi_{ij}}} \tag{11.55}$$

(We have followed [11.10] in omitting a minor empirical correction factor proposed by Mason and Saxena.)

Equation (11.54) is accurate to about 2 % and eqn. (11.55) to about 4% for mixtures of nonpolar gases. For higher accuracy or for mixtures with polar components, refer to [11.10, 11.11].

Example 11.4

Compute the transport properties of normal air at 300 K.

SOLUTION. The mass composition of air was given in Example 11.1. Using the methods of Example 11.1, we obtain the mole fractions as $x_{N_2} = 0.7808$, $x_{O_2} = 0.2095$, and $x_{Ar} = 0.0093$.

We first compute μ and k for the three species to illustrate the use of eqns. (11.51) to (11.53), although we could simply use tabled data in eqns. (11.54) and (11.55). From Tables 11.1 and 11.2, we obtain

Species	σ (Å)	ε/k_B (K)	M	Ω_μ
N_2	3.798	71	28.02	0.9588
O_2	3.467	107	32.00	1.058
Ar	3.542	93	39.95	1.020

Substitution of these values into eqn. (11.51) yields

Species	$\mu_{\text{calc.}}$ (kg/m·s)	μ_{expt} (kg/m·s)
N_2	1.770×10^{-5}	1.784×10^{-5}
O_2	2.057×10^{-5}	2.063×10^{-5}
Ar	2.284×10^{-5}	2.29×10^{-5}

where we show experimental values from Appendix A for comparison. We then read c_p from Appendix A and use eqn. (11.52) and (11.53) to get the thermal conductivities of the components:

Species	c_p (J/kg·K)	k_{calc} (W/m·K)	k_{expt} (W/m·K)
N_2	1040.8	0.02500	0.0259
O_2	920.3	0.02569	0.02676
Ar	521.6	0.01782	0.01766

The predictions are thus accurate within about 1% for μ and within about 4% for k.

To compute μ_m and k_m, we use eqns. (11.54) and (11.55) and the experimental values of μ and k. Identifying N_2, O_2, and Ar as species 1, 2, and 3, we get

$$\begin{aligned} \phi_{12} &= 0.9931, \quad \phi_{21} = 1.006 \\ \phi_{13} &= 1.046, \quad \phi_{31} = 0.9418 \\ \phi_{23} &= 1.057, \quad \phi_{32} = 0.9401 \end{aligned}$$

and $\phi_{ii} = 1$. The sums appearing in the denominators are

$$\sum x_j \phi_{ij} = \begin{cases} 0.9986 & \text{for} \quad i = 1 \\ 1.005 & \text{for} \quad i = 2 \\ 0.9416 & \text{for} \quad i = 3 \end{cases}$$

When they are substituted in eqns. (11.54) and (11.55), these values give

$$\mu_{m,\text{calc}} = 1.848 \times 10^{-5}\ \text{kg/m·s}, \quad \mu_{m,\text{expt}} = 1.853 \times 10^{-5}\ \text{kg/m·s}$$
$$k_{m,\text{calc}} = 0.02600\ \text{W/m·K}, \quad k_{m,\text{expt}} = 0.02614\ \text{W/m·K}$$

so the mixture values are also predicted within 3 and 5%, respectively.

Finally, we need c_{p_m} to compute the Prandtl number of the mixture. This is merely the mass weighted average of c_p, or $\sum_i m_i c_{p_i}$, and it is equal to 1006 J/kg·K. Then

$$\text{Pr} = (\mu c_p/k)_m = (1.848 \times 10^{-5})(1006)/0.02600 = 0.715.$$

This is only 0.3% above the tabled value of 0.713. The reader may wish to compare these values with those obtained directly using the values for air in Table 11.1 or to explore the effects of neglecting argon in the preceding calculations. ■

11.5 The equation of species conservation

Conservation of species

Just as we formed an equation of energy conservation in Chapter 6, we now form an equation of *species conservation* that applies to each substance in a mixture. In addition to accounting for the convection and diffusion of each species, we must allow the possibility that a particular species is created or destroyed by chemical reactions occuring in the bulk medium (so-called *homogeneous reactions*). Reactions on surfaces surrounding the medium (*heterogeneous reactions*) would be accounted for using boundary conditions.

We consider, in the usual way, an arbitrary control volume, R, with a boundary, S, as shown in Fig. 11.8. The control volume is fixed in space, with fluid moving through it. Species i may accumulate in R, it may travel in and out of R by bulk convection or by diffusion, and it may be created within R by homogeneous reactions. The rate of creation of species i is denoted as $\dot{r}_i$(kg/m^3·s); since chemical reactions conserve mass, the net mass creation is $\dot{r} = \sum \dot{r}_i = 0$. The rate of change of species i in R is then

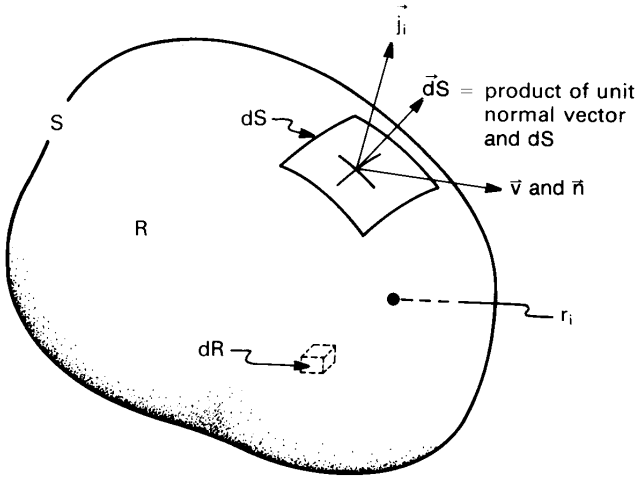

Figure 11.8 Control volume in a fluid-flow and mass-diffusion field.

described by the following balance:

$$\underbrace{\frac{d}{dt}\int_R \rho_i \, dR}_{\substack{\text{rate of increase} \\ \text{of } i \text{ in } R}} = -\int_S \vec{n}_i \cdot d\vec{S} + \int_R \dot{r}_i \, dR$$

$$= -\underbrace{\int_S \rho_i \vec{v} \cdot d\vec{S}}_{\substack{\text{rate of convection} \\ \text{of } i \text{ out of } R}} - \underbrace{\int_S \vec{j}_i \cdot d\vec{S}}_{\substack{\text{diffusion of } i \\ \text{out of } R}} + \underbrace{\int_R \dot{r}_i \, dR}_{\substack{\text{rate of creation} \\ \text{of } i \text{ in } R}} \qquad (11.56)$$

This species conservation statement is identical to our energy conservation statement, eqn. (6.36) on page 279, except that mass of species i has taken the place of energy and heat.

We may convert the surface integrals to volume integrals using Gauss's theorem [eqn. (2.8)] and rearrange the result to find:

$$\int_R \left[\frac{\partial \rho_i}{\partial t} + \nabla \cdot (\rho_i \vec{v}) + \nabla \cdot \vec{j}_i - \dot{r}_i \right] dR = 0 \qquad (11.57)$$

Since the control volume is selected arbitrarily, the integrand must be identically zero. Thus, we obtain the general form of the species conservation equation:

$$\boxed{\frac{\partial \rho_i}{\partial t} + \nabla \cdot (\rho_i \vec{v}) = -\nabla \cdot \vec{j}_i + \dot{r}_i} \qquad (11.58)$$

We may obtain a mass conservation equation for the entire mixture by summing eqn. (11.58) over all species and applying eqns. (11.1), (11.17), and (11.22) and the requirement that there be no net creation of mass:

$$\sum_i \left[\frac{\partial \rho_i}{\partial t} + \nabla \cdot (\rho_i \vec{v}) \right] = \sum_i (-\nabla \cdot \vec{j}_i + \dot{r}_i)$$

so that

$$\frac{\partial \rho}{\partial t} + \nabla \cdot (\rho \vec{v}) = 0 \tag{11.59}$$

This equation applies any mixture, including those with varying density (see Problem 6.36).

Incompressible mixtures. For an incompressible mixture, $\nabla \cdot \vec{v} = 0$ (see Sect. 6.2 or Problem 11.22), and the second term in eqn. (11.58) can be written

$$\nabla \cdot (\rho_i \vec{v}) \equiv \vec{v} \cdot \nabla \rho_i + \rho_i \underbrace{\nabla \cdot \vec{v}}_{=0} = \vec{v} \cdot \nabla \rho_i \tag{11.60}$$

We may compare the resulting, incompressible species equation to the incompressible energy equation, eqn. (6.37)

$$\frac{D\rho_i}{Dt} = \frac{\partial \rho_i}{\partial t} + \vec{v} \cdot \nabla \rho_i = -\nabla \cdot \vec{j}_i + \dot{r}_i \tag{11.61}$$

$$\rho c_p \frac{DT}{Dt} = \rho c_p \left(\frac{\partial T}{\partial t} + \vec{v} \cdot \nabla T \right) = -\nabla \cdot \vec{q} + \dot{q} \tag{6.37}$$

We see, then, that: the reaction term, $\dot{r}_i$, is analogous to the heat generation term, $\dot{q}$; the diffusional mass flux, $\vec{j}_i$, is analogous to the heat flux, $\vec{q}$; and that $d\rho_i = \rho \, dm_i$ is analogous to $\rho c_p dT$.

We can use Fick's law to eliminate $\vec{j}_i$ in eqn. (11.61). If the product $(\rho \mathcal{D}_{im})$ is independent of (x, y, z)—if it is spatially uniform—then eqn. (11.61) becomes

$$\boxed{\frac{D}{Dt} m_i = \mathcal{D}_{im} \nabla^2 m_i + \dot{r}_i / \rho} \tag{11.62}$$

where the substantial derivative, D/Dt, is defined in eqn. (6.38). If, instead, ρ and $\mathcal{D}_{im}$ are *each* spatially uniform, then

$$\frac{D\rho_i}{Dt} = \mathcal{D}_{im}\nabla^2\rho_i + \dot{r}_i \tag{11.63}$$

The equation of species conservation and its particular forms may also be stated in molar form, using c_i or x_i, N_i, and J_i^* (see Problem 11.24.) Molar analysis sometimes has advantages over mass-based analysis, as we discover in Section 11.6.

Interfacial boundary conditions

The equation of species conservation, like any differential equation, cannot be solved until boundary conditions are specified. We are already familiar with the general issue of boundary conditions from our study of the heat equation. To find a temperature distribution, we specified temperatures or heat fluxes at the boundaries of the domain of interest. Likewise, to find a concentration distribution, we must specify the concentration or flux of species i at the boundaries of the medium of interest.

The interfaces we consider are always assumed to be in local thermodynamic equilibrium. Thus, for example, temperature is continuous at the interface between two media: the adjacent media cannot have different temperatures at their common boundary because this would violate the Zeroth Law of Thermodynamics. Concentration, on the other hand, need *not* be continuous across an interface, even in a state of thermodynamic equilibrium. Water in a drinking glass, for example, has discontinous a change in the concentration of water at both its interface with the glass and its interface with the air above.

In mass transfer problems, we are normally interested in situations in which the species being transferred has some finite solubility in the media on both sides of an interface. For example, gaseous ammonia is absorbed into water in some types of refrigeration cycles. A gaseous mixture containing some finite mass fraction of ammonia will produce some different mass fraction of ammonia just inside an adjacent body of water, as shown in Fig. 11.9.

To characterize the conditions at such an interface, we introduce imaginary surfaces, s and u, very close to either side of the interface. In the ammonia absorption process, then, we have a mass fraction $m_{\mathrm{NH_3},s}$ on the gas side of the interface and a *different* mass fraction $m_{\mathrm{NH_3},u}$ on the liquid side.

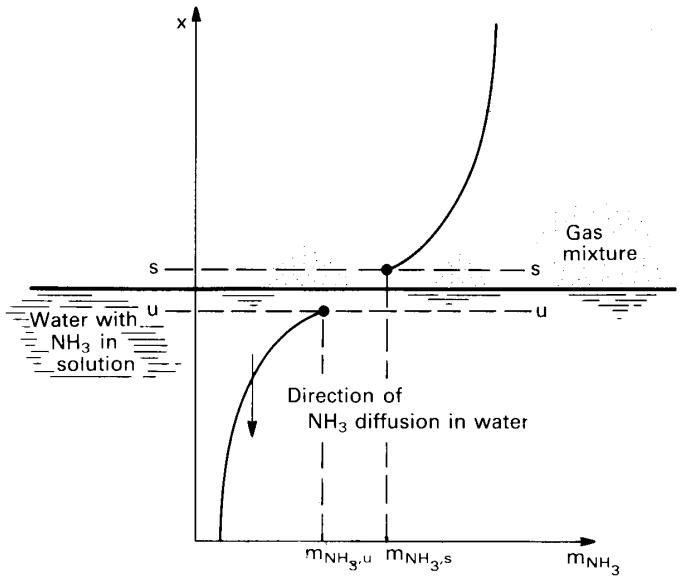

Figure 11.9 Absorption of ammonia into water.

In many mass transfer problems, we must find the concentration distribution of a species in one medium given only its concentration at the interface in the *adjacent* medium. We might wish to find the distribution of ammonia in the body of water knowing only the concentration of ammonia on the gas side of the interface. This would force us to find $m_{\mathrm{NH_3},u}$ from $m_{\mathrm{NH_3},s}$ and the interfacial temperature and pressure, since $m_{\mathrm{NH_3},u}$ is the appropriate boundary condition for the medium in question.

Thus, for the general mass transfer boundary condition, we must specify not only the concentration of species i in the medium adjacent to the medium of interest but also the *solubility* of species i from one medium to the other. The solubility depends on the nature of the media in question, the temperature and pressure, and the concentration of substance i in either medium. Although a detailed study of solubility and phase equilibria is far beyond our scope (see, for example, [11.23]), we illustrate these concepts with the following simple solubility relations.

For a gas mixture in contact with a liquid mixture, two simplified relationships dictate the vapor composition. When the liquid is rich in species i, the partial pressure of species i in the gas phase, p_i, can be

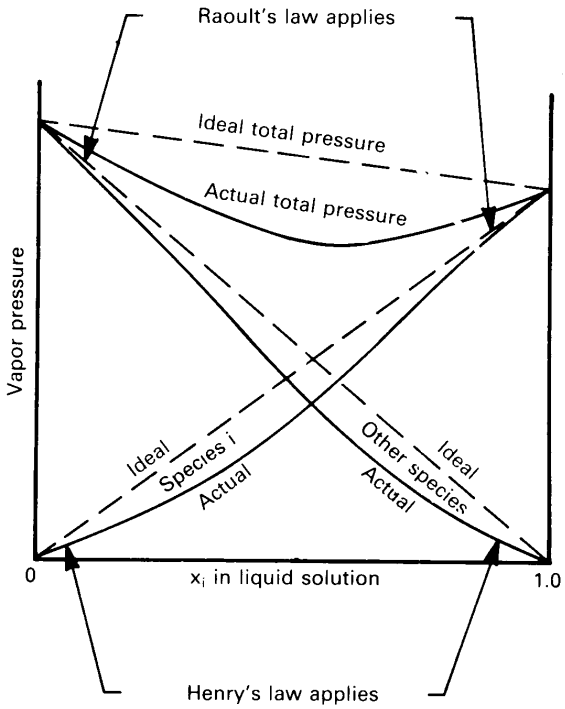

Figure 11.10 Typical partial and total vapor-pressure plot for the vapor in contact with a liquid solution, illustrating the region of validity of Raoult's and Henry's laws.

characterized approximately with *Raoult's law*, which says that

$$p_i = p_{\text{sat},i}\, x_i \tag{11.64}$$

where $p_{\text{sat},i}$ is the saturation pressure of pure i at the interface temperature and x_i is the mole fraction of i in the liquid. When the species i is dilute in the liquid, *Henry's law* applies. It says that

$$p_i = H\, x_i \tag{11.65}$$

where H is an empirical constant that is tabulated in the literature. Figure 11.10 shows how the vapor pressure varies over a liquid mixture and indicates the regions of validity of Raoult's and Henry's laws.

If the vapor pressure were to obey Raoult's law over the entire range of liquid composition, we would have what is called an *ideal solution*. When x_i is much below unity, the ideal solution approximation is usually very poor.

Example 11.5

A tray of water sits outside on a warm day. If the air temperature is 33°C and evaporation cools the water surface to 29°C, what is the concentration of water vapor above the liquid surface?

SOLUTION. Raoult's law applies almost exactly in this situation, since it happens that the concentration of air in water is virtually nil. Thus, $p_{H_2O,s} = p_{sat,H_2O}(29°C)$ by eqn. (11.64). From a steam table, we read $p_{sat}(29°C) = 4.008$ kPa and compute, from eqn. (11.16),

$$x_{H_2O,s} = p_{sat}/p_{atm} = 4.008/101.325 = 0.0396$$

Equation (11.9) gives

$$m_{H_2O,s} = \frac{(0.0396)(18.02)}{[(0.0396)(18.02) + (1 - 0.0396)(28.96)]}$$
$$= 0.0250$$ ■

Stationary media

Let us now focus attention on nonreacting systems for which $\dot{r}_i$ is zero in eqn. (11.62). There are several special cases of this equation.

When there are no reactions and $\vec{v} = 0$, eqn. (11.62) reduces to

$$\frac{\partial m_i}{\partial t} = \mathcal{D}_{im}\nabla^2 m_i \tag{11.66}$$

which is called the *mass diffusion equation* and which has the same form as the equation of heat conduction. Solutions for mass transfer in stationary media are entirely analogous to those for heat conduction when the boundary conditions are the same. Generally, this equation applies in solids or in stationary fluids when the mass flux, $|\vec{n}|$, is very small and transport is purely diffusive.

Example 11.6

A semi-infinite stationary medium (medium 1) has an initially uniform concentration, $m_{i,0}$ of species i. From time $t = 0$ onward, we place the end plane at $x = 0$ in contact with a second medium (medium 2) with a concentration $m_{i,s}$. What is the resulting distribution of species in medium 1?

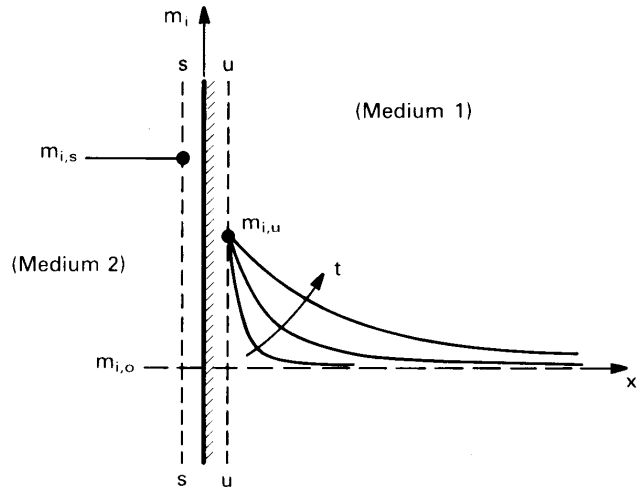

Figure 11.11 Mass diffusion into a semi-infinite stationary medium.

SOLUTION. Once $m_{i,s}$ and the solubility data are known, $m_{i,u}$ can be applied as the boundary condition at $x = 0$ for $t > 0$ (see Fig. 11.11). Our mathematical problem then becomes

$$\frac{\partial m_i}{\partial t} = \mathcal{D}_{im_1} \frac{\partial^2 m_i}{\partial x^2} \tag{11.67}$$

with

$$m_i = m_{i,0} \quad \text{for} \quad t = 0 \quad (\text{all } x)$$
$$m_i = m_{i,u} \quad \text{for} \quad t > 0 \quad (x = 0)$$

This is exactly the mathematical form of the problem of transient heat diffusion to a semi-infinite region (Section 5.6), and its solution is completely analogous to eqn. (5.50):

$$\frac{m_i - m_{i,u}}{m_{i,0} - m_{i,u}} = \text{erf}\left(\frac{x}{2\sqrt{\mathcal{D}_{im_1} t}}\right) \qquad \blacksquare$$

The reader can solve all sorts of steady diffusion problems by direct analogy to the methods of Chapters 4 and 5.

Mass transfer with specified velocity fields

Mass transfer can alter the velocity field in a given situation. This is apparent from the definition of the mass average velocity in eqn. (11.17),

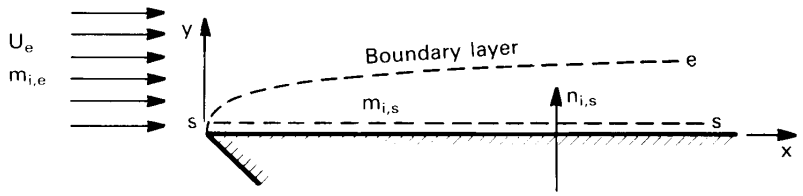

Figure 11.12 Concentration boundary layer on a flat plate.

when species with different velocities and partial densities are present. Mass transfer can drive individual species in a different direction from that of the imposed flow (which is driven by, say, a pressure gradient.) We have noted that the mass flow is composed of contributions of both bulk convection and diffusion:

$$\vec{n}_i = \rho_i \vec{v} + \vec{j}_i$$

In some cases, the bulk transport is largely determined by the given flow field, and the mass transfer problem reduces to determining $\vec{j}_i$ as a small component of $\vec{n}_i$.

As a concrete example, consider a laminar flat-plate boundary layer flow in which species i is transferred from the wall to the free stream, as shown in Fig. 11.12. (Free stream values, at the edge of the b.l., are labeled with the subscript e.) If the concentration difference, $m_{i,s} - m_{i,e}$, is small, then the mass flux of i through the wall, $n_{i,s}$, is small compared to the bulk mass transfer, n, in the streamwise direction. Hence, we expect the velocity field to be influenced only slightly by mass transfer from the wall, so that $\vec{v}$ is essentially that for the Blasius boundary layer. It follows that the boundary layer approximations are applicable and that the species equation can be reduced to

$$u\frac{\partial m_i}{\partial x} + v\frac{\partial m_i}{\partial y} = \mathcal{D}_{im}\frac{\partial^2 m_i}{\partial y^2} \tag{11.68a}$$

where $\vec{v}$ is the velocity from the Blasius solution, eqn. (6.19). The b.c.'s are

$$m_i(y \to \infty) = m_{i,e}, \quad m_i(x = 0) = m_{i,e}, \quad m_i(y = 0) = m_{i,s}$$

This is fully analogous to the heat transfer problem for a flat plate flow

with an isothermal wall:

$$u\frac{\partial T}{\partial x} + v\frac{\partial T}{\partial y} = \alpha\frac{\partial^2 T}{\partial y^2} \tag{11.68b}$$

where $\vec{v}$ is the Blasius value and the b.c.'s are

$$T(y \to \infty) = T_e, \quad T(x = 0) = T_e, \quad T(y = 0) = T_s$$

We can therefore find $n_{i,s}$ by analogy to our previous solution for q_w. We return to this sort of heat and mass transfer analogy in Section 11.7.

Steady mass transfer

Equation (11.58) makes it clear that steady mass transfer without reactions is governed by the equation

$$\boxed{\nabla \cdot \vec{n}_i = 0} \tag{11.69}$$

or, in one dimension,

$$\frac{dn_i}{dx} = 0 \tag{11.70}$$

that is, n_i is independent of x.

Example 11.7

A solid slab of species 1 has different concentrations of species 2 at the inside of each of its faces, as shown in Fig. 11.13. What is the mass transfer rate of species 2 through the slab?

SOLUTION. The mass transfer rate through the slab satisfies

$$\frac{dn_2}{dx} = 0$$

For a solid, $\vec{v} \cong 0$, so $n_2 \cong j_2$ and with Fick's law we have

$$\frac{dn_2}{dx} \cong \frac{dj_2}{dx} = \frac{d}{dx}\left(-\rho\mathcal{D}_{21}\frac{dm_2}{dx}\right) = 0$$

If $\rho\mathcal{D}_{21} \cong$ constant, the right side gives

$$\frac{d^2 m_2}{dx^2} = 0$$

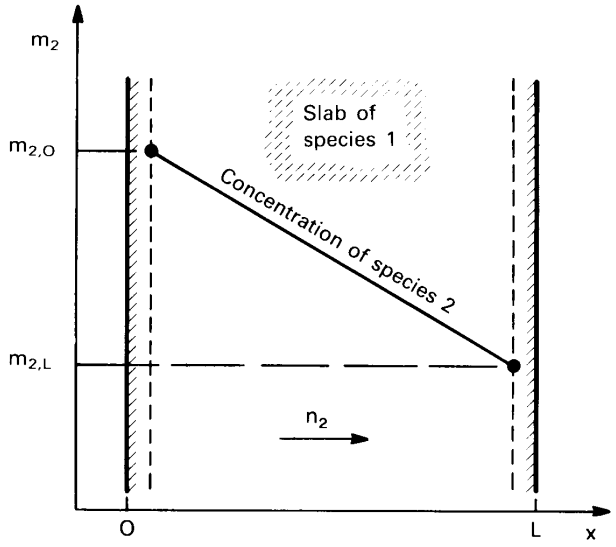

Figure 11.13 One-dimensional, steady diffusion in a slab.

Integrating and applying the boundary conditions, $m_2(x = 0) = m_{2,0}$ and $m_2(x = L) = m_{2,L}$, we obtain the concentration distribution:

$$m_2(x) = m_{2,0} + (m_{2,L} - m_{2,0}) \left(\frac{x}{L}\right)$$

and the mass flux is then

$$n_2 \cong j_2 = -\frac{\rho \mathcal{D}_{21}}{L} (m_{2,L} - m_{2,0}) \tag{11.71}$$

This, in essence, is the same kind of calculation we made in Example 2.2 in Chapter 2. ■

11.6 Steady mass transfer through a stagnant layer

In 1874, Stefan presented his solution to the problem of evaporation from a liquid pool at the bottom of a vertical tube over which a gas flows. This configuration, often called a *Stefan tube*, is shown in Fig. 11.14. Vapor leaving the liquid surface diffuses through the gas in the tube and is carried away by the gas flow across top of the tube. If the gas stream itself has only a relatively small concentration of vapor, then diffusion is driven by the higher concentration of vapor over the liquid pool that arises from the vapor pressure of the liquid. This process can be kept in

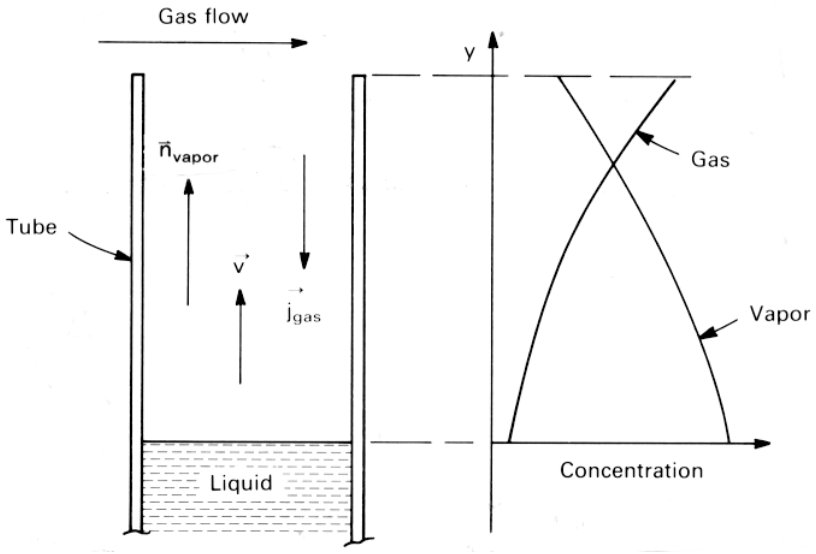

Figure 11.14 The Stefan tube.

a steady state, since the constant replacement of the gas at the top of the tube maintains the upper surface conditions. The Stefan tube has often been used to measure diffusion coefficients.

Will convection occur in this arrangement? If the liquid species has a higher molecular weight than the gas species, the density of the mixture in the tube decreases with the height above the liquid surface. The mixture is then buoyantly stable and natural convection will not occur. However, mass transfer is still not purely diffusive in this problem.

There is a net upward flow of evaporating vapor in the steady state but a negligible downflow of gas (assuming that the liquid is saturated with the gas and thus is unable to absorb more.) Yet because there is a concentration gradient of vapor, there must also be an opposing concentration gradient of gas and an associated diffusional mass flux of gas [cf. eqn. (11.22)]. For the gas in the tube to have a net diffusion flux when it is stationary, there must be an *induced* upward convective velocity against which the gas diffuses. The velocity at the liquid surface can be obtained, using eqns. (11.21) and (11.22), as

$$v = -j_{\text{gas,surface}}/\rho_{\text{gas,surface}} = j_{\text{vapor,surface}}/\rho_{\text{gas,surface}}$$

In this situation, mass transfer has a decisive effect on the velocity field.

This problem may be generalized to a stagnant horizontal layer of

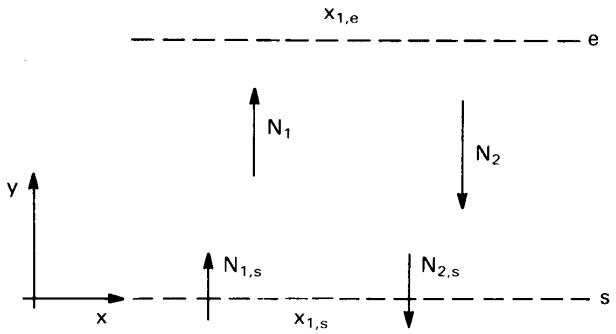

Figure 11.15 Mass flow across a stagnant horizontal layer.

a two-component fluid having different concentrations of the components at each boundary, as shown in Fig. 11.15. The components will diffuse across the layer and, in general, may each have a nonzero mass flux through the layer. If there is no imposed horizontal velocity, the mass transfer will induce none, but there may be a net vertical velocity produced by the upward or downward transfer of mass. Thus, both convection and diffusion are likely to occur. In this section, we analyze the general problem of steady mass transfer across a stagnant layer and then consider some particular cases. The results obtained here form an important prototype for our subsequent analyses of convective mass transfer.

The solution of the mass transfer problem begins with an appropriate form of the equation of species conservation. Since the mixture composition varies along the length of the tube, the density varies as well. However, if we take the temperature and pressure to be constant, the molar concentration of the mixture does not change through the tube. The system is then most easily analyzed using the molar form of species conservation.

For one-dimensional steady mass transfer, the mole fluxes N_1 and N_2 have only vertical components and depend only on the vertical coordinate, y. Therefore, using $n_i = M_i N_i$, we get, from eqn. (11.70),

$$\frac{dN_1}{dy} = \frac{dN_2}{dy} = 0$$

so that N_1 and N_2 are constant at the s-surface values, $N_{1,s}$ and $N_{2,s}$. These constants will be positive for upward mass flow. (For the orientations in Fig. 11.15, $N_{1,s} > 0$ and $N_{2,s} < 0$.) This is a fairly clear example of steady-flow species conservation.

Recalling the general expression for N_i and introducing Fick's law, we write

$$N_1 = x_1 N - c\mathcal{D}_{12}\frac{dx_1}{dy} = N_{1,s} \tag{11.72}$$

Here we have allowed for the possibility of a nonzero vertical convective transport, $x_1 N$, induced by mass transfer. The total mole flux, N, must be constant at its s-surface value; by eqn. (11.24), this is

$$N = N_{1,s} + N_{2,s} = N_s \tag{11.73}$$

Substituting this result into eqn. (11.72), we obtain a differential equation for x_1:

$$c\mathcal{D}_{12}\frac{dx_1}{dy} = N_s x_1 - N_{1,s} \tag{11.74}$$

In this equation, x_1 is a function of y, the N's are constants, and $c\mathcal{D}_{12}$ depends on temperature and pressure. If the temperature and pressure can be taken as constant in the stagnant layer, so, too, can $c\mathcal{D}_{12}$. Direct integration then yields

$$\frac{N_s y}{c\mathcal{D}_{12}} = \ln\left(N_s x_1 - N_{1,s}\right) + \text{ constant} \tag{11.75}$$

We need to fix the constant and the two mole fluxes, $N_{1,s}$ and $N_{2,s}$. To do this, we apply the boundary conditions at the ends of the tube. The first boundary condition is

$$x_1 = x_{1,s} \quad \text{at} \quad y = 0$$

and it requires that

$$\text{constant} = -\ln(N_s x_{1,s} - N_{1,s}) \tag{11.76}$$

so

$$\frac{N_s y}{c\mathcal{D}_{12}} = \ln\left(\frac{N_s x_1 - N_{1,s}}{N_s x_{1,s} - N_{1,s}}\right) \tag{11.77}$$

The second boundary condition is

$$x_1 = x_{1,e} \quad \text{at} \quad y = L$$

which yields

$$\frac{N_s L}{c\mathcal{D}_{12}} = \ln\left(\frac{x_{1,e} - N_{1,s}/N_s}{x_{1,s} - N_{1,s}/N_s}\right) \tag{11.78}$$

or

$$\boxed{N_s = \frac{c\mathcal{D}_{12}}{L} \ln\left(1 + \frac{x_{1,e} - x_{1,s}}{x_{1,s} - N_{1,s}/N_s}\right)} \tag{11.79}$$

If we know the ratio $N_{1,s}/N_s$ for a given problem, we can find the overall mass flux, N_s, explicitly. This ratio, which depends on the specific problem at hand, can be fixed by considering the rates at which the species pass through the s-surface and forms the last boundary condition.

Example 11.8

Find the evaporation rate for the Stefan tube described at the beginning of this section.

SOLUTION. Let species 1 be the species of the liquid and species 2 be the gas. The e-surface in our analysis is at the mouth of the tube and the s-surface is just above the surface of the liquid. The gas flow over the top may contain some concentration of the liquid species, $x_{1,e}$, and the vapor pressure of the liquid pool produces a concentration $x_{1,s}$. Only vapor is transferred through the s-surface, since the gas is assumed to be essentially insoluble and will not be absorbed into gas-saturated liquid. Thus, $N_{2,s} = 0$, and $N_s = N_{1,s} = N_{\text{vapor},s}$ is just the evaporation rate of the liquid. The ratio $N_{1,s}/N_s$ is unity, and the rate of evaporation is

$$N_s = N_{\text{vapor},s} = \frac{c\mathcal{D}_{12}}{L} \ln\left(1 + \frac{x_{1,e} - x_{1,s}}{x_{1,s} - 1}\right) \tag{11.80}$$

■

Example 11.9

What will happen in the Stefan tube if the gas is bubbled up through the liquid at some fixed rate, N_{gas}?

SOLUTION. In this case, we obtain a single equation for $N_{1,s} = N_{\text{vapor},s}$, the evaporation rate:

$$N_{\text{gas}} + N_{1,s} = \frac{c\mathcal{D}_{12}}{L} \ln\left(1 + \frac{x_{1,e} - x_{1,s}}{x_{1,s} - N_{1,s}/(N_{1,s} + N_{\text{gas}})}\right) \tag{11.81}$$

This equation determines $N_{1,s}$, but it must be solved iteratively. ■

Once we have found the mole fluxes, we may compute the concentration distribution, $x_1(y)$, using eqn. (11.77):

$$x_1(y) = \frac{N_{1,s}}{N_s} + (x_{1,s} - N_{1,s}/N_s)\exp(N_s y/c\mathcal{D}_{12}) \tag{11.82}$$

Alternatively, we may eliminate N_s between eqns. (11.77) and (11.78) to obtain the concentration distribution in a form that depends only on the ratio $N_{1,s}/N_s$:

$$\frac{x_1 - N_{1,s}/N_s}{x_{1,s} - N_{1,s}/N_s} = \left(\frac{x_{1,e} - N_{1,s}/N_s}{x_{1,s} - N_{1,s}/N_s}\right)^{y/L} \tag{11.83}$$

Example 11.10

Find the concentration distribution of water vapor in a helium–water Stefan tube at 325 K and 1 atm. The tube is 20 cm in length. Assume the helium stream at the top of the tube to have a mole fraction of water equal to 0.01.

SOLUTION. Let water be species 1 and helium be species 2. The vapor pressure of the liquid water is approximately the saturation pressure at the water temperature. Using the steam tables, we get $p_v = 1.341 \times 10^4$ Pa and, from eqn. (11.16),

$$x_{1,s} = \frac{1.341 \times 10^4 \text{ Pa}}{101,325 \text{ Pa}} = 0.1323$$

We use eqn. (11.14) to evaluate the mole concentration in the tube:

$$c = \frac{101,325}{8314.5(325)} = 0.03750 \text{ kmol/m}^3$$

From eqn. (11.42) we obtain $\mathcal{D}_{12}(325\text{ K}, 1\text{ atm}) = 0.0001067\text{ m}^2/\text{s}$. Then eqn. (11.80) gives the molar evaporation rate:

$$N_{1,s} = \frac{0.03750(1.067 \times 10^{-4})}{0.20} \ln\left(1 + \frac{0.01 - 0.1323}{0.1323 - 1}\right)$$
$$= 2.638 \times 10^{-6}\text{ kmol/m}^2\cdot\text{s}$$

This corresponds to a mass evaporation rate:

$$n_{1,s} = 4.754 \times 10^{-5}\text{ kg/m}^2\cdot\text{s}$$

The concentration distribution of water vapor [eqn. (11.82)] is

$$x_1(y) = 1 - 0.8677\exp(0.6593y)$$

where y is expressed in meters. ■

The present analysis has two serious shortcomings when it is applied to real Stefan tubes. First, it applies only when the evaporating species is heavier than the gas into which it evaporates. If the evaporating species is lighter, then the density increases toward the top of the tube and buoyant instability can give rise to natural convection. (This is discussed in [11.24].)

The second limitation is the assumption that conditions are isothermal within the tube. Because a heat sink is associated with the latent heat of vaporization, the gas mixture tends to cool near the interface. The resulting temperature variations within the tube can affect the assumption that $c\mathcal{D}_{12}$ is constant and can potentially contribute to buoyancy effects as well. Since Stefan tubes are widely used to measure diffusion coefficients, the preservation of isothermal conditions has received some attention in the literature.

A mass-based analysis of convection problems often becomes more convenient than a molar analysis because it can be related directly to the mass-averaged velocity used in the equations of fluid motion. The problem dealt with in this section can be solved on a mass basis, assuming a constant value of $\rho\mathcal{D}_{12}$ (see Problem 11.33). However, if the two species have greatly differing molecular weights or if the mixture composition changes strongly across the layer, then ρ can vary significantly within the layer and the molar analysis yields better results (see Problem 11.34). Nevertheless, the mass-based solution of this problem provides an important approximation in our analysis of convective mass transfer in the next section.

11.7 Mass transfer coefficients

Scope

We have found that in convective *heat* transfer problems, it is useful to express the heat flux from a surface, q, as the product of a heat transfer coefficient, h, and a driving force for heat transfer, ΔT—at least when h is not strongly dependent on ΔT. Thus,

$$q = h\left(T_{\text{body}} - T_{\infty}\right) \tag{1.17}$$

In convective *mass* transfer problems, we would also like to express the mass flux from a surface, $\dot{m}''$, as the product of a mass transfer coefficient and a driving force for mass transfer. Heat and mass transfer were shown to be very similar processes in Section 11.5, so it seems reasonable that the previous results for heat transfer coefficients might be adapted to the problem of mass transfer. However, because of the strong influence mass transfer can have on the convective velocity field, the flow effects of a mass flux from a wall must also be considered in modeling mass convection processes.

The mass transfer coefficient is developed in three stages in this section: First, we define it and derive the appropriate driving force for mass transfer. Next, we relate the mass transfer coefficient at finite mass transfer rates to that at very low mass transfer rates, using a simple model for the mass convection boundary layer. Finally, we present the analogy between the low-rate mass transfer coefficient and the heat transfer coefficients of previous chapters. In following these steps, we create the apparatus for solving a wide variety of mass transfer problems using methods and results from Chapters 6, 7, and 8.

The mass transfer coefficient and the mass transfer driving force

Figure 11.16 shows a boundary layer over a wall through which there is a net mass transfer, $\dot{m}''$, of the various species in the direction normal to the wall. In particular, we focus on species i. In the free stream, i has a concentration $m_{i,e}$; at the wall, it has a concentration $m_{i,s}$.

The mass flux of i leaving the wall is obtained from eqn. (11.21):

$$n_{i,s} = m_{i,s}\dot{m}'' + j_{i,s} \tag{11.84}$$

It is desirable to express $\dot{m}''$ in terms of the concentrations $m_{i,s}$ and $m_{i,e}$. By analogy to the definition of the heat transfer coefficient, we define the

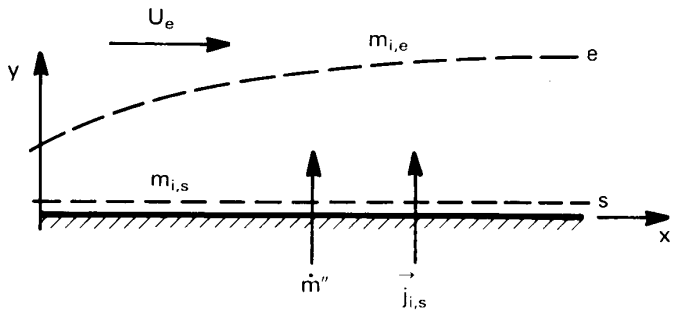

Figure 11.16 The mass concentration boundary layer.

mass transfer coefficient for species i, $g_{m,i}$ kg/m^2·s, as

$$g_{m,i} \equiv j_{i,s} / (m_{i,s} - m_{i,e}) \tag{11.85}$$

Thus,

$$n_{i,s} = m_{i,s}\dot{m}'' + g_{m,i}(m_{i,s} - m_{i,e}) \tag{11.86}$$

It is important to recognize that the mass transfer coefficient is based on the *diffusive* transfer from the wall, just as h is. Equation (11.86) may be rearranged as

$$\dot{m}'' = g_{m,i}\left(\frac{m_{i,e} - m_{i,s}}{m_{i,s} - n_{i,s}/\dot{m}''}\right) \tag{11.87}$$

which express the total mass transfer $\dot{m}''$, through the wall as the product of the mass transfer coefficient and a ratio of concentrations. This ratio is called the *mass transfer driving force* for species i:

$$B_{m,i} \equiv \left(\frac{m_{i,e} - m_{i,s}}{m_{i,s} - n_{i,s}/\dot{m}''}\right) \tag{11.88}$$

The ratio of mass fluxes in the denominator is called the *mass fraction in the transferred state*, denoted as $m_{i,t}$:

$$m_{i,t} \equiv n_{i,s}/\dot{m}'' \tag{11.89}$$

The mass fraction in the transferred state is simply the fraction of the total mass flux, $\dot{m}''$, which is made up of species i. It is not really a mass fraction in the sense of Section 11.2 because it can have any value from $-\infty$ to $+\infty$, depending on the relative magnitudes of $\dot{m}''$ and $n_{i,s}$. If, for example, $n_{1,s} \cong -n_{2,s}$ in a binary mixture, then $\dot{m}''$ is very small and both $m_{1,t}$ and $m_{2,t}$ are very large.

Equations (11.87), (11.88), and (11.89) provide a formulation of mass transfer problems in terms of a mass transfer coefficient, $g_{m,i}$, and a driving force for mass transfer, $B_{m,i}$:

$$\boxed{\dot{m}'' = g_{m,i} B_{m,i}} \tag{11.90}$$

where

$$\boxed{B_{m,i} = \left(\frac{m_{i,e} - m_{i,s}}{m_{i,s} - m_{i,t}} \right), \qquad m_{i,t} = n_{i,s} / \dot{m}''} \tag{11.91}$$

Equation (11.90) is the mass transfer analog of eqn. (1.17).

These relations are based on an arbitrary species, i. The mass transfer rate may equally well be calculated using any species in a mixture; one obtains the same result for each. This is well illustrated in a binary mixture for which one may show (Problem 11.36) that

$$g_{m,1} = g_{m,2} \quad \text{and} \quad B_{m,1} = B_{m,2}$$

In many situations, only one species is transferred at the wall. If species i is the only one passing through the wall, then $n_{i,s} = \dot{m}''$, so that $m_{t,i} = 1$. The mass transfer driving force is simply

$$\boxed{B_{m,i} = \left(\frac{m_{i,e} - m_{i,s}}{m_{i,s} - 1} \right) \begin{array}{l} \text{one species} \\ \text{transferred} \end{array}} \tag{11.92}$$

and it depends only on the actual mass fractions, $m_{i,e}$ and $m_{i,s}$. The evaporation of vapor from a liquid surface is an important example of single-species transfer.

Example 11.11

A pan of hot water with a surface temperature of 75°C is placed in an air stream that has a mass fraction of water equal to 0.05. If the average mass transfer coefficient for water over the pan is $\overline{g_{m,H_2O}} = 0.0169$ kg/m^2·s and the pan has a surface area of 0.04 m^2, what is the evaporation rate?

SOLUTION. Only water vapor passes through the liquid surface, since air is not strongly absorbed into water under normal conditions. Thus,

we use eqn. (11.92) for the driving force for mass transfer. Reference to a steam table shows the saturation pressure of water to be 0.381 atm at 75°C, so

$$x_{H_2O,s} = 0.381/1 = 0.381$$

from which we obtain

$$m_{H_2O,s} = 0.277$$

so that

$$B_{i,m} = \frac{0.05 - 0.277}{0.277 - 1.0} = 0.314$$

Thus,

$$\begin{aligned} \dot{m}_{H_2O} &= \dot{m}''(0.04\ \text{m}^2) = (0.0169\ \text{kg/m}^2\cdot\text{s})(0.314)(0.04\ \text{m}^2) \\ &= 0.000212\ \text{kg/s} = 764\ \text{gm/hr} \end{aligned}$$

■

The effect of mass transfer rates on the mass transfer coefficient

We still face the task of finding the mass transfer coefficient, $g_{m,i}$. The most obvious way to do this would be to apply the same methods we used to find the heat transfer coefficient in Chapters 6 through 8—numerical or analytical solution of the momentum and species equations or direct experimental simulation of the mass transfer problem. These approaches are often used for specific mass transfer problems, but they are one level more complicated than the analogous heat transfer problems, since the flow field is coupled to the mass transfer rate. Simple correlations and analytical formulas such as those used to calculate h are not so readily available for mass transfer problems. We instead employ a widely used approximate method that allows us to calculate $g_{m,i}$ from corresponding results for h in a given geometry by applying a correction for the effect of finite mass transfer rates.

To isolate the effect of $\dot{m}''$ on the mass transfer coefficient, we first define the mass transfer coefficient at zero net mass transfer, $g^*_{m,i}$:

$$g^*_{m,i} \equiv \lim_{\dot{m}'' \to 0} g_{m,i}$$

As the mass transfer rate becomes very small, eqn. (11.86) shows that

$$n_{i,s} \cong j_{i,s} \cong g^*_{m,i}\,(m_{i,s} - m_{i,e})$$

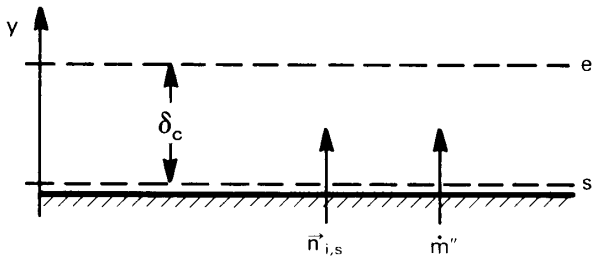

Figure 11.17 A stagnant film.

Thus, $g^*_{m,i}$ characterizes mass transfer when rates are low enough that mass flow occurs primarily by diffusion. Although $g_{m,i}$ depends directly on the rate of mass transfer, $g^*_{m,i}$ does not; it is determined by flow geometry and physical properties. If we introduce an appropriate model for the mass transfer through a boundary layer, we can express $g_{m,i}$ in terms of $g^*_{m,i}$ and the mass transfer driving force. This will make the determination of the mass transfer coefficient much simpler with little sacrifice of accuracy.

One way of modeling mass transfer effects on $g_{m,i}$ is simply to consider transport across a *stagnant film*—a stationary layer of fluid with no horizontal gradients in it, as shown in Fig. 11.17. This layer may be viewed as a first approximation to the real boundary layer, in which the fluid near the wall is slowed by the no-slip condition. The film thickness, δ_c, is an effective local concentration boundary layer thickness. If concentrations are fixed on either of the horizontal boundaries of the layer, this becomes the configuration dealt with in the previous section (i.e., Fig. 11.15). Thus, the solution obtained in the previous section—eqn. (11.79)—also gives the rate of mass transfer across the stagnant film.

It is convenient to use the mass-based analog of the mole-based eqn. (11.79) in the present mass-based analysis. This analog can be shown to be (Problem 11.33)

$$\dot{m}'' = \frac{\rho \mathcal{D}_{im}}{\delta_c} \ln\left(1 + \frac{m_{i,e} - m_{i,s}}{m_{i,s} - n_{i,s}/\dot{m}''}\right)$$

which can be recast in the more suggestive form

$$\dot{m}'' = \frac{\rho \mathcal{D}_{im}}{\delta_c} \left[\frac{\ln(1 + B_{m,i})}{B_{m,i}}\right] B_{m,i} \tag{11.93}$$

Comparing this equation with eqn. (11.90), we see that

$$g_{m,i} = \frac{\rho \mathcal{D}_{im}}{\delta_c} \left[\frac{\ln(1 + B_{m,i})}{B_{m,i}}\right]$$

When $\dot{m}''$ approaches zero,

$$g^*_{m,i} = \lim_{\dot{m}'' \to 0} g_{m,i} = \lim_{B_{m,i} \to 0} g_{m,i} = \frac{\rho \mathcal{D}_{im}}{\delta_c}$$

which corresponds to one-dimensional diffusion through a slab of thickness δ_c [cf. eqn. (11.71)]. Hence,

$$\boxed{g_{m,i} = g^*_{m,i} \left[\frac{\ln(1 + B_{m,i})}{B_{m,i}} \right]} \tag{11.94}$$

We see that the value of $g^*_{m,i}$ depends on an effective concentration boundary layer thickness, δ_c, which is determined by solving the convection problem for $\dot{m}'' \to 0$. In other words, the correct value of δ_c, and thus $g^*_{m,i}$, may be found for *any* configuration by an independent analysis. Our model and result for finite mass transfer rates are thus justified for a wide variety of convection problems. We now have a correction for finite mass transfer rates to be used in conjunction with low-rate results. (Analogous stagnant film analyses of heat and momentum transport may also be made, as discussed in Problem 11.37.)

The group $[\ln(1 + B_{m,i})]/B_{m,i}$ is called the *blowing factor*. It accounts for mass transfer effects on the velocity field. When $B_{m,i} > 0$, we have mass flow away from the wall (or *blowing*.) In this case, the blowing factor is always a positive number less than unity, so blowing *reduces* $g_{m,i}$. When $B_{m,i} < 0$, we have mass flow toward the wall (or *suction*), and the blowing factor is a positive number greater than unity. Thus, $g_{m,i}$ is *increased* by suction. These trends may be better understood if we note that wall suction removes the slow fluid at the wall and thins the b.l. The thinner b.l. offers less resistance to mass transfer. Likewise, blowing tends to thicken the boundary layer, increasing the resistance to mass transfer.

The stagnant film b.l. model ignores details of the flow in the b.l. and focuses on the balance of mass fluxes across it. It is equally valid for both laminar and turbulent flows.

Low mass transfer rates: The analogy between heat and mass transfer

To complete the solution of the mass transfer problem, we must find $g^*_{m,i}$ for a given geometry. We do this by returning to the analogy between

heat and mass transfer that exists when the mass transfer rates are low enough that they do not affect the velocity field.

We have seen in Sect. 11.5 that the equation of species conservation and the energy equation were quite similar in an incompressible flow. If there are no reactions and no heat generation, then eqns. (11.61) and (6.37) can be written as

$$\frac{\partial \rho_i}{\partial t} + \vec{v} \cdot \nabla \rho_i \;\; = -\nabla \cdot \vec{j}_i$$

$$\rho c_p \left(\frac{\partial T}{\partial t} + \vec{v} \cdot \nabla T \right) = -\nabla \cdot \vec{q}$$

In each case, the conservation equation expresses changes in the amount of heat or energy per unit volume that results from convection by a given velocity field and from diffusion under either Fick's or Fourier's law.

We may identify the analogous quantities in these equations. For capacity per unit volume, we have

$$d\rho_i \Longleftrightarrow \rho c_p dT \qquad \text{or} \qquad \rho \, dm_i \Longleftrightarrow \rho c_p dT \tag{11.95a}$$

From the flux laws, we have

$$\vec{j}_i = -\rho \mathcal{D}_{im} \nabla m_i = -\mathcal{D}_{im} (\rho \nabla m_i)$$

$$\vec{q} = -k \nabla T \qquad\quad = -\frac{k}{\rho c_p} \left(\rho c_p \nabla T \right)$$

so that

$$\mathcal{D}_{im} \Longleftrightarrow \frac{k}{\rho c_p} = \alpha \qquad \text{or} \qquad \rho \mathcal{D}_{im} \Longleftrightarrow \frac{k}{c_p} \tag{11.95b}$$

This result further implies that

$$\text{Sc} = \frac{\nu}{\mathcal{D}_{im}} \quad \Longleftrightarrow \quad \text{Pr} = \frac{\nu}{\alpha} = \frac{\mu c_p}{k} \tag{11.95c}$$

Finally, from the transfer coefficients, we have[7]

$$\vec{j}_{i,s} = g^*_{m,i} \, (m_{i,s} - m_{i,e}) = \left(\frac{g^*_{m,i}}{\rho} \right) \rho \, (m_{i,s} - m_{i,e})$$

$$\vec{q}_s = h^* \, (T_s - T_e) \qquad\quad = \left(\frac{h^*}{\rho c_p} \right) \rho c_p \, (T_s - T_e)$$

[7] We henceforth denote by h^* the heat transfer coefficient at zero net mass transfer, since high mass flux can alter the heat transfer coefficient, h, just as it does the mass transfer coefficient $g_{m,i}$. This is discussed further in Section 11.8.

so that

$$g^*_{m,i} \Longleftrightarrow \frac{h^*}{c_p} \tag{11.95d}$$

From these comparisons, we see that the solution of a heat convection problem becomes the solution of a low-rate mass convection problem upon replacing the variables in the heat transfer problem with the mass transfer variables given by eqns. (11.95). Solutions for convective heat transfer coefficients are usually expressed in terms of the Nusselt number as a function of Reynolds and Prandtl number

$$\mathrm{Nu}_x = \frac{h^* x}{k} = \frac{(h^*/c_p)x}{k/c_p} = \mathrm{fn}\,(\mathrm{Re}_x, \mathrm{Pr}) \tag{11.96}$$

For convective mass transfer problems, we expect the same functional dependence after we make the substitutions indicated above. Thus, if we replace h^*/c_p by $g^*_{m,i}$, k/c_p by $\rho\mathcal{D}_{i,m}$, and Pr by Sc, we obtain

$$\boxed{\mathrm{Nu}_{m,x} \equiv \frac{g^*_{m,i} x}{\rho \mathcal{D}_{im}} = \mathrm{fn}\,(\mathrm{Re}_x, \mathrm{Sc})} \tag{11.97}$$

where $\mathrm{Nu}_{m,x}$, the Nusselt number for mass transfer, is defined as indicated. Nu_m is sometimes called the *Sherwood number*[8], written as Sh.

Example 11.12

Calculate the mass transfer coefficient for Example 11.11 if the air speed is 5 m/s, the length of the pan in the flow direction is 20 cm, and the air temperature is 25°C.

SOLUTION. The water surface is essentially a flat plate, as shown in Fig. 11.18. To find the appropriate equation for the Nusselt number, we must first compute Re_L.

The properties are evaluated at the average film temperature, (75+25)/2 = 50°C, and the *film composition*,

$$m_{f,\mathrm{H_2O}} = (0.050 + 0.277)/2 = 0.164$$

[8]Thomas K. Sherwood (1903–1976) obtained his doctoral degree at M.I.T. under Warren K. Lewis in 1929 and served as a professor of Chemical Engineering there from 1930 to 1969. His research dealt with mass transfer and related industrial processes. Sherwood was also the author of a very influential textbook on mass transfer.

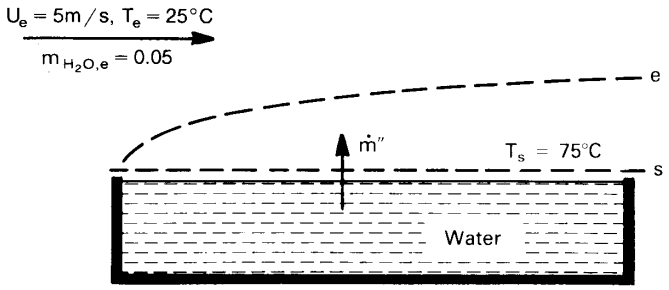

Figure 11.18 Evaporation from a tray of water.

For these conditions, we find the mixture molecular weight from eqn. (11.8) as $M_f = 26.34$ kg/kmol. Thus, from the ideal gas law,

$$\rho_f = (101,325)(26.34)/(8314.5)(323.15) = 0.993 \text{ kg/m}^3$$

From Appendix A, we get $\mu_{\text{air}} = 1.959 \times 10^{-5}$ kg/m·s, and eqn. (11.51) yields $\mu_{\text{water vapor}} = 1.172 \times 10^{-5}$ kg/m·s. Then eqn. (11.54), with $x_{H_2O,f} = 0.240$ and $x_{\text{air},f} = 0.760$, yields

$$\mu_f = 1.77 \times 10^{-5} \text{ kg/m·s} \quad \text{and} \quad \nu_f = (\mu/\rho)_f = 1.78 \times 10^{-5} \text{m}^2/\text{s}$$

and $\text{Re}_L = 5(0.2)/(1.78 \times 10^{-5}) = 56,200$, so the flow must be laminar.

The appropriate Nusselt number is obtained from the mass transfer version of eqn. (6.68):

$$\overline{\text{Nu}}_{m,L} = 0.664 \, \text{Re}_L^{1/2} \text{Sc}^{1/3}$$

Equation (11.42) yields $\mathcal{D}_{H_2O,\text{air}} = 2.929 \times 10^{-5} \text{m}^2/\text{s}$, so

$$\text{Sc} = 1.78/2.929 = 0.608$$

and

$$\overline{\text{Nu}}_{m,L} = 133$$

Hence,

$$\overline{g^*_{m,H_2O}} = \overline{\text{Nu}_{m,L}}(\rho \mathcal{D}_{H_2O,\text{air}}/L) = 0.0194 \text{ kg/m}^2\text{·s}$$

Finally,

$$\overline{g_{m,H_2O}} = 0.0194 \ln(1.309)/0.309 = 0.0169 \text{ kg/m}^2\text{·s}$$

In this case, the blowing factor is 0.871—slightly less than unity. Thus, mild blowing has reduced the mass transfer coefficient. ■

When we apply the analogy between heat transfer and mass transfer to calculate $g^*_{m,i}$, we must consider the boundary condition at the wall. We dealt with two common types of wall condition in the study of heat transfer: uniform temperature and uniform heat flux. The analogous mass transfer wall conditions are uniform concentration and uniform mass flux. We used the mass transfer analog of the uniform wall temperature solution in the preceding example, since the mass fraction of water vapor over the liquid surface was *uniform* over the whole pan. Had the mass flux been uniform at the wall, we would have used the analog of a uniform heat flux solution.

When the mass transfer driving force is small enough, the low-rate mass transfer coefficient itself is an adequate approximation to the actual mass transfer coefficient. This is because the blowing factor tends toward unity as $B_{m,i} \longrightarrow 0$:

$$\lim_{B_{m,i} \to 0} \frac{\ln(1 + B_{m,i})}{B_{m,i}} = 1$$

Thus, for small values of $B_{m,i}$, $g_{m,i} \cong g^*_{m,i}$.

The calculation of mass transfer proceeds in one of two ways for low rates of mass transfer. One way is if the ratio $n_{i,s}/\dot{m}''$ is fixed at a finite value while $\dot{m}'' \longrightarrow 0$. (This would be the case when only one species is transferred and $n_{i,s}/\dot{m}'' = 1$.) Then the mass flux at low rates is

$$\dot{m}'' \cong g^*_{m,i} B_{m,i} \tag{11.98}$$

In this case, convective and diffusive contributions to $n_{i,s}$ are of the same order of magnitude.

If, on the other hand, $n_{i,s}$ is finite while $\dot{m}'' \longrightarrow 0$, then

$$n_{i,s} \cong j_{i,s} \cong g^*_{m,i}(m_{i,s} - m_{i,e}) \tag{11.99}$$

The transport in this case is purely diffusive. Problem 11.43 illustrates how this occurs in the process of catalysis.

An estimate of the blowing factor when $B_{m,i}$ is small often reveals that adequate results will be obtained using low-rate theory. This can considerably reduce the complexity of a calculation. If, for example, $B_{m,i} = 0.06$, then $[\ln(1 + B_m)]/B_m = 0.97$ and an error of only 3 percent is introduced by assuming low rates. This level of accuracy is adequate for most engineering calculations.

Natural convection in mass transfer

In Chapter 8 we saw that the density differences produced by temperature variations can lead to flow and convection in a fluid. Variations in fluid composition can also produce density variations that result in natural convection mass transfer. This type of natural convection flow is still governed by eqn. (8.3):

$$u\frac{\partial u}{\partial x} + v\frac{\partial u}{\partial y} = (1 - \rho_\infty/\rho)g + \nu\frac{\partial^2 u}{\partial y^2}$$

but the species equation is now used in place of the energy equation in determining the distribution of density. Rather than solving eqn. (8.3) and the species equation for specific mass transfer problems, we again turn to the analogy between heat and mass transfer.

In analyzing natural convection heat transfer, we eliminated ρ from eqn. (8.3) using $(1 - \rho_\infty/\rho) = \beta(T - T_\infty)$, and the resulting Grashof and Rayleigh numbers came out in terms of an appropriate $\beta\Delta T$ instead of $\Delta\rho/\rho$. These groups could just as well be written for the heat transfer problem as

$$\mathrm{Gr}_L = \frac{g\Delta\rho L^3}{\rho\nu^2} \quad \text{and} \quad \mathrm{Ra}_L = \frac{g\Delta\rho L^3}{\rho\alpha\nu} = \frac{g\Delta\rho L^3}{\mu\alpha} \tag{11.100}$$

although $\Delta\rho$ would still have to be evaluated from ΔT.

With Gr and Pr expressed in terms of density differences instead of temperature differences, the analogy between heat transfer and low-rate mass transfer may be used directly to adapt natural convection heat transfer predictions to the prediction of natural convection mass transfer. As before, we replace Nu by Nu_m and Pr by Sc. But this time we also write

$$\mathrm{Ra}_L = \mathrm{Gr}_L\mathrm{Sc} = \frac{g\Delta\rho L^3}{\mu\mathcal{D}_{12}} \tag{11.101}$$

and calculate Gr_L as in eqn. (11.100). The density difference must now be calculated from the concentration difference.

Example 11.13

31.3 mg/cm^2·hr of helium is slowly bled through a porous vertical wall, 40 cm high, into the surrounding air. Both the helium and the

air are at 300 K, and the environment is at 1 atm. What is the average concentration of helium at the wall?

SOLUTION. This is a uniform wall flux, natural convection problem. The appropriate Nusselt number is obtained from the mass transfer analog of eqn. (8.43):

$$(\overline{\mathrm{Nu}}_{m,L})^{5/4} - 0.68(\overline{\mathrm{Nu}_{m,L}})^{1/4} = \frac{0.67(\mathrm{Ra}_L^*)^{1/4}}{[1 + (0.492/\mathrm{Sc})^{9/16}]^{4/9}}$$

with

$$\mathrm{Ra}_L^* = \frac{g\Delta\rho\dot{m}''L^4}{\mu\rho\mathcal{D}^2_{\mathrm{He,air}}\overline{B_{m,\mathrm{He}}}}$$

The problem is to find a value of $\overline{m_{\mathrm{He},s}}$ that satisfies $\dot{m}'' = \overline{g_{m,\mathrm{He}}}\,\overline{B_{m,\mathrm{He}}}$. The mass transfer coefficient, $\overline{g_{m,\mathrm{He}}}$, depends on $\overline{m_{\mathrm{He},s}}$, so an iterative solution is required.

As a first guess, we pick $\overline{m_{\mathrm{He},s}} = 0.01$. Then the film composition is $\overline{m_{\mathrm{He},f}} = (0.010 + 0)/2 = 0.005$, since $m_{\mathrm{He},e} = 0$. The usual calculations give the film and wall densities as

$$\rho_f = 1.141 \text{ kg/m}^3 \quad \text{and} \quad \rho_s = 1.107 \text{ kg/m}^3$$

and the diffusion coefficient as

$$\mathcal{D}_{\mathrm{He,air}} = 7.119 \times 10^{-5} \text{ m}^2/\text{s}.$$

Reference to Appendix A shows that μ_{air} is close to μ_{He} at 300 K, so at this low concentration of helium we take

$$\mu_f \cong \mu_{\mathrm{air}} = 1.853 \times 10^{-5} \text{ kg/m}\cdot\text{s}.$$

The corresponding Schmidt number is Sc = 0.2281. Furthermore,

$$\rho_e = \rho_{\mathrm{air}} = 1.183 \text{ kg/m}^3$$

Now, because the concentration difference is small, we test the blowing factor to see if the low-rate theory is adequate:

$$B_{m,\mathrm{He}} = \frac{m_{\mathrm{He},e} - m_{\mathrm{He},s}}{m_{\mathrm{He},s} - 1} = \frac{-0.01}{0.01 - 1} = 0.0101$$

and

$$\frac{\ln(1 + B_{m,\mathrm{He}})}{B_{m,\mathrm{He}}} = 0.995$$

Thus, the low-rate approach to this problem is almost exact. We can then set

$$\dot{m}'' = \overline{g^*_{m,\mathrm{He}}}\,\overline{B_{m,\mathrm{He}}}$$

and we need not introduce the log term into subsequent calculations.

Since $\dot{m}''/\overline{B_{m,\mathrm{He}}} = \overline{g^*_{m,\mathrm{He}}}$, we may divide the Nusselt number equation we started with by $(\overline{g^*_{m,\mathrm{He}}})^{1/4}$. Using the physical property data, we get

$$\overline{g^*_{m,\mathrm{He}}}\left[\frac{0.40}{1.141(7.119\times10^{-5})}\right]^{5/4} - 0.68\left[\frac{0.40}{1.141(7.119\times10^{-5})}\right]^{1/4} = \frac{0.67}{[1 + (0.492/0.2281)^{9/16}]^{4/9}} \times \left[\frac{9.806(1.183 - 1.107)(0.40)^4}{1.853\times10^{-5}(1.141)(7.119\times10^{-5})^2}\right]^{1/4}$$

This yields

$$\overline{g^*_{m,\mathrm{He}}} = 0.00711\ \mathrm{kg/m^2\cdot s}$$

The average mass fraction at the wall corresponding to this value of $\overline{g^*_{m,\mathrm{He}}}$ is found from $\overline{B_{m,\mathrm{He}}}$:

$$\overline{B_{m,\mathrm{He}}} = \dot{m}''/\overline{g^*_{m,\mathrm{He}}} = 31.3(10^{-6})(10^4)/(0.00711)(3600) = 0.0122$$

so that

$$\overline{m_{\mathrm{He},s}} = 0.0123$$

which is only 20 percent higher than our initial guess of 0.01.

Using the value above as our second guess for $\overline{m_{\mathrm{He},s}}$, we repeat the preceding calculations with revised values for the densities. The results are

$$\overline{g^*_{m,\mathrm{He}}} = 0.00736\ \mathrm{kg/m^2\cdot s}$$

and

$$\overline{m_{\mathrm{He},s}} = 0.0120$$

Thus, our second guess put us within 3 percent of the first result, and a third guess should not be needed. ■

Thus far, we have treated separately the cases of thermally driven and concentration-driven natural convection. If *both* temperature and density vary, the appropriate Gr or Ra may be calculated using density differences based on the local m_i and T, *provided* that the Prandtl and Schmidt numbers are about the same (that is, the Lewis number $\cong 1$). This is usually true in gases. If the Lewis number is far from unity, the analogy between heat and mass transfer breaks down in the solution of those natural convection problems that involve both heat and mass transfer.

11.8 Simultaneous heat and mass transfer

Some of the most important engineering mass transfer processes are those that occur simultaneously with heat transfer. Cooling towers, drying equipment, combustion chambers, and humidifiers are just a few of the kinds of equipment in which heat and mass transfer are intimately coupled. In this section we introduce a procedure for calculating the effect of mass transfer on the heat transfer coefficients that were developed in previous chapters without reference to mass transfer.

In a flow with mass transfer, the transport of enthalpy by individual species must enter the energy balance along with heat conduction through the fluid mixture. Each species in a mixture carries its own enthalpy, h_i. For a steady flow without internal heat generation, we may rewrite the energy balance, eqn. (6.36), as

$$-\int_S (-k\nabla T)\cdot d\vec{S} - \int_S \left(\sum_i \rho_i h_i \vec{v}_i\right)\cdot d\vec{S} = 0$$

where the second term accounts for enthalpy transport by each species in the mixture. The usual procedure of applying Gauss's theorem and requiring the integrand to vanish identically gives

$$\nabla\cdot\left(-k\nabla T + \sum_i \rho_i h_i \vec{v}_i\right) = 0 \tag{11.102}$$

This steady-state equation expresses conservation of the total energy flux—the sum of heat conduction and enthalpy transport.

Let us restrict attention to the transport of a single species, i, across a boundary layer. We again use the stagnant film model for the thermal

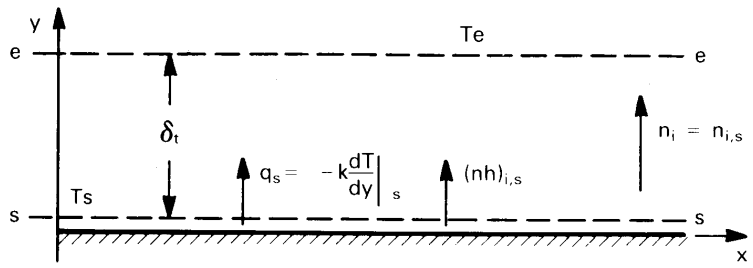

Figure 11.19 Energy transport in a stagnant film.

boundary layer and consider the flow of energy (see Fig. 11.19). Equation (11.102) now simplifies to

$$\frac{d}{dy}\left(-k\frac{dT}{dy} + \rho_i h_i v_i\right) = 0 \tag{11.103}$$

From eqn. (11.70) for steady, one-dimensional flow,

$$\frac{d}{dy}(\rho_i v_i) = \frac{dn_i}{dy} = 0$$

so

$$n_i = \text{constant} = n_{i,s}$$

If we neglect pressure variations (as in Sect. 6.3), the enthalpy may be written as $h_i = c_{p,i}(T - T_{\text{ref}})$, and eqn. (11.103) becomes

$$\frac{d}{dy}\left(-k\frac{dT}{dy} + n_{i,s}c_{p,i}T\right) = 0$$

Integrating twice and applying the boundary conditions

$$T(y = 0) = T_s \quad \text{and} \quad T(y = \delta_t) = T_e$$

we obtain the temperature profile of the stagnant film:

$$\frac{T - T_s}{T_e - T_s} = \frac{\exp\left(\frac{n_{i,s}c_{p,i}}{k}y\right) - 1}{\exp\left(\frac{n_{i,s}c_{p,i}}{k}\delta_t\right) - 1} \tag{11.104}$$

The temperature distribution may be used to find the heat transfer coefficient according to its definition [eqn. (6.5)]:

$$h \equiv \frac{-k\left.\dfrac{dT}{dy}\right|_s}{T_s - T_e} = \frac{n_{i,s}c_{p,i}}{\exp\left(\dfrac{n_{i,s}c_{p,i}}{k}\delta_t\right) - 1} \tag{11.105}$$

Equation (11.105) can be related to the heat transfer coefficient at zero mass transfer, h^*—called h in the previous chapters—by taking the limit as $n_{i,s}$ goes to zero:

$$h^* \equiv \lim_{n_{i,s}\to 0} h = \frac{k}{\delta_t} \tag{11.106}$$

Thus the low-rate heat transfer coefficient, h^*, is the same as that for conduction through a fluid layer of thickness δ_t, in agreement with the stagnant film concept. Because we presume that h^* has been obtained for a given geometry by conventional heat convection analysis, eqn. (11.106) really defines the effective thermal boundary layer thickness, δ_t, rather than h^*.

The substitution of eqn. (11.106) into eqn. (11.105) yields

$$\boxed{h = \frac{n_{i,s}c_{p,i}}{\exp(n_{i,s}c_{p,i}/h^*) - 1}} \tag{11.107}$$

Equation (11.107) shows the primary effects of mass transfer on h. When $n_{i,s}$ is large and positive—the blowing case—h becomes small. Thus, blowing decreases the heat transfer coefficient, just as it decreases the mass transfer coefficient. Likewise, when $n_{i,s}$ is large and negative—the suction case—h becomes very large; so suction increases the heat transfer coefficient as well as the mass transfer coefficient.

At this point, it is well to consider what reference state should be used to approximate variable property effects. In Section 11.7, we calculated $g^*_{m,i}$ (and thus $g_{m,i}$) at the film temperature *and* film composition, as though mass transfer were occurring at the mean mixture composition and temperature. This is because $g^*_{m,i}$ occurs in the limit as $B_{m,i} \longrightarrow 0$; in this limit, the stagnant layer takes on the film composition as the mass transfer rate vanishes. We evaluate $g^*_{m,i}$ the same way when heat transfer occurs simultaneously.

To approximate the effect of variable properties on h, we must select reference states for h^* and $c_{p,i}$. Both h^* and $c_{p,i}$ must be evaluated at

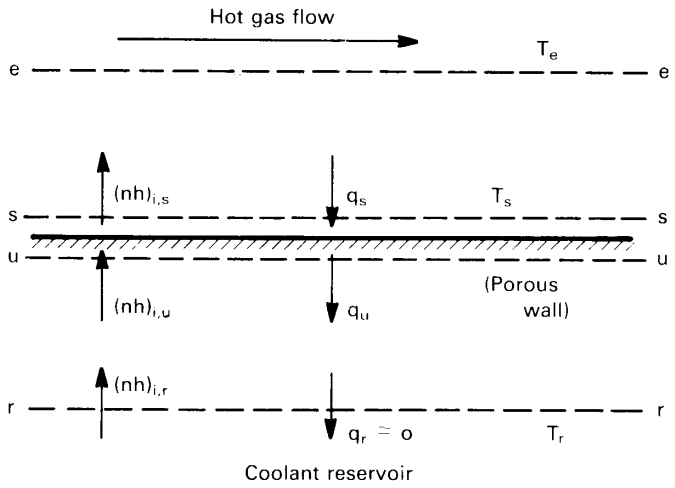

Figure 11.20 Transpiration cooling.

the film temperature, and $c_{p,i}$ is independent of composition. However, the heat transfer coefficient at zero mass transfer, h^*, occurs in the limit as $n_{i,s}$ goes to zero. In this limit, there are no concentration gradients in the stagnant film and the film has the composition of the free stream. Thus, h^* is best approximated at the film temperature and free stream composition.

Energy balances in simultaneous heat and mass transfer

To calculate simultaneous heat and mass transfer rates, one must generally look at the energy balance below the wall as well as across the boundary layer. Consider, for example, the process of *transpiration cooling*, shown in Fig. 11.20. Here a wall exposed to high temperature gases is protected by injecting a cooler gas into the flow through a porous section of the surface. A portion of the heat transfer to the wall is taken up in raising the temperature (or, more specifically, the enthalpy) of the transpired gas, and blowing serves to reduce h below h^* as well. This process is frequently used to cool turbine blades and combustion chamber walls.

Let us construct an energy balance for a steady state in which the wall has reached a temperature T_s. The enthalpy and heat fluxes are as shown in Fig. 11.20. We take the coolant reservoir to be far enough back from the surface that temperature gradients at the r-surface are negligible and the conductive heat flux, q_r, is zero. An energy balance between the r-

and u-surfaces gives

$$n_{i,r}h_{i,r} = n_{i,u}h_{i,u} - q_u \tag{11.108}$$

and between the u- and s-surfaces,

$$n_{i,u}h_{i,u} - q_u = n_{i,s}h_{i,s} - q_s \tag{11.109}$$

Since there is no change in the enthalpy of the transpired species when it passes through the interface,

$$h_{i,u} = h_{i,s} \tag{11.110}$$

and since the process is steady, conservation of mass gives

$$n_{i,r} = n_{i,u} = n_{i,s} \tag{11.111}$$

Thus, eqn. (11.109) reduces to

$$q_s = q_u \tag{11.112}$$

The flux q_u is merely the conductive heat flux into the wall, while q_s is the convective heat transfer,

$$q_s = h(T_e - T_s) \tag{11.113}$$

(The reader should take care to distinguish the heat transfer coefficient, h, from the enthalpy, h_i.)

Combining eqns. (11.108) through (11.113), we find

$$n_{i,s}(h_{i,s} - h_{i,r}) = h(T_e - T_s) \tag{11.114}$$

This equation shows that, at steady state, the heat convection to the wall is absorbed by the enthalpy rise of the transpired gas. Writing the enthalpy as $h_i = c_{p,i}(T_s - T_{\text{ref}})$, we obtain

$$n_{i,s}c_{p,i}(T_s - T_r) = h(T_e - T_s) \tag{11.115}$$

or

$$T_s = \frac{hT_e + n_{i,s}c_{p,i}T_r}{h + n_{i,s}c_{p,i}} \tag{11.116}$$

It is left as an exercise (Problem 11.46) to show that

$$T_s = T_r + (T_e - T_r)\exp(-n_{i,s}c_{p,i}/h^*) \tag{11.117}$$

The wall temperature decreases exponentially to T_r as the mass flux of the transpired gas increases. Transpiration cooling is also enhanced by injecting a gas with a high specific heat.

A common variant of this process is *sweat cooling*, in which a *liquid* is bled through the porous wall. The liquid is vaporized by convective heat flow to the wall, and the latent heat of vaporization acts as a sink. Figure 11.20 also represents this process. The balances, eqns. (11.108) and (11.109), as well as mass conservation, eqn. (11.111), still apply. However, the enthalpies at the interface now differ by the latent heat of vaporization:

$$h_{i,u} + h_{fg} = h_{i,s} \tag{11.118}$$

Thus, eqn. (11.112) becomes

$$q_s = q_u + h_{fg} n_{i,s}$$

and eqn. (11.114) takes the form

$$n_{i,s}[h_{fg} + c_{p,i_f}(T_s - T_r)] = h(T_e - T_s) \tag{11.119}$$

where c_{p,i_f} is the specific heat of *liquid i*. Since the latent heat is generally much larger than the sensible heat, eqn. (11.119) reflects the greater efficiency of sweat cooling as compared to transpiration cooling.

When the rate of mass transfer is small, we approximate h by h^*, just as we approximated g_m by g_m^* at low mass transfer rates. The approximation $h = h^*$ may be tested by considering the ratio $n_{i,s}c_{p,i}/h^*$ in eqn. (11.107). For example, if $n_{i,s}c_{p,i}/h^* = 0.06$, then $h/h^* = 0.97$, and $h = h^*$ within an error of only 3 percent. One common situation in which heat and mass transfer rates are given by low-rate approximations is the evaporation of water into air at low or moderate temperatures, as in the following example.

Example 11.14

The humidity of air is commonly measured with a *sling psychrometer*. A wet cloth is wrapped about the bulb of one thermometer, as shown in Fig. 11.21. This so-called *wet-bulb* thermometer is mounted, along with a second *dry-bulb* thermometer, on a swivel handle, and the pair are "slung" in a rotary motion until they reach steady state.

The wet-bulb thermometer is cooled, as the latent heat of the vaporized water is given up, until it reaches the temperature at which

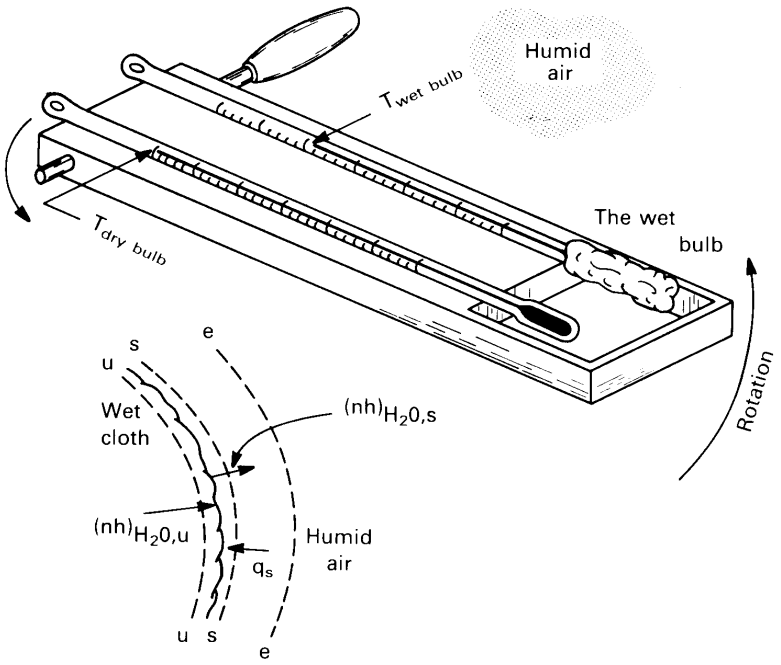

Figure 11.21 The wet bulb of a sling psychrometer.

the rate of cooling by evaporation just balances the rate of convective heating by the warmer air. This temperature, which is called the *wet-bulb temperature*, is directly related to the amount of water in the surrounding air.[9]

Find the relationship between the wet-bulb temperature and the amount of water in the ambient air.

SOLUTION. The highest air temperatures likely to be encountered in meteorological practice are fairly low, so the rate of mass transfer should be small. We can test this suggestion by choosing a situation that should maximize the evaporation rate—say, ambient air at a high temperature of 120°F and bone-dry air ($m_{H_2O,e} = 0$)—and then computing the resulting value of the blowing factor as an upper bound:

$$x_{H_2O} \lesssim p_{sat}(120°F)/1\ \text{atm} = 0.115$$

[9]The wet-bulb temperature for air–water systems is very nearly the *adiabatic saturation temperature* of the air–water mixture. This is the temperature reached by the mixture if it is brought to saturation with water by adding water vapor without adding heat. It is a thermodynamic property of an air–water combination.

so

$$m_{\mathrm{H_2O},s} \lesssim 0.0750$$

Thus,

$$B_{m,\mathrm{H_2O}} \lesssim 0.0811$$

and

$$\left[1 - \frac{\ln(1 + B_{m,\mathrm{H_2O}})}{B_{m,\mathrm{H_2O}}}\right] \lesssim 0.038$$

This means that under the worst normal circumstances, the low-rate theory should deviate by only 4 percent from the actual rate of evaporation. We assume that this estimate holds for the heat transfer as well, although this assumption must be tested *a posteriori* by computing $n_{\mathrm{H_2O},s} c_{p,\mathrm{H_2O}}/h^*$.

There is no heat flux through the u-surface once it reaches the wet-bulb temperature, so the energy balance between the u- and s-surfaces is

$$n_{\mathrm{H_2O},s} h_{\mathrm{H_2O},s} - q_s = n_{\mathrm{H_2O},u} h_{\mathrm{H_2O},u}$$

or

$$n_{\mathrm{H_2O},s} h_{fg}|_{T_{\text{wet-bulb}}} = h(T_e - T_{\text{wet-bulb}})$$

Since low rates are indicated, this can be written as

$$g^*_{m,\mathrm{H_2O}} B_{m,\mathrm{H_2O}} h_{fg}|_{T_{\text{wet-bulb}}} = h^*(T_e - T_{\text{wet-bulb}}) \tag{11.120}$$

Since the transfer coefficients depend on the geometry and flow rates of the psychrometer, it would appear that $T_{\text{wet-bulb}}$ should depend on the device used to measure it. However, we can use the analogy between heat and mass transfer and results given in Chapter 7 to write

$$\frac{h^* D}{k} = C\ \mathrm{Re}^a \mathrm{Pr}^b$$

and

$$\frac{g^*_m D}{\rho \mathcal{D}_{12}} = C\ \mathrm{Re}^a \mathrm{Sc}^b$$

where C is a constant, $a \cong 1/2$, and $b \cong 1/3$. Thus,

$$\frac{h^*}{g_m^* c_p}\frac{\mathcal{D}_{12}}{\alpha} = \left(\frac{\mathrm{Pr}}{\mathrm{Sc}}\right)^b$$

Both $\alpha/\mathcal{D}_{12}$ and Sc/Pr are equal to the Lewis number, Le. Hence,

$$\frac{h^*}{g_m^* c_p} = \mathrm{Le}^{1-b} \cong \mathrm{Le}^{2/3} \tag{11.121}$$

This type of relationship between h^* and g_m^* was first developed by W. K. Lewis in 1922 for the case in which Le = 1 [11.25]. (The Lewis number for air–water systems, Lewis's primary interest, is about 0.847, so the approximation was not too bad.) The more general form, eqn. (11.121), is another Reynolds-Colburn type of analogy, similar to eqn. (6.75), which was subsequently given by Chilton and Colburn [11.26] in 1934. Equation (11.121) shows that the ratio of h^* to g_m^* depends primarily on the physical properties of the mixture, rather than the geometry or flow rate.

Equation (11.120) can now be written as

$$\frac{\mathrm{Le}^{-2/3}}{c_p} h_{fg}\Big|_{T_{\text{wet-bulb}}} B_{m,\mathrm{H_2O}} = T_e - T_{\text{wet-bulb}} \tag{11.122}$$

This expression can be solved iteratively with a steam table to obtain the wet-bulb temperature as a function of the dry-bulb temperature, T_e, and the humidity of the air, $m_{\mathrm{H_2O},e}$. The psychrometric charts found in engineering handbooks and thermodynamics texts may be generated in this way. We ask the reader to make such calculations in Problem 11.48. ■

The wet-bulb temperature is a helpful concept in many phase-change processes. When a body (without internal heat sources) evaporates or sublimes, it approaches a "wet-bulb" temperature at which convective heating is balanced by latent heat removal; and it will stay at that temperature until the phase-change process is complete. Thus, the wet-bulb temperature appears in the evaporation of water droplets, the sublimation of dry ice, the combustion of fuel sprays, and so on.

Thermal radiation and chemical reactions

If significant thermal radiation falls on the surface through which mass is transferred, the energy balances must account for this additional heat

flux. For example, suppose that thermal radiation were present during transpiration cooling. Radiant heat flux, $q_{\text{rad},e}$, originating above the e-surface would be absorbed *below* the u-surface.[10] Thus, eqn. (11.108) becomes

$$n_{i,r}h_{i,r} = n_{i,u}h_{i,u} - q_u - \alpha q_{\text{rad},e} \tag{11.123}$$

while eqn. (11.109) is unchanged. Similarly, thermal radiation emitted by the wall is taken to originate below the u-surface, so eqn. (11.123) is now

$$n_{i,r}h_{i,r} = n_{i,u}h_{i,u} - q_u - \alpha q_{\text{rad},e} + q_{\text{rad},u} \tag{11.124}$$

or, since reflected radiation has little effect on the balance,

$$n_{i,r}h_{i,r} = n_{i,u}h_{i,u} - q_u - (H - B) \tag{11.125}$$

for an opaque surface (where H and B are defined in Section 10.4).

The heat and mass transfer analyses in this section and Section 11.7 require that the transferred species undergo no homogeneous reactions. If the species do enter into reactions in the medium through which they are transferred, the mass balances of Section 11.7 are invalid, because the mass flux of a reacting species will vary across the region of reaction. Likewise, the energy balance of this section will fail because it does not include the heat of reaction. The energy analysis may be correctly stated by leaving eqn. (11.102) in terms of enthalpy and including each species transferred in the reacting medium. Correction of the mass transfer analysis is far more involved.

For heterogeneous reactions, the complications are not so severe. Reactions at the boundaries require that we incorporate the heat of reaction released between the s- and u-surfaces and the proper stoichiometry of the fluxes to and from the surface. The heat transfer coefficient [eqn. (11.107)] must also be modified to account for the transfer of more than one species. All of these considerations become important in the study of combustion, which is another intriguing arena of mass transfer theory.

[10] Remember that the s- and u-surfaces are fictitious elements of the enthalpy balances at the phase interface. The apparent space between them need be only a few molecules thick. Thermal radiation is therefore absorbed below the u-surface.

Problems

11.1 Derive: (a) eqns. (11.8); (b) eqns. (11.9).

11.2 A 1000 liter cylinder at 300 K contains a gaseous mixture composed of 0.10 kmol of NH_3, 0.04 kmol of CO_2, and 0.06 kmol of He. (a) Find the mass fraction for each species and the pressure in the cylinder. (b) After the cylinder is heated to 600 K, what are the new mole fractions, mass fractions, and molar concentrations? (c) The cylinder is now compressed isothermally to a volume of 600 liters. What are the molar concentrations, mass fractions, and partial densities? (d) If 0.40 kg of gaseous N_2 is injected into the cylinder while the temperature remains at 600 K, find the mole fractions, mass fractions, and molar concentrations. [(a) $m_{CO_2} = 0.475$; (c) $c_{CO_2} = 0.0667$ kmol/m^3; (d) $x_{CO_2} = 0.187$.]

11.3 Planetary atmospheres show significant variations of temperature and pressure in the vertical direction. Observations suggest that the atmosphere of Jupiter has the following composition at the tropopause level:

$$\begin{aligned}
\text{number density of } H_2 &= 5.7 \times 10^{21} \text{ (molecules/m}^3\text{)} \\
\text{number density of He} &= 7.2 \times 10^{20} \text{ (molecules/m}^3\text{)} \\
\text{number density of } CH_4 &= 6.5 \times 10^{18} \text{ (molecules/m}^3\text{)} \\
\text{number density of } NH_3 &= 1.3 \times 10^{18} \text{ (molecules/m}^3\text{)}
\end{aligned}$$

Find the mole fraction and partial density of each species at this level if $p = 0.1$ atm and $T = 113$ K. Estimate the number densities at the level where $p = 10$ atm and $T = 400$ K, deeper within the Jovian troposphere. (Deeper in the Jupiter's atmosphere, the pressure may exceed 10^5 atm.)

11.4 Using the definitions of the fluxes, velocities, and concentrations, derive eqn. (11.35) from eqn. (11.28) for *binary* diffusion.

11.5 Show that $\mathcal{D}_{12} = \mathcal{D}_{21}$ in a binary mixture.

11.6 Fill in the details involved in obtaining eqn. (11.32) from eqn. (11.31).

11.7 Batteries commonly contain an aqueous solution of sulfuric acid with lead plates as electrodes. Current is generated by

the reaction of the electrolyte with the electrode material. At the negative electrode, the reaction is

$$\mathrm{Pb}(s) + \mathrm{SO}_4^{2-} \rightleftharpoons \mathrm{PbSO}_4(s) + 2e^-$$

where the (s) denotes a solid phase component and the charge of an electron is -1.609×10^{-19} coulombs. If the current density at such an electrode is $J = 5$ milliamperes/cm^2, what is the mole flux of SO_4^{2-} to the electrode? (1 amp =1 coulomb/s.) What is the mass flux of SO_4^{2-}? At what mass rate is PbSO_4 produced? If the electrolyte is to remain electrically neutral, at what rate does H^+ flow toward the electrode? Hydrogen does not react at the negative electrode. [$\dot{m}''_{\mathrm{PbSO}_4} = 7.83 \times 10^{-5}$ kg/m$^2\cdot$s.]

11.8 The salt concentration in the ocean increases with increasing depth, z. A model for the concentration distribution in the upper ocean is

$$S = 33.25 + 0.75 \tanh(0.026z - 3.7)$$

where S is the salinity in grams of salt per kilogram of ocean water and z is the distance below the surface in meters. (a) Plot the mass fraction of salt as a function of z. (The region of rapid transition of $m_{\mathrm{salt}}(z)$ is called the *halocline*.) (b) Ignoring the effects of waves or currents, compute $j_{\mathrm{salt}}(z)$. Use a value of $\mathcal{D}_{\mathrm{salt,water}} = 1.5 \times 10^{-5}$ cm^2/s. Indicate the position of maximum diffusion on your plot of the salt concentration. (c) The upper region of the ocean is well mixed by wind-driven waves and turbulence, while the lower region and halocline tend to be calmer. Using $j_{\mathrm{salt}}(z)$ from part (b), make a simple estimate of the amount of salt carried upward in one week in a 5 km^2 horizontal area of the sea.

11.9 In *catalysis*, one gaseous species reacts with another on a passive surface (the catalyst) to form a gaseous product. For example, butane reacts with hydrogen on the surface of a nickel catalyst to form methane and propane. This heterogeneous reaction, referred to as *hydrogenolysis*, is

$$\mathrm{C_4H_{10}} + \mathrm{H_2} \xrightarrow{\mathrm{Ni}} \mathrm{C_3H_8} + \mathrm{CH_4}$$

The molar rate of consumption of C_4H_{10} per unit area in the reaction is $\dot{R}_{C_4H_{10}} = A(e^{-\Delta E/R^\circ T})p_{C_4H_{10}}p_{H_2}^{-2.4}$, where $A = 6.3 \times 10^{10}$ kmol/m^2·s, $\Delta E = 1.9 \times 10^8$ J/kmol, and p is in atm. (a) If $p_{C_4H_{10},s} = p_{C_3H_8,s} = 0.2$ atm, $p_{CH_4,s} = 0.17$ atm, and $p_{H_2,s} = 0.3$ atm at a nickel surface with conditions of 440°C and 0.87 atm total pressure, what is the rate of consumption of butane? (b) What are the mole fluxes of butane and hydrogen to the surface? What are the mass fluxes of propane and ethane away from the surface? (c) What is $\dot{m}''$? What are v, v^*, and $v_{C_4H_{10}}$? (d) What is the diffusional mole flux of butane? What is the diffusional mass flux of propane? What is the flux of Ni? [(b) $n_{CH_4,s} = 0.0441$ kg/m^2·s; (d) $j_{C_3H_8} = 0.121$ kg/m^2·s.]

11.10 Consider two chambers held at temperatures T_1 and T_2, respectively, and joined by a small insulated tube. The chambers are filled with a binary gas mixture, with the tube open, and allowed to come to steady state. If the Soret effect is taken into account, what is the concentration difference between the two chambers? Assume that an effective mean value of the thermal diffusion ratio is known.

11.11 Compute $\mathcal{D}_{12}$ for oxygen gas diffusing through nitrogen gas at $p = 1$ atm, using eqns. (11.39) and (11.42), for $T = 200$ K, 500 K, and 1000 K. Observe that eqn. (11.39) shows large deviations from eqn. (11.42), even for such simple and similar molecules.

11.12 (a) Compute the binary diffusivity of each of the noble gases when they are individually mixed with nitrogen gas at 1 atm and 300 K. Plot the results as a function of the molecular weight of the noble gas. What do you conclude? (b) Consider the addition of a small amount of helium ($x_{He} = 0.04$) to a mixture of nitrogen ($x_{N_2} = 0.48$) and argon ($x_{Ar} = 0.48$). Compute $\mathcal{D}_{He,m}$ and compare it with $\mathcal{D}_{Ar,m}$. Note that the higher concentration of argon does not improve its ability to diffuse through the mixture.

11.13 (a) One particular correlation shows that gas phase diffusion coefficients vary as $T^{1.81}$ and p^{-1}. If an experimental value of $\mathcal{D}_{12}$ is known at T_1 and p_1, develop an equation to predict $\mathcal{D}_{12}$ at T_2 and p_2. (b) The diffusivity of water vapor (1) in air (2) was

measured to be 2.39×10^{-5} m^2/s at 8°C and 1 atm. Provide a formula for $\mathcal{D}_{12}(T, p)$.

11.14 Kinetic arguments lead to the *Stefan-Maxwell equation* for a dilute-gas mixture:

$$\nabla x_i = \sum_{j=1}^{n} \frac{c_i c_j}{c^2 \mathcal{D}_{ij}} \left(\frac{\vec{J}_j^*}{c_j} - \frac{\vec{J}_i^*}{c_i} \right)$$

(a) Derive eqn. (11.44) from this, making the appropriate assumptions. (b) Show that if $\mathcal{D}_{ij}$ has the same value for each pair of species, then $\mathcal{D}_{im} = \mathcal{D}_{ij}$.

11.15 Compute the diffusivity of methane in air using (a) eqn. (11.42) and (b) Blanc's law. For part (b), treat air as a mixture of oxygen and nitrogen, ignoring argon. Let $x_{\text{methane}} = 0.05$, $T = 420$°F, and $p = 10$ psia. [(a) $\mathcal{D}_{CH_4,\text{air}} = 7.66 \times 10^{-5}$ m^2/s; (b) $\mathcal{D}_{CH_4,\text{air}} = 8.13 \times 10^{-5}$ m^2/s.]

11.16 Diffusion of solutes in liquids is driven by the chemical potential, μ. Work is required to move a mole of solute A from a region of low chemical potential to a region of high chemical potential; that is,

$$dW = d\mu_A = \frac{d\mu_A}{dx}\, dx$$

under isothermal, isobaric conditions. For an ideal (very dilute) solute, μ_A is given by

$$\mu_A = \mu_0 + R^\circ T \ln(c_A)$$

where μ_0 is a constant. Using an elementary principle of mechanics, derive the Nernst-Einstein equation. Note that the solution must be assumed to be very dilute.

11.17 A dilute aqueous solution at 300 K contains potassium ions, K^+. If the velocity of aqueous K^+ ions is 6.61×10^{-4} cm^2/s·V per unit electric field (1 V/cm), estimate the effective radius of K^+ ions in an aqueous solution. Criticize this estimate. (The charge of an electron is -1.609×10^{-19} coulomb and a volt = 1J/coulomb.)

11.18 (a) Obtain diffusion coefficients for: (1) dilute CCl_4 diffusing through liquid methanol at 340 K; (2) dilute benzene diffusing through water at 290 K; (3) dilute ethyl alcohol diffusing through water at 350 K; and (4) dilute acetone diffusing through methanol at 370 K. (b) Estimate the effective radius of a methanol molecule in a dilute aqueous solution. [(a) $\mathcal{D}_{\text{acetone,methanol}} = 6.8 \times 10^{-9}$ m^2/s.]

11.19 If possible, calculate values of the viscosity, μ, for methane, hydrogen sulfide, and nitrous oxide, under the following conditions: 250 K and 1 atm, 500 K and 1 atm, 250 K and 2 atm, 250 K and 12 atm, 500 K and 12 atm.

11.20 (a) Show that $k = (5/2)\mu c_v$ for a monatomic gas. (b) Obtain Eucken's formula for the Prandtl number of a dilute gas:

$$\text{Pr} = 4\gamma/(9\gamma - 5)$$

(c) Recall that for an ideal gas, $\gamma \cong (D + 2)/D$, where D is the number of modes of energy storage of its molecules. Obtain an expression for Pr as a function of D and describe what it means. (d) Use Eucken's formula to compute Pr for gaseous Ar, N_2, and H_2O. Compare the result to data in Appendix A over the range of temperatures. Explain the results obtained for steam as opposed to Ar and N_2. (Note that for each mode of vibration, there are two modes of energy storage but that vibration is normally inactive until T is very high.)

11.21 A student is studying the combustion of a premixed gaseous fuel with the following molar composition: 10.3% methane, 15.4% ethane, and 74.3% oxygen. She passes 0.006 ft^3/s of the mixture (at 70°F and 18 psia) through a smooth 3/8 inch I.D. tube, 47 inches long. (a) What is the pressure drop? (b) The student's advisor recommends preheating the fuel mixture, using a Nichrome strip heater wrapped around the last 5 inches of the duct. If the heater produces 0.8 W/inch, what is the wall temperature at the outlet of the duct? Let $c_{p,\text{CH}_4} = 2280$ J/kg·K, $\gamma_{\text{CH}_4} = 1.3$, $c_{p,\text{C}_2\text{H}_6} = 1730$ J/kg·K, and $\gamma_{\text{C}_2\text{H}_6} = 1.2$, and evaluate the properties at the inlet conditions.

11.22 (a) Work Problem 6.36. (b) A fluid is said to be incompressible if the density of a fluid particle does not change as it moves about

in the flow (i.e., if $D\rho/Dt = 0$). Show that an incompressible flow satisfies $\nabla \cdot \vec{u} = 0$. (c) How does the condition of incompressibility differ from that of "constant density"? Describe a flow that is incompressible but that does not have "constant density."

11.23 Carefully derive eqns. (11.62) and (11.63). Note that ρ is not assumed constant in eqn. (11.62).

11.24 Derive the equation of species conservation on a molar basis, using c_i rather than ρ_i. Also obtain an equation in c_i alone, similar to eqn. (11.63) but without the assumption of incompressibility. What assumptions must be made to obtain the latter result?

11.25 Find the following concentrations: (a) the mole fraction of air in solution with water at 5°C and 1 atm, exposed to air at the same conditions, $H = 4.88 \times 10^4$ atm; (b) the mole fraction of ammonia in air above an aqueous solution, with $x_{NH_3} = 0.05$ at 0.9 atm and 40°C and $H = 1522$ mm Hg; (c) the mole fraction of SO_2 in an aqueous solution at 15°C and 1 atm, if $p_{SO_2} = 28.0$ mm Hg and $H = 1.42 \times 10^4$ mm Hg; and (d) the partial pressure of ethylene over an aqueous solution at 25°C and 1 atm, with $x_{C_2H_4} = 1.75 \times 10^{-5}$ and $H = 11.4 \times 10^3$ atm.

11.26 Use a steam table to estimate (a) the mass fraction of water vapor in air over water at 1 atm and 20°C, 50°C, 70°C, and 90°C; (b) the partial pressure of water over a 3 percent-by-weight aqueous solution of HCl at 50°C; (c) the boiling point at 1 atm of salt water with a mass fraction $m_{NaCl} = 0.18$. [(c) $T_{B.P.} = 101.8$°C.]

11.27 A large copper fitting is plated with a layer of nickel. Suppose that the interface conditions are such that the concentration of nickel within the copper at the interface, $m_{Ni,u}$, is 0.02. The plated fitting is to be used in a high-temperature environment. The diffusivity of nickel in copper is

$$\mathcal{D}_{Ni,Cu} = (1.1 \text{ cm}^2/\text{s}) \exp\left[-(2.25 \times 10^8 \text{ J/kmol})/R^\circ T\right]$$

between 620°C and 1080°C, where T is in K. Estimate the concentration of nickel at a depth of 2 mm below the surface of

the copper after 2 years at each of the following temperatures: 650°C, 800°C, and 950°C.

11.28 (a) Write eqn. (11.68a) and the b.c.'s in terms of a nondimensional mass fraction, ψ, analogous to the dimensionless temperature in eqn. (6.42). (b) For $\nu = \mathcal{D}_{im}$, relate ψ to the Blasius function, f, for flow over a flat plate. (c) Note the similar roles of Pr and Sc in the two boundary layer transport processes. Infer the mass concentration analog of eqn. (6.55) and sketch the concentration and momentum b.l. profiles for $\mathrm{Sc} \ll 1$, $\mathrm{Sc} = 1$, and $\mathrm{Sc} \gg 1$.

11.29 When Sc is large, momentum diffuses more easily than mass, and the concentration b.l. thickness, δ_c, is much less than the momentum b.l. thickness, δ. On a flat plate, the small part of the velocity profile within the concentration b.l. is approximately $u/U_e = 3y/2\delta$. Compute $\mathrm{Nu}_{m,x}$ based on this velocity profile, assuming a constant wall concentration. (*Hint*: Use the mass transfer analogs of eqn. (6.47) and (6.50) and note that $q_w/\rho c_p$ becomes $j_{i,s}/\rho$.).

11.30 Consider a one-dimensional, binary gaseous diffusion process in which species 1 and 2 diffuse in opposite directions along the z-axis at equal molar rates. This process is known as *equimolar counter-diffusion*. (a) What are the relations between N_1, N_2, J_1^*, and J_2^*? (b) If steady state prevails and conditions are isothermal and isobaric, what is the concentration of species 1 as a function of z? (c) Write the mole flux in terms of the difference in partial pressure of species 1 between locations z_1 and z_2.

11.31 Consider steady mass diffusion from a small sphere. When convection is negligible, the mass flux in the radial direction is $n_{r,i} = j_{r,i} = -\rho\mathcal{D}_{im}dm_i/dr$. If the concentration is $m_{i,\infty}$ far from the sphere and $m_{i,s}$ at its surface, use a mass balance to obtain the surface mass flux in terms of the overall concentration difference (assuming that $\rho\mathcal{D}_{im}$ is constant). Then apply the definition eqns. (11.85) and (11.97) to show that $\mathrm{Nu}_{m,D} = 2$ for this situation.

11.32 An experimental Stefan tube is 6 cm in diameter and 30 cm from the liquid surface to the top. It is held at 10°C and 8.0×10^4 Pa. Pure argon flows over the top and liquid CCl_4 is at the

bottom. The pool level is maintained while 0.69 ml of liquid CCl_4 evaporates during a period of 8 hours. What is the diffusivity of carbon tetrachloride in argon measured under these conditions? The specific gravity of liquid CCl_4 is 1.59 and its vapor pressure is $\log_{10} p_v = 8.004 - 1771/T$, where p_v is expressed in mm Hg and T in K.

11.33 Repeat the analysis given in Section 11.6 on the basis of *mass* fluxes, assuming that $\rho\mathcal{D}_{im}$ is constant and neglecting any buoyancy-driven convection. Obtain the analog of eqn. (11.79).

11.34 In Sections 11.5 and 11.6, it was assumed at points that $c\mathcal{D}_{12}$ or $\rho\mathcal{D}_{12}$ was independent of position. (a) If the mixture composition (e.g., x_1) varies in space, this assumption may be poor. Using eqn. (11.42) and the definitions from Section 11.2, examine the composition dependence of these two groups. For what type of mixture is $\rho\mathcal{D}_{12}$ most sensitive to composition? What does this indicate about molar versus mass-based analysis? (b) How do each of these groups depend on pressure and temperature? Is the analysis of Section 11.6 really limited to isobaric conditions? (c) Do the Prandtl and Schmidt numbers depend on composition, temperature, or pressure?

11.35 A Stefan tube contains liquid bromine at 320 K and 1.2 atm. Carbon dioxide flows over the top and is also bubbled up through the liquid at the rate of 40 ml/hr. If the distance from the liquid surface to the top is 16 cm and the diameter is 3 cm, what is the evaporation rate of Br_2? ($p_{\text{sat},Br_2} = 0.680$ bar at 320 K.) [$N_{Br_2,s} = 1.90 \times 10^{-6}$ kmol/m$^2\cdot$s.]

11.36 Show that $g_{m,1} = g_{m,2}$ and $B_{m,1} = B_{m,2}$ in a binary mixture.

11.37 Demonstrate that stagnant film models of the momentum and thermal boundary layers reproduce the proper dependence of $C_{f,x}$ and Nu_x on Re_x and Pr. Using eqns. (6.31) and (6.55) to obtain the dependence of δ and δ_t on Re_x and Pr, show that stagnant film models gives eqns. (6.33) and (6.58) within a constant on the order of unity. [The constants in these results will differ from the exact results because the effective b.l. thicknesses of the stagnant film model are not the same as the exact values—see eqn. (6.57).]

11.38 (a) What is the largest value of the mass transfer driving force when one species is transferred? What is the smallest value? (b) Plot the blowing factor as a function of $B_{m,i}$ for one species transferred. Indicate on your graph the regions of blowing, suction, and low-rate mass transfer. (c) Verify the two limits used to show that $g^*_{m,i} = \rho \mathcal{D}_{im}/\delta_c$.

11.39 Nitrous oxide is bled through the surface of a porous 3/8 in. O.D. tube at 0.025 liter/s per meter of tube length. Air flows over the tube at 25 ft/s. Both the air and the tube are at 18°C, and the ambient pressure is 1 atm. Estimate the mean concentration of N_2O at the tube surface. (*Hint*: First estimate the concentration using properties of pure air; then correct the properties if necessary.)

11.40 Gases are sometimes absorbed into liquids through *film absorbtion*. A thin film of liquid is run down the inside of a vertical tube through which flows the gas to be absorbed. Analyze this process under the following assumptions: The film flow is laminar and of constant thickness, δ_0, with a velocity profile given by eqn. (8.47). The gas is only slightly soluble in the liquid, so that it does not penetrate far beyond the liquid surface and so that liquid properties are unaffected by it. The gas concentration at the s- and u-surfaces does not vary along the length of the tube. The inlet concentration of gas in the liquid is $m_{1,0}$. Show that the mass transfer is given by

$$\mathrm{Nu}_{m,x} = \left(\frac{u_0 x}{\pi \mathcal{D}_{12}}\right)^{1/2} \quad \text{with} \quad u_0 = \frac{(\rho_f - \rho_g) g \delta_0^2}{2\mu_f}$$

The mass transfer coefficient here is based on the concentration difference between the u-surface and the bulk liquid at $m_{1,0}$ (*Hint*: The small penetration assumption can be used to reduce the species equation for the film to the diffusion equation, eqn. (11.66).)

11.41 Benzene vapor flows through a 3 cm I.D. vertical tube. A thin film of initially pure water runs down the inside wall of the tube at a flow rate of 0.3 liter/s. If the tube is 0.5 m long and 40°C, estimate the rate (in kg/s) at which benzene is absorbed into water over the entire length of the tube. The mass fraction of

benzene at the u-surface is 0.206. (*Hint*: Use the result stated in Problem 11.40. Obtain δ_0 from the results in Chapter 8.)

11.42 A certain commercial mothball consists of a 1.0 inch diameter sphere of naphthalene ($C_{10}H_8$) that is hung by a wire in the closet. The solid naphthalene slowly sublimates to vapor, which drives off the moths. What is the lifetime of this mothball in a closet with a mean temperature of 68°F? Use the following data:

$$\sigma = 618 \text{ Å}, \qquad \varepsilon/k_B = 561.5 \text{ K} \quad \text{for} \quad C_{10}H_8,$$

and, for solid naphthalene,

$$\rho_{C_{10}H_8} = 71.47 \text{ lb}_m/\text{ft}^3 \text{ at } 68°\text{F}$$

The vapor pressure (in mm Hg) of solid naphthalene is given approximately by $\log_{10} p_v = 11.450 - 3729.3/(T \text{ K})$. The latent heat of sublimation and evaporation rate are low enough that the wet-bulb temperature is essentially the ambient temperature. Evaluate the integral you obtain numerically.

11.43 Consider the process of catalysis as described in Problem 11.9. The mass transfer process involved is the diffusion of the reactants to the surface and diffusion of products away from it. (a) What is $\dot{m}''$ in catalysis? (b) Reaction rates in catalysis are of the form:

$$\dot{R}_{\text{reactant}} = A\, e^{-\Delta E/R^\circ T} (p_{\text{reactant}})^n (p_{\text{product}})^m \text{ kmol/m}^2\cdot\text{s}$$

for the rate of consumption of a reactant per unit surface area. The p's are partial pressures and A, ΔE, n, and m are constants. Suppose that $n = 1$ and $m = 0$ for the reaction $B + C \longrightarrow D$. Approximate the reaction rate, in terms of mass, as

$$\dot{r}_B = A' e^{-\Delta E/R^\circ T} \rho_{B,s} \text{ kg/m}^2\cdot\text{s}$$

and find the rate of consumption of B in terms of $m_{B,e}$ and the mass transfer coefficient for the geometry in question. (c) The ratio $\text{Da} \equiv \rho A' e^{-\Delta E/R^\circ T}/g_m^*$ is called the *Damkohler number*. Explain its significance in catalysis. What features dominate the process when Da approaches 0 or ∞? What temperature range characterizes each?

11.44 One typical kind of mass exchanger is a fixed-bed catalytic reactor. A flow chamber of length L is packed with a catalyst bed. A gas mixture containing some species i to be consumed by the catalytic reaction flows through the bed at a rate $\dot{m}$. The effectiveness of such a exchanger (cf. Chapter 3) is

$$\varepsilon = 1 - e^{-\text{NTU}}, \quad \text{where NTU} = g_{m,\text{oa}} PL/\dot{m}$$

where $g_{m,\text{oa}}$ is the overall mass transfer coefficient for the catalytic packing, P is the surface area per unit length, and ε is defined in terms of mass fractions. In testing a 0.5 m catalytic reactor for the removal of ethane, it is found that the ethane concentration drops from a mass fraction of 0.36 to 0.05 at a flow rate of 0.05 kg/s. The packing is known to have a surface area of 11 m^2. What is the exchanger effectiveness? What is the overall mass transfer coefficient in this bed?

11.45 (a) Perform the integration to obtain eqn. (11.104). Then take the derivative and the limit needed to get eqns. (11.105) and (11.106). (b) What is the general form of eqn. (11.107) when more than one species is transferred?

11.46 (a) Derive eqn. (11.117) from eqn. (11.116). (b) Suppose that 1.5 m^2 of the wing of a spacecraft re-entering the earth's atmosphere is to be cooled by transpiration; 900 kg of the vehicle's weight is allocated for this purpose. The low-rate heat transfer coefficient is about 1800 $W/m^2 \cdot K$ in the region of interest, and the hottest portion of re-entry is expected to last 3 minutes. If the air behind the shock wave ahead of the wing is at 2500°C and the reservior is at 5°C , which of these gases—H_2, He, and N_2—keeps the surface coolest? (Of course, the result for H_2 is invalidated by the fact that H_2 would burn under these conditions.)

11.47 Dry ice (solid CO_2) is used to cool medical supplies transported by a small plane to a remote village in Alaska. A roughly spherical chunk of dry ice, 5 cm in diameter, falls from the plane through air at 5°C with a terminal velocity of 15 m/s. If steady state is reached quickly, what are the temperature and sublimation rate of the dry ice? The latent heat of sublimation is 574 kJ/kg and $\log_{10} p_v(\text{mm Hg}) = 9.9082 - 1367.3/\text{T K}$. The

temperature will be well below the "sublimation point" of CO_2, which is $-78.6°C$ at 1 atm. Use the heat transfer relation for spheres in a laminar flow, $\overline{\mathrm{Nu}}_D = 2 + 0.3\,\mathrm{Re}_D^{0.6}\,\mathrm{Pr}^{1/3}$. (*Hint*: first estimate the surface temperature using properties for pure air; then correct the properties as necessary.)

11.48 The following data were taken at a weather station over a period of several months:

Date	$T_{\text{dry-bulb}}$	$T_{\text{wet-bulb}}$
3/15	15.5°C	11.0°C
4/21	22.0	16.8
5/13	27.3	25.8
5/31	32.7	20.0
7/4	39.0	31.2

Use eqn. (11.122) to find the mass fraction of water in the air at each date. Compare these values to values obtained using a psychrometric chart.

11.49 Biff Harwell has taken Deb sailing. Deb, and Biff's towel, fall into the harbor. Biff rescues them both from a passing dolphin and then spreads his wet towel out to dry on the fiberglas foredeck of the boat. The incident solar radiation is 1050 W/m^2; the ambient air is at 31°C, with $m_{\mathrm{H_2O}} = 0.017$; the wind speed is 8 knots relative to the boat (1 knot = 1.151 mph); $\varepsilon_{\text{towel}} \cong \alpha_{\text{towel}} \cong 1$; and the sky has the properties of a black body at 280 K. The towel is 3 ft long in the windward direction and 2 ft wide. Help Biff figure out how rapidly (in kg/s) water evaporates from the towel.

11.50 Steam condenses on a 25 cm high, cold vertical wall in a low-pressure condenser unit. The wall is isothermal at 25°C, and the ambient pressure is 8000 Pa. Air has leaked into the unit and has reached a mass fraction of 0.04. The steam–air mixture is at 45°C and is blown downward past the wall at 8 m/s. (a) Estimate the rate of condensation on the wall. (*Hint*: The surface of the condensate film is *not* at the mixture or wall temperature.) (b) Compare the result of part (a) to condensation without air in the steam. What do you conclude?

References

[11.1] W. C. Reynolds. *Energy, from Nature to Man*. McGraw-Hill Book Company, New York, 1974.

[11.2] S. Chapman and T. G. Cowling. *The Mathematical Theory of Nonuniform Gases*. Cambridge University Press, New York, 2nd edition, 1964.

[11.3] J. O. Hirschfelder, C. F. Curtiss, and R. B. Bird. *Molecular Theory of Gases and Liquids*. John Wiley & Sons, Inc., New York, 1964.

[11.4] R. K. Ghai, H. Ertl, and F. A. L. Dullien. Liquid diffusion of non-electrolytes: Part 1. *AIChE J.*, 19(5):881–900, 1973.

[11.5] C. L. Tien and J. H. Lienhard. *Statistical Thermodynamics*. Hemisphere Publishing Corp., Washington, D.C., rev. edition, 1978.

[11.6] R. A. Svehla. Estimated viscosities and thermal conductivities of gases at high temperatures. NASA TR R-132, 1962. (Nat. Tech. Inf. Svcs. N63-22862).

[11.7] C. R. Wilke and C. Y. Lee. Estimation of diffusion coefficients for gases and vapors. *Ind. Engr. Chem.*, 47:1253, 1955.

[11.8] J. O. Hirschfelder, R. B. Bird, and E. L. Spotz. The transport properties for non-polar gases. *J. Chem. Phys.*, 16(10):968–981, 1948.

[11.9] R. C. Weast, editor. *Handbook of Chemistry and Physics*. Chemical Rubber Co., Cleveland, Ohio, 56th edition, 1976.

[11.10] R. C. Reid, J. M. Prausnitz, and B. E. Poling. *The Properties of Gases and Liquids*. McGraw-Hill Book Company, New York, 4th edition, 1987.

[11.11] J. Millat, J. H. Dymond, and C. A. Nieto de Castro. *Transport Properties of Fluids: Their Correlation, Prediction and Estimation*. Cambridge University Press, Cambridge, UK, 1996.

[11.12] G. E. Childs and H. J. M. Hanley. Applicability of dilute gas transport property tables to real gases. *Cryogenics*, 8:94–97, 1968.

[11.13] R. B. Bird, J. O. Hirschfelder, and C. F. Curtiss. The equation of state and transport properties of gases and liquids. In *Handbook of Physics*. McGraw-Hill Book Company, New York, 1958.

[11.14] C. Cercignani. *Rarefied Gas Dynamics*. Cambridge University Press, Cambridge, UK, 2000.

[11.15] A. Einstein. *Investigations of the Theory Brownian Movement*. Dover Publications, Inc., New York, 1956. (This book is a collection of Einstein's original papers on the subject, which were published between 1905 and 1908.).

[11.16] W. Sutherland. A dynamical theory of diffusion for nonelectrolytes and the molecular mass of albumin. *Phil. Mag., Ser. 6*, 9(54):781–785, 1905.

[11.17] H. Lamb. *Hydrodynamics*. Dover Publications, Inc., New York, 6th edition, 1945.

[11.18] J. C. M. Li and P. Chang. Self-diffusion coefficient and viscosity in liquids. *J. Chem. Phys.*, 23(3):518–520, 1955.

[11.19] S. Glasstone, K. J. Laidler, and H. Eyring. *The Theory of Rate Processes*. McGraw-Hill Book Company, New York, 1941.

[11.20] C. J. King, L. Hsueh, and K-W. Mao. Liquid phase diffusion of nonelectrolytes at high dilution. *J. Chem. Engr. Data*, 10(4):348–350, 1965.

[11.21] C. R. Wilke. A viscosity equation for gas mixtures. *J. Chem. Phys.*, 18(4):517–519, 1950.

[11.22] E. A. Mason and S. C. Saxena. Approximate formula for the thermal conductivity of gas mixtures. *Phys. Fluids*, 1(5):361–369, 1958.

[11.23] J. M. Prausnitz, R. N. Lichtenthaler, and E. G. de Azevedo. *Molecular Thermodynamics of Fluid-Phase Equilibria*. Prentice-Hall, Englewood Cliffs, N.J., 2nd edition, 1986.

[11.24] E. M. Sparrow, G. A. Nunez, and A. T. Prata. Analysis of evaporation in the presence of composition-induced natural convection. *Int. J. Heat Mass Transfer*, 28(8):1451–1460, 1985.

[11.25] W. K. Lewis. The evaporation of a liquid into a gas. *Mech. Engr.*, 44(7):445–446, 1922.

[11.26] T. H. Chilton and A. P. Colburn. Mass transfer (absorption) coefficients: Prediction from data on heat transfer and fluid friction. *Ind. Eng. Chem.*, 26:1183–1187, 1934.

Part VI

Appendices

A. Some thermophysical properties of selected materials

A *primary source* of thermophysical properties is a document in which the experimentalist who obtained the data reports the details and results of his or her measurements. The term *secondary source* generally refers to a document, based on primary sources, that presents other peoples' data and does so critically. This appendix is neither a primary nor a secondary source, since it has been assembled from a variety of secondary and even tertiary sources.

We attempted to cross-check the data against different sources, and this often led to contradictory values. Such contradictions are usually the result of differences between the experimental samples that are reported or of differences in the accuracy of experiments themselves. We resolved such differences by judging the source, by reducing the number of significant figures to accommodate the conflict, or by omitting the substance from the table. The resulting numbers will suffice for most calculations. However, the reader who needs high accuracy should be sure of the physical constitution of the material and then should seek out one of the relevant secondary data sources.

The format of these tables is quite close to that established by R. M. Drake, Jr., in his excellent appendix on thermophysical data [A.1]. However, although we use a few of Drake's numbers directly in Table A.6, many of his other values have been superseded by more recent measurements. One secondary source from which many of the data here were obtained was the Purdue University series *Thermophysical Properties of Matter* [A.2]. The Purdue series is the result of an enormous property-gathering effort carried out under the direction of Y. S. Touloukian and several coworkers. The various volumes in the series are dated since

1970, and addenda were issued throughout the following decade. In more recent years, IUPAC, NIST, and other agencies have been developing critically reviewed, standard reference data for various substances, some of which are contained in [A.3, A.4, A.5, A.6, A.7, A.8, A.9, A.10, A.11]. We have taken many data for fluids from those publications. A third secondary source that we have used is the G. E. *Heat Transfer Data Book* [A.12].

Numbers that did not come directly from [A.1], [A.2], [A.12] or the sources of standard reference data were obtained from a large variety of manufacturers' tables, handbooks, other textbooks, and so on. No attempt has been made to document all these diverse sources and the various compromises that were made in quoting them.

Table A.1 gives the density, specific heat, thermal conductivity, and thermal diffusivity for various metallic solids. These values were obtained from volumes 1 and 4 of [A.2] or from [A.3] whenever it was possible to find them there. Most thermal conductivity values in the table have been rounded off to two significant figures. The reason is that k is sensitive to very minor variations in physical structure that cannot be detailed fully here. Notice, for example, the significant differences between pure silver and 99.9% pure silver, or between pure aluminum and 99% pure aluminum. Additional information on the characteristics and use of these metals can be found in the ASM *Metals Handbook* [A.13].

The effect of temperature on thermal conductivity is shown for most of the metals in Table A.1. The specific heat capacity is shown only at 20°C. For most materials, the heat capacity is much lower at cryogenic temperatures. For example, c_p for alumimum, iron, molydenum, and titanium decreases by two orders of magnitude as temperature decreases from 200 K to 20 K. On the other hand, for most of these metals, c_p changes more gradually for temperatures between 300 K and 800 K, varying by tens of percent to a factor of two. At still higher temperatures, some of these metals (iron and titanium) show substantial spikes in c_p, which are associated with solid-to-solid phase transitions.

Table A.2 gives the same properties as Table A.1 (where they are available) but for nonmetallic substances. Volumes 2 and 5 of [A.2] and also [A.3] provided many of the data here, and they revealed even greater variations in k than the metallic data did. For the various sands reported, k varied by a factor of 500, and for the various graphites by a factor of 50, for example. The sensitivity of k to small variations in the packing of fibrous materials or to the water content of hygroscopic materials forced us to restrict many of the k values to a single significant figure.

The data for polymers come mainly from their manufacturers' data and are substantially less reliable than, say, those given in Table A.1 for metals. The values quoted are mainly those for room temperature. In processing operations, however, most of these materials are taken to temperatures of several hundred degrees Celsius, at which they flow more easily. The specific heat capacity may double from room temperature to such temperatures. These polymers are also produced in a variety of modified forms; and in many applications they may be loaded with significant portions of reinforcing fillers (e.g., 10 to 40% by weight glass fiber). The fillers, in particular, can have a significant effect on thermal properties.

Table A.3 gives ρ, c_p, k, α, ν, Pr, and β for several liquids. Data for water are from [A.7] and [A.14]; they are in agreement with IAPWS recommendations through 1998. Data for ammonia are from [A.4, A.15, A.16], data for carbon dioxide are from [A.5, A.6, A.8], and data for oxygen are from [A.9, A.10]. Data for HFC-134a, HCFC-22, and nitrogen are from [A.11] and [A.17]. For these liquids, ρ has uncertainties less than 0.2%, c_p has uncertainties of 1–2%, while μ and k have typical uncertainties of 2–5%. Uncertainties may be higher near the critical point. Thermodynamic data for methanol follow [A.18]. Data for mercury follow [A.3] and [A.19]. Volumes 3, 6, 10, and 11 of [A.2] gave many of the other values of c_p, k, and $\mu = \rho\nu$, and occasional independently measured values of α. Additional values came from [A.20]. Values of α that disagreed only slightly with $k/\rho c_p$ were allowed to stand. Densities for other substances came from [A.20] and a variety of other sources. A few values of ρ and c_p were taken from [A.21].

Table A.5 provides thermophysical data for saturated vapors. The sources and the uncertainties are as described for gases in the next paragraph.

Table A.6 gives thermophysical properties for gases at 1 atmosphere pressure. The values were drawn from a variety of sources: air data are from [A.22, A.23], except for ρ and c_p above 850 K which came from [A.24]; argon data are from [A.25, A.26, A.27]; ammonia data were taken from [A.4, A.15, A.16]; carbon dioxide properties are from [A.5, A.6, A.8]; carbon monoxide properties are from [A.17]; helium data are from [A.28, A.29, A.30]; nitrogen data came from [A.31]; oxygen data are from [A.9, A.10]; water data were taken from [A.7] and [A.14] (in agreement with IAPWS recommendations through 1998); and a few high-temperature hydrogen data are from [A.20] with the remainding hydrogen data drawn from [A.1]. Uncertainties in these data vary among the

gases; typically, ρ has uncertainties of 0.02–0.2%, c_p has uncertainties of 0.2–2%, μ has uncertainties of 0.3–3%, and k has uncertainties of 2–5%. The uncertainties are generally lower in the dilute gas region and higher near the saturation line or the critical point. The values for hydrogen and for low temperature helium have somewhat larger uncertainties.

Table A.7 lists values for some fundamental physical constants, as given in [A.32]. Table A.8 points out physical data that are listed in other parts of this book.

References

[A.1] E. R. G. Eckert and R. M. Drake, Jr. *Analysis of Heat and Mass Transfer*. McGraw-Hill Book Company, New York, 1972.

[A.2] Y. S. Touloukian. *Thermophysical Properties of Matter*. vols. 1–6, 10, and 11. Purdue University, West Lafayette, IN, 1970 to 1975.

[A.3] C. Y. Ho, R. W. Powell, and P. E. Liley. Thermal conductivity of the elements: A comprehensive review. *J. Phys. Chem. Ref. Data*, 3, 1974. Published in book format as Supplement No. 1 to the cited volume.

[A.4] A. Fenghour, W. A. Wakeham, V. Vesovic, J. T. R. Watson, J. Millat, and E. Vogel. The viscosity of ammonia. *J. Phys. Chem. Ref. Data*, 24(5):1649–1667, 1995.

[A.5] A. Fenghour, W. A. Wakeham, and V. Vesovic. The viscosity of carbon dioxide. *J. Phys. Chem. Ref. Data*, 27(1):31–44, 1998.

[A.6] V. Vesovic, W. A. Wakeham, G. A. Olchowy, J. V. Sengers, J. T. R. Watson, and J. Millat. The transport properties of carbon dioxide. *J. Phys. Chem. Ref. Data*, 19(3):763–808, 1990.

[A.7] C.A. Meyer, R. B. McClintock, G. J. Silvestri, and R.C. Spencer. *ASME Steam Tables*. American Society of Mechanical Engineers, New York, NY, 6th edition, 1993.

[A.8] R. Span and W. Wagner. A new equation of state for carbon dioxide covering the fluid region from the triple-point temperature to 1100 K at pressures up to 800 MPa. *J. Phys. Chem. Ref. Data*, 25 (6):1509–1596, 1996.

[A.9] A. Laesecke, R. Krauss, K. Stephan, and W. Wagner. Transport properties of fluid oxygen. *J. Phys. Chem. Ref. Data*, 19(5):1089–1122, 1990.

[A.10] R. B. Stewart, R. T. Jacobsen, and W. Wagner. Thermodynamic properties of oxygen from the triple point to 300 K with pressures to 80 MPa. *J. Phys. Chem. Ref. Data*, 20(5):917–1021, 1991.

[A.11] R. Tillner-Roth and H. D. Baehr. An international standard formulation of the thermodynamic properties of 1,1,1,2-tetrafluoroethane (HFC-134a) covering temperatures from 170 K to 455 K at pressures up to 70 MPa. *J. Phys. Chem. Ref. Data*, 23: 657–729, 1994.

[A.12] R. H. Norris, F. F. Buckland, N. D. Fitzroy, R. H. Roecker, and D. A. Kaminski, editors. *Heat Transfer Data Book*. General Electric Co., Schenectady, NY, 1977.

[A.13] ASM Handbook Committee. *Metals Handbook*. ASM, International, Materials Park, OH, 10th edition, 1990.

[A.14] A. H. Harvey, A. P. Peskin, and S. A. Klein. *NIST/ASME Steam Properties*. National Institute of Standards and Technology, Gaithersburg, MD, March 2000. NIST Standard Reference Database 10, Version 2.2.

[A.15] R. Tufeu, D. Y. Ivanov, Y. Garrabos, and B. Le Neindre. Thermal conductivity of ammonia in a large temperature and pressure range including the critical region. *Ber. Bunsenges. Phys. Chem.*, 88:422–427, 1984.

[A.16] R. Tillner-Roth, F. Harms-Watzenberg, and H. D. Baehr. Eine neue Fundamentalgleichung fuer Ammoniak. *DKV-Tagungsbericht*, 20: 167–181, 1993.

[A.17] E. W. Lemmon, A. P. Peskin, M. O. McLinden, and D. G. Friend. *Thermodynamic and Transport Properties of Pure Fluids — NIST Pure Fluids*. National Institute of Standards and Technology, Gaithersburg, MD, September 2000. NIST Standard Reference Database Number 12, Version 5. Property values are based upon the most accurate standard reference formulations then available.

[A.18] K. M. deReuck and R. J. B. Craven. *Methanol: International Thermodynamic Tables of the Fluid State-12*. Blackwell Scientific Publications, Oxford, 1993. Developed under the sponsorship of the International Union of Pure and Applied Chemistry (IUPAC).

[A.19] N. B. Vargaftik, Y. K. Vinogradov, and V. S. Yargin. *Handbook of Physical Properties of Liquids and Gases*. Begell House, Inc., New York, 3rd edition, 1996.

[A.20] N. B. Vargaftik. *Tables on the Thermophysical Properties of Liquids and Gases*. Hemisphere Publishing Corp., Washington, D.C., 2nd edition, 1975.

[A.21] E. W. Lemmon, M. O. McLinden, and D. G. Friend. Thermophysical properties of fluid systems. In W. G. Mallard and P. J. Linstrom, editors, *NIST Chemistry WebBook, NIST Standard Reference Database Number 69*. National Institute of Standards and Technology, Gaithersburg, MD, 2000. http://webbook.nist.gov.

[A.22] K. Kadoya, N. Matsunaga, and A. Nagashima. Viscosity and thermal conductivity of dry air in the gaseous phase. *J. Phys. Chem. Ref. Data*, 14(4):947–970, 1985.

[A.23] R.T. Jacobsen, S.G. Penoncello, S.W. Breyerlein, W.P. Clark, and E.W. Lemmon. A thermodynamic property formulation for air. *Fluid Phase Equilibria*, 79:113–124, 1992.

[A.24] E.W. Lemmon, R.T. Jacobsen, S.G. Penoncello, and D. G. Friend. Thermodynamic properties of air and mixtures of nitrogen, argon, and oxygen from 60 to 2000 K at pressures to 2000 MPa. *J. Phys. Chem. Ref. Data*, 29(3):331–385, 2000.

[A.25] Ch. Tegeler, R. Span, and W. Wagner. A new equation of state for argon covering the fluid region for temperatures from the melting line to 700 K at pressures up to 1000 MPa. *J. Phys. Chem. Ref. Data*, 28(3):779–850, 1999.

[A.26] B. A. Younglove and H. J. M. Hanley. The viscosity and thermal conductivity coefficients of gaseous and liquid argon. *J. Phys. Chem. Ref. Data*, 15(4):1323–1337, 1986.

[A.27] R. A. Perkins, D. G. Friend, H. M. Roder, and C. A. Nieto de Castro. Thermal conductivity surface of argon: A fresh analysis. *Intl. J. Thermophys.*, 12(6):965–984, 1991.

[A.28] R. D. McCarty and V. D. Arp. A new wide range equation of state for helium. *Adv. Cryo. Eng.*, 35:1465–1475, 1990.

[A.29] V. D. Arp, R. D. McCarty, and D. G. Friend. Thermophysical properties of helium-4 from 0.8 to 1500 K with pressures to 2000 MPa. Technical Note 1334, National Institute of Standards and Technology, Boulder, CO, 1998.

[A.30] E. Bich, J. Millat, and E. Vogel. The viscosity and thermal conductivity of pure monatomic gases from their normal boiling point up to 5000 K in the limit of zero density and at 0.101325 MPa. *J. Phys. Chem. Ref. Data*, 19(6):1289–1305, 1990.

[A.31] B. A. Younglove. Thermophysical properties of fluids: Argon, ethylene, parahydrogen, nitrogen, nitrogen trifluoride, and oxygen. *J. Phys. Chem. Ref. Data*, 11, 1982. Published in book format as Supplement No. 1 to the cited volume.

[A.32] P. J. Mohr and B. N. Taylor. CODATA recommended values of the fundamental physical constants: 1998. *J. Phys. Chem. Ref. Data*, 28(6):1713–1852, 1999.

Table A.1 Properties of metallic solids

	Properties at 20°C				*Thermal Conductivity, k* (W/m·K)									
Metal	ρ (kg/m^3)	c_p (J/kg·K)	k (W/m·K)	α (10^{-5} m^2/s)	−170°C	−100°C	0°C	100°C	200°C	300°C	400°C	600°C	800°C	1000°C
Aluminums														
Pure	2,707	905	237	9.61	302	242	236	240	238	234	228	215	≈95 (liq.)	
99% pure			211		220	206	209							
Duralumin (≈4% Cu, 0.5% Mg)	2,787	883	164	6.66		126	164	182	194					
Alloy 6061-T6	2,700	896	167	6.90			166	172	177	180				
Alloy 7075-T6	2,800	841	130	5.52	76	100	121	137	172	177				
Chromium	7,190	453	90	2.77	158	120	95	88	85	82	77	69	64	62
Cupreous metals														
Pure Copper	8,954	384	398	11.57	483	420	401	391	389	384	378	366	352	336
DS-C15715*	8,900	≈384	365	≈10.7			367	355	345	335	320			
Beryllium copper (2.2% Be)	8,250	420	103	2.97				117						
Brass (30% Zn)	8,522	385	109	3.32	73	89	106	133	143	146	147			
Bronze (25% Sn)§	8,666	343	26	0.86										
Constantan (40% Ni)	8,922	410	22	0.61	17	19	22	26	35					
German silver (15% Ni, 22% Zn)	8,618	394	25	0.73	18	19	24	31	40	45	48			
Gold	19,320	129	318	12.76	327	324	319	313	306	299	293	279	264	249
Ferrous metals														
Pure iron	7,897	447	80	2.26	132	98	84	72	63	56	50	39	30	29.5
Cast iron (4% C)	7,272	420	52	1.70										
Steels (C ≤ 1.5%)‖														
AISI 1010††	7,830	434	64	1.88		70	65	61	55	50	45	36	29	
0.5% carbon	7,833	465	54	1.47			55	52	48	45	42	35	31	29
1.0% carbon	7,801	473	43	1.17			43	43	42	40	36	33	29	28
1.5% carbon	7,753	486	36	0.97			36	36	36	35	33	31	28	28

* Dispersion-strengthened copper (0.3% Al_2O_3 by weight); strength comparable to stainless steel.
§ Conductivity data for this and other bronzes vary by a factor of about two.
‖ k and α for carbon steels can vary greatly, owing to trace elements.
†† 0.1% C, 0.42% Mn, 0.28% Si; hot-rolled.

Table A.1 Properties of metallic solids…*continued.*

	Properties at 20°C				*Thermal Conductivity, k* (W/m·K)									
Metal	ρ (kg/m^3)	c_p (J/kg·K)	k (W/m·K)	α (10^{-5} m^2/s)	−170°C	−100°C	0°C	100°C	200°C	300°C	400°C	600°C	800°C	1000°C
Stainless steels:														
AISI 304	8,000	400	13.8	0.4				15	17$^+$	19$^-$	21	25		
AISI 316	8,000	460	13.5	0.37		12		15	16	17$^+$	19$^-$	21$^+$	24	26$^+$
AISI 347	8,000	420	15	0.44		13		16$^+$	18$^-$	19	20	23	26	28
AISI 410	7,700	460	25	0.7				25$^+$	26	27	27$^+$	28$^+$		
AISI 446	7,500	460						18	19$^-$	19	20	21	22	
Lead	11,373	130	35	2.34	40	37	36	34	33	32	17 (liq.)	20 (liq.)		
Magnesium	1,746	1023	156	8.76	169	160	157	154	152	150	148	145	89 (liq.)	
Mercury†					32	30	7.8 (liq.)							
Molybdenum	10,220	251	138	5.38	175	146	139	135	131	127	123	116	109	103
Nickels														
Pure	8,906	445	91	2.30	156	114	94	83	74	67	64	69	73	78
Inconel X-750¶	8,510	442	11.6	0.23	8.8	10.6	11.3	13.0	14.7	16.0	18.3	21.8	25.3	29
Nichrome (24% Fe, 16% Cr)	8,250	448		0.34				13						
Nichrome V (20% Cr)	8,410	466	13	0.33			12	14	15	17	19			
Platinum	21,450	133	71	2.50	78	73	72	72	72	73	74	77	80	84
Silicon‡	2,330	705.5	153	9.31	856	342	168	112	82	66	54	38	29	25
Silver														
99.99$^+$% pure	10,524	236	427	17.19	449	431	428	422	417	409	401	386	370	176 (liq.)
99.9% pure	10,524	236	411	16.55		422	405		373	367	364			
Tin†	7,304	≈ 220	67	4.17	85	76	68	63	60	32 (liq.)	34 (liq.)	38 (liq.)		
Titanium														
Pure†	4,540	523	22	0.93	31	26	22	21	20	20	19	21	21	22
Ti-6%Al-4%V	4,430	580	7.1	0.28				7.8	8.8	10	12$^-$			
Tungsten	19,350	133	178	6.92	235	223	182	166	153	141	134	125	122	114
Uranium	18,700	116	28	1.29	22	24	27	29	31	33	36	41	46	
Zinc	7,144	388	121	4.37	124	122	122	117	110	106	100	60 (liq.)		

† Polycrystalline form. ‡ Single crystal form. ¶ 73% Ni, 15% Cr, 6.75% Fe, 2.5% Ti, 0.85% Nb, 0.8% Al, 0.7% Mn, 0.3% Si.

Table A.2 Properties of nonmetallic solids

Material	*Temperature Range* (°C)	*Density* ρ (kg/m^3)	*Specific Heat* c_p (J/kg·K)	*Thermal Conductivity* k (W/m·K)	*Thermal Diffusivity* α (m^2/s)
Aluminum oxide (Al_2O_3)					
plasma sprayed coating	20			≈ 4	
polycrystalline (98% dense)	0		725	40	
	27	3900	779	36	1.19×10^{-5}
	127		940	26	
	577		1200	10	
	1077		1270	6.1	
	1577		1350	5.6	
single crystal (sapphire)	0		725	52	
	27	3980	779	46	1.48×10^{-5}
	127		940	32	
	577		1180	13	
Asbestos					
Cement board	20			0.6	
Fiber, densely packed	20	1930		0.8	
Fiber, loosely packed	20	980		0.14	
Asphalt	20–25			0.75	
Beef	25				1.35×10^{-7}
Brick					
B & W, K-28 insulating	300			0.3	
	1000			0.4	
Cement	10	720		0.34	
Common	0–1000			0.7	
Chrome	100			1.9	
Facing	20			1.3	
Firebrick, insulating	300	2000	960	0.1	5.4×10^{-8}
	1000			0.2	
Carbon					
Diamond (type IIb)	20	≈3250	510	1350.0	8.1×10^{-4}
Graphites	20	≈1730	≈710	k varies with structure	
AGOT graphite					
⊥ to extrusion axis	0			141	
	27	1700	800	138	
	500		1600	59.1	
∥ to extrusion axis	0			230	
	27	1700	800	220	
	500		1600	93.6	
Pyrolitic graphite					
⊥ to layer planes	0			10.6	
	27	2200	710	9.5	
	227			5.4	
	1027			1.9	

Table A.2…*continued.*

Material	*Temperature Range* (°C)	*Density* ρ (kg/m^3)	*Specific Heat* c_p (J/kg·K)	*Thermal Conductivity* k (W/m·K)	*Thermal Diffusivity* α (m^2/s)
Pyrolitic graphite *(con't)*					
‖ to layer planes	0			2230	
	27	2200	710	2000	
	227			1130	
	1027			400	
Cardboard	0–20	790		0.14	
Clay					
Fireclay	500–750			1.0	
Sandy clay	20	1780		0.9	
Coal					
Anthracite	900	≈1500		≈0.2	
Brown coal	900			≈0.1	
Bituminous in situ		≈1300		0.5–0.7	3 to 4×10^{-7}
Concrete					
Limestone gravel	20	1850		0.6	
Portland cement	90	2300		1.7	
Sand : cement (3 : 1)	230			0.1	
Sand and gravel	20			1.8	
Slag cement	20			0.14	
Corkboard (medium ρ)	30	170		0.04	
Egg white	20				1.37×10^{-7}
Glass					
Lead	36	3040		1.2	
Plate	20	2500		1.3	
Pyrex (borosilicate)	60–100	2210	753	1.3	7.8×10^{-7}
Soda	20	2590		0.7	
Window	46	2490		1.3	
Glass wool	20	64–160		0.04	
Ice	0	917	2100	2.215	1.15×10^{-6}
Ivory	80			0.5	
Kapok	30			0.035	
Lunar surface dust (high vacuum)	250	1500±300	≈600	≈0.0006	$\approx 7 \times 10^{-10}$
Magnesia (85%)	38			0.067	
	93			0.071	
	150			0.074	
	204			0.08	
Magnesium oxide					
polycrystalline (98% dense)	27	3500	900	48	1.5×10^{-5}
single crystal	27	3580	900	60	1.9×10^{-5}

Table A.2…*continued.*

Material	*Temperature Range* (°C)	*Density* ρ (kg/m^3)	*Specific Heat* c_p (J/kg·K)	*Thermal Conductivity* k (W/m·K)	*Thermal Diffusivity* α (m^2/s)
Polymers					
acrylic (PMMA, Plexiglas)	25	1180		0.17	
acrylonitrile butadiene styrene (ABS)		1060		0.14–0.31	
epoxy, bisphenol A (EP), cast		1150		0.17–0.52	
epoxy/glass-cloth laminate (G-10, FR4)		1800	≈1600	0.29	$\approx 1.0 \times 10^{-7}$
polyethylene (PE)					
HDPE		960	2260	0.33	1.5×10^{-7}
LDPE		920	≈2100	0.33	$\approx 1.7 \times 10^{-7}$
polypropylene (PP)		905	1900	0.17–0.20	
polystyrene (PS)		1040	≈ 1350	0.10–0.16	
polyvinylchloride (PVC)		≈1450		0.12–0.17	
polytetrafluoroethylene (PTFE, Teflon)		≈2200	1050	0.24	$\approx 1.0 \times 10^{-7}$
acetyl (POM, Delrin)	−18–100	1420	1470	0.30–0.37	
polyamide (PA)					
nylon 6,6	0–49	1120	1470	0.25	1.5×10^{-7}
nylon 6,12	0–49	1060	1680	0.22	1.2×10^{-7}
polycarbonate (PC, Lexan)	23	1200	1250	0.29	1.9×10^{-7}
polyimide (PI)		1430	1130	0.35	2.2×10^{-7}
Rock wool	−5	≈130		0.03	
	93			0.05	
Rubber (hard)	0	1200	2010	0.15	6.2×10^{-8}
Silica aerogel	0	140		0.024	
	120	136		0.022	
Silo-cel (diatomaceous earth)	0	320		0.061	
Silicon dioxide					
Fused silica glass					
	0		703	1.33	
	27	2200	745	1.38	8.4×10^{-7}
	227		988	1.62	
Single crystal (quartz)					
⊥ to c-axis	0		709	6.84	
	27	2640	743	6.21	
	227		989	3.88	
∥ to c-axis	0		709	11.6	
	27	2640	743	10.8	
	227		989	6.00	

Table A.2…*continued.*

Material	*Temperature Range* (°C)	*Density* ρ (kg/m^3)	*Specific Heat* c_p (J/kg·K)	*Thermal Conductivity* k (W/m·K)	*Thermal Diffusivity* α (m^2/s)
Soil (mineral)					
Dry	15	1500	1840	1.	4×10^{-7}
Wet	15	1930		2.	
Stone					
Granite (NTS)	20	≈2640	≈820	1.6	$\approx 7.4 \times 10^{-7}$
Limestone (Indiana)	100	2300	≈900	1.1	$\approx 5.3 \times 10^{-7}$
Sandstone (Berea)	25			≈3	
Slate	100			1.5	
Wood (perpendicular to grain)					
Ash	15	740		0.15–0.3	
Balsa	15	100		0.05	
Cedar	15	480		0.11	
Fir	15	600	2720	0.12	7.4×10^{-8}
Mahogany	20	700		0.16	
Oak	20	600	2390	0.1–0.4	
Pitch pine	20	450		0.14	
Sawdust (dry)	17	128		0.05	
Sawdust (dry)	17	224		0.07	
Spruce	20	410		0.11	
Wool (sheep)	20	145		0.05	

Table A.3 Thermophysical properties of saturated liquids

Temperature								
K	°C	ρ (kg/m^3)	c_p (J/kg·K)	k (W/m·K)	α (m^2/s)	ν (m^2/s)	Pr	β (K^{-1})
				Ammonia				
200	−73	728	4227	0.803	2.61×10^{-7}	6.967×10^{-7}	2.67	0.00147
220	−53	706	4342	0.733	2.39	4.912	2.05	0.00165
240	−33	682	4488	0.665	2.19	3.738	1.70	0.00182
260	−13	656	4548	0.600	2.01	3.007	1.50	0.00201
280	7	629	4656	0.539	1.84	2.514	1.37	0.00225
300	27	600	4800	0.480	1.67	2.156	1.29	0.00258
320	47	568	5018	0.425	1.49	1.882	1.26	0.00306
340	67	532	5385	0.372	1.30	1.663	1.28	0.00387
360	87	490	6082	0.319	1.07	1.485	1.39	0.00542
380	107	436	7818	0.267	0.782	1.337	1.71	0.00952
400	127	345	22728	0.216	0.276	1.214	4.40	0.04862
				Carbon dioxide				
220	−53	1166	1962	0.176	7.70×10^{-8}	2.075×10^{-7}	2.70	0.00318
230	−43	1129	1997	0.163	7.24	1.809	2.50	0.00350
240	−33	1089	2051	0.151	6.75	1.588	2.35	0.00392
250	−23	1046	2132	0.139	6.21	1.402	2.26	0.00451
260	−13	999	2255	0.127	5.61	1.245	2.22	0.00538
270	−3	946	2453	0.115	4.92	1.110	2.26	0.00677
280	7	884	2814	0.102	4.10	0.993	2.42	0.00934
290	17	805	3676	0.0895	3.03	0.887	2.93	0.0157
300	27	679	8698	0.0806	1.36	0.782	5.73	0.0570
302	29	634	15787	0.0845	0.844	0.756	8.96	0.119
				Freon 12 (dichlorodifluoromethane)				
180	−93	1664	834	0.124	8.935×10^{-8}			
200	−73	1610	856	0.1148	8.33			
220	−53	1555	873	0.1057	7.79	3.2×10^{-7}	4.11	0.00263
240	−33	1498	892	0.0965	7.22	2.60	3.60	
260	−13	1438	914	0.0874	6.65	2.26	3.40	
280	7	1374	942	0.0782	6.04	2.06	3.41	
300	27	1305	980	0.0690	5.39	1.95	3.62	
320	47	1229	1031	0.0599	4.72	1.9	4.03	
340	67		1097	0.0507				

Table A.3: saturated liquids…*continued*

Temperature								
K	°C	ρ (kg/m^3)	c_p (J/kg·K)	k (W/m·K)	α (m^2/s)	ν (m^2/s)	Pr	β (K^{-1})
				Glycerin (or glycerol)				
273	0	1276	2200	0.282	1.00×10^{-7}	0.0083	83,000	
293	20	1261	2350	0.285	0.962	0.001120	11,630	0.00048
303	30	1255	2400	0.285	0.946	0.000488	5,161	0.00049
313	40	1249	2460	0.285	0.928	0.000227	2,451	0.00049
323	50	1243	2520	0.285	0.910	0.000114	1,254	0.00050
				20% glycerin, 80% water				
293	20	1047	3860	0.519	1.28×10^{-7}	1.681×10^{-6}	13.1	0.00031
303	30	1043	3860	0.532	1.32	1.294	9.8	0.00036
313	40	1039	3915	0.540	1.33	1.030	7.7	0.00041
323	50	1035	3970	0.553	1.35	0.849	6.3	0.00046
				40% glycerin, 60% water				
293	20	1099	3480	0.448	1.20×10^{-7}	3.385×10^{-6}	28.9	0.00041
303	30	1095	3480	0.452	1.22	2.484	20.4	0.00045
313	40	1090	3570	0.461	1.18	1.900	16.1	0.00048
323	50	1085	3620	0.469	1.19	1.493	12.5	0.00051
				60% glycerin, 40% water				
293	20	1154	3180	0.381	1.04×10^{-7}	9.36×10^{-6}	90.0	0.00048
303	30	1148	3180	0.381	1.04	6.89	66.3	0.00050
313	40	1143	3240	0.385	1.04	4.44	42.7	0.00052
323	50	1137	3300	0.389	1.04	3.31	31.8	0.00053
				80% glycerin, 20% water				
293	20	1209	2730	0.327	0.99×10^{-7}	4.97×10^{-5}	502	0.00051
303	30	1203	2750	0.327	0.99	2.82	282	0.00052
313	40	1197	2800	0.327	0.98	1.74	178	0.00053
323	50	1191	2860	0.331	0.97	1.14	118	0.00053
				Helium I and Helium II				

- k for He I is about 0.020 W/m·K near the λ-transition (≈ 2.17 K).
- k for He II below the λ-transition is hard to measure. It appears to be about 80,000 W/m·K between 1.4 and 1.75 K and it might go as high as 340,000 W/m·K at 1.92 K. These are the highest conductivities known (cf. copper, silver, and diamond).

Table A.3: saturated liquids...*continued*

Temperature								
K	°C	ρ (kg/m^3)	c_p (J/kg·K)	k (W/m·K)	α (m^2/s)	ν (m^2/s)	Pr	β (K^{-1})
				HCFC-22 (R22)				
160	−113	1605	1061	0.1504	8.82×10^{-8}	7.10×10^{-7}	8.05	0.00163
180	−93	1553	1061	0.1395	8.46	4.77	5.63	0.00170
200	−73	1499	1064	0.1291	8.09	3.55	4.38	0.00181
220	−53	1444	1076	0.1193	7.67	2.79	3.64	0.00196
240	−33	1386	1100	0.1099	7.21	2.28	3.16	0.00216
260	−13	1324	1136	0.1008	6.69	1.90	2.84	0.00245
280	7	1257	1189	0.0918	6.14	1.61	2.62	0.00286
300	27	1183	1265	0.0828	5.53	1.37	2.48	0.00351
320	47	1097	1390	0.0737	4.83	1.17	2.42	0.00469
340	67	990.1	1665	0.0644	3.91	0.981	2.51	0.00756
360	87	823.4	3001	0.0575	2.33	0.786	3.38	0.02388
				Heavy water (D_2O)				
589	316	740	2034	0.0509	0.978×10^{-7}	1.23×10^{-7}	1.257	
				HFC-134a (R134a)				
180	−93	1564	1187	0.1391	7.49×10^{-8}	9.45×10^{-7}	12.62	0.00170
200	−73	1510	1205	0.1277	7.01	5.74	8.18	0.00180
220	−53	1455	1233	0.1172	6.53	4.03	6.17	0.00193
240	−33	1397	1266	0.1073	6.06	3.05	5.03	0.00211
260	−13	1337	1308	0.0979	5.60	2.41	4.30	0.00236
280	7	1271	1360	0.0890	5.14	1.95	3.80	0.00273
300	27	1199	1432	0.0803	4.67	1.61	3.45	0.00330
320	47	1116	1542	0.0718	4.17	1.34	3.21	0.00433
340	67	1015	1750	0.0631	3.55	1.10	3.11	0.00657
360	87	870.1	2436	0.0541	2.55	0.883	3.46	0.0154
				Lead				
644	371	10,540	159	16.1	1.084×10^{-5}	2.276×10^{-7}	0.024	
755	482	10,442	155	15.6	1.223	1.85	0.017	
811	538	10,348	145	15.3	1.02	1.68	0.017	

Table A.3: saturated liquids…*continued*

Temperature								
K	°C	ρ (kg/m^3)	c_p (J/kg·K)	k (W/m·K)	α (m^2/s)	ν (m^2/s)	Pr	β (K^{-1})
				Mercury				
234	−39		141.5	6.97	3.62×10^{-6}	1.5×10^{-7}	0.041	
250	−23		140.5	7.32	3.83	1.4	0.037	
300	27	13,529	139.3	8.34	4.43	1.1	0.025	0.000181
350	77	13,407	137.7	9.15	4.96	0.98	0.020	0.000181
400	127	13,286	136.6	9.84	5.42	0.88	0.016	0.000181
500	227	13,048	135.3	11.0	6.23	0.73	0.012	0.000183
600	327	12,809	135.5	12.0	6.91	0.71	0.010	0.000187
700	427	12,567	136.9	12.7	7.38	0.67	0.0091	0.000195
800	527	12,318	139.8	12.8	7.43	0.64	0.0086	0.000207
				Methyl alcohol (methanol)				
260	−13	823	2336	0.2164	1.126×10^{-7}	$\approx 1.3\times10^{-6}$	≈ 11.5	0.00113
280	7	804	2423	0.2078	1.021	≈ 0.9	≈ 8.8	0.00119
300	27	785	2534	0.2022	1.016	≈ 0.7	≈ 6.9	0.00120
320	47	767	2672	0.1965	0.959	≈ 0.6	≈ 6.3	0.00123
340	67	748	2856	0.1908	0.893	≈ 0.44	≈ 4.9	0.00135
360	87	729	3036	0.1851	0.836	≈ 0.36	≈ 4.3	0.00144
380	107	710	3265	0.1794	0.774	≈ 0.30	≈ 4.1	0.00164
				NaK (eutectic mixture of sodium and potassium)				
366	93	849	946	24.4	3.05×10^{-5}	5.8×10^{-7}	0.019	
672	399	775	879	26.7	3.92	2.67	0.0068	
811	538	743	872	27.7	4.27	2.24	0.0053	
1033	760	690	883			2.12		
				Nitrogen				
70	−203	838.5	2014	0.162	9.58×10^{-8}	2.62×10^{-7}	2.74	0.00513
77	−196	807.7	2040	0.147	8.90	2.02	2.27	0.00564
80	−193	793.9	2055	0.140	8.59	1.83	2.13	0.00591
90	−183	745.0	2140	0.120	7.52	1.38	1.83	0.00711
100	−173	689.4	2318	0.101	6.29	1.09	1.74	0.00927
110	−163	621.5	2743	0.0818	4.80	0.894	1.86	0.0142
120	−153	523.4	4507	0.0633	2.68	0.730	2.72	0.0359

Table A.3: saturated liquids...*continued*

Temperature								
K	°C	ρ (kg/m^3)	c_p (J/kg·K)	k (W/m·K)	α (m^2/s)	ν (m^2/s)	Pr	β (K^{-1})
				Oils (some approximate viscosities)				
273	0			MS-20		0.0076	100,000	
339	66			California crude (heavy)		0.00008		
289	16			California crude (light)		0.00005		
339	66			California crude (light)		0.000010		
289	16			Light machine oil (ρ = 907)		0.00016		
339	66			Light machine oil (ρ = 907)		0.000013		
289	16			SAE 30		0.00044	$\approx$ 5,000	
339	66			SAE 30		0.00003		
289	16			SAE 30 (Eastern)		0.00011		
339	66			SAE 30 (Eastern)		0.00001		
289	16			Spindle oil (ρ = 885)		0.00005		
339	66			Spindle oil (ρ = 885)		0.000007		
				Oxygen				
60	−213	1282	1673	0.195	9.09×10^{-8}	4.50×10^{-7}	4.94	0.00343
70	−203	1237	1678	0.181	8.72	2.84	3.26	0.00370
80	−193	1190	1682	0.167	8.33	2.08	2.49	0.00398
90	−183	1142	1699	0.153	7.88	1.63	2.07	0.00436
100	−173	1091	1738	0.139	7.33	1.34	1.83	0.00492
110	−163	1036	1807	0.125	6.67	1.13	1.70	0.00575
120	−153	973.9	1927	0.111	5.89	0.974	1.65	0.00708
130	−143	902.5	2153	0.0960	4.94	0.848	1.72	0.00953
140	−133	813.2	2691	0.0806	3.67	0.741	2.01	0.0155
150	−123	675.5	5464	0.0643	1.74	0.639	3.67	0.0495

Table A.3: saturated liquids...*continued*

Temperature								
K	°C	ρ (kg/m^3)	c_p (J/kg·K)	k (W/m·K)	α (m^2/s)	ν (m^2/s)	Pr	β (K^{-1})
				Water				
273.16	0.01	999.8	4220	0.5610	1.330×10^{-7}	17.91×10^{-7}	13.47	-6.80×10^{-5}
275	2	999.9	4214	0.5645	1.340	16.82	12.55	-3.55×10^{-5}
280	7	999.9	4201	0.5740	1.366	14.34	10.63	4.36×10^{-5}
285	12	999.5	4193	0.5835	1.392	12.40	8.91	0.000112
290	17	998.8	4187	0.5927	1.417	10.85	7.66	0.000172
295	22	997.8	4183	0.6017	1.442	9.600	6.66	0.000226
300	27	996.5	4181	0.6103	1.465	8.568	5.85	0.000275
305	32	995.0	4180	0.6184	1.487	7.708	5.18	0.000319
310	37	993.3	4179	0.6260	1.508	6.982	4.63	0.000361
320	47	989.3	4181	0.6396	1.546	5.832	3.77	0.000436
340	67	979.5	4189	0.6605	1.610	4.308	2.68	0.000565
360	87	967.4	4202	0.6737	1.657	3.371	2.03	0.000679
373.15	100.0	958.3	4216	0.6791	1.681	2.940	1.75	0.000751
400	127	937.5	4256	0.6836	1.713	2.332	1.36	0.000895
420	147	919.9	4299	0.6825	1.726	2.030	1.18	0.001008
440	167	900.5	4357	0.6780	1.728	1.808	1.05	0.001132
460	187	879.5	4433	0.6702	1.719	1.641	0.955	0.001273
480	207	856.5	4533	0.6590	1.697	1.514	0.892	0.001440
500	227	831.3	4664	0.6439	1.660	1.416	0.853	0.001645
520	247	803.6	4838	0.6246	1.607	1.339	0.833	0.001909
540	267	772.8	5077	0.6001	1.530	1.278	0.835	0.002266
560	287	738.0	5423	0.5701	1.425	1.231	0.864	0.002783
580	307	697.6	5969	0.5346	1.284	1.195	0.931	0.003607
600	327	649.4	6953	0.4953	1.097	1.166	1.06	0.005141
620	347	586.9	9354	0.4541	0.8272	1.146	1.39	0.009092
640	367	481.5	25,940	0.4149	0.3322	1.148	3.46	0.03971
642	369	463.7	34,930	0.4180	0.2581	1.151	4.46	0.05679
644	371	440.7	58,910	0.4357	0.1678	1.156	6.89	0.1030
646	373	403.0	204,600	0.5280	0.06404	1.192	18.6	0.3952
647.0	374	357.3	3,905,000	1.323	0.00948	1.313	138.	7.735

Table A.4 Some latent heats of vaporization, h_{fg} (kJ/kg)

T(K)	Water	Ammonia	CO_2	HCFC-22	HFC-134a	Mercury	Methanol	Nitrogen	Oxygen
60									238.4
70								208.1	230.5
80								195.7	222.3
90								180.5	213.2
100								161.0	202.6
110								134.3	189.7
120				300.4				92.0	173.7
130				294.0					153.1
140				287.9					125.2
150				281.8					79.2
160				275.9					
180				264.3	257.4				
200		1474		252.9	245.7		1310		
220		1424	344.9	241.3	233.9		1269		
230		1397	328.0	235.2	227.8		1258		
240		1369	309.6	228.9	221.5		1247		
250		1339	289.3	222.2	215.0		1235		
260		1307	266.5	215.1	208.2		1222		
270		1273	240.1	207.5	201.0		1209		
273	2501	1263	230.9	205.0	198.6	306.8	1205		
280	2485	1237	208.6	199.4	193.3	306.6	1196		
290	2462	1199	168.1	190.5	185.0	306.2	1181		
300	2438	1158	103.7	180.9	176.1	305.8	1166		
310	2414	1114		170.2	166.3	305.5	1168		
320	2390	1066		158.3	155.5	305.1	1150		
330	2365	1015		144.7	143.3	304.8	1116		
340	2341	957.9		128.7	129.3	304.4	1096		
350	2315	895.2		109.0	112.5	304.1	1078		
360	2290	824.8		81.8	91.0	303.8	1054		
373	2257	717.0				303.3	1022		
400	2183	346.9				302.4	945		
500	1828					299.2	391		
600	1173					295.9			
700						292.3			

Table A.5 Thermophysical properties of saturated vapors ($p \neq 1$ atm).

T (K)	p (MPa)	ρ (kg/m^3)	c_p (J/kg·K)	k (W/m·K)	μ (kg/m·s)	Pr	β (K^{-1})
			Ammonia				
200	0.008651	0.08908	2076	0.0197	6.952×10^{-6}	0.733	0.005141
220	0.03379	0.3188	2160	0.0201	7.485	0.803	0.004847
240	0.1022	0.8969	2298	0.0210	8.059	0.883	0.004724
260	0.2553	2.115	2503	0.0223	8.656	0.973	0.004781
280	0.5509	4.382	2788	0.0240	9.266	1.08	0.005042
300	1.062	8.251	3177	0.0264	9.894	1.19	0.005560
320	1.873	14.51	3718	0.0296	10.56	1.33	0.006462
340	3.080	24.40	4530	0.0339	11.33	1.51	0.008053
360	4.793	40.19	5955	0.0408	12.35	1.80	0.01121
380	7.140	67.37	9395	0.0546	14.02	2.42	0.01957
400	10.30	131.1	34924	0.114	18.53	5.70	0.08664
			Carbon dioxide				
220	0.5991	15.82	930.3	0.0113	1.114×10^{-5}	0.917	0.006223
230	0.8929	23.27	1005.	0.0122	1.169	0.962	0.006615
240	1.283	33.30	1103.	0.0133	1.227	1.02	0.007223
250	1.785	46.64	1237.	0.0146	1.290	1.09	0.008154
260	2.419	64.42	1430.	0.0163	1.361	1.19	0.009611
270	3.203	88.37	1731.	0.0187	1.447	1.34	0.01203
280	4.161	121.7	2277.	0.0225	1.560	1.58	0.01662
290	5.318	172.0	3614.	0.0298	1.736	2.10	0.02811
300	6.713	268.6	11921.	0.0537	2.131	4.73	0.09949
302	7.027	308.2	23800.	0.0710	2.321	7.78	0.2010
			HCFC-22 (R22)				
160	0.0005236	0.03406	479.2	0.00398	6.69×10^{-6}	0.807	0.006266
180	0.003701	0.2145	507.1	0.00472	7.54	0.810	0.005622
200	0.01667	0.8752	539.1	0.00554	8.39	0.816	0.005185
220	0.05473	2.649	577.8	0.00644	9.23	0.828	0.004947
240	0.1432	6.501	626.2	0.00744	10.1	0.847	0.004919
260	0.3169	13.76	688.0	0.00858	10.9	0.877	0.005131
280	0.6186	26.23	769.8	0.00990	11.8	0.918	0.005661
300	1.097	46.54	885.1	0.0116	12.8	0.977	0.006704
320	1.806	79.19	1071.	0.0140	14.0	1.07	0.008801
340	2.808	133.9	1470.	0.0181	15.7	1.27	0.01402
360	4.184	246.7	3469.	0.0298	19.3	2.24	0.04233

Table A.5: saturated vapors ($p \neq 1$ atm)...*continued.*

T (K)	p (MPa)	ρ (kg/m^3)	c_p (J/kg·K)	k (W/m·K)	μ (kg/m·s)	Pr	β (K^{-1})
HFC-134a (R134a)							
180	0.001128	0.07702	609.7	0.00389	6.90×10^{-6}	1.08	0.005617
200	0.006313	0.3898	658.6	0.00550	7.75	0.929	0.005150
220	0.02443	1.385	710.9	0.00711	8.59	0.859	0.004870
240	0.07248	3.837	770.5	0.00873	9.40	0.829	0.004796
260	0.1768	8.905	841.8	0.0104	10.2	0.826	0.004959
280	0.3727	18.23	929.6	0.0121	11.0	0.845	0.005421
300	0.7028	34.19	1044.	0.0140	11.9	0.886	0.006335
320	1.217	60.71	1211.	0.0163	12.9	0.961	0.008126
340	1.972	105.7	1524.	0.0197	14.4	1.11	0.01227
360	3.040	193.6	2606.	0.0274	17.0	1.62	0.02863
Nitrogen							
70	0.03854	1.896	1082.	0.00680	4.88×10^{-6}	0.776	0.01525
77	0.09715	4.437	1121.	0.00747	5.41	0.812	0.01475
80	0.1369	6.089	1145.	0.00778	5.64	0.830	0.01472
90	0.3605	15.08	1266.	0.00902	6.46	0.906	0.01553
100	0.7783	31.96	1503.	0.0109	7.39	1.02	0.01842
110	1.466	62.58	2062.	0.0144	8.58	1.23	0.02646
120	2.511	125.1	4631.	0.0235	10.6	2.09	0.06454
Oxygen							
60	0.0007258	0.04659	947.5	0.00486	3.89×10^{-6}	0.757	0.01688
70	0.006262	0.3457	978.0	0.00598	4.78	0.781	0.01471
80	0.03012	1.468	974.3	0.00711	5.66	0.776	0.01314
90	0.09935	4.387	970.5	0.00826	6.54	0.769	0.01223
100	0.2540	10.42	1006.	0.00949	7.44	0.789	0.01207
110	0.5434	21.28	1101.	0.0109	8.36	0.847	0.01277
120	1.022	39.31	1276.	0.0126	9.35	0.951	0.01462
130	1.749	68.37	1600.	0.0149	10.5	1.13	0.01868
140	2.788	116.8	2370.	0.0190	12.1	1.51	0.02919
150	4.219	214.9	6625.	0.0318	15.2	3.17	0.08865

Table A.5: saturated vapors ($p \neq 1$ atm)...*continued.*

T (K)	p (MPa)	ρ (kg/m^3)	c_p (J/kg·K)	k (W/m·K)	μ (kg/m·s)	Pr	β (K^{-1})
			Water vapor				
273.16	0.0006177	0.004855	1884	0.01707	0.9216×10^{-5}	1.02	0.003681
275.0	0.0006985	0.005507	1886	0.01717	0.9260	1.02	0.003657
280.0	0.0009918	0.007681	1891	0.01744	0.9382	1.02	0.003596
285.0	0.001389	0.01057	1897	0.01773	0.9509	1.02	0.003538
290.0	0.001920	0.01436	1902	0.01803	0.9641	1.02	0.003481
295.0	0.002621	0.01928	1908	0.01835	0.9778	1.02	0.003428
300.0	0.003537	0.02559	1914	0.01867	0.9920	1.02	0.003376
305.0	0.004719	0.03360	1920	0.01901	1.006	1.02	0.003328
310.0	0.006231	0.04366	1927	0.01937	1.021	1.02	0.003281
320.0	0.01055	0.07166	1942	0.02012	1.052	1.02	0.003195
340.0	0.02719	0.1744	1979	0.02178	1.116	1.01	0.003052
360.0	0.06219	0.3786	2033	0.02369	1.182	1.01	0.002948
373.15	0.1014	0.5982	2080	0.02510	1.227	1.02	0.002902
380.0	0.1289	0.7483	2110	0.02587	1.250	1.02	0.002887
400.0	0.2458	1.369	2218	0.02835	1.319	1.03	0.002874
420.0	0.4373	2.352	2367	0.03113	1.388	1.06	0.002914
440.0	0.7337	3.833	2560	0.03423	1.457	1.09	0.003014
460.0	1.171	5.983	2801	0.03766	1.526	1.13	0.003181
480.0	1.790	9.014	3098	0.04145	1.595	1.19	0.003428
500.0	2.639	13.20	3463	0.04567	1.665	1.26	0.003778
520.0	3.769	18.90	3926	0.05044	1.738	1.35	0.004274
540.0	5.237	26.63	4540	0.05610	1.815	1.47	0.004994
560.0	7.106	37.15	5410	0.06334	1.901	1.62	0.006091
580.0	9.448	51.74	6760	0.07372	2.002	1.84	0.007904
600.0	12.34	72.84	9181	0.09105	2.135	2.15	0.01135
620.0	15.90	106.3	14,940	0.1267	2.337	2.76	0.02000
640.0	20.27	177.1	52,590	0.2500	2.794	5.88	0.07995
642.0	20.76	191.5	737,900	0.2897	2.894	7.37	0.1144
644.0	21.26	211.0	1,253,000	0.3596	3.034	10.6	0.1988
646.0	21.77	243.5	3,852,000	0.5561	3.325	23.0	0.6329
647.0	22.04	286.5	53,340,000	1.573	3.972	135.	9.274

Table A.6 Thermophysical properties of gases at atmospheric pressure (101325 Pa)

T (K)	ρ (kg/m^3)	c_p (J/kg·K)	μ (kg/m·s)	ν (m^2/s)	k (W/m·K)	α (m^2/s)	Pr
			Air				
100	3.605	1039	0.711×10^{-5}	0.197×10^{-5}	0.00941	0.251×10^{-5}	0.784
150	2.368	1012	1.035	0.437	0.01406	0.587	0.745
200	1.769	1007	1.333	0.754	0.01836	1.031	0.731
250	1.412	1006	1.606	1.137	0.02241	1.578	0.721
260	1.358	1006	1.649	1.214	0.02329	1.705	0.712
270	1.308	1006	1.699	1.299	0.02400	1.824	0.712
280	1.261	1006	1.747	1.385	0.02473	1.879	0.711
290	1.217	1006	1.795	1.475	0.02544	2.078	0.710
300	1.177	1007	1.857	1.578	0.02623	2.213	0.713
310	1.139	1007	1.889	1.659	0.02684	2.340	0.709
320	1.103	1008	1.935	1.754	0.02753	2.476	0.708
330	1.070	1008	1.981	1.851	0.02821	2.616	0.708
340	1.038	1009	2.025	1.951	0.02888	2.821	0.707
350	1.008	1009	2.090	2.073	0.02984	2.931	0.707
400	0.8821	1014	2.310	2.619	0.03328	3.721	0.704
450	0.7840	1021	2.517	3.210	0.03656	4.567	0.703
500	0.7056	1030	2.713	3.845	0.03971	5.464	0.704
550	0.6414	1040	2.902	4.524	0.04277	6.412	0.706
600	0.5880	1051	3.082	5.242	0.04573	7.400	0.708
650	0.5427	1063	3.257	6.001	0.04863	8.430	0.712
700	0.5040	1075	3.425	6.796	0.05146	9.498	0.715
750	0.4704	1087	3.588	7.623	0.05425	10.61	0.719
800	0.4410	1099	3.747	8.497	0.05699	11.76	0.723
850	0.4150	1110	3.901	9.400	0.05969	12.96	0.725
900	0.3920	1121	4.052	10.34	0.06237	14.19	0.728
950	0.3716	1131	4.199	11.30	0.06501	15.47	0.731
1000	0.3528	1142	4.343	12.31	0.06763	16.79	0.733
1100	0.3207	1159	4.622	14.41	0.07281	19.59	0.736
1200	0.2940	1175	4.891	16.64	0.07792	22.56	0.738
1300	0.2714	1189	5.151	18.98	0.08297	25.71	0.738
1400	0.2520	1201	5.403	21.44	0.08798	29.05	0.738
1500	0.2352	1211	5.648	23.99	0.09296	32.64	0.735

Table A.6: gases at 1 atm...*continued.*

T (K)	ρ (kg/m^3)	c_p (J/kg·K)	μ (kg/m·s)	ν (m^2/s)	k (W/m·K)	α (m^2/s)	Pr
			Argon				
100	4.982	547.4	0.799×10^{-5}	0.160×10^{-5}	0.00632	0.232×10^{-5}	0.692
150	3.269	527.7	1.20	0.366	0.00939	0.544	0.673
200	2.441	523.7	1.59	0.652	0.01245	0.974	0.669
250	1.950	522.2	1.95	1.00	0.01527	1.50	0.668
300	1.624	521.5	2.29	1.41	0.01787	2.11	0.667
350	1.391	521.2	2.59	1.86	0.02029	2.80	0.666
400	1.217	520.9	2.88	2.37	0.02256	3.56	0.666
450	1.082	520.8	3.16	2.92	0.02470	4.39	0.666
500	0.9735	520.7	3.42	3.51	0.02675	5.28	0.666
550	0.8850	520.6	3.67	4.14	0.02870	6.23	0.665
600	0.8112	520.6	3.91	4.82	0.03057	7.24	0.665
650	0.7488	520.5	4.14	5.52	0.03238	8.31	0.665
700	0.6953	520.5	4.36	6.27	0.03412	9.43	0.665
			Ammonia				
240	0.8888	2296	8.06×10^{-6}	0.907×10^{-5}	0.0210	0.1028×10^{-4}	0.882
273	0.7719	2180	9.19	1.19	0.0229	0.1361	0.874
323	0.6475	2176	11.01	1.70	0.0274	0.1943	0.876
373	0.5589	2238	12.92	2.31	0.0334	0.2671	0.866
423	0.4920	2326	14.87	3.01	0.0407	0.3554	0.850
473	0.4396	2425	16.82	3.82	0.0487	0.4565	0.838
			Carbon dioxide				
220	2.4733	783	11.06×10^{-6}	4.472×10^{-6}	0.01090	0.05628×10^{-4}	0.795
250	2.1657	804	12.57	5.804	0.01295	0.07437	0.780
300	1.7973	853	15.02	8.357	0.01677	0.1094	0.764
350	1.5362	900	17.40	11.33	0.02092	0.1513	0.749
400	1.3424	942	19.70	14.68	0.02515	0.1989	0.738
450	1.1918	980	21.88	18.36	0.02938	0.2516	0.730
500	1.0732	1013	24.02	22.38	0.03354	0.3085	0.725
550	0.9739	1047	26.05	26.75	0.03761	0.3688	0.725
600	0.8938	1076	28.00	31.33	0.04159	0.4325	0.724

Table A.6: gases at 1 atm…*continued.*

T(K)	ρ (kg/m^3)	c_p (J/kg·K)	μ (kg/m·s)	ν (m^2/s)	k (W/m·K)	α (m^2/s)	Pr
			Carbon monoxide				
250	1.367	1042	1.54×10^{-5}	1.13×10^{-5}	0.02306	1.62×10^{-5}	0.697
300	1.138	1040	1.77	1.56	0.02656	2.24	0.694
350	0.975	1040	1.99	2.04	0.02981	2.94	0.693
400	0.853	1039	2.19	2.56	0.03285	3.70	0.692
450	0.758	1039	2.38	3.13	0.03571	4.53	0.691
500	0.682	1040	2.55	3.74	0.03844	5.42	0.691
600	0.5687	1041	2.89	5.08	0.04357	7.36	0.690
700	0.4874	1043	3.20	6.56	0.04838	9.52	0.689
800	0.4265	1046	3.49	8.18	0.05297	11.9	0.689
900	0.3791	1049	3.77	9.94	0.05738	14.4	0.689
1000	0.3412	1052	4.04	11.8	0.06164	17.2	0.689
			Helium				
50	0.9732	5201	0.607×10^{-5}	0.0624×10^{-4}	0.0476	0.0940×10^{-4}	0.663
100	0.4871	5194	0.953	0.196	0.0746	0.295	0.664
150	0.3249	5193	1.25	0.385	0.0976	0.578	0.665
200	0.2437	5193	1.51	0.621	0.118	0.932	0.667
250	0.1950	5193	1.76	0.903	0.138	1.36	0.665
300	0.1625	5193	1.99	1.23	0.156	1.85	0.664
350	0.1393	5193	2.22	1.59	0.174	2.40	0.663
400	0.1219	5193	2.43	1.99	0.190	3.01	0.663
450	0.1084	5193	2.64	2.43	0.207	3.67	0.663
500	0.09753	5193	2.84	2.91	0.222	4.39	0.663
600	0.08128	5193	3.22	3.96	0.252	5.98	0.663
700	0.06967	5193	3.59	5.15	0.281	7.77	0.663
800	0.06096	5193	3.94	6.47	0.309	9.75	0.664
900	0.05419	5193	4.28	7.91	0.335	11.9	0.664
1000	0.04877	5193	4.62	9.46	0.361	14.2	0.665
1100	0.04434	5193	4.95	11.2	0.387	16.8	0.664
1200	0.04065	5193	5.27	13.0	0.412	19.5	0.664
1300	0.03752	5193	5.59	14.9	0.437	22.4	0.664
1400	0.03484	5193	5.90	16.9	0.461	25.5	0.665
1500	0.03252	5193	6.21	19.1	0.485	28.7	0.665

Table A.6: gases at 1 atm...*continued.*

T (K)	ρ (kg/m^3)	c_p (J/kg·K)	μ (kg/m·s)	ν (m^2/s)	k (W/m·K)	α (m^2/s)	Pr
			Hydrogen				
30	0.8472	10840	1.606×10^{-6}	1.805×10^{-6}	0.0228	0.0249×10^{-4}	0.759
50	0.5096	10501	2.516	4.880	0.0362	0.0676	0.721
100	0.2457	11229	4.212	17.14	0.0665	0.2408	0.712
150	0.1637	12602	5.595	34.18	0.0981	0.475	0.718
200	0.1227	13540	6.813	55.53	0.1282	0.772	0.719
250	0.09819	14059	7.919	80.64	0.1561	1.130	0.713
300	0.08185	14314	8.963	109.5	0.182	1.554	0.706
350	0.07016	14436	9.954	141.9	0.206	2.031	0.697
400	0.06135	14491	10.86	177.1	0.228	2.568	0.690
450	0.05462	14499	11.78	215.6	0.251	3.164	0.682
500	0.04918	14507	12.64	257.0	0.272	3.817	0.675
600	0.04085	14537	14.29	349.7	0.315	5.306	0.664
700	0.03492	14574	15.89	455.1	0.351	6.903	0.659
800	0.03060	14675	17.40	569	0.384	8.563	0.664
900	0.02723	14821	18.78	690	0.412	10.21	0.675
1000	0.02451	14968	20.16	822	0.445	12.13	0.678
1100	0.02227	15165	21.46	965	0.488	14.45	0.668
1200	0.02050	15366	22.75	1107	0.528	16.76	0.661
1300	0.01890	15575	24.08	1273	0.568	19.3	0.660
			Nitrogen				
100	3.484	1072	6.80×10^{-6}	1.95×10^{-6}	0.00988	0.0265×10^{-4}	0.738
200	1.711	1043	12.9	7.54	0.0187	0.105	0.720
300	1.138	1041	18.0	15.8	0.0260	0.219	0.721
400	0.8533	1044	22.2	26.0	0.0326	0.366	0.711
500	0.6826	1055	26.1	38.2	0.0388	0.539	0.709
600	0.5688	1074	29.5	51.9	0.0448	0.733	0.708
700	0.4876	1096	32.8	67.3	0.0508	0.951	0.708
800	0.4266	1120	35.8	83.9	0.0567	1.19	0.707
900	0.3792	1143	38.7	102.	0.0624	1.44	0.709
1000	0.3413	1165	41.5	122.	0.0680	1.71	0.711
1100	0.3103	1184	44.2	142.	0.0735	2.00	0.712
1200	0.2844	1201	46.7	164.	0.0788	2.31	0.712
1400	0.2438	1229	51.7	212.	0.0889	2.97	0.715
1600	0.2133	1250	56.3	264.	0.0984	3.69	0.715

Table A.6: gases at 1 atm…*continued.*

T (K)	ρ (kg/m^3)	c_p (J/kg·K)	μ (kg/m·s)	ν (m^2/s)	k (W/m·K)	α (m^2/s)	Pr
			Oxygen				
100	3.995	935.6	0.738×10^{-5}	0.185×10^{-5}	0.00930	0.249×10^{-5}	0.743
150	2.619	919.8	1.13	0.431	0.01415	0.587	0.733
200	1.956	914.6	1.47	0.754	0.01848	1.03	0.730
250	1.562	915.0	1.79	1.145	0.02244	1.57	0.729
300	1.301	919.9	2.07	1.595	0.02615	2.19	0.730
350	1.114	929.1	2.34	2.101	0.02974	2.87	0.731
400	0.9749	941.7	2.59	2.657	0.03324	3.62	0.734
450	0.8665	956.4	2.83	3.261	0.03670	4.43	0.737
500	0.7798	972.2	3.05	3.911	0.04010	5.29	0.739
600	0.6498	1003	3.47	5.340	0.04673	7.17	0.745
700	0.5569	1031	3.86	6.930	0.05309	9.24	0.750
800	0.4873	1054	4.23	8.673	0.05915	11.5	0.753
900	0.4332	1073	4.57	10.56	0.06493	14.0	0.757
1000	0.3899	1089	4.91	12.59	0.07046	16.6	0.759
			Steam (H_2O vapor)				
373.15	0.5976	2080	12.28×10^{-6}	20.55×10^{-6}	0.02509	2.019×10^{-5}	1.018
393.15	0.5652	2021	13.04	23.07	0.02650	2.320	0.994
413.15	0.5365	1994	13.81	25.74	0.02805	2.622	0.982
433.15	0.5108	1980	14.59	28.56	0.02970	2.937	0.973
453.15	0.4875	1976	15.38	31.55	0.03145	3.265	0.966
473.15	0.4665	1976	16.18	34.68	0.03328	3.610	0.961
493.15	0.4472	1980	17.00	38.01	0.03519	3.974	0.956
513.15	0.4295	1986	17.81	41.47	0.03716	4.357	0.952
533.15	0.4131	1994	18.63	45.10	0.03919	4.758	0.948
553.15	0.3980	2003	19.46	48.89	0.04128	5.178	0.944
573.15	0.3840	2013	20.29	52.84	0.04341	5.616	0.941
593.15	0.3709	2023	21.12	56.94	0.04560	6.077	0.937
613.15	0.3587	2034	21.95	61.19	0.04784	6.554	0.934
673.15	0.3266	2070	24.45	74.86	0.05476	8.100	0.924
773.15	0.2842	2134	28.57	100.5	0.06698	11.04	0.910
873.15	0.2516	2203	32.62	129.7	0.07990	14.42	0.899
973.15	0.2257	2273	36.55	161.9	0.09338	18.20	0.890
1073.15	0.2046	2343	40.38	197.4	0.1073	22.38	0.882

Table A.7 Physical constants from 1998 CODATA. The 1σ uncertainties of the last two digits are stated in parentheses.

Avogadro's number, N_A	$6.02214199\ (47) \times 10^{26}$	molecules/kmol
Boltzmann's constant, k_B	$1.3806503\ (24) \times 10^{-23}$	J/K
Universal gas constant, R°	8314.472 (15)	J/kmol·K
Speed of light in vacuum, c	299,792,458 (0)	m/s
Standard acceleration of gravity, g	9.80665 (0)	m/s^2
Stefan-Boltzmann constant, σ	$5.670400\ (40) \times 10^{-8}$	W/m^2K^4

Table A.8 Additional physical property data in the text

Page no.	*Data*
28	Electromagnetic wave spectrum
52, 53	Additional thermal conductivities of metals, liquids, and gases
429, 430	Surface tension
490	Total emittances
565	Lennard-Jones constants and molecular weights
566	Collision integrals
572	Molal specific volumes and latent heats

B. Units and conversion factors

The reader is certainly familiar with the *Système International d' Unités* (the "S.I. System") and will probably make primary use of it in later work. But the need to deal with English units will remain with us for many years to come. We therefore list some conversion factors from English units to S.I. units in this appendix. Many more conversion factors and an extensive discussion of the S.I. system and may be found in [B.1]. The dimensions that are used consistently in the subject of heat transfer are length, mass, force, energy, temperature, and time. We generally avoid using both force and mass dimensions in the same equation, since force is always expressible in dimensions of mass, length, and time, and vice versa. We do not make a practice of eliminating energy in terms of force times length because the accounting of work and heat is often kept separate in heat transfer problems. The text makes occasional reference to electrical units; however, these are conventional and do not have counterparts in the English system, so no electrical units are discussed here.

We present conversion factors in the form of multipliers that may be applied to English units so as to obtain S.I units. For example, the relationship between Btu and J is

$$1 \text{ Btu} = 1055.04 \text{ J}. \tag{B.1}$$

Thus, a given number of Btu may be multiplied by 1055.04 to obtain the equivalent number of joules. We denote this in our tabulation as

$$\text{J} = 1055.04 \times \text{Btu}. \tag{B.2}$$

although the meaning of the multiplier is clearer if we rearrange eqn. (B.1) to display a conversion factor whose numerical worth is unity:

$$1 = 1055.04 \, \frac{\text{J}}{\text{Btu}}$$

Table B.1 SI Multiplying Factors

Multiple	*Prefix*	*Symbol*	*Multiple*	*Prefix*	*Symbol*
10^{24}	yotta	Y	10^{-24}	yocto	y
10^{21}	zetta	Z	10^{-21}	zepto	z
10^{18}	exa	E	10^{-18}	atto	a
10^{15}	peta	P	10^{-15}	femto	f
10^{12}	tera	T	10^{-12}	pico	p
10^{9}	giga	G	10^{-9}	nano	n
10^{6}	mega	M	10^{-6}	micro	μ
10^{3}	kilo	k	10^{-3}	milli	m
10^{2}	hecto	h	10^{-2}	centi	c
10^{1}	deka	da	10^{-1}	deci	d

The latter form is quite useful in changing units within more complex equations. For example, the conversion factor

$$1 = 0.0001663 \ \frac{\text{m/s}}{\text{furlong/fortnight}}$$

could be multiplied by a velocity, on just one side of an equation, to convert it from furlongs per fortnight[1] to meters per second.

Note that the S.I. units may have prefixes placed in front of them to indicate multiplication by various powers of ten. For example, the prefix "k" denotes multiplication by 1000 (e.g., 1 km = 1000 m). The complete set of S.I. prefixes is given in Table B.1.

Table B.2 provides multipliers for a selection of common units.

References

[B.1] B. N. Taylor. *Guide to the Use of the International System of Units (SI)*. National Institute of Standards and Technology, Gaithersburg, MD, 1995. NIST Special Publication 811. May be downloaded from NIST's web pages.

[1] Shortly after World War II, a group of staff physicists at Boeing Airplane Co. answered angry demands by engineers that calculations be presented in English units with a report translated entirely into such dimensions as these.

Table B.2 Selected Conversion Factors

Dimension	SI	=	*multiplier*	×	*other unit*
Density	kg/m^3	=	16.018	×	lbm/ft^3
	kg/m^3	=	10^3	×	g/cm^3
Diffusivity (α, ν, $\mathcal{D}$)	m^2/s	=	0.092903	×	ft^2/s
	m^2/s	=	10^{-6}	×	centistokes
Energy	J	=	1055.04	×	Btu[a]
	J	=	4.1868	×	cal[b]
	J	=	10^{-7}	×	erg
Energy per unit mass	J	=	2326.0	×	Btu/lbm
	J	=	4186.8	×	cal/g
Flow rate	m^3/s	=	6.3090×10^{-5}	×	gal/min (gpm)
	m^3/s	=	4.7195×10^{-4}	×	ft^3/min (cfm)
	m^3/s	=	10^{-3}	×	L/s
Force	N	=	10^{-5}	×	dyne
	N	=	4.4482	×	lbf
Heat flux	W/m^2	=	3.154	×	$Btu/hr\cdot ft^2$
	W/m^2	=	10^4	×	W/cm^2
Heat transfer coefficient	W/m^2K	=	5.6786	×	$Btu/hr\cdot ft^2{}^\circ F$
Length	m	=	10^{-10}	×	ångströms (Å)
	m	=	0.0254	×	inches
	m	=	0.3048	×	feet
	m	=	201.168	×	furlongs
	m	=	1609.34	×	miles
	m	=	3.0857×10^{16}	×	parsecs
Mass	kg	=	0.45359	×	lbm
	kg	=	14.594	×	slug

Table B.2…*continued.*

Dimension	SI	=	*multiplier*	×	*other unit*
Power	W	=	0.022597	×	ft·lbf/min
	W	=	0.29307	×	Btu/hr
	W	=	745.700	×	hp
Pressure	Pa	=	133.32	×	mmHg (@0°C)
	Pa	=	248.84	×	inH_2O (@60°F)
	Pa	=	3376.9	×	inHg (@60°F)
	Pa	=	6894.8	×	psi
	Pa	=	10^5	×	bar
	Pa	=	101325	×	atm
Specific heat capacity	J/kg·K	=	4186.8	×	Btu/lbm·°F
	J/kg·K	=	4186.8	×	cal/g·°C
Temperature	K	=	5/9	×	°R
	K	=	°C + 273.15		
	K	=	(°F + 459.67)/1.8		
Thermal conductivity	W/m·K	=	0.14413	×	Btu·in/hr·ft^2°F
	W/m·K	=	1.7307	×	Btu/hr·ft°F
	W/m·K	=	418.68	×	cal/s·cm°C
Viscosity (dynamic)	Pa·s	=	10^{-3}	×	centipoise
	Pa·s	=	1.4881	×	lbm/ft·s
	Pa·s	=	47.880	×	lbf·s/ft^2
Volume	m^3	=	10^{-3}	×	L
	m^3	=	3.7854×10^{-3}	×	gallons
	m^3	=	0.028317	×	ft^3

[a] The British thermal unit, originally defined as the heat that raises 1 lbm of water 1°F, has several values that depend mainly on the initial temperature of the water warmed. The above is the International Table (*i.e.*, steam table) Btu. A "mean" Btu of 1055.87 J is also common. Related quantities are: 1 therm = 10^5 Btu; 1 quad = 10^{15} Btu ≈ 1 EJ; 1 ton of refrigeration = 12,000 Btu/hr absorbed.

[b] The calorie represents the heat that raises 1 g of water 1°C. Like the Btu, the calorie has several values that depend on the initial temperature of the water warmed. The above is the International Table calorie, or IT calorie. A "thermochemical" calorie of 4.184 J has also been in common use. The dietitian's "Calorie" is actually 1 kilocalorie.

C. Nomenclature

Arbitrary constants, coefficients, and functions introduced in context are not included here; neither are most geometrical dimensions. Dimensions of symbols are given in S.I. units in parenthesis after the definition. Symbols without dimensions are noted with (–), where it is not obvious.

A, A_c, A_h, A_j	area (m^2) or function defined in eqn. (9.39); cross-sectional area (m^2); area of heater (m^2); jet cross-sectional area (m^2)
B	radiosity (W/m^2), or the function defined in Fig. 8.14.
$B_{m,i}$	mass transfer driving force, eqn. (11.88) (–)
b.c.	boundary condition
b.l.	boundary layer
C, C_c, C_h	heat capacity rate (W/K) or electrical capacitance (s/ohm) or correction factor in Fig. 7.16; heat capacity rate for hot and cold fluids (W/K)
$\overline{C}$	average thermal molecular speed
C_f	skin friction coefficient (–) [eqn. (6.33)]
C_{sf}	surface roughness factor (–). (see Table 9.2)
c, c_p, c_v	specific heat, specific heat at constant pressure, specific heat at constant volume ($J/kg \cdot K$)
c	molar concentration of a mixture ($kmol/m^3$) or damping coefficient ($N \cdot s/m$)
c	partial molar concentration of a species i ($kmol/m^3$)
c_o	speed of light, 2.99792458×10^8 m/s
D or d	diameter (m)
D_h	hydraulic diameter, $4A_c/P$ (m)
$\mathcal{D}_{12}, \mathcal{D}_{im}$	binary diffusion coefficient for species 1 diffusing in species 2, effective binary diffusion coefficient for species i diffusing in mixture m, (m^2/s)
E, E_0	voltage, initial voltage (V)
e, e_λ	emissive power of a black body (W/m^2) or energy equivalent of mass (J); monochromatic emissive power ($W/m^2 \cdot \mu m$)
F	LMTD correction factor (–) or $(\text{Re}_{TP}/\text{Re}_f)^{0.8}$ (–)

$F(t)$ time-dependent driving force (N)

F_{1-2} view factor

$\mathcal{F}_{1-2}$ transfer factor

f Darcy-Weisbach friction factor(–) [eqn. (3.24)] or Blasius function of η (–)

f_v frequency of vibration (Hz)

G superficial mass flux $= \dot{m}/A_{\text{pipe}}$

g, g_{eff} gravitational body force (m/s^2), effective g defined in eqn. (8.60) (m/s^2)

$g_{m,i}$ mass transfer coefficient for species i, ($\text{kg/m}^2\cdot\text{s}$)

H height of ribbon (m), head (m), irradiance (W/m^2), or Henry's law constant (N/m^2)

$h, \overline{h}$ local heat transfer coefficient ($\text{W/m}^2\text{K}$), or enthalpy (J/kg), or height (m), or Planck's constant ($6.6260755 \times 10^{-34}$ J·s); average heat transfer coefficient.

$\hat{h}$ specific enthalpy (J/kg)

h_c interfacial conductance ($\text{W/m}^2\text{K}$)

h_{fg}, h_{sf}, h_{sg} latent heat of vaporization (J/kg), latent heat of fusion (J/kg), latent heat of sublimation (J/kg)

h'_{fg} latent heat corrected for sensible heat

$\hat{h}_i$ specific enthalpy of species i (J/kg)

h^* heat transfer coefficient at zero mass transfer, in Chapter 11 only ($\text{W/m}^2\text{K}$)

I electric current (amperes) or number of isothermal increments (–)

$\vec{i}, \vec{j}, \vec{k}$ unit vectors in the x, y, z directions

i intensity of radiation ($\text{W/m}^2\cdot$ steradian)

$I_0(x)$ modified Bessel function of the first kind of order zero

i.c. initial condition

$J_0(x), J_1(x)$ Bessel function of the first kind of order zero, of order one

$\vec{j}_i$ diffusional mass flux of species i ($\text{kg/m}^2\cdot\text{s}$)

$\vec{J}$ electric current density (amperes/m^2)

$\vec{J}_i^*$ diffusional mole flux of species i ($\text{kmol/m}^2\cdot\text{s}$)

k thermal conductivity ($\text{W/m}^2\text{K}$)

k_{B} Boltzmann's constant, $1.3806503 \times 10^{-23}$ J/K

k_T thermal diffusion ratio (–)

L any characteristic length (m)

L_e mean beam length (m)

LMTD logarithmic mean temperature difference

ℓ an axial length or length into the paper or mean free molecular path (m or Å) or mixing length (m)

M molecular weight (of mixture if not subscripted) (kg/kmol)

m fin parameter, $\sqrt{\overline{h}P/kA}$ (m^{-1})

m_0 rest mass (kg)

$\dot{m}$ mass flow rate (kg/s), also mass flux per unit width ($\text{kg/m}\cdot\text{s}$)

m_i mass fraction of species i (–)

$\dot{m}''$ scalar mass flux of a mixture ($kg/m^2 \cdot s$)

N number of adiabatic channels (–) or number of rows in a rod bundle (–)

$\vec{N}$ mole flux (of mixture if not subscripted) ($kmol/m^2 \cdot s$)

N_A Avogadro's number, $6.02214199 \times 10^{26}$ molecules/kmol

$\mathcal{N}$ number density (of mixture if not subscripted) ($molecules/m^3$)

$\vec{n}$ mass flux (of mixture if not subscripted) ($kg/m^2 \cdot s$), unit normal vector

n summation index (–) or nucleation site density ($sites/m^2$)

P factor (–) defined in eqn. (3.14) or pitch of a tube bundle (m) or perimeter (m)

p pressure (N/m^2)

p_i partial pressure of species i (N/m^2)

Q rate of heat transfer (W)

$q, \vec{q}$ heat flux (W/m^2)

q_b, q_{FC}, q_i defined in context of eqn. (9.36)

$q_{\max}$ or q_{burnout} peak boiling heat flux (W/m^2)

$q_{\min}$ minimum boiling heat flux (W/m^2)

$\dot{q}$ volumetric heat generation (W/m^3)

R factor defined in eqn. (3.14) (–), radius (m), electrical resistance (ohm), or region (m^3)

R ideal gas constant per unit mass, R°/M (for mixture if not subscripted) ($J/kg \cdot K$)

R° ideal gas constant, 8314.472 ($J/kmol \cdot K$)

R_t, R_f thermal resistance (K/W or $m^2 \cdot K/W$), fouling resistance ($m^2 \cdot K/W$)

$r, \vec{r}$ radial coordinate (m), position vector (m)

r_{crit} critical radius of insulation (m)

$\dot{r}_i$ volume rate of creation of mass of species i ($kg/m^3 \cdot s$)

S entropy (J/K), or surface (m^2), or shape factor (N/I), or function defined in Fig. 9.22

S_L, S_T rod bundle spacings (m). See Fig. 7.13

s specific entropy ($J/kg \cdot K$)

T, T_c temperature (°C, K); thermodynamic critical temperature (K)

$\boldsymbol{T}$ time constant, $\rho c V/\overline{h}A$ (s)

$\mathbf{T}$ a long time over which properties are averaged (s)

t time (s)

U overall heat transfer coefficient (W/m^2K); internal thermodynamic energy (J); characteristic velocity (m/s)

$u, u_{\text{av}}, \overline{u}$ local x-direction fluid velocity (m/s) or specific energy (J/kg); average velocity over an area (m/s); local time-averaged velocity (m/s);

$\vec{u}, u_c, u_g$ vectorial velocity (m/s); characteristic velocity (m/s) [see eqn. (8.18)]; Helmholtz-unstable velocity (m/s)

$\hat{u}$	specific internal energy (J/kg)
V	volume (m^3); voltage (V)
V_m	molal specific volume (m^3/kmol)
v	local y-direction fluid velocity (m/s)
$\vec{v}$	mass-average velocity, in Chapter 11 only (m/s)
$\vec{v}_i$	average velocity of species i (m/s)
$\vec{v}^*$	mole average velocity (m/s)
Wk	rate of doing work (W)
w	z-direction velocity (m/s) or width (m)
X_{tt}	Martinelli parameter (–)
x, y, z	Cartesian coordinates (m); x is also used to denote any unknown quantity
x_i	mole fraction of species i (–)
x	quality of steam

Greek symbols

α	thermal diffusivity, $k/\rho c_p$ (m^2/s), or helix angle (rad.)
α, α_g	absorptance (–); gaseous absorptance (–)
β	coefficient of thermal expansion (K^{-1}) or relaxation factor (–), or $h\sqrt{\alpha t}/k$, or coefficient of viscous friction (–)
β_λ	monochromatic extinction coefficient (m^{-1})
Γ, Γ_c	$\dot{g}L^2/k\Delta T$, mass flow rate in film (kg/m·s)
γ	c_p/c_v; electrical conductivity (V/ohm·m^2)
γ_λ	monochromatic scattering coefficient (m^{-1})
ΔE	Activation energy of reaction (J/kmol)
Δp	pressure drop in any system (N/m^2)
ΔT	any temperature difference; various values are defined in context.
$\delta, \delta_c, \delta_t, \delta_t'$	flow boundary layer thickness (m) or condensate film thickness (m); concentration boundary layer thickness (m); thermal boundary layer thickness (m); h/k (m).
ε	emittance (–); heat exchanger effectiveness (–); roughness (m); fin efficiency (–)
$\varepsilon_A, \varepsilon_{AB}$	potential well depth for molecules of A, for collisions of A and B (J)
ε_g	gaseous emittance (–)
$\varepsilon_m, \varepsilon_h$	eddy diffusivity of mass (–), of heat (–)
η	independent variable of Blasius function, $y\sqrt{u_\infty/\nu x}$ (–)
η_f	fin efficiency
Θ	a ratio of two temperature differences (–)
θ	$(T - T_\infty)$ (K) or angular coordinate (rad)
ζ	$x/\sqrt{\alpha t}$
κ_λ	monochromatic absorption coefficient (m^{-1})
$\lambda, \lambda_c, \lambda_H$	wavelength (m) or eigenvalue (m^{-1}); critical Taylor wavelength (m); Helmholtz-unstable wavelength (m)

$\lambda_d, \lambda_{d_1}, \lambda_{d_2}$ most dangerous Taylor-unstable wavelength (m); subscripts denote one- and two-dimensional values

$\hat{\lambda}$ dimensionless eigenvalue (–)

μ dynamic viscosity (kg/m·s) or chemical potential (J/mol)

ν kinematic viscosity, μ/ρ (m^2/s)

ξ x/L or $x\sqrt{\omega/2\alpha}$; also $(x/L+1)$ or x/L (–)

ρ mass density (kg/m^3) or reflectance (–)

ρ_i partial density of ith species (kg/m^3)

σ surface tension (N/m) or Stefan-Boltzmann constant 5.670400×10^{-8} ($W/m^2 \cdot K^4$)

σ_A, σ_{AB} collision cross section of molecules of A, for collisions of A with B (Å)

τ transmissivity (–) or dimensionless time ($T/\boldsymbol{T}$) or shear stress (N/m^2) or length of travel in b.l. (m)

τ_w, τ_{yx} shear stress on a wall (N/m^2), shear stress in the x-direction on the plane normal to the y-direction (N/m^2)

τ_δ shear stress exerted by liquid film (N/m^2)

Φ $\Delta T/(\dot{q}L^2/k)$ or fraction of total heat removed (see Fig. 5.10) (–)

ϕ angular coordinate (rad), or δ_t/δ (–), or factor defined in context of eqn. (6.103) (–)

ϕ_{ij} weighting functions for mixture viscosity or thermal conductivity (–)

χ $d\Theta/d\zeta$

ψ $\omega L^2/\alpha$

Ω ωt

$\Omega_D, \Omega_k, \Omega_\mu$ collision integral for diffusivity, thermal conductivity, or dynamic viscosity (–)

ω frequency of a wave or of rotation (rad/s) or solid angle (sr)

General subscripts

av, avg denoting bulk or average values

b, body denoting any body

b denoting a black body

c denoting the critical state

D denoting a value based on D

e, e_t denoting a dynamical entry length or a free stream variable; denoting a thermal entry length

i denoting initial or inside value, or a value that changes with the index i, or values for the ith species in a mixture

f, g denoting saturated liquid and vapor states

in denoting a value at the inlet

L denoting a value based on L or at the left-hand side

m denoting values for mixtures

max, min denoting maximum or minimum values

NB denoting nucleate boiling

n denoting a value that changes with the index n

o denoting outside, in most cases

out	denoting a value at the outlet
R	denoting a value based on R or at the right-hand side
s	denoting values above an interface
sfc	denoting conditions at a surface
sup, sat, sub	denoting superheated, saturated, or subcooled states
TP	denoting a two-phase value
w	denoting conditions at a wall
u	denoting values below an interface
x	denoting a local value at a given value of x
∞	denoting conditions in a fluid far from a surface
λ	denoting radiative properties evaluated at a particular wavelength

General superscript

*	denoting values for zero net mass transfer (used in Chapter 11 only)

Dimensionless parameters

Bi	Biot number, hL/k_{body}
Bo	Bond number, $L^2 g(\rho_f - \rho_g)/\sigma$
Da	Damkohler number, $\rho \text{A}' \exp(-\Delta E/R^\circ T)/g_m^*$
Ec	Eckert number, $u^2/(c_p \Delta T)$
Fo	Fourier number, $\alpha t/L^2$
Fr	Froude number, $U^2/(gL)$
Gr_L	Grashof number, $g\beta\Delta T L^3/\nu^2$ (for heat transfer), or $g(\Delta\rho/\rho)L^3/\nu^2$
Gz	Graetz number, $\text{RePr}D/x$
H'	L' based on $L \equiv H$
Ja	Jakob number, $c_p \Delta T/h_{fg}$
j	Colburn j-factor, $\text{St}\,\text{Pr}^{2/3}$
Ku	Kutateladze number, $(\pi/24)(q_{\max}/q_{\max_z})$
L'	$L\sqrt{g(\rho_f - \rho_g)/\sigma}$
Le	Lewis number, $\text{Sc}/\text{Pr} = \alpha/\mathcal{D}_{im}$
Ma	Mach number, $u/$(sound speed)
NTU	number of transfer units, $UA/C_{\min}$
Nu_L	Nusselt number, hL/k_{fluid}
$\text{Nu}_{m,L}$	Nusselt number for mass transfer (or Sherwood number) $g_{m,i}^* L/(\rho \mathcal{D}_{im})$
Pe_L	Péclét number, $UL/\alpha = \text{Re}\,\text{Pr}$
Pr, Pr_t	Prandtl number, $\mu c_p/k = \nu/\alpha$; turbulent Prandtl number, $\varepsilon_m/\varepsilon_h$
Ra_L,	Rayleigh number, $\text{Gr}\,\text{Pr} = g\beta\Delta T L^3/(\nu\alpha)$ for heat transfer; $g(\Delta\rho/\rho)L^3/(\nu\mathcal{D}_{12})$ for mass transfer
Ra_L^*	$\text{Ra}_L \text{Nu}_L = g\beta q_w L^4/(k\nu\alpha)$
$\text{Re}_L, \text{Re}_c, \text{Re}_f$	Reynolds number, UL/ν; condensation Re equal to Γ_c/μ; Re for liquid
Sc	Schmidt number for species i in mixture m, $\nu/\mathcal{D}_{im}$
Sh_L	Sherwood number, $g_{m,i}^* L/(\rho \mathcal{D}_{im})$
St	Stanton number, $\text{Nu}/(\text{Re}\,\text{Pr}) = h/(\rho c_p u)$
Str	Strouhal number, $f_v D/u_\infty$
We_L	Weber number, $\rho_g U_\infty^2 L/\sigma$
Π	any dimensionless group

Citation Index

A

Al-Arabi and El-Riedy (1976), 386, 418
Arp, McCarty, and Friend (1998), 635, 639
Arpaci (1991), 46, 223, 251
ASM Handbook Committee (1990), 634, 637
Aung (1987), 392, 419

B

Baehr and Stephan (1998), 195, 207, 250
Barrow and Sitharamarao (1971), 380, 417
Bejan and Lage (1990), 378, 416
Bejan (1995), 46
Bell, Taborek, and Fenoglio (1970), 466, 468, 470, 482
Bellman and Pennington (1954), 436, 479
Berenson (1960), 452–454, 481
Bich, Millat, and Vogel (1990), 635, 639
Binney, Dong, and Lienhard (1986), 431, 479
Bird, Hirschfelder, and Curtiss (1958), 568, 628
Bird, Stewart, and Lightfoot (1960), 47
Boelter, Cherry, Johnson, and Martinelli (1965), 45, 196, 225, 227, 250, 333, 360, 462, 481
Boussinesq (1877), 303, 316
Bowman, Mueller, and Nagle (1940), 110, 129
Bromley, LeRoy, and Robbers (1953), 459, 481
Bromley (1950), 450, 451, 480
Bronowski (1973), 208, 251
Buckingham (1914), 143, 180
Buckingham (1915), 143, 180

C

Carslaw and Jaeger (1959), 46, 203, 214, 220, 221, 223, 234, 236, 250
Catton (1978), 392, 418
Cebeci (1974), 384, 385, 417
Cercignani (2000), 569, 628
Chapman and Cowling (1964), 561, 562, 628
Chen and Armaly (1987), 392, 419
Chen (1963), 460, 463, 481
Childs and Hanley (1968), 568, 628
Chilton and Colburn (1934), 614, 629
Churchill and Bernstein (1977), 346, 347, 361
Churchill and Chu (1975), 370, 382, 383, 416, 417
Churchill and Ozoe (1973), 292, 296, 316
Churchill (1976), 307, 316
Churchill (1977), 392, 418
Clausing and Berton (1989), 388, 418
Colburn (1933), 333, 360
Collier and Thome (1994), 47, 460, 466, 469, 470, 481
Considine (1975), 122, 130
Corriher (1997), 244, 251

D

Ded and Lienhard (1972), 448, 480
deReuck and Craven (1993), 635, 637
Dergarabedian (1953), 219, 251

Dhir and Lienhard (1971), 402, 405, 419, 450, 480
Dhir (1975), 395, 396, 419
Drew and Mueller (1937), 423, 479
Duffie and Beckman (1991), 534, 542
Dukler and Taitel (1985), 469, 482
Dunn and Reay (1982), 475, 482

E

Eckert and Drake (1972), 633–636
Eckert and Drake (1987), 46, 223, 251, 371, 416
Einstein (1956), 570, 629

F

Farlow, Thompson, and Rosner (1976), 155, 180
Fenghour, Wakeham, and Vesovic (1998), 634–636
Fenghour, Wakeham, Vesovic, Watson, Millat, and Vogel (1995), 634–636
Fourier (1955), 45
Fraas (1989), 122, 130
Fujii and Imura (1972), 386, 389, 417

G

Gardner and Taborek (1977), 111, 129
Gebhart, Jaluria, Mahajan, and Sammakia (1988), 387, 418
Ghai, Ertl, and Dullien (1973), 561, 628
Giedt (1949), 345, 361
Glasstone, Laidler, and Eyring (1941), 571, 629
Gnielinski (1976), 336, 360
Goldstein (1938), 371, 373, 416
Graetz (1885), 328, 360
Gregorig, Kern, and Turek (1974), 407, 408, 419

H

Hahne and Grigull (1975), 232–234, 251
Harvey, Peskin, and Klein (2000), 635, 637
Hatfield and Edwards (1981), 389, 418
Heisler (1947), 196, 250
Hennecke and Sparrow (1970), 166, 167, 180
Hewitt (1998), 47, 122, 130
Hirschfelder, Bird, and Spotz (1948), 564, 628
Hirschfelder, Curtiss, and Bird (1964), 561–563, 568, 628
Ho, Powell, and Liley (1974), 634–636
Holman (1981), 518, 530, 542
Hottel and Sarofim (1967), 47, 526, 542
Hsu and Graham (1986), 47, 466, 482
Hsu (1962), 431, 479
Hubbert (1971), 530, 542

I

International Association for the Properties of Water and Steam (1994), 429, 479

J

Jacobsen, Penoncello, Breyerlein, Clark, and Lemmon (1992), 635, 638
Jakob (1949), 46
Jasper (1972), 430, 479
Jeglic, Switzer, and Lienhard (1980), 203, 251
Jeglic (1962), 203, 250

K

Kadambi and Drake (1959), 389, 418
Kadoya, Matsunaga, and Nagashima (1985), 635, 638
Kalish and Dwyer (1967), 351, 361
Karimi (1977), 406, 407, 419
Katto (1978), 466, 482
Kaviany (1995), 46
Kays and Crawford (1993), 46, 292, 316, 327, 328, 359
Kays and London (1984), 47, 115, 116, 122, 129
Kern and Kraus (1972), 171, 180
Kern (1950), 122, 129
Kheyrandish and Lienhard (1985), 458, 481

King, Hsueh, and Mao (1965), 571, 629
Kraus (1955), 380, 381, 417
Kreith and Kreider (1978), 534, 543
Kreith (1973), 331, 332, 360
Kutateladze (1948), 443, 480

L

Laesecke, Krauss, Stephan, and Wagner (1990), 634–636
Lamb (1945), 440, 479, 570, 629
Lemmon, Jacobsen, Penoncello, and Friend (2000), 635, 638
Lemmon, McLinden, and Friend (2000), 635, 638
Lemmon, Peskin, McLinden, and Friend (2000), 635, 637
Leonard, Sun, and Dix (1976), 451, 480
Lewis (1922), 614, 629
Li and Chang (1955), 571, 629
Libby (1996), 310, 316
Lienhard and Dhir (1973), 443, 444, 448, 480
Lienhard and Witte (1985), 455, 481
Lienhard and Wong (1964), 452, 481
Lienhard, Dhir, and Riherd (1973), 443, 448, 480
Lienhard (1966), 343, 344, 361
Lienhard (1973), 386, 417
Lloyd and Moran (1974), 388, 418
Lubarsky and Kaufman (1955), 338, 339, 360
Lyon (1952), 339, 361

M

Marto (1998), 408, 409, 419, 472, 482
Mason and Saxena (1958), 574, 629
McAdams (1954), 46
McCarty and Arp (1990), 635, 638
Meyer, McClintock, Silvestri, and Spencer (1993), 634–636
Millat, Dymond, and Nieto de Castro (1996), 567, 568, 574, 628
Mills (1999), 195, 250
Mills (2001), 47
Modest (1993), 47
Mohr and Taylor (1999), 636, 639
Morse and Feshbach (1953), 233, 251

N

Nakai and Okazaki (1975), 346, 361
Norris, Buckland, Fitzroy, Roecker, and Kaminski (1977), 634, 637
Nukiyama (1934), 421, 478
Nusselt (1915), 369, 416
Nusselt (1916), 396, 419

O

Okado and Watanabe (1988), 430, 479
Oppenheim (1956), 512, 542

P

Pera and Gebhart (1973), 386, 387, 417, 418
Perkins, Friend, Roder, and Nieto de Castro (1991), 635, 638
Perry, Green, and Maloney (1997), 122, 130
Perry (1941), 78, 91
Petukhov (1970), 335, 336, 360
Pioro (1999), 433, 479
Pitschmann and Grigull (1970), 451, 480
Plesset and Zwick (1954), 219, 251
Pope (2000), 310, 316
Poulikakos (1994), 46
Prausnitz, Lichtenthaler, and de Azevedo (1986), 580, 629

R

Raithby and Hollands (1998), 385, 388, 389, 392, 417
Ramilison and Lienhard (1987), 455, 481
Rayleigh (1915), 143, 180
Reed (1987), 339, 361
Reid, Prausnitz, and Poling (1987), 567–569, 571, 573, 574, 628
Restrepo and Glicksman (1974), 389, 418
Reynolds (1874), 297, 316
Reynolds (1974), 549, 628
Rich (1953), 386, 417
Rohsenow and Choi (1961), 46

Rohsenow and Hartnett (1973), 65, 91, 431, 457, 479
Rohsenow, Hartnett, and Cho (1998), 47, 353, 361
Rohsenow (1952), 432–435, 479
Rohsenow (1956), 398, 419
Rose, Uehara, Koyama, and Fujii (1999), 408, 409, 420
Rose, Utaka, and Tanasawa (1999), 472, 482
Rüdenberg (1925), 232, 234, 251

S

Sadasivan and Lienhard (1987), 400, 419, 450, 480
Sanders and Holman (1972), 369, 416
Schetz (1984), 46
Schlichting and Gersten (2000), 47
Schlichting (1968), 265, 272, 289, 306, 315
Schneider (1955), 171, 180
Schneider (1963), 203, 250
Scriven (1959), 219, 251
Seban and Shimazaki (1951), 339, 361
Sellars, Tribus, and Klein (1956), 328, 360
Sernas (1969), 436, 479
Shah and Bhatti (1987), 328, 329, 360
Shah and London (1978), 328, 360
Shah and Sekulic (1998), 80, 91, 122, 130
Shamsundar (1982), 111, 129
Sharan and Lienhard (1985), 458, 481
Shekriladze and Gomelauri (1966), 470, 482
Sieder and Tate (1936), 335, 360
Siegel and Howell (1992), 47, 497, 504, 526, 542
Span and Wagner (1996), 634–636
Sparrow and Cess (1978), 47, 489, 518, 530, 542
Sparrow and Gregg (1959), 399, 400, 405, 419
Sparrow and Gregg (1961), 380, 417
Sparrow and Lin (1963), 409, 420
Sparrow, Nunez, and Prata (1985), 592, 629
Stewart, Jacobsen, and Wagner (1991), 634, 635, 637
Streeter and Wylie (1979), 142, 147, 180
Strock (1959), 78, 91
Sun and Lienhard (1970), 448, 480
Sutherland (1905), 570, 629
Svehla (1962), 564, 628

T

Taborek (1979), 121, 129
Taylor (1995), 663, 664
Tegeler, Span, and Wagner (1999), 635, 638
Tien and Lienhard (1978), 283, 315, 562, 563, 573, 628
Tien (1975), 475, 483
Tillner-Roth and Baehr (1994), 634, 635, 637
Tillner-Roth, Harms-Watzenberg, and Baehr (1993), 635, 637
Touloukian (1970 to 1975), 633–636
Tubular Exchanger Manufacturer's Association (1959 and 1978), 80, 91, 94, 110, 122, 129
Tufeu, Ivanov, Garrabos, and Neindre (1984), 635, 637

U

U.S. Department of Commerce (1977), 534, 543

V

Vargaftik, Vinogradov, and Yargin (1996), 635, 638
Vargaftik (1975), 635, 638
Vesovic, Wakeham, Olchowy, Sengers, Watson, and Millat (1990), 634–636
Vliet (1969), 386, 417

W

Weast (1976), 567, 628
Westwater and Breen (1962), 451, 481
Wheeler (1959), 65, 91
Whitaker (1972), 307, 316

White (1974), 323, 359
White (1991), 46, 260, 305, 315
Wilke and Lee (1955), 564, 628
Wilke (1950), 574, 629
Wilkinson (2000), 47
Winter and Barsch (1971), 475, 482
Witte and Lienhard (1982), 455, 481
Witte (1968), 460, 481
Woodruff and Westwater (1979), 472, 482

Y

Yamagata, Hirano, Nishiwaka, and Matsuoka (1955), 432, 479
Yang (1987), 392, 418
Younglove and Hanley (1986), 635, 638
Younglove (1982), 635, 639
Yovanovich (1998), 232, 251
Yuge (1960), 385, 417

Z

Zuber (1959), 218, 251, 442, 443, 452, 480

Ž

Žukauskas (1972), 350, 351, 361

Subject Index

A

Absorptance, 29, 495–497
  gaseous, 522–530
Adiabatic saturation temperature, 612
Air
  composition, 552
  thermophysical properties, 656
Avogadro's number, 551, 661

B

Baker plot, modified, 466
Batteries, lead-acid, 616
Beer's law, 524
Bernoulli equation, 268
Biot number, 24
  for fins, 157–160
  for lumped capacity behavior, 24
Biot, J.B., 24
Black body, 28–29
  emissive power, 489
  Stefan-Boltzmann law, 30
Black, J., 255
Blanc's law, 569
Blasius, H., 268
Blowing, 598
Blowing factor, 598
Boiling, 421–469
  Forced convection boiling, 457–466
    in external flows, 457–460
    in tubes, 460–466
  peak heat flux, *see* Peak heat flux
  pool boiling, 421–457
    boiling curve, 423–426
    effect of surface condition, 453–456
    film boiling, 426, 450–451
    gravitational influences, 457
    hysteresis, 421–423
    inception, 428–432
    minimum heat flux, 452–453
    nucleate boiling, 428–435
    Rohsenow correlation, 432
    slugs and columns, 424
    subcooling, 456
    transition boiling, 426, 453–456
  small objects, 446, 451
Boiling crisis, *see* Peak Heat Flux
Boltzmann's constant, 32, 552, 661
Bond number, 446
Bonilla, C.F, 444
Boundary conditions, 70, 134–135
Boundary layers, 19, 255–310
  Blasius solution, 268–272
  concentration b.l., 583–585, 593–598
  laminar momentum b.l.
    forced convection, 262–278
    natural convection, 364–382
    thickness, 269, 375
  laminar thermal b.l.
    effect of Pr, 285–286, 290
    forced convection, 278–297
    natural convection, 364–382
    thickness, 290
  relation to transient conduction, 213
  turbulent b.l., 299–310
  turbulent transition
    forced convection, 258–260
    natural convection, 379, 382, 387
Boussinesq, J., 303
Bubble growth, 217–219, 428–435

Buckingham pi-theorem, 143–146
applications of, 146–150
Buckingham, E., 143
Bulk enthalpy, 319
Bulk temperature, 319–322, 340–342
Bulk velocity, 319
Burnout, *see* Peak Heat Flux
Burton, R.
The Anatomy of Melancholy, 363

C

Caloric, 3
Carbon oxidation, 556–558
Catalysis, 602, 617, 625
catalytic reactor, 626
Cervantes, M. de
Don Quixote, 49
Chen, J.C., 462
Chilton, T.H., 444
Colburn j-factor, 298
Colburn equation, 333
Colburn, A.P., 297, 298, 444
Collision cross-sections, 564–565
Collision integrals, 564–565, 568, 573
Condensation
dropwise condensation, 470–472
film condensation, 394–409
cone, 405
conservation equations for, 395–398
dimensional analysis, 394–395
effective gravity, 402
helical tube, 406
horizontal cylinder, 404
inclined plate, 404
latent heat correction, 400
noncondensible gases, 409, 627
rotating disk, 405
sphere, 405
tube bundles, 408
turbulent transition, 406–408
vertical plate, 395–402
forced convective condensation, 469–470
Conduction, 10–19, 49–74, 133–173, 181–239
dimensional analysis of semi-infinite region, 209–210
steady, 142–155
transient, 182–184
fins, 155–173
heat diffusion equation
multidimensional, 49–56
one-dimensional, 17–19
lumped capacity, *see* Lumped capacity solutions
multidimensional, 138–142
steady, 223–235
transient, 235–239
one-dimensional steady, 58–62, 136–137
one-dimensional transient, 191–223
cylinder, 195–196
heat removal during, 196–200
one-term solutions, 206
slab, 191–196
sphere, 195–196
temperature response charts, 196–206
semi-infinite region, 208–223
contact of two, 219–221
convection at surface, 213–216
heat flux to, 216
oscillating surface temperature, 221–223
step-change of q_w, 216–217
step-change of T_w, 209–213
shape factors, 229–235
table of, 233, 234
thermal resistance, *see* Thermal resistance
volumetric heating, 54
periodic, 203–206
steady, 58–61, 136–137, 150–155
well-posed problems, 133–135
Conductivity, *see* Thermal conductivity
Configuration factor, *see* View factor, 32
Conrad, J.
Heart of Darkness, 547
Conservation of energy, *see* Energy equation or Heat diffusion equation
Conservation of mass

general equation, 315
relation to species conservation, 578
steady incompressible flow, 262–264
Conservation of momentum, 265–268
Conservation of species, *see* Species conservation
Contact resistance, *see* Thermal resistance
Continuity equation, *see* Conservation of mass
Convection, 19–22
topics, *see* Boiling, Boundary layers, Condensation, Forced convection, Heat transfer coefficient, or Natural convection
Conversion factors, 663–667
example of development, 14
Cooling towers, 548–549
Correlations, critically evaluating, 352–354
Critical heat flux (CHF), *see* Peak heat flux
Cross flow, 342–352
cylinders
flow field, 342–345
heat transfer, 345–348
tube bundles, 348–352

D

Dalton's law of partial pressures, 552
Damkohler number, 625
Darcy-Weisbach friction factor, 121, 332
Departure from nucleate boiling (DNB), *see* Peak Heat Flux
Diffusion coefficient, 64, 558–571
binary gas mixtures, 563–569
dilute liquid solutions, 569–571
hydrodynamic model for liquid solutions, 570–571
kinetic theory model for gases, 559–562
multicomponent gas mixtures, 569
Diffusional mass flux, 554
Fick's law for, 558–562
Diffusional mole flux, 555
Fick's law for, 561
Diffusivity, *see* Thermal diffusivity
Dilute gas, 559, 568
Dimensional analysis, 142–155
Dirichlet conditions, 134
Dittus-Boelter equation, 333
Dry ice, 626
Dufour effect, 562

E

Earth, age of, Kelvin's estimate, 249
Eckert number, 294
Eddy diffusivity
for heat, 304
for momentum, 303
Effectiveness, *see* Heat exchangers or Fins
Eigenvalue, 192
Einstein, A., 147, 570
Electromagnetic spectrum, 28
Emittance, 489–492
diffuse and specular, 492–493
gaseous, 522–530
monochromatic, 489
Energy equation, 278–280
analogy to momentum equation, 281–282
for boundary layers, 280
for pipe flow, 321
with mass transfer, 606
Entropy production, 9
for lumped capacity system, 24
Entry length, *see* Internal flow
Equimolar counter-diffusion, 622
Error function, 211
Evaporation, 611–614

F

Falling liquid films, 311, 395–397
Fick's law, 63, 548, 558–562
Film absorption, 624
Film boiling, *see* Boiling
Film coefficient, *see* Heat transfer coefficient
Film composition, 600, 608

Film condensation, *see* Condensation
Film temperature, 281, 294, 380, 608
Fins, 155–173
  condition for one-dimensionality, 157–158
  design considerations, 168–169
  effectiveness, 168
  efficiency, 168
  purpose of, 155
  root temperature, 166–168
  variable cross-section, 169–173
  very long fins, 165
  with tip heat transfer, 163–165
  without tip heat transfer, 160–163
First law of thermodynamics, 7–8
Flux, *see* Heat flux or Mass flux
Flux plot, 224–229
Forced convection, 20
  boiling, *see* Boiling, forced convection
  boundary layers, *see* Boundary layers
  condensation, *see* Condensation
  cross flow, *see* Cross flow
  cylinders, 346–347
  flat plates
    laminar, uniform q_w, 295–297
    laminar, uniform T_w, 290–293
    turbulent, 305–308
    unheated starting length, 292
  spheres, 627
  tube bundles, 349–352
  within tubes, *see* Internal flow
Fourier number, 183
Fourier series conduction solutions, 191–195
  one-term approximations, 206
Fourier's law, 10–17, 50–51
Fourier, J.B.J., 10
  The Analytical Theory of Heat, 3, 10, 133
Free convection, *see* Natural convection
Free molecule flow, 569
Friction coefficient, *see* Darcy-Weisbach friction factor or Skin friction coefficient
Froude number, 149
Fully developed flow, *see* Internal flow
Functional replacement, method of, 142

G

Gaseous radiation, 522–530
  absorption, scattering, and extinction coefficients, 523–525
  Beer's law, 524
  flames, 530
  mean beam length, 526
Gauss's theorem, 55, 279, 577, 606
Gnielinski equation, 336
Graetz number, 328
Grashof number, 369
  for mass transfer, 603
Grashof, F., 369
Gravity
  effect on boiling, 457
  g-jitter, 383
  g_{eff} for condensation, 402
  standard acceleration of, 661
Gray body, 489, 495–497, 512–522
  electrical analogy for heat exchange, 512–522
  transfer factor, *see* Transfer factor
Greenhouse effect, 533

H

Hagan, G., 324
Hagan-Poiseuille flow, 324
Halocline, 617
Heat, 3
Heat capacity, *see* Specific heat capacity
Heat conduction, *see* Conduction
Heat convection, *see* Convection
Heat diffusion equation
  multidimensional, 49–56
  one-dimensional, 17–19
Heat exchangers, 93–123
  counterflow, 93, 102, 117
  cross-flow, 94, 112, 118
  design of, 120–123

effectiveness-NTU method, 114–120
function and configuration, 93–97
Logarithmic mean temperature difference, *see* Logarithmic mean temperature difference
mean temperature difference in, 97–107
microchannel, 327
parallel flow, 93, 102, 117
relationship to isothermal pipe flow, 340–341
shell-and-tube, 94, 112, 118
single-stream limit, 119–120, 341
with variable U, 108
Heat flux, defined, 10–13
Heat pipe, 473–475
Heat transfer, 3
modes of, 10–34
Heat transfer coefficient, 20–21
average, 20, 292–293
effect of mass transfer, 606–609
overall, 74–82
Heisler charts, 196
Helmholtz instability, 438–441
Henry's law, 581
Hohlraum, 29
Hot-wire anemometer, 348
Hydraulic diameter, 341
Hydrodynamic theory of CHF, *see* Peak Heat Flux

I

Ideal gas law for mixtures, 551–552
Ideal solution, 581
Incompressible flow, 263–264, 278, 578, 621
Indices, method of, 142
Initial condition, 134
Insulation
critical radius of, 72–74
superinsulation, 16
Integral conservation equations
for energy, 286–290
for momentum, 272–275
Intensity of radiation, 493–494
Interfacial boundary conditions, 579–582
Internal flow
bulk energy equation, 321
bulk enthalpy, 319
bulk temperature, 319–322
for uniform q_w, 325
for uniform T_w, 340–341
bulk velocity, 319
entry length
laminar hydrodynamic, 323
laminar thermal, 327–328
turbulent, 330–331
friction factor
laminar flow, 334
turbulent flow, 332–335
fully developed
hydrodynamically, 319, 323–324
thermally, 319–322
hydraulic diameter, 341
laminar heat transfer
developing flow, 327–330
uniform q_w, fully developed, 324–327
uniform T_w, fully developed, 327
laminar temperature profiles, 321–322
laminar velocity profile
developing flow, 319
fully developed, 323–324
noncircular ducts, 342
turbulent, 330–340
turbulent heat transfer, 332–340
Gnielinski equation, 336
liquid metals, 337–340
variable property effects, 336
turbulent transition, 259
Irradiance, 512

J

Jakob number, 394
Jakob, M., 218, 394
Jupiter, atmosphere of, 616

K

Kinetic theory of gases
average molecular speed, 563

Chapman-Enskog theory, 563
diffusion coefficient
elementary model, 559–561
exact, 563–565
limitations of, 567–569
mean free path, 283, 563
thermal conductivity
elementary model, 283–284
gas mixtures, 574
monatomic gas, 572
viscosity
elementary model, 283–284
gas mixtures, 574
monatomic gas, 572
Kirchhoff's law, 495–497
Kirchhoff, G.R., 495
Kolmogorov scales of turbulence, 315

L

L'Hospital's rule, 106
Laplace's equation, 223
Laplacian, 56, 223
Lardner, D.
The Steam Engine Familiarly Explained and Illustrated, 93
Leibnitz's rule, 273
Lennard-Jones intermolecular potential, 563–564
Lewis number, 559
Lewis, W.K., 559, 600, 614
Liquid metal heat transfer
effect of Pr, 285–286
in tube bundles, 351–352
in tubes, 337–340
laminar boundary layer, 291–293
Logarithmic mean temperature difference (LMTD), 97–114
correction factors, 108–114
defined, 105
limitations on, 107–108
Lummer, O.R., 31
Lumped capacity solutions, 22–26, 182–190
dimensional analysis of, 183–184
electrical/mechanical analogies, 184–186
in natural convection, 377–378
second order, 187–190
with heat generation, 137
with variable ambient temperature, 186–187

M

Mach number, 294
Martinelli parameter, 462
Martinelli, R.C., 462
Mass average velocity, 553
Mass conservation, *see* Conservation of mass
Mass diffusion equation, 582
Mass exchangers, 626
Mass flux, 554
Mass fraction, 550
in the transferred state, 594
Mass transfer, 547–615
analogy to heat transfer, 63, 582, 584, 586, 598–600
evaporation, 611–614
forced convective, 593–602
natural convective, 603–606
through a stagnant layer, 586–592
mass-based solution, 597
with simultaneous heat transfer, 606–615
Mass transfer coefficients, 593–606
at low rates, 598–602
analogy of heat and mass transfer, 598–602
effect of mass transfer rate on, 596–598
variable property effects, 608
Mass transfer driving force, 593–596
at low rates, 602
one species transferred, 595
Material derivative, 280
Mean beam length, 526
Mean free path, 283
rigid sphere molecules, 563
Melville, H.
Moby Dick, 317
Microchannel heat exchanger, 327
Mixed convection, 392
Mixing-cup temperature, *see* Bulk temperature
Mixtures

binary, 559
composition of, 550–553
molecular weight of, 551
of ideal gases, 551–553
specific heat of, 576
transport properties, 562–576
gas diffusion coefficients, 563–569
liquid diffusion coefficients, 569–571
thermal conductivity of gas mixtures, 571–576
viscosity of gas mixtures, 571–576
velocities and fluxes in, 553–558
Mobility, 570
Molar concentration, 550
Mole flux, 555
Mole fraction, 551
Mole-average velocity, 555
Molecular weight, 550–551, 565
Momentum equation, 265–268
Momentum integral method, *see* Integral conservation equations
Moody diagram, 334
Mothballs, 625

N

Natural convection, 20, 363–393
dimensional analysis, 367–370
governing equations, 365–368
horizontal cylinders, 382–384
in enclosures, 391
in mass transfer, 603–606
inclined and horizontal plates, 386–389
spheres, 384–386
subermerged bodies, 386
turbulent, 370, 379, 387
validity of b.l. approximations, 380–382
variable-property effects, 380, 388
vertical cylinders, 384
vertical plates, 367–379
analysis compared to data, 378–379
Squire-Eckert analysis, 371–376
wide-range correlation, 378
with forced convection, 392
with uniform heat flux, 390–391
Navier-Stokes equation, 265
Nernst-Einstein equation, 570, 619
Neumann conditions, 134
Newcomen's engine, 181
Newton's law of cooling, 20
Newton's law of viscous shear, 267
Newton, Isaac, 19
Nomenclature, 667–673
NTU, number of transfer units, 115
Nucleate boiling, *see* Boiling
Nukiyama, S., 421–423
Number density, 551
Nusselt number, defined, 261
average, 293, 296
for developing internal flow, 328–329
for fully developed internal flow, 325
for mass transfer, 600
Nusselt, E.K.W., 115, 261, 369, 396, 402, 408

O

Ocean, salt concentration in, 617
Ohm's law, 63
gray body radiation analogy, 512–522
thermal resistance analogy, *see* Thermal resistance
Overall heat transfer coefficient, 74–82
typical values, 79

P

Péclét number, 338
Partial density, 550
Partial pressure, 551
Peak heat flux, 426, 436–449
external flows, 458–459
general expression for, 442
horizontal plate, 442–445
internal flows, 466
various configurations, 445–449
very small objects, 446

Zuber-Kutateladze prediction, 444
Petukhov equation, 335
Physical constants, 661
Pi-theorem, *see* Buckingham pi-theorem
Pipe flow, *see* Internal flow
Planck's constant, 32
Planck's law, 32
Planck, M., 31
Pohlhausen, K., 272, 289
Poiseuille's law, 324
Poiseuille, J., 324
Prandtl number, 282–285
Eucken formula, 620
relation to b.l. thickness, 285–286, 290
turbulent Prandtl number, 304
Prandtl, L., 256, 257, 268, 301
Pringsheim, E., 31
Properties of substances, *see* Thermophysical property data
Property reference state, *see* Film temperature or Film composition
Psychrometer, sling, 611
Pumping power, 120

Q

Quenching, 449

R

Radiation, *see* Thermal radiation
Radiation heat transfer coefficient, 498
Radiation shield, 33–34, 501
Radiosity, 512
Raoult's law, 581
Rayleigh number, 369
for mass transfer, 603
for uniform wall heat flux, 391
Rayleigh, Lord (J.W. Strutt), 143
Reactions
heterogeneous, 556, 576, 615, 617, 625
homogeneous, 576, 615
Reflectance, 29
diffuse and specular, 492–493
Relativity, theory of, 148
Resistance, *see* Thermal resistance
Resistance thermometer, 421
Reversibility and heat transfer, 8
Reynolds number, 257
for two-phase flow, 463–464
Reynolds, O., 258, 297
Reynolds-Colburn analogy
for laminar flow, 297–299
for mass transfer, 614
for turbulent flow, 303–305
Richardson, L.F., 299

S

S.I. System, 14, 663–667
Samurai sword, 208–209
Savery's engine, 181
Schmidt number, 559
Schmidt, E., 261, 559
Second law of thermodynamics, 8–10
Self-diffusion, 560, 563
Separation of variables solutions, 138–142
Shakespeare, Wm.
Macbeth, 421
Venus and Adonis, 487
Sherwood number, 600
Sherwood, T.K., 600
Sieder-Tate equation, 335
Similarity transformations, 212, 268–270
Simultaneous heat and mass transfer, 606–615
energy balances for, 609–611, 614–615
Skin drag, *see* Skin friction coefficient
Skin friction coefficient, 273
for laminar flow, 275–276
for turbulent flow, 306
for turbulent pipe flow, 332–337
versus profile drag, 298
Solar energy, 530–535
solar collectors, 534–535
wavelength distribution, 491
Solubility, 580
Soret effect, 562, 618
Species conservation, 576–586

boundary conditions for, 579–582
equation of, 576–579
for stationary media, 582–585
for steady state, 585–586
Species-average velocity, 553
Specific heat capacity, 18, 278
for mixtures, 576
Specific heat ratio, 573
Speed of light in vacuum, 32, 661
Stagnant film model, 597–598, 623
Stanton number, 298
Stefan tube, 586
Stefan, J., 586
Stefan-Boltzmann constant, 30, 661
Stefan-Boltzmann law, 30
Stefan-Maxwell equation, 619
Stegosaurus, 155
Steradian, defined, 493
Stokes' law, 570
Stokes, G.G., 570
Stokes-Einstein equation, 570
Stream function, 262–264
Streamlines, 262
String rule, 537
Strouhal number, 344
Sublimation, 614, 625, 626
Suction, 598
Surface roughness effects
on friction factor, 333
on nucleation, 431–432
on pool boiling, 453–456
on turbulent transition, 307
Surface tension, 429–431
Sutherland, W., 570
Sweat cooling, 611

T

Taylor instability, 436–438
Taylor, G.I., 436
Temperature gradient, defined, 50
Temperature response charts, 196–206
Thermal conductivity, 12–16, 51
equations for gases, 571–576
Eucken correction, 573
simple kinetic theory model, 283–284
temperature dependence, 50–51
Thermal diffusion, 562
Thermal diffusivity, 19
Thermal expansion, coefficient of, 367
for an ideal gas, 369
Thermal radiation, 26–34, 487–535
black body, 28–32
black body exchange, 499–511
diffuse and specular, 492–493
gaseous, *see* Gaseous radiation
gray body, 489
gray body exchange, 495–497
algebraic solutions, 519–522
electrical analogy, 512–522
with a specified wall flux, 516
with an adiabatic surface, 515
infrared radiation, 28–29
intensity, 493–494
Kirchhoff's law, 495–497
monochromatic emissive power, 30
one body surrounding another, 497–499
Planck's law, 32
radiant exchange described, 32–34
radiation shield, 33–34, 501
selective surface, 491
solar, 530–535
Stefan-Boltzmann law, 30
transfer factor, *see* Transfer factor
view factor, *see* View factor
wavelength distribution, 28–32, 489–491
Wein's law, 31
Thermal resistance, 62–66
contact resistance, 64–66
defined, 62
for a cylinder, 69
for a slab, 62
for convection, 72
fouling resistance, 79–82
in parallel, 77–78
in series, 72–74, 76
Ohm's law analogy, 62–63
Thermophysical property data, 633
accuracy of, 633–636
density, 640–660
dynamic viscosity, 656–660

emittance
gases, 522–530
surfaces, 490
gases at 1 atm pressure, 656–660
kinematic viscosity, 646–660
latent heat of vaporization, 652
liquid metals, 646–651
metallic solids, 640–642
mixtures, *see* Mixtures
molecular weights, 565
nonmetallic solids, 642–645
Prandtl number, 646–660
saturated liquids, 646–651
saturated vapors, 653–655
specific heat capacity, 640–660
surface tension, 429–431
thermal conductivity, 15, 52, 53, 640–660
thermal diffusivity, 640–660
thermal expansion coefficient, 646–655
vapor pressure, 653–655
$CCl_4(l)$, 623
$CO_2(s)$, 627
napthalene, 625
Time constant, 23, 184, 188
Transfer factor, 32, 489
parallel plates, 498
two diffuse bodies, 499, 514
two specular bodies, 499
Transmittance, 29
Transpiration cooling, 609–611
Transport laws, 8
Tube bundles, 348–352
Tube flow, *see* Internal flow
Turbulence, 299–310
eddy diffusivities, 303–304
internal flow, 330–340
lengthscales of, 301–302, 315
Reynolds-Colburn analogy, 303–305
transition to, 258–260
Two-phase flow
heat transfer
boiling, 460–466
condensing, 469–470
regimes
for horizontal tubes, 466–469
without gravity force, 460

U

Units, 663–667
Universal gas constant, 552, 661

V

Verne, J.
Around the World in 80 Days, 5
View factor, 32, 499–511
between small and large objects, 508
examples of view factor algebra, 499, 509–511
general integral for, 502–504
reciprocity relation, 504
some three-dimensional configurations, 506, 507
some two-dimensional configurations, 505
summation rule, 500
View factors
string rule, 537
Viscosity
correction for temperature dependence of, 336
dynamic, 256
gas mixtures, 574
kinematic, 257
monatomic gas, 572
Newton's law of viscous shear, 267
simple kinetic theory model, 283–284
Sutherland formula for gases, 314
von Kármán, T., 272
Vortex shedding, 342–345

W

Watt, James, 181
Weber number, 458
Wein's law, 31
Wet-bulb temperature, 611–614
Wetting agent, 470

Y

Yamagata equation, 432